

The uptake mechanism of synthetic siderophore conjugates in Gram-negative bacteria

Von der Naturwissenschaftlichen Fakultät der
Gottfried Wilhelm Leibniz Universität Hannover

zur Erlangung des Grades

Doktorin der Naturwissenschaften (Dr. rer. nat.)

genehmigte Dissertation

von

Yi-Hui Lai, Master of Science (Taiwan)

2021

Keywords: *Escherichia coli*; siderophore; metabolomics

Schlagworte zum Inhalt: *Escherichia coli*; Siderophor; Metabolomics

Referent: Prof. Dr. rer. nat. Mark Brönstrup

Korreferent: Prof. Dr. rer. nat. Natalia Tschowri

Tag der Promotion: 13.10.2021

Abstract

Drug resistance in bacteria becomes a serious challenge in the clinic, so it is exigent to seek novel and effective antibiotic treatment options. By hijacking the siderophore transport system, siderophore-antibiotic conjugates are actively imported to the pathogen, boosting antibiotic efficacy via increased intracellular accumulation. However, the underlying transport mechanisms and the bacterial response to exposure to siderophore drugs are poorly understood. In this Thesis, a novel siderophore-conjugate named LP-600 was characterized, displaying excellent activity against both laboratory and uropathogenic *E. coli*. *E. coli* displaying triple knockout of *fepA*, *cirA* and *fiu* is resistant to LP-600, suggesting that outer membrane receptors FepA, CirA, and Fiu contribute to the uptake of siderophore-conjugates and antibacterial activity. To understand the resistance mechanism and potential targets, LP-600 resistant clones were generated by serial passages, followed by whole genome sequencing. Two point mutations were identified in genomes of LP-600-resistant clones in the proteins *exbB* (Excretes an inhibitor of colicin B) and *cyo B* (Cytochrome bo(3) ubiquinol oxidase subunit 1) at positions *exbB163** and *cyoBG269D*, respectively. Additionally, *E. coli* showed a paradoxical re-growth, a phenomenon coined the ‘Eagle-effect’ in other systems, upon treatment of LP-600 at concentrations 16 times above the minimum inhibitory concentration (MIC). Co-treatment with LP-600 and the β -lactamase inhibitor sulbactam significantly diminished the effect in *E. coli*. To decipher the mechanism behind the Eagle effect, transcriptomic and metabolome analysis were conducted. Joint pathway mapping from transcriptome and metabolome results revealed enrichment in pathways about amino acid metabolism including L-arginine, L-lysine degradation, and polyamine biosynthesis pathways upon regrowth conditions Eagle, compared with a sub-MIC treatment of LP-600. In addition, LP-600 induces expression of genes involved in SOS response and $\epsilon 14$ prophage upon regrowth conditions Eagle. Taken together, the work of this Thesis not only characterizes a novel and potent anti-bacterial compound, but also provides insight into the systemic bacterial responses towards siderophore-antibiotic conjugate exposure.

Keywords

Escherichia coli; siderophore; metabolomics

Zusammenfassung

Die Antibiotikaresistenz von Bakterien wird vor allem in der Klinik zu einer ernsthaften Herausforderung. Daher ist es dringend erforderlich, nach neuen und wirksamen Behandlungsmöglichkeiten für bakterielle Infektionen zu suchen. Durch die Ausnutzung des Siderophor-Transportsystems werden Siderophor-Antibiotika-Konjugate aktiv in den Erreger eingebracht. Damit wird die Antibiotikawirksamkeit durch eine erhöhte intrazelluläre Akkumulation gesteigert. Die zugrundeliegenden Transportmechanismen und die bakterielle Reaktion auf die Exposition gegenüber Siderophor-Wirkstoffen sind Gegenstand dieser Arbeit. In dieser Studie wurde ein neues Siderophor-Konjugat namens LP-600 charakterisiert, das sowohl gegen Laborstämme als auch gegen ein uropathogenes Isolat von *E. coli* eine hervorragende Aktivität aufweist. *E. coli* mit Dreifach-Knockout von *fepA*, *cirA* und *fiu* zeigt Resistenz gegen LP-600, was darauf hindeutet, dass die Außenmembranrezeptoren FepA, CirA und Fiu zur Aufnahme von Siderophor-Konjugaten und zur antibakteriellen Aktivität beitragen. Um den Resistenzmechanismus sowie mögliche Zielstrukturen zu verstehen, wurden LP-600-resistente Klone durch serielle Passagen erzeugt, gefolgt von einer Sequenzierung des Gesamtgenoms. Zwei Punktmutationen wurden in Genomen von LP-600-resistenten Klonen in den Proteinen exbB (sekretiert einen Inhibitor von Colicin B) und Cyo B (Cytochrom bo (3) Ubichinoloxidase-Untereinheit 1) an den Positionen exbB163 * bzw. cyoBG269D identifiziert. Zusätzlich zeigte *E. coli* ein paradoxes Wiederwachstum - ein Phänomen, das in anderen Systemen als „Eagle-Effekt“ bezeichnet wird - bei Behandlung mit LP-600 in Konzentrationen höher der 16-fachen minimalen Hemmkonzentration (MHK). Die gleichzeitige Behandlung mit LP-600 und dem β -Lactamase-Inhibitor Sulbactam verringerte den Effekt in *E. coli* signifikant. Um den Mechanismus hinter diesem Effekt zu entschlüsseln, wurden Transkriptom- und Metabolomanalysen durchgeführt. Die gemeinsame Kartierung der Pathogenantwort anhand der Transkriptom- und Metabolomdaten zeigte eine Anreicherung in Signalwegen des Aminosäurestoffwechsels - einschließlich L-Arginin, L-Lysin-Abbau und Polyamid-Biosynthesewege - unter ‚Eagle‘-Bedingungen, verglichen mit einer Sub-MHK-Behandlung von LP-600. Zudem induziert LP-600 unter diesen Bedingungen die Expression von Genen, die an der SOS-Reaktion und dem e14-Prophagen beteiligt sind. Zusammengefasst charakterisiert diese Studie nicht nur einen potenten

antiinfektiösen Wirkstoff, sondern bietet auch Einblick in die systemischen bakteriellen Reaktionen auf die Exposition von Siderophor-Antibiotika-Konjugaten.

Schlagworte zum Inhalt: *Escherichia coli*; Siderophor; Metabolomics

Table of contents

Abstract.....	i
Zusammenfassung	ii
Table of contents.....	iv
List of Figures	viii
List of tables.....	x
Abbreviations	xi
1. Introduction	1
1.1 Antibiotics	1
1.1.1 Mode of actions.....	1
1.1.1.1 Nucleic acid synthesis	2
1.1.1.2 Protein synthesis	3
1.1.1.3 Cell wall synthesis.....	5
1.1.1.4 Membrane integrity.....	6
1.1.2 Antibiotic resistance	7
1.1.3 Antibiotic resistance mechanisms.....	8
1.1.3.1 Modification of drug target.....	9
1.1.3.2 Inactivation of drug	9
1.1.3.3 Reduction of drug accumulation	11
1.2 Iron and iron acquisition.....	11
1.2.1 Iron acquisition	12
1.2.2 Siderophores	12
1.2.2.1 Enterobactin.....	14

1.2.2.2	MECAM.....	15
1.2.2.3	Sideromycins	15
1.3	<i>E. coli</i>	17
1.3.1	Antibiotic uptake	17
1.3.2	Siderophore transport system in <i>E. coli</i>	18
1.3.2.1	Outer membrane receptors.....	18
1.3.2.2	Ton machinery	19
1.3.2.3	Periplasmic binding protein and ABC transporter	20
1.3.2.4	Iron release from siderophore	20
1.4	Eagle effect.....	21
1.5	Metabolomics	23
1.5.1	Introduction of metabolomics.....	23
1.5.2	Workflow of metabolomics.....	24
1.6	Transcriptomics	27
2.	Aim of the thesis	29
3.	Materials and methods.....	30
3.1	Strains	30
3.2	Plasmids	30
3.3	Recombineering/Lambda red-mediated gene deletion	31
3.4	Growth recovery assay	34
3.5	Determination of minimum inhibitory concentrations (MICs)	35
3.6	Bacterial cell viability assay	35
3.7	Generation of LP-600-resistant clones and bioinformatic analysis of whole genome sequence	35
3.8	Determination of β -lactamase activity	36
3.9	Protein expression in <i>E. coli</i>	36
3.10	Quantitative RT-PCR	37
3.11	RNA isolation and transcriptome analysis	38

3.12 Metabolomics sample preparation	39
3.13 LC-MS/MS measurement and data analysis.....	39
3.14 Statistics analysis and bioinformatics	43
4. Results.....	44
4.1 LP-117, a novel synthetic siderophore, induced growth recovery in enterobactin-deleted <i>E. coli</i> in a FepA dependent manner. 44	
4.2 Siderophore-conjugate LP-600 and LP-624 display antibacterial activity against both laboratory and pathogenic <i>E. coli</i> ..	48
4.3 Catecholate siderophore receptors- FepA, CirA and Fiu, are required for LP-600 and LP-624 mediated antibacterial activity in <i>E. coli</i>	51
4.4 LP-600 resistant clones reveal single nucleotide variants in <i>cyoB</i> and <i>exbB</i> gene.	53
4.5 The siderophore uptake system functions in LP-600 resistant clones	55
4.6 Complementation of ExbB in <i>E. coli</i> Δ <i>exbB</i> restored susceptibility to LP-600	56
4.7 High-dose treatments of LP-600 induce a paradoxical growth of <i>E. coli</i>	59
4.8 Treatment with LP-600 at high, Eagle effect-inducing concentrations induces a modest increase in β -lactamase activity in <i>E. coli</i> 63	
4.9 Transcriptome analysis	65
4.9.1 Transcriptomic analysis of <i>E. coli</i> following treatments with LP-600.....	65
4.9.2 Transcriptome profile and differentially expressed genes following treatment with LP-600 at sub-MIC.....	71
4.9.3 Transcriptome profile and differentially expressed genes following treatment with LP-600 at high, Eagle effect-inducing concentrations.....	73
4.10 Metabolomic analysis	80
4.10.1 Metabolomic analysis of <i>E. coli</i> following treatments with LP-600.....	80
4.10.2 Metabolomic profile following treatment with LP-600 at sub-MIC.....	83
4.10.3 Metabolomic profiles following treatment with LP-600 at high, Eagle effect-inducing concentrations	87
4.11 Joint pathway mapping from transcriptome and metabolome results.....	91
5. Discussion	94
5.1 The uptake route of LP-600.	94
5.1.1 The role of ExbB in LP-600-mediated anti-bacterial activity in <i>E. coli</i>	95

5.1.2 The role of CyoB in LP-600-mediated anti-bacterial activity in <i>E. coli</i>	96
5.2 The metabolic and transcriptional response to sub-MIC level of LP-600.....	97
5.3 The mechanism of LP-600-induced Eagle effect:.....	98
5.3.1 The role of beta-lactamase in LP-600-induced Eagle effect.	98
5.3.2 Pathways involved in the Eagle effect.	99
Summary and outlook	103
References.....	105
Appendices.....	115
I. Summary of statistical results of whole genome sequencing for “recover” clones.....	115
II. Single nucleotide variants of “recover” clones and susceptibility	115
III. Differentially expressed gene of CL1 and CL2	115
IV. Significantly enriched terms in CL1 and CL2	119
V. Differentially expressed gene of LH1 and LH2	120
VI. Significantly enriched terms in LH1 and LH2	176
VII. Significantly regulated metabolites table of CL1 and CL2	189
VIII. Significantly regulated metabolites table of LH1 and LH2.....	194
IX. Over-representation analysis for differentially regulated metabolites in LH1 and LH2.....	202
X. Top 100 differential pathways	203
XI. MS and MS/MS identification.....	206
Acknowledgment.....	277
Curriculum vitae	278

List of Figures

Figure 1. Bacterial protein synthesis. aa-tRNA: aminoacyl-tRNA, A: aminoacyl site, E: exit site, P: peptidyl site.	4
Figure 2. Structure and mode of action β -lactam.	6
Figure 3. Mediators of antibiotic resistance.	8
Figure 4. β -Lactamase-catalyzed hydrolysis of ampicillin.	10
Figure 5. Examples of different types of natural siderophores.	13
Figure 6. Enterobactin biosynthesis in <i>E. coli</i>	14
Figure 7. Structure of the MECAM.	15
Figure 8. The structure and drug design of cefiderocol.	16
Figure 9. Ribbon representations of outer membrane siderophore receptor FepA from <i>E. coli</i>	19
Figure 10. Ferric iron transport system in <i>E. coli</i>	19
Figure 11. Antibiotic concentration versus CFU curves of resistance, persistence, and Eagle effect.	21
Figure 12. Scheme and result of growth recovery assay.	45
Figure 13. FepA is required for LP-117 uptake in <i>E. coli</i> under iron-limited medium.	47
Figure 14. Structures and molecular weights of LP-600 and LP-624.	48
Figure 15. Antibacterial activity of LP-600 and LP-624 against <i>E. coli</i>	50
Figure 16. Scheme of siderophore uptake system in <i>E. coli</i>	52
Figure 17. The siderophore uptake system does not abolish in LP-600 resistant clones.	56
Figure 18. Over-expression of ExbB163*, but not of CyoB G269D displays LP-600 resistance in <i>E. coli</i>	57
Figure 19. Antibacterial activity of LP-600 against <i>E. coli</i> in the presence or absence of CCCP.	59
Figure 20. Laboratory and pathogenic <i>E. coli</i> show paradoxical growth under high concentrations of LP-600.	61
Figure 21. Antibacterial activity of LP-600 against gene modification strains involved in siderophore uptake pathways of <i>E. coli</i>	62
Figure 22. The role of beta-lactamase in the LP-600 induced Eagle effect.	64
Figure 23. The growth curve of wild type <i>E. coli</i> treated without or with LP-600.	66
Figure 24. Multidimensional scaling (MDS) analysis of <i>E. coli</i> transcriptomes from the treatments of vehicle control (DMSO), low-dose (0.0625 μ g/mL), high-dose (128 μ g/mL) of LP-600 during mid-exponential phase ($OD_{600} = 0.5$) or stationary phase ($OD_{600} = 1.0$).	67
Figure 25. Heat map of top 100 variant genes from samples treated with DMSO, low-dose (0.0625 μ g/mL), high-dose (128 μ g/mL) of LP-600 during mid-exponential phase ($OD_{600} = 0.5$) or stationary phase ($OD_{600} = 1.0$).	71
Figure 26. Venn diagram of differentially expressed genes (DEGs) comparing low-dose (0.0625 μ g/mL) treatment of LP-600 with vehicle control.	71
Figure 27. Volcano plot of differentially expressed genes under low-dose treatment of LP-600 (0.0625 μ g/mL) during mid-exponential phase (at $OD_{600} = 0.5$).	73
Figure 28. Volcano plot of differentially expressed genes under low-dose treatment of LP-600 (0.0625 μ g/mL) during stationary phase (at $OD_{600} = 1.0$).	73
Figure 29. Networks of functional enrichment with significantly up-regulated genes in both LH1 and LH2.	75
Figure 30. Volcano plots of differentially expressed genes upon the high-dose treatment of LP-600 (128 μ g/mL) comparing with low-dose (0.0625 μ g/mL) LP-600 treatments at $OD_{600} = 0.5$	76
Figure 31. Networks of selected functional enrichment with significantly up-regulated genes in LH1.	77
Figure 32. Functional enrichment of networks with significantly down-regulated genes in LH1.	78
Figure 33. Volcano plots of differentially expressed genes upon the high-dose treatment of LP-600 (128 μ g/mL) comparing with low-dose (0.0625 μ g/mL) LP-600 treatment at $OD_{600} = 1.0$	79
Figure 34. Functional enrichment of networks with differentially expressed genes in LH2.	80
Figure 35. MDS analysis of <i>E. coli</i> metabolomes from indicated culture conditions obtained by UPLC-ESI-QToF experiments using C18 or HILIC columns in positive or negative mode.	82

Figure 36. Venn diagram represents the amounts of identified metabolites by different separation methods (C18 and HILIC columns) and ionization modes (positive and negative electrospray ionization).	83
Figure 37. Regulation of identified metabolites in CL1.	85
Figure 38. Regulation of identified metabolites in CL2.	86
Figure 39. Top 100 significantly regulated metabolites in LH1.	88
Figure 40. Regulation of identified metabolites in LH2.	90
Figure 41. Scatter diagram of ORA (over-representation analysis) for significantly regulated metabolites in both LH1 and LH2.	91
Figure 42. Summary of enriched pathways of differentially expressed genes and metabolites upon the Eagle effect.	93

List of tables

Table 1. Examples of common antibiotics.	1
Table 2. Priority Pathogens List and major antibiotic class affected by resistance.	7
Table 3. β -Lactamases.	10
Table 4. The Eagle effect of different bacteria	22
Table 5. List of genomic modification strains used in this study.....	30
Table 6. List of primers for lambda red-mediated gene deletion.....	31
Table 7. List of primers for colony PCR	33
Table 8. List of primers for quantitative RT-PCR.	38
Table 9. List of parameters applied in Metaboscope.	40
Table 10. Antibacterial activity of LP-600 and LP-624 against non-pathogenic and uropathogenic <i>E. coli</i>	49
Table 11. Antibacterial activity of LP-600, ampicillin and cefiderocol against gene modification strains involved in siderophore uptake pathways of <i>E. coli</i>	52
Table 12. Single nucleotide variants and antimicrobial susceptibility of LP-600-resistant clones.	54
Table 13. Summary of statistical results of whole genome sequencing for four LP-600-resistant clones.....	54

Abbreviations

ABC	ATP-binding cassette
Amp	Ampicillin
Amx	Amoxicillin
AST	Arginine succinyltransferase
CFU	Colony-forming unit
Ctrl	Control (untreated)
EB	Enterobactin
ESI	Electrospray ionization
FAD	Flavin adenine dinucleotide
FC	Fold change
FDR	False discovery rate
FMN	Flavin mononucleotide
FQ	Fluoroquinolone
GC	Gas chromatography
GNPS	Global Natural Product Social Molecular Networking
HILIC	Hydrophilic interaction liquid chromatography
Kan	Kanamycin
log ₂ -FC	Fold change of log ₂ -transformed data
LPE	Lyso-phosphatidylethanolamine
LPG	Lyso-phosphatidylglycol
LPS	Lipopolisaccharide
m/z	Mass-to-charge ratio of the molecular ion
MDR	Multi-drug resistant
MDS	Multidimensional scaling
MECAM	1,3,5-Tris (N, N', N' '- 2,3-dihydroxybenzoyl) aminomethylbenzene
MIC	Minimum inhibitory concentration
mRNA	Messenger ribonucleic acid

MS	Mass spectrometry
NAD	Nicotinamide adenine nucleotide
NADP	Nicotinamide adenine dinucleotide phosphate
NAG	N-acetylglucosamine
NAM	N-acetylmuramic acid
OBC	Optimal bactericidal concentration
OD ₆₀₀	Optical density at $\lambda = 600$ nm
OMR	Outer membrane receptor
PBP	Penicillin binding proteins
PE	Phosphatidylethanolamine
PG	Phosphatidylglycol
PMF	Proton-motive force
QQQ	Triple quadrupole
Q-TOF	Quadrupole-TOF
ROS	Reactive oxygen species
rRNA	Ribosomal ribonucleic acid
RT	Reverse transcription
SAM	S-adenosyl-L-methionine
SNP	Single nucleotide polymorphism
sub-MIC	Concentrations under the minimum inhibitory concentration
TMD	Transmembrane domains
TOF	Time of flight
tRNA	Transfer ribonucleic acid
UPEC	Uropathogenic E. coli
UPLC	Ultra-Performance Liquid Chromatography
UPLC	Ultra Performance Liquid Chromatography
WT	Wild type

1. Introduction

1.1 Antibiotics

Antibiotics, a type of anti-bacterial compounds, are able to kill bacteria (bactericidal) or inhibit bacterial growth (bacteriostatic). Antibiotics are widely used and play a key role in infection treatment since the discovery of penicillin by Alexander Fleming in 1928 ¹. The medical uses of antibiotics are not only confined to treating infectious diseases such as nosocomial infections, but also include measures for preventing infections in immunocompromised populations such as people with HIV (human immunodeficiency viruses) or patients taking immunosuppressive drugs after surgery ². In addition, the demand for antibiotics is increasing around the world ³. A study among 76 countries from 2000 to 2015 revealed that antibiotic consumption increased by 65% from 21.1 to 34.8 billion defined daily doses (DDDs), and the rate of antibiotic consumption increased by 39% (from 11.3 to 15.7) DDDs per 1,000 inhabitants per day ³. In the European Union/European Economic Area (EU/EEA), there was an average total antibiotic consumption of 20.1 DDD per 1,000 inhabitants per day during 2009 and 2018 ⁴. In the United States, over 50% of inpatients received at least one antibiotic during their stay in hospital and at least 270 million antibiotic prescriptions were applied in 2015 ⁵. Considering the high demand and wide application, antibiotics play a key role in the modern health care system.

1.1.1 Mode of actions

Antibiotics can be classified into four main types on the basis of mechanism of action: nucleic acid, protein, cell wall synthesis, and membrane integrity (Table 1).

Table 1. Examples of common antibiotics ⁶.

Mode of action	Target	Antibiotic classes (examples in brackets)
Nucleic acid synthesis	DNA gyrase	Quinolones (nalidixic acid, ciprofloxacin, levofloxacin and gemifloxacin)
	Folate metabolism (Enzymes in tetrahydrofolate biosynthesis)	Sulfonamides, Trimethoprim

	RNA polymerase	Rifamycins (rifampicin)
Protein synthesis	30S subunit	Tetracyclines, Aminoglycosides
	50S subunit	Chloramphenicol, macrolides, Oxazolidinones
Cell wall synthesis	Penicillin-binding protein	β -lactams (ampicillin)
	D-alanyl D-alanine	Glycopeptides (vancomycin)
Membrane integrity	Cell Membrane	Lipopeptides (daptomycins)
	Lipopolysaccharides (LPS)	Polymyxins (polymyxin B)

1.1.1.1 Nucleic acid synthesis

Nucleic acid synthesis is essential for bacterial survival, so certain types of compounds interfere with the synthesis of nucleic acid as antibiotics. For instance, quinolones, a member of a large group of broad-spectrum bacteriocidal (e.g. nalidixic acid, ciprofloxacin, levofloxacin or gemifloxacin), are active against both Gram-positive and negative as well as *Mycobacterium tuberculosis* by targeting DNA synthesis⁷. Quinolones inhibit the activity of topoisomerase II and topoisomerase IV involved in the modulation of chromosomal supercoiling⁸⁻¹⁰. Despite topoisomerase II and topoisomerase IV have a general similarity of functions, quinolones have different topoisomerase targets across species. Previous studies showed that the primary target of quinolones in Gram-negative bacteria (e.g. *E. coli*) is topoisomerase II¹¹, while quinolones primarily target topoisomerase VI in some Gram-positive bacteria such as *Streptococcus pneumoniae*¹². Ciprofloxacin, for example, targets *E. coli* DNA gyrase that is a topoisomerase II enzyme for the introduction of negative supercoil of double-stranded DNA (dsDNA) and resealing the nicked ends during DNA replication^{10,11}. During DNA replication, gyrase containing two subunits of gyrase A (GyrA) and B (GyrB) nicks each strand of DNA, forming a stable complex with DNA^{10,13}. Subsequently, the broken strands pass the other strands of DNA, enabling topological relaxation followed by resealing of two strands of DNA. By covalently complexing with gyrase, quinolones trap gyrase at the DNA cleavage stage and preventing strand rejoining, leading to DNA replication arrest, double strand break of DNA and eventually cell death^{7,13}.

In addition to direct interfering with DNA replication, antibiotics such as sulfonamide and trimethoprim target the folate pathway, leading to the arrest of DNA synthesis. For example, sulfonamides inhibit the activity of dihydropteroate synthase, which is an enzyme involved in the upstream of tetrahydrofolate synthesis. Tetrahydrofolate is a key cofactor in the thymidine synthesis, and the blockade of tetrahydrofolate synthesis leads to inhibition of DNA replication^{14,15}. Sulfonamides compete with p-amino benzoic acid for binding dihydropteroate synthase, blocking folate metabolism and then shutting down DNA synthesis. Besides, antibiotics such as trimethoprim target folic acid synthesis by inhibiting the activity of dihydrofolate reductase involved downstream of tetrahydrofolate synthesis¹⁵. In medical use, a combination of sulfonamides and trimethoprim shows a synergistic effect and reduces resistance¹⁴.

Apart from DNA synthesis, antibiotics like rifampin act as the inhibitor of transcription¹⁴. Rifamycins can bind to the β -subunit (encoded by *rpoB*) of a DNA-bound as well as actively transcribing RNA polymerase, inhibiting DNA-dependent transcription.

1.1.1.2 Protein synthesis

In bacteria, full ribosomes (size: 70S) are composed of 30S and 50S subunits and responsible for protein synthesis. During protein synthesis, there are three main steps: initiation, elongation and termination^{7,16} (Figure 1). Firstly, the intact ribosome forms. With the help of initiation factors, 30S and the 50S ribosomal subunits form a 70S complex accompanied with the first aminoacyl-tRNA (aa-tRNA) (tRNA with the first amino acid) paired with cognate mRNA in the peptidyl (P) site of the ribosome¹⁶. Subsequently, during the elongation, the subsequent aminoacyl-tRNA occupies the aminoacyl (A) site of ribosome and then peptide chain elongates by transferring the first aminoacyl-tRNA to the second. After transfer the peptide chain to the second aminoacyl-tRNA, the disassociated tRNA accommodates the E (exit) site for release from ribosome. The translation continues with the elongation process cycle with the following aminoacyl-tRNA. Lastly, the translation occurs when a nonsense codon occupies the A site, leading to the release of polypeptide chain, tRNA and the dissociation of ribosomal complex^{7,16}.

Antibiotics can interfere with protein synthesis by targeting 30S and 50S subunits. Antibiotics like tetracyclines and aminoglycosides target 30S subunits, while chloramphenicol, macrolides, and oxazolidinones target 50S subunits⁷. For example, aminoglycosides, highly polar and positively-

charged antibacterial drugs, interfere with proofreading function during translation by interacting with 16S rRNA of 30S ribosomal subunit^{6,17}. Without a proper proofreading process, it results in mismatches of codons and anticodons and thereby inaccurate translation. Similar to aminoglycosides, tetracyclines binds to 16S rRNA of 30S subunit to block tRNA binding to the A site, thereby inhibiting protein synthesis. Furthermore, chloramphenicol interacts with 50S subunit to avoid ribosomal binding to t-RNA, interfering with peptide bond formation and stopping protein synthesis¹⁴.

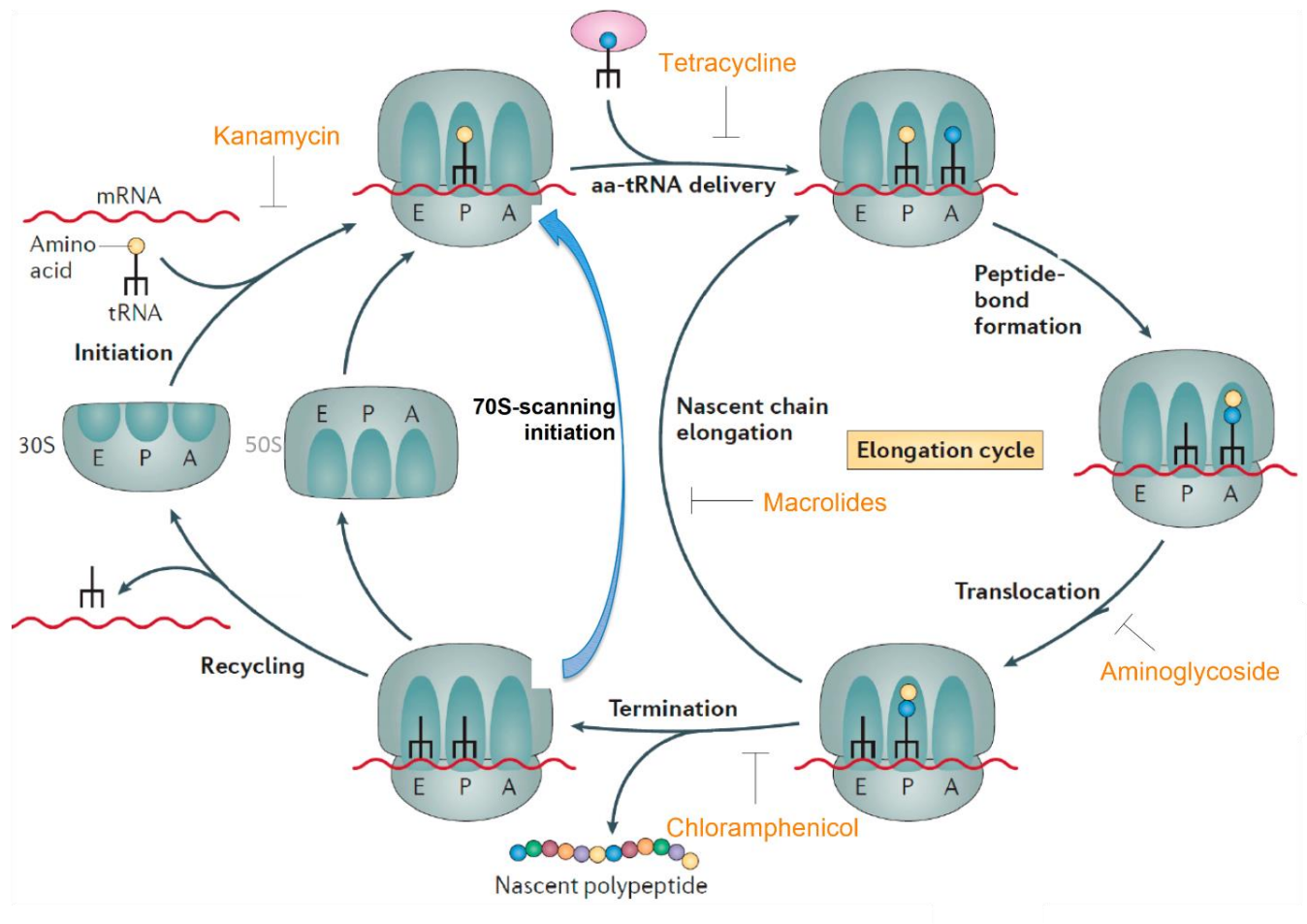


Figure 1. Bacterial protein synthesis. aa-tRNA: aminoacyl-tRNA, A: aminoacyl site, E: exit site, P: peptidyl site. Modified from¹⁶.

1.1.1.3 Cell wall synthesis

The peptidoglycan layer is a polymeric mesh-like layer outside the plasma membrane, forming cell wall. The peptidoglycan layer is composed of glycan strands of repeating units of N-acetylglucosamine (NAG) and N-acetylmuramic acid (NAM) crosslinked by peptides¹⁸. The integrity of peptidoglycan layer is essential for bacteria, because it contributes to protein anchoring on the cell surface as a scaffold, cell shape, maintenance of structural integrity during growth, cell division as well as osmotic stress^{18,19}.

Considering that the peptidoglycan layer is important to bacterial survival, there are various classes of antibiotics targeting to cell wall for antibiotic actions. For example, β -lactam antibiotics, the biggest class of antibiotics, are a type of compounds containing β -lactam ring that is a structural analog of the peptidoglycan motif D-alanyl-D-alanine (Figure 2)²⁰. D-alanyl-D-alanine is the terminal amino acid residues on the precursor N-acetylglucosamine/ N-acetylmuramic acid (NAG/NAM)-peptide subunits of a peptidoglycan layer. Penicillin binding proteins (PBPs), a kind of transpeptidases, catalyzes the final step in the synthesis of peptidoglycan- cross-linking of peptides. PBP recognizes D-alanyl-D-alanine as its substrate to form a covalent bond between D-alanine on two different side chains (Figure 2B). β -lactam suppresses this crosslinking (transpeptidation) of the nascent peptidoglycan layer by irreversible binding to PBP's active site, thereby disrupting the synthesis of cell wall²¹. Furthermore, interference of cross-linkage leads to an accumulation of peptidoglycan precursors, triggering the breakdown of existing peptidoglycan by autolytic hydrolases. Consequently, the antibacterial activity of β -lactam antibiotics is further promoted. Besides, glycopeptides such as vancomycin block cell wall synthesis in a different way. Vancomycin binds to D-alanyl D-alanine to prevent the interaction between D-alanyl D-alanine and PBP, suppressing the cell-wall synthesis⁶.

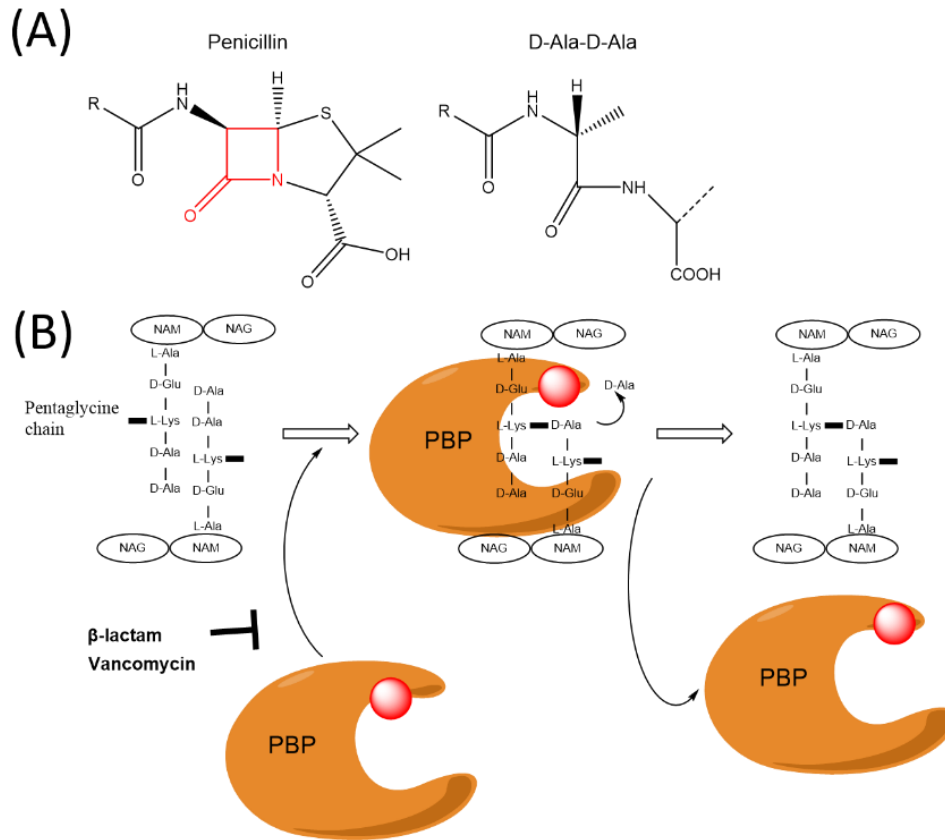


Figure 2. Structure and mode of action β -lactam. (A) Structures of penicillin and D-alanyl-D-alanine, β -lactam ring is highlighted in red²⁰. (B) Mode of action of β -lactam antibiotics.

1.1.1.4 Membrane integrity

The maintenance of cell membrane integrity is essential to bacterial survival. The structure of cell envelopes of Gram-positive and Gram-negative bacteria varies. The cell envelope of Gram-positive bacteria contains a layer of membrane and a thick peptidoglycan layer, whereas, the cell envelope of Gram-negative bacteria is composed of an outer membrane, a peptidoglycan layer, and an inner membrane^{6,14,22}. Thus, groups of compounds disrupt membrane structure for anti-bacterial activity. For example, daptomycin, a lipopeptide antibiotic, is applied in the treatment of infections caused by Gram-positive organisms^{23,24}. Daptomycin can insert into membrane and aggregate in the membrane, leading to pore formation, then rapid depolarization of membrane. Membrane depolarization causes the loss of membrane potential and thus interference of several reactions in bacteria, leading to eventually bacterial death^{23,24}. In addition to membrane depolarization, interference of physicochemical properties of the cytoplasmic membrane was

found to contribute to daptomycin-mediated cell death ²⁵. Another example is polymyxins (e.g. polymyxin B, polymyxins E also known as colistin) which are peptides with a fatty acid chain is used to treat Gram-negative bacterial infections ¹⁴. Polymyxins interact with lipopolysaccharides (LPS) of the outer membrane, subsequently disrupt both outer and inner membrane structures ¹⁴.

1.1.2 Antibiotic resistance

The emerging antibiotic resistance becomes a global crisis. World Health Organization announced that antibiotics become increasingly ineffective as drug resistance spreads globally leading to the difficulty to treat infections, thus antimicrobial resistance is a global threat and influences anyone anywhere. In EU/EEA countries, for example, population-weighted average antibiotics consumption for treating multidrug-resistant (MDR) bacterial infections exhibits a significant increase during 2009-2018 ⁴. Globally, at least 0,7 million annual deaths are attributed to antimicrobial resistance (AMR), and the number was estimated to increase to 10 million by 2050 ²⁶. In 2017, WHO published a list of global priority pathogens that urgently require solutions for treatment (Table 2) ²⁷. Among this list, ESKAPE (*Enterococcus faecium*, *Staphylococcus aureus*, *Klebsiella pneumoniae*, *Acinetobacter baumannii*, *Pseudomonas aeruginosa*, and *Enterobacter* species) pathogens were designated as being growingly involved in infectious diseases ²⁸. Therefore, the world has an urgent need for more effective antibiotic strategies.

Table 2. Priority Pathogens List and major antibiotic class affected by resistance ²⁷.

Level	Pathogen	Antibiotics Resistance	
Priority 1: Critical	<i>Acinetobacter baumannii</i>	Carbapenem	β-lactam
	<i>Pseudomonas aeruginosa</i>	Carbapenem	β-lactam
	Enterobacteriaceae ⁺	Carbapenem	β-lactam
		3rd generation -cephalosporin	β-lactam
Priority 2: High	<i>Enterococcus faecium</i>	Vancomycin	Glycopeptides
	<i>Staphylococcus aureus</i>	Methicillin	β-lactam
		Vancomycin	Glycopeptides
	<i>Helicobacter pylori</i>	Clarithromycin	Macrolides

	Campylobacter spp.	Fluoroquinolone	Quinolone
	Salmonella spp.	Fluoroquinolone	Quinolone
	Neisseria gonorrhoeae	Fluoroquinolone	Quinolone
		3rd generation -cephalosporin	β -lactam
Priority 3: Medium	Streptococcus pneumonia	Penicillin -non-susceptible	β -lactam
	Haemophilus influenza,	Ampicillin	β -lactam
	Shigella spp.	Fluoroquinolone	Quinolone

+ Enterobacteriaceae includes: *Klebsiella pneumonia*, *Escherichia coli*, *Enterobacter* spp., *Serratia* spp., *Proteus* spp., and *Providencia* spp., *Morganella* spp.

1.1.3 Antibiotic resistance mechanisms

Bacteria develop a variety of resistance mechanisms to survive in the presence of antibiotics (Figure 3). Among resistance mechanisms, there are three major categories: modification of drug target, inactivation of drug, reduction of drug accumulation ²⁹.

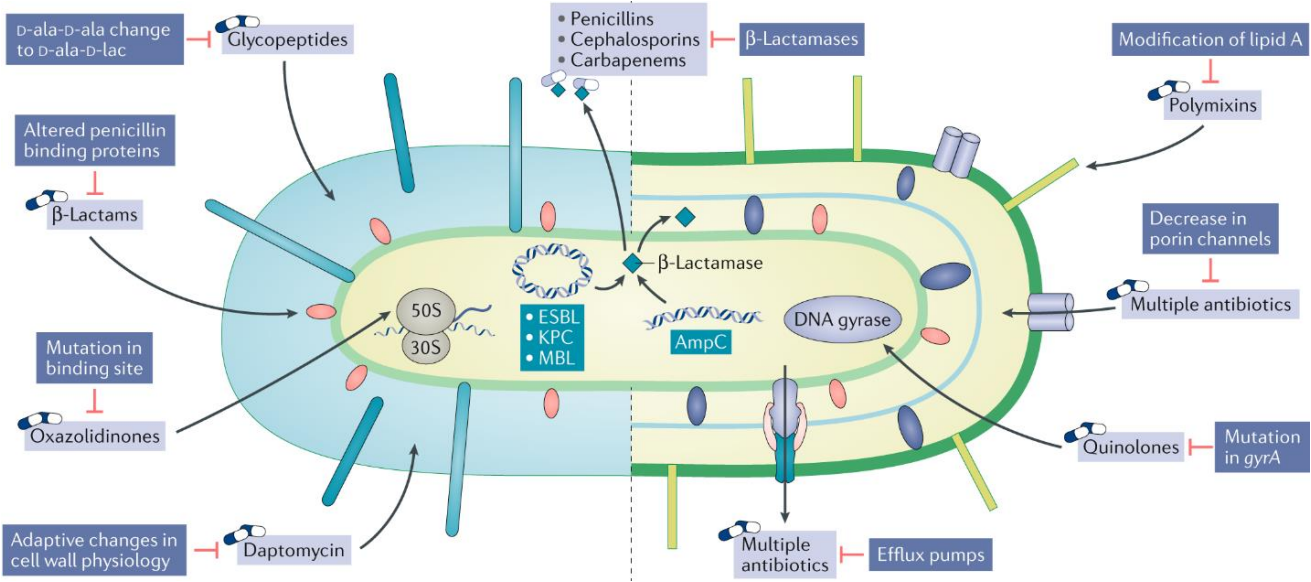


Figure 3. Mediators of antibiotic resistance. (taken from ³⁰)

1.1.3.1 Modification of drug target

Bacteria modify the antibiotic target site, diminishing the affinity or avoiding the binding of the antibiotics. To reach this goal, bacteria can display mutations in genes encoding drug targets. For instance, studies found that fluoroquinolone resistance most commonly occurs by *gyrA* and *parC* gene mutations that are in the quinolone-binding region of the enzyme ²¹. In addition to spontaneous mutations, bacteria can modify target site mediated by plasmids. For example, increasing plasmid-mediated quinolone resistance (PMQR) among pathogens such as *Enterobacter* spp. was found. Qnr-family proteins contribute to PMQR by bind directly to DNA gyrase antibiotic target, thereby reducing the antibacterial activity of fluoroquinolone ³¹.

1.1.3.2 Inactivation of drug

Pathogens destroy or neutralize antibiotics through chemical modifications with the help of certain enzymes encoded by chromosomal or plasmid genes. Such enzymes are especially prevalent in Gram-negative bacteria ²¹. A representative example is β -lactamase that inactivates β -lactam-antibiotics by breaking the β -lactam ring via hydrolysis (Figure 4) ²¹. More than 2000 β -lactamases enabling resistance to one or more β -lactams (e.g. penicillin, cephalosporin) have been reported ³². β -Lactamases represent the most important resistance mechanism for β -lactam antibiotics, especially in Gram-negative ESKAPE pathogens ²¹. According to primary molecular structures, there are four classes of β -lactamases ³² (Table 3). The largest cluster of β -lactamase-class A is capable of inactivating most β -lactam classes including the third-generation oxyimino-cephalosporin and carbapenem, which is the major concern of their prevalence among β -lactam-resistant *Enterobacteriaceae* ^{27,32}. Besides, several “priority” pathogens such as *Pseudomonas*, *Enterobacter* express class C lactamases such as AmpC, contributing to carbapenem and extended-spectrum cephalosporins resistance. In contrast to class A, class D enzymes are prevalent in *P. aeruginosa* as well as *A. baumannii* ^{32,33}.

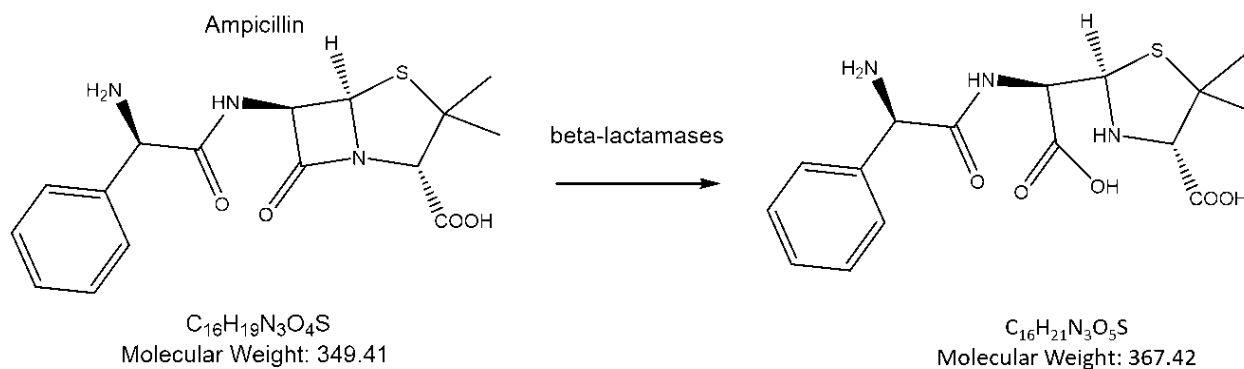


Figure 4. β -Lactamase-catalyzed hydrolysis of ampicillin.

Table 3. β -Lactamases³²⁻³⁴.

Class	Type	Characteristics	Examples of Enzymes
A	Narrow-spectrum β lactamases	Hydrolyze penicillin	Staphylococcal penicillinase, TEM-1, TEM-2, SHV-1
	Extended-spectrum β -lactamases (ESBL)	Hydrolyze cephalosporins, penicillin	SHV-2, CTX-M-15, PER-1, VEB-1
	carbapenemases	Hydrolyze carbapenems	KPC-1, IMI-1, SME-1
B	Metallo- β -lactamases	Hydrolyze carbapenems	VIM-1, IMP-1, NDM-1
C	Cephalosporinases	Hydrolyze cephamycins and some oxyimino β lactams; inducible; chromosomally mediated	AmpC, P99, ACT-1, CMY-2, FOX-1, MIR-1
D	OXA-type enzymes	Hydrolyze carbapenems, oxacillin, oxyimino β -lactams; produced by <i>P. aeruginosa</i> and <i>A. baumannii</i>	OXA enzymes

Another enzymatic modification occurs in the aminoglycosides resistance. Aminoglycoside modifying enzymes such as nucleotidyltransferases, phosphotransferases, and acetyltransferases catalyze the O-adenylation, O-phosphorylation and N-acetylation, thereby deactivating

aminoglycosides¹⁷. Aminoglycoside modifying enzymes constitute the most prevalent resistance mechanism of aminoglycosides in clinics.

1.1.3.3 Reduction of drug accumulation

The third general mechanism is to reduce drug accumulation by either increasing efflux of drug or decreasing drug uptake. Downregulation or lack of certain membrane channels such as porins reduces drug uptake for antibiotic resistance. For example, the mutation of OprD porin in *P. aeruginosa* results in a reduction of carbapenem susceptibility³⁵. In addition, actively extruding drugs out of bacteria contributes to resistance. There are six main families of efflux pumps related to antibiotic resistance: resistance-nodulation-division (RND), major facilitator superfamily (MFS), multidrug and toxic compound extrusion (MATE), small multidrug resistance (SMR), ATP-binding cassette (ABC), and proteobacterial antimicrobial compound efflux (PACE) families³⁶. Especially RND-type efflux pump-mediated resistance occurs frequently among Gram-negative bacteria. For instance, the overexpression of AcrAB-TolC contributes to antibiotic resistance in multidrug-resistant *K. pneumoniae* and *E. coli*³⁶.

1.2 Iron and iron acquisition

Iron is essential for most living organisms from bacteria to human. In vivo, iron, by shifting between ferric (Fe^{3+}) and ferrous (Fe^{2+}) oxidation states, serves as a redox catalyst and participates in heme- and iron-sulfur cluster proteins involved in numbers of reactions such as DNA synthesis, respiration, metabolism of oxygen and nitrogen^{37,38}. Yet, iron is scarce at a concentration as low as 10^{-9} to 10^{-18} M in an aerobic environment and 10^{-24} M in the host^{39,40}. At neutral pH, iron dominantly forms insoluble ferric hydroxide, because a soluble and bioavailable form of iron (Fe^{2+}) is rapidly oxidized to Fe^{3+} and subsequently becomes insoluble hydroxides^{37,38} in the presence of oxygen. Besides, iron is tightly controlled in the living organism to prevent iron toxicity. For example, excessive iron can generate hydroxyl radicals with reactive oxygen species (ROS) via Fenton reaction, resulting in DNA and protein damage. Thus, iron availability is a considerable challenge but essential for life.

1.2.1 Iron acquisition

For survival, living organisms develop diverse systems to secure the iron demand. In humans, the majority of iron is stored intracellularly, complexed with hemoglobin inside erythrocytes⁴¹, and extracellularly sequestered by transferrin that is a glycoprotein responsible for iron transport through blood plasma. Dietary ferric iron is reduced by ferric reductases in apical brush border of enterocytes and then transported into cells by the DMT1 transporter for cellular usage or storage⁴¹. To make use of iron, released ferrous iron from enterocytes subsequently binds to transferrin and shuttles into target sites⁴². The rest of iron binds to plasma molecules including citrate and albumin⁴³. On the other hand, bacteria develop diverse strategies to secure their iron resource in the host. In bacteria, iron can be obtained via the uptake of host proteins such as lactoferrin, transferrin and heme-bound hemoglobin⁴⁴ in host environment. Alternatively, bacteria synthesize siderophores, a class of low-molecule-weight (500–1500 Da) molecules with substantially higher affinity to iron, for iron acquisition⁴⁵. For example, enterobactin, one of the most common siderophores in *E. coli*, forms an iron-enterobactin complex (Fe^{3+} -Ent) with a dissociation constant (K_d) of 10^{-49} M that enables to dissociate iron from host proteins including transferrin ($K_d = 10^{-20}$ M)^{46,47}.

Due to the scarcity and essentiality of iron, a war for iron acquisition occurs between host and pathogens. To prevent iron stealing from pathogens, neutrophils produce lipocalin 2 (Lcn2, or neutrophil gelatinase-associated lipocalin (NGAL)) to sequester the prototypic catecholate siderophore such as enterobactin. However, numbers of enteric pathogens encode salmochelin, a glycosylated-enterobactin which is resistant to sequestering by Lcn2, thus evading the host immunity⁴⁸. Besides, bacteria such as *P. aeruginosa* and *S. aureus* can take up xenosiderophores that are produced by other microbes^{49,50}, providing a benefit for bacterial survival. Therefore, the acquisition of iron is crucial for survival as well as the battle between host and pathogens.

1.2.2 Siderophores

Siderophores, iron chelators secreted by several phyla of microorganisms from bacteria to fungi, complex with iron and shuttle iron into organisms⁴⁵. There are more than 500 types of siderophores that have been discovered from microbes and plants⁴⁵ since the first siderophore mycobactin was discovered in 1950s from *Mycobacterium johnei*⁵¹. Rather than a ribosomal-

dependent manner, the biosynthesis of siderophore relies on non-ribosomal peptide synthetases (NRPS) or NRPS-independent synthetases (NIS) pathway^{52,53}. Negatively charged oxygen atoms have the highest affinity to Fe^{3+} , so siderophores thus utilize charged oxygens as donor atoms to tighten the interaction with iron⁴⁵. Siderophores can be categorized into three main classes based on the moieties donating the oxygen ligands for Fe^{3+} coordination: catecholates, hydroxamates, and carboxylates⁴⁷ (Figure 5), which form a stable hexadentate, octahedral complex with iron (III)⁴⁷. The most efficient form of siderophores is an octahedral 1:1 complex with Fe^{3+} by arranging iron center around hexadentate ligands^{45,54}. Among three types of siderophores, catecholate displays the highest ferric iron affinity than others at physiological pH 7.4⁴⁵. By contrast, carboxylate displays a high affinity of iron at acidic pH where catecholate and hydroxamate siderophores remain protonated. Besides, siderophore can have a mix of structures combining more than one class. For example, aerobactin includes hydroxamate and carboxylate moieties⁵⁴.

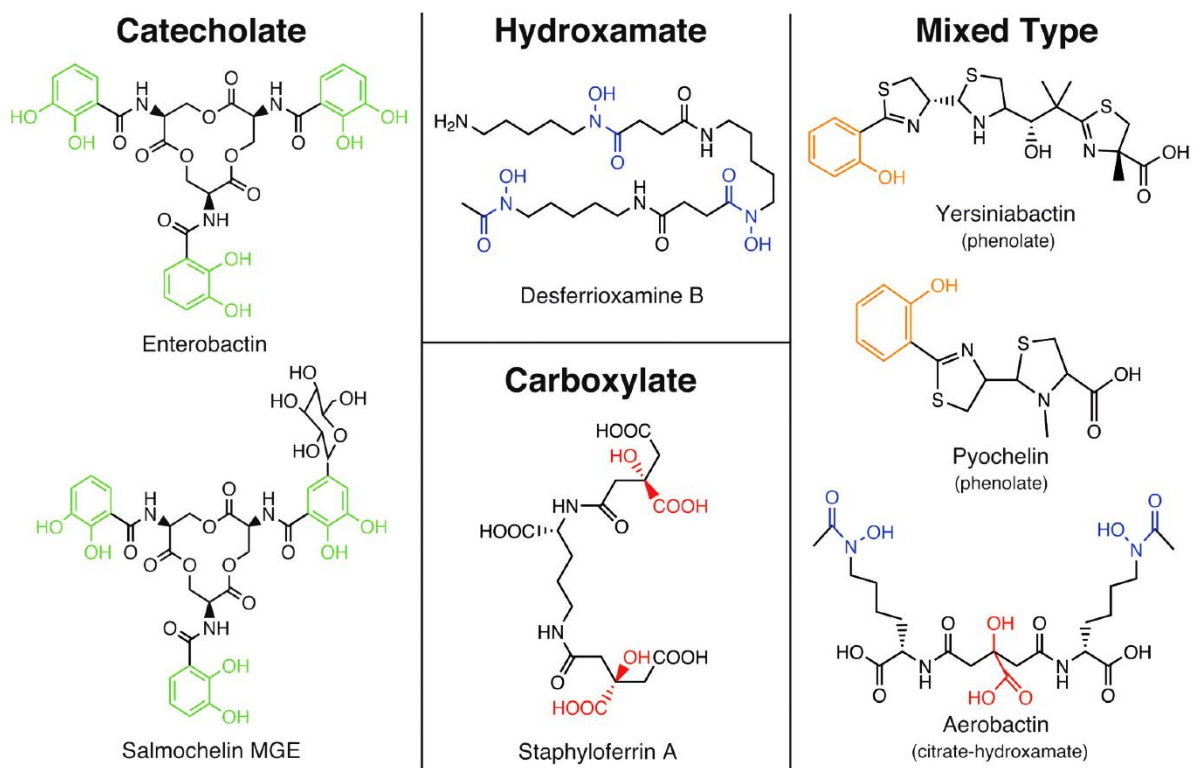


Figure 5. Examples of different types of natural siderophores (taken from⁴⁷).

1.2.2.1 Enterobactin

Enterobactin, a siderophore first isolated first from *Salmonella typhimurium* in 1970⁵⁵, is made of three units of catechol moieties (2,3-dihydroxybenzoylserine with in a central trilactone backbone (Figure 6). In addition to *S. typhimurium*, various bacteria such as *E. coli* produce enterobactin. Furthermore, enterobactin can be applied as a xenosiderophore by several bacteria including *P. aeruginosa*⁴⁹. Fe³⁺-enterobactin is a stable complex with a formation constant $K_{f,Fe^{3+}} = 10^{49} M^{-1}$ which is considerably higher than numbers of synthetic chelators such as EDTA ($K_{f,Fe^{3+}} \sim 10^{25} M^{-1}$)⁴⁵, making it one of the most competent siderophores.

In *E. coli*, the synthesis of enterobactin starts from chorismate, an aromatic amino acid precursor and contains two main steps: the conversion of chorismate to DHB (2,3-dihydroxybenzoate) and the synthesis of enterobactin from DHB and L-serine⁵⁶ (Figure 6). To yield DHB from chorismate, a series of enzymes, EntC (isochorismate synthase), EntB (isochorismatase) and EntA (2,3-dihydro-2,3-dihydroxy- benzoate dehydrogenase) are involved. Subsequently, EntDEF, with the bifunctional enzyme EntB, converts DHB to enterobactin⁵⁷.

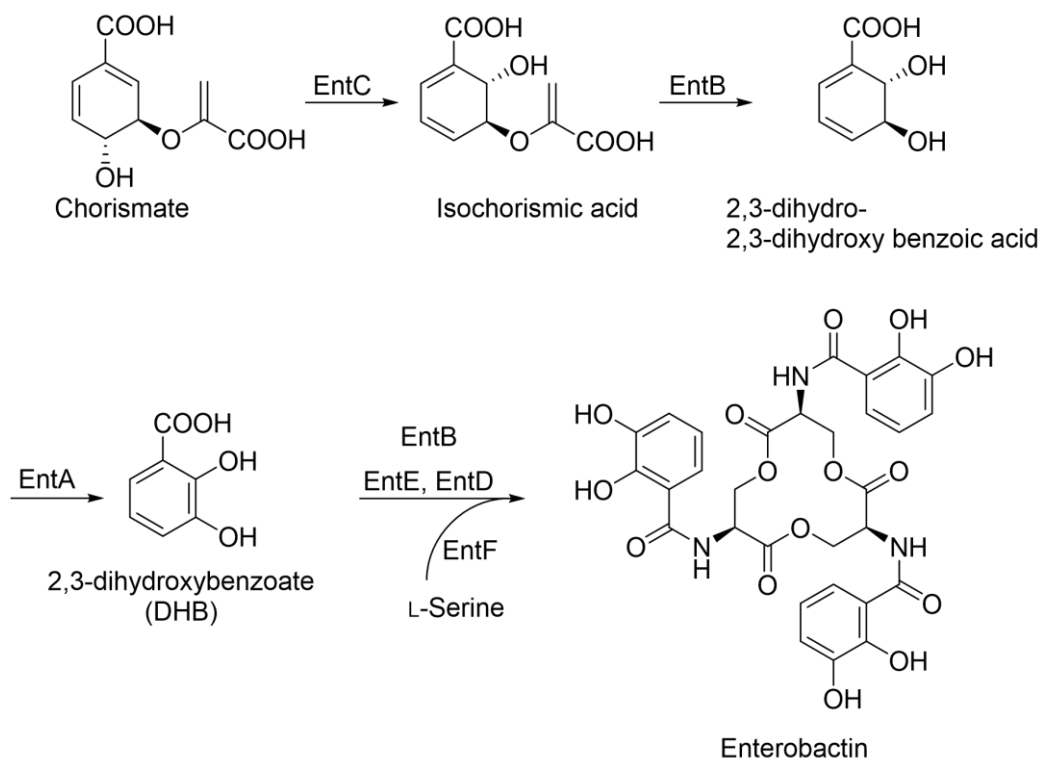


Figure 6. Enterobactin biosynthesis in *E. coli*.

1.2.2.2 MECAM

In the synthetic siderophore MECAM (1,3,5-Tris (N, N', N'- 2,3-dihydroxybenzoyl) aminomethylbenzene), first described in 1978⁵⁸, the trilactone backbone of enterobactin is replaced with an aromatic core (Figure 7). MECAM forms ferric-MECAM with iron, which can be transported as efficiently as ferric-enterobactin across outer membrane and thus supply iron into bacteria. Besides, studies revealed that ferric-MECAM inhibits the uptake of ferric-enterobactin⁵⁹ and protects bacteria from killing by colicin B which is a type of bacteriocin relying on enterobactin receptor to enter into bacteria⁶⁰. These studies indicate that MECAM is a potent siderophore for bacteria but also might use the enterobactin receptor for its uptake. Yet, subsequent iron import into cytoplasm by MECAM is almost 10 times slower than that by enterobactin⁶¹. Given the siderophore property and accumulation in the periplasm, MECAM might become a potential siderophore scaffold linked to antibiotic targeting to the periplasm.

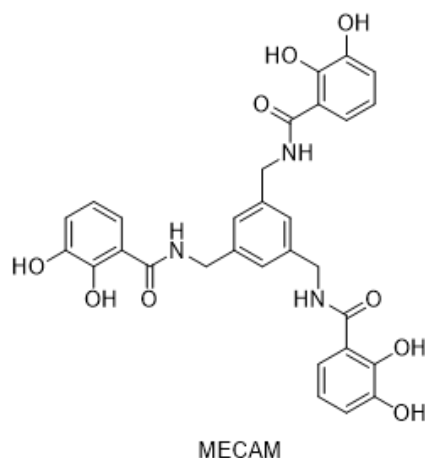


Figure 7. Structure of the MECAM⁵⁸.

1.2.2.3 Sideromycins

Limited drug uptake is common in challenging-to-treat Gram-negative bacteria due to the innate barrier of the outer membrane. To overcome the uptake limitation, sideromycin uses siderophore as a vector to link covalently to antibiotics, smuggling antibiotics as a Trojan horse into bacteria by hijacking siderophore-acquisition. Given that siderophore uptake is essential for bacterial survival, Trojan horse strategy not only enhances the drug accumulation but also significantly decreases permeability-mediated resistance³⁵. Moreover, sideromycins can be widely used by

applying various types of siderophore scaffolds or antibiotics. For instance, several potent enterobactin-antibiotics conjugates such as enterobactin-ampicillin or, enterobactin-ciprofloxacin have been reported ^{62,63}.

Accumulating studies reported a number of potent natural and synthetic sideromycins. For instance, albomycin, a natural sideromycin, serves as a seryl-tRNA synthetase inhibitor with a ferrichrome siderophore group and a thioribosyl pyrimidine ⁶⁴. Albomycin shows effective growth inhibition of both Gram-positive and Gram-negative bacteria ^{64,65}. In addition to natural sideromycin, accumulating studies describe numbers of synthetic sideromycins. Among various siderophores, catechol generally has the highest Fe^{3+} affinity at physiological pH 7.4 ⁴⁵, making it a potential candidate for the Trojan horse strategy. One of the successful examples is cefiderocol (Figure 8), a catechol siderophore-cephalosporin antibiotic, recently was approved for medical use in the USA in 2019 ⁶⁶. Cefiderocol is active against several pathogens including *Enterobacter* spp., *Klebsiella* spp., *Proteus* spp., *Shigella flexneri*, *Salmonella* spp., *Vibrio* spp., *Acinetobacter* spp., *Pseudomonas* spp. ³⁵. Notably, cefiderocol exhibits a promising antibacterial activity in carbapenem-resistant strains such as carbapenem-resistant *Acinetobacter baumannii*, *Stenotrophomonas maltophilia* ⁶⁷. This demonstrates that the Trojan-horse approach is a promising strategy to overcome the current challenge of antibiotics.

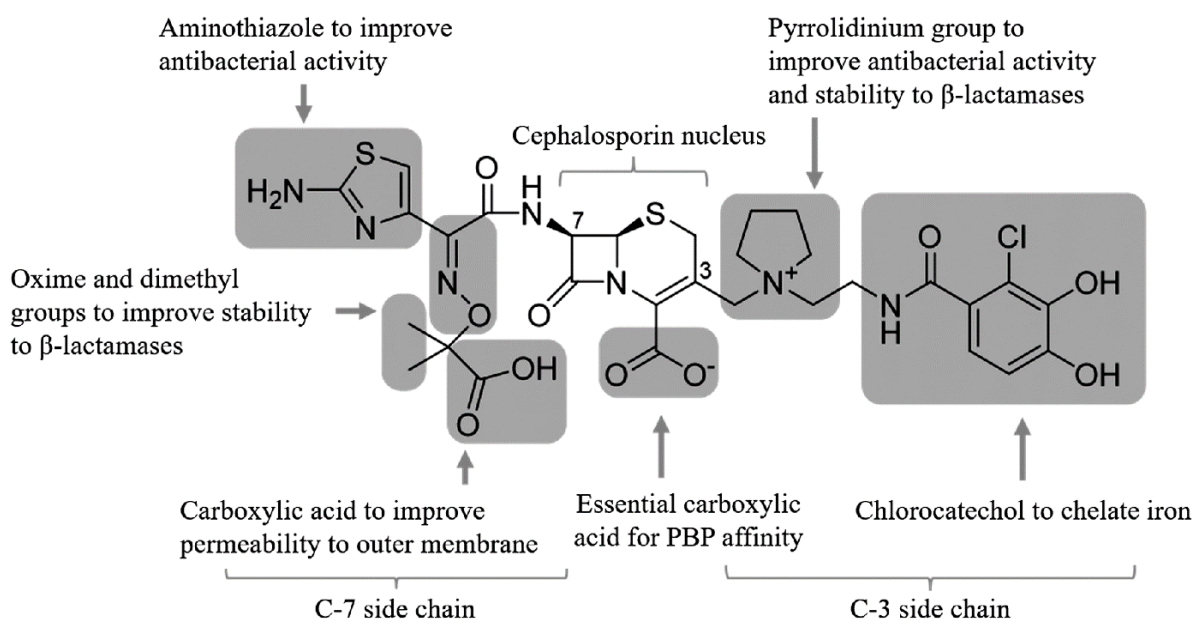


Figure 8. The structure and drug design of cefiderocol (taken from ⁶⁸).

Siderophore receptors mediate sideromycin uptake. For example, it was shown that FhuA, a ferrichrome transporter, is crucial for the antibacterial activity of the ferrichrome-antibiotic conjugate albomycin. Furthermore, it was shown that double knockout of catecholate receptors *cirA*, *fiu* and knockout of *piuA* increased the MIC of cefiderocol in *E. coli* and *P. aeruginosa* by 16-fold respectively ³⁵. In contrast, deficiency in porin oprD (carbapenem permeation porin) or overexpression of the MexAB-OprM efflux pump had modest effects on cefiderocol activity in *P. aeruginosa* ³⁵. These studies suggested that sideromycins hijack siderophore uptake system and might be able to overcome the porin-mediated resistance of antibiotics.

1.3 *E. coli*

E. coli contributes to a major cause of bacteremia and urinary tract infection (UTI) ⁶⁹. Most strains of *E. coli* such as commensal and laboratory K-12 strains are harmless, but certain pathogenic strains lead to serious conditions such as septic shock in host ⁷⁰. A variety of virulence factors such as iron-acquisition factors, LPS and toxins benefits the growth of pathogenic strains of *E. coli* during infection ⁷⁰. For example, multiple types of siderophores are crucial for colonizing uropathogenic *E. coli* (UPEC) under iron-limited environment such as bladder, contributing to about 90% of UTI ⁷¹. In addition to the prevalence of *E. coli* infections, multi-drug resistant *E. coli* such as ESBL-producing *E. coli*, is a critical problem waiting for solutions ²⁷.

1.3.1 Antibiotic uptake

E. coli, similar to other Gram-negative, is composed of cell wall comprising a thin layer of peptidoglycan and an outer membrane, periplasm, inner membrane as well as cytoplasm. Antibiotic uptake is especially challenging in Gram-negative bacteria, because their surface is composed of an asymmetric bilayer of lipopolysaccharides (LPS) in the outer leaflet and phospholipids in the inner leaflet ²². Tightly packed LPS and phospholipids make the outer membrane a selective barrier for both hydrophobic and hydrophilic compounds, including most antibiotics ²². On the other hand, multidrug efflux pumps reinforce the barrier by expelling antibiotics from bacteria.

Hydrophobic compounds diffuse across the outer membrane to a limited degree because of the LPS-containing bilayer ⁷², while small, hydrophilic antibiotics depend on pore-forming porins

(transporters responsible for the uptake of compounds less than 600 Daltons) to penetrate the outer membrane^{21,22}. In *E. coli*, porins OmpF and OmpC constitute the major entrance path for small hydrophilic compounds of less than 600 Daltons such as β -lactams⁷³.

1.3.2 Siderophore transport system in *E. coli*

E. coli has multiple systems to obtain iron (II) and iron (III). *E. coli* can obtain free ferrous ion via porin on the outer membrane and FeoABC transporter anchored in the inner membrane. Due to the scarcity of ferrous iron, siderophore is a more common way for iron acquisition in *E. coli*. Because ferric iron–siderophore complexes exceed the molecular weight cut-off of porins, *E. coli* has specific outer membrane receptors for siderophore uptake. Apart from outer membrane receptors, there are three components involved in siderophore uptake, i.e. the Ton complex (TonB-ExbB-ExbD complex), a periplasmic binding protein, and the ATP-driven transporter (or ATP binding cassette transporter, ABC transporter) anchoring in inner membrane⁷⁴.

1.3.2.1 Outer membrane receptors

In *Escherichia coli* K-12, there are six TBDTs (TonB-dependent transporters) transporting various sources of iron (FepA, FecA, FhuA, FhuE, Fiu, and Cir) and one TBDT importing vitamin B12 (btuB)⁷⁵. TBDTs share a similar protein structure comprising a 22 antiparallel β -stranded β -barrel and an N-terminal globular domain⁷⁶ (Figure 9). Distinct outer membrane receptors transport different types of siderophores. For instance, there are three main catecholate receptors expressed in all strains of *E. coli*: FepA, the receptor for enterobactin; Fiu and Cir, receptors for enterobactin degradation products such as DBS (2,3-dihydroxybenzoyl-1-serine)⁴⁵, while FecA is the receptor for ferric-citrate (Figure 10).

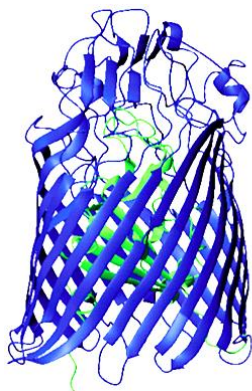


Figure 9. Ribbon representations of outer membrane siderophore receptor FepA from *E. coli* (adapted from ⁷⁶). The β -barrel is colored blue. The α - β globular domain is colored green.

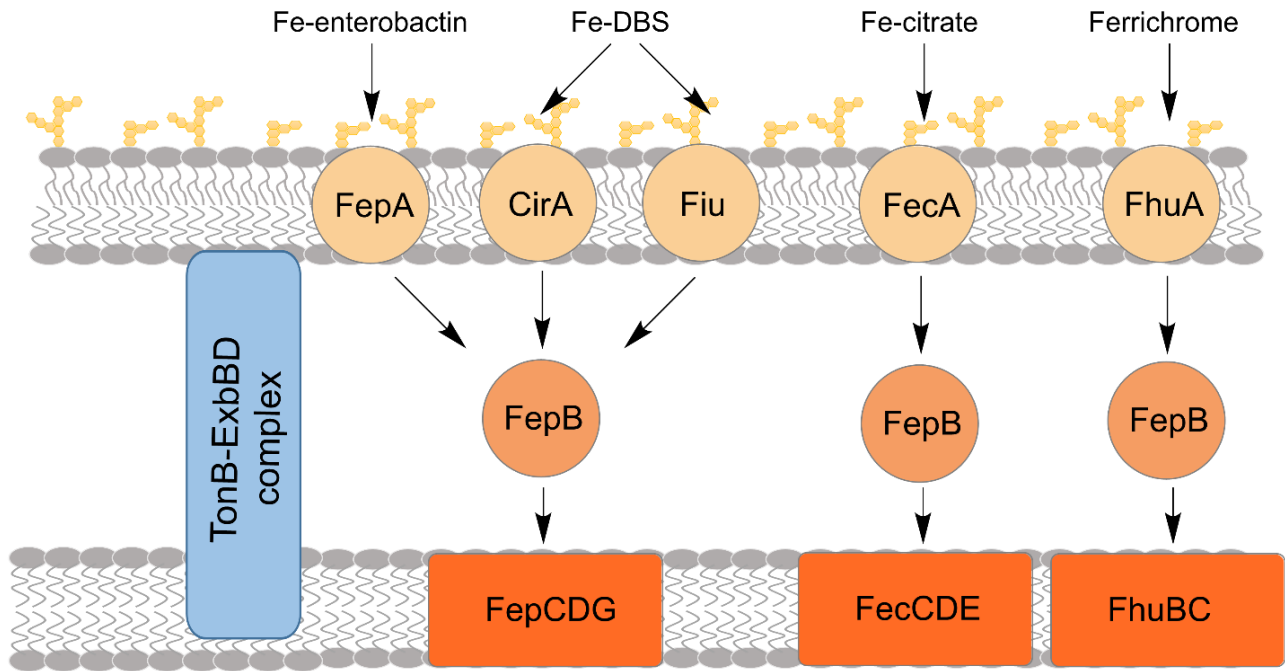


Figure 10. Ferric iron transport system in *E. coli* ⁴⁵. Iron-loaded siderophores (for example, Fe-enterobactin) are imported by outer-membrane receptors such as FepA, a periplasmic-binding protein (FepB) and an ABC transporter (FepCDG). With the help of TonB–ExbBD complex, the iron-loaded siderophores are imported across the outer membrane and then shuttled to the corresponding ABC transporter located in the inner membrane by periplasmic-binding protein. DBS: 2,3-dihydroxybenzoyl-serine.

1.3.2.2 Ton machinery

While binding to iron-siderophore complex, the TBDT undergoes a conformational change, opening the channel and thereby translocating the siderophore across the outer membrane. This process is coupled with energy supply of proton-motive force (PMF) by Ton complex. Ton complex comprises three members: the inner membrane-anchored, periplasm-spanning TonB and the inner membrane-embedded ExbB and ExbD proteins with a cellular ratio of 1:7:2. ExbB functions as a scaffolding protein for stabilizing the Ton machinery complex. ExbB has three transmembrane domains (TMDs) with the majority of the protein residing in the cytoplasm, whereas ExbD and TonB are anchored by single N-terminal TMDs, with most of the residues located in the periplasm ^{77,78}. During siderophore transport, ExbB and ExbD firstly harvest the

cytoplasmic membrane PMF and transmit it to TonB, energizing TonB and facilitating its conformational change. Energized TonB subsequently interacts with the TonB motif of the outer membrane receptor so that siderophore import is enabled ^{74,79}.

1.3.2.3 Periplasmic binding protein and ABC transporter

In the periplasm, a particular ferric-siderophore is delivered by a periplasmic binding protein to the cytosolic uptake systems that belong to a class of ABC transporters comprising permease units with ATP hydrolysis activity. For example, the catecholate siderophore enterobactin relies on a FepA receptor, periplasmic binding protein FepB, and FepCDG ABC transporters for its import. FhuABCD and FecABCDE target ferrichrome and ferric citrate, respectively ⁴⁵. Notably, receptors for the same types of siderophore can share the same part of transporters: CirA, Fiu, FepA all use FepBCDG for siderophore import. Therefore, multiple iron-acquisition systems meet the iron demand in *E. coli*.

1.3.2.4 Iron release from siderophore

After crossing the inner membrane, iron-siderophore liberates iron in the cytoplasm by enzymatic conversions. For instance, ferric-triscatecholates like ferric-enterobactin can be either directly reduced by ferric triscatecholate reductase YqjH or undergo hydrolysis by esterases such as Fes prior to reduction ^{80,81}, thereby releasing ferrous iron for further use. After iron release, apo-siderophore is degraded or released through resistance/nodulated/cell division (RND)-class efflux pumps like TolC associated with AcrB, AcrD, or MdtABC ⁸². Thus, free ferrous iron can participate in cytosolic reactions or be stored in liable iron pool ^{80,81}.

Once Fe²⁺ is available in the cytoplasm, Fe²⁺ not only gets involved in several cellular functions, but also regulates the iron-acquisition system. Gene expression of siderophore uptake systems is suppressed when iron is abundant and increased under iron starvation; this control is mediated by Fur (ferric-uptake regulator), an iron-responsive transcription factor. When iron is rich, Fur binds to Fe²⁺, suppresses a series of genes for iron-acquisition by binding the Fur box in the promoter regions. By contrast, under low-iron conditions, Fe²⁺ dissociates from the Fur, driving the transcription of genes involved in iron uptake via releasing Fur from the operator sequence ^{83,84}.

1.4 Eagle effect

The Eagle effect describes a phenomenon where increased concentrations of an antibiotic above the optimal bactericidal concentration (OBC) lead to an increase of bacterial growth, rather than a decrease, as observed in normal cases. The effect was named after Harry Eagle who first reported the “more antibiotic more growth” effect on various types of bacteria such as *S. aureus* upon penicillin treatment^{85,86}. It is clearly different from resistance and persistence phenotypes in response to antibiotics. Resistance occurs when bacteria are able to grow in the presence of antibiotics at high concentrations. Resistant bacteria exhibit a substantially increased minimal inhibitory concentration (MIC). In contrast, persistence occurs when a subpopulation of bacteria survives in the presence of antibiotics beyond the concentration that is able to kill the majority of the susceptible population. Persistence is believed to be acquired from a spontaneous, uninherited, reversible switch between normal and persister states⁸⁷. Unlike Eagle effect, higher antibiotic concentrations are able to kill bacterial persisters. The curves depicting the relationship between antibiotic concentrations versus CFU curves under resistance, persistence and the Eagle effect are shown in Figure 11.

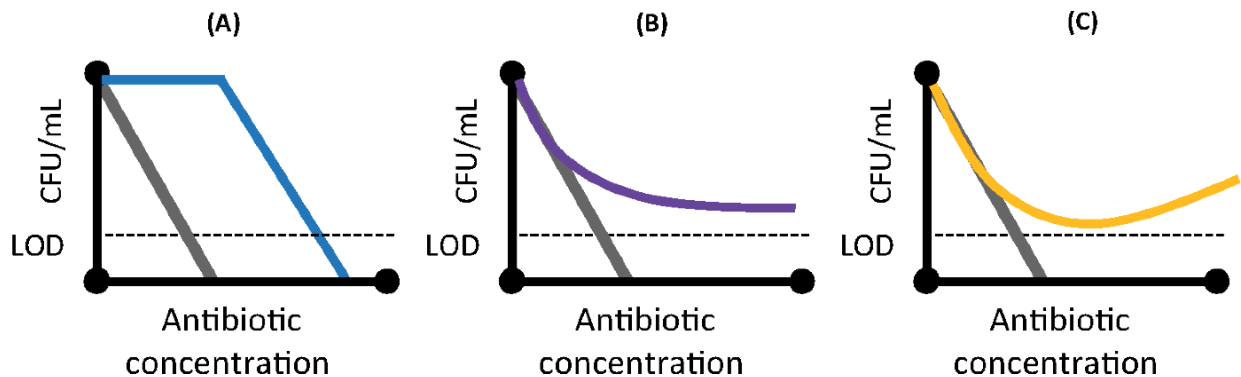


Figure 11. Antibiotic concentration versus CFU curves of resistance (A), persistence (B), and Eagle effect (C). The gray line in each panel stands for the typical CFU curve of susceptible strain with increasing antibiotic concentration. CFU, colony-forming unit; LOD, limit of detection (taken from⁸⁸).

Previous studies described an Eagle effect in a wide range of pathogens such as Group B *Streptococcus*, *Clostridium difficile*, *E. coli* upon diverse kinds of antibiotic (e.g. cell-wall synthesis or DNA gyrase inhibitors) (Table 4)^{89,90}. In addition to in vitro observations, it was reported that reduced dosage of penicillin improves the treatments of bacterial infection in patients

⁹¹. Besides, Eagle effect has been reported in animal models. For example, a reduced dose of cefmenoxime treatment exhibits more potent inhibition of *Proteus vulgaris* in a mouse model ⁹².

However, the underlying mechanism of Eagle effect remains largely unknown. There are some proposed mechanisms that have been reported in response to different classes of antibiotics ⁸⁸. Firstly, Luan and colleagues suggested that a reduced ROS level contributes to the high-dose paradoxical growth in response to a quinolone antibiotic - nalidixic acid - in *E. coli*. It was found that nalidixic acid-associated Eagle effect decreased ROS, and an exogenous supplement of hydrogen peroxide abolished this effect ⁹³. Secondly, a high level of β -lactamase expression might cause the β -lactam-associated Eagle effect. In *P. vulgaris*, the presence of β -lactamase inhibitor but also β -lactamase-deficient strains abolished the Eagle effect in response to cefmenoxime ⁹⁴, implying that bacteria might enhance β -lactamase expression triggered by a high-level of β -lactam to ensure their survival. Yet, whether a common mechanism of the Eagle effect shared among species as well as various classes of antibiotics exists, that is marked by key molecules, is still not clear.

Table 4. The Eagle effect of different bacteria (adapted from ⁸⁸).

Antibiotic target	Antibiotic class	Antibiotics	Organisms
Cell-wall synthesis	β -lactam	penicillin	<i>Staphylococcus aureus</i> , <i>Enterococcus faecalis</i> ^{89,90}
		amoxicillin	Non-toxigenic <i>Corynebacterium diphtheria</i> ⁹⁵
		cefmenoxime	<i>Proteus vulgaris</i> ⁹⁴
	Glycopeptides	vancomycin	<i>Enterococcus faecalis</i> ⁹⁶
DNA synthesis	Quinolones	nalidixic acid	<i>Escherichia coli</i> ⁹³
Aminoglycosides	Protein synthesis	gentamicin	<i>Klebsiella pneumoniae</i> ⁹⁷

1.5 Metabolomics

1.5.1 Introduction of metabolomics

Multiple -omics techniques (i.e., genomics, transcriptomics, proteomics, and metabolomics) have been widely applied in research in recent decades, providing a comprehensive view of a biological system. Metabolomics is the systematic study of substrates and products of small molecule metabolism from cells, tissues or organisms. The metabolome represents a set of downstream products of the dynamic interactions between genes, transcripts, and proteins, reflecting the metabolic phenotype associated with certain endogenous or environmental factors ⁹⁸. Metabolomics includes two approaches: targeted and untargeted metabolomics. A targeted metabolomics approach aims at identification and quantification of a limited set of pre-defined metabolites. On the contrary, an untargeted approach detects both known and unknown metabolites ⁹⁹, and the interpretation of data from untargeted experiments is highly dependent on a thorough and accurate metabolite annotation. However, unlike proteomics, data identification is a fundamental challenge for untargeted metabolomics. In proteomics, proteins or peptides can be sequenced and identified by matching identified peptides against in-silico fragmentation spectra, whereas metabolites lack common structural building blocks whose fragmentation is easily predictable ⁹⁹.

Metabolomics has been applied in several fields of research as well as in clinical studies. For example, pharmacometabonomics refers to direct measurement of metabolites from body fluids (e.g. plasma, serum, urine, etc.) for the evaluation of the metabolism of drugs, monitoring the pharmacokinetic profile of a compound. Moreover, each cell or tissue has a unique metabolic ‘fingerprint’, so metabolomics can apply to biomarker identification in the disease diagnosis and prognosis ⁹⁸. In infection research, metabolomics serves to study the influence of different factors on the metabolism of the host during infection, but also enables a better understanding of the set of microorganism metabolites in response to environmental stimuli such as antibiotic treatments ¹⁰⁰. For instance, by investigating antibiotics-treated metabolome, Zampieri et al. revealed that common metabolic responses exist among antibiotics with different modes of action ¹⁰¹. Besides, it was reported that, antibiotics such as β -lactams, aminoglycosides, quinolones can lead to reactive

oxygen species (ROS) production, so that antibacterial activities are enhanced by the induction of series of metabolic changes ¹⁰².

Accumulating studies demonstrated that the metabolome modulates physiological functions as well as other levels of omics including genome, epigenome, transcriptome and proteome ⁹⁸. In recent decades, research studies focusing on the interplay between metabolomics and other omics layers have emerged. For example, studies identified glucose, fatty acids as modulators for insulin secretion and sensitivity by post-translational modification of proteins ¹⁰³. Besides, succinate and α -ketoglutarate, intermediates involved in tricarboxylic acid cycle, modulate the immune response through gene expression and epigenetic reprogramming ^{104,105}.

Furthermore, integrating data among metabolomics and other omics can provide a systemic understanding of the physiological response under specific conditions. For instance, Bar et al. reported more than 76% of the profiled metabolite prediction based on host genetics, gut microbiome, and untargeted serum metabolome ¹⁰⁶. Bar et al. also uncovered new associations between metabolite levels and single nucleotide polymorphisms ¹⁰⁶. Additionally, Suhre et al. identified 37 genetic loci that are highly relevant to metabolic traits in blood by combining genome-wide association studies (GWAS) and metabolomics ¹⁰⁷, providing new insight on the association between disease-linked loci with metabolites. Therefore, the integration of metabolomics with other omics enables to provide overview of interplay of transcripts and metabolites, facilitating to uncover underlying mechanisms.

1.5.2 Workflow of metabolomics

The workflow of metabolomics includes experimental design, metabolite extraction, sample analysis and data analysis. For experimental design, it is critical to select groups of samples as well as the goal of the experiments. Secondly, metabolite extraction comprises metabolic quenching steps and extraction methods tailored to specific classes of metabolites. The efficient quench of biochemical processes at a given time point is extremely important for metabolomics, because the abundance of metabolites varies even in a very short period. The extraction solvent is also important, because it enables to solubilize as many metabolites as possible ¹⁰⁰, usually coupled with the addition of selected compounds as internal standards. Thirdly, during sample analysis, metabolites are often separated by chromatography before detection. Main chromatography

methods include high-performance liquid chromatography (HPLC), gas chromatography (GS), or capillary electrophoresis (CE). These are usually coupled with mass spectrometry (MS), and/or (rarely) with nuclear magnetic resonance spectrometry (NMR). Finally, the measured data require further processing, with key steps being feature extraction, metabolite identification, and statistical analysis ¹⁰⁰.

Among various separation methods, LC and GC are the most widely used methods in metabolomics. The gaseous phase offers a better separation for compounds than LC, yet LC-MS enables to detect a larger pool of intact metabolites without the chemical derivatization that is generally required prior to GC analysis ¹⁰⁸. In LC-MS, samples are injected onto a packed column containing a stationary phase ¹⁰⁰. Metabolites can be further separated based on different partition coefficients between the eluotropic mobile phase and stationary phase ¹⁰⁰. Based on distinct stationary phases, there are normal-phase LC, reverse-phase LC such as C18 as well as hydrophilic interaction liquid chromatography (HILIC) ¹⁰⁰. Reverse-phase LC is commonly used for the separation of hydrophobic and mid-polar compounds (e.g., lipids), while HILIC is more common for polar compounds.

A mass spectrometer comprises a source for ionization of the molecules, an analyzer for separation of metabolites based on their mass-to-charge (m/z) ratio, and a detector for registering their quantity. For ionization, there are two major ionization methods applied in metabolomics: electrospray ionization (ESI) and electron impact (EI) ionization. In HPLC-MS, ESI is the standard, because ESI enables ionization of a large group of molecules (small molecules less than 1,000 amu, peptides, proteins) without a strong fragmentation of molecular ions ¹⁰⁹. In ESI, liquid-containing analytes are dispersed by electrospray in a positive (positive mode) or negative potential (mode) into aerosol. ESI requires certain volatile buffers such as ammonium acetate or ammonium formate to reduce the possible interference from salts and enhance ion formation with solvent evaporation ¹⁰⁹. While the aerosol passes through a capillary with a high potential difference ($\sim\pm 3\text{--}6$ kV) into a vacuum stage, the solvent evaporates from a charged droplet ¹¹⁰. Small molecules usually are single-charged, while multiply charged species commonly occur among larger molecules ¹¹¹. During solvent evaporation, the charged droplets decay into many smaller droplets. Subsequently, the charged molecules are then detected by the analyzer.

After ionization, the first mass analyzer (provide single MS) separates molecule ions via their mass-to-charge ratio (m/z). There are various options for single-configuration mass analyzers such as quadrupole (Q), time of flight (TOF), or Orbitrap. TOF and Orbitrap provide high mass resolution, while quadrupole analyzers have generally high sensitivity in single ion monitoring mode, but limited resolution and mass accuracy¹⁰⁹. Ions that are mass-selected in MS are split into fragment ions by photodissociation, collision-induced dissociation or ion-molecule reactions¹¹². Subsequently, tandem-configuration mass analyzers like triple-quadrupole ion trap (QTrap), triple quadrupole (QqQ) and quadrupole-TOF (Q-TOF) separate those fragments based on their m/z -ratio. Take Q-TOF as an example, the quadrupole sends selected ions of interest to a collision cell for fragmentation. The fragments then pass across an accelerating potential, and are mass-analyzed based on their detected flight time. Besides, among tandem mass analyzers, Q-TOF is more suitable for global profiling and metabolite identification (including isotopomer analysis) due to its higher mass-resolution, which enables mass accuracy with errors in a part per million (ppm) level¹⁰⁰. By contrast, QqQ and Qtrap are more used in targeted metabolomics due to their high sensitivity¹⁰⁹.

To extract features, data processing requires peak detection and retention time alignment⁹⁹. Notably, features are not equal to metabolites. A single metabolite can have more than one feature, that corresponds to isotopes, different adducts, or in-source fragments with different m/z values. Finally, metabolites can be identified by matching experimental MS and MS/MS data with local libraries created by commercial or synthesized standards as well as by matching retention times. Besides, databases such as METLIN, Human Metabolome DataBase (HMDB)¹¹³, ECMDB¹¹⁴, GNPS (<http://gnps.ucsd.edu/>)¹¹⁵ provide MS or MS/MS spectrum information for further metabolite annotation. In untargeted MS-based metabolomics, metabolite identification is still a fundamental challenge. Compared to metabolomics, peptides their fragmentation patterns in proteomics are relatively predictable because most of the peptide sequences can be inferred from genomic sequences and predictable after experimental processes such as enzymatic digestion⁹⁹. By contrast, in metabolomics, the set of metabolites making up the metabolome cannot be directly predicted from the genome. The broad range of chemical classes which make up the metabolome, and the wide range of polarities and abundances provide a huge challenge for analytical chemistry. Identification of metabolites can be challenging, because fragmentation patterns can be relatively uninformative, which might result from the difficulty to compare similar fragments with different

species, the variation between fragmentation patterns caused by analytical conditions such as ionization and collision energy ⁹⁹. Even *in-silico* metabolite databases provide guidance and in some cases validation, they will not fit all metabolomic studies ⁹⁹. For more confident metabolite identification, data from MS/MS fragmentation and retention times from a reference standard are required ⁹⁹. In addition, high-resolution, high-mass accuracy and isotope ratio measurements are crucial to provide MS and MS/MS data for metabolite identification, because they allow to determine or narrow down the molecular formula of metabolites and their fragments. Additionally, MS/MS fragmentation data can be used for determining the most probable composition of molecules ¹¹⁶.

1.6 Transcriptomics

The term transcriptomics describes technologies for examining the complete set of transcripts in a cell, tissues or an organism, providing a systemic view on the profile of gene expression under particular conditions of a biological system. Transcriptomics is critical for discovering the underlying mechanisms of development and disease. Yet, since not all RNAs are transcribed into proteins (e.g. rRNA, sRNA), the transcriptome does not directly correlate to the protein expression as well as “phenotype”, while metabolome reflects the metabolic phenotype associated with certain endogenous or environmental stimuli ⁹⁸.

Transcriptomics is widely applied in studying bacterial response to antibiotics treatment, providing a systemic perspective on the drug-bacteria interaction as well as a potential mode of action of an antibiotic. For instance, large-scale transcriptomic studies from O’Rourke et al. and Boshoff et al. provide new insights for predicting mode of actions based upon the differential gene expression profiles upon antibiotic treatments in *E. coli* and *Mycobacterium tuberculosis*, respectively ^{117,118}. Besides, antibiotic-treated transcriptomes are commonly applied to study the resistance mechanism ^{119,120}. For example, by transcriptomic analysis, Erickson et al. revealed that a set of key genes involved in membrane structure, cell mobility, and metabolism are associated with adaptive resistance which facilitates transient tolerance and the emergence of drug resistance ¹¹⁹. Therefore, transcriptomics approach can be used for understanding global drug response but also the underlying mechanism of antibiotics.

For the transcriptome analysis, two key techniques have been developed: hybridization and sequence-based approaches ¹²¹. Hybridization-based methods incubate fluorescently labeled cDNA with custom-made microarrays, so it highly relies on existing knowledge of genome information ¹²¹. Another limitation of microarray methods concerns high background signals contributed by cross-hybridization ¹²². By contrast, sequence-based approaches such as RNA-seq, which use a high-throughput cDNA sequencing to capture all sequences ¹²³, are more commonly used because of their higher resolution and broader application (e.g. discovery of novel transcripts ¹²⁴, alternative splicing ¹²⁵).

A general experiment procedure for RNA-seq includes three main steps: conversion of a cDNA library, adaptor attachment, and then high-throughput sequencing ¹²¹. To generate cDNA, two methods are applied: RNA or cDNA fragmentation. For cDNA fragmentation method, RNA molecules are firstly converted into cDNA via oligo-dT primers, followed by sonication or DNase I treatment to generate DNA fragments, whereas RNA fragmentation method directly digests RNA into small RNA fragments and then converted those small RNA fragments into cDNA. Secondly, adaptors are added into either one or both ends of small cDNA fragments. Thirdly, each molecule is then sequenced via single- or paired-end sequencing. After sequencing, the raw data is formatted in a FASTQ file. For further RNA-seq data analysis, a general workflow includes five main steps: preprocessing of raw data, read alignment, transcriptome reconstruction, quantification, and data analysis ¹²⁶. RNA-seq data are first subjected to quality control (QC) assessment such as adaptor trimming and quality trimming. Adaptor trimming is to remove adaptor sequences for later read alignment. Quality trimming is to remove the ends of reads showing base quality, preventing the mismatch from alignment ¹²⁶. The trimmed data is then used to align reads against corresponding reference genomes. Subsequently, transcriptome reconstruction serves to identify all transcripts expressed in a sample and their abundance can be estimated using read mapping data for quantification. Finally, differential expression analysis is performed using statistical methods ¹²⁶.

2. Aim of the thesis

Limited antibiotic uptake is a great challenge in treating Gram-negative bacteria due to the abundance of lipopolysaccharides and phospholipids in the outer membrane. To overcome the physical barrier from outer membrane, siderophore-antibiotic conjugates hijack the iron transport system that is essential to bacterial growth due to iron scarcity, boosting drug uptake and efficacy. However, the underlying transport mechanism and the bacterial response to exposure to siderophore drugs are poorly understood.

Even though siderophore-antibiotic conjugates were reported and shown activity against several bacteria, more effective siderophore-antibiotic conjugates are still needed. To generate novel siderophore-antibiotic conjugate, the first goal of the thesis was to identify suitable siderophore scaffolds from different chemical series by investigating their uptake in *E. coli* via growth recovery assay.

Secondly, after the most promising candidate was identified, the second goal was to characterize a synthetic siderophore-antibiotic conjugate named LP-600 in terms of antibacterial activity and its uptake route in *E. coli*. Thirdly, the resistance mechanism and potential targets of LP-600 in *E. coli* should be studied.

In the course of the antibacterial studies, a paradoxical re-growth upon treatment of LP-600 above 16 times the minimum inhibitory concentration was observed, a phenomenon coined the ‘Eagle-effect’ in other systems. However, the mechanism and systemic view on the Eagle effect is poorly understood and Eagle effects induced by siderophore-antibiotic conjugate have not been reported yet. Hence, the fourth aim of the thesis was to investigate the global molecular response associated with the LP-600-induced Eagle effect in *E. coli* on the transcriptome and metabolome level.

3. Materials and methods

3.1 Strains

The Keio collection strain of *E. coli* wild type strain BW25113 and genetically modified strains were purchased from Horizon (Cambridge, UK). In this study, several deletion strains were generated by lambda red recombinase system ¹²⁷ are listed in Table 5.

Table 5. List of genomic modification strains used in this study.

Strain	Reference or source	Strains	Reference or source
BW25113	Horizon cat. # OEC5042	$\Delta entA \Delta fepA$	This study
$\Delta entA$	This study	$\Delta entA \Delta fecA$	This study
$\Delta fepA$	This study	$\Delta entA \Delta fhuA$	This study
$\Delta fepB$	This study	$\Delta entA \Delta cirA$	This study
$\Delta fepD$	This study	$\Delta entA \Delta fiu$	This study
$\Delta tonB$	Horizon cat. # OEC4987-200829327	$\Delta fepA \Delta cirA$	This study
$\Delta cyoB$	Horizon cat. # OEC4987-200825978	$\Delta fepA \Delta fiu$	This study
$\Delta exbB$	Horizon cat. # OEC4987-213606445	$\Delta cirA \Delta fiu$	This study
$\Delta tolC$	Horizon cat. # OEC4987-213607439	$\Delta fepA \Delta cirA \Delta fiu$	This study
$\Delta ampC$	Horizon cat. # OEC4987-200828975		

3.2 Plasmids

To generate protein-expressing plasmids, sequences encoding FepA, CyoB and ExbB were amplified from chromosomal DNA of wild type or LP-600 resistant clones by PCR amplification. FepA sequence was cloned into BamHI and HindIII sites of pQE 80L (Qiagen cat.# 32943) vector. CyoB and ExbB sequences were cloned into XhoI and XbaI sites of pSF-OXB15 (Sigma-Aldrich cat. # OGS558) vector. The primers used for PCR amplification are listed below.

Primer	Sequence
BamHI-fepA F	CGCGGATCCATGAACAAGAAGATTCATTC
HindIII-fepA R	CCCAAGCTTTCAGAAGTGGGTGTTTACGC
XhoI-cyoB F	CCGCTCGAGATGTTTCGGAAAATTATCACTTGATG
XbaII-cyoB R	GCTCTAGATCAGTTGCCATTTTTTCAGCCCTGCC
XhoI-exbB F	CCGCTCGAGGTGGGTAATAATTTAATGCAGACGG
XbaII-exbB R	GCTCTAGATTATCCTGCGCGTAATTTTTGTGCG

3.3 Recombineering/Lambda red-mediated gene deletion

Gene deletion was conducted via lambda red recombineering in *E. coli* wild type BW25113¹²⁷ or indicated strains. Targeted genes on the corresponding locus were replaced by homologous recombination with chloramphenicol cassette with FRT sequence which is flanked by 50 base pairs of upstream and downstream of the targeted gene. Chloramphenicol cassette was amplified from pKD3 by PCR with the primers containing corresponding upstream and downstream of the gene sequence. The primers are listed in Table 6. For expression of lambda red system, the plasmid pKD46, encoding lambda red genes with araBAD promoter, was transformed into the target strain and grown at 30 ° C. Strain with pKD46 were further grown until the early exponential phase (OD₆₀₀ = 0.2) followed by the induction of "lambda red" proteins Gam, Exo and Beta by supplementation of 0.2 % arabinose. Bacterial cultures were grown up to an OD₆₀₀ of 0.6 and transformed with the PCR product. The transformed cells were recovered for 2 hours at 37 ° C. and then selected on an agar plate with chloramphenicol (25 µg/mL). Indicated gene deletion strains were obtained and checked by colony PCR with the primers listed in Table 7.

Table 6. List of primers for lambda red-mediated gene deletion

Primer	Sequence
entA-K-F	AACCCGACCATCGACGCCTGGTGGGAAGCTACTCTCCCGCGAGGTGAAATAGT GTAGGCTGGAGCTGCTTC

entA-K-R	GCTGGTGGCGTTCAGTTCGTCGAGCGTTAAATGGCGTTTCCAGATCATGCATG GGAATTAGCCATGGTCC
fepA-K-F	CCGCATCCGGCATGAACGACGCGCACTTTGTCAACAATCTGACGTTAGCAGT GTAGGCTGGAGCTGCTTC
fepA-K-R	CGACCATGCCCCGACAGTTGCAATTCGTGGCAAAAATGCAGGAATAAAACAAT GGGAATTAGCCATGGTCC
fecA-K-F	CAACATAATCACATTCAGCTAAAAGCCCGGCAAGCCGGGCGTTAACACAGT GTAGGCTGGAGCTGCTTC
fecA-K-R	TTCTCGTTCGACTCATAGCTGAACACAACAAAAATGATGATGGGGAAGGTAT GGGAATTAGCCATGGTCC
fhuA-K-F	ATAATCATTCTCGTTTACGTTATCATTCACTTTACATCAGAGATATACCAGTG TAGGCTGGAGCTGCTTC
fhuA-K-R	AACAGCCAACCTTGTGAAATGGGCACGGAAATCCGTGCCCAAAAGAGAAAA TGGGAATTAGCCATGGTCC
K-fepB-F	CGCAGGTGACAGCGTCCGACAGTTAATGCTTAAACAGCGCCTTAAGCCTGT GTAGGCTGGAGCTGCTTC
K-fepB-R	AATTTGTCATTACGCCCTTAACCTTATTAATAACAGGAAGCTGATTTGTGATG GGAATTAGCCATGGTCC
K-fepD-F	GGTGATGAGTAATCGGCGAGAGACGTAAATCATGCACCACCTCGCGTTTTGT GTAGGCTGGAGCTGCTTC
K-fepD-R	AAATAAGATCGATAACGATAATTAATTTTCATTATCATGGAAGTTCGTATGATG GGAATTAGCCATGGTCC
K-fes-F	GGTGGCAGTCGAAACATGGCCCCGGAATGGCAGCGTCTGAATGACGAAATGGT GTAGGCTGGAGCTGCTTC
K-fes-R	ATCATCGAAGGGATTACTGAATGCCATATTCAACTCCTGTCATGGAAAAGAT GGGAATTAGCCATGGTCC
K-fecD-F	ACCGTCAGATTTTCAGTTCGTAAAGTCATTTATCGCATTCTCACAAGCAAGTG TAGGCTGGAGCTGCTTC

K-fecD-R	GCGCTGATTGGCAGCCCTTGCTTTGTCTGGCTTGTGAGGAGGCGAGGATGAT GGGAATTAGCCATGGTCC
K-fhuB-F	GCAATGCACTTTGTGCGCGTTCTGGATAACGCCATCGGAGGTAAAGCGTGGT GTAGGCTGGAGCTGCTTC
K-fhuB-R	CAGGCGTACAGGGCCGTTATATGGAAAAATTAACGGCTCTGCTTTCTCAAAT GGGAATTAGCCATGGTCC
K-cirA-F	GCAGTATTTACTGAAGTGAAAGTCCGCCGTCGCCGGGCATCTTCTCAGTGTA GGCTGGAGCTGCTTC
K-cirA-R	TGTGAGCGATAACCCATTTTATTTTCGTAGTTACCTCATGGAGATATGGAATG GGAATTAGCCATGGTCC
K-fiu-F	GTACATCATACAATTTCTCCAAAAAGTGGGGCCTGCGCCCCACATCTGAAGT GTAGGCTGGAGCTGCTTC
K-fiu-R	TTTCTCGTGGCAGTGAAAATTTCAACATATAAGAAAAAGTCACCTGCAAAAT GGGAATTAGCCATGGTCC

Table 7. List of primers for colony PCR

Primer	Sequence
entA-C-F	AACCCGACCA TCGACGCCTG
entA-C-R	GCTGGTGGCGTTCAGTTCGT
fepA-C-F	CCGCATCCGG CATGAACGAC GCGCA
fepA-C-R	CGACCATGCCCGACAGTTGCAATTC
fecA-C-F	CAACATAATC ACATTCCAGC TAAAA
fecA-C-R	TTCTCGTTCGACTCATAGCTGAACA
fhuA-C-F	ATAATCATTC TCGTTTACGT TATCA
fhuA-C-R	AACAGCCAACTTGTGAAATGGGCAC
C-fepB-F	CGCAGGTGACAGCGTCCGACAGTTA
C-fepB-R	AATTTGTCATTACGCCCTTAACCTT

C-fepD-F	GGTGATGAGTAATCGGCGAGAGACG
C-fepD-R	AAATAAGATCGATAACGATAATTAA
C-fes-F	GGTGGCAGTCGAAACATGGCCCGGA
C-fes-R	ATCATCGAAGGGATTACTGAATGCC
C-fecD-F	ACCGTCAGATTTTCAGTTCGTAAAG
C-fecD-R	GCGCTGATTGGCAGCCCTTGCTTTG
C-fhuB-F	GCAATGCACTTTGTGCGCGTTCTGG
C-fhuB-R	CAGGCGTACAGGGCCGTTATATGGA
C-cirA-F	GCAGTATTTA CTGAAGTGAA AGTCC
C-cirA-R	TGTGAGCGATAACCCATTTTATTTT
C-fiu-F	GTACATCATA CAATTTCTCC AAAAA
C-fiu-R	TTTCTCGTGGCAGTGAAAATTTCA

3.4 Growth recovery assay

Colonies from *E. coli* strains were transferred from agar-plates into 5 ml of Mueller-Hinton broth (MHB) for overnight cultures at 37°C. The cultures were diluted in MHB to OD₆₀₀ = 0.1 and grown until exponential phase (OD₆₀₀ = 0.5). Each strain was harvested by centrifugation, three-time washing step in PBS and then diluted into OD₆₀₀ = 0.01 in 1XLMR medium (KH₂PO₄ = 176 mM, NaOH = 100 mM, (NH₄)₂SO₄ = 12.6 mM, MgSO₄ = 2 mM, FeCl₃ × 6 H₂O = 0.1 μM, CaCl₂ = 0.8 μM, MnCl₂ × 4 H₂O = 0.2 μM, ZnSO₄ × 7 H₂O = 0.2 μM, CoCl₂ × 6 H₂O = 0.04 μM, CuCl₂ = 0.08 μM, NiCl₂ × 6 H₂O = 0.04 μM, Na₂MoO₄ × 2 H₂O = 0.08 μM, Na₂SeO₃ = 0.08 μM, H₃BO₄ = 0.08 μM, glycerol = 0.02%, pH = 7.4). Bacterial cultures were dispensed in LMR in the presence of indicated compounds at 10 μM (LP-177, LP-450¹²⁸), enterobactin as a positive control, or DMSO as a negative control) in 96-well plates. Plates were incubated for 48 hours at 37 °C and followed by OD₆₀₀ measurement in a plate-spectrophotometer (BioTek Synergy 5).

3.5 Determination of minimum inhibitory concentrations (MICs)

For iron-depleted Mueller Hinton Broth (MHB) preparation, MHB was treated with Chelex® (Bio-Rad cat.# 142-2842], Hercules, CA, USA) for two hours at room temperature, followed by filtration with a 0.2-micron filter, supplemented with $\text{ZnSO}_4 = 10 \mu\text{M}$, $\text{CaCl}_2 = 0.5 \text{ mM}$, $\text{MgSO}_4 = 0.5 \text{ mM}$, adjusted pH to 7.4¹²⁹. Serial two-fold dilution of tested antibiotics were prepared and dispensed in half-area 96-well plates (Greiner cat. # 675161). Overnight cultures of each strain were diluted into $\text{OD}_{600} = 0.1$ and harvested when reaching the exponential phase ($\text{OD}_{600} = 0.5$). Bacterial pellets were harvested, washed three times in PBS, diluted into $\text{OD}_{600} = 0.01$ in iron-depleted MHB medium, then transferred to wells with dispensed antibiotic solution in half-area 96-well plates. The plates were incubated for 24 hours at 37 °C, followed by an OD_{600} measurement in a plate-spectrophotometer as mentioned above.

3.6 Bacterial cell viability assay

Bacterial cultures were collected from the exponential phase as mentioned above. Bacterial cultures were diluted into $\text{OD}_{600} = 0.05$ in iron-depleted MHB medium, dispensed into cavities of a 96-well plate filled with a panel of antibiotics, then incubated at 37°C. The bacterial cell viability was examined with the BacTiter-Glo™ Microbial Cell Viability assay (Promega, Mannheim, Germany, cat. # G8230) Cultures from 96-well plate were taken at 1, 2, 4, and 6 hours after incubation, mixed with the BacTiter-Glo™ reagent in equal volume to the bacterial culture, and dispensed into a new 96-well plate. The luminescence was measured in a microplate luminometer with a Synergy 4 system (BioTek, Bad Friedrichshall, Germany). The luminescence values were normalized by the medium control.

3.7 Generation of LP-600-resistant clones and bioinformatic analysis of whole genome sequence

To generate resistance in *E. coli* K-12 BW25113, cell suspensions with a cell density equal to 10^8 CFU/ml were grown in chelating Mueller-Hinton broth as mentioned before containing LP-600 in a concentration of 2x MIC (2 $\mu\text{g/ml}$) at 37 °C under shaking (180 rpm). Cultures that displayed visible growth after 24h ($\text{OD}_{600} > 0.1$ units) were exposed to higher drug concentrations (4, 8, 16 $\mu\text{g/ml}$). Four of the original cultures survived 21 passages ($\text{MIC} \geq 16 \mu\text{g/ml}$). To exclude general

drug-resistant clones, resistant clones were subject to ampicillin, kanamycin or cefiderocol (Haoyuan Chemexpress cat.1225208-94-5), and the clones that were only resistant to LP-600 were selected. Genomic DNA was isolated from the four resistant clones and from the parental strain control using the DNeasy Blood and Tissue Kit (Qiagen). The whole-genome sequence analysis was performed by the Genome Analytics Research Group at the Helmholtz Centre for Infection Research.

According to the manufacturer's protocols, the library was generated from 0.2 mg DNA for PCR amplification with 4 cycles by applying NEBNext Ultra II FS DNA Library Prep Kit for Illumina (New England BioLabs)¹³⁰. The libraries were sequenced on an Illumina MiSeq system (600 cycle) using MiSeq Reagent Kit v3 with an average of 1 million reads per DNA sample, paired-end mode, 2 x300 bp read length, and ~100x genome coverage. Libraries of DNA fragments with an average length of 580 bp were prepared according to the manufacturer's instructions¹³⁰. Sequences were quality controlled and adapter clipped by using the fastq-mcf tool of ea-utils¹³¹. The sequences of parental control and four resistant clones were mapped to the reference genome *E. coli* BW25113 (GenBank: CP009273.1) by Snippy¹³² to find substitutions and insertions/deletions.

3.8 Determination of β -lactamase activity

The β -lactamase activity was determined by β -lactamase activity assay kit (Sigma cat. # MAK22) following the manufacturer's instruction. Culture supernatants and pellets were harvested. Bacterial pellets were lysed by sonication for 5 minutes on ice, followed by centrifugation at 12,000 g for five minutes, and the cell lysate was collected. Culture supernatant and cell lysate were dispensed into a 96-well plate and mixed with reaction buffer containing nitrocefin, which is a substrate of β -lactamase. The absorbance (A_{490}) of each well was measured with the microplate reader (BioTek Synergy5) in kinetic mode for two hours at room temperature.

3.9 Protein expression in *E. coli*

To prepare electro-competent cells, overnight cultures of *E. coli* $\Delta FepA$, $\Delta cyoB$, and $\Delta exbB$ were diluted into $OD_{600} = 0.1$ and grown in 10 mL LB, and then harvested when reaching the exponential phase ($OD_{600} = 0.5$). Bacterial pellets were harvested g for ten minutes and then washed in ddH₂O

three times and in 10 % sterile glycerol for two times by centrifugation at 6000 xg at 4 °C. The supernatant was discarded and the pellet is resuspended in 1 mL 10 % sterile glycerol (4°C) and again centrifuged at 6000 xg for 15 minutes at 4°C. 100 µL aliquots of this bacteria solution were prepared for further electroporation.

By electroporation, pQE FepA, pSF CyoB, or pSF ExbB were transformed into strains $\Delta FepA$, $\Delta cyoB$ and $\Delta exbB$, respectively. Transformed cells were spread onto kanamycin (50 µg/mL)-containing LB agar plates and grown overnight at 37°C. For protein expression of CyoB and ExbB, a single colony of bacteria was picked followed by inoculation as mentioned. For FepA protein expression, cells were grown with the addition of 1 mM isopropyl β -D-thiogalactopyranoside (IPTG) (Thermo Fisher Scientific cat. # R0392) for protein induction. The effectiveness of overexpression was determined by real-time PCR. All constructs were verified by PCR amplification, restriction enzyme analysis and sequencing.

3.10 Quantitative RT-PCR

Total RNAs from bacteria pellets were isolated via RNAeasy Mini Kit (Qiagen, cat. #74104) following the manufacturer's recommendations. 2500 ng of total RNA was reverse-transcribed to cDNA using RevertAid H Minus First Strand cDNA Synthesis Kit (Thermo Scientific, cat. #K1632) following the manufacturer's instructions. To determine the amount of cDNA by qPCR, 100 ng cDNA was mixed with primers and amplified using LightCycler® 480 SYBR Green I Master (Roche, cat. # 04887352001) following the manufacturer's instructions. The program for real-time was set as follows: 95°C for 10 min, 40 cycles of 95°C for 15 seconds, annealing temperature (60°C) for 1 minute, and 72°C for 15 seconds. The real-time PCR was performed using Roche LightCycler® 480 system. All values of interesting genes were normalized to the housekeeping gene- *rpoB* mRNA as an internal control using the $2^{-\Delta\Delta Ct}$ method, where $\Delta\Delta Ct = \Delta Ct$ test sample (Ct target gene-Ct internal control) - ΔCt untreated wild type sample (Ct target gene-Ct internal control). All data were presented as fold change relative to the untreated wild type sample. Expression levels of the target genes were presented as mean \pm SEM (standard error of the mean). Primers used to detect specific mRNA are listed in Table 8.

Table 8. List of primers for quantitative RT-PCR.

Primer	Sequence
fepA-F	GGAATACGCGAGTTACGGGT
fepA-R	ACCGTCTGTATCGCCAGAAC
rpoB-F	TCCGTATTCCCGATTCAGAG
rpoB-R	TCACCAGACGCAGTTTAACG
cyoB-q-F	ATGTTTCGGAAAATTATCACT
cyoB-q-R	CTTACCGAAGTAAGTGATCA
exbB-q-F	GTGGGTAATAATTTAATGCA
exbB-q-R	AAGAAGATTGCCCAGGTGAC
exB735-F	TTAAAGCGATGCTGGGTGAT

3.11 RNA isolation and transcriptome analysis

Overnight cultures of each strain were diluted into $OD_{600} = 0.1$ and harvested until reaching exponential phase ($OD_{600} = 0.5$). Bacterial pellets were harvested, washed three times in PBS, diluted into $OD_{600} = 0.01$ in iron-depleted MHB medium. 2 ml of *E. coli* BW25113 were challenged with LP-600 at the concentration of 0.0625, 128 $\mu\text{g/ml}$ or DMSO as vehicle control. Bacterial cultures were grown and pelleted by centrifuge at $OD_{600} = 0.5$ and 1.0, respectively. RNA was extracted by applying the RNAeasy Mini Kit (Qiagen cat. 74104) and followed by the DNase treatment (Qiagen cat. 79254). Total RNA quality and integrity were assessed using the 5200 Fragment Analyzer System (Agilent Technologies). By applying NEBNext® Ultra™ II Directional RNA Library Prep Kit (New England BioLabs), total RNA library was generated from 1 μg total RNA after rRNA depletion through Ribo-off rRNA Depletion Kit (Bacteria) (Vazyme BioTech Co.Ltd.). The libraries were sequenced on Illumina NovaSeq 6000 with an average of 10×10^6 reads per RNA sample by using NovaSeq 6000 S1 PE Reagent Kit (100 cycles). The image data of sequencing was transformed into raw reads and saved in FASTQ format. Quality control and adapter clipping were done using fastq-mcf tool of ea-utils¹³³, followed by mapping to the

genome of *E. coli* strain BW25113 (genebank: CP009273.1) via Rockhopper tool ¹³⁴. The raw counts of reads were normalized differential expression analysis were performed with the R package-limma (version 3.42.2) ¹³⁵. T-test correction was obtained by false discovery rate correction through the Benjamini-Hochberg method ¹³⁶. The cutoffs of differentially expressed genes are absolute log₂ fold change of 1 and a corrected *p*-value of 0.05. Functional enrichment analysis and putative protein-protein interaction network of differentially expressed genes were performed by online STRING tool ¹³⁷ with default settings (minimum required interaction score = medium confidence 0.4, a threshold of false discovery rate = 0.05).

3.12 Metabolomics sample preparation

Wild type *E. coli* cultures were prepared as mentioned above, treated without or with LP-600 at indicated concentrations and grown until OD₆₀₀ = 0.5 and 1.0, respectively. For intrametabolome extraction, bacterial cultures were pelleted by centrifugation at 9000 xg for 10 min at 4°C, followed by washing with ice-cold 0.9 % NaCl and transferring into 2-ml Eppendorf tubes. The pellets were submitted to shock-freezing in liquid nitrogen and thawed three times at room temperature, respectively. The pellets were resuspended in 600 µl of ice-cold 100% methanol that was spiked with glipizide (Acros) as an internal standard at a concentration of 1200 µg/ml. The suspension was frozen in liquid nitrogen again, thawed, and 600 µl of ddH₂O were added, followed by two additional freeze-thaw-sonication cycles. Extracts were centrifuged for 10 minutes at 13,000 g. The supernatant was collected into fresh Eppendorf tubes and dried overnight in a speedvac. The dried metabolite extracts were reconstituted in 45 µl 1:1 methanol/H₂O containing trimethoprim (Sigma-Aldrich cat. # T7883) at a concentration of 200 µg/ml and nortriptyline (Sigma-Aldrich) at a concentration of 200 µg/ml as internal controls for normalization.

3.13 LC-MS/MS measurement and data analysis

To analyze metabolomics samples, 3 µl of metabolome extracts per sample were analyzed by HR-LCMS. For the LC separation, an Ultimate 3000 UHPLC-system was used (Dionex/Thermo Scientific, Dreieich, Germany) and a maxis HD UHR-TOF mass spectrometer (Bruker, Bremen, Germany), equipped with an Apollo II electrospray source for measuring the HR-mass data. Full scans (50–1500 Da) were performed for electrospray ionization (ESI). To generate ions, a capillary voltage of 4500 V and the MS input is applied. The separation was done with a Kinetex 1.7 µm

C18 150 x 2.1 mm diameter column (Phenomenex, USA) at a flow rate of 300 μ l/min. Samples were analyzed in both positive and negative modes with solvent A (water plus 0.1% formic acid) and solvent B (acetonitrile + 0.1% formic acid). The elution was run as follows: 1% B from 0 to 2 minutes, and a linear gradient from 1% to 100% B for 2 to 20 minutes, 100% B from 20 to 25 minutes, and the gradient from 100% to 1% B from 25 to 30 minutes. To analyze more polar metabolites, a hydrophilic interaction liquid chromatography (HILIC) separation mode was used. An Acquity UPLC BEH Amide 1.7 μ m, 150 x 2.1mm column (Waters Corp., USA) at a flow rate of 300 μ l/min was applied for separation. Samples were analyzed in both positive and negative ion mode with solvent A: Water with 20mM ammonium formate and solvent B: 95% acetonitrile, 5% water with 20mM ammonium formate. The elution was run as follows: 100% B from 0 to 2 minutes, and a linear gradient from 100% to 50% B from 2 to 20 minutes, 50% B from 24 minutes, after this was returning to 100% B. For internal calibration, sodium formate was infused into the system as a calibrant during the first 0.3 min of each run. For lock mass calibration, hexakis (2,2-difluoroethoxy) phosphazene was used with 622.0290 m/z for positive and 556.0020 m/z for negative ion mode. MS/MS fragmentation was conducted by collision-induced dissociation of the five most abundant ions per MS scan with collision energy between 14-110 eV depending on the mass and charge of the parent ions.

Raw data were analyzed by Metaboscape 4.0 software with indicated parameters in Table 9. Metabolites were annotated by matching the retention time, MS and MS/MS fragmentation patterns with the in-house library of 600 metabolites as pure chemical standards, commercial libraries including LipidBlast (with 14048 metabolites) and Bruker MetaboBase (482025 metabolites), Bruker HMDB Metabolite Library (824 metabolites). Features were putatively identified by matching MS/MS fragmentation patterns as well as exact masses to in-house library or open-source MS/MS libraries such as ECMDB ¹¹⁴, HMDB ¹¹³, GNPS ¹¹⁵ or theoretical MS/MS fragmentation patterns from MetFrag ¹³⁸.

Table 9. List of parameters applied in Metaboscape.

Parameters	Positive	Negative
ferraWorkflow_minCorrelation	0.8	0.8
ferraWorkflow_lockMass	622.0290	556. 0020

ferraWorkflow_GroupFeatures_rtDelta	10	10
ferraWorkflow_chargeMax	3	3
ferraWorkflow_rtMaxInSeconds	1680	1680
ferraWorkflow_ForeachAnalysisMsms_MsmsExtractionWorkflow – ConsolidateMsmsPeaklists_method	average	average
msmsExtractionCompassResult_fillNonDeconvolutedValue	0	0
ferraWorkflow_substanceClass	small molecules	small molecules
ferraWorkflow_rtMinInSeconds	12	12
ferraWorkflow_ForeachAnalysis_FeatureFinder_ClusterDeisotoping_ featureIntervalMethod	FWHM	FWHM
ferraWorkflow_seedIntensityThreshold	500	500
ferraWorkflow_enableLockMass	true	true
ferraWorkflow_useIsotopePatternCoverage	false	false
ferraWorkflow_ForeachAnalysisMsms_MsmsExtractionWorkflow – MsmsDeisotoping_relativeAbundanceThreshold	0.005	0.005
ferraWorkflow_targetedExtractionMinClusterSize	3	3
ferraWorkflow_maxClusterOverlap	0.1	0.1
ferraWorkflow_ForeachAnalysisMsms_MsmsExtractionWorkflow – ConsolidateMsmsPeaklists_groupByCollisionEnergy	true	true
ferraWorkflow_mzMin	75	75
ferraWorkflow_ForeachAnalysis_FeatureFinder_ClusterDeisotoping_ ng_	2	2

areaCalculationScale		
ferraWorkflow_minExistFraction	0.55	0.55
ferraWorkflow_CreateRecursiveTargets_threshold	3	3
ferraWorkflow_ForeachAnalysisMsms_MsmsExtraction Workflow_MsmsDeisotoping_proteomics	true	true
msmsExtractionCompassResult_fillStrategy	topN	topN
ferraWorkflow_uffMinSeedClusterSize	7	7
ferraWorkflow_maxIsotopePatternError	0.2	0.2
ferraWorkflow_CreateBatchFeatures_minGroupSize	3	3
ferraWorkflow_minCorrelatedFraction	0.55	0.55
ferraWorkflow_mzMax	1000	1000
ferraWorkflow_areaIntensity	false	false
ferraWorkflow_enableMsmsExtraction	true	true
ferraWorkflow_minNumClusters	1	1
ferraWorkflow_uffMinClusterSize	2	2
processingWorkflowId	Ferra3d	Ferra3d
polarity	positive	negative
Deconvolution.eicCorrelation	0.8	0.8
persistOnlyConsensusIsotopePattern	false	false
Deconvolution.primaryIon	[M+H] ⁺	[M-H] ⁻
Deconvolution.seedIons	[M+Na] ⁺ , [M+K] ⁺	[M+Cl] ⁻
Deconvolution.commonIons	[M-H ₂ O+H] ⁺ , [2M+H] ⁺ , [M+NH ₄] ⁺ , [M- CO ₂ +H] ⁺	[M-H-H ₂ O] ⁻

sampleGroupFilterType	percentage	percentage
sampleGroupPresenceFilterValue	100	100
nupfTimeStamp	1.60215E+12	1.6E+12
nupfWorkflowVersion	3.4	3.4

3.14 Statistics analysis and bioinformatics

Statistics analysis for metabolomics data was calculated by R packages- stats (version 3.6.3). T-test correction was obtained by false discovery rate correction through Benjamini-Hochberg method ¹³⁶. The threshold for significant features is corrected p-value (false discovery rate, FDR) < 0.05 and absolute value of fold change > 1.5. Lists of significantly regulated metabolites were further annotated with pathway information from the EcoCyc database ¹³⁹ and MetaboAnalyst ¹⁴⁰. For visualization of data, the R packages: pheatmap (version 1.0.12), ggplot2 (version 3.3.0), limma (version 3.42.2), EnhancedVolcano (version 1.4.0), RDAVIDWebService (version 4.0.3) ¹⁴¹, the software Cytoscape ¹⁴² and the add-in Enrichment Map ¹⁴³ were used.

4. Results

4.1 LP-117, a novel synthetic siderophore, induced growth recovery in enterobactin-deleted *E. coli* in a FepA dependent manner.

To generate novel antibiotics based on siderophore-conjugates, several artificial siderophores were designed and synthesized¹²⁸. *E. coli* BW25113 and certain single-gene deletion mutants from the Keio collection as a model were applied to study the efficacy of siderophores and their conjugates. *E. coli* BW25113, one of the most common laboratory strains, is primarily a genetic derivative of *E. coli* K-12. BW25113 was created in Barry L. Wanner's laboratory and used as a parent strain for developing the Keio collection comprising nearly 4,000 single-gene deletion mutants via bacteriophage lambda red recombination engineering^{127,144}. To identify potential synthetic siderophores and investigate their uptake in *E. coli*, a growth recovery assay in *E. coli* was conducted. In iron-limited condition, wild type K-12 strain is able to grow due to endogenous siderophore production. By contrast, *E. coli* Δ entA is unable to grow under iron-limited condition due to the lack of endogenous siderophore production (Figure 12A), because Δ entA strain is an enterobactin-depleted strain which lacks a key gene- entA encoding 2,3-dihydro-2,3-dihydroxybenzoate dehydrogenase involved in enterobactin synthesis (see Figure 6). Upon supplementation with exogenous enterobactin, *E. coli* Δ entA recovered growth in iron-limited medium (Figure 12A and B). Thus, enterobactin serves as a positive control in this so-called growth recovery assay. Using this assay, the uptake of several artificial siderophores was assessed by a growth recovery assay. A novel MECAM-based catecholate siderophore named LP-117 (Figure 12B and C) was identified, exhibiting equivalent or comparable growth recovery to the *E. coli* Δ entA strain in iron-limited condition (Figure 12B).

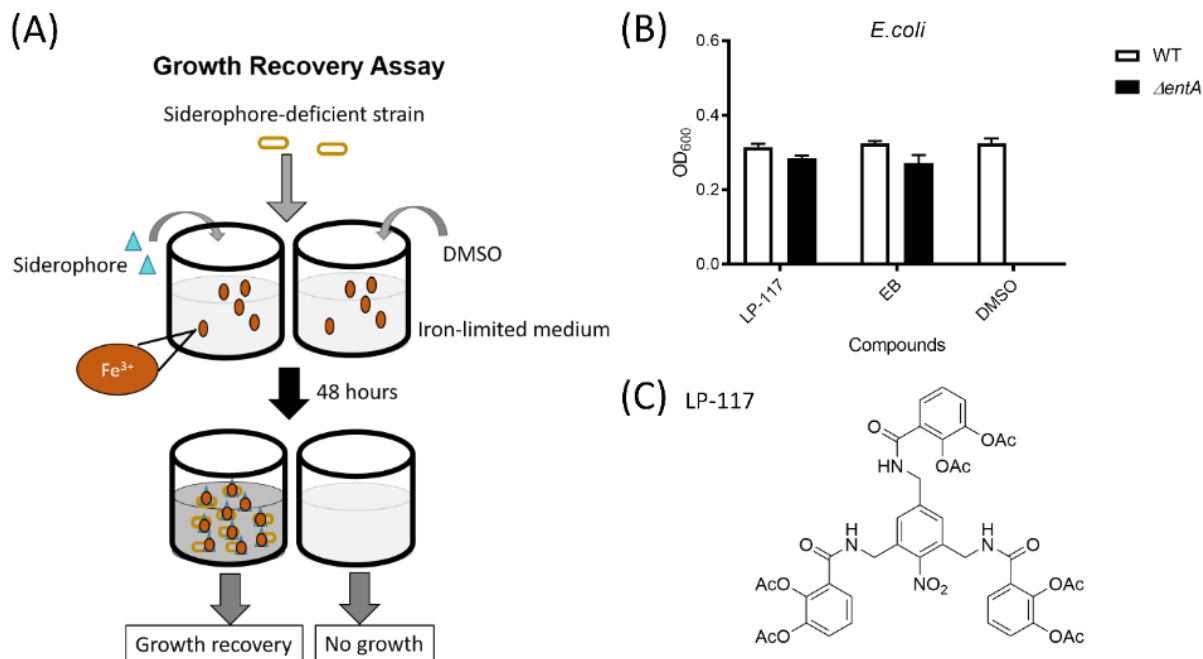


Figure 12. Scheme and result of growth recovery assay. (A) Scheme of procedure for growth recovery assay. (B) *E. coli* BW25113 (wild type, WT) and the enterobactin-deficient strain ($\Delta entA$) cultures were treated with DMSO (solvent control), enterobactin (EB) or LP-117 in iron-limited medium. The growth of *E. coli* K12 BW25113 (WT) and the enterobactin deficient strain ($\Delta entA$) was determined by the OD₆₀₀ after 48-hour compound treatment. (C) The structure of LP-117.

To characterize receptors involved in LP-117 uptake, growth recovery assay was conducted in double knockout strains that harbor the first gene deletion in one outer membrane receptor and the second knockout in *entA* gene. To obtain the gene deletion strains, lambda red recombineering was applied to introduce the deletion of the second gene in *E. coli* $\Delta entA$ strain¹²⁷. Chloramphenicol cassette flanked with FRT sequence and plasmid expressing lambda red system was introduced into *E. coli* $\Delta entA$ strain. By homologous recombination, the targeted gene on the corresponding locus was replaced with chloramphenicol cassette for further clone selection. The detailed procedures are mentioned in the section of materials and methods. With deletion of *entA*, *E. coli* $\Delta entA$ strain is able to grow in iron-limited condition with the supplement of siderophore because of the expression of iron-siderophore acquisition system. With the second deletion in *fepA* gene, $\Delta entA\Delta fepA$ strain shows growth defect in growth recovery assay in the presence of enterobactin (Figure 13A), suggesting that *fepA* is a key molecule involved in enterobactin uptake. Similar to enterobactin, a growth defect was observed in $\Delta entA\Delta fepA$ strain following treatment of LP-117,

whereas LP-117 treatment still enabled growth recovery in $\Delta entA\Delta fecA$, $\Delta entA\Delta fhuA$, $\Delta entA\Delta cirA$, and $\Delta entA\Delta fiu$ strains (Figure 13A). These results suggest that only FepA is the key receptor for LP-117 uptake instead of FecA, FhuA, CirA, and Fiu.

To further confirm the role of FepA in LP-117 uptake, FepA receptors were reintroduced by expressing a plasmid encoding full-length FepA in $\Delta entA\Delta fepA$ strain, followed by a growth recovery assay with supplement of LP-117 (Figure 13B). The level of *fepA* expression was monitored by real-time PCR (Figure 13C). Complementation of FepA in $\Delta entA\Delta fepA$ strain rescues growth under LP-117 treatment in iron-limited condition, indicating that FepA, but not the other catechol receptors CirA and Fiu, was essential for LP-117 uptake in *E. coli* under iron-depleted conditions. Besides, to further conjugate LP-117 to antibiotics, the siderophore-LP-697 was synthesized, which is based on LP-117, but carries an additional linker. Similar to LP-117, LP-697 shows a growth recovery in $\Delta entA$ (Figure 13D and E). Thus, LP-697 was applied for siderophore conjugation.

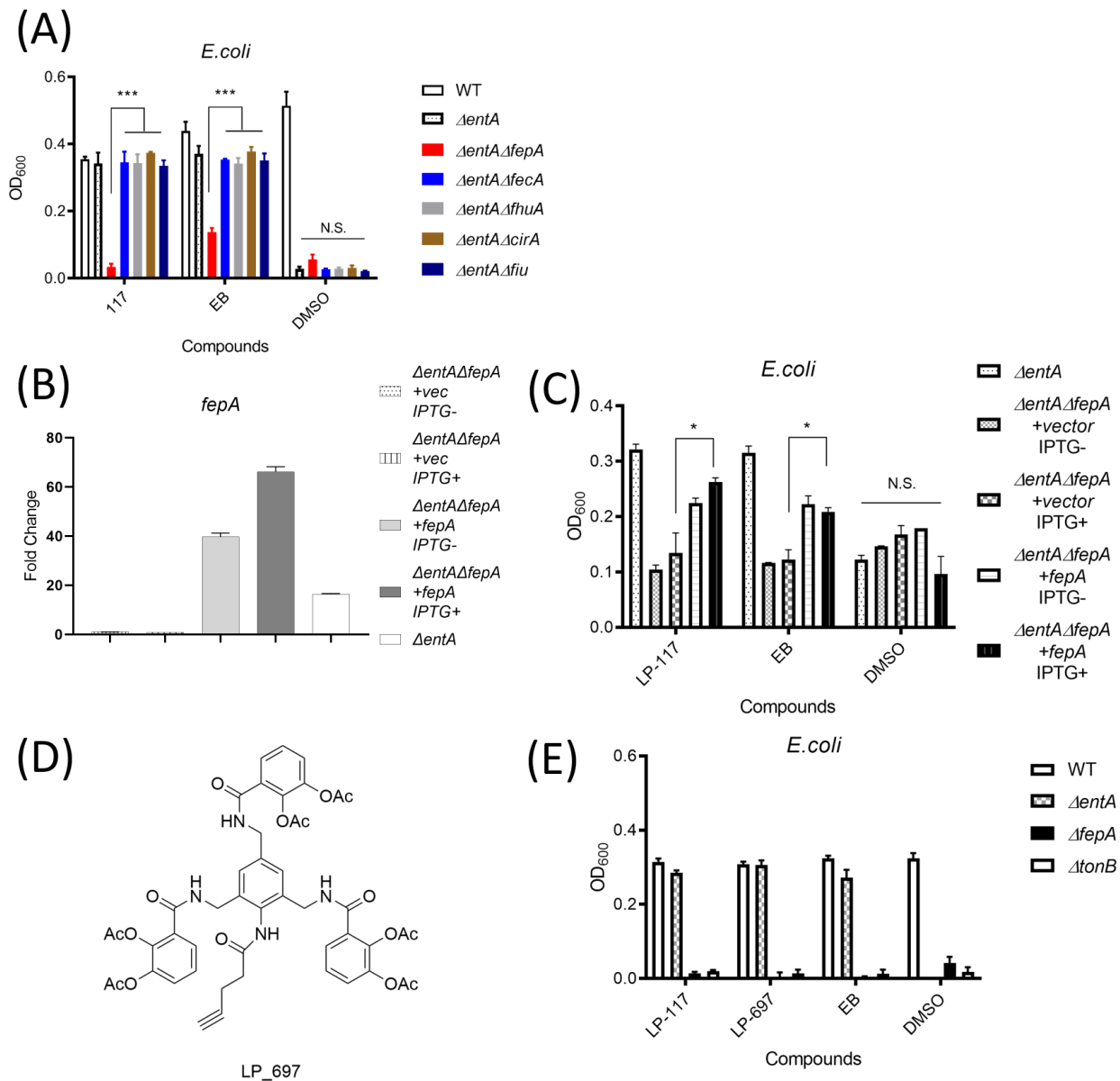


Figure 13. FepA is required for LP-117 uptake in *E. coli* under iron-limited medium. (A) Cultures of WT, single or double knockout of *entA* with the outer membrane receptors were treated with indicated compounds and grown as mentioned above. (B) The RNA expression of *fepA* from the cultures in (C). Bacterial pellets were harvested, followed by RNA extraction. Reverse transcription was performed followed by real-time PCR. Gene expression was normalized against reference gene *RpoB* and given as relative to $\Delta entA \Delta fecA$ +vec control. (C) Indicated strains harboring IPTG-driven *fepA* expression plasmid or vector control were treated with LP-117, EB or DMSO in LMR medium. (D) The structure of LP-697. (E) Indicated *E. coli* strains were treated with LP-117, LP-697, EB (enterobactin), or DMSO for growth recovery assay. Bars represent the means and standard deviations of one representative experiment done in

triplicate. Results shown are means and standard deviations of one representative experiment done in triplicate. * $P < 0.05$ (Student t test). *** $P < 0.001$ (Student t test).

4.2 Siderophore-conjugate LP-600 and LP-624 display antibacterial activity against both laboratory and pathogenic *E. coli*.

Based on LP-697 siderophore, the compounds LP-600 and LP-624 were prepared, that linked LP-697 to ampicillin and amoxicillin, respectively (Figure 14A and B). To address the antibacterial activity of these siderophore conjugates, minimum inhibitory concentration (MIC) assay against laboratory strain *E. coli* BW25113¹⁴⁴ in iron-depleted Mueller Hinton broth (MHB) was performed. LP-600 and LP-624 both exerted remarkably high antibacterial activity against *E. coli* (Figure 15A and Table 10) with MIC values of 2 $\mu\text{g/mL}$ (LP-600: 1.45 μM , LP-624: 1.43 μM). By contrast, the MICs of ampicillin and amoxicillin were 16 $\mu\text{g/mL}$ (45.79 μM) and 8 $\mu\text{g/mL}$ (21.89 μM), respectively. Besides, deletion of *entA* decreased the MICs for LP-600 and LP-624 by 4-fold was found (Table 10).

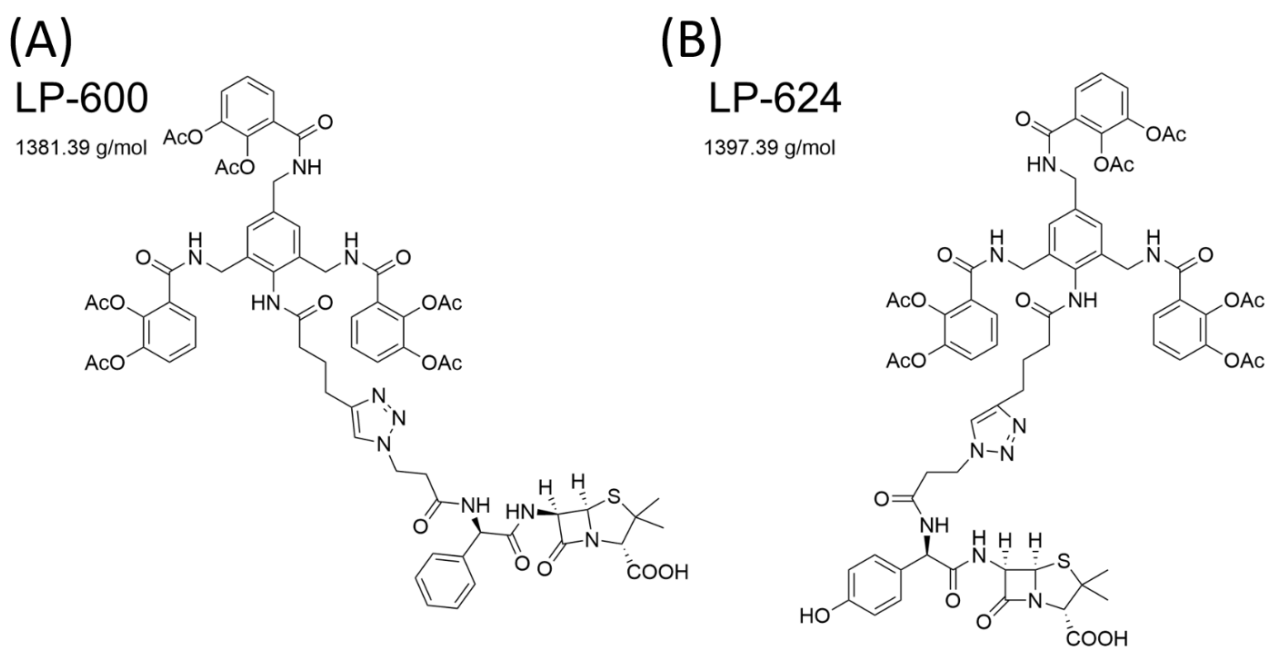


Figure 14. Structures and molecular weights of LP-600 (A) and LP-624 (B).

Table 10. Antibacterial activity of LP-600 and LP-624 against non-pathogenic and uropathogenic *E. coli*.

	MIC ($\mu\text{g/mL}$)		
	WT	ΔentA	UPEC
	K-12		536
Amp	16	16	8
Amx	8	8	4
LP-600	2	0.5	1
LP-624	2	0.5	2

Furthermore, an antibacterial assay against the uropathogenic strain UPEC 536 was performed. Unlike BW25113 strain that produces only enterobactin, UPEC 536 produces multiple siderophores including enterochelin, yersiniabactin, salmochelin¹⁴⁵ that contribute to the virulence of UPEC. Notably, LP-600 and LP-624 displayed promising antibacterial activities against UPEC 536 with MIC's of 1 $\mu\text{g/mL}$ and 2 $\mu\text{g/mL}$, respectively (Figure 15B and Table 10), suggesting that *E. coli* enabled uptake of LP-600 and LP-624 even in the presence of multiple siderophores. On the other hand, time-killing kinetics for *E. coli* treated with LP-600 or LP-624 were assessed by quantifying the bacterial ATP level, which is an indicator of metabolically active cells and thereby for bacterial viability¹⁴⁶. LP-600 exerted a killing effect on *E. coli* starting after two-hour treatment. After six-hour treatment of LP-600 at concentrations of one-time and eight-times the MICs, ATP levels were significantly reduced in comparison with untreated control or ampicillin (Figure 15C). Likewise, the bacterial viability largely decreased under the treatment of LP-624 compared to the amoxicillin (Figure 15D). Additionally, considering the influence of iron on siderophore uptake, whether LP-600 and LP-624 were active against *E. coli* in iron-rich conditions were checked. Both LP-600 still show antibacterial activity against *E. coli* in regular MHB, even the MICs increase 8-times in comparison to the MICs in iron-depleted MHB (Figure 15E and F). These results suggest that LP-600 and LP-624 are potential antibiotics against both laboratory as well as pathogenic *E. coli*.

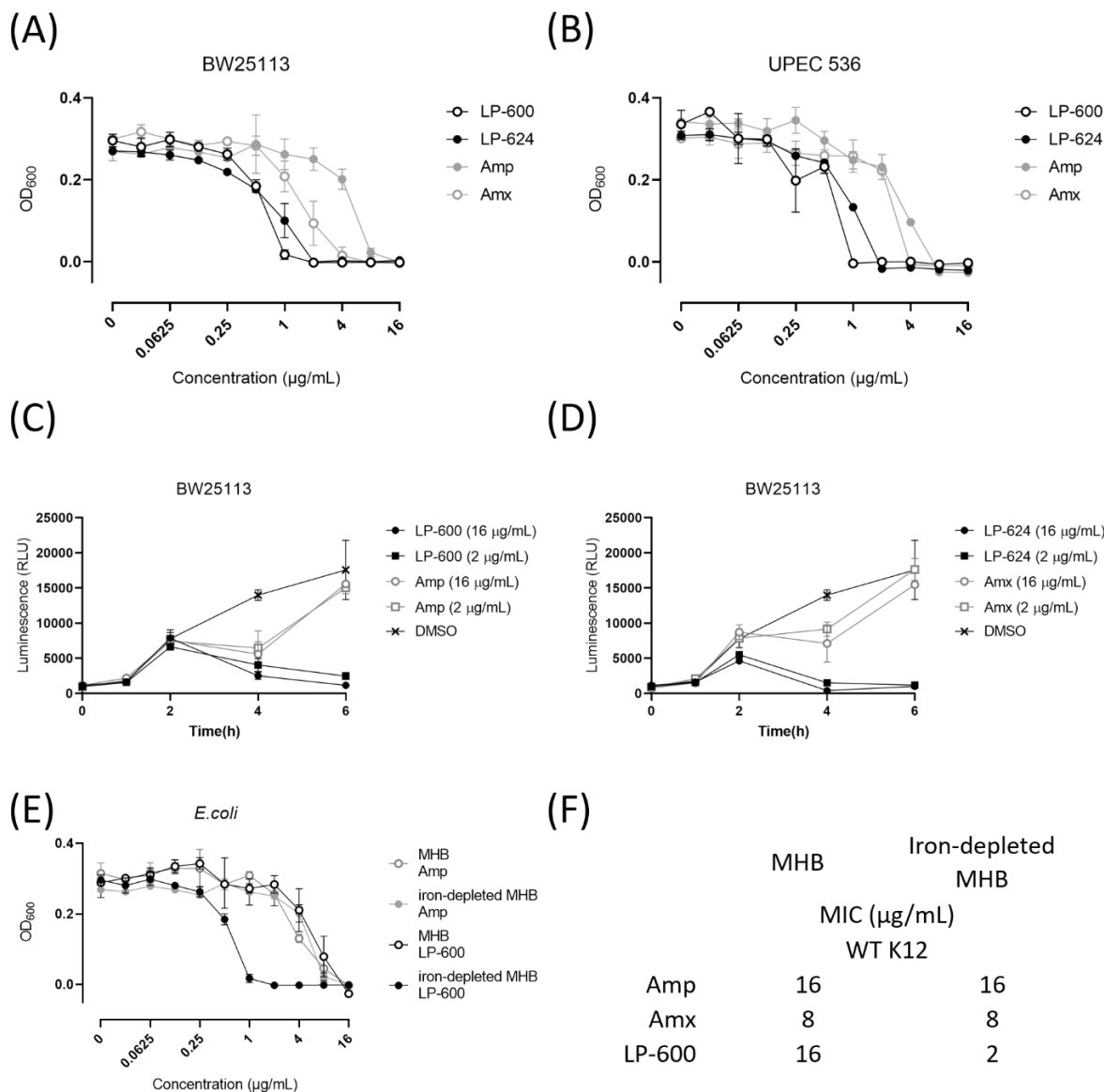


Figure 15. Antibacterial activity of LP-600 and LP-624 against *E. coli*. Antibacterial activity assay against BW25113 (A) or UPEC 536 (B) with LP-600, LP-624, ampicillin, and amoxicillin was assessed by OD_{600} measurement after 24-hour antibiotic treatment in iron-depleted MHB. Time-kill curves for *E. coli* treated with LP-600 and ampicillin (C), LP-624 and amoxicillin (D) at 2 or 16 $\mu\text{g/mL}$ in iron-depleted MHB. Cell viability at 1, 2, 4 and 6 hours after incubation with antibiotics was determined by a BacTiter-Glo™ assay. DMSO treated group served as a growth control. Antibacterial activity of LP-600 against *E. coli* in MHB and iron-depleted MHB (E and F). BW25113 was treated with LP-600 or ampicillin and incubated in MHB or iron-depleted MHB for 24 hours, followed by OD_{600} measurement. Representative results of $n = 3$. Amp: ampicillin. Amx: amoxicillin.

4.3 Catecholate siderophore receptors- FepA, CirA and Fiu, are required for LP-600 and LP-624 mediated antibacterial activity in *E. coli*.

To understand the role of siderophore uptake pathway in LP-600 activity in *E. coli*, different knockout strains involved in siderophore uptake pathway were treated with LP-600. Growth recovery experiments have shown that FepA is essential for LP-117 uptake (Chapter 4.1 and Figure 13), so the role of outer membrane receptors for catecholate siderophores in antibacterial activity of LP-600 was first examined. Surprisingly, strains with single deletions of catecholate receptor genes such as *fepA*, *cirA*, or *fiu* as well as the double knockout strains $\Delta fepA\Delta cirA$, $\Delta fepA\Delta fiu$, $\Delta cirA\Delta fiu$ showed susceptibility to LP-600 (Table 11). In contrast, *E. coli* displaying triple knockout of *fepA*, *cirA* and *fiu* is resistant to LP-600. Similarly, only triple knockout of *fepA*, *cirA* and *fiu* was found to be resistant to cefiderocol, a commercial catechol conjugate to β -lactam⁶⁸, even though a remarkable 64-fold increase in the MIC of cefiderocol was observed in the $\Delta cirA\Delta fiu$ strain. Thus, these results suggest that LP-600 can be taken up by FepA, CirA, and Fiu catechol receptors in *E. coli*, and each of them shows a redundant role in cases when one or two of the receptors are impaired.

Moreover, the influence of downstream components of the catechol siderophore pathway on antimicrobial activities of LP-600 was examined (Figure 16). The Ton machinery is composed of TonB, ExbB and ExbD, facilitating cargo uptake from cognate receptors such as FepA⁴⁵. Both LP-600 and cefiderocol are inactive against a $\Delta tonB$ strain. Interestingly, $\Delta exbB$ strain shows full resistance to only LP-600, but only impaired sensitivity to cefiderocol (Table 11), indicating ExbB might play a specific role in LP-600-mediated antibacterial activity against *E. coli*.

On the other hand, depletion of *fepB*, a periplasmic protein responsible for shutting corresponding cargo from catechol receptors to ABC transporters in the inner membrane⁴⁵, increases merely two-fold MIC of LP-600 than in wild type *E. coli*. To investigate whether the import system of siderophore from inner membrane into cytoplasm is required for the LP-600 activity against *E. coli*, the antibacterial activity of LP-600 was examined in $\Delta fepD$ strain. The $\Delta fepD$ strain, which is defective in catechol import from inner membrane to cytoplasm, was susceptible to LP-600, suggesting that transporting LP-600 into periplasm space is sufficient for LP-600-mediated

antibacterial activities (Table 11). Therefore, these results demonstrate all three catecholate receptors-FepA, CirA and Fiu might contribute to LP-600 uptake in *E. coli*.

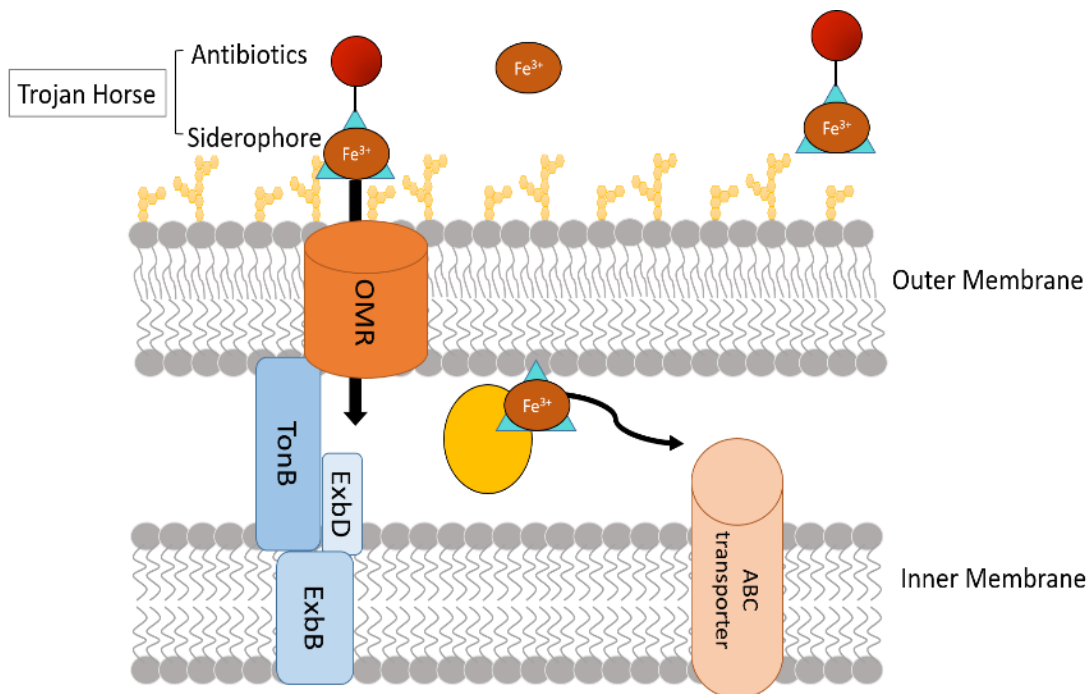


Figure 16. Scheme of siderophore uptake system in *E. coli*.

Table 11. Antibacterial activity of LP-600, ampicillin and cefiderocol against gene modification strains involved in siderophore uptake pathways of *E. coli*.

	MIC ($\mu\text{g/mL}$)		
	LP-600	Amp	CEF
WT	2	16	0.25
ΔfepA	4	16	0.125
ΔcirA	4	16	0.5
Δfiu	2	16	0.5
$\Delta\text{fepA}\Delta\text{cirA}$	2	16	0.125
$\Delta\text{fepA}\Delta\text{fiu}$	2	16	0.5
$\Delta\text{cirA}\Delta\text{fiu}$	4	16	16
$\Delta\text{fepA}\Delta\text{cirA}\Delta\text{fiu}$	>128	16	>16
ΔtonB	>128	16	>16
ΔexbB	>128	16	4
ΔfepB	4	16	0.0625
ΔfepD	2	16	0.0625

The K-12 strains WT (BW25113) or indicated knockout strains were treated with indicated antibiotics for 24 hours in iron-depleted MHB followed by OD₆₀₀ measurement as mentioned above. Amp: ampicillin. CEF: cefiderocol.

4.4 LP-600 resistant clones reveal single nucleotide variants in *cyoB* and *exbB* gene.

To understand the resistance mechanism of *E. coli* toward LP-600, LP-600 resistant clones in *E. coli* K-12 BW25113 were generated by serial passage under LP-600 challenge. To generate LP-600-resistant clones, *E. coli* BW25113 was treated with LP-600 (0-16 ug/mL) in iron-deficient MHB. Cultures displaying visible growth (OD₆₀₀> 0.1) after 24-hour LP-600 treatment were exposed to the higher dose of LP-600 (4-16 ug/mL). Four of the original clones survived after 21 passages (MIC >16 µg/ml) (Table 12). To exclude general drug-resistant clones, resistant clones were subject to ampicillin, kanamycin or cefiderocol and the clones resistant to LP-600 were selected. Genomic DNA from four clones surviving 21 passages (MIC>16 ug/mL) were isolated, followed by whole genome sequence and bioinformatics analysis, identifying single nucleotide variants in four resistant clones. Besides, these four clones are resistant to LP-624 as well. Whole-genome sequencing from the four resistant clones and parental clone was performed via Illumina MiSeq system. The results of parental control and four resistant clones were mapped to the reference genome *E. coli* BW25113 (GenBank: CP009273.1) containing 4,631,469 base pairs by Snippy¹³² to find substitutions and insertions/deletions. The statistical results of sequence are listed in Table 13.

Two single nucleotide mutations were found among the four LP-600-resistant clones. Firstly, a single nucleotide mutation observed in all four clones displays a replacement of guanine to adenine at the position of 806 in the gene encoding cytochrome o ubiquinol oxidase subunit I (*cyoB*) (Table 12). This point mutation results in an exchange of glycine to aspartate at the position of 269 (G269D) of expressed protein. *cyoABCD* genes encode and form a terminal cytochrome bo oxidase complex which is the main terminal oxidases in the aerobic respiratory chain in *E. coli* and catalyzes the four-electron reduction of molecular oxygen to water^{147,148}. Besides, the cytochrome bo terminal oxidase serves as supplier of PMF by pumping proton¹⁴². Previous studies showed that CyoB contributes to proton translocation so that plays a key role in PMF generation¹⁴⁸. Previous studies have shown some key sites of CyoB playing an important role in PMF generation^{148,149}. For example, mutation in CyoB D135, a highly conserved amino acid, prevents proton pumping from electron transfer-activity¹⁴⁸. Secondly, a nucleotide mutation, found in the third and fourth

clone, led to thymine instead of cytosine at position 487 in gene-biopolymer transport protein exbB which is one of component in Ton machinery^{74,79}. This point mutation at position 163 leads to a stop codon mutation from glutamine (Q163*) of encoding protein. Both CyoB G269D and ExbB Q163* have not been reported from previous studies.

Table 12. Single nucleotide variants and antimicrobial susceptibility of LP-600-resistant clones.

Clone	Type of variant	Gene	Mutation (DNA)	Mutation (protein)	MIC (µg/mL)			
					LP-600	Amp	Kan	CEF
Clone 1	SNP	cyoB	G > A	Gly269Asp	>16	16	2	0.125
	SNP	exbB	C > T	Gln163*				
Clone 2	SNP	cyoB	G > A	Gly269Asp	>16	16	2	0.125
	SNP	exbB	C > T	Gln163*				
Clone 3	SNP	cyoB	G > A	Gly269Asp	>16	16	2	0.125
Clone 4	SNP	cyoB	G > A	Gly269Asp	>16	16	2	0.125

SNP: Single nucleotide polymorphism. Amp: ampicillin. Kan: kanamycin. CEF: cefiderocol.

Table 13. Summary of statistical results of whole genome sequencing for four LP-600-resistant clones.

	Number of fragments	Average length (bp)	Total base count	Average depth	Percentage coverage of reference genome
Parental genome					
Fragment	1004273	301	301272850	53.3	100
Written	996322				
Non-written	851				
Clone 1					
Fragments	1420630	300	404550050	75.3	100
Written	1409359				
Non-written	1286				

Clone 2					
Fragments	1308499	300	373231276	69.5	100
Written	1299605				
Non-written	1347				
Clone 3					
Fragments	1518924	300	428039546	80.5	100
Written	1505838				
Non-written	1389				
Clone 4					
Fragments	1451979	300	418014672	77.1	100
Written	1442124				
Non-written	1912				

4.5 The siderophore uptake system functions in LP-600 resistant clones

It is believed that ExbB serves as a supplier of proton motive force (PMF) for conformational change of TonB and outer membrane receptor, facilitating siderophore uptake^{78,150}. The ExbB Q163* mutation has not been reported. Given that ExbB forms a complex with TonB for facilitating the siderophore uptake⁷⁴, whether the resistance towards LP-600 resulted from an impaired siderophore uptake system was examined. All of the resistant clones were still able to grow in iron-limited medium (Figure 17A), indicating that the uptake of enterobactin is functional in resistant clones. Moreover, to evaluate whether LP-600 resistant clones enable the uptake of LP-117, *entA* gene in full-length was deleted in four resistant clones that were then investigated the ability to recover growth in the presence of LP-117. With the deletion of *entA*, the "new" four LP-600 resistant clones displayed growth recovery upon supplementation with LP-117 (Figure 17B), further confirming that siderophore uptake system does not abolish in LP-600 resistant clones. On the other hand, unlike $\Delta entA$ LP-600 resistant clones, double knockout strains of *entA* and full-length *exbB* showed no growth recovery in the presence of LP-117 in iron-limited

medium. Thus, these results indicate that neither CyoB G269D nor ExbB Q163* impairs the uptake of enterobactin and LP-117. Notably, deletion of full-length ExbB impairs LP-117 uptake in *E. coli*. These results confirm that the uptake system of siderophore in LP-600 resistant clones is not abolished. According to the peptide sequence, ExbB 163 is located in the third transmembrane domain (TMD) (TMD3)⁷⁸. Mutation of ExbB Q163* leads to an encoding truncated form of ExbB lacking the third transmembrane domain and the cytoplasmic carboxy-terminal⁷⁸. Previous study reported that the role of TMD 1 and 2 is to stabilize the Ton machinery, while the role of TMD 3 in signal transduction⁷⁸. Therefore, the resistant clones with ExbB Q163* mutation take up enterobactin and LP-117 might hint that TMD 1 and TMD 2, but not TMD 3, plays the key role in siderophore uptake (Figure 17).

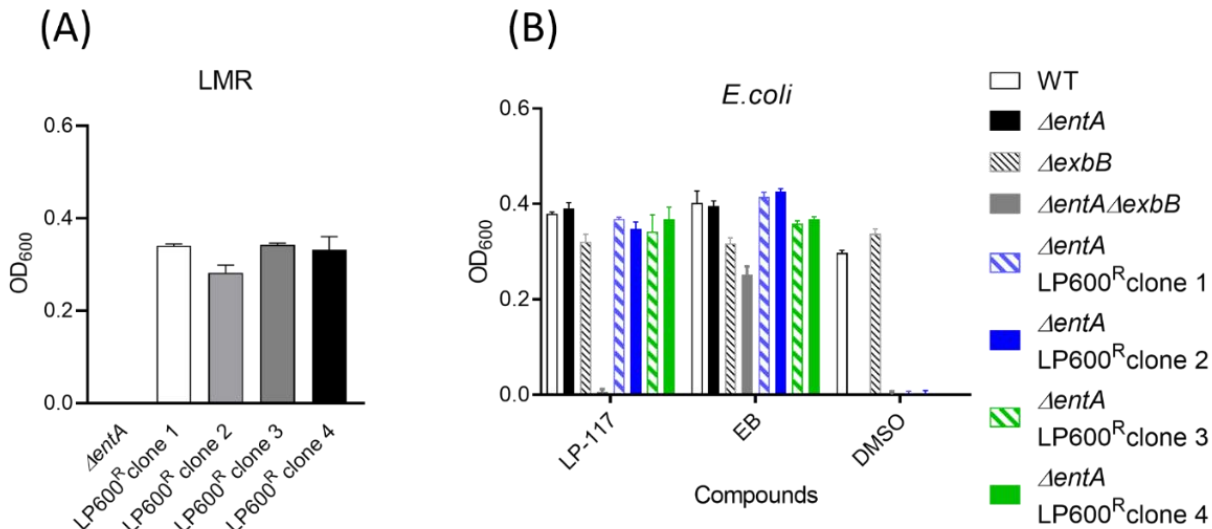


Figure 17. The siderophore uptake system does not abolish in LP-600 resistant clones. The siderophore uptake system does not abolish in LP-600 resistant clones. (A) Cultures of $\Delta entA$, four LP-600 resistant clones were grown in LMR medium. (B) Indicated strains were treated with LP-117, enterobactin (EB), or DMSO in LMR medium, followed by OD₆₀₀ measurement after 48-hour compound treatment. Representative results of n = 3.

4.6 Complementation of ExbB in *E. coli* $\Delta exbB$ restored susceptibility to LP-600

To investigate the effect of CyoB G269D and ExbB Q163* on the anti-bacterial activity of LP-600, CyoB G269D or ExbB Q163*-expressing plasmid was reintroduced into $\Delta cyoB$ and $\Delta exbB$,

respectively. Over-expression of ExbB Q163* in $\Delta exbB$ clone is sufficient for resistance against LP-600 up to 16 $\mu\text{g/mL}$, while over-expressing either wild type ExbB or vector control show susceptibility to LP-600 (Figure 18A). The expression efficiency was confirmed by real-time qPCR (Figure 18B). However, reintroducing either wild type CyoB or CyoB G269D expressing plasmid in $\Delta cyoB$ strain shows no resistance to LP-600 (Figure 18C). The complementation efficiency was confirmed by real-time qPCR (Figure 18D). In line with this, a “reverse” susceptibility to LP-600 in LP-600 resistant clone no. 3 and no. 4 was observed. This “reverse” susceptibility to LP-600 was not observed in LP-600 resistant clone no. 1 and 2 (with only one single nucleotide mutation in the *exbB* gene) after a few passages. Further whole-genome sequence analysis confirms no additional genetic mutation occurred among those “recovery” clones and the statistical results of sequence are listed in Appendix I and II. These results indicate that mutation of ExbB163*, but not CyoB G269D, plays an essential role in LP-600 resistance in *E. coli*.

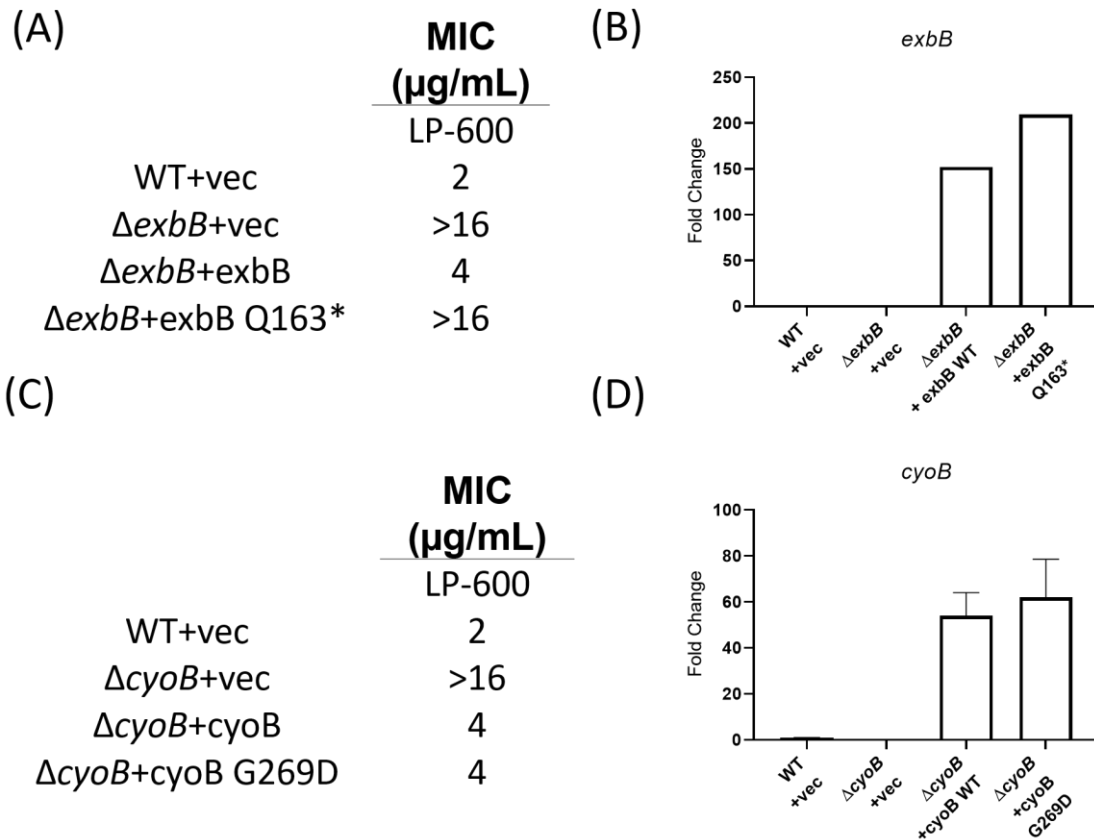


Figure 18. Over-expression of ExbB163*, but not of CyoB G269D displays LP-600 resistance in *E. coli*.

(A) The MICs of LP-600 against $\Delta exbB$ with a plasmid expressing wild-type, Q163* of ExbB, or vector

control. (C) The MICs of LP-600 against *ΔcyoB* with a plasmid expressing wild-type, G269D of CyoB, or vector control. (B)The RNA expression of *exbB* from the cultures shown in (A), and the (D) RNA expression of *cyoB* from the cultures shown in (C). Bacterial pellets were harvested, followed by RNA extraction. Reverse transcription was performed followed by real-time PCR. Gene expression was normalized against reference gene *rpoB* and given as relative to WT+vec control. Bars represent the means and standard deviations of one representative experiment done in triplicate. Results shown are means and standard deviations of one representative experiment done in triplicate. Vec: vector control.

Considering both ExbB and CyoB contribute to the PMF, whether PMF played an important role in antibacterial activity of LP-600 was examined. The presence of CCCP (carbonyl cyanide *m*-chlorophenylhydrazine), an inhibitor of PMF¹⁵¹, has little effect on the MIC values of LP-600 against LP-600-resistant clones as well as wild type strains (Figure 19). These results indicate that PMF is not essential for antibacterial activity of LP-600, but also not required for ExbB163*-mediated resistance to LP-600 in *E. coli*. Collectively, these results confirm the role of ExbB Q163* in LP-600 mediated anti-microbial activity, instead of general siderophore uptake. It is likely that ExbB Q163* blocks specifically uptake of LP-600 instead of siderophore such as enterobactin and LP-117, yet it has to be further explored.

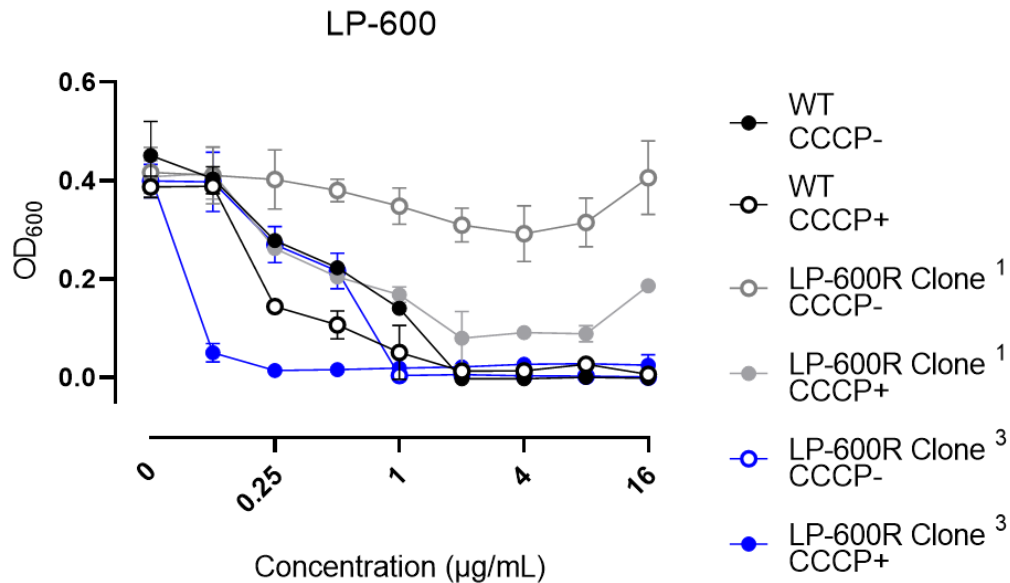


Figure 19. Antibacterial activity of LP-600 against *E. coli* in the presence or absence of CCCP. The indicated strains were treated with LP-600 for 24 hours with or without CCCP in iron-depleted Mueller Hinton broth followed by OD₆₀₀ measurement. Representative results of n = 3.

4.7 High-dose treatments of LP-600 induce a paradoxical growth of *E. coli*.

LP-600 has antibacterial activities against laboratory K-12 BW25113 and uropathogenic *E. coli* 536 strains with minimum inhibitory concentrations (MICs) 2 µg/mL and 1 µg/mL, respectively. Surprisingly, BW25113 and UPEC 536 display paradoxical re-growths upon treatment of LP-600 at concentrations more than 16 times the MIC (Figure 20A and B). This “more compounds - less killing” effect, a phenomenon coined the ‘Eagle-effect’⁸⁵, is a paradoxical growth treated with antibiotics at a higher concentration than the optimal bactericidal concentration (OBC). Eagle effect was named after Harry Eagle who first reported the effect on various types of bacteria such as *S. aureus* upon penicillin treatment^{85,86}. Besides, Eagle effect was previously found in a variety of pathogens as well as antibiotics⁸⁵. In previous studies, a few proposed mechanisms have been reported in response to different classes of antibiotics: a reduced ROS level might contributed to quinolone-induced Eagle effect in *E. coli*⁹³; β-lactamase might cause the β-lactam-associated Eagle effect⁹⁴. Yet, the underlying mechanism of the Eagle effect remains largely unknown. To investigate the LP-600-induced Eagle effect, a growth kinetic assay was conducted by measurement of optical density at a wavelength of 600 nm (OD₆₀₀). In growth kinetic analysis, the lag phase in growth under high-dose LP-600 (64-128 µg/mL) exposure is remarkably delayed from two hours to 7 and half hours compared to the growth of vehicle control (Figure 20C). Notably, after an approximate 20-hour treatment of LP-600, the high-dose treatments reach similar OD₆₀₀ values as the vehicle control, whereas a low dose of 2 µg/mL led to sustained growth inhibition. Furthermore, to examine whether the culture showing the Eagle effect became resistant to the antibiotic, the panels of LP-600 or ampicillin against “Eagle cultures” which are from the cultures displaying the Eagle effect after 24 hours treatment of 128 µg/mL of LP-600 were investigated. After re-treatment of LP-600, bacteria from the Eagle cultures are still susceptible to LP-600 as well as ampicillin and exhibit the Eagle effect, implying that the Eagle effect might result from a transient phenomenon instead of permanent resistance upon high-dose antibiotic treatment (Figure 20D).

To understand whether the Eagle effect is a general phenomenon resulting from antibiotic exposure at a very high concentration, whether ampicillin that causes the Eagle effect in *E. coli* was first investigated. *E. coli* displays no Eagle effect upon exposure to ampicillin up to 256 times (4096 $\mu\text{g}/\text{mL}$) the MIC (Figure 20E). Besides, to examine whether siderophore-conjugates other than LP-600 cause the Eagle effect in *E. coli*, the panel of cefiderocol, which is a commercial catecholate- β -lactam conjugate, against *E. coli* was evaluated. No Eagle effect up to 256 times (64 $\mu\text{g}/\text{mL}$) the MIC of cefiderocol was observed (Figure 20E). On the other hand, the role of iron availability in LP-600-induced Eagle effect was investigated. Interestingly, *E. coli* demonstrates no Eagle effect under the treatment of LP-600 (up to 512 $\mu\text{g}/\text{mL}$) in non-iron depleted Mueller Hinton Broth (Figure 20F). These results suggested that this Eagle effect in *E. coli* is specifically induced by LP-600 rather than by general β -lactam or siderophore-conjugated antibiotics, and it occurs in an iron-dependent manner.

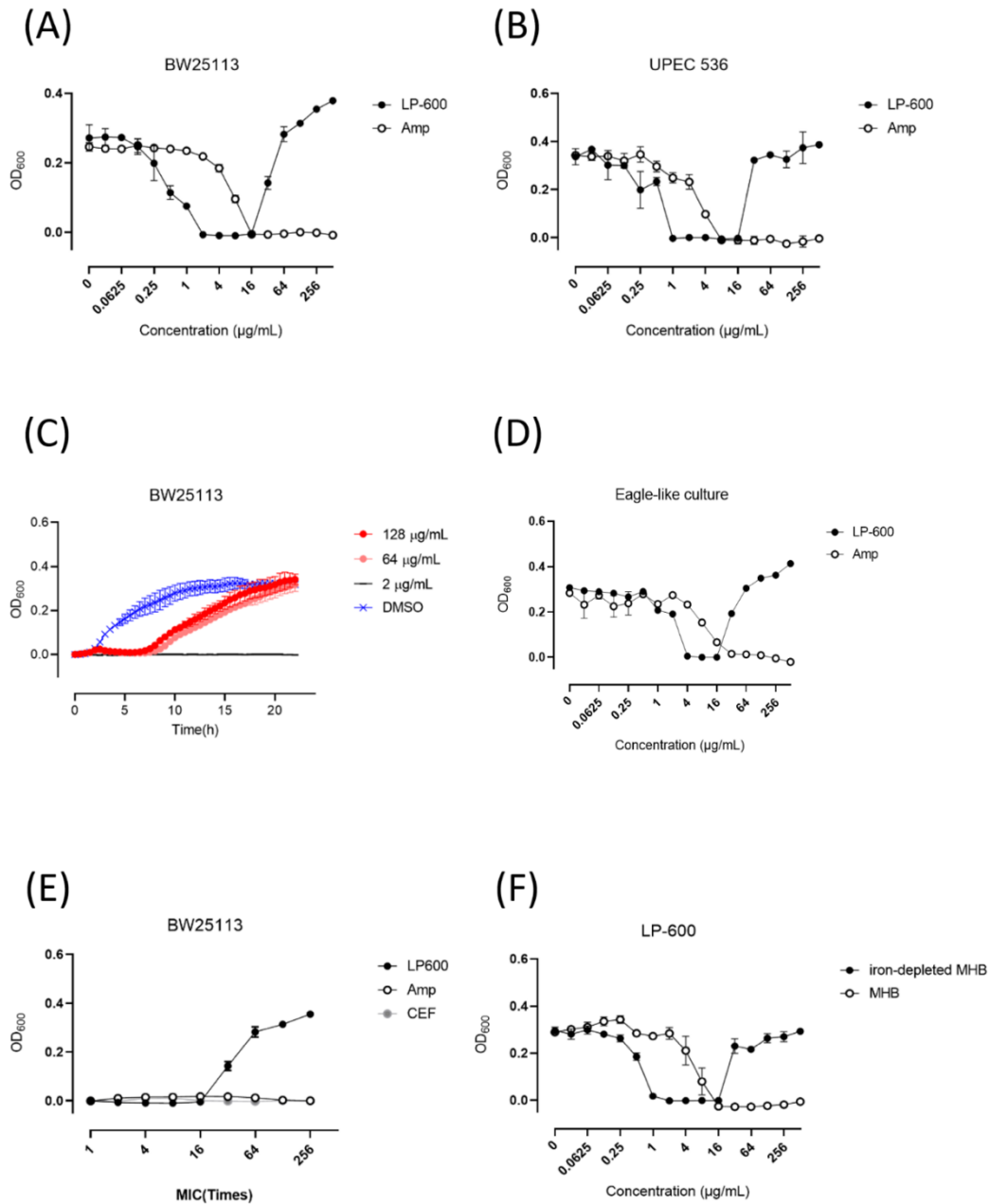


Figure 20. Laboratory and pathogenic *E. coli* show paradoxical growth under high concentrations of LP-600. (A-B) The K-12 BW25113 strain (A) and UPEC 536 (B) were treated with indicated antibiotics for 24 hours in iron-depleted Mueller Hinton broth followed by OD₆₀₀ measurement. (C) BW25113 were treated with LP-600 or DMSO (vehicle control) and followed by the growth kinetic analysis via OD₆₀₀ measurement (D) BW25113 cultures were treated with 128 μg/mL of LP-600 for 24 hours. The cultures were then harvested after washing in PBS, treated with LP-600 or ampicillin for 24-hour, followed by OD₆₀₀ measurement. (E) BW25113 *E. coli* cultures were treated at ranging concentrations of LP-600 (2- 512

μg/mL), ampicillin (16- 4096 μg/mL), or cefiderocol (0.25- 64 μg/mL) with a dilution factor of two for 24 hours followed by OD₆₀₀ measurement. (F) BW25113 was treated with LP-600 with iron-depleted MHB as mentioned above or MHB for 24 hours, followed by OD₆₀₀ measurement.

Moreover, to investigate whether siderophore uptake plays a role in the LP-600-induced Eagle effect, whether high-dose LP-600 induces Eagle effects in strains that are lacking genes involved in enterobactin biosynthesis pathway (*entA*), outer membrane receptors in iron-acquisition system (*fepA*, *fecA*, *fhuA*, *cirA*, *fiu*), shuttle and import system of catechol siderophore from periplasm through inner membrane (*fepB*, *fepD*) were examined. Yet, all of those knockout strains involved in siderophore uptake display Eagle effect upon high-dose LP-600 stimuli (Figure 21). Additionally, high-dose LP-600 induces the Eagle effect in the knockout of *tolC*, involved in drug efflux pump and enterobactin secretion¹⁵². These results suggest that neither siderophore uptake nor efflux is essential for LP-600-induced Eagle effect.

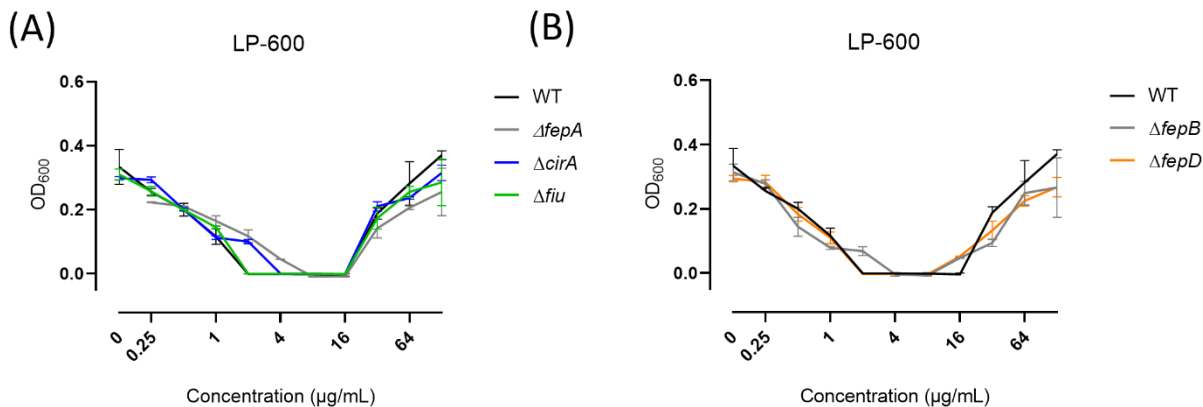


Figure 21. Antibacterial activity of LP-600 against gene modification strains involved in siderophore uptake pathways of *E. coli*. (A) The receptor knockout strains- *fepA*, *cirA*, and *fiu* were treated with LP-600 for 24 hours in iron-depleted Mueller Hinton broth followed by OD₆₀₀ measurement. (B) The knockout strains of *fepB* and *fepD* were treated with LP-600 for 24 hours in iron-depleted Mueller Hinton broth followed by OD₆₀₀ measurement.

4.8 Treatment with LP-600 at high, Eagle effect-inducing concentrations induces a modest increase in β -lactamase activity in *E. coli*

A previous study showed that co-treatment of β -lactam inhibitor with β -lactam abolishes β -lactam-induced Eagle effect in *P. vulgaris*⁹⁴, indicating that β -lactam-induced Eagle effect might attribute to the expression of β -lactamase. To answer this question, the Eagle effect upon co-administration of LP-600 and the β -lactamase inhibitor-sulbactam in *E. coli* was examined. Sulbactam has a β -lactam ring that inhibits β -lactamase activity by covalently binding to β -lactamases¹⁵³ and is widely applied in the treatment combining with ampicillin for infectious diseases¹⁵⁴. Sulbactam exhibits modest antibacterial activity against *E. coli* with the MIC of 64 $\mu\text{g/mL}$ (Figure 22A and B). Intriguingly, co-treatment of LP-600 with 16 $\mu\text{g/mL}$ of sulbactam displays no observable growth of *E. coli* (Figure 22C). Additionally, co-treatment of sulbactam at the concentration of 8 $\mu\text{g/mL}$ and LP-600 remarkably decreases bacterial growth after 24-hour incubation and extends the lag phase to reach exponential growth in comparison with LP-600 treatment alone in *E. coli*. Furthermore, to investigate the role of β -lactamase in LP-600-induced Eagle effect, the role of AmpC in the Eagle effect was examined. Gene *ampC* encodes the chromosomal β -lactamase and mutation in *ampC* was found to contribute to β -lactam tolerance and resistance in clinical isolates^{155,156}. Deletion of *ampC* has little effect on Eagle effect upon LP-600 stimulation even though it has a two-fold decrease in the MIC of LP-600 in *E. coli* (Figure 22D). In line with this, no significant increase in *ampC* expression in transcript level upon LP-600 treatment (128 $\mu\text{g/mL}$) compared to vehicle control or sub-MIC treatment of LP-600 (0.0625 $\mu\text{g/mL}$) (Appendix V) was observed. Moreover, to investigate whether the increase in β -lactamase activity contributes to the Eagle effect, β -lactamase activity in *E. coli* treated with different concentrations of LP-600 was evaluated. After 24-hour LP-600 treatment, there is no significant increase in β -lactamase activity from the cultures shown Eagle effect (32-128 $\mu\text{g/mL}$) comparing to the cultures treated with sub-MIC of LP-600 (0.0625-0.5 $\mu\text{g/mL}$) (Figure 22E) as well as untreated control. Likewise, there is no significant difference in β -lactamase activity between the supernatants collected from cultures treated with different concentrations of LP-600 (Figure 22F).

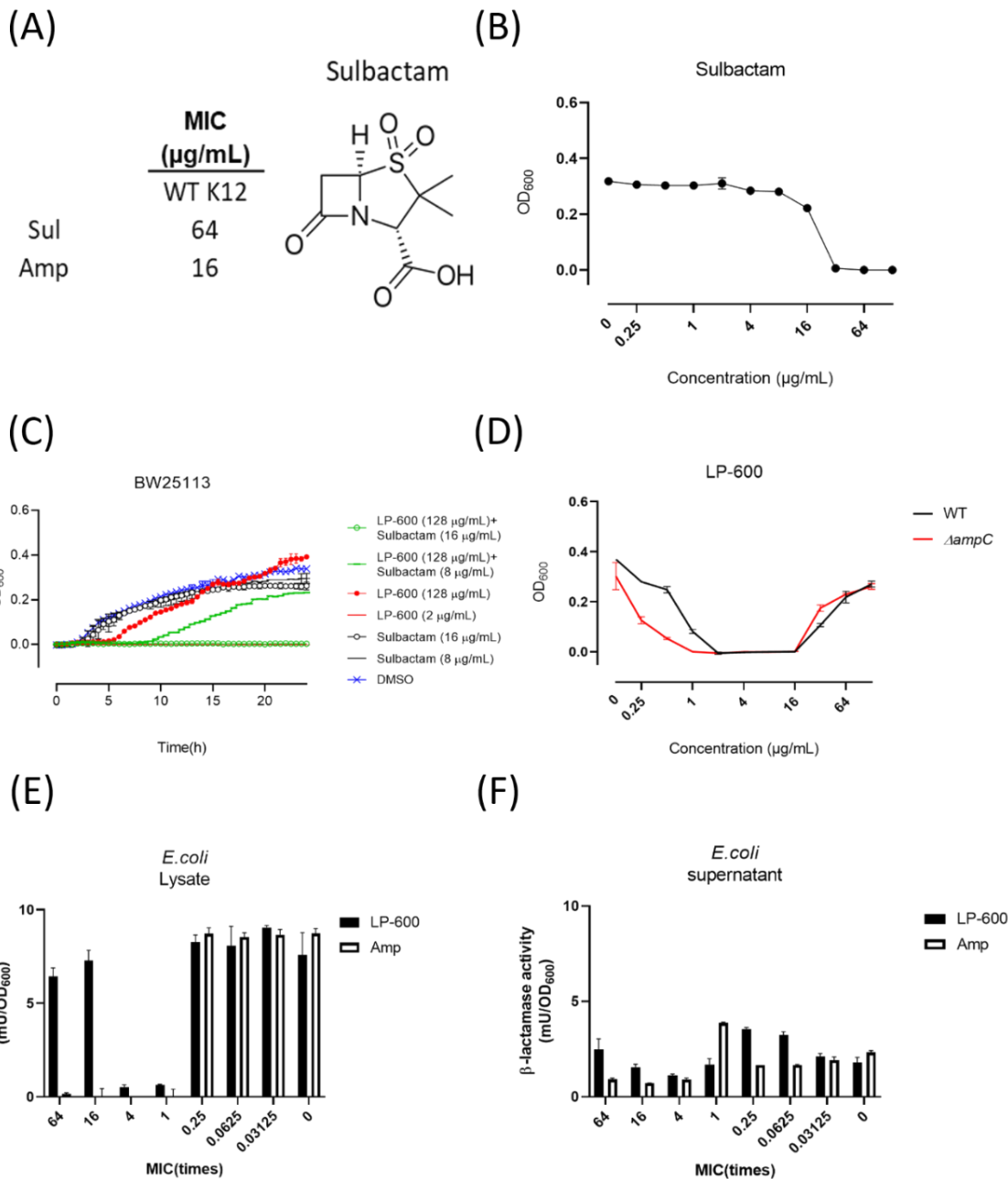


Figure 22. The role of beta-lactamase in the LP-600 induced Eagle effect. (A) The structure and MIC of sulbactam in *E. coli*. (B) WT strain of *E. coli* was treated sulbactam for 24 hours at concentrations of 0.125-128 $\mu\text{g/mL}$ with a serial dilution factor of two. (C) BW25113 were treated with LP-600 or DMSO (vehicle control) with or without sulbactam, followed by the growth kinetic analysis via OD_{600} measurement for 24 hours. (D) WT and $\Delta ampC$ were treated with LP-600 with indicated concentrations for 24 hours in iron-depleted Mueller Hinton broth followed by OD_{600} measurement. (E and F) WT *E. coli* cultures were treated LP-600 for 24 hours, and the β -lactamase activity of bacterial lysate (E) and supernatant (F) were measured.

4.9 Transcriptome analysis

4.9.1 Transcriptomic analysis of *E. coli* following treatments with LP-600

Both transcriptomics and metabolomics approaches are widely applied to study the interaction between antibiotics and microorganisms^{157,158}. Metabolites coordinate a rapid response to environmental changes such as antibiotic stresses¹⁵⁹ and modulate gene expression^{101,160}. In reverse, transcriptional regulation can modulate the metabolic flux by modulating expression of certain key genes¹⁶¹. To gain a global view of LP-600-induced Eagle effect on the *E. coli* over time, both gene expression and metabolic change under LP-600 treatment was investigated during both exponential phase ($OD_{600} = 0.5$) and stationary phase ($OD_{600} = 1.0$). To characterize genes differentially expressed in the Eagle effect cultures, *E. coli* was treated as follows: vehicle control (DMSO), low-dose (sub-MIC level, $0.0625 \mu\text{g/mL}$) and high-dose (Eagle-dose, $128 \mu\text{g/mL}$) treatment of LP-600 and compared the transcriptomes upon treatments. Overall, six groups of samples were generated, i.e. ctrl $OD_{600} = 0.5$, low-dose $OD_{600} = 0.5$, high-dose $OD_{600} = 0.5$, ctrl $OD_{600} = 1.0$, low-dose $OD_{600} = 1.0$, high-dose $OD_{600} = 1.0$. Then, the transcriptomes between the groups were compared between cultures that were harvested from the same OD_{600} value. The growth curves of harvested cultures for omics analysis upon different doses of LP-600 treatment are shown in Figure 23. To reach the $OD_{600} = 0.5$, both vehicle control and low-dose groups exhibit a similar growth curve, while the high-dose group took additional six hours to reach the mid-exponential phase than the other two groups. Interestingly, after 15-hour treatments, all three groups reach similar OD_{600} values.

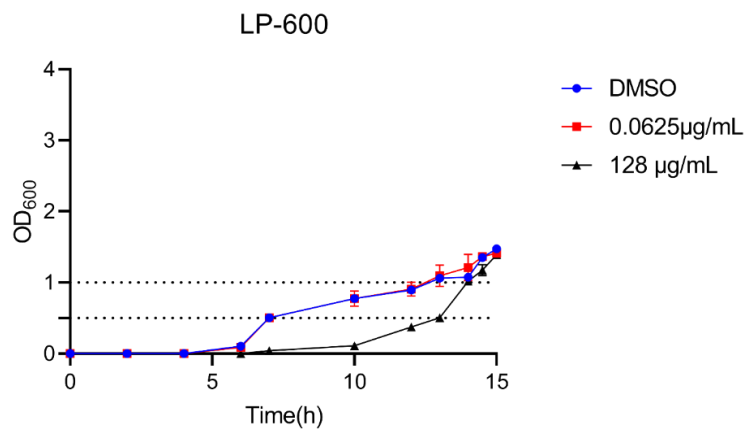


Figure 23. The growth curve of wild type *E. coli* treated without or with LP-600. Wild type *E. coli* was treated with DMSO (vehicle control), low-dose (0.0625 $\mu\text{g/mL}$), high-dose (128 $\mu\text{g/mL}$) of LP-600, followed by OD_{600} measurement over time.

With the help of RNA sequencing, 4079 transcripts were annotated by mapping the obtained short reads to the genome of BW25113 *E. coli* strain (genebank: CP009273.1). To examine the effect of LP-600 treatment on transcriptome, multidimensional scaling (MDS) analysis was performed. MDS represents the level of dissimilarity between objects in a dataset and is commonly used in omics studies to find relationships between samples¹⁶². MDS is a visualization method that transforms and decomposes the correlated variables among samples in a dataset by reducing its dimensionality, expressing high dimensional data in low dimensional space and preserving the similarities between objects¹⁶². In this study, Log-CPM (log counts per million) values in transcriptome data were applied into MDS analysis via R package-limma¹³⁵. A MDS plot projects the distances from the first two. The x- and y-axis is representative of Euclidean distances between samples. Distances between each pair of samples on the plot is the root-mean-square deviation of the log2-fold-changes for the genes most distinguishing each pair of samples¹³⁵. Distances on the MDS plot stand for the leading log2-fold-change between the samples for the genes¹³⁵. In other words, the smaller the distance between samples in the MDS projection, the more similar are their corresponding transcriptomes.

The MDS result for transcriptomes from different treatments and growth phases were plotted into a two-dimension plot shown in Figure 24. In general, all samples from the same condition (same treatment and same growth phase) cluster together, indicating that those clusters share the most similarity and groups of triplicates show consistency and low variance. As expected, different growth phases separated the clusters in MDS plot. There are three main clusters distributed separately in MDS: the first cluster contains the three groups that are harvested at the stationary phase ($\text{OD}_{600} = 1.0$) with or without LP-600 treatments, the second includes two groups that are treated without or with low-dose LP-600 and harvested during mid-exponential phase, and the third cluster is from samples of high-dose LP-600 treatment harvested during mid-exponential phase. Especially, the third cluster clearly separates from the other two clusters, indicating that high-dose treatment of LP-600 triggers a unique condition during mid-exponential phase. In addition, among stationary groups, the clusters from both vehicle control and low-dose treatment

are separated from high-dose group. Likewise, during mid-exponential phase, samples from low-dose treatment of LP-600 are close to the untreated group. Therefore, the MDS result suggests that the high-dose LP-600 treatment significantly influences gene expression in comparison to low-dose LP-600 or untreated control.

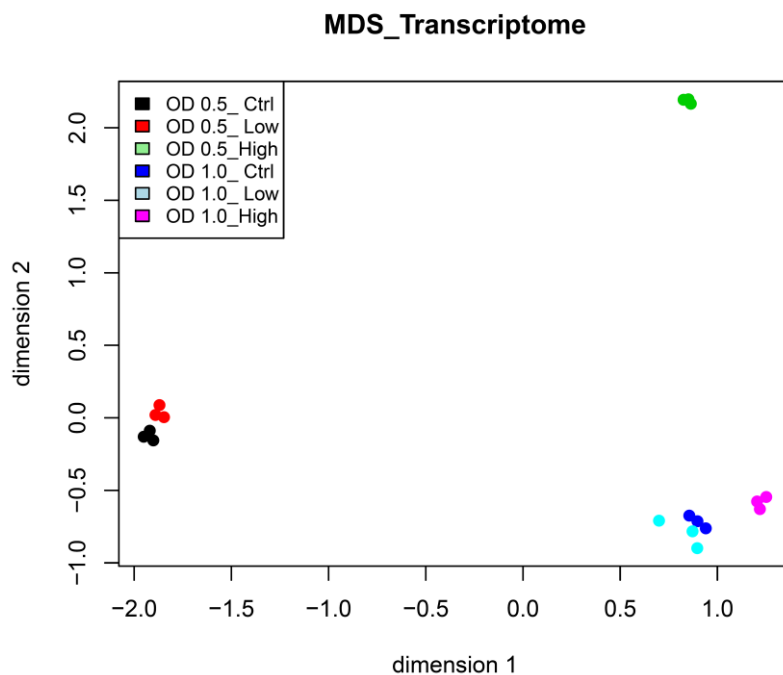


Figure 24. Multidimensional scaling (MDS) analysis of *E. coli* transcriptomes from the treatments of vehicle control (DMSO), low-dose (0.0625 $\mu\text{g}/\text{mL}$), high-dose (128 $\mu\text{g}/\text{mL}$) of LP-600 during mid-exponential phase ($\text{OD}_{600} = 0.5$) or stationary phase ($\text{OD}_{600} = 1.0$). Log-CPM (log counts per million) values among samples were applied in MDS analysis with the R package-limma.

To further investigate the influence of LP-600 treatment on individual gene expression, top 100 variant genes under different treatments and growth phases are represented as a heat map with hierarchical clustering, visualizing the similarities and dissimilarities between distinct transcriptomic samples (Figure 25). The pheatmap package in R was applied for calculating a matrix of euclidean distances from the log CPM (log counts per million) for the top 100 most variable genes¹⁶³. Hierarchical clustering of the samples showed that high-dose LP-600 treatments display the most different expressions compared to the counterpart harvested at the same OD_{600} value, while samples treated with low-dose LP-600 and vehicle control (DMSO) for individual

group displaying more similar gene expression pattern. Besides, among six groups in triplicates, it could be classified into three groups through column-wised hierarchical clustering: control and low-dose OD₆₀₀ = 0.5, high-dose OD₆₀₀ = 0.5, and OD₆₀₀ = 1.0. Notably, group of high-dose OD₆₀₀ = 0.5 shows more similarity to OD₆₀₀ = 1.0 groups under column-wised hierarchical cluster, which might correlate to the close time-points between high-dose OD₆₀₀ = 0.5 and OD₆₀₀ = 1.0 groups. Overall, the hierarchical cluster among samples suggests that high-dose LP-600 treatment has a great effect on gene expression in comparison with low-dose LP-600 treatment or vehicle control.

In contrast to column-wised hierarchical cluster that shows the variance among samples, row-wised hierarchical cluster allows the identification the clusters of genes showing similar or distinct expression patterns under certain treatments. Among top 100 variant expressed genes, there are three most distinct gene clusters associated with LP-600-induced Eagle effect (Figure 25). To understand the relationship among those genes, putative or experiment-based protein-protein interaction networks were analyzed in STRING database¹³⁷. Besides, to understand the functions of groups of genes, functional enrichment analysis via STRING¹³⁷ and DAVIDWebService (version 4.0.3) was conducted¹⁴¹. For functional enrichment analysis, genes are selectively classified based on GO (gene ontology), KEGG (Kyoto Encyclopedia of Genes and Genomes), annotated keywords by UniProt, and local network cluster of STRING¹³⁷. The first cluster is a group of genes that show especially down-regulated upon high-dose LP-600 treatment during both mid-exponential and stationary phases (Figure 25). The first cluster is composed of 28 genes (*ansB*, *hyaA*, *hyuA*, *nrfA*, *nrfB*, *nrfC*, *nrfD*, *ssnA*, *tdcA*, *tdcB*, *tdcC*, *tdcD*, *tdcE*, *tdcF*, *tdcG*, *tnaB*, *uacT*, *xanQ*, *xdhD*, *yehC*, *ygeW*, *ygeX*, *ygeY*, *ygfK*, *ygfM*, *ynfF*, *ynfG*, *yqfG*) which are enriched in functions about selenocompound metabolism (*hyuA*, *ssnA*, *xdhD*, *ygeW*, *ygeX*, *ygeY*, *ygfK*, *ygfM*) and amidohydrolase-related, L-threonine catabolic process to propionate (*tdcA*, *tdcB*, *tdcD*, *tdcE*, *tdcF*, *tdcG*), and Metal-binding (*hyaA*, *hyuA*, *nrfA*, *nrfB*, *nrfC*, *ssnA*, *xdhD*, *ygeY*, *ygfK*, *ynfF*, *ynfG*). The second cluster, including only six genes (*dmsA*, *dmsB*, *hyaB*, *ompW*, *yehD*, *yhbU*), is down-regulation only during mid-exponential phase upon high-dose LP-600 treatment. Among the second cluster, anaerobic respiration (*hyaB*, *dsmA*, and *dsmB*) was found enriched. The third cluster of genes is especially up-regulated under high-dose LP-600 treatment during mid-exponential phase, but shows intermediate expression during stationary phase. The third cluster contains 13 genes (*croE*, *intE*, *malK*, *pinE*, *recN*, *stfP*, *tisB*, *wcaF*, *xisE*, *ymfJ*, *ymfL*, *ymfM*, *ymfR*). Among the third cluster, nine out of 13 genes involved in bacteriophage T4, Gp38, and tail fibre

assembly (*croE*, *intE*, *pinE*, *sffP*, *xisE*, *yjfJ*, *yjfL*, *yjfM*, *yjfR*). Especially, these nine genes belong to e14 prophage that is one of defective prophage elements integrated into the *E. coli* chromosome¹³⁹. Even most of genes in e14 element are annotated as putative proteins with unknown functions, certain genes such as over-expression of *yjfM* are associated with SOS-induced cell division inhibition^{164,165}. The up-regulated genes in e14 prophage elements might hint that the SOS response contributes to the Eagle effect upon high-dose treatment of LP-600. Therefore, these clusters and enrichment analysis suggested that high-dose LP-600 induces not only a paradoxical growth but also unique transcript expressions.

Top 100 most variable genes

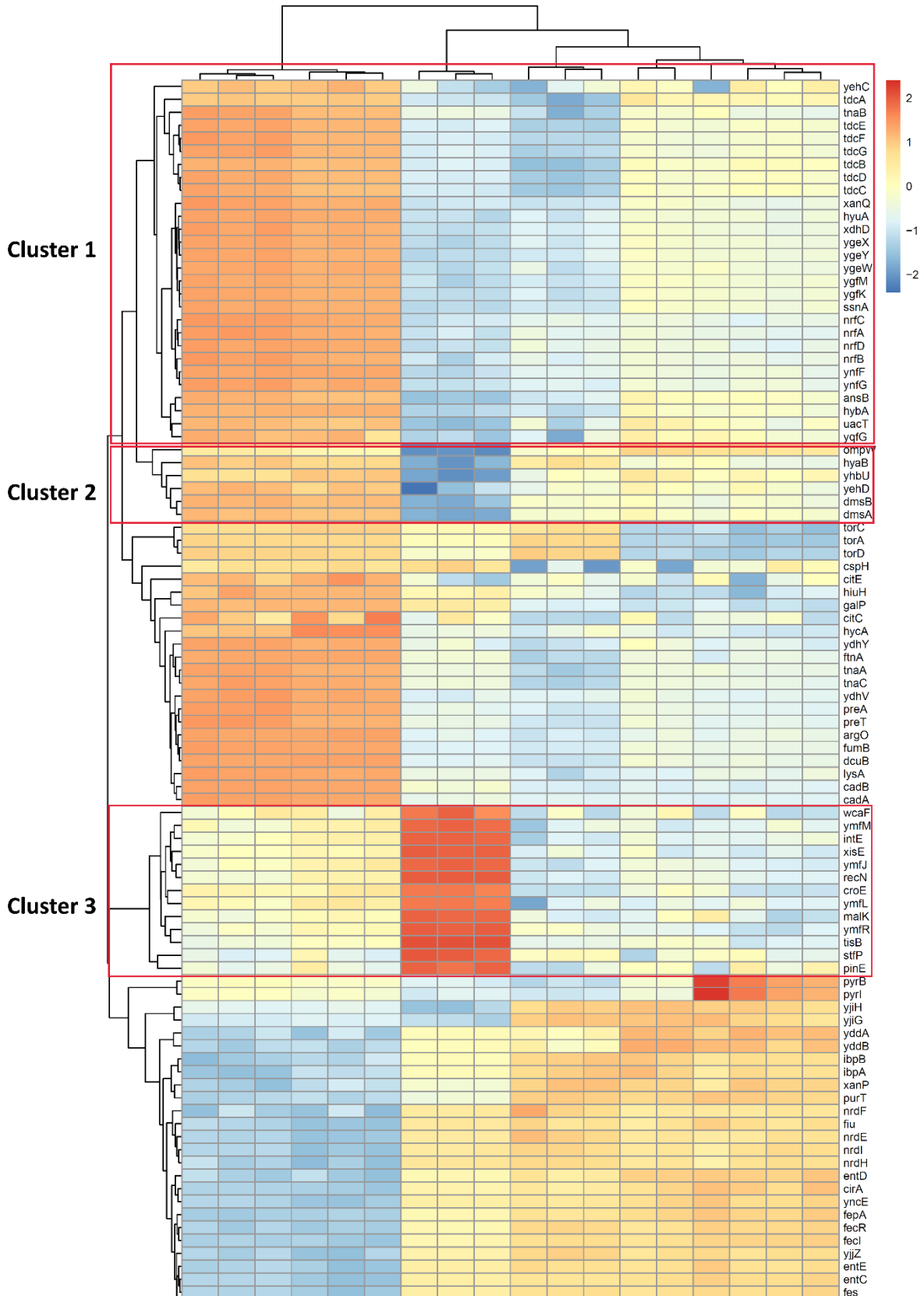


Figure 25. Heat map of top 100 variant genes from samples treated with DMSO, low-dose (0.0625 $\mu\text{g/mL}$), high-dose (128 $\mu\text{g/mL}$) of LP-600 during mid-exponential phase ($\text{OD}_{600} = 0.5$) or stationary phase ($\text{OD}_{600} = 1.0$). Three clusters of genes are highlighted and labeled. Log-CPM (counts per million) values were calculated and scaled. Samples with relatively high expression of a given gene are colored in red and samples with relatively low expression are expressed in blue. Intermediate expression are colored in lighter colors. Samples and genes are ordered according to hierarchical clustering and dendrograms are displayed for sample clustering. The heat map with dendrograms was generated by the R package limma.

4.9.2 Transcriptome profile and differentially expressed genes following treatment with LP-600 at sub-MIC

To understand the influence of LP-600 treatment in a sub-MIC dose on gene expression, low-dose LP-600-treated (0.0625 $\mu\text{g/mL}$) transcriptomes were compared to the transcriptomes of vehicle control. Of all 4079 profiled transcripts, only 72 and 35 transcripts are differentially expressed upon low-dose LP-600 treatments during mid-exponential ($\text{OD}_{600} = 0.5$) and stationary phases ($\text{OD}_{600} = 1.0$), respectively. There are only less than 2% genes shown significant expression upon low-dose LP-600 treatment compared to vehicle control at both growth phases. Between two conditions of growing phases under low-dose treatment of LP-600, there are only three genes (*bdm*, *yjiY*, *ymfJ*) are differentially expressed in both conditions with a cut-off for of adjusted p-value (false discovery rate, FDR) < 0.05 and absolute value of $\log_2\text{FC} > 1$ (Figure 26, for more details, see Appendix III).

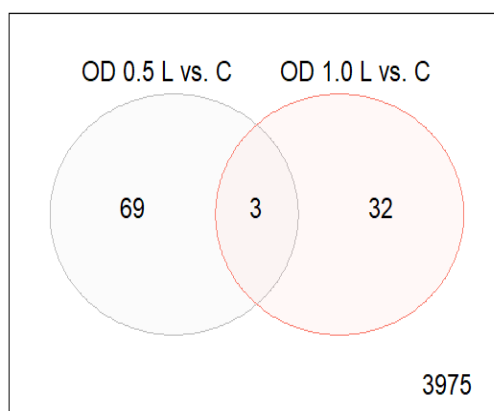


Figure 26. Venn diagram of differentially expressed genes (DEGs) comparing low-dose (0.0625 $\mu\text{g/mL}$) treatment of LP-600 with vehicle control. (A) The Venn diagram represents the number of differentially expressed genes in: low-dose treatment of LP-600 versus vehicle control (DMSO) at $\text{OD}_{600} = 0.5$ (OD 0.5

exponential ($OD_{600} = 0.5$) and stationary phases ($OD_{600} = 1.0$), respectively (for more details, see Appendix V). The comparison of high-dose over low-dose of LP-600 treatment at $OD_{600} = 0.5$ (LH1) shows 1182 transcripts are differentially expressed with a cut-off for of FDR (false discovery rate) < 0.05 and absolute value of $\log_2FC > 1$. By contrast, only 592 differentially expressed transcripts were found in the comparison of high-dose with low-dose of LP-600 treatment at $OD_{600} = 1.0$ (LH2). By comparing the differentially expressed genes in LH1 versus LH2, 303 genes show significant expression in both transcriptomes.

To understand the functions of these 303 differentially expressed genes shared between LH1 and LH2, functional enrichment analysis was conducted. Functional enrichment analysis commonly generates several redundant enrichment terms because a single gene can be annotated with more than one functional term. Rather than using enrichment analysis and presenting as a STRING network that visualizes the interaction networks between individual genes, the add-in Enrichment Map in Cytoscape combining with RDAVIDWebService (version 4.0.3)¹⁴¹ was applied for visualizing the networks between enriched terms. The more overlapping genes share among two terms, the more lines links between two terms. In contrast, a group of genes is only annotated in an enriched term, so the term will have no connection with any term. In functional enrichment analysis, 22 categories were found enriched among these 303 genes (for more details, see Appendix V) and the category composed of the most abundant gene counts (71 genes that account for around 23% of these genes) is metal-binding (for more details, see Appendix V). The network of enrichment terms with differentially expressed genes among both LH1 and LH2 is shown in Figure 29. In the enrichment network, categories can be classified into clusters based on how many overlapping genes are shared between terms. Each line between two terms means there are overlapping genes between two terms. The more lines are, the more overlapping genes are. The biggest cluster shown in Figure 29 is associated with iron and metal-associated functions. In addition, there are categories involved in some metabolic processes such as purine metabolism and amino acid metabolism such as L-threonine catabolic process to propionate and arginine catabolic process to succinate (Figure 29 and Appendix VI). Hence, these results might suggest potential functions and metabolic change involved in LP-600-induced Eagle effect.

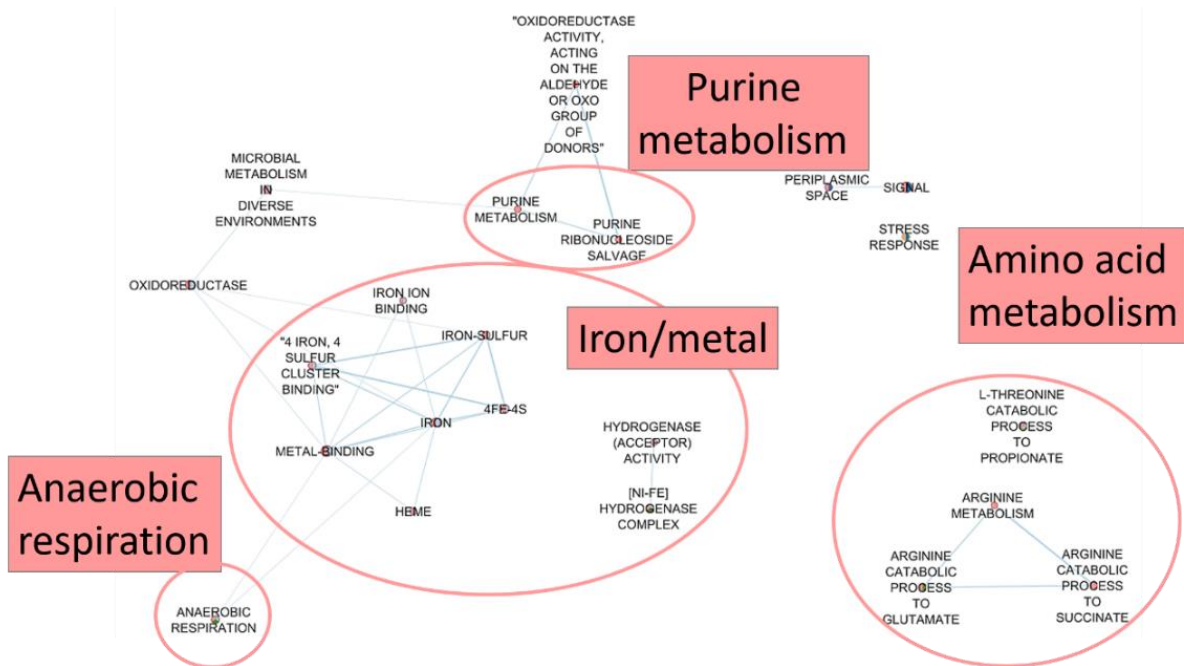


Figure 29. Networks of functional enrichment with significantly up-regulated genes in both LH1 and LH2. Each node represents an enrichment category and is labeled with the annotation. The line between two nodes represents genes overlapping in two nodes. LH1: the comparison of high-dose over low-dose of LP-600 treatment at $OD_{600} = 0.5$. LH2: the comparison of high-dose over low-dose of LP-600 treatment at $OD_{600} = 1.0$.

To explore the details of individual gene expression in the LH1 setup, the transcriptome result with adjusted p-values (FDRs) and fold changes are shown as volcano plot in Figure 30. Among 1182 differentially expressed genes in LH1, 771 transcripts are up-regulated while 421 are down-regulated.

belonging to Fur (Ferric uptake regulation) regulon ¹³⁹ (Figure 31 and see more details in Appendix VI). Besides, genes involved in SOS response such as *tisB* and *recN* (a full list of genes are shown in Appendix VI) are also in the third cluster ‘f the most variable genes in Figure 25. Considering previous studies have shown some of e14 prophage genes contribute to SOS induced cell division inhibition ^{164,165}, the up-regulation of SOS response gene as well as e14 prophages upon high-dose LP-600 treatment might hint that the e14 prophages-mediated SOS response contributes to the Eagle effect.

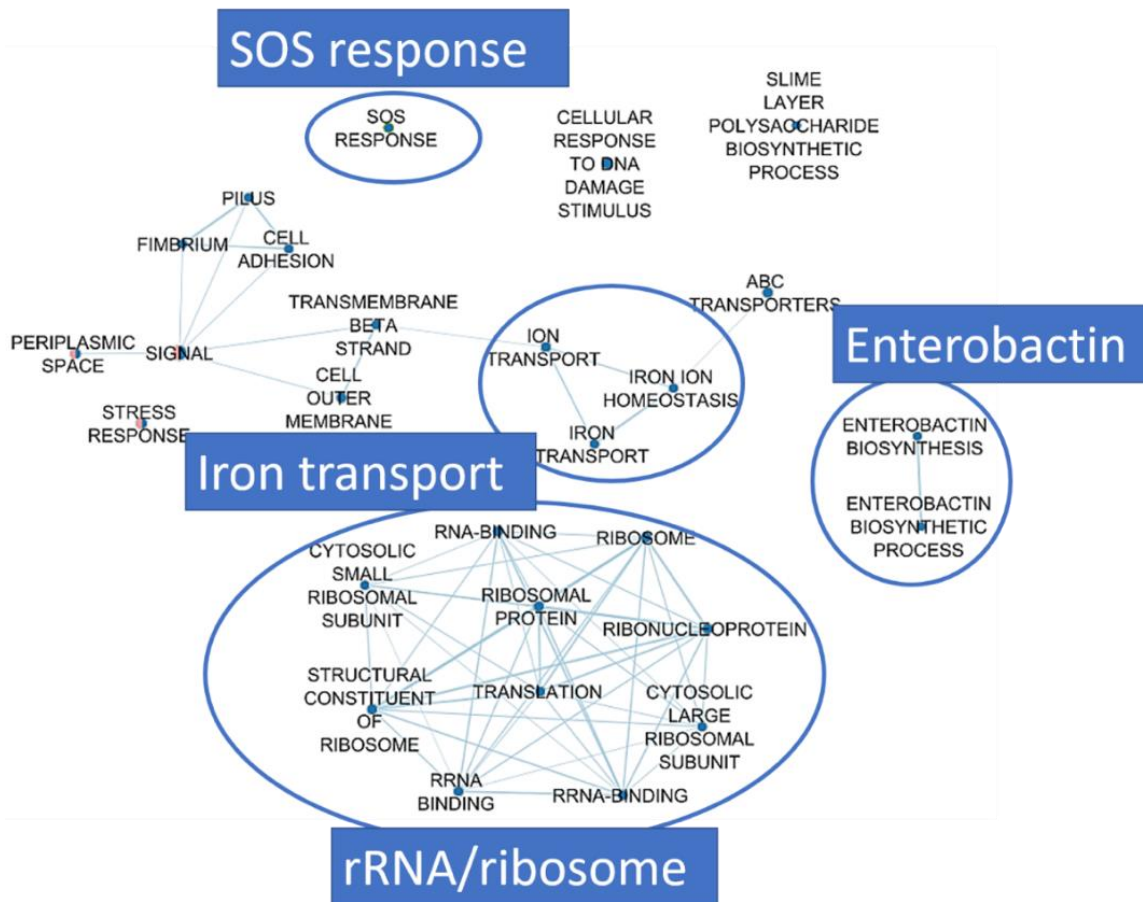


Figure 31. Networks of selected functional enrichment with significantly up-regulated genes in LH1. Each node represents an enrichment category and is labeled with the annotation. The line between two nodes represents genes overlapping in two nodes. LH1: the comparison of high-dose over low-dose of LP-600 treatment at $OD_{600} = 0.5$.

By contrast, there are 53 enrichment categories shared among down-regulated genes in LH1 (Appendix VI). Among top ten most significantly enriched categories in down-regulated genes, they can be classified into clusters such as ion and metal-associated (iron-sulfur, iron and metal-binding, etc.), electron transport and anaerobic respiration (Figure 30). In addition to the top ten categories, several terms are involved in other pathways: thiamine-associated functions (metabolism, thiamine diphosphate biosynthetic process, etc.), nitrogen metabolism, carbon metabolism (carbon metabolism and citrate cycle) (Figure 32 and Appendix VI) were found down-regulated in LH1.

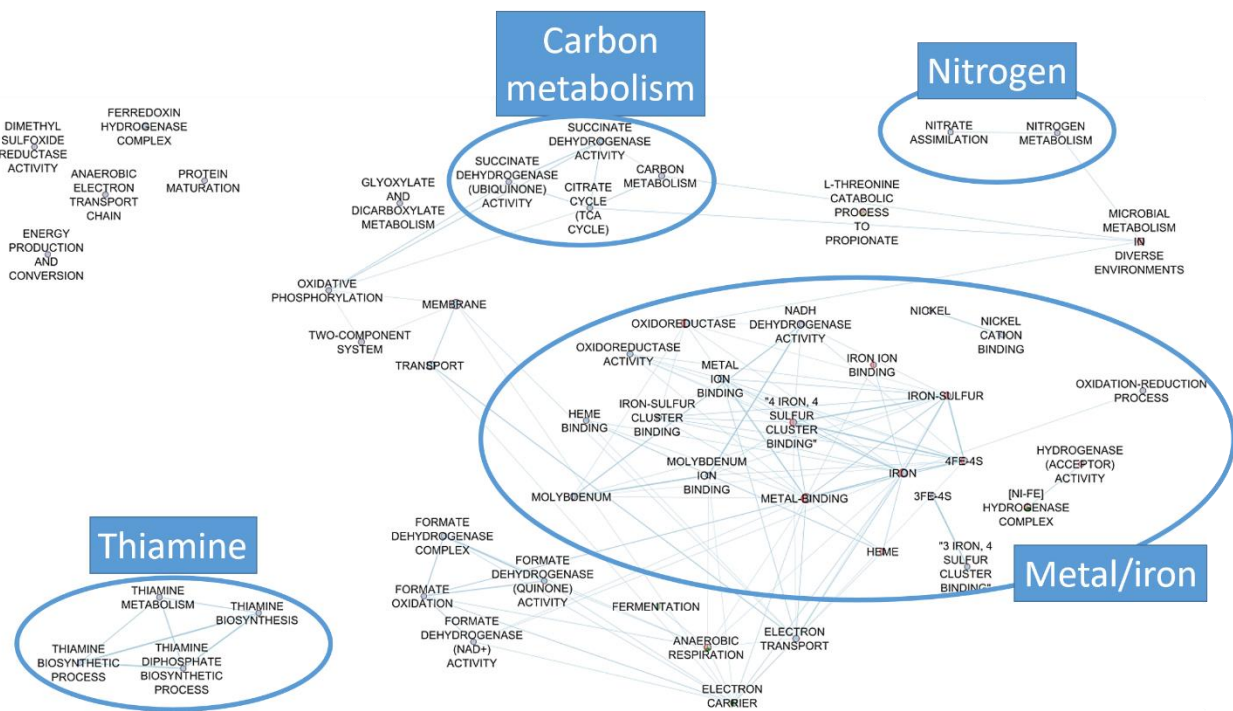


Figure 32. Functional enrichment of networks with significantly down-regulated genes in LH1. Each node represents an enrichment category and is labeled with the annotation. The line between two nodes represents genes overlapping in two nodes. LH1: the comparison of high-dose over low-dose of LP-600 treatment at $OD_{600} = 0.5$.

On the other hand, 283 out of 592 differentially expressed transcripts are up-regulated while 313 genes are down-regulated. The transcriptome result with p-values and fold changes are shown as volcano plot in Figure 33. Besides, the functional enrichment analysis was performed for the differentially expressed genes in LH2. There are 17 enriched terms are found in differentially expressed genes in LH2 and are shown in Figure 34 (see more details on Appendix VI). Among

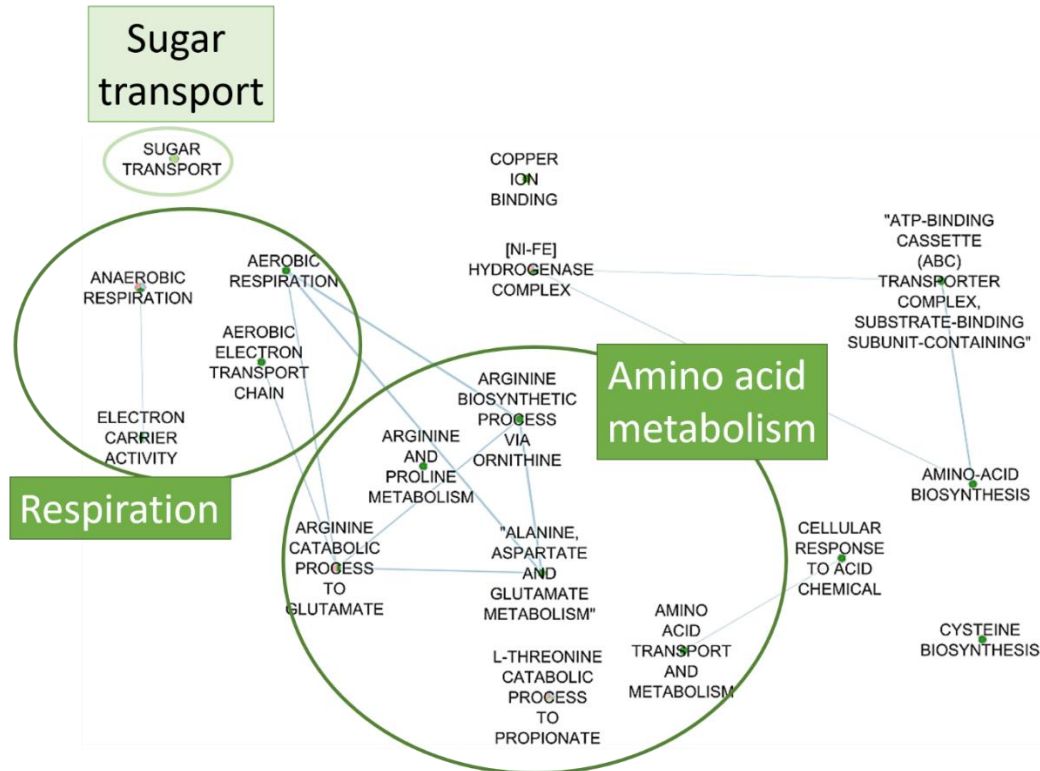


Figure 34. Functional enrichment of networks with differentially expressed genes in LH2. Each node represents an enrichment category and is labeled with the annotation. The line between two nodes represents genes overlapping in two nodes. LH2: the comparison of high-dose over low-dose of LP-600 treatment at $OD_{600} = 1.0$. Nodes and clusters are labeled in dark green for terms with up-regulation genes, whereas light green represents a term with down-regulated genes.

4.10 Metabolomic analysis

4.10.1 Metabolomic analysis of *E. coli* following treatments with LP-600

To understand the response of *E. coli* to LP-600 treatment, a complementary -omics method was applied and the metabolome was investigated. To be able to compare and relate results from both omics experiments, samples for metabolomic analysis were harvested from the same batch as for transcriptome analysis: six groups with three types of treatment (vehicle control, low-dose, high-dose of LP-600) which were harvested at mid-exponential ($OD_{600} = 0.5$) and stationary phase ($OD_{600} = 1.0$). For each sample, bacterial pellets were harvested, washed and lysed to perform the extraction of endo-metabolites. Untargeted metabolomics analysis was conducted by combining different analytical approaches using UPLC-ESI-QToF in both positive and negative modes and

with separation methods including C18 or HILIC column. The raw data obtained were processed by MetaboScape for peak picking and feature detection. As a result, lists of features were obtained by MetaboScape software with a cutoff of retention time ($0.3 \text{ min} \leq \text{RT} \leq 28 \text{ min}$). In six groups of samples with individual triplicates, 2846 and 606 features were detected with C18 column in positive and negative mode, respectively. 1547 and 501 features were obtained via HILIC column in positive and negative mode, respectively.

To obtain an overview of endo-metabolites among samples, the resulting feature tables submitted to a MDS analysis using R package-limma as mentioned above to characterize the most dissimilar and similar metabolites among groups under LP-600 treatments at different concentrations. The MDS results from different treatments and growth phases are shown with a two-dimensional plot representing Euclidean distances between samples in Figure 35. In positive mode of C18 column analysis, all samples harvested from the same OD_{600} values distribute closely, becoming a big cluster except for the samples of high-dose treatment at $\text{OD}_{600} = 0.5$ far separating from the others (Figure 35). This behavior suggests that all triplicates have a consistent pattern under the same treatments and conditions. Likewise, with C18 column, metabolomes recorded in a negative mode display a similar distribution pattern in MDS analysis as shown in Figure 35. In the negative mode with C18, the features detected among samples form two clusters that are separated in the MDS plot. The samples harvested at the same OD_{600} value are closely together except for one of the low-dose treated samples of $\text{OD}_{600} = 0.5$ that was separated along dimension 2 from the samples collected at the same OD. These results indicate that the cultures from the Eagle effect at $\text{OD}_{600} = 0.5$ display the most distinguished metabolome from the other two treatments at the same OD_{600} values, which is in agreement with the MDS result of transcriptome.

On the other hand, in positive mode of HILIC column analysis, groups under three treatments at the $\text{OD}_{600} = 1.0$ forms a cluster closely (Figure 35). By contrast, the groups under three treatments at the $\text{OD}_{600} = 0.5$ relatively separated from each other and distributed among dimension 2. And the high-dose group is distant from the low-dose and untreated groups. In the MDS of HILIC analysis in negative mode, samples of low-dose treatment and untreated control at $\text{OD}_{600} = 0.5$ remain close, whereas the high-dose group harvested at the same OD value is separated along dimension 2 (Figure 35). The samples from the $\text{OD}_{600} = 1.0$ separate from groups of OD_{600} of 0.5 along the dimension 1. Among groups of OD_{600} of 1.0, unexpectedly, low-dose treated group is

distant from the untreated and high-dose treatment that are clustered together. As a result, MDS results demonstrate that all triplicates among groups behave consistently with little variance. Additionally, the results indicate that high-dose LP-600 greatly affects both metabolome and transcriptome, especially, during the mid-exponential phase at $OD_{600} = 0.5$.

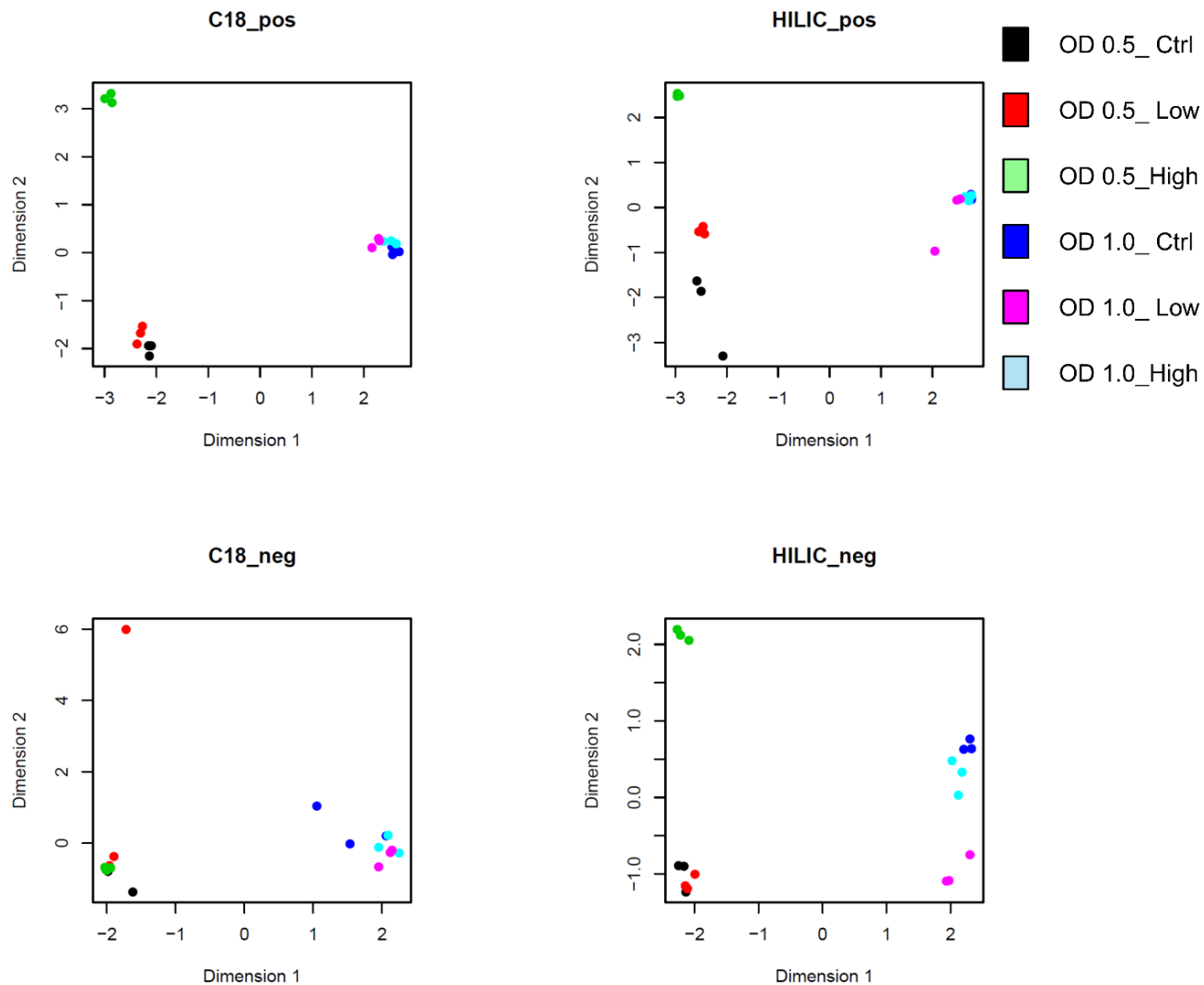


Figure 35. MDS analysis of *E. coli* metabolomes from indicated culture conditions obtained by UPLC-ESI-QToF experiments using C18 or HILIC columns in positive or negative mode.

4.10.2 Metabolomic profile following treatment with LP-600 at sub-MIC

For metabolite annotation, metabolite identification was done by matching the retention time, exact mass as well as the MS/MS spectra with an in-house metabolite library, commercial libraries (including LipidBlast, Bruker MetaboBase, and Bruker HMDB Metabolite Library) or by comparing the MS/MS spectra (combined with exact mass and m/z values) with online public databases including ECMDB¹¹⁴, HMDB¹¹³, GNPS¹¹⁵ or theoretical MS/MS fragmentation patterns from MetFrag¹³⁸. With C18 approach, there are 161 and 130 metabolites successfully annotated among 2846 and 606 features in positive and negative mode, respectively. In HILIC analysis, 38 and 21 metabolites among 1547 and 501 features in positive and negative mode were identified, respectively. In total, there are 257 unique metabolites annotated from the four analytic approaches (C18 and HILIC columns in both positive and negative modes) as displayed in a Venn diagram (Figure 36).

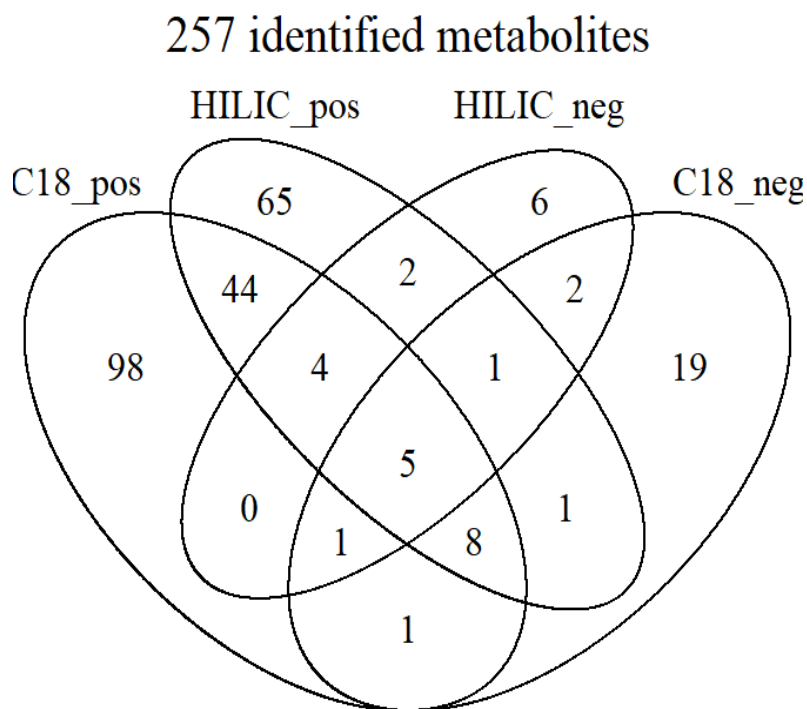


Figure 36. Venn diagram represents the amounts of identified metabolites by different separation methods (C18 and HILIC columns) and ionization modes (positive and negative electrospray ionization).

To identify the significantly regulated metabolites under the treatment of LP-600 at sub-MIC (0.0625 $\mu\text{g/mL}$), the abundance of individual features from the treatment group with the respective untreated control was compared. The fold changes and adjusted p-value of each feature were calculated via R with the package of stats (version 3.6.3) for T-test correction through Benjamini-Hochberg method. Significantly regulated features were listed the thresholds of adjusted p-value (false discovery rate, FDR) < 0.05 and absolute fold change > 1.5 .

The comparison of samples treated with a low-dose of LP-600 with the untreated control harvested at $\text{OD}_{600} = 0.5$ (CL1) resulted in a total of 777 significantly regulated features among four analytic methods. Out of 777, 109 significantly regulated features were annotated, resulting in an annotation of 98 significantly regulated metabolites. The result table is shown in Appendix VII. 98 metabolites were further categorized into defined classes based on chemical taxonomy from HMDB or ECMDB libraries. The significantly regulated metabolites of CL1 with respective fold changes and chemical classifications are shown in a bar plot (Figure 37). In CL1, the largest chemical class among significantly regulated metabolites comprised amino acid, peptides and analogs. Five out of the top ten up-regulated metabolites corresponded to lipid class, corresponding to five lipid compounds: LPE(15:0), LPE(16:0), LPE(18:1), PE(16:0-17:1), LPE(17:1) (Figure 37); while the most down-regulated among the annotated features are peptides, NAD (Nicotinamide adenine dinucleotide) and nicotinamide.

On the other hand, in CL2 (comparing low-dose treatment of LP-600 with vehicle control at $\text{OD}_{600} = 1.0$), 66 significantly regulated features that were annotated to 58 metabolites and further categorized into chemical classes. The metabolites were further categorized into chemical taxonomical classes. Consequently, the most abundant metabolites belong to amino acid, peptides and analogs class, followed by the second class-nucleosides, nucleotides and analogs (Figure 38). Similar to CL1, top ten up-regulated metabolites in CL2 include lipid-associated compounds: LPE(18:1), LPG(18:1), LPE(16:1), LPE(17:1). By contrast, the classes among the top ten most down-regulated metabolites are more diverse: peptides, carboxylic acids and derivatives (N-acetylcadaverine), organonitrogen compounds (cadaverine), purines and purine derivatives.

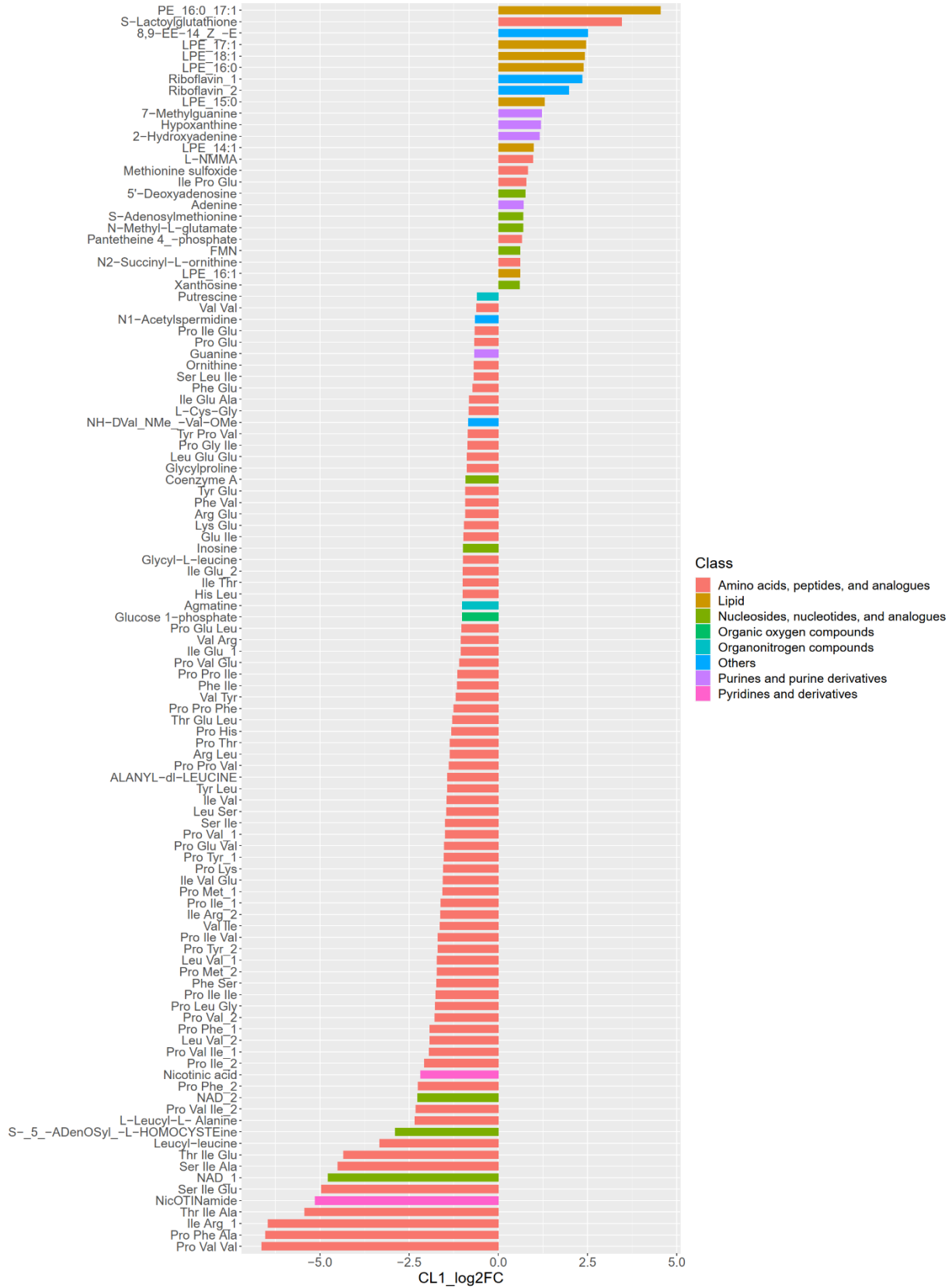


Figure 37. Regulation of identified metabolites in CL1. The \log_2 -fold change was plotted on the x-axis for all identified metabolites in CL1. CL1: significantly regulated metabolites by comparing low-dose (0.0625 $\mu\text{g}/\text{mL}$) treatment of LP-600 with untreated control (DMSO) at $\text{OD}_{600} = 0.5$. The classes of metabolites are highlighted with indicated colors. LPE: lyso-phosphatidylethanolamines. LPG: lyso-phosphatidylglycerols.

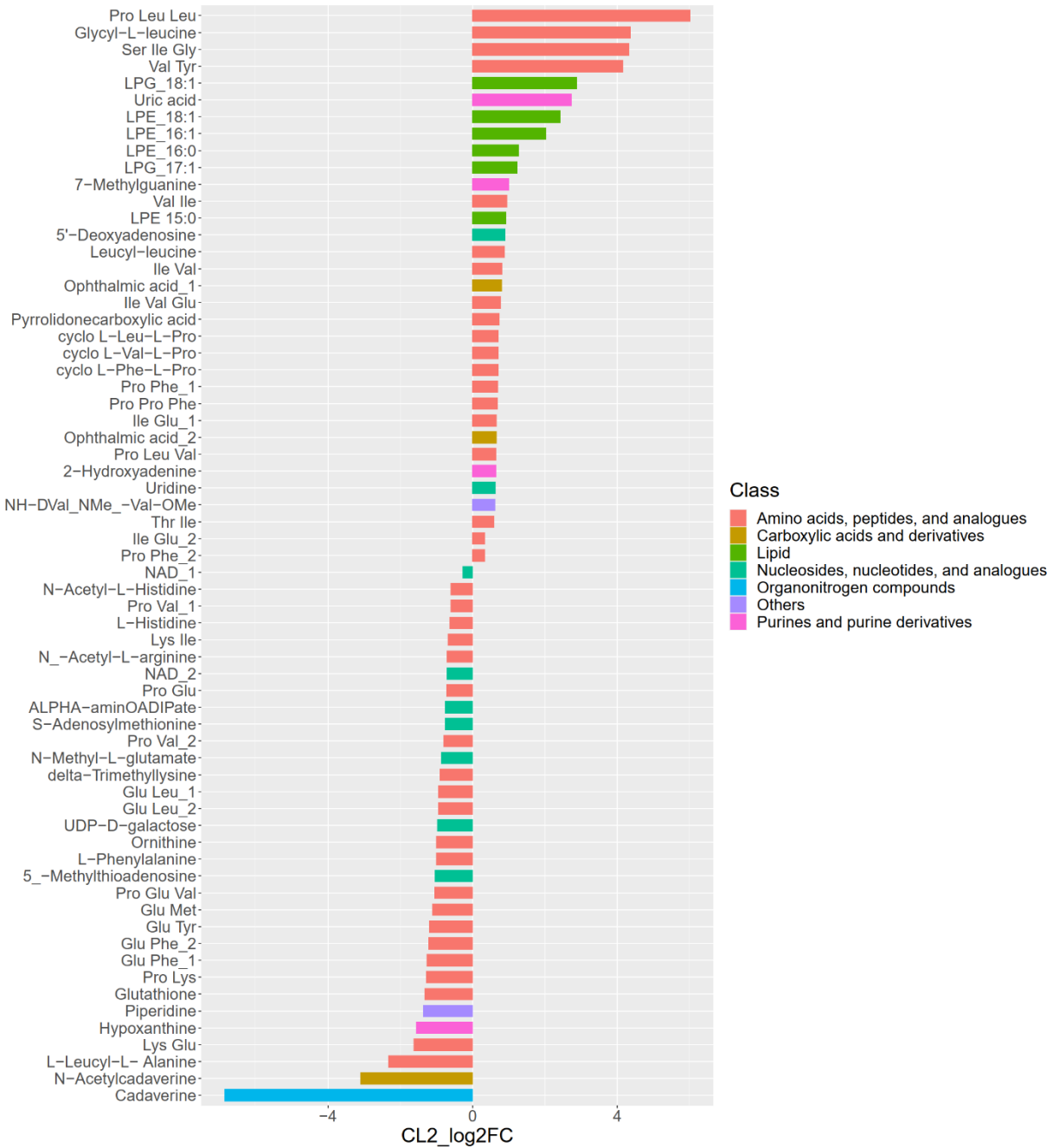


Figure 38. Regulation of identified metabolites in CL2. The \log_2 -fold change was plotted on the x-axis for all identified metabolites in CL2. CL2: significantly regulated metabolites by comparing low-dose (0.0625 $\mu\text{g}/\text{mL}$) treatment of LP-600 with untreated control (DMSO) at $\text{OD}_{600} = 0.5$. The classes of metabolites are highlighted with indicated colors. LPE: lyso-phosphatidylethanolamines. LPG: lyso-phosphatidylglycerols.

$\mu\text{g/mL}$) treatment of LP-600 with untreated control (DMSO) at $\text{OD}_{600} = 1.0$. The classes of metabolites are highlighted with indicated colors. LPE: lyso-phosphatidylethanolamines. LPG: Lyso-phosphatidylglycerols.

Moreover, CL1 and CL2 share 28 significantly regulated metabolites in common (see more details in Appendix VII). In order to correlate the metabolite list with biological metabolic pathways, over-representation analysis (ORA) was performed with the help of enrichment analysis on the website- MetaboAnalyst (<https://www.metaboanalyst.ca/faces/home.xhtml>) with a KEGG library of *E. coli* K12¹⁴⁰, detecting enrichment of metabolites within biological categories or pathways. However, neither significantly regulated metabolites in CL1 nor CL2 show significant enrichment in any KEGG pathway. Similarly, the 28 significantly regulated metabolites found in both CL1 and CL2 show no enrichment under ORA analysis. Notably, even there no matched metabolites in KEGG pathways, there are ten lipids exhibiting over-production in either CL1, CL2 or both conditions (Appendix VII). LPG and LPE are lysophospholipids (LPLs) that are metabolic intermediates during membrane degradation under stress¹⁶⁶, so the up-regulation of LPLs might indicate the stress response for *E. coli* under LP-600 treatment.

4.10.3 Metabolomic profiles following treatment with LP-600 at high, Eagle effect-inducing concentrations

To identify the significantly regulated features and metabolites upon conditions that induce the Eagle effect, the abundance of individual features from the high-dose treatment was compared with the respective low-dose group, in order to rule out generally significantly regulated features upon LP-600 treatment. The significantly regulated features were obtained with the threshold of FDR (false discovery rate) < 0.05 and absolute fold change > 1.5 . In LH1 (comparing high-dose with low-dose treatment of LP-600 at $\text{OD}_{600} = 0.5$), 945 significantly regulated features were found among four analytic methods, resulting in the identification of 174 differentially regulated metabolites. On the other hand, in LH2 (comparing high-dose with low-dose treatment of LP-600 at $\text{OD}_{600} = 1.0$), out of a total 253 significantly regulated features, 71 metabolites were identified. The significantly regulated metabolites with respective fold changes and chemical classifications are shown in the bar plot (Figure 39 and Figure 40). The whole results of significantly regulated metabolites with p-values and fold changes of LH1 and LH2 are shown in Appendix VIII.

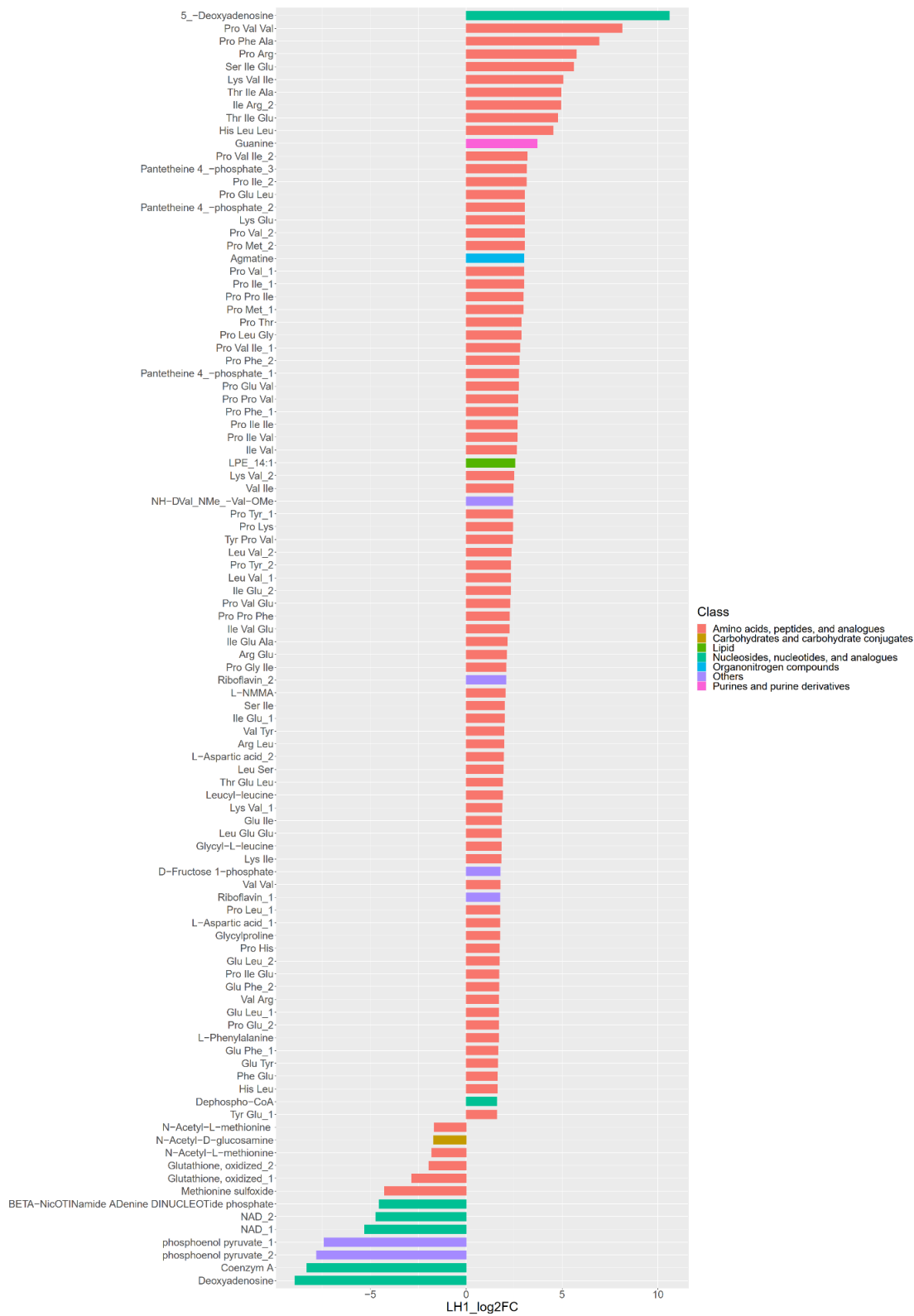


Figure 39. Top 100 significantly regulated metabolites in LH1. The log₂-fold change was plotted on the x-axis for all identified metabolites in LH1. LH1: significantly regulated metabolites by comparing low-dose

(0.0625 $\mu\text{g/mL}$) treatment of LP-600 with untreated control (DMSO) at $\text{OD}_{600} = 0.5$. The classes of metabolites are highlighted with indicated colors. LPE: lyso-phosphatidylethanolamines. LPG: lyso-phosphatidylglycerols.

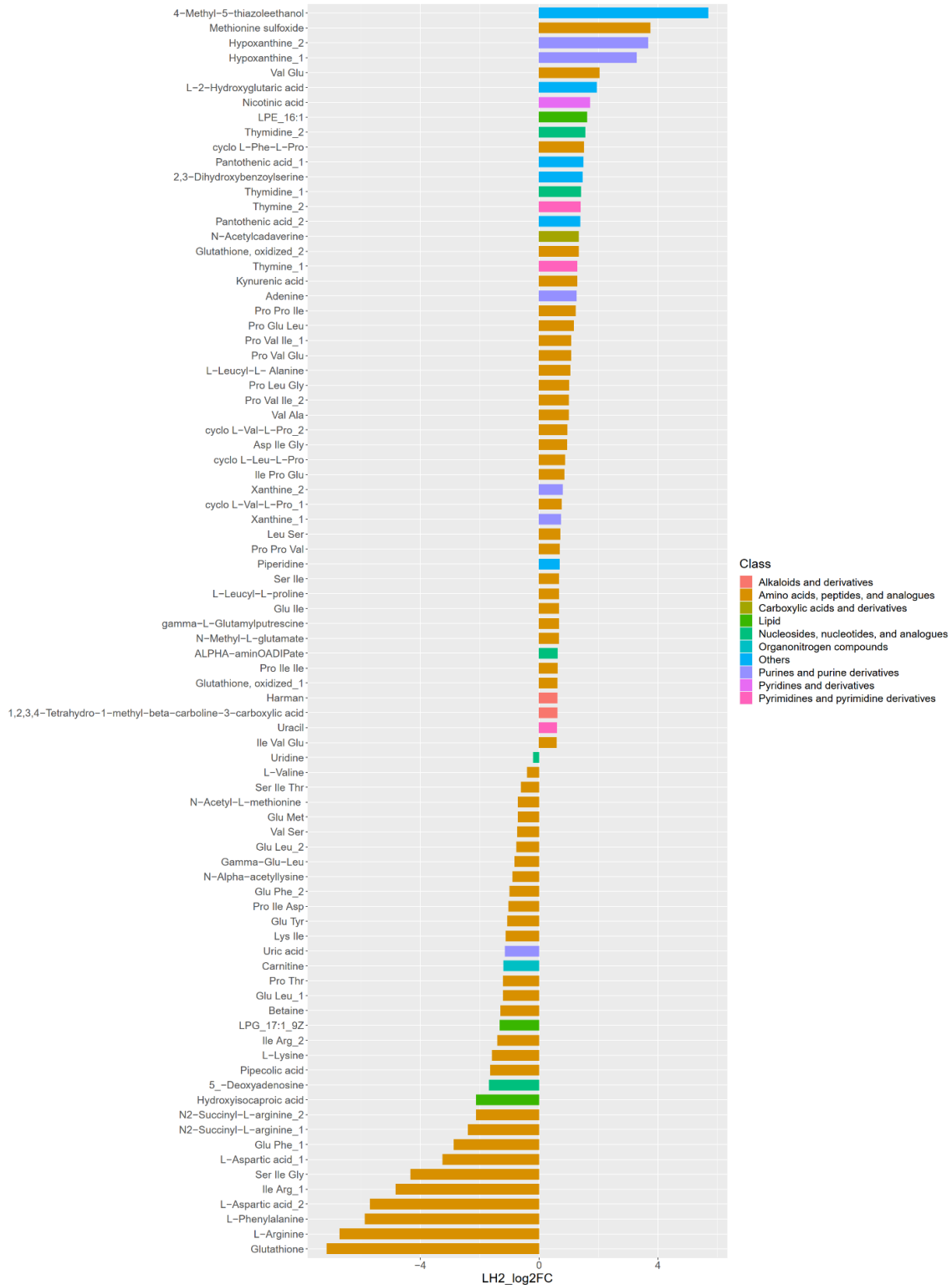


Figure 40. Regulation of identified metabolites in LH2. The log₂-fold change was plotted on the x-axis for all identified metabolites in LH2. LH2: significantly regulated metabolites by comparing low-dose (0.0625 µg/mL) treatment of LP-600 with untreated control (DMSO) at OD₆₀₀ = 1.0. The classes of metabolites are highlighted with indicated colors. LPE: lyso-phosphatidylethanolamines. LPG: lyso-phosphatidylglycerols.

Fifty two (52) differentially regulated metabolites are found commonly in both LH1 and LH2 conditions. Of those, the majority of compounds (41 metabolites) are classified into amino acids, peptides and analogs (78.8%). In ORA analysis, LH1 metabolome relates to six functions as following: glutathione metabolism, arginine and proline metabolism, arginine biosynthesis, nicotinate and nicotinamide metabolism, aminoacyl-tRNA biosynthesis, D-Glutamine and D-glutamate metabolism, whereas the list of metabolites that were exclusively regulated under LH2 conditions shows no significant enrichment in any terms with differentially regulated metabolites (Figure 41). Furthermore, in LH1, the most significantly enriched term is glutathione metabolism that is associated with ten significantly regulated metabolites (glutathione, oxidized glutathione, NADP, L-glutamic acid, pyroglutamic acid, ornithine, putrescine, spermidine, and cadaverine). Besides, L-arginine-associated enriched classification in Figure 41 supports the enrichment analysis results for transcriptome in Figure 29, indicating that the potential role of L-arginine in LP-600-induced Eagle effect. On the other hand, among common significantly regulated metabolites in both LH1 and LH2, only five out of 52 significantly regulated metabolites (L-phenylalanine; L-arginine; L-aspartic acid; L-valine; L-lysine) contribute to the enrichment in aminoacyl-tRNA biosynthesis (Figure 41, see more details in Appendix IX).

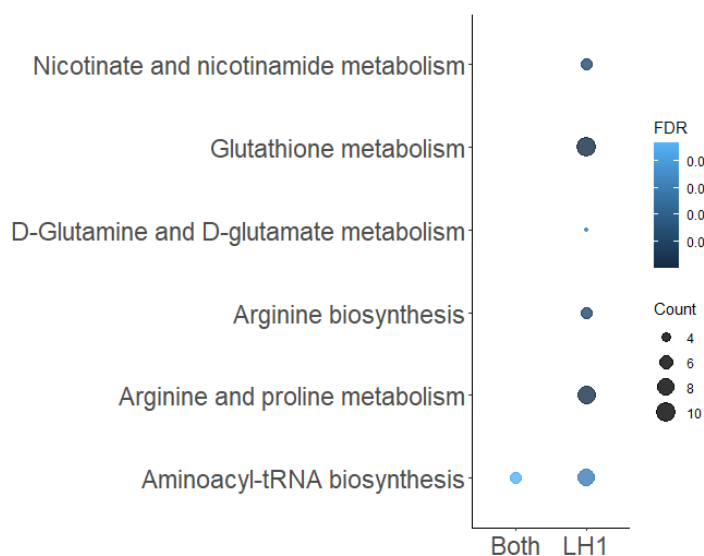


Figure 41. Scatter diagram of ORA (over-representation analysis) for significantly regulated metabolites in both LH1 and LH2. Y-axis label represents enriched pathways. Size and color of the circle represent counts of significantly regulated metabolites enriched in pathways and enrichment significance, respectively. LH1: significantly regulated metabolites comparing high-dose treatment of LP-600 with the low-dose at $OD_{600} = 0.5$; LH2: significantly regulated metabolites comparing high-dose treatment of LP-600 with the low-dose at $OD_{600} = 1.0$. FDR: false discovery rate.

4.11 Joint pathway mapping from transcriptome and metabolome results

Considering the samples for the transcriptome and metabolome analysis of LC-MS were prepared from the same batch, metabolome and transcriptome data were correlated with each other. To further understand the effect of high-dose LP-600 on both transcriptome and metabolome, differential pathway perturbation analysis was conducted with both transcriptome and metabolome results through EcoCyc¹³⁹ by mapping differentially expressed genes or metabolites upon the Eagle effect into metabolic pathways. In contrast to the enrichment analysis in STRING or DAVIDWebService, differential pathway perturbation mainly focuses on known metabolic pathways, so the putative function (e.g. e14 prophages) or protein functions such as SOS response are not included in the database of differential pathway perturbation analysis.

The top 100 differential pathways are shown in Appendix X. Several pathways such as enterobactin biosynthesis and threonine degradation were found as mentioned in transcriptomic results, but either key intermediates or end products are not annotated from the untargeted metabolomics. As a result, only a limited number of pathways such as polyamine biosynthesis (cadaverine, putrescine and aminopropylcadaverine biosynthesis) and L-arginine degradation were identified among significantly regulated genes and metabolites under the Eagle effect (by comparing high-dose with low-dose treatment of LP-600) at two growth phases (Figure 42).

Cadaverine, putrescine, and aminopropylcadaverine are all polyamines which are small aliphatic molecules with two or more amino groups that have a net positive charge at physiological pH¹⁶⁷. *E. coli* produces four types of polyamines, putrescine, spermidine, cadaverine, and aminopropylcadaverine^{168,169}. Polyamines modulate several cellular functions such as ribosomal activities and cell permeability and protection from stress^{167,170,171}. It has been shown that antioxidant properties of polyamines reduce oxidative stress, protecting DNA and proteins from

oxidative stress, and thus causes enhancement of antibiotic tolerance and survival ¹⁷². In *E. coli*, the diamine putrescine can be produced by two resources: decarboxylation of ornithine, decarboxylation of arginine followed by hydrolysis of agmatine. For spermidine generation, putrescine and an aminopropyl group from S-adenosyl-L-methionine(SAM) yield triamine spermidine ¹⁶⁸. Cadaverine is produced via lysine decarboxylation ¹⁶⁸. Under high-dose LP-600 treatment, key metabolites including agmatine, SAM (S-adenosyl-L-methionine) shows significantly over-produced at OD₆₀₀ = 0.5 but no significant expressed later at OD₆₀₀ = 1.0. Besides, two types of polyamines, spermidine and cadaverine, over-produce upon high-dose treatment of LP-600, whereas putrescine is significantly down-regulated (Figure 42). On the other hand, key cognate genes *speB* (encoding agmatinase) and *idcC* (encoding lysine decarboxylase 2) are up-regulated during the Eagle effect at the OD₆₀₀ = 1.0. These results indicate that polyamine biosynthesis might contribute to the LP-600-induced Eagle effect.

On the other hand, several differentially expressed genes and metabolites in L-arginine degradation via arginine succinyltransferase (AST) were found (Figure 42). L-arginine is involved in protein synthesis, but also a precursor for putrescine biosynthesis in *E. coli* ¹⁶⁸. In *E. coli*, L-arginine degradation includes the following superpathways: L-arginine degradation II via arginine succinyltransferase (AST) pathway, L-arginine degradation III (arginine decarboxylase/agmatinase pathway), superpathway of L-arginine and L-ornithine degradation, and superpathway of L-arginine, putrescine, and 4-aminobutanoate degradation ^{173,174}. Among those superpathways, L-arginine degradation via AST pathway contributes to the major arginine-degrading pathway in *E. coli* ^{173,174}, producing glutamate and succinate that further enter into TCA cycle, satisfying the nitrogen requirement. Under both growth phases, high-dose LP-600 induces genes involved in AST pathway (*astA*, *astB*, *astC*, *astD*, *astE*) up-regulated with at least fold change of four, comparing with the low-dose treatment (Figure 42). In addition, the upstream metabolites such as L-arginine and N²-succinyl-L-arginine are up-regulated at LH1, while they are down-regulated at a later time point (LH2). Glutamate, one of the end products in AST pathway, shows down-regulation at LH1. Previous studies reported the change of amino acid metabolisms confers persisters and antibiotic resistance ¹⁷⁵⁻¹⁷⁷. Thus, the induction of certain amino acid pathways such as L-arginine degradation might correlate to the tolerance of *E. coli* to high-dose LP-600.

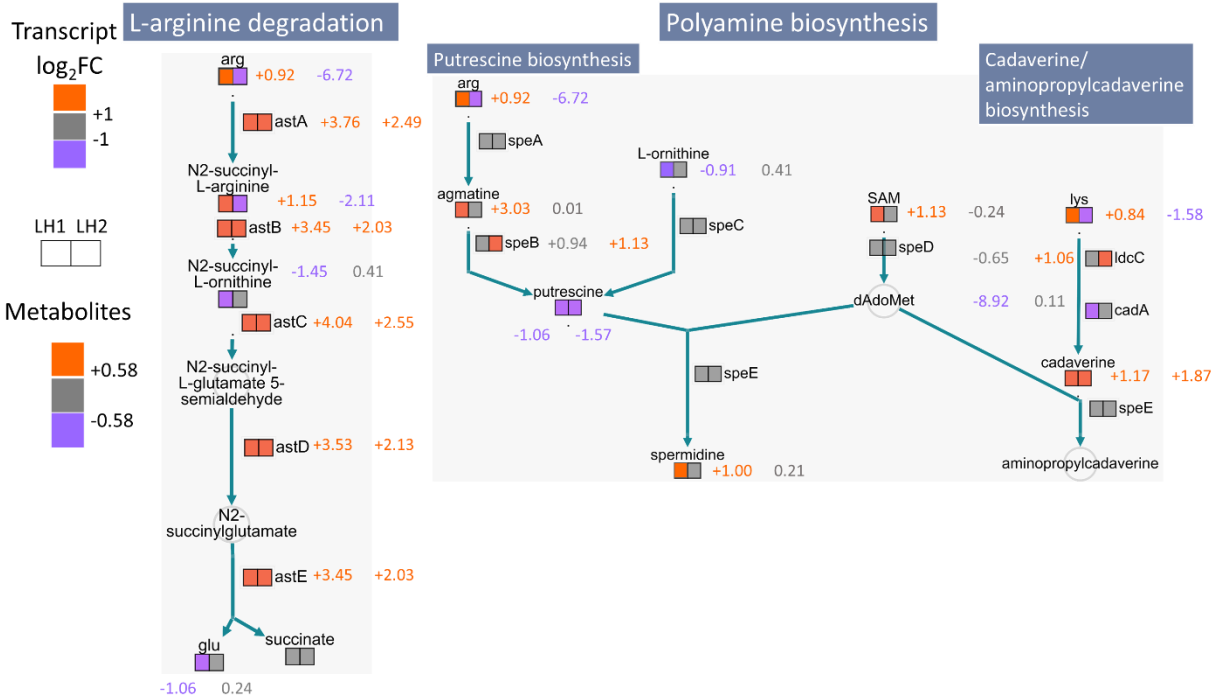


Figure 42. Summary of enriched pathways of differentially expressed genes and metabolites upon the Eagle effect. Significantly regulated metabolites were obtained by subtracting the log₂-mean values of high-dose condition from the log₂-mean values of low-dose group grown at the same condition. The threshold for significantly regulation of metabolites is FDR < 0.05 and absolute fold change > 1.5, whereas the threshold for differential expression of genes is FDR < 0.05 and log₂FC > 1. The up-regulation and down-regulated entries were expressed in red, purple, respectively. The non-significant expression is represented in gray. LH1: significantly regulated metabolites or genes upon the Eagle effect at exponential phase. LH2: significantly regulated metabolites or genes upon the Eagle effect during stationary phase.

5. Discussion

5.1 The uptake route of LP-600.

Antibiotic resistance is a major threat to the modern health system¹⁷⁸. For the development of novel antibiotics the cell wall with the additional outer membrane of Gram-negative bacteria poses a hurdle for antibiotic entry, dramatically reducing the drug efficacy. The siderophore-antibiotic conjugate concept is a promising strategy to overcome the current challenge by hijacking the iron acquisition system that is essential for microbial survival. However, the mechanism on how siderophore-antibiotic conjugates works and bacterial response to such a new class of antibiotics remains largely unknown.

This study demonstrated the anti-bacterial activity of LP-600 against *E. coli* and demonstrated that only triple knockout of three catecholate receptors (FepA, CirA, and Fiu) conferred resistance to LP-600 in *E. coli* (Table 11), suggesting that LP-600 is able to use multiple siderophore receptors to facilitate its uptake into bacteria. Interestingly, only FepA is required for the LP-117 (Figure 13), the siderophore-core of LP-600, to induce growth recovery, which indicates that the outer membrane receptors differentiate between LP-600 and LP-117. A previous study showed that double knockout of catecholate receptors *cirA* and *fiu* substantially increase the MIC of cefiderocol (64-fold), a commercial catecholate-beta-lactam conjugate, in *E. coli*³⁵. In contrast, double knockout of *cirA* and *fiu* displays only a two-fold increase in MIC of LP-600 (Table 11), suggesting that the receptors dependencies of LP-600 and cefiderocol are different. Considering the specificity of siderophore-OMR interaction, different compound structures may contribute to their selectivity on siderophore-acquisition receptors.

In addition to receptors for catecholate siderophores, TonB and ExbB play important role in LP-600-mediated anti-bacterial activity in *E. coli*. TonB deletion strain shows resistance to LP-600 and cefiderocol (> 64-fold MIC) (Table 11). On the other hand, ExbB, another component in Ton machinery, deletion strain exhibits higher resistance to LP-600 (> 64-fold MIC), compared to cefiderocol (16-fold MIC) in *E. coli*. Moreover, in Figure 17, double knockout of *entA* and *exbB* ($\Delta entA \Delta exbB$) is unable to grow in an iron-limited medium in the presence of LP-117. By contrast, $\Delta entA \Delta exbB$ shows growth recovery in the presence of enterobactin while iron level is limited (Figure 17). These results confirm the key biomolecules involved in the uptake of LP-600 in *E.*

coli. Further studies on how OMRs differentiate LP-600 from LP-117, and on the role of ExbB in LP-117 as well as LP-600 uptake are needed.

5.1.1 The role of ExbB in LP-600-mediated anti-bacterial activity in *E. coli*.

There is limited knowledge about how the resistance mechanism of siderophore-antibiotic conjugate. It was found that the loss of siderophore transporters such as CirA and Fiu contribute to the resistance of siderophore-conjugate^{35,179}. In this study, two sites of single nucleotide mutation in LP-600-resistant clones were identified. The first mutation was found in gene locus of *exbB* resulting in a stop codon mutation from glycine (Q163*) of encoding protein (Table 12). Complementation of ExbB Q163*, but not wild type of ExbB, into $\Delta exbB$ strain shows resistance to LP-600 in *E. coli* (Figure 18A), further confirming the role of ExbB Q163* in anti-bacterial activity of LP-600. Previous studies showed that ExbB is an integral cytoplasmic membrane (CM) protein with three transmembrane domains^{77,78}. It is believed that ExbB has three functions: as a scaffold on stabilizing the structure of Ton machinery^{77,78}, supplier of proton motive force (PMF) for conformational changes of TonB and the associated outer membrane receptor, and signal transduction^{78,150}. According to the peptide sequence, ExbB Q163* leads to a truncated form of ExbB lacking the third transmembrane domain (TMD3) and the cytoplasmic carboxy-terminal⁷⁸, although the boundaries of the TMD 3 have not been fully established because there are studies showing different ranges of TMD 3 such as residues 177 to 199¹⁸⁰ or 162 to 194¹⁸¹. By site-directed mutagenesis, the team of Baker found key residues located in three TMDs of ExbB and proposed that the role of TMD 1 is to mainly interact with the TMD of TonB, the role of TMD 2 is in the interaction with ExbD and the role of TMD 3 is to transduce signals⁷⁸. The importance of TMD 1 and TMD 2 in the interactions between ExbB and TonB, ExbD might explain why the resistant clones with ExbB Q163* mutation is able to take up either enterobactin or LP-117 (Figure 17), suggesting that this truncated form of ExbB does not abolish siderophore uptake. Yet, the role of TMD 3 has not been firmly determined. Other studies demonstrated that the mutagenesis of certain residues in TMD 3 and cytoplasmic carboxy terminus of ExbB disrupts the assembly of Ton machinery and ferrichrome uptake^{78,182}, which is different from our observation in LP-600-resistant clones with ExbB Q163* were still able to recover growth in the presence of siderophores (such as enterobactin or LP-117) under iron-limited conditions (Figure 17). These results indicate

that the truncated form of ExbB Q163* is not essential for siderophore uptake, but it might play a key role in LP-600 entry into *E. coli*.

On the other hand, considering the role of ExbB in PMF^{78,150}, whether co-treatment of CCCP interrupted the anti-bacterial activity of LP-600 was examined. Figure 19 demonstrates that the presence of CCCP, an inhibitor of PMF¹⁵¹, does not alter the MIC values of LP-600 against LP-600-resistant clones with ExbB163* mutation as well as wild type strains. The findings suggest that PMF is not essential for LP-600-mediated anti-bacterial activity, but also that ExbB163* mutation-mediated LP-600 resistance cannot be attributed to a change in PMF. There are still questions that have to be explored. Firstly, how the truncated form of ExbB Q163* influences the structures and functions of Ton machinery. Secondly, quantification of intracellular accumulation of LP-600 could confirm the importance of Q163* ExbB for LP-600 uptake; However, LP-600 and its metabolites (e.g. a hydrolyzed form of LP-600) was not found in the metabolomic analysis (data not shown). Hence, these results confirm that ExbB is a key molecule for LP-600 activity against *E. coli*.

5.1.2 The role of CyoB in LP-600-mediated anti-bacterial activity in *E. coli*.

Apart from ExbB, a single nucleotide mutation in *cyoB* leading to a G269D change in the protein CyoB was found in all LP-600-resistant clones (Table 12). The protein CyoB (cytochrome bo(3) ubiquinol oxidase subunit I) functions as the major terminal oxidase in the aerobic respiratory chain of *E. coli* and contributes to PMF generation^{183,184}. However, unlike ExbB Q163*, reintroducing CyoB G269D into $\Delta cyoB$ strain is unable to restore the resistance to LP-600 in *E. coli* (Figure 18C). Cultures from LP-600-resistant clones with only one mutation site in *cyoB*, instead of with the second mutation site on *exbB*, were sensitive to LP-600 (MIC = 2 $\mu\text{g/mL}$) after a few passages (Appendix I and II). This recovery of resistance can be explained by different studies regarding transient resistance. Antibiotic resistance could result from permanent resistance that is usually associated with genetic mutations, acquisition of resistance elements through either vertical or horizontal transfer¹⁸⁵, or from transient, phenotypic resistance allowing bacteria to temporarily survive upon antibiotic exposure¹⁸⁶. Previous studies demonstrated that dormancy evades the drug target or alters gene expression to generate a resistant phenotype rather than genetic mutation¹⁸⁵. A further whole-genome sequence confirms no additional genetic mutation

occurred among those “recovery” clones (Appendix I and II). Thus, these results indicate phenotypic variation exists among generations even without the new genetic mutation.

On the other hand, the question how CyoB G269D interferes antibacterial activity of LP-600 arises. Wistrand-Yuen et al. identified a CyoB G283D mutation in *Salmonella enterica* that was exposed to sub-MIC levels of streptomycin and acquired a high-level of drug resistance¹⁸⁷. Given that streptomycin is an aminoglycoside, the uptake of streptomycin depends on electron transport as well as membrane potential for passing through both outer and inner membrane¹⁸⁸. Wistrand-Yuen *et al* suggested that CyoB G283D decreases the membrane potential so that reduces streptomycin uptake and enables drug resistance. Another study from Lázár revealed that the mutation of CyoB involved aminoglycoside resistance via the reduction of PMF¹⁸⁹. Considering that CyoB G269D mutation existed in all LP-600-resistant clones (Table 12) and the role of CyoB in membrane potential, CyoB G269D might impede the LP-600 uptake for bacterial survival by reducing membrane potential as well as PMF even though CyoB G269D alone is not sufficient for complete resistance to LP-600.

5.2 The metabolic and transcriptional response to sub-MIC level of LP-600.

Metabolism plays a central role in coordinating a rapid response to environmental changes such as stresses¹⁵⁹. Accumulating studies demonstrated the antibiotic resistance is associated with several metabolic functions such as amino acid biosynthesis and ROS production^{190,191}. Yet, the interplay between antibiotics and metabolic changes and the consequences on bacterial function and drug resistance deserved further and deeper characterization. In this study, both transcriptome and metabolome upon LP-600 treatment were investigated, gaining a deeper view on the interaction between LP-600 and bacteria as well as the LP-600 mechanism of action.

Even though cultures from sub-MIC treatment of LP-600 and vehicle control cluster closely and exhibit a similar growth rate in growth curve and MDS plots (Figure 23, Figure 24 and Figure 35), numbers of differentially expressed genes and metabolites were found. Only three out of 72 (CL1) and 35 (CL2) differentially expressed genes were found in both transcriptomes. But no enriched classification were found in either these three genes or 72 genes of CL1. By contrast, among 35 differentially expressed genes in CL2, enriched terms involved in maltodextrin transport

(Appendix III) were found in up-regulated genes of CL2, indicating the potential pathways involved in LP-600 treatment.

In addition, a number of lipid-associated metabolites-LPG and LPE significantly increases upon sub-MIC level of LP-600 (Appendix VII). LPG and LPE belong to lysophospholipids (LPLs) which are generated as metabolic intermediates during membrane degradation as well as phospholipid synthesis¹⁶⁶. In pathogenic bacteria, LPE was found accumulated and associated with pathogenic or survival advantages under stress conditions^{166,192}. For example, a previous study from Davydova's team addressed the accumulation of LPE of Gram-negative bacteria *Yersinia Pseudotuberculosis*, under the parasitic phase, and found that the lipid contributes to conformational rearrangement of outer membrane protein OmpF, thereby hindering permeability for β -lactam antibiotics and increasing the MIC of β -lactam antibiotics¹⁹³. These studies might explain the up-regulation of LPLs upon sub-MIC of LP-600 treatment which causes the change of membrane composition so that counteracts the antibiotic stress for growth.

5.3 The mechanism of LP-600-induced Eagle effect:

5.3.1 The role of beta-lactamase in LP-600-induced Eagle effect.

A high dose of LP-600 induces the Eagle effect in *E. coli* (Figure 20). Eagle effect was firstly addressed in 1950s and reported in numbers of microorganisms upon various classes of antibiotics^{85,86}, however, the mechanism of the Eagle effect remains largely unknown. One of proposed mechanisms of Eagle effect is the induction of β -lactamase against β -lactam contributing to paradoxical antibacterial activity. Ikeda et al. addressed the essential role of β -lactamase in β -lactam-induced Eagle effect in *P. vulgaris*⁹⁴. The team of Ikeda found that the presence of β -lactamase inhibitor or β -lactamase-deficiency strains abolish β -lactam (such as cephalosporins)-induced Eagle effect in *P. vulgaris*⁹⁴. In line with this, co-treatment of sulbactam and LP-600 abolishes LP-600-induced Eagle effect in *E. coli* (Figure 22C). However, there is no comparable increase in β -lactamase activity between the "Eagle-dose" and the sub-MIC level of LP-600 (Figure 22E and F) after 24-hour treatment of LP-600. On the transcriptome level, *ampC*, the main chromosomal gene encoding β -lactamase, displayed no significant up-regulation upon high-dose LP-600 compared to sub-MIC level treatment of LP-600 during both mid-exponential and stationary phases (Appendix V)^{155,156}. These results indicate that it is less likely to induce a high

level of β -lactamase expression during the Eagle effect at least in the phases of stationary and mid-exponential phases. Therefore, it remains to be explored whether and when the β -lactamase abundance increases in LP-600-induced Eagle effect and it could not exclude that other mechanisms attributed to the synergic effect of sulbactam and LP-600.

5.3.2 Pathways involved in the Eagle effect.

Here demonstrated LP-600-induced Eagle effect greatly influences the expression of genes and metabolites involved in several metabolic pathways involving amino acids or polyamine (Figure 29 and Figure 42). For example, in transcriptomes from mid-exponential and stationary phases (LH1 and LH2), high-dose LP-600 reduces gene expression involved in threonine catabolic process to propionate (*tdcABCDE*), whereas enhances the expression of genes regarding arginine (*astABCDE*) and lysine (*gabDT*) pathways (Figure 30 and Appendix V). In line with transcriptomic results, metabolic intermediates involved in arginine degradation shows expressed significantly under high-dose LP-600 treatment (Figure 42). The association between amino acid metabolism and antibiotic tolerance are consistent with previous researches that reported the shift of amino acid metabolism confers persisters and antibiotic resistance¹⁷⁵⁻¹⁷⁷. Furthermore, Lebeaux et al. revealed that elevated *L*-arginine abundance enhance susceptibility to aminoglycoside treatment in *E. coli* by increasing PMF^{194,195}. In this study, a reduction of *L*-arginine and an increase in gene expression involved in arginine degradation in condition was found (Figure 42). Collectively, these results indicate that amino acids such as *L*-arginine might contribute to the LP-600-induced Eagle effect.

On the other hand, genes and metabolites involved in polyamine biosynthesis are differentially regulated upon Eagle effect (Figure 42). Polyamine modulates several metabolic pathways and cellular functions such as cell permeability upon antibiotic treatment^{167,170,171}. The increase in polyamines such as cadaverine and spermidine upon high-dose LP-600 treatment supports Tkachenko et al.'s finding that is polyamine induction upon sub-MIC of β -lactam treatment¹⁷⁰. Besides, Tkachenko et al. reported that polyamines protect DNA and proteins from oxidative stress, thereby enhancing antibiotic tolerance and survival¹⁷², whereas Kwon et al. showed that the exogenous supplement of polyamine decreases MIC of β -lactam in *E. coli*¹⁹⁶ and the underlying mechanism remains unknown. It is likely that induction of endogenous polyamine

protects *E. coli* from stress under high-dose LP-600 treatment, yet the role of polyamine in LP-600-induced Eagle effect has to be further explored.

In addition to amino acid metabolism, an SOS response might play an important role in Eagle effect. Previous studies suggested that SOS response, a global response to DNA damage or antibiotics treatment, is associated with the evolution of resistance under treatment with antibiotics such as β -lactams and DNA-damaging fluoroquinolones^{197,198}. During SOS response, stress or DNA damage activates transcription factor-RecA to stimulate self-cleavage of LexA, leading to the expression of SOS genes for repair¹⁹⁸. For example, Dörr et al. showed that overexpressing *tisB*, one of the SOS genes, significantly increased the level of persister cells that are phenotypic variants with antibiotics tolerances¹⁹⁹. Dörr et al. also revealed that TisB-dependent persisters were highly tolerant to many antibiotics, indicating that SOS response and TisB provide survival benefits for bacterial under antibiotic exposure by altering the PMF and interfering with antibiotic uptake. In line with their findings, in this study, a cluster of genes involved in SOS response belonging to the LexA regulon (such as *tisB*, *dinB*, *cho*, *umuC*, *recN* etc.), are significantly induced in samples shown Eagle effect during the mid-exponential phase (LH1) (Figure 31 and Appendix V). Additionally, the up-regulated e14 prophage genes (*croE*, *intE*, *pinE*, *sffP*, *xisE*, *yfmJ*, *yfmL*, *yfmM*, *yfmR*) in LH1 (Appendix V and Figure 25) might contribute to Eagle effect upon SOS response. Most genes in e14 element encode proteins with unknown functions and only a few genes such as *yfmM* are found to have an association with SOS-induced cell division inhibition and filamentation^{164,165}. Ansari et al. demonstrated that over-expression of *yfmM* causes filamentation by inhibiting cell division during SOS response¹⁶⁵. Filamentation can be induced by SOS response during stress such as β -lactam treatment^{197,200}, resulting in elongated cells that are growing in the absence of cell division. Besides, Miller et al. reported that β -lactam-induced SOS response and filamentation enable survival to antibiotic exposure by reducing the demand for cell wall synthesis¹⁹⁷. The induction SOS and e14 prophage gene in mid-exponential phase instead of stationary phase imply that the quick SOS response of *E. coli* to LP-600 might enable survival by halting the cell division and reducing the cell wall synthesis. Therefore, induction of SOS response as well those cell division inhibition mediated by e14 prophages might contribute to the Eagle effect, yet it remains to be further explored.

In addition to the metabolites involved in the above-mentioned pathways, up-regulated metabolites such as hypoxanthine, guanine and thymidine either in LH1 or LH2 and down-regulated metabolites (NAD) may play a role in the Eagle effect (Figure 39 and Figure 40). These metabolites are also reported in a study by Su et al., who identified a number of metabolites responsible for classification of the strains as UPECs or non-UPECs. Moreover, these metabolites were modulated by siderophore biosynthesis²⁰¹. Another study from Karlsen et al addressed hypoxanthine and guanine and their potential to serve as biomarkers during *E. coli*-mediated UTI²⁰². Furthermore, Su and colleagues suggested a list of 23 metabolites involved in three main pathways (amino acid metabolism, carbohydrate and energy metabolism, nucleotide metabolism-associated metabolic pathways) which play a key role in virulence and survival for UPEC under human urine²⁰¹.

In transcriptomic results shown in Figure 29, genes involved in purine and pyrimidine metabolism are differentially expressed in both LH1 and LH2 conditions. Besides, Belenky et al. found a decrease in purine/pyrimidine level (guanine and guanosine) and an increase in xanthine (which is a marker of purine catabolism) in response to several classes of antibiotics such as ampicillin, claiming that this increase in turnover of nucleotides attributes to a general DNA damage in response to antibiotic^{102,203}. In LH2 condition, the increase of xanthine abundance supports the idea, yet a general decrease in nucleotides such as guanine was not found (Appendix VIII). Purine and pyrimidine metabolism may contribute to Eagle effect and provide the survival benefit in response to antibiotic exposure. Yet, the detailed mechanism remains to be further explored.

In summary of metabolomic and transcriptomic results, the high-dose LP-600 treatment significantly influences gene expression as well as metabolite abundance in comparison to low-dose LP-600 or untreated control. Especially, the samples from high-dose LP-600 treatment during exponential phase display the most variance from other conditions (Figure 24 and Figure 35). Furthermore, SOS response and e14 prophage genes are highly induced only in LH1 condition, indicating that their quick response might be an initiator for defense mechanism contributing to the Eagle effect (Appendix V and Figure 30). On the other hand, in LH2 condition, much less differentially expressed genes as well as significantly regulated metabolites were found compared to LH1 (Appendix V, Figure 33 and Figure 41). Besides, both transcriptomes and metabolomes in LH2 condition affect mainly metabolic pathways such as amino acid metabolism rather than

specific gene regulons or signal pathways, which might suggest a general adaption for high-dose antibiotic exposure during the stationary phase.

Summary and outlook

This study provides new insights into the resistance mechanism of synthetic siderophore-LP-600 in *E. coli*. Complementation and growth recovery assays confirmed the important role of ExbB Q163* in the resistance to LP-600 in *E. coli*, rather than siderophore uptake. Further quantification of LP-600 via LC-MS method in the LP-600-resistant clones with ExbB Q163* could clarify the question of whether ExbB Q163* contributes to resistance to LP-600 due to the interference with LP-600 uptake or other mechanisms.

Besides, it is the first study about Eagle effect triggered by siderophore-based antibiotics and the multi-omics results for Eagle effect. In the transcriptomic study, it was found that clusters of SOS response and $\epsilon 14$ prophage genes were significantly up-regulated at the early time-point at high compound concentration, indicating that SOS-mediated survival reactions such as DNA repair, filamentation or persister formation might contribute to the Eagle effect. Additionally, upon the Eagle effect, both transcriptome and metabolome reveal a dramatic change of pathways involved in amino acid and polyamine metabolism. Open questions remain about the role of SOS response in the Eagle effect, the key modulators that drive the Eagle effect, and the interplay between those metabolic pathways. To characterize key moderators, examining whether high-dose LP-600 induces the Eagle effect in the knockout of $\epsilon 14$ prophages or a series of SOS response genes is needed. Besides, a targeted metabolomics approach can be applied to confirm the metabolic changes in pathways associated with differentially expressed genes, elucidating the role of individual metabolic pathways under the LP-600-induced Eagle effect. Such a targeted approach would assure that the majority of important metabolites on such pathways, that remained partially undetected in the untargeted method, are quantified.

Moreover, since the Eagle effect has been found in several organisms upon treatments of antibiotics with distinct modes of action, it remains unclear that whether a general mechanism exists to trigger the effect upon various antibiotic treatments. To answer the question, whether LP-600 induces a paradoxical growth in other bacterial species that were previously reported to show an “Eagle effect” should be investigated. A further multi-omic study across species can characterize whether a “general” mechanism or key pathway exists.

In summary, this study identified receptors- FepA, CirA, and Fiu all getting involved in LP-600-mediated antimicrobial activity in *E. coli*. In addition, by the generation of LP-600-resistant clones, a point mutation in gene *exbB* (encoding Q163* ExbB) is essential for the antibacterial activity of LP-600 that is confirmed by complementation assay in Δ *exbB* strain. On the other hand, surprisingly, above 16-times the MIC of LP-600 induces the Eagle effect that can be diminished upon co-treatment of β -lactamase inhibitor. In metabolome and transcriptome results, several amino acid metabolomic pathways such as L-arginine degradation, L-threonine catabolism are differentially regulated upon Eagle effect. In addition, LP-600 induces expression of genes involved in SOS response and ϕ 14 prophage upon regrowth conditions Eagle. Taken together, this study identifies not only a potential anti-infective compound but also provides a systemic insight into the bacterial responses to siderophore-antibiotic conjugate exposure, facilitating the future study for the Eagle effect.

References

1. Lewis, K. Platforms for antibiotic discovery. *Nat. Rev. Drug Discov.* **12**, 371–387 (2013).
2. In Switzerland: World Health Organization. Prevention of Hospital-Acquired Infections. *Dep. Commun. Dis. Response, World Heal. Organ.* **17**, 422–426 (2016).
3. Klein, E. Y. *et al.* Global increase and geographic convergence in antibiotic consumption between 2000 and 2015. *Proc. Natl. Acad. Sci. U. S. A.* **115**, E3463–E3470 (2018).
4. European Centre for Disease Prevention and Control. Antimicrobial consumption in the EU/EEA, annual epidemiological report for 2018. *Eur. Cent. Dis. Prev. Control* 1–24 (2019).
5. Control, D. & States, U. Outpatient Antibiotic Prescriptions—United States, 2015. 1–3 (2017).
6. Garima Kapoor, Saurabh Saigal, A. E. Action and resistance mechanisms of antibiotics: A guide for clinicians. *J. Anaesthesiol. Clin. Pharmacol.* **34**, 46–50 (2018).
7. Kohanski, M. A., Dwyer, D. J. & Collins, J. J. How antibiotics kill bacteria: From targets to networks. *Nat. Rev. Microbiol.* **8**, 423–435 (2010).
8. Chen, C. R., Malik, M., Snyder, M. & Drlica, K. DNA gyrase and topoisomerase IV on the bacterial chromosome: Quinolone-induced DNA cleavage. *J. Mol. Biol.* **258**, 627–637 (1996).
9. Drlica, K. & Zhao, X. DNA gyrase, topoisomerase IV, and the 4-quinolones. *Microbiol. Mol. Biol. Rev.* **61**, 377–392 (1997).
10. Hooper, D. C. Mode of action of fluoroquinolones. *Drugs* **58**, 6–10 (1999).
11. Gellert, M., Mizuuchi, K., O'dea, M. H. & Nasht, H. A. DNA gyrase: An enzyme that introduces superhelical turns into DNA (*Escherichia coli*/ATP-dependent reaction/superhelix density). **73**, 3872–3876 (1976).
12. Muñoz, R. & De La Campa, A. G. ParC subunit of DNA topoisomerase IV of *Streptococcus pneumoniae* is a primary target of fluoroquinolones and cooperates with DNA gyrase A subunit in forming resistance phenotype. *Antimicrob. Agents Chemother.* **40**, 2252–2257 (1996).
13. Drlica, K., Malik, M., Kerns, R. J. & Zhao, X. Quinolone-mediated bacterial death. *Antimicrob. Agents Chemother.* **52**, 385–392 (2008).
14. Yoneyama, H. & Katsumata, R. Antibiotic resistance in bacteria and its future for novel antibiotic development. *Biosci. Biotechnol. Biochem.* **70**, 1060–1075 (2006).
15. Fernández-Villa, D., Aguilar, M. R. & Rojo, L. Folic acid antagonists: Antimicrobial and immunomodulating mechanisms and applications. *Int. J. Mol. Sci.* **20**, 1–30 (2019).
16. Nikolay, R., Schmidt, S., Schlömer, R., Deuerling, E. & Nierhaus, K. H. Ribosome assembly as antimicrobial target. *Antibiotics* **5**, 1–13 (2016).
17. Tolmasky, M. S. R. and M. E. Aminoglycoside Modifying Enzymes. *Drug Resist Updat.* **13**, 151–171 (2010).
18. Vollmer, W., Blanot, D. & De Pedro, M. A. Peptidoglycan structure and architecture. *FEMS Microbiol. Rev.* **32**, 149–167 (2008).
19. Typas, A., Banzhaf, M., Gross, C. A. & Vollmer, W. From the regulation of peptidoglycan synthesis to bacterial growth and morphology. *Nat. Rev. Microbiol.* **10**, 123–136 (2012).
20. Hamed, R. B. *et al.* The enzymes of β -lactam biosynthesis. *Nat. Prod. Rep.* **30**, 21–107 (2013).

21. De Oliveira, D. M. P. *et al.* Antimicrobial resistance in ESKAPE pathogens. *Clin. Microbiol. Rev.* **33**, 1–49 (2020).
22. Delcour, A. H. Outer Membrane Permeability and Antibiotic Resistance. *Biochim Biophys Acta.* **1794**, 808–816 (2008).
23. Miller, W. R., Bayer, A. S. & Arias, C. A. Mechanism of action and resistance to daptomycin in *Staphylococcus aureus* and enterococci. *Cold Spring Harb. Perspect. Med.* **6**, 1–16 (2016).
24. Pogliano, J., Pogliano, N. & Silverman, J. A. Daptomycin-mediated reorganization of membrane architecture causes mislocalization of essential cell division proteins. *J. Bacteriol.* **194**, 4494–4504 (2012).
25. Grein, F. *et al.* Ca²⁺-Daptomycin targets cell wall biosynthesis by forming a tripartite complex with undecaprenyl-coupled intermediates and membrane lipids. *Nat. Commun.* **11**, 1–11 (2020).
26. Neill, J. O. ' . Antimicrobial Resistance: Tackling a crisis for the health and wealth of nations. *Rev. Antimicrob. Resist.* (2014).
27. Prioritization of pathogens to guide discovery, research and development of new antibiotics for drug-resistant bacterial infections, including tuberculosis. *Switz. World Heal. Organ.* (2017).
28. Rice, L. B. Federal funding for the study of antimicrobial resistance in nosocomial pathogens: No ESKAPE. *J. Infect. Dis.* **197**, 1079–1081 (2008).
29. C Reygaert, W. An overview of the antimicrobial resistance mechanisms of bacteria. *AIMS Microbiol.* **4**, 482–501 (2018).
30. Wang, T. Z., Kodiyankal, R. P. L. & Calfee, D. P. Antimicrobial resistance in nephrology. *Nat. Rev. Nephrol.* **15**, 463–481 (2019).
31. Robicsek, A., Jacoby, G. A. & Hooper, D. C. The worldwide emergence of plasmid-mediated quinolone resistance. *Lancet Infect. Dis.* **6**, 629–640 (2006).
32. Toussaint, K. A. & Gallagher, J. C. β -Lactam/ β -Lactamase Inhibitor Combinations: From Then to Now. *Ann. Pharmacother.* **49**, 86–98 (2015).
33. Poirel, L. & Nordmann, P. Carbapenem resistance in *Acinetobacter baumannii*: Mechanisms and epidemiology. *Clin. Microbiol. Infect.* **12**, 826–836 (2006).
34. Pai, H. *et al.* Carbapenem resistance mechanisms in *Pseudomonas aeruginosa* clinical isolates. *Antimicrob. Agents Chemother.* **45**, 480–484 (2001).
35. Akinobu Ito, Takafumi Sato, Merime Ota, Miki Takemura, Toru Nishikawa, Shinsuke Toba, Naoki Kohira, Satoshi Miyagawa, Naoki Ishibashi, Shuhei Matsumoto, Rio Nakamura, Masakatsu Tsuji, Y. Y. In Vitro Antibacterial Properties of Cefiderocol, a Novel Siderophore Cephalosporin, against Gram-Negative Bacteria. *Antimicrob Agents Chemother* **62**, e01454-17 (2017).
36. Li, X. Z., Plésiat, P. & Nikaido, H. The challenge of efflux-mediated antibiotic resistance in Gram-negative bacteria. *Clin. Microbiol. Rev.* **28**, 337–418 (2015).
37. Nairz, M. & Weiss, G. Iron in infection and immunity. *Mol. Aspects Med.* **75**, 100864 (2020).
38. Crandon, J. L. *et al.* Adaptation-Based Resistance to Siderophore-Conjugated Antibacterial Agents by *Pseudomonas aeruginosa*. *Antimicrob. Agents Chemother.* **57**, 4197–4207 (2013).
39. Gueriot, M. Lou. Microbial iron transport. *Annu Rev Microbiol* **48**, 743–72 (1994).
40. Raymond, K. N., Allred, B. E. & Sia, A. K. Coordination Chemistry of Microbial Iron Transport. *Acc. Chem. Res.* **48**, 2496–2505 (2015).
41. Cassat, J. E. & Skaar, E. P. Iron in infection and immunity. *Cell Host Microbe* **13**, 509–519 (2013).

42. Skaar, E. P. The Battle for Iron between Bacterial Pathogens and Their Vertebrate Hosts. *PLoS Pathog.* **6**, e1000949 (2010).
43. Winter, W. E., Bazydlo, L. A. L. & Harris, N. S. The molecular biology of human iron metabolism. *Lab Med.* **45**, 92–102 (2014).
44. Ouyang, Z. & Isaacson, R. Identification and characterization of a novel ABC iron transport system, fit, in *Escherichia coli*. *Infect. Immun.* **74**, 6949–6956 (2006).
45. Hider, R. C. & Kong, X. Chemistry and biology of siderophores. *Nat. Prod. Rep.* **27**, 637 (2010).
46. Loomis, L. D. & Raymond, K. N. Solution Equilibria of Enterobactin and Metal-Enterobactin Complexes. *Inorg. Chem.* **30**, 906–911 (1991).
47. Holden, V. I. & Bachman, M. A. Diverging roles of bacterial siderophores during infection. *Metallomics* **7**, 986–995 (2015).
48. Abergel, R. J., Moore, E. G., Strong, R. K. & Raymond, K. N. Microbial evasion of the immune system: Structural modifications of enterobactin impair siderocalin recognition. *J. Am. Chem. Soc.* **128**, 10998–10999 (2006).
49. Poole, K., Young, L. & Neshat, S. Enterobactin-mediated iron transport in *Pseudomonas aeruginosa*. *J. Bacteriol.* **172**, 6991–6996 (1990).
50. Endicott, N. P., Lee, E. & Wenczewicz, T. A. Structural Basis for Xenosiderophore Utilization by the Human Pathogen *Staphylococcus aureus*. *ACS Infect. Dis.* **3**, 542–553 (2017).
51. FRANCIS, J., MACTURK, H. M., MADINAVEITIA, J. & SNOW, G. A. Mycobactin, a growth factor for *Mycobacterium johnei*. I. Isolation from *Mycobacterium phlei*. *Biochem. J.* **55**, 596–607 (1953).
52. Kadi, N. & Challis, G. L. *Chapter 17 Siderophore Biosynthesis. A Substrate Specificity Assay for Nonribosomal Peptide Synthetase-Independent Siderophore Synthetases Involving Trapping of Acyl-Adenylate Intermediates with Hydroxylamine. Methods in Enzymology* vol. 458 (Elsevier Inc., 2009).
53. Cassandra S Carroll, M. M. M. Ironing out siderophore biosynthesis: a review of non-ribosomal peptide synthetase (NRPS)-independent siderophore synthetases. *Crit Rev Biochem Mol Biol* **53**, 356–381 (2018).
54. Miethke, M. & Marahiel, M. A. Siderophore-Based Iron Acquisition and Pathogen Control. *Microbiol. Mol. Biol. Rev.* **71**, 413–451 (2007).
55. Pollack, J. R. & Neilands, J. B. Enterobactin, an iron transport compound from *Salmonella typhimurium*. *Biochem. Biophys. Res. Commun.* **38**, 989–992 (1970).
56. Dosselaere, F. & Vanderleyden, J. *A metabolic node in action: Chorismate-utilizing enzymes in microorganisms. Critical Reviews in Microbiology* vol. 27 (2001).
57. Gehring, A. M., Bradley, K. A. & Walsh, C. T. Enterobactin biosynthesis in *Escherichia coli*: Isochorismate lyase (EntB) is a bifunctional enzyme that is phosphopantetheinylated by EntD and then acylated by ente using ATP and 2,3-dihydroxybenzoate. *Biochemistry* **36**, 8495–8503 (1997).
58. Venuti, M. C., Rastetter, W. H. & Neilands, J. B. 1,3,5-Tris(N, N',N-2 dihydroxybenzoyl)aminomethylbenzene, a Synthetic Iron Chelator Related to Enterobactin. *J. Med. Chem.* **22**, 123–124 (1979).
59. Matzanke, B. F. *et al.* *Escherichia coli* iron enterobactin uptake monitored by Mossbauer spectroscopy. *J. Bacteriol.* **167**, 674–680 (1986).
60. Heidinger, S., Braun, V., Pecoraro, V. L. & Raymond, K. N. Iron supply to *Escherichia coli* by synthetic analogs of enterochelin. *J. Bacteriol.* **153**, 109–115 (1983).
61. Harris, W. R. *et al.* *Coordination Chemistry of Microbial Iron Transport Compounds*. 19. Stability Constants and

- Electrochemical Behavior of Ferric Enterobactin and Model Complexes. *J. Am. Chem. Soc.* **101**, 6097–6104 (1979).
62. Neumann, W., Sassone-Corsi, M., Raffatellu, M. & Nolan, E. M. Esterase-Catalyzed Siderophore Hydrolysis Activates an Enterobactin-Ciprofloxacin Conjugate and Confers Targeted Antibacterial Activity. *J. Am. Chem. Soc.* **140**, 5193–5201 (2018).
 63. Zheng, T. & Nolan, E. M. Enterobactin-mediated delivery of β -lactam antibiotics enhances antibacterial activity against pathogenic *Escherichia coli*. *J. Am. Chem. Soc.* **136**, 9677–9691 (2014).
 64. Braun, V., Pramanik, A., Gwinner, T., Köberle, M. & Bohn, E. Sideromycins: Tools and antibiotics. *BioMetals* **22**, 3–13 (2009).
 65. Braun, V., Gunthner, K., Hantke, K. & Zimmermann, L. Intracellular activation of albomycin in *Escherichia coli* and *Salmonella typhimurium*. *J. Bacteriol.* **156**, 308–315 (1983).
 66. Andrei, S., Droc, G. & Stefan, G. FDA approved antibacterial drugs: 2018-2019. *Discoveries* **7**, e102 (2019).
 67. Falcone, M. *et al.* Cefiderocol as rescue therapy for *Acinetobacter baumannii* and other carbapenem-resistant Gram-Negative infections in ICU patients. *Clin. Infect. Dis.* 1–4 (2020) doi:10.1093/cid/ciaa1410.
 68. Sato, T. & Yamawaki, K. Cefiderocol: Discovery, Chemistry, and in Vivo Profiles of a Novel Siderophore Cephalosporin. *Clin. Infect. Dis.* **69**, S538–S543 (2019).
 69. Flores-Meireles, A., Walker, J., Caparon, M. & Hultgren, S. Urinary tract infections: epidemiology, mechanisms of infection and treatment options. *Nat. Rev. Microbiol.* **13**, 269–284 (2015).
 70. Sarowska, J. *et al.* Virulence factors, prevalence and potential transmission of extraintestinal pathogenic *Escherichia coli* isolated from different sources: Recent reports. *Gut Pathog.* **11**, 1–16 (2019).
 71. Terlizzi, M. E., Gribaudo, G. & Maffei, M. E. UroPathogenic *Escherichia coli* (UPEC) infections: Virulence factors, bladder responses, antibiotic, and non-antibiotic antimicrobial strategies. *Front. Microbiol.* **8**, (2017).
 72. Nikaido, H. & Vaara, M. Molecular basis of bacterial outer membrane permeability. *Microbiol. Rev.* **49**, 1–32 (1985).
 73. Nikaido, H., Rosenberg, E. Y. & Foulds, J. Porin channels in *Escherichia coli*: Studies with β -lactams in intact cells. *J. Bacteriol.* **153**, 232–240 (1983).
 74. Faraldo-Gómez, J. D. & Sansom, M. S. P. Acquisition of siderophores in gram-negative bacteria. *Nat. Rev. Mol. Cell Biol.* **4**, 105–116 (2003).
 75. Higgs, P. I., Larsen, R. A. & Postle, K. Quantification of known components of the *Escherichia coli* TonB energy transduction system: TonB, ExbB, ExbD and FepA. *Mol. Microbiol.* **44**, 271–281 (2002).
 76. Krewulak, K. D. & Vogel, H. J. Structural biology of bacterial iron uptake. *Biochim. Biophys. Acta - Biomembr.* **1778**, 1781–1804 (2008).
 77. Kopp, D. R. & Postle, K. The Intrinsically Disordered Region of ExbD is Required for Signal Transduction. *bioRxiv* **202**, (2019).
 78. Baker, K. R. & Postle, K. Mutations in *Escherichia coli* ExbB transmembrane domains identify scaffolding and signal transduction functions and exclude participation in a proton pathway. *J. Bacteriol.* **195**, 2898–2911 (2013).
 79. Braun, V. Surface signaling: Novel transcription initiation mechanism starting from the cell surface. *Arch. Microbiol.* **167**, 325–331 (1997).
 80. Miethke, M. Molecular strategies of microbial iron assimilation: From high-affinity complexes to cofactor assembly systems. *Metallomics* **5**, 15–28 (2013).
 81. Cooper, S. R., McArdle, J. V & Raymond, K. N. Siderophore electrochemistry: relation to intracellular iron release

- mechanism. *Proc. Natl. Acad. Sci. U. S. A.* **75**, 3551–4 (1978).
82. Wilson, B. R., Bogdan, A. R., Miyazawa, M., Hashimoto, K. & Tsuji, Y. Siderophores in Iron Metabolism: From Mechanism to Therapy Potential. *Trends Mol. Med.* **22**, 1077–1090 (2016).
 83. Escolar, L., Pérez-Martín, J. & De Lorenzo, V. Opening the iron box: Transcriptional metalloregulation by the fur protein. *J. Bacteriol.* **181**, 6223–6229 (1999).
 84. Hantke, K. Iron and metal regulation in bacteria. *Curr. Opin. Microbiol.* **4**, 172–177 (2001).
 85. Eagle, H. & Musselmann, A. D. The rate of bactericidal action of penicillin in vitro as a function of its concentration, and its paradoxically reduced activity at high concentrations against certain organisms. *J. Exp. Med.* **88**, 99–131 (1948).
 86. Eagle, H. A paradoxical zone phenomenon in the bactericidal action of penicillin in vitro. *Science.* **107**, 44–45 (1948).
 87. Kussell, E., Kishony, R., Balaban, N. Q. & Leibler, S. Bacterial persistence: A model of survival in changing environments. *Genetics* **169**, 1807–1814 (2005).
 88. Anggia Prasetyoputri, Angie M. Jarrad, Matthew A. Cooper, M. A. T. B. The Eagle Effect and Antibiotic-Induced Persistence: Two Sides of the Same Coin? *Trends Microbiol.* **27**, 339–354 (2019).
 89. Jarrad, A. M. *et al.* Detection and investigation of eagle effect resistance to vancomycin in *Clostridium difficile* With an ATP-bioluminescence assay. *Front. Microbiol.* **9**, 1–9 (2018).
 90. Piddock, L. J. V., Walters, R. N. & Diver, J. M. Correlation of quinolone MIC and inhibition of DNA, RNA, and protein synthesis and induction of the SOS response in *Escherichia coli*. *Antimicrob. Agents Chemother.* **34**, 2331–2336 (1990).
 91. Noone, P. Paradoxical effect of penicillin in-vivo. *J Antimicrob Chemother.* **15**, 507–508 (1985).
 92. Ikeda, Y., Fukuoka, Y., Motomura, K., Yasuda, T. & Nishino, T. Paradoxical activity of β -lactam antibiotics against *Proteus vulgaris* in experimental infection in mice. *Antimicrob. Agents Chemother.* **34**, 94–97 (1990).
 93. Luan, G., Hong, Y., Drlica, K. & Zhao, X. Suppression of reactive oxygen species accumulation accounts for paradoxical bacterial survival at high quinolone concentration. *Antimicrob. Agents Chemother.* **62**, 1–13 (2018).
 94. Ikeda, Y. & Nishino, T. Paradoxical antibacterial activities of β -lactams against *Proteus vulgaris*: Mechanism of the paradoxical effect. *Antimicrob. Agents Chemother.* **32**, 1073–1077 (1988).
 95. Grandière-Pérez, L. *et al.* Eagle effect in *Corynebacterium diphtheriae*. *J. Infect. Dis.* **191**, 2118–2120 (2005).
 96. McKay, G. A. *et al.* Time-kill kinetics of oritavancin and comparator agents against *Staphylococcus aureus*, *Enterococcus faecalis* and *Enterococcus faecium*. *J. Antimicrob. Chemother.* **63**, 1191–1199 (2009).
 97. V Lorian, R P Silletti, F X Biondo, C. C. D. F. Paradoxical effect of aminoglycoside antibiotics on the growth of Gram-negative bacilli. *J Antimicrob Chemother* **5**, 613–616 (1979).
 98. Rinschen, M. M., Ivanisevic, J., Giera, M. & Siuzdak, G. Identification of bioactive metabolites using activity metabolomics. *Nat. Rev. Mol. Cell Biol.* **20**, 353–367 (2019).
 99. Schrimpe-Rutledge, A. C., Codreanu, S. G., Sherrod, S. D. & McLean, J. A. Untargeted Metabolomics Strategies—Challenges and Emerging Directions. *J. Am. Soc. Mass Spectrom.* **27**, 1897–1905 (2016).
 100. Fernández-García, M., Rojo, D., Rey-Stolle, F., García, A. & Barbas, C. *Metabolomic-Based Methods in Diagnosis and Monitoring Infection Progression. Experientia supplementum* (2012) vol. 109 (2018).
 101. Zampieri, M., Zimmermann, M., Claassen, M. & Sauer, U. Nontargeted Metabolomics Reveals the Multilevel Response to Antibiotic Perturbations. *Cell Rep.* **19**, 1214–1228 (2017).
 102. Belenky, P. *et al.* Bactericidal Antibiotics Induce Toxic Metabolic Perturbations that Lead to Cellular Damage. *Cell Rep.*

- 13**, 968–980 (2015).
103. Yang, Q., Vijayakumar, A. & Kahn, B. B. Metabolites as regulators of insulin sensitivity and metabolism. *Nat. Rev. Mol. Cell Biol.* **19**, 654–672 (2018).
 104. Tannahill, G. M. *et al.* Succinate is an inflammatory signal that induces IL-1 β through HIF-1 α . *Drugs* **496**, 238–242 (1999).
 105. Liu, P. S. *et al.* A-Ketoglutarate Orchestrates Macrophage Activation Through Metabolic and Epigenetic Reprogramming. *Nat. Immunol.* **18**, 985–994 (2017).
 106. Bar, N. *et al.* A reference map of potential determinants for the human serum metabolome. *Nature* **588**, 135–140 (2020).
 107. Suhre, K. *et al.* Human metabolic individuality in biomedical and pharmaceutical research. *Nature* **477**, 54–62 (2011).
 108. Fiehn, O. *et al.* Metabolite profiling for plant functional genomics. *Nat. Biotechnol.* **18**, 1157–1161 (2000).
 109. Nagana Gowda, G. A. & Djukovic, D. Overview of mass spectrometry-based metabolomics: Opportunities and challenges. *Methods Mol. Biol.* **1198**, 3–12 (2014).
 110. Van Berkel, G. J. & Kertesz, V. Using the electrochemistry of the electrospray ion source. *Anal. Chem.* **79**, 5510–5520 (2007).
 111. Banerjee, S. & Mazumdar, S. Electrospray Ionization Mass Spectrometry: A Technique to Access the Information beyond the Molecular Weight of the Analyte. *Int. J. Anal. Chem.* **2012**, 1–40 (2012).
 112. Chakraborty, P. & Pradeep, T. The emerging interface of mass spectrometry with materials. *NPG Asia Mater.* **11**, (2019).
 113. Wishart, D. S. *et al.* HMDB 4.0: The human metabolome database for 2018. *Nucleic Acids Res.* **46**, D608–D617 (2018).
 114. Sajed, T. *et al.* ECMDDB 2.0: A richer resource for understanding the biochemistry of E. coli. *Nucleic Acids Res.* **44**, D495–D501 (2016).
 115. Wang, M. *et al.* Sharing and community curation of mass spectrometry data with Global Natural Products Social Molecular Networking. *Nat. Biotechnol.* **34**, 828–837 (2016).
 116. Kind, T. & Fiehn, O. Seven Golden Rules for heuristic filtering of molecular formulas obtained by accurate mass spectrometry. *BMC Bioinformatics* **8**, 1–20 (2007).
 117. O’Rourke, A. *et al.* Mechanism-of-action classification of antibiotics by global transcriptome profiling. *Antimicrob. Agents Chemother.* **64**, 1–15 (2020).
 118. Boshoff, H. I. M. *et al.* The transcriptional responses of Mycobacterium tuberculosis to inhibitors of metabolism. Novel insights into drug mechanisms of action. *J. Biol. Chem.* **279**, 40174–40184 (2004).
 119. Keesha E. Erickson, a Peter B. Otoupal, a A. C. Transcriptome-Level Signatures in Gene Expression and Gene Expression Variability during Bacterial Adaptive Evolution. *Am. Soc. Microbiol.* **2**, 1–17 (2017).
 120. Domínguez, Á. *et al.* Transcriptomics as a tool to discover new antibacterial targets. *Biotechnol. Lett.* **39**, 819–828 (2017).
 121. Wang, Z., Gerstein, M. & Snyder, M. RNA-Seq: a revolutionary tool for transcriptomics. *Nat. Rev. Genet.* **10**, 57–63 (2009).
 122. Royce, T. E., Rozowsky, J. S. & Gerstein, M. B. Toward a universal microarray: Prediction of gene expression through nearest-neighbor probe sequence identification. *Nucleic Acids Res.* **35**, 1–10 (2007).
 123. Lowe, R., Shirley, N., Bleackley, M., Dolan, S. & Shafee, T. Transcriptomics technologies. *PLoS Comput. Biol.* **13**, 1–23 (2017).

124. Denoeud, F. *et al.* Annotating genomes with massive-scale RNA sequencing. *Genome Biol.* **9**, (2008).
125. Wang, E. T. *et al.* Alternative isoform regulation in human tissue transcriptomes. *Nature* **456**, 470–476 (2008).
126. Yang, I. S. & Kim, S. Analysis of Whole Transcriptome Sequencing Data: Workflow and Software. *Genomics Inform.* **13**, 119 (2015).
127. Datsenko, K. A. & Wanner, B. L. One-step inactivation of chromosomal genes in *Escherichia coli* K-12 using PCR products. *Proc. Natl. Acad. Sci. U. S. A.* **97**, 6640–5 (2000).
128. Pinkert, L. *Synthese von Siderophor-Antibiotika- Konjugaten als neuartige antibakterielle Wirkstoffe.* Leibniz Universität Hannover (2021).
129. Hackel, M. A. *et al.* Reproducibility of broth microdilution MICs for the novel siderophore cephalosporin, cefiderocol, determined using iron-depleted cation-adjusted Mueller-Hinton broth. *Diagn. Microbiol. Infect. Dis.* **94**, 321–325 (2019).
130. Illumina. Preparing Samples for Sequencing Genomic DNA.
131. Aronesty, E. ea-utils : ‘Command-line tools for processing biological sequencing data’. <https://github.com/ExpressionAnalysis/ea-utils> (2011).
132. T., S. Snippy: fast bacterial variant calling from NGS reads. <https://github.com/tseemann/snippy>.
133. Aronesty, E. ea-utils : ‘Command-line tools for processing biological sequencing data’. (2011).
134. Tjaden, B. De novo assembly of bacterial transcriptomes from RNA-seq data. *Genome Biol.* **16**, 1–10 (2015).
135. Ritchie, M. E. *et al.* Limma powers differential expression analyses for RNA-sequencing and microarray studies. *Nucleic Acids Res.* **43**, e47 (2015).
136. Benjamini, Y. & Hochberg, Y. Controlling the False Discovery Rate: A Practical and Powerful Approach to Multiple Testing. *J. R. Stat. Soc. Series B* (**57**), 289–300 (1995).
137. Szklarczyk, D. *et al.* STRING v11: Protein-protein association networks with increased coverage, supporting functional discovery in genome-wide experimental datasets. *Nucleic Acids Res.* **47**, D607–D613 (2019).
138. Ruttkies, C., Schymanski, E. L., Wolf, S., Hollender, J. & Neumann, S. MetFrag relaunched: Incorporating strategies beyond in silico fragmentation. *J. Cheminform.* **8**, 1–16 (2016).
139. Keseler, I. M. *et al.* The EcoCyc database: Reflecting new knowledge about *Escherichia coli* K-12. *Nucleic Acids Res.* **45**, D543–D550 (2017).
140. Pang, Z., Chong, J., Li, S. & Xia, J. Metaboanalyst 3.0: Toward an optimized workflow for global metabolomics. *Metabolites* **10**, (2020).
141. Fresno, C. & Fernández, E. A. RDAVIDWebService: A versatile R interface to DAVID. *Bioinformatics* **29**, 2810–2811 (2013).
142. Otasek, D., Morris, J. H., Bouças, J., Pico, A. R. & Demchak, B. Cytoscape Automation: Empowering workflow-based network analysis. *Genome Biol.* **20**, 1–15 (2019).
143. Merico, D., Isserlin, R., Stueker, O., Emili, A. & Bader, G. D. Enrichment map: A network-based method for gene-set enrichment visualization and interpretation. *PLoS One* **5**, (2010).
144. Baba, T. *et al.* Construction of *Escherichia coli* K-12 in-frame, single-gene knockout mutants: The Keio collection. *Mol. Syst. Biol.* **2**, (2006).
145. Brzuszkiewicz, E. *et al.* How to become a uropathogen: Comparative genomic analysis of extraintestinal pathogenic *Escherichia coli* strains. *Proc. Natl. Acad. Sci.* **103**, 12879–12884 (2006).

146. Promega. BacTiter-Glo™ Microbial Cell Viability Assay. 67 (2012).
147. Puustinen, A., Finel, M., Haltia, T., Gennis, R. B. & Wikström, M. Properties of the Two Terminal Oxidases of *Escherichia coli*. *Biochemistry* **30**, 3936–3942 (1991).
148. J W Thomas, A Puustinen, J O Alben, R B Gennis, M. W. Substitution of asparagine for aspartate-135 in subunit I of the cytochrome bo ubiquinol oxidase of *Escherichia coli* eliminates proton-pumping activity. *Biochemistry* **32**, 10929–10928 (1993).
149. Abramson, J. *et al.* The structure of the ubiquinol oxidase from *Escherichia coli* and its ubiquinone binding site. *Nat. Struct. Biol.* **7**, 910–917 (2000).
150. Skare, J. T., Ahmer, B. M. M., Seachord, C. L., Darveau, R. P. & Postle, K. Energy transduction between membranes. TonB, a cytoplasmic membrane protein, can be chemically cross-linked in vivo to the outer membrane receptor FepA. *J. Biol. Chem.* **268**, 16302–16308 (1993).
151. Kasianowicz, J., Benz, R. & McLaughlin, S. The kinetic mechanism by which CCCP (carbonyl cyanide m-Chlorophenylhydrazone) transports protons across membranes. *J. Membr. Biol.* **82**, 179–190 (1984).
152. Bleuel, C. *et al.* TolC is involved in enterobactin efflux across the outer membrane of *Escherichia coli*. *J. Bacteriol.* **187**, 6701–6707 (2005).
153. Drawz, S. M. & Bonomo, R. A. Three decades of β -lactamase inhibitors. *Clin. Microbiol. Rev.* **23**, 160–201 (2010).
154. E Wald, J S Reilly, C D Bluestone, D. C. Sulbactam/ampicillin in the treatment of acute epiglottitis in children. *Rev Infect Dis.* **8**, S617-9 (1986).
155. Bergstrom, S. & Normark, S. β -Lactam resistance in clinical isolates of *Escherichia coli* caused by elevated production of the ampC-mediated chromosomal β -lactamase. *Antimicrob. Agents Chemother.* **16**, 427–433 (1979).
156. G Nicoletti , A Speciale, F Caccamo, F. R. Sulbactam/ampicillin in the treatment of otitis and sinusitis. *J Int Med Res* **19**, 29A-35A (1991).
157. Han, M.-L. *et al.* Comparative Metabolomics and Transcriptomics Reveal Multiple Pathways Associated with Polymyxin Killing in *Pseudomonas aeruginosa*. *mSystems* **4**, 1–18 (2019).
158. Stokes, J. M., Lopatkin, A. J., Lobritz, M. A. & Collins, J. J. Bacterial Metabolism and Antibiotic Efficacy. *Cell Metab.* **30**, 251–259 (2019).
159. Link, H., Fuhrer, T., Gerosa, L., Zamboni, N. & Sauer, U. Real-time metabolome profiling of the metabolic switch between starvation and growth. *Nat. Methods* **12**, 1091–1097 (2015).
160. Lempp, M. *et al.* Systematic identification of metabolites controlling gene expression in *E. coli*. *Nat. Commun.* **10**, (2019).
161. Yeang, C. H. Integration of metabolic reactions and gene regulation. *Mol. Biotechnol.* **47**, 70–82 (2011).
162. Tzeng, J., Lu, H. & Li, W. H. Multidimensional scaling for large genomic data sets. *BMC Bioinformatics* **9**, 1–17 (2008).
163. Perry, M. heatmaps: Flexible Heatmaps for Functional Genomics and Sequence Features. R package version 1.14.0. (2020).
164. Mehta, P., Casjens, S. & Krishnaswamy, S. Analysis of the lambdoid prophage element ϕ 14 in the *E. coli* K-12 genome. *BMC Microbiol.* **13**, 1–13 (2004).
165. Shirin Ansari, James C Walsh , Amy L Bottomley , Iain G Duggin , Catherine Burke, E. J. H. A newly identified prophage-encoded gene, ymfM, causes SOS-inducible filamentation in *Escherichia coli*. *J Bacteriol* *Bacteriol* (2021) doi:10.1128/JB.00646-20.
166. Lei Zheng, Yibin Lin, Shuo Lu, Jiazhe Zhang, and M. B. Biogenesis, transport and remodeling of lysophospholipids in

- Gram-negative bacteria. *Biochim Biophys Acta Mol Cell Biol Lipids* **1862**, 1404–1413 (2017).
167. Shah, P. & Swiatlo, E. A multifaceted role for polyamines in bacterial pathogens. *Mol. Microbiol.* **68**, 4–16 (2008).
 168. Charlier, D. & Glansdorff, N. Biosynthesis of Arginine and Polyamines. *EcoSal Plus* **1**, (2004).
 169. Charlier, D. & Bervoets, I. Regulation of arginine biosynthesis, catabolism and transport in Escherichia coli. *Amino Acids* **51**, 1103–1127 (2019).
 170. A G Tkachenko, M S Shumkov, A. V. A. Adaptive functions of Escherichia coli polyamines in response to sublethal concentrations of antibiotics. *Mikrobiologiya* **78**, 32–41 (2009).
 171. Ha, H. C. *et al.* The natural polyamine spermine functions directly as a free radical scavenger. *Proc. Natl. Acad. Sci. U. S. A.* **95**, (1998).
 172. Tkachenko, A. G., Akhova, A. V., Shumkov, M. S. & Nesterova, L. Y. Polyamines reduce oxidative stress in Escherichia coli cells exposed to bactericidal antibiotics. *Res. Microbiol.* **163**, 83–91 (2012).
 173. Schneider, B. L., Kiupakis, A. K. & Reitzer, L. J. Arginine catabolism and the arginine succinyltransferase pathway in Escherichia coli. *J. Bacteriol.* **180**, 4278–4286 (1998).
 174. Reitzer, L. Catabolism of Amino Acids and Related Compounds. *EcoSal Plus* **1**, (2005).
 175. Amato, S. M. *et al.* The role of metabolism in bacterial persistence. *Front. Microbiol.* **5**, 1–9 (2014).
 176. Peng, B. *et al.* Exogenous Alanine and/or Glucose plus Kanamycin Kills Antibiotic-Resistant Bacteria. *Cell Metab.* **21**, 249–262 (2015).
 177. Martínez, J. L. & Rojo, F. Metabolic regulation of antibiotic resistance. *FEMS Microbiol. Rev.* **35**, 768–789 (2011).
 178. Prestinaci, F., Pezzotti, P. & Pantosti, A. Antimicrobial resistance: A global multifaceted phenomenon. *Pathog. Glob. Health* **109**, 309–318 (2015).
 179. Nikaïdo, H. & Rosenberg, E. Y. Cir and Fiu proteins in the outer membranes of Escherichia coli catalyze transport of monomeric catechols: Study with β -lactam antibiotics containing catechol and analogous groups. *J. Bacteriol.* **172**, 1361–1367 (1990).
 180. Karlsson, M., Hannavy, K. & Higgins, C. F. ExbB acts as a chaperone-like protein to stabilize TonB in the cytoplasm. *Mol. Microbiol.* **8**, 389–396 (1993).
 181. Kampfenkel, K. & Braun, V. Topology of the ExbB protein in the cytoplasmic membrane of Escherichia coli. *J. Biol. Chem.* **268**, 6050–6057 (1993).
 182. Jana, B., Manning, M. & Postle, K. Mutations in the ExbB cytoplasmic carboxy terminus prevent energy-dependent interaction between the TonB and ExbD periplasmic domains. *J. Bacteriol.* **193**, 5649–5657 (2011).
 183. Wikström, M. *et al.* Mechanism of proton translocation by the respiratory oxidases. The histidine cycle. *BBA - Bioenerg.* **1187**, 106–111 (1994).
 184. Price, C. E. & Driessen, A. J. M. Biogenesis of membrane bound respiratory complexes in Escherichia coli. *Biochim. Biophys. Acta - Mol. Cell Res.* **1803**, 748–766 (2010).
 185. Alekshun, M. N. & Levy, S. B. Molecular Mechanisms of Antibacterial Multidrug Resistance. *Cell* **128**, 1037–1050 (2007).
 186. Keren, I., Kaldalu, N., Spoering, A., Wang, Y. & Lewis, K. Persister cells and tolerance to antimicrobials. *FEMS Microbiol. Lett.* **230**, 13–18 (2004).
 187. Wistrand-Yuen, E. *et al.* Evolution of high-level resistance during low-level antibiotic exposure. *Nat. Commun.* **9**, (2018).

188. Bryan, L. E. & Kwan, S. Roles of ribosomal binding, membrane potential, and electron transport in bacterial uptake of streptomycin and gentamicin. *Antimicrob. Agents Chemother.* **23**, 835–845 (1983).
189. Lázár, V. *et al.* Bacterial evolution of antibiotic hypersensitivity. *Mol. Syst. Biol.* **9**, (2013).
190. Lee, H. H., Molla, M. N., Cantor, C. R. & Collins, J. J. Bacterial charity work leads to population-wide resistance. *Nature* **467**, 82–85 (2010).
191. Brynildsen, M. P., Winkler, J. A., Spina, C. S., MacDonald, I. C. & Collins, J. J. Potentiating antibacterial activity by predictably enhancing endogenous microbial ROS production. *Nat. Biotechnol.* **31**, 160–165 (2013).
192. Liudmila Davydova, Nina Sanina, Svetlana Bakholdina, A. S. and A. Z. High relative content of lysophospholipids of *Helicobacter pylori* mediates increased risk for ulcer disease. *FEMS Immunol. Med. Microbiol.* **44**, 17–23 (2005).
193. Davydova, L., Stenkova, A., Sanina, N., Zabolotnaya, A. & Bakholdina, S. Effect of adaptive changes of lysophosphatidylethanolamine content on ampicillin resistance of *Yersinia pseudotuberculosis*. in *ACM International Conference Proceeding Series* 122–127 (2018). doi:10.1145/3301879.3301901.
194. Lebeaux, D. *et al.* pH-mediated potentiation of aminoglycosides kills bacterial persisters and eradicates in vivo biofilms. *J. Infect. Dis.* **210**, 1357–1366 (2014).
195. Deng, W. *et al.* L-lysine potentiates aminoglycosides against *Acinetobacter baumannii* via regulation of proton motive force and antibiotics uptake. *Emerg. Microbes Infect.* **9**, 639–650 (2020).
196. Kwon, D. H. & Lu, C. D. Polyamine effects on antibiotic susceptibility in bacteria. *Antimicrob. Agents Chemother.* **51**, 2070–2077 (2007).
197. Miller, C. *et al.* SOS response induction by β -lactams and bacterial defense against antibiotic lethality. *Science*. **305**, 1629–1631 (2004).
198. Podlesek, Z. & Žgur Bertok, D. The DNA Damage Inducible SOS Response Is a Key Player in the Generation of Bacterial Persister Cells and Population Wide Tolerance. *Front. Microbiol.* **11**, 1–8 (2020).
199. Dörr, T., Vulić, M. & Lewis, K. Ciprofloxacin causes persister formation by inducing the TisB toxin in *Escherichia coli*. *PLoS Biol.* **8**, 29–35 (2010).
200. Park, M. *et al.* Plasticity-Induced Growth of Dendritic Spines by Exocytic Trafficking from Recycling Endosomes. *Neuron* **52**, 817–830 (2006).
201. Su, Q., Guan, T., He, Y. & Lv, H. Siderophore Biosynthesis Governs the Virulence of Uropathogenic *Escherichia coli* by Coordinately Modulating the Differential Metabolism. *J. Proteome Res.* **15**, 1323–1332 (2016).
202. Karlsen, H. & Dong, T. Biomarkers of urinary tract infections: State of the art, and promising applications for rapid strip-based chemical sensors. *Anal. Methods* **7**, 7961–7975 (2015).
203. Xi, H., Schneider, B. L. & Reitzer, L. Purine catabolism in *Escherichia coli* and function of xanthine dehydrogenase in purine salvage. *J. Bacteriol.* **182**, 5332–5341 (2000).

Appendices

I. Summary of statistical results of whole genome sequencing for “recover” clones

Clone 3					
Fragments	495639	301	126417775	26.4	100
Written	494434				
Non-written	162				
Clone 4					
Fragments	678482	301	144121524	36.2	100
Written	676259				
Non-written	322				

II. Single nucleotide variants of “recover” clones and susceptibility

Clone	Type of variant	Gene	Mutation (DNA)	Mutation (protein)	MIC (µg/mL)			
					LP-600	Amp	Kan	CEF
R1	SNP	cyoB	G > A	Gly269Asp	2	16	2	0.125
R2	SNP	cyoB	G > A	Gly269Asp	2	16	2	0.125

III. Differentially expressed gene of CL1 and CL2

Symbol	Product	CL1_logFC	CL1_adj.P	CL2_logFC	CL2_adj.P	Sig
apt	adenine phosphoribosyltransferase	1.01	1.56E-02	-0.62	5.36E-02	CL1
arpA	ankyrin repeat protein	1.10	4.57E-02	-0.48	3.37E-01	CL1
blr	beta-lactam resistance membrane protein; divisome-associated protein	1.21	6.95E-03	0.10	8.32E-01	CL1
bsmA	bioflm peroxide resistance protein	-1.22	1.32E-02	0.42	3.50E-01	CL1
chpS	antitoxin of the ChpBS toxin-antitoxin system	-1.08	7.81E-04	0.09	6.80E-01	CL1

cnu	nucleoid-associated oriC-binding protein; H-NS and StpA stabilizing factor	1.22	1.18E-02	-0.37	3.72E-01	CL1
cstA	carbon starvation protein involved in peptide utilization; APC peptide transporter family protein	-1.12	3.46E-06	-0.07	6.96E-01	CL1
cysA	sulfate/thiosulfate transporter subunit	-1.04	8.08E-03	-0.01	9.77E-01	CL1
cysH	phosphoadenosine phosphosulfate reductase; PAPS reductase, thioredoxin dependent	-1.07	2.78E-02	0.03	9.42E-01	CL1
cysI	sulfite reductase, beta subunit, NAD(P)-binding, heme-binding	-1.10	8.83E-03	0.13	7.65E-01	CL1
dusC	tRNA-dihydrouridine synthase C	1.45	5.81E-03	-0.36	1.90E-01	CL1
ecpA	ECP pilin	-1.09	3.36E-02	0.29	5.46E-01	CL1
emrD	multidrug efflux system protein	1.24	1.84E-07	-0.29	2.05E-02	CL1
endA	DNA-specific endonuclease I	1.33	3.19E-03	0.41	2.03E-01	CL1
garP	putative (D)-galactarate transporter	-1.23	6.60E-04	-0.45	2.46E-01	CL1
gfcB	O-antigen capsule production lipoprotein	1.57	5.38E-03	0.21	6.73E-01	CL1
glnU	tRNA-Gln	-1.07	7.81E-04	0.29	1.84E-01	CL1
glnW	tRNA-Gln	-1.15	1.41E-04	0.43	3.29E-02	CL1
gpt	xanthine phosphoribosyltransferase; xanthine-guanine phosphoribosyltransferase	1.52	1.08E-04	-0.90	1.29E-03	CL1
gsk	inosine/guanosine kinase	1.05	2.11E-03	-0.61	3.16E-02	CL1
gtrA	CPS-53 (KpLE1) prophage; bactoprenol-linked glucose translocase (flippase)	1.06	2.91E-02	-0.61	1.20E-01	CL1
guaB	IMP dehydrogenase	1.03	8.83E-04	-0.12	6.74E-01	CL1
hycA	regulator of the transcriptional regulator FhIA	1.39	4.19E-05	0.84	3.17E-01	CL1
hycB	hydrogenase 3, Fe-S subunit	1.52	1.76E-04	0.15	8.53E-01	CL1
hydN	formate dehydrogenase-H, [4Fe-4S] ferredoxin subunit	1.42	7.52E-05	0.43	1.64E-01	CL1
intE	e14 prophage; putative integrase	1.10	8.67E-03	-0.08	8.82E-01	CL1
leuW	tRNA-Leu	-1.12	1.37E-03	0.10	7.13E-01	CL1
ligB	DNA ligase, NAD(+)-dependent	-1.09	1.63E-03	0.00	9.97E-01	CL1
lysQ	tRNA-Lys	1.52	1.27E-03	-0.44	1.20E-01	CL1
lysZ	tRNA-Lys	1.10	2.97E-04	-0.37	5.44E-02	CL1
metT	tRNA-Met	-1.04	5.86E-03	0.00	9.89E-01	CL1

metU	tRNA-Met	-1.05	1.53E-03	0.46	4.91E-02	CL1
mltF	membrane-bound lytic transglycosylase F, murein hydrolase	1.08	6.09E-03	-0.21	3.67E-01	CL1
mntP	putative Mn(2+) efflux pump, mntR-regulated	2.14	4.57E-03	-0.17	7.88E-01	CL1
mtr	tryptophan transporter of high affinity	-1.02	1.94E-03	0.14	4.97E-01	CL1
nikA	nickel-binding, heme-binding periplasmic protein	1.04	1.66E-02	0.03	9.54E-01	CL1
nupC	nucleoside (except guanosine) transporter	1.30	1.84E-07	-0.10	4.12E-01	CL1
puuA	glutamate--putrescine ligase	-1.15	1.06E-05	-0.45	3.95E-02	CL1
pyrD	dihydro-orotate oxidase, FMN-linked	1.15	4.71E-03	-0.58	2.74E-02	CL1
quuD	DLP12 prophage; putative antitermination protein	2.37	3.25E-02	1.19	1.85E-01	CL1
recE	Rac prophage; exonuclease VIII, 5' -> 3' specific dsDNA exonuclease	-1.29	5.34E-05	0.08	7.16E-01	CL1
recN	recombination and repair protein	1.40	1.84E-07	0.78	2.19E-04	CL1
rpsU	30S ribosomal subunit protein S21	1.13	9.10E-03	-0.43	2.61E-01	CL1
thrA	Bifunctional aspartokinase/homoserine dehydrogenase 1	-1.15	5.90E-05	-0.56	2.14E-02	CL1
tsx	nucleoside channel, receptor of phage T6 and colicin K	1.16	3.23E-06	0.23	1.27E-01	CL1
tusA	mnm(5)-s(2)U34-tRNA 2-thiolation sulfurtransferase	1.08	2.93E-02	-0.77	1.96E-02	CL1
umuC	DNA polymerase V, subunit C	1.01	1.41E-04	0.09	5.85E-01	CL1
wcaD	putative colanic acid polymerase	2.00	1.61E-02	0.09	8.96E-01	CL1
xylF	D-xylose transporter subunit	-1.18	3.48E-05	0.24	1.47E-01	CL1
xylG	fused D-xylose transporter subunits of ABC superfamily: ATP-binding components	-1.06	2.44E-03	0.39	1.52E-01	CL1
yahM	uncharacterized protein	1.40	1.08E-02	0.62	3.79E-01	CL1
yaiY	DUF2755 family inner membrane protein	-1.76	7.29E-04	-0.89	7.87E-03	CL1
ybaV	putative competence-suppressing periplasmic helix-hairpin-helix DNA-binding protein	-1.07	1.22E-03	0.10	6.36E-01	CL1
ybdD	DUF466 family protein	-1.03	2.64E-04	0.13	4.90E-01	CL1
ybjG	undecaprenyl pyrophosphate phosphatase	1.06	2.64E-04	-0.37	6.80E-02	CL1
ycaD	putative MFS-type transporter	1.37	2.13E-05	-0.66	2.60E-03	CL1
ycjW	LacI family putative transcriptional repressor	1.08	3.32E-02	-0.80	3.22E-02	CL1

ydiY	acid-inducible putative outer membrane protein	1.48	5.73E-05	-0.93	2.60E-03	CL1
yfcC	putative inner membrane transporter, C4-dicarboxylate anaerobic carrier family	1.17	1.52E-04	0.09	7.33E-01	CL1
yhjV	putative transporter	1.02	1.66E-02	-0.49	9.38E-02	CL1
ymfL	e14 prophage; putative DNA-binding transcriptional regulator	1.32	4.42E-02	-0.05	9.68E-01	CL1
ymfM	e14 prophage; uncharacterized protein	1.69	3.68E-02	-0.36	7.50E-01	CL1
ymgG	UPF0757 family protein	2.15	9.23E-03	-0.73	2.23E-02	CL1
ynaK	Rac prophage; conserved protein	1.77	3.33E-02	-0.08	8.95E-01	CL1
yoel	uncharacterized protein	1.38	5.60E-03	-0.95	5.14E-03	CL1
yqeI	putative transcriptional regulator	1.75	3.32E-02	-0.63	2.01E-01	CL1
yqiH	putative periplasmic pilin chaperone	2.39	1.20E-02	-0.18	8.38E-01	CL1
yqiI	fimbrial protein	1.59	3.40E-02	0.21	7.56E-01	CL1
ytfI	uncharacterized protein	1.03	3.47E-02	0.18	7.18E-01	CL1
asnA	asparagine synthetase A	-0.93	7.29E-04	1.18	3.71E-04	CL2
croE	e14 prophage; putative DNA-binding transcriptional regulator	0.65	3.15E-01	2.94	1.14E-02	CL2
cusF	periplasmic copper- and silver-binding protein	-0.47	6.31E-01	2.09	4.14E-02	CL2
cyoA	cytochrome o ubiquinol oxidase subunit II	-0.14	5.79E-01	-1.15	3.41E-04	CL2
essD	DLP12 prophage; putative phage lysis protein	0.99	2.77E-01	-1.30	4.27E-02	CL2
flxA	Qin prophage; uncharacterized protein	0.53	5.54E-01	-2.48	9.39E-03	CL2
fryB	putative enzyme IIB component of PTS	0.10	9.34E-01	2.02	1.69E-02	CL2
glnA	glutamine synthetase	-0.08	7.02E-01	-1.12	1.86E-04	CL2
glnK	nitrogen assimilation regulatory protein for GlnL, GlnE, and AmtB	-0.16	8.79E-01	-1.96	8.20E-03	CL2
ilvB	acetolactate synthase 2 large subunit	-0.08	7.78E-01	-1.11	3.41E-04	CL2
ilvX	uncharacterized protein	1.20	1.06E-01	-1.54	3.17E-02	CL2
lamB	maltose outer membrane porin (maltoporin)	1.03	6.80E-02	1.50	1.89E-02	CL2
lsrC	autoinducer 2 import system permease protein	-0.54	3.13E-01	1.01	4.51E-02	CL2
malE	maltose transporter subunit	-0.09	9.27E-01	2.18	1.31E-02	CL2
malF	maltose transporter subunit	0.37	5.38E-01	1.87	3.01E-03	CL2
malG	maltose transporter subunit	0.50	3.81E-01	1.11	2.23E-02	CL2

malK	fused maltose transport subunit, ATP-binding component of ABC superfamily/regulatory protein	0.86	3.21E-01	2.11	2.89E-02	CL2
mokB	regulatory peptide	-0.40	1.07E-01	1.02	3.38E-04	CL2
proM	tRNA-Pro	0.67	2.77E-01	-1.11	2.05E-02	CL2
pspD	peripheral inner membrane phage-shock protein	0.19	8.55E-01	1.02	3.61E-02	CL2
tisB	toxic membrane persister formation peptide, LexA-regulated	0.86	1.09E-03	1.44	4.36E-05	CL2
tnaB	tryptophan transporter of low affinity	-0.65	1.46E-01	1.08	1.68E-02	CL2
torC	trimethylamine N-oxide (TMAO) reductase I, cytochrome c-type subunit	0.56	9.68E-03	1.29	3.14E-02	CL2
uacT	uric acid permease	-0.26	5.50E-01	1.29	2.13E-02	CL2
uraA	uracil permease	0.66	4.99E-01	-1.51	4.17E-02	CL2
valV	tRNA-Val	1.00	3.75E-02	-1.28	2.13E-02	CL2
valW	tRNA-Val	0.90	5.00E-02	-1.22	2.47E-02	CL2
yahA	c-di-GMP-specific phosphodiesterase	1.03	7.90E-02	-1.79	6.45E-04	CL2
yahL	uncharacterized protein	0.54	3.94E-01	-1.61	4.17E-02	CL2
yigI	4HBT thioesterase family protein	-0.60	8.83E-03	-1.01	6.85E-04	CL2
yjcH	DUF485 family inner membrane protein	-0.32	5.46E-01	-1.06	9.55E-03	CL2
ymgA	RcsB connector protein for regulation of biofilm	-0.11	7.27E-01	-1.00	3.02E-02	CL2
bdm	biofilm-dependent modulation protein	-2.54	1.41E-04	-1.12	1.56E-02	both
yjiY	putative transporter	-1.01	2.10E-03	2.18	1.59E-04	both
ymfJ	e14 prophage; uncharacterized protein	1.54	1.37E-03	1.27	4.14E-02	both

IV. Significantly enriched terms in CL1 and CL2

Category	Term	Count	%	Genes	List Total	FDR	Sig	Reg
GOTERM_BP_DIR ECT	Maltodextrin transport	5	14.3	MALK, LAMB, MALG, MALF, MALE	24	4.41E-07	CL2	UP
GOTERM_CC_DIR ECT	Maltose transport complex	4	11.4	MALK, MALG, MALF, MALE	22	2.63E-05	CL2	UP

GOTERM_BP_DIRECTORY	Maltose transport	4	11.4	MALK, MALG, MALF, MALE	24	7.19E-05	CL2	UP
GOTERM_MF_DIRECTORY	Maltose-transporting atpase activity	3	8.6	MALK, MALG, MALF	21	0.00526	CL2	UP
UP_KEY_WORDS	Sugar transport	6	17.1	MALK, FRYB, LAMB, MALG, MALF, MALE	32	0.031789	CL2	UP

V. Differentially expressed gene of LH1 and LH2

Symbol	Product	LH1_logFC	LH1_adj.P	LH2_logFC	LH2_adj.P	Sig
aaeB	p-hydroxybenzoic acid efflux system component	1.15	3.56E-07	0.17	1.60E-01	LH1
aceE	pyruvate dehydrogenase, decarboxylase component E1, thiamine triphosphate-binding	-1.85	6.26E-10	-0.57	6.77E-04	LH1
aceF	pyruvate dehydrogenase, dihydrolipoyltransacetylase component E2	-1.65	6.62E-09	-0.65	4.15E-04	LH1
acrE	cytoplasmic membrane lipoprotein	3.99	5.16E-04	-0.17	8.57E-01	LH1
acrS	acrAB operon transcriptional repressor	2.13	4.39E-02	-1.42	2.68E-01	LH1
adk	adenylate kinase	-1.01	2.63E-10	-0.59	6.03E-07	LH1
aegA	putative oxidoreductase, FeS binding subunit/NAD/FAD-binding subunit	-2.18	2.01E-09	-0.70	2.63E-04	LH1
afuC	CP4-6 prophage; putative ferric transporter subunit	1.31	4.48E-05	0.09	6.18E-01	LH1
agaS	tagatose-6-phosphate ketose/aldose isomerase	1.27	1.46E-03	-0.63	6.37E-02	LH1
ahpF	alkyl hydroperoxide reductase, F52a subunit, FAD/NAD(P)-binding	-1.01	1.82E-07	0.57	1.69E-04	LH1
ais	putative LPS core heptose(II)-phosphate phosphatase	1.69	1.63E-02	1.14	1.40E-01	LH1
alaA	valine-pyruvate aminotransferase 2	-1.30	1.59E-10	-0.37	2.20E-04	LH1
alaC	valine-pyruvate aminotransferase 3	-2.19	1.93E-14	0.11	1.73E-01	LH1
aldA	aldehyde dehydrogenase A, NAD-linked	1.66	5.27E-09	0.72	1.36E-04	LH1
aldB	aldehyde dehydrogenase B	1.75	2.67E-09	0.53	2.59E-03	LH1
alx	putative membrane-bound redox modulator	1.15	1.77E-05	0.09	7.05E-01	LH1
ampC	penicillin-binding protein; beta-lactamase, intrinsically weak	-1.74	6.22E-09	-0.79	1.10E-04	LH1

ampG	muropeptide transporter	-1.18	8.12E-09	-0.47	2.17E-04	LH1
araC	ara regulon transcriptional activator; autorepressor	1.39	1.62E-10	-0.67	1.05E-06	LH1
araF	L-arabinose transporter subunit	-1.34	7.12E-09	-0.91	2.05E-07	LH1
araG	fused L-arabinose transporter subunits of ABC superfamily: ATP-binding components	-1.08	2.70E-07	-0.67	5.46E-06	LH1
argF	ornithine carbamoyltransferase 2, chain F; CP4-6 prophage	1.29	3.09E-08	0.33	1.04E-02	LH1
argI	ornithine carbamoyltransferase 1	2.39	1.02E-07	0.43	2.15E-01	LH1
argO	arginine transporter	-4.57	2.89E-14	-0.80	1.49E-04	LH1
argT	lysine/arginine/ornithine transporter subunit	1.79	7.92E-10	0.86	5.02E-06	LH1
argU	tRNA-Arg	1.26	2.48E-03	-0.87	3.67E-02	LH1
aroM	AroM family protein	2.04	8.74E-11	0.73	5.45E-06	LH1
arpA	ankyrin repeat protein	-1.32	6.16E-03	-0.60	1.76E-01	LH1
aslB	putative AslA-specific sulfatase-maturing enzyme	1.21	1.68E-05	-0.62	5.73E-04	LH1
asnU	tRNA-Asn	2.94	1.89E-05	-0.70	2.31E-01	LH1
asnV	tRNA-Asn	2.61	1.96E-04	-0.13	8.69E-01	LH1
aspC	aspartate aminotransferase, PLP-dependent	-1.18	2.81E-09	-0.74	2.72E-06	LH1
asr	acid shock-inducible periplasmic protein	1.15	2.99E-03	0.95	2.29E-02	LH1
bamE	lipoprotein component of BamABCDE OM biogenesis complex	1.72	4.38E-07	-0.91	8.10E-04	LH1
bax	putative glucosaminidase	1.78	2.20E-09	-0.43	6.08E-03	LH1
bdcA	c-di-GMP-binding biofilm dispersal mediator protein	1.53	3.40E-06	-0.43	3.39E-02	LH1
bdm	biofilm-dependent modulation protein	2.09	7.72E-05	-0.69	1.00E-01	LH1
bfd	bacterioferritin-associated ferredoxin	4.21	1.99E-11	-0.43	1.89E-03	LH1
bglH	carbohydrate-specific outer membrane porin, cryptic	1.63	2.23E-03	-0.63	2.38E-01	LH1
bioF	8-amino-7-oxononanoate synthase	1.18	4.15E-03	-0.99	2.74E-03	LH1
bsmA	biofilm peroxide resistance protein	1.95	4.51E-05	0.55	1.19E-01	LH1
cadA	lysine decarboxylase, acid-inducible	-8.92	1.68E-17	0.11	6.30E-01	LH1
cadB	putative lysine/cadaverine transporter	-8.37	2.24E-16	-0.74	9.04E-02	LH1
caiC	putative crotonobetaine/carnitine-CoA ligase	-1.17	1.74E-04	0.12	5.04E-01	LH1
caiE	stimulator of CaiD and CaiB enzyme activities	1.07	1.67E-02	0.24	4.65E-01	LH1

casA	CRISP RNA (crRNA) containing Cascade antiviral complex protein	1.25	4.44E-05	0.11	6.23E-01	LH1
ccmC	heme exporter subunit	-1.24	1.81E-06	-0.35	2.32E-02	LH1
ccmD	cytochrome c biogenesis protein	-1.33	1.09E-04	-0.44	4.74E-02	LH1
ccmE	periplasmic heme chaperone	-1.09	4.53E-05	-0.30	8.38E-02	LH1
cedA	cell division modulator	1.05	2.69E-02	-0.02	9.52E-01	LH1
chaA	calcium/sodium:proton antiporter	1.24	1.79E-06	-0.21	2.21E-01	LH1
chaC	cation transport regulator	1.47	1.19E-09	0.90	2.66E-07	LH1
chbA	N,N'-diacetylchitobiose-specific enzyme IIA component of PTS	1.50	9.16E-06	-0.31	1.38E-01	LH1
chbB	N,N'-diacetylchitobiose-specific enzyme IIB component of PTS	1.51	4.96E-07	-0.06	7.45E-01	LH1
chbC	N,N'-diacetylchitobiose-specific enzyme IIC component of PTS	1.53	1.95E-06	0.13	6.13E-01	LH1
chbF	phospho-chitobiase; general 6-phospho-beta-glucosidase activity	1.30	1.34E-07	-0.09	4.96E-01	LH1
chbR	repressor of chb operon for N,N'-diacetylchitobiose utilization	1.20	9.13E-06	-0.26	1.28E-01	LH1
cho	endonuclease of nucleotide excision repair	2.06	1.05E-08	-0.64	2.03E-03	LH1
chpS	antitoxin of the ChpBS toxin-antitoxin system	1.06	8.56E-05	-0.53	3.00E-03	LH1
citC	[citrate [pro-3S]-lyase] ligase	-3.22	1.82E-03	-1.60	2.02E-01	LH1
citD	citrate lyase, acyl carrier (gamma) subunit	-3.40	4.76E-04	-0.14	9.03E-01	LH1
citE	citrate lyase, citryl-ACP lyase (beta) subunit	-5.23	8.84E-05	0.05	9.66E-01	LH1
citF	citrate lyase, citrate-ACP transferase (alpha) subunit	-2.87	4.38E-07	0.35	2.27E-01	LH1
citX	apo-citrate lyase phosphoribosyl-dephospho-CoA transferase	-3.99	1.14E-05	0.24	6.52E-01	LH1
cohE	e14 prophage; repressor protein phage e14	1.80	2.90E-08	-0.34	7.15E-02	LH1
corA	magnesium/nickel/cobalt transporter	1.45	1.15E-08	0.26	3.19E-02	LH1
cpdB	2':3'-cyclic-nucleotide 2'-phosphodiesterase	-1.58	5.43E-11	-0.87	1.56E-07	LH1
cpsB	mannose-1-phosphate guanylyltransferase	1.69	6.78E-05	0.10	6.91E-01	LH1
cpsG	phosphomannomutase	1.31	2.20E-03	0.46	1.93E-01	LH1
cra	transcriptional repressor-activator for carbon metabolism	-1.44	3.14E-11	-0.66	1.74E-06	LH1
csgA	curlin subunit, amyloid curli fibers, cryptic	1.99	5.32E-04	0.50	1.58E-01	LH1

csgB	curlin nucleator protein, minor subunit in curli complex	2.49	2.70E-03	0.70	2.28E-01	LH1
cspA	RNA chaperone and antiterminator, cold-inducible	-1.07	9.18E-06	0.09	6.40E-01	LH1
cspB	Qin prophage; cold shock protein	-2.30	1.02E-06	0.41	2.26E-01	LH1
cspG	cold shock protein homolog, cold-inducible	-2.42	6.13E-06	0.38	3.96E-01	LH1
cvrA	putative cation/proton antiporter	-1.50	9.03E-06	-0.25	2.29E-01	LH1
cycA	D-alanine/D-serine/glycine transporter	1.26	1.43E-08	0.54	2.84E-04	LH1
cydB	cytochrome d terminal oxidase, subunit II	-1.54	6.05E-11	-0.88	1.25E-06	LH1
cydX	cytochrome d (bd-I) ubiquinol oxidase subunit X	-1.01	1.08E-07	-0.77	1.10E-06	LH1
cysP	thiosulfate-binding protein	1.12	1.33E-02	-0.01	9.79E-01	LH1
cysU	sulfate/thiosulfate ABC transporter permease	1.27	4.87E-03	0.75	1.34E-02	LH1
ddpB	D-ala-D-ala transporter subunit	1.29	7.20E-04	0.94	9.66E-04	LH1
ddpC	D-ala-D-ala transporter subunit	1.19	5.85E-03	0.54	4.62E-02	LH1
ddpD	D,D-dipeptide permease system, ATP-binding component	1.05	3.39E-03	0.80	1.50E-03	LH1
dicB	Qin prophage; cell division inhibition protein	2.77	1.14E-03	-0.10	9.12E-01	LH1
dinB	DNA polymerase IV	2.75	1.24E-14	0.11	2.27E-01	LH1
dinF	oxidative stress resistance protein; putative MATE family efflux pump; UV and mitomycin C inducible protein	2.01	2.02E-11	0.06	6.76E-01	LH1
dinG	ATP-dependent DNA helicase	1.15	4.64E-07	0.01	9.35E-01	LH1
dinI	DNA damage-inducible protein I	2.80	7.22E-11	-0.94	1.39E-03	LH1
dinJ	antitoxin of YafQ-DinJ toxin-antitoxin system	1.22	3.24E-06	-0.02	9.10E-01	LH1
dinQ	UV-inducible membrane toxin, DinQ-AgrB type I toxin-antitoxin system	1.43	1.66E-06	-0.15	4.29E-01	LH1
dksA	transcriptional regulator of rRNA transcription, DnaK suppressor protein	1.06	1.03E-08	0.47	1.92E-04	LH1
dmlA	D-malate oxidase, NAD-dependent; putative tartrate dehydrogenase	-1.33	9.26E-06	0.02	9.35E-01	LH1
dmsA	dimethyl sulfoxide reductase, anaerobic, subunit A	-6.32	1.79E-12	-0.19	3.91E-01	LH1
dmsB	dimethyl sulfoxide reductase, anaerobic, subunit B	-6.21	2.74E-10	0.21	3.76E-01	LH1
dmsC	dimethyl sulfoxide reductase, anaerobic, subunit C	-5.29	1.40E-11	0.16	4.39E-01	LH1
dmsD	twin-argininine leader-binding protein for DmsA and TorA	-2.32	1.07E-13	-0.22	8.69E-03	LH1

dppF	dipeptide transporter	1.00	2.09E-02	0.52	2.05E-01	LH1
dsdA	D-serine dehydratase	-1.09	2.70E-05	-0.60	1.87E-03	LH1
dsrB	uncharacterized protein	1.10	1.79E-02	0.33	5.10E-01	LH1
dtpC	dipeptide and tripeptide permease	-3.30	7.20E-11	-0.14	4.97E-01	LH1
dusB	tRNA-dihydrouridine synthase B	1.92	1.05E-10	0.07	6.13E-01	LH1
eamB	cysteine and O-acetylserine exporter	1.24	1.18E-03	0.15	4.46E-01	LH1
ebgR	transcriptional repressor	-1.02	2.15E-07	-0.76	4.19E-06	LH1
ecnB	entericidin B membrane lipoprotein	1.01	8.58E-06	1.00	2.06E-06	LH1
ecpA	ECP pilin	1.52	6.54E-04	-0.26	4.84E-01	LH1
ecpB	ECP production pilus chaperone	1.88	1.75E-03	-0.42	3.61E-01	LH1
ecpR	putative transcriptional regulator for the ecp operon	2.81	6.83E-04	-0.13	8.96E-01	LH1
efeB	deferrochelataase, periplasmic	2.10	8.48E-06	-0.38	6.04E-02	LH1
efeO	inactive ferrous ion transporter EfeUOB	2.61	1.00E-07	-0.16	3.57E-01	LH1
elfD	putative periplasmic pilin chaperone	1.41	4.46E-02	-0.42	5.43E-01	LH1
emrY	putative multidrug efflux system	1.04	6.16E-03	-0.24	6.00E-01	LH1
entA	2,3-dihydro-2,3-dihydroxybenzoate dehydrogenase	5.15	2.18E-10	-0.24	2.35E-01	LH1
entB	isochorismatase	5.40	5.71E-11	-0.27	2.00E-01	LH1
entC	isochorismate synthase 1	6.37	1.05E-12	-0.48	3.98E-03	LH1
entE	2,3-dihydroxybenzoate-AMP ligase component of enterobactin synthase multienzyme complex	6.27	4.78E-11	-0.06	8.10E-01	LH1
entF	enterobactin synthase multienzyme complex component, ATP-dependent	4.71	1.72E-12	0.06	7.79E-01	LH1
entH	enterobactin synthesis proofreading thioesterase	4.57	4.27E-07	-0.22	3.02E-01	LH1
entS	enterobactin exporter, iron-regulated	3.90	7.85E-13	-0.26	6.87E-03	LH1
erpA	iron-sulfur cluster insertion protein	1.25	2.96E-08	-0.19	1.36E-01	LH1
essQ	Qin prophage; putative S lysis protein	1.46	3.73E-02	0.42	6.59E-01	LH1
eutS	putative ethanol utilization carboxysome structural protein	1.33	2.31E-02	-0.90	3.67E-03	LH1
evgA	response regulator in two-component regulatory system with EvgS	-2.32	1.13E-08	-0.22	2.40E-01	LH1
evgS	hybrid sensory histidine kinase in two-component regulatory system with EvgA	-2.18	3.82E-09	0.35	3.45E-02	LH1

exbB	membrane spanning protein in TonB-ExbB-ExbD complex	2.37	2.67E-09	-0.48	1.72E-02	LH1
exbD	membrane spanning protein in TonB-ExbB-ExbD complex	2.84	1.01E-11	-0.25	4.82E-02	LH1
fabB	3-oxoacyl-[acyl-carrier-protein] synthase I	-1.35	6.39E-10	-0.04	7.70E-01	LH1
fadA	3-ketoacyl-CoA thiolase (thiolase I)	3.58	5.42E-10	0.97	9.10E-04	LH1
fadB	fused 3-hydroxybutyryl-CoA epimerase/delta(3)-cis-delta(2)-trans-enoyl-CoA isomerase/enoyl-CoA hydratase/3-hydroxyacyl-CoA dehydrogenase	4.00	1.31E-10	0.80	4.06E-03	LH1
fadH	2,4-dienoyl-CoA reductase, NADH and FMN-linked	2.95	8.89E-10	-0.40	6.37E-02	LH1
fadI	beta-ketoacyl-CoA thiolase, anaerobic, subunit	1.73	7.53E-07	0.46	4.35E-02	LH1
fadJ	fused enoyl-CoA hydratase and epimerase and isomerase/3-hydroxyacyl-CoA dehydrogenase	1.44	2.31E-06	0.84	6.26E-04	LH1
fadM	long-chain acyl-CoA thioesterase III	2.39	7.68E-07	-0.16	4.44E-01	LH1
fdhE	formate dehydrogenase formation protein	-1.19	1.82E-09	-0.05	6.14E-01	LH1
fdhF	formate dehydrogenase-H, selenopolypeptide subunit	-4.03	8.36E-15	-0.50	1.76E-04	LH1
fdnG	formate dehydrogenase-N, alpha subunit, nitrate-inducible	-4.00	3.90E-13	-0.88	4.95E-06	LH1
fdnH	formate dehydrogenase-N, Fe-S (beta) subunit, nitrate-inducible	-2.98	9.23E-11	-0.68	1.46E-04	LH1
fdnI	formate dehydrogenase-N, cytochrome B556 (gamma) subunit, nitrate-inducible	-2.37	1.73E-08	-0.17	2.87E-01	LH1
fdoG	formate dehydrogenase-O, large subunit	-1.59	5.89E-10	0.34	1.26E-02	LH1
fdoH	formate dehydrogenase-O, Fe-S subunit	-1.79	8.94E-10	0.41	8.77E-03	LH1
fdoI	formate dehydrogenase-O, cytochrome b556 subunit	-1.81	6.48E-10	0.43	5.01E-03	LH1
fdrA	putative NAD(P)-binding acyl-CoA synthetase	1.56	7.43E-04	-0.34	3.72E-01	LH1
feaR	transcriptional activator for tynA and feaB	1.88	2.04E-08	-0.48	5.62E-03	LH1
fecA	ferric citrate outer membrane transporter	1.53	1.07E-05	-0.04	8.37E-01	LH1
fecB	iron-dicitrate transporter subunit	1.23	2.93E-05	-0.33	3.23E-02	LH1
fecC	iron-dicitrate transporter subunit	1.06	2.14E-04	-0.58	1.54E-03	LH1
fecD	iron-dicitrate transporter subunit	1.20	1.95E-03	-0.32	1.40E-01	LH1
fecI	RNA polymerase, sigma 19 factor	3.37	4.94E-12	0.01	9.69E-01	LH1
fecR	FecI pro-sigma factor; transmembrane signal transducer for ferric citrate transport; periplasmic	3.56	2.86E-10	0.26	1.16E-01	LH1

	FecA:ferric citrate sensor and cytoplasmic FecI ECF sigma factor activator					
fepA	iron-enterobactin outer membrane transporter	4.53	9.82E-13	-0.77	1.63E-04	LH1
fepB	iron-enterobactin transporter subunit	3.47	4.68E-11	-0.09	4.62E-01	LH1
fepC	iron-enterobactin transporter subunit	3.06	7.07E-08	-0.44	9.78E-03	LH1
fepD	iron-enterobactin transporter subunit	2.72	1.72E-12	-0.54	3.30E-06	LH1
fepG	iron-enterobactin transporter subunit	2.85	2.21E-08	-0.56	8.73E-04	LH1
fes	enterobactin/ferric enterobactin esterase	5.41	2.69E-12	-0.06	6.87E-01	LH1
fetA	iron exporter, ATP-binding subunit, ABC transporter FetAB subunit; peroxide resistance protein	-1.22	3.34E-06	-0.43	2.07E-02	LH1
fetB	iron exporter permease subunit, ABC transporter FetAB; peroxide resistance protein	-1.55	6.56E-08	-0.09	5.91E-01	LH1
fhuA	ferrichrome outer membrane transporter	3.20	4.71E-14	0.01	9.14E-01	LH1
fhuB	fused iron-hydroxamate transporter subunits of ABC superfamily: membrane components	1.85	1.11E-05	0.22	3.45E-01	LH1
fhuC	iron-hydroxamate transporter subunit	1.97	6.02E-09	0.37	9.61E-03	LH1
fhuD	iron-hydroxamate transporter subunit	1.88	1.01E-07	0.10	5.20E-01	LH1
fhuE	ferric-rhodotorulic acid outer membrane transporter	4.08	7.90E-12	-0.05	7.21E-01	LH1
fhuF	ferric iron reductase involved in ferric hydroxamate transport	3.60	2.31E-13	-0.30	4.83E-02	LH1
fieF	ferrous iron and zinc transporter	1.04	6.23E-10	0.11	1.58E-01	LH1
fimC	periplasmic chaperone	2.39	4.44E-06	-0.85	2.51E-04	LH1
fimI	fimbrial protein involved in type 1 pilus biosynthesis	2.36	4.28E-06	-0.78	1.12E-03	LH1
fis	global DNA-binding transcriptional dual regulator	2.04	7.17E-09	0.28	7.84E-02	LH1
fiu	catecholate siderophore receptor Fiu	4.66	3.39E-09	0.08	7.50E-01	LH1
flgE	flagellar hook protein	-1.05	1.62E-03	-0.61	1.03E-02	LH1
flgF	flagellar component of cell-proximal portion of basal-body rod	-1.44	2.39E-03	-0.59	4.55E-02	LH1
fliE	flagellar basal-body component	1.33	3.71E-02	-0.57	2.45E-01	LH1
fliL	flagellar biosynthesis protein	-1.11	1.75E-02	-0.32	3.40E-01	LH1
fliN	flagellar motor switching and energizing component	-1.51	3.66E-02	0.59	2.44E-01	LH1
flu	CP4-44 prophage; antigen 43 (Ag43) phase-variable biofilm formation autotransporter	-1.31	1.32E-03	-0.51	9.91E-02	LH1
frdA	fumarate reductase (anaerobic) catalytic and NAD/flavoprotein subunit	-2.87	1.93E-14	-0.95	9.91E-08	LH1

frdB	fumarate reductase (anaerobic), Fe-S subunit	-2.93	2.89E-14	-0.63	1.30E-05	LH1
frdC	fumarate reductase (anaerobic), membrane anchor subunit	-2.90	1.79E-12	-0.55	7.13E-04	LH1
frdD	fumarate reductase (anaerobic), membrane anchor subunit	-2.93	1.92E-11	-0.59	1.96E-03	LH1
frlB	fructoselysine-6-P-deglycase	1.50	3.75E-09	0.26	6.23E-02	LH1
fruA	fused fructose-specific PTS enzymes: IIBcomponent/IIC components	1.64	8.70E-11	0.98	1.24E-07	LH1
fruB	fused fructose-specific PTS enzymes: IIA component/HPr component	2.53	1.22E-11	0.48	2.16E-03	LH1
fruK	fructose-1-phosphate kinase	2.04	4.10E-11	0.94	4.90E-07	LH1
fsaB	fructose-6-phosphate aldolase 2	-1.04	3.34E-04	-0.77	2.70E-04	LH1
fusA	protein chain elongation factor EF-G, GTP-binding	1.24	2.32E-09	0.51	4.04E-04	LH1
fxsA	suppressor of F exclusion of phage T7	1.39	1.95E-03	-0.97	2.10E-03	LH1
galM	aldose 1-epimerase; type-1 mutarotase	-1.11	7.27E-11	0.01	8.83E-01	LH1
galP	D-galactose transporter	-1.51	1.96E-10	0.24	1.43E-01	LH1
garK	glycerate kinase I	-1.12	2.72E-08	0.54	3.86E-05	LH1
garL	alpha-dehydro-beta-deoxy-D-glucarate aldolase	-1.74	1.91E-07	0.06	8.12E-01	LH1
garP	putative (D)-galactarate transporter	-1.07	2.32E-03	-0.20	5.56E-01	LH1
garR	tartronate semialdehyde reductase	-2.23	1.59E-10	0.28	9.02E-02	LH1
gatA	galactitol-specific enzyme IIA component of PTS	-1.40	8.35E-09	-0.76	5.75E-05	LH1
gatZ	D-tagatose 1,6-bisphosphate aldolase 2, subunit	-1.08	8.39E-08	-0.58	4.10E-04	LH1
gcvH	glycine cleavage complex lipoylprotein	-1.28	3.13E-10	0.46	9.01E-05	LH1
gcvP	glycine decarboxylase, PLP-dependent, subunit (protein P) of glycine cleavage complex	-1.46	7.59E-10	0.47	1.92E-03	LH1
gcvT	aminomethyltransferase, tetrahydrofolate-dependent, subunit (T protein) of glycine cleavage complex	-1.40	1.07E-12	0.41	3.52E-05	LH1
glcC	glycolate-inducible glc operon transcriptional repressor; autorepressor	1.04	1.74E-05	0.32	5.03E-02	LH1
glcF	glycolate oxidase 4Fe-4S iron-sulfur cluster subunit	1.22	1.21E-08	0.69	8.44E-06	LH1
gldA	glycerol dehydrogenase, NAD+ dependent; 1,2-propanediol:NAD+ oxidoreductase	-2.87	3.14E-12	-0.70	4.87E-05	LH1
glgA	glycogen synthase	-1.34	5.57E-09	0.19	1.48E-01	LH1
glgB	1,4-alpha-glucan branching enzyme	-1.18	4.71E-08	0.06	6.60E-01	LH1

glgC	glucose-1-phosphate adenylyltransferase	-1.31	4.24E-09	0.01	9.56E-01	LH1
glgP	glycogen phosphorylase	-1.34	1.35E-08	0.17	2.34E-01	LH1
glgS	motility and biofilm regulator	1.18	1.98E-04	-0.31	1.86E-01	LH1
glnA	glutamine synthetase	-1.24	2.45E-07	0.52	3.54E-03	LH1
glpC	anaerobic sn-glycerol-3-phosphate dehydrogenase, C subunit, 4Fe-4S iron-sulfur cluster	-1.46	4.10E-05	-0.77	1.77E-03	LH1
gltB	glutamate synthase, large subunit	-1.39	1.73E-04	-0.06	8.43E-01	LH1
glxR	tartronate semialdehyde reductase, NADH-dependent	1.48	3.35E-04	0.47	1.88E-01	LH1
glyV	tRNA-Gly	2.22	1.81E-10	-0.32	3.38E-02	LH1
glyX	tRNA-Gly	2.29	3.57E-10	-0.25	1.13E-01	LH1
glyY	tRNA-Gly	2.08	3.04E-07	-0.09	6.94E-01	LH1
gmd	GDP-D-mannose dehydratase, NAD(P)-binding	3.76	5.06E-07	0.27	5.25E-01	LH1
gnsA	putative phosphatidylethanolamine synthesis regulator	-1.41	1.82E-05	-0.12	7.23E-01	LH1
grxA	glutaredoxin 1, redox coenzyme for ribonucleotide reductase (RNR1a)	-1.87	1.17E-04	-0.23	6.46E-01	LH1
gsiA	glutathione transporter ATP-binding protein, ABC superfamily	-1.19	1.99E-05	0.70	2.35E-03	LH1
gsk	inosine/guanosine kinase	-1.21	7.72E-05	-0.45	3.66E-02	LH1
gspA	general secretory pathway component, cryptic	1.33	3.89E-04	0.11	7.21E-01	LH1
gspC	general secretory pathway component, cryptic	1.66	6.07E-03	0.27	7.45E-01	LH1
gss	fused glutathionylspermidine amidase/glutathionylspermidine synthetase	-1.17	4.30E-09	0.01	8.94E-01	LH1
guaB	IMP dehydrogenase	1.30	2.24E-06	-0.94	1.04E-04	LH1
guaD	guanine deaminase	-3.61	5.66E-14	-0.57	1.84E-04	LH1
gudD	(D)-glucarate dehydratase 1	-1.31	4.30E-09	0.29	7.60E-03	LH1
gudP	putative D-glucarate transporter	-1.36	7.84E-05	-0.16	4.49E-01	LH1
hcaR	hca operon transcriptional regulator	1.88	4.64E-09	-0.13	3.83E-01	LH1
hcp	hybrid-cluster [4Fe-2S-2O] protein in anaerobic terminal reductases	-3.79	1.97E-09	-0.55	1.54E-02	LH1
hcr	HCP oxidoreductase, NADH-dependent	-3.81	9.40E-11	-0.56	3.35E-03	LH1
hda	ATPase regulatory factor involved in DnaA inactivation	-1.14	1.26E-05	-0.91	4.14E-05	LH1

hha	modulator of gene expression, with H-NS	1.59	3.43E-04	-0.97	7.05E-03	LH1
hicA	mRNA interferase toxin of the HicAB toxin-antitoxin system	1.19	9.53E-05	-0.45	1.53E-02	LH1
hicB	antitoxin for the HicAB toxin-antitoxin system	1.14	3.01E-05	-0.52	3.84E-03	LH1
hinT	purine nucleoside phosphoramidase, dadA activator protein	-1.18	9.48E-10	0.34	7.65E-04	LH1
hlyE	hemolysin E	-1.96	3.36E-07	0.38	5.83E-02	LH1
hofO	DNA catabolic protein	-1.12	4.93E-03	-0.70	2.39E-03	LH1
hokB	toxic polypeptide, small	-1.24	2.74E-05	-0.73	1.54E-04	LH1
hokD	Qin prophage; small toxic polypeptide	1.50	3.04E-07	0.33	3.06E-02	LH1
hscC	Hsp70 family chaperone Hsc62, binds to RpoD and inhibits transcription	-1.26	1.51E-06	-0.46	6.97E-03	LH1
hslJ	heat-inducible lipoprotein involved in novobiocin resistance	1.80	1.63E-07	0.61	2.92E-03	LH1
hslO	heat shock protein Hsp33	1.03	4.38E-07	0.70	1.27E-05	LH1
hspQ	heat shock protein involved in degradation of mutant DnaA; hemimethylated oriC DNA-binding protein	2.36	2.99E-12	0.74	4.15E-06	LH1
hsrA	putative multidrug or homocysteine efflux system	-1.24	1.94E-06	-0.14	3.83E-01	LH1
htpX	putative endopeptidase	1.16	2.82E-08	-0.57	1.80E-04	LH1
htrE	putative outer membrane usher protein	1.55	1.47E-04	0.16	7.23E-01	LH1
hybD	maturation protease for hydrogenase 2	-3.24	6.44E-13	-0.84	5.78E-06	LH1
hybE	hydrogenase 2-specific chaperone	-3.31	3.88E-12	-0.81	1.75E-05	LH1
hybF	protein involved with the maturation of hydrogenases 1 and 2	-3.18	4.06E-11	-0.76	8.95E-05	LH1
hybG	hydrogenase 2 accessory protein	-2.98	1.14E-10	-0.59	1.71E-03	LH1
hycA	regulator of the transcriptional regulator Fh1A	-5.61	1.48E-09	0.37	5.31E-01	LH1
hycB	hydrogenase 3, Fe-S subunit	-4.88	2.24E-08	0.93	6.29E-02	LH1
hycC	hydrogenase 3, membrane subunit	-2.89	3.10E-09	0.19	3.75E-01	LH1
hycD	hydrogenase 3, membrane subunit	-2.27	5.74E-06	0.02	9.44E-01	LH1
hycE	hydrogenase 3, large subunit	-2.32	4.76E-09	0.20	1.81E-01	LH1
hycF	formate hydrogenlyase complex iron-sulfur protein	-1.89	8.99E-05	0.31	2.99E-01	LH1
hycG	hydrogenase 3 and formate hydrogenase complex, HycG subunit	-1.06	2.37E-04	0.32	5.13E-02	LH1

hydN	formate dehydrogenase-H, [4Fe-4S] ferredoxin subunit	-1.98	1.30E-07	0.18	4.10E-01	LH1
hyfH	hydrogenase 4, Fe-S subunit	-1.53	4.40E-04	0.38	9.15E-02	LH1
hypD	hydrogenase maturation protein	-3.41	8.40E-11	-0.57	4.05E-03	LH1
hypE	carbamoyl dehydratase, hydrogenases 1,2,3 maturation protein	-2.26	2.57E-12	0.21	3.15E-02	LH1
hypF	carbamoyl phosphate phosphatase and maturation protein for [NiFe] hydrogenases	-1.86	1.33E-10	-0.52	7.22E-05	LH1
ibpA	heat shock chaperone	2.72	4.55E-06	0.24	4.50E-01	LH1
ibpB	heat shock chaperone	3.53	2.08E-05	0.28	3.04E-01	LH1
infB	translation initiation factor IF-2	1.11	2.07E-07	0.32	3.43E-02	LH1
insJ	IS150 transposase A	1.52	1.00E-05	-0.21	3.80E-01	LH1
insK	IS150 transposase B	2.43	1.10E-06	-0.34	3.19E-01	LH1
iraM	RpoS stabilizer during Mg starvation, anti-RssB factor	1.99	3.97E-03	-0.13	8.84E-01	LH1
iraP	anti-RssB factor, RpoS stabilizer during Pi starvation; anti-adaptor protein	1.97	1.93E-06	-0.04	8.39E-01	LH1
iroK	3-hydroxypropionic acid resistance peptide	1.64	3.84E-04	-0.16	6.46E-01	LH1
iscA	FeS cluster assembly protein	1.19	1.97E-07	0.12	4.36E-01	LH1
iscR	isc operon transcriptional repressor; suf operon transcriptional activator; oxidative stress- and iron starvation-inducible; autorepressor	1.37	2.77E-08	-0.14	3.33E-01	LH1
iscU	iron-sulfur cluster assembly scaffold protein	1.05	5.43E-07	0.18	2.10E-01	LH1
ivbL	ilvB operon leader peptide	1.04	2.98E-03	0.86	3.95E-03	LH1
katG	catalase-peroxidase HPI, heme b-containing	-3.46	1.84E-15	-0.20	4.01E-02	LH1
kdgT	2-keto-3-deoxy-D-gluconate transporter	1.39	3.19E-05	-0.31	1.23E-01	LH1
kdpA	potassium translocating ATPase, subunit A	1.78	2.40E-05	-0.96	6.00E-03	LH1
kdpD	fused sensory histidine kinase in two-component regulatory system with KdpE; signal sensing protein	1.67	4.89E-10	-0.63	1.02E-04	LH1
kdpE	response regulator in two-component regulatory system with KdpD	1.09	1.56E-07	-0.14	1.95E-01	LH1
lacY	lactose permease	1.40	7.69E-04	0.09	8.31E-01	LH1
lamB	maltose outer membrane porin (maltoporin)	3.36	2.40E-08	-0.91	3.37E-02	LH1
ldrA	toxic polypeptide, small	-1.79	1.69E-03	-0.13	5.58E-01	LH1
ldtC	L,D-transpeptidase linking Lpp to murein	1.47	1.16E-06	0.63	1.68E-03	LH1

leuA	2-isopropylmalate synthase	1.91	3.18E-09	0.58	3.31E-04	LH1
leuB	3-isopropylmalate dehydrogenase, NAD(+)-dependent	1.57	3.23E-08	0.73	1.83E-05	LH1
leuC	3-isopropylmalate dehydratase large subunit	1.52	2.31E-06	0.69	7.98E-04	LH1
leuD	3-isopropylmalate dehydratase small subunit	1.49	6.76E-06	0.71	5.50E-04	LH1
leuL	leu operon leader peptide	1.70	1.24E-02	0.75	1.90E-01	LH1
leuP	tRNA-Leu	3.83	5.04E-05	1.16	2.13E-01	LH1
leuV	tRNA-Leu	3.98	5.01E-06	1.17	1.24E-01	LH1
lexA	transcriptional repressor of SOS regulon	1.99	1.54E-13	-0.30	1.37E-03	LH1
lit	e14 prophage; cell death peptidase, inhibitor of T4 late gene expression	2.26	1.11E-08	-0.31	1.97E-01	LH1
livJ	leucine/isoleucine/valine transporter subunit	2.20	1.49E-11	0.04	7.79E-01	LH1
lldD	L-lactate dehydrogenase, FMN-linked	1.28	6.79E-06	0.57	7.56E-03	LH1
lldP	L-lactate permease	2.00	3.50E-09	1.00	1.52E-05	LH1
lldR	dual role activator/repressor for lldPRD operon	1.23	2.22E-04	0.83	3.55E-03	LH1
lnt	apolipoprotein N-acyltransferase	-1.56	2.84E-09	0.36	9.37E-03	LH1
lolB	lipoprotein localization factor	-1.19	1.81E-10	0.06	4.62E-01	LH1
lolC	lipoprotein-releasing system transmembrane protein	-1.02	1.39E-07	-0.07	5.86E-01	LH1
lpd	lipoamide dehydrogenase, E3 component is part of three enzyme complexes	-1.06	6.52E-09	-0.35	2.23E-03	LH1
lpoB	OM lipoprotein stimulator of MrcB transpeptidase	-1.06	9.46E-09	0.57	1.70E-05	LH1
lpp	murein lipoprotein	-1.57	3.25E-09	0.06	7.21E-01	LH1
lsrA	autoinducer 2 import ATP-binding protein	1.90	7.50E-05	0.22	5.58E-01	LH1
lsrB	autoinducer 2-binding protein	1.02	3.21E-03	0.46	1.37E-01	LH1
lsrC	autoinducer 2 import system permease protein	1.65	3.62E-04	0.53	1.36E-01	LH1
lsrD	autoinducer 2 import system permease protein	1.59	3.87E-04	0.49	1.39E-01	LH1
lsrK	autoinducer-2 (AI-2) kinase	1.16	5.67E-04	0.43	1.36E-01	LH1
lsrR	lsr operon transcriptional repressor	1.11	5.24E-04	0.27	2.99E-01	LH1
lysA	diaminopimelate decarboxylase, PLP-binding	-3.97	1.99E-11	-0.68	1.66E-02	LH1
lysC	lysine-sensitive aspartokinase 3	-2.19	1.22E-11	0.07	5.51E-01	LH1
lysU	lysine tRNA synthetase, inducible	-1.06	7.26E-09	-0.34	3.08E-03	LH1

maa	maltose O-acetyltransferase	1.07	7.42E-04	-0.59	2.59E-02	LH1
maeB	malic enzyme: putative oxidoreductase/putative phosphotransacetylase	-1.06	2.92E-08	-0.62	4.95E-05	LH1
malF	maltose transporter subunit	3.04	8.69E-08	-0.79	2.72E-02	LH1
malG	maltose transporter subunit	2.47	7.66E-07	-0.43	1.86E-01	LH1
malM	maltose regulon periplasmic protein	3.31	1.19E-08	-0.23	4.57E-01	LH1
malS	alpha-amylase	1.75	3.56E-08	0.09	5.90E-01	LH1
marB	mar operon regulator, periplasmic	2.32	4.44E-09	-0.98	2.24E-04	LH1
mcrC	5-methylcytosine-specific restriction enzyme McrBC, subunit McrC	-2.11	1.98E-09	-0.84	7.08E-05	LH1
mdtH	multidrug resistance efflux transporter conferring overexpression resistance to norfloxacin and enoxacin	-2.58	4.54E-11	0.12	3.75E-01	LH1
menD	2-succinyl-5-enolpyruvyl-6-hydroxy-3-cyclohexene-1-carboxylate synthase; SEPHCHC synthase	-1.20	4.48E-09	-0.16	1.25E-01	LH1
menH	2-succinyl-6-hydroxy-2, 4-cyclohexadiene-1-carboxylate synthase	-1.01	2.92E-07	0.09	4.41E-01	LH1
metE	5-methyltetrahydropteroyltriglutamate-homocysteine S-methyltransferase	1.03	3.95E-03	0.37	1.12E-01	LH1
metK	S-adenosylmethionine synthetase	1.26	4.10E-06	-0.76	2.65E-04	LH1
mgtA	magnesium transporter	3.37	2.87E-11	-0.43	4.25E-02	LH1
minC	cell division inhibitor	-1.18	3.40E-11	-0.29	4.12E-04	LH1
minD	membrane ATPase of the MinC-MinD-MinE system	-1.12	2.09E-10	-0.23	7.61E-03	LH1
minE	cell division topological specificity factor	-1.21	5.57E-09	-0.21	3.79E-02	LH1
mlrA	transcriptional activator of csgD and csgBA	1.07	2.83E-07	0.56	1.04E-04	LH1
mltD	putative membrane-bound lytic murein transglycosylase D	1.44	6.39E-10	-0.50	2.20E-04	LH1
mltF	membrane-bound lytic transglycosylase F, murein hydrolase	1.13	5.43E-05	-0.48	1.76E-02	LH1
mngA	fused 2-O-a-mannosyl-D-glycerate specific PTS enzymes: IIA component/IIB component/IIC component	1.63	2.90E-05	0.02	9.30E-01	LH1
mntH	manganese/divalent cation transporter	2.18	8.54E-09	0.62	9.14E-03	LH1
mokB	regulatory peptide	-1.25	2.49E-05	-0.74	1.84E-04	LH1
mgo	malate dehydrogenase, FAD/NAD(P)-binding domain	1.32	2.24E-06	-0.05	7.92E-01	LH1

mqsA	antitoxin for MqsR toxin; transcriptional repressor	1.81	3.19E-06	-0.20	3.58E-01	LH1
mqsR	GCU-specific mRNA interferase toxin of the MqsR-MqsA toxin-antitoxin system; biofilm/motility regulator; anti-repressor	1.84	2.34E-06	0.03	8.76E-01	LH1
mraZ	RsmH methyltransferase inhibitor	1.10	6.56E-08	0.08	4.87E-01	LH1
mtgA	biosynthetic peptidoglycan transglycosylase	-1.08	7.16E-08	-0.93	5.47E-08	LH1
mtr	tryptophan transporter of high affinity	2.01	6.42E-08	-0.22	1.80E-01	LH1
nadA	quinolinate synthase, subunit A	1.52	4.75E-10	-0.21	8.29E-02	LH1
nagC	N-acetylglucosamine-inducible nag divergent operon transcriptional repressor	-1.11	3.31E-10	0.14	7.93E-02	LH1
nanA	N-acetylneuraminate lyase	1.40	1.05E-09	-0.09	5.12E-01	LH1
nanM	N-acetylneuraminic acid mutarotase	1.16	8.19E-09	0.95	9.68E-07	LH1
napC	quinol dehydrogenase, electron source for NapAB	-1.48	7.36E-06	-0.70	7.90E-04	LH1
narG	nitrate reductase 1, alpha subunit	-5.55	1.84E-15	0.34	7.46E-03	LH1
narH	nitrate reductase 1, beta (Fe-S) subunit	-4.80	1.84E-15	0.51	5.68E-05	LH1
narI	nitrate reductase 1, gamma (cytochrome b(NR)) subunit	-4.29	3.90E-13	0.39	6.84E-03	LH1
narJ	molybdenum-cofactor-assembly chaperone subunit (delta subunit) of nitrate reductase 1	-4.83	7.30E-14	0.38	4.39E-03	LH1
narK	nitrate/nitrite transporter	-3.94	5.37E-09	-0.21	3.65E-01	LH1
narQ	sensory histidine kinase in two-component regulatory system with NarP (NarL)	-1.27	2.78E-07	-0.45	1.40E-03	LH1
narV	nitrate reductase 2 (NRZ), gamma subunit	1.27	2.05E-06	0.59	1.56E-03	LH1
narW	nitrate reductase 2 (NRZ), delta subunit (assembly subunit)	1.08	9.87E-06	0.63	1.45E-03	LH1
ndk	multifunctional nucleoside diphosphate kinase and apyrimidinic endonuclease and 3'-phosphodiesterase	1.24	1.53E-07	-0.70	6.52E-05	LH1
nei	endonuclease VIII/5-formyluracil/5-hydroxymethyluracil DNA glycosylase	-1.70	4.58E-08	0.70	1.03E-04	LH1
nhaA	sodium-proton antiporter	1.33	9.42E-09	0.60	2.31E-04	LH1
nhaB	sodium:proton antiporter	-1.16	1.82E-09	-0.49	3.73E-05	LH1
nhoA	N-hydroxyarylamine O-acetyltransferase	1.16	4.02E-07	0.16	2.08E-01	LH1
nikB	nickel transporter subunit	-4.84	2.36E-08	-0.69	2.39E-03	LH1
nikC	nickel transporter subunit	-3.88	6.02E-11	-0.16	1.84E-01	LH1
nikD	nickel transporter subunit	-3.59	8.28E-10	-0.32	2.53E-02	LH1

nikE	nickel transporter subunit	-2.35	2.62E-08	-0.44	5.27E-03	LH1
nirB	nitrite reductase, large subunit, NAD(P)H-binding	-3.30	1.08E-11	-0.16	3.49E-01	LH1
nirD	nitrite reductase, NAD(P)H-binding, small subunit	-3.10	1.85E-07	-0.65	4.14E-02	LH1
nrdD	anaerobic ribonucleoside-triphosphate reductase	-1.39	5.06E-06	0.79	1.44E-03	LH1
nrdG	anaerobic ribonucleotide reductase activating protein	-1.73	1.16E-04	0.96	7.98E-04	LH1
nrdH	hydrogen donor for NrdEF electron transport system; glutaredoxin-like protein	5.02	5.57E-09	0.74	2.44E-04	LH1
nrdI	NrdEF cluster assembly flavodoxin	5.01	4.62E-10	0.76	1.25E-04	LH1
nrfA	nitrite reductase, formate-dependent, cytochrome	-5.52	3.75E-13	-0.38	5.26E-02	LH1
nrfB	nitrite reductase, formate-dependent, penta-heme cytochrome c	-6.00	5.05E-11	-0.61	3.08E-02	LH1
nrfC	formate-dependent nitrite reductase, 4Fe4S subunit	-6.00	2.98E-12	-0.50	4.01E-02	LH1
nrfD	formate-dependent nitrite reductase, membrane subunit	-5.57	4.81E-12	-0.37	7.60E-02	LH1
nrfE	heme lyase (NrfEFG) for insertion of heme into c552, subunit NrfE	-3.32	7.20E-11	0.27	1.23E-01	LH1
nrfF	heme lyase (NrfEFG) for insertion of heme into c552, subunit NrfF	-2.30	1.85E-05	0.21	5.12E-01	LH1
nrfG	heme lyase (NrfEFG) for insertion of heme into c552, subunit NrfG	-2.18	2.58E-05	0.07	8.20E-01	LH1
nth	DNA glycosylase and apyrimidinic (AP) lyase (endonuclease III)	1.57	1.60E-06	0.51	6.34E-03	LH1
ogrK	positive regulator of P2 growth (insertion of P2 ogr gene into the chromosome)	1.84	2.03E-04	-0.67	8.74E-02	LH1
ompC	outer membrane porin protein C	-1.26	6.37E-06	-0.28	2.10E-01	LH1
ompG	outer membrane porin G	2.89	4.86E-03	-0.13	9.21E-01	LH1
ompN	outer membrane pore protein N, non-specific	2.26	6.98E-05	0.74	1.48E-01	LH1
ompX	outer membrane protein X	1.17	3.24E-09	0.82	1.00E-06	LH1
oxc	oxalyl CoA decarboxylase, ThDP-dependent	1.02	1.28E-02	-0.37	3.57E-01	LH1
paaA	ring 1,2-phenylacetyl-CoA epoxidase subunit	1.47	9.37E-06	-0.07	8.51E-01	LH1
paaB	putative ring 1,2-phenylacetyl-CoA epoxidase subunit	1.47	1.51E-02	0.67	3.65E-01	LH1
paaC	ring 1,2-phenylacetyl-CoA epoxidase subunit	1.53	4.36E-05	0.95	9.04E-03	LH1
paaD	ring 1,2-phenylacetyl-CoA epoxidase subunit	1.23	5.63E-04	0.97	5.52E-03	LH1

paaG	1,2-epoxyphenylacetyl-CoA isomerase, oxepin-CoA-forming	1.20	1.88E-03	0.28	3.19E-01	LH1
paaJ	3-oxoadipyl-CoA/3-oxo-5,6-dehydrosuberil-CoA thiolase	1.02	9.42E-06	0.43	4.41E-03	LH1
paaZ	fused oxepin-CoA hydrolase/3-oxo-5,6-dehydrosuberil-CoA semialdehyde dehydrogenase	1.13	6.34E-04	0.13	5.27E-01	LH1
pck	phosphoenolpyruvate carboxykinase	-1.04	2.21E-08	-0.59	6.03E-05	LH1
pdxH	pyridoxine 5'-phosphate oxidase	-1.38	6.29E-10	-0.68	2.38E-06	LH1
pdxK	pyridoxal-pyridoxamine kinase/hydroxymethylpyrimidine kinase	-1.60	2.71E-09	-0.62	6.09E-05	LH1
pepD	aminoacyl-histidine dipeptidase (peptidase D)	-1.19	2.56E-10	-0.04	7.03E-01	LH1
pepT	peptidase T	-1.01	4.44E-09	0.14	1.39E-01	LH1
pgaA	biofilm adhesin polysaccharide PGA secretin; OM porin; poly-beta-1,6-N-acetyl-D-glucosamine export protein	-2.18	2.58E-06	-0.42	1.54E-01	LH1
pgaB	poly-beta-1,6-N-acetyl-D-glucosamine (PGA) N-deacetylase outer membrane export lipoprotein	-1.16	1.57E-03	-0.79	7.18E-03	LH1
pheA	chorismate mutase and prephenate dehydratase, P-protein	2.19	1.67E-09	0.89	7.18E-05	LH1
phnH	ribophosphonate triphosphate synthase subunit	2.48	5.25E-03	0.20	7.96E-01	LH1
phnL	ribophosphonate triphosphate synthase subunit; putative ABC transporter ATP-binding protein	1.26	1.48E-02	0.56	1.03E-01	LH1
phoA	bacterial alkaline phosphatase	1.39	5.26E-09	0.15	1.74E-01	LH1
phoE	outer membrane phosphoporin protein E	1.52	1.32E-02	0.50	5.31E-01	LH1
pinE	e14 prophage; site-specific DNA recombinase	4.59	1.44E-05	-1.13	2.84E-01	LH1
plaP	putrescine importer, low affinity	1.41	2.32E-07	-0.17	3.22E-01	LH1
pntA	pyridine nucleotide transhydrogenase, alpha subunit	-1.22	7.19E-10	-0.41	3.41E-04	LH1
pntB	pyridine nucleotide transhydrogenase, beta subunit	-1.23	1.16E-07	-0.22	1.38E-01	LH1
polB	DNA polymerase II	1.95	2.84E-12	0.71	1.86E-06	LH1
preA	dihydropyrimidine dehydrogenase, NADH-dependent, subunit C	-4.57	1.02E-14	-0.95	1.24E-05	LH1
priB	primosomal protein N	1.19	7.75E-08	0.18	2.07E-01	LH1
proV	glycine betaine transporter subunit	2.18	1.12E-07	-0.10	6.58E-01	LH1
proW	glycine betaine transporter subunit	2.64	2.21E-06	0.08	7.97E-01	LH1
proX	glycine betaine transporter subunit	2.54	1.99E-06	-0.38	1.73E-01	LH1

prpB	2-methylisocitrate lyase	4.81	1.54E-03	0.39	5.08E-01	LH1
prpC	2-methylcitrate synthase	2.70	3.33E-03	0.23	6.67E-01	LH1
prpD	2-methylcitrate dehydratase	1.83	2.39E-02	0.32	5.68E-01	LH1
prpE	propionate--CoA ligase	1.48	4.21E-05	0.15	4.06E-01	LH1
psiE	phosphate starvation inducible protein	1.09	1.81E-02	0.73	5.39E-02	LH1
pstS	periplasmic phosphate binding protein, high-affinity	1.29	7.28E-09	-0.28	1.66E-02	LH1
ptwF	tRNA-OTHER	2.00	5.46E-03	-0.49	3.70E-01	LH1
purD	phosphoribosylglycinamide synthetase phosphoribosylamine-glycine ligase	1.01	7.20E-06	0.30	1.14E-02	LH1
purT	phosphoribosylglycinamide formyltransferase 2	1.82	1.99E-06	0.04	7.41E-01	LH1
puuA	glutamate--putrescine ligase	1.02	7.51E-07	0.69	2.96E-04	LH1
puuD	gamma-glutamyl-gamma-aminobutyrate hydrolase	1.15	2.36E-08	0.51	1.02E-03	LH1
puuP	putrescine importer	1.29	1.25E-06	0.29	1.04E-01	LH1
racC	Rac prophage; uncharacterized protein	3.00	2.81E-03	-0.05	9.56E-01	LH1
ravA	hexameric AAA+ MoxR family ATPase, putative molecular chaperone	-1.43	6.73E-10	-0.11	2.97E-01	LH1
rbbA	ribosome-associated ATPase: ATP-binding protein/ATP-binding membrane protein	-1.76	4.64E-09	-0.17	3.15E-01	LH1
rbfA	30s ribosome binding factor	1.04	5.89E-06	0.35	2.01E-02	LH1
rbsD	putative cytoplasmic sugar-binding protein	1.07	6.33E-09	-0.76	1.19E-06	LH1
rclC	reactive chlorine species (RCS) stress resistance inner membrane protein	1.68	5.50E-04	0.22	6.40E-01	LH1
rcnA	membrane protein conferring nickel and cobalt resistance	1.32	8.57E-04	-0.97	6.91E-04	LH1
rcnB	periplasmic modulator of Ni and Co efflux	1.16	9.94E-05	-0.71	8.00E-03	LH1
rcaA	transcriptional regulator of colanic acid capsular biosynthesis	4.30	1.65E-05	0.08	8.80E-01	LH1
recA	DNA recombination and repair protein; ssDNA-dependent ATPase; synaptase; ssDNA and dsDNA binding protein forming filaments; ATP-dependent homologous DNA strand exchanger; recombinase A; LexA autocleavage cofactor	2.71	1.93E-14	-0.57	6.09E-06	LH1
recE	Rac prophage; exonuclease VIII, 5' -> 3' specific dsDNA exonuclease	1.06	1.77E-05	0.30	5.50E-02	LH1
recX	regulatory protein for RecA	3.48	1.80E-11	0.45	9.05E-02	LH1

relB	Qin prophage; bifunctional antitoxin of the RelE-RelB toxin-antitoxin system/ transcriptional repressor	1.41	4.25E-06	0.20	2.65E-01	LH1
relE	Qin prophage; toxin of the RelE-RelB toxin-antitoxin system	1.33	4.13E-08	0.24	6.33E-02	LH1
rhaT	L-rhamnose:proton symporter	1.48	1.94E-06	0.24	8.34E-02	LH1
rihA	ribonucleoside hydrolase 1	-1.28	9.62E-10	-1.00	3.16E-08	LH1
rimM	16S rRNA processing protein	1.34	2.64E-11	0.17	5.99E-02	LH1
rlmN	dual specificity 23S rRNA m(2)A2503, tRNA m(2)A37 methyltransferase, SAM-dependent	1.24	3.63E-06	0.60	2.36E-03	LH1
rluE	23S rRNA pseudouridine(2457) synthase	-1.17	3.26E-05	-0.26	1.53E-01	LH1
rmf	ribosome modulation factor	2.12	9.50E-10	0.71	1.94E-03	LH1
rmuC	DNA recombination protein	2.25	3.78E-13	-0.70	1.73E-06	LH1
rnI	CP4-57 prophage; RNase LS	-1.33	9.38E-09	-0.24	5.28E-02	LH1
rplA	50S ribosomal subunit protein L1	1.14	8.89E-10	0.20	5.28E-02	LH1
rplB	50S ribosomal subunit protein L2	1.83	2.76E-09	0.69	9.33E-04	LH1
rplC	50S ribosomal subunit protein L3	1.83	1.53E-09	0.59	2.12E-03	LH1
rplD	50S ribosomal subunit protein L4	1.79	2.89E-09	0.65	1.41E-03	LH1
rplE	50S ribosomal subunit protein L5	1.03	2.82E-09	0.21	4.71E-02	LH1
rplF	50S ribosomal subunit protein L6	1.46	2.80E-10	0.27	3.12E-02	LH1
rplI	50S ribosomal subunit protein L9	1.43	8.03E-10	0.30	1.52E-02	LH1
rplK	50S ribosomal subunit protein L11	1.01	6.58E-09	0.13	2.04E-01	LH1
rplM	50S ribosomal subunit protein L13	1.11	1.93E-09	0.30	6.72E-03	LH1
rplO	50S ribosomal subunit protein L15	1.79	7.66E-11	0.30	3.05E-02	LH1
rplP	50S ribosomal subunit protein L16	1.56	2.84E-08	0.61	2.28E-03	LH1
rplQ	50S ribosomal subunit protein L17	1.51	1.31E-09	0.33	1.91E-02	LH1
rplR	50S ribosomal subunit protein L18	1.69	2.12E-10	0.28	4.52E-02	LH1
rplS	50S ribosomal subunit protein L19	1.59	3.12E-11	0.42	1.62E-04	LH1
rplV	50S ribosomal subunit protein L22	1.76	2.07E-08	0.64	2.96E-03	LH1
rplW	50S ribosomal subunit protein L23	1.81	2.15E-09	0.69	5.58E-04	LH1
rpmC	50S ribosomal subunit protein L29	1.61	2.15E-08	0.61	1.84E-03	LH1
rpmD	50S ribosomal subunit protein L30	1.78	8.23E-11	0.25	5.26E-02	LH1

rpmE	50S ribosomal subunit protein L31	1.21	3.24E-08	0.76	9.64E-06	LH1
rPMF	50S ribosomal subunit protein L32	1.20	4.44E-09	0.47	3.12E-04	LH1
rpmH	50S ribosomal subunit protein L34	1.00	3.68E-04	-0.02	9.29E-01	LH1
rpmJ	50S ribosomal subunit protein L36	1.14	2.73E-09	0.38	1.00E-03	LH1
rpoA	RNA polymerase, alpha subunit	1.37	2.81E-09	0.34	1.71E-02	LH1
rpsB	30S ribosomal subunit protein S2	1.20	7.22E-11	0.04	6.54E-01	LH1
rpsC	30S ribosomal subunit protein S3	1.66	1.70E-08	0.64	2.44E-03	LH1
rpsD	30S ribosomal subunit protein S4	1.26	1.47E-09	0.33	8.58E-03	LH1
rpsE	30S ribosomal subunit protein S5	1.69	7.22E-11	0.24	6.09E-02	LH1
rpsF	30S ribosomal subunit protein S6	1.21	1.77E-08	0.17	1.86E-01	LH1
rpsG	30S ribosomal subunit protein S7	1.10	4.30E-10	0.48	4.95E-05	LH1
rpsH	30S ribosomal subunit protein S8	1.38	1.92E-10	0.32	6.37E-03	LH1
rpsI	30S ribosomal subunit protein S9	1.30	4.76E-10	0.36	2.78E-03	LH1
rpsJ	30S ribosomal subunit protein S10	1.84	5.60E-09	0.55	6.16E-03	LH1
rpsK	30S ribosomal subunit protein S11	1.11	3.79E-09	0.25	2.93E-02	LH1
rpsM	30S ribosomal subunit protein S13	1.04	4.37E-09	0.27	1.59E-02	LH1
rpsN	30S ribosomal subunit protein S14	1.16	2.04E-09	0.29	1.36E-02	LH1
rpsP	30S ribosomal subunit protein S16	1.22	1.20E-10	0.16	6.36E-02	LH1
rpsQ	30S ribosomal subunit protein S17	1.56	6.19E-08	0.64	1.54E-03	LH1
rpsR	30S ribosomal subunit protein S18	1.43	4.20E-09	0.27	3.79E-02	LH1
rpsS	30S ribosomal subunit protein S19	1.76	1.91E-08	0.68	1.46E-03	LH1
rrrQ	Qin prophage; putative lysozyme	2.53	4.83E-03	-0.03	9.76E-01	LH1
rseC	SoxR iron-sulfur cluster reduction factor component; with R _{sx} ABCDEG	-1.10	1.78E-06	0.09	5.48E-01	LH1
rspA	bifunctional D-altronate/D-mannonate dehydratase	3.76	4.54E-06	0.56	2.10E-01	LH1
rspB	putative Zn-dependent NAD(P)-binding oxidoreductase	4.03	9.60E-07	0.49	2.05E-01	LH1
rspR	transcriptional repressor for rspAB	-1.33	2.01E-07	-0.53	1.50E-03	LH1
rsxA	SoxR iron-sulfur cluster reduction factor component; inner membrane protein of electron transport complex	1.37	2.73E-09	-0.01	9.28E-01	LH1

rsxB	SoxR iron-sulfur cluster reduction factor component; putative iron-sulfur protein	1.38	7.53E-09	0.48	5.75E-04	LH1
rsxC	SoxR iron-sulfur cluster reduction factor component; putative membrane-associated NADH oxidoreductase of electron transport complex	1.73	4.12E-09	0.83	1.33E-05	LH1
rsxD	SoxR iron-sulfur cluster reduction factor component; putative membrane protein of electron transport complex	1.94	3.48E-06	0.56	2.11E-02	LH1
rsxE	SoxR iron-sulfur cluster reduction factor component; electron transport inner membrane NADH-quinone reductase	2.00	1.08E-07	0.27	1.20E-01	LH1
rsxG	SoxR iron-sulfur cluster reduction factor component; putative membrane protein of electron transport complex	1.76	1.14E-05	0.45	5.50E-02	LH1
rutE	putative malonic semialdehyde reductase	1.26	3.63E-02	0.61	1.25E-01	LH1
ruvA	component of RuvABC resolvase, regulatory subunit	1.67	6.44E-13	-0.23	4.01E-03	LH1
ruvB	ATP-dependent DNA helicase, component of RuvABC resolvase	1.19	3.40E-11	0.04	6.09E-01	LH1
rzoR	Rac prophage; putative lipoprotein	1.26	1.64E-02	0.22	5.58E-01	LH1
sbmC	DNA gyrase inhibitor	2.63	1.07E-13	0.73	1.21E-06	LH1
sbp	sulfate transporter subunit	2.52	8.66E-06	0.72	4.63E-02	LH1
sdaB	L-serine dehydratase 2	2.73	8.37E-09	0.75	5.05E-03	LH1
sdaC	putative serine transporter	2.16	8.88E-08	-0.21	4.50E-01	LH1
sdhA	succinate dehydrogenase, flavoprotein subunit	-1.08	2.39E-06	0.45	1.22E-02	LH1
sdhB	succinate dehydrogenase, FeS subunit	-1.06	2.73E-04	0.29	2.58E-01	LH1
sdiA	quorum-sensing transcriptional activator	1.86	2.01E-09	0.65	1.12E-03	LH1
secY	preprotein translocase membrane subunit	1.55	2.40E-10	0.36	9.59E-03	LH1
selC	tRNA-Sec	2.38	7.63E-03	-0.58	5.20E-01	LH1
serA	D-3-phosphoglycerate dehydrogenase	-1.43	1.11E-08	-0.28	4.65E-02	LH1
serS	seryl-tRNA synthetase, also charges selenocysteinyl-tRNA with serine	-1.49	4.52E-13	-0.11	1.58E-01	LH1
setC	putative arabinose efflux transporter	3.08	2.32E-03	0.08	9.12E-01	LH1
sfmD	putative outer membrane export usher protein	1.42	3.45E-06	-0.45	9.98E-02	LH1
sfmH	FimA homolog	2.22	4.00E-03	-0.78	3.35E-01	LH1
shoB	toxic membrane protein	1.00	1.24E-02	-0.57	1.16E-01	LH1

sixA	phosphohistidine phosphatase	1.11	1.40E-08	0.36	1.64E-03	LH1
smrA	DNA endonuclease	1.60	2.04E-06	0.06	7.72E-01	LH1
srlQ	D-arabinose 5-phosphate isomerase	-1.09	1.12E-06	-0.53	8.54E-04	LH1
stfP	e14 prophage; uncharacterized protein	5.53	8.34E-07	1.39	7.99E-02	LH1
stfQ	Qin prophage; putative side tail fiber assembly protein	1.25	6.15E-04	-0.32	1.83E-01	LH1
sthA	pyridine nucleotide transhydrogenase, soluble	-1.28	3.66E-09	0.25	4.05E-02	LH1
sugE	multidrug efflux system protein	-1.22	1.50E-07	0.44	3.12E-03	LH1
sulA	SOS cell division inhibitor	2.83	4.71E-14	-0.22	8.91E-02	LH1
symE	toxic peptide regulated by antisense sRNA symR	1.97	5.67E-06	-0.69	3.37E-02	LH1
tauB	taurine transporter subunit	1.24	2.61E-02	0.88	6.98E-03	LH1
tfaE	e14 prophage; putative tail fiber assembly protein	3.23	1.20E-07	-0.30	5.18E-01	LH1
tfaP	e14 prophage; uncharacterized protein	4.52	2.10E-08	-0.74	1.29E-01	LH1
thiC	phosphomethylpyrimidine synthase	-2.19	2.74E-09	-0.09	6.66E-01	LH1
thiE	thiamine phosphate synthase (thiamine phosphate pyrophosphorylase)	-2.03	1.26E-06	0.10	7.24E-01	LH1
thiF	adenylyltransferase, modifies ThiS C-terminus	-1.89	6.74E-06	-0.04	8.94E-01	LH1
thiG	thiamine biosynthesis ThiGH complex subunit	-1.79	3.11E-06	-0.14	6.11E-01	LH1
thiH	tyrosine lyase, involved in thiamine-thiazole moiety synthesis	-1.87	1.37E-06	-0.10	7.07E-01	LH1
thiK	thiamine kinase	-1.23	1.06E-06	0.27	6.87E-02	LH1
thiM	hydroxyethylthiazole kinase	-1.14	3.23E-08	-0.55	1.95E-05	LH1
thiS	immediate sulfur donor in thiazole formation	-1.87	5.46E-05	-0.02	9.62E-01	LH1
thrS	threonyl-tRNA synthetase	-1.42	3.98E-11	-0.17	8.56E-02	LH1
thrU	tRNA-Thr	1.03	2.19E-04	-0.92	4.33E-04	LH1
tisB	toxic membrane persister formation peptide, LexA-regulated	4.67	1.84E-15	-0.86	1.98E-05	LH1
tktA	transketolase I, thiamine triphosphate-binding	-1.10	4.30E-09	-0.95	1.86E-07	LH1
tomB	Hha toxicity attenuator; conjugation-related protein	1.37	1.32E-03	-0.85	2.38E-02	LH1
tonB	membrane spanning protein in TonB-ExbB-ExbD transport complex	2.20	9.67E-10	-0.63	3.05E-04	LH1
topB	DNA topoisomerase III	-1.08	2.61E-07	-0.42	4.17E-03	LH1

torS	hybrid sensory histidine kinase in two-component regulatory system with TorR	-1.52	7.35E-09	0.15	1.64E-01	LH1
torT	periplasmic sensory protein associated with the TorRS two-component regulatory system	-1.74	6.93E-08	-0.07	6.15E-01	LH1
torY	TMAO reductase III (TorYZ), cytochrome c-type subunit	1.72	5.24E-05	-0.13	6.45E-01	LH1
tpr	protamine-like protein	3.05	7.90E-08	-0.78	8.71E-02	LH1
trmD	tRNA m(1)G37 methyltransferase, SAM-dependent	1.56	1.43E-11	0.28	9.05E-03	LH1
trpD	fused glutamine amidotransferase (component II) of anthranilate synthase/anthranilate phosphoribosyl transferase	1.72	5.20E-06	0.72	2.59E-04	LH1
trpE	component I of anthranilate synthase	2.51	1.09E-07	0.42	7.88E-03	LH1
truB	tRNA pseudouridine synthase B: tRNA pseudouridine(55) synthase and putative tmRNA pseudouridine(342) synthase	1.01	1.49E-05	0.29	7.57E-02	LH1
tsaA	tRNA-Thr(GGU) m(6)t(6)A37 methyltransferase, SAM-dependent	-1.13	4.09E-05	-0.81	8.98E-04	LH1
tsf	translation elongation factor EF-Ts	1.04	4.20E-09	0.36	1.14E-03	LH1
tsgA	putative transporter	1.39	3.06E-04	0.52	3.47E-02	LH1
tusC	mnm(5)-s(2)U34-tRNA synthesis 2-thiolation protein	-1.23	1.42E-07	0.18	1.40E-01	LH1
tusD	sulfurtransferase for 2-thiolation step of mnm(5)-s(2)U34-tRNA synthesis	-1.00	4.22E-07	0.06	6.19E-01	LH1
ugd	UDP-glucose 6-dehydrogenase	1.37	2.54E-07	-0.13	4.04E-01	LH1
uhpB	sensory histidine kinase in two-component regulatory system with UhpA	1.31	2.87E-06	0.62	5.63E-04	LH1
uhpC	membrane protein regulates uhpT expression	1.58	6.57E-06	0.44	1.75E-02	LH1
uhpT	hexose phosphate transporter	3.47	5.71E-10	0.21	3.91E-01	LH1
uidA	beta-D-glucuronidase	1.61	2.21E-08	-0.23	1.74E-01	LH1
uidB	glucuronide transporter	1.49	6.53E-07	-0.18	3.43E-01	LH1
uidC	putative outer membrane porin for beta-glucuronides porin protein	1.86	4.57E-05	-0.04	9.21E-01	LH1
umuC	DNA polymerase V, subunit C	3.75	4.76E-15	-0.02	9.11E-01	LH1
umuD	DNA polymerase V, subunit D	3.58	7.40E-14	0.25	1.22E-01	LH1
uspC	universal stress protein	-1.48	1.47E-06	-0.59	9.44E-04	LH1
uvrB	excinuclease of nucleotide excision repair, DNA damage recognition component	1.36	1.56E-11	0.61	1.31E-06	LH1

uvrC	excinuclease UvrABC, endonuclease subunit	-1.50	6.80E-09	0.39	9.02E-03	LH1
uvrD	DNA-dependent ATPase I and helicase II	1.01	4.44E-09	0.37	6.07E-04	LH1
uvrY	response regulator in two-component regulatory system with BarA	-1.09	2.10E-08	-0.16	1.40E-01	LH1
uxuA	mannonate hydrolase	1.76	3.09E-11	-0.81	7.91E-07	LH1
uxuB	D-mannonate oxidoreductase, NAD-dependent	1.26	2.80E-07	-0.35	2.68E-02	LH1
valV	tRNA-Val	1.50	2.90E-05	-0.42	3.84E-01	LH1
valW	tRNA-Val	1.58	9.16E-06	-0.32	4.99E-01	LH1
viaA	stimulator of RavA ATPase activity; von Willebrand factor domain protein	-1.49	2.58E-10	0.40	4.96E-04	LH1
waaB	UDP-D-galactose:(glucosyl)lipopolysaccharide-1, 6-D-galactosyltransferase	1.34	8.56E-07	0.64	3.25E-04	LH1
waaG	glucosyltransferase I	1.28	6.68E-10	0.66	1.00E-06	LH1
waaH	LPS(HepIII)-glucuronic acid glycosyltransferase	1.29	7.84E-06	-0.10	7.29E-01	LH1
waaP	kinase that phosphorylates core heptose of lipopolysaccharide	1.28	3.30E-06	0.69	2.34E-04	LH1
waaR	UDP-D-galactose:(glucosyl)lipopolysaccharide-alpha-1,3-D-galactosyltransferase	1.13	1.80E-06	0.49	1.04E-03	LH1
waaS	lipopolysaccharide core biosynthesis protein	1.44	1.10E-06	0.85	3.12E-05	LH1
waaZ	lipopolysaccharide core biosynthesis protein	1.02	1.06E-05	0.49	1.94E-03	LH1
wcaA	putative glycosyl transferase	4.20	1.55E-05	-0.25	5.89E-01	LH1
wcaB	putative acyl transferase	2.41	8.32E-04	0.33	5.43E-01	LH1
wcaC	putative glycosyl transferase	1.88	7.89E-04	0.47	2.14E-01	LH1
wcaD	putative colanic acid polymerase	1.55	9.02E-04	0.19	6.77E-01	LH1
wcaE	putative glycosyl transferase	1.97	9.43E-03	-0.15	8.76E-01	LH1
wcaF	putative acyl transferase	3.45	2.60E-04	-0.81	4.99E-01	LH1
wcaG	bifunctional GDP-fucose synthetase: GDP-4-dehydro-6-deoxy-D-mannose epimerase/ GDP-4-dehydro-6-L-deoxygalactose reductase	2.51	3.71E-05	0.56	1.68E-01	LH1
wcaH	GDP-mannose mannosyl hydrolase	2.56	7.92E-04	-0.18	7.46E-01	LH1
wcaI	putative glycosyl transferase	2.18	6.75E-05	-0.31	3.38E-01	LH1
wcaJ	colanic biosynthesis UDP-glucose lipid carrier transferase	1.64	3.67E-04	0.44	1.46E-01	LH1
wcaK	colanic acid biosynthesis protein	1.14	6.71E-04	0.38	1.03E-01	LH1

wrbA	NAD(P)H:quinone oxidoreductase	-1.68	5.03E-11	0.77	2.43E-06	LH1
wza	colanic acid export protein; outer membrane auxillary lipoprotein	3.36	1.37E-04	-0.85	4.24E-01	LH1
wzb	colanic acid production protein-tyrosine-phosphatase; Wzc-P dephosphorylase	3.81	2.00E-05	-0.63	4.10E-01	LH1
wzc	colanic acid production tyrosine-protein kinase; autokinase; Ugd phosphorylase	3.29	1.99E-06	0.10	7.81E-01	LH1
wzxC	putative colanic acid exporter	1.02	4.92E-03	-0.06	8.25E-01	LH1
xanP	xanthine permease	1.88	4.73E-04	0.65	1.25E-02	LH1
xapA	purine nucleoside phosphorylase II	1.42	6.18E-04	-0.27	3.40E-01	LH1
xdhB	xanthine dehydrogenase, FAD-binding subunit	-4.26	4.81E-13	-0.95	7.53E-06	LH1
xdhC	xanthine dehydrogenase, Fe-S binding subunit	-3.58	4.86E-12	-0.81	5.78E-05	LH1
xisE	e14 prophage; putative excisionase	4.56	1.69E-10	-0.16	7.81E-01	LH1
xylH	D-xylose ABC transporter permease subunit	1.11	4.12E-05	-0.16	3.91E-01	LH1
yaaJ	putative transporter	-1.09	1.22E-05	0.11	5.51E-01	LH1
yaaX	DUF2502 family putative periplasmic protein	1.09	3.01E-02	-0.21	6.93E-01	LH1
yacH	uncharacterized protein	2.88	4.20E-09	0.06	7.29E-01	LH1
yadC	putative fimbrial-like adhesin protein	1.89	2.56E-05	0.07	9.10E-01	LH1
yadK	putative fimbrial-like adhesin protein	1.88	1.05E-04	-0.19	6.94E-01	LH1
yadL	putative fimbrial-like adhesin protein	1.30	4.80E-03	-0.35	5.20E-01	LH1
yadM	putative fimbrial-like adhesin protein	1.22	3.22E-02	0.92	1.74E-01	LH1
yadN	putative fimbrial-like adhesin protein	2.78	1.46E-02	-0.11	9.24E-01	LH1
yafE	putative S-adenosyl-L-methionine-dependent methyltransferase	-1.20	3.70E-08	0.38	1.50E-03	LH1
yafN	antitoxin of the YafO-YafN toxin-antitoxin system	1.95	1.64E-08	0.21	3.55E-01	LH1
yafO	mRNA interferase toxin of the YafO-YafN toxin-antitoxin system	1.57	1.08E-07	0.41	6.13E-02	LH1
yafP	putative acyl-CoA transferase	1.44	7.46E-06	0.64	5.80E-02	LH1
yafZ	CP4-6 prophage; conserved protein	-1.01	4.40E-03	0.82	1.09E-02	LH1
yagK	CP4-6 prophage; conserved protein	1.54	2.58E-05	-0.23	5.31E-01	LH1
yagL	CP4-6 prophage; DNA-binding protein	1.60	6.00E-03	0.17	7.99E-01	LH1
yagU	DUF1440 family inner membrane protein	-1.34	3.66E-08	-0.09	5.30E-01	LH1

yahA	c-di-GMP-specific phosphodiesterase	2.18	3.38E-06	-0.02	9.64E-01	LH1
yahD	ankyrin repeat protein	-1.59	3.26E-05	-0.77	3.97E-02	LH1
yahO	periplasmic protein, function unknown, YhcN family	1.57	8.09E-09	0.14	3.78E-01	LH1
yaiC	diguanylate cyclase, cellulose regulator	1.20	8.32E-04	0.84	3.75E-03	LH1
yaiY	DUF2755 family inner membrane protein	3.05	5.36E-08	-0.27	3.06E-01	LH1
ybaN	DUF454 family inner membrane protein	1.30	8.07E-06	-0.23	1.12E-01	LH1
ybaO	putative DNA-binding transcriptional regulator	1.19	8.29E-03	-0.76	3.37E-02	LH1
ybaQ	putative DNA-binding transcriptional regulator	2.07	4.24E-08	0.81	1.71E-04	LH1
ybbW	putative allantoin transporter	1.24	1.99E-02	-0.23	6.96E-01	LH1
ybcL	inactive polymorphonuclear leukocyte migration suppressor; DLP12 prophage; secreted protein, UPF0098 family	1.18	5.85E-03	0.94	6.50E-04	LH1
ybcM	DLP12 prophage; putative DNA-binding transcriptional regulator	1.18	4.34E-06	0.30	8.02E-02	LH1
ybdR	putative Zn-dependent NAD(P)-binding oxidoreductase	1.93	4.91E-09	0.98	4.43E-06	LH1
ybdZ	stimulator of EntF adenylation activity, MbtH-like	5.68	5.89E-09	0.22	1.28E-01	LH1
ybeD	UPF0250 family protein	1.74	9.45E-05	-0.02	9.61E-01	LH1
ybeR	uncharacterized protein	2.40	1.00E-02	-0.12	9.05E-01	LH1
ybeT	Sell family TPR-like repeat protein	1.46	3.57E-02	0.94	3.14E-01	LH1
ybeX	putative ion transport	-1.13	7.20E-11	0.36	1.64E-04	LH1
ybgD	putative fimbrial-like adhesin protein	1.96	1.22E-02	0.79	5.06E-01	LH1
ybgQ	putative outer membrane protein	2.38	3.92E-04	0.00	9.98E-01	LH1
ybhD	putative DNA-binding transcriptional regulator	1.53	2.35E-03	-0.11	7.75E-01	LH1
ybhH	putative PrpF family isomerase	3.71	2.47E-05	0.27	7.24E-01	LH1
ybhI	putative transporter	1.71	1.03E-03	0.11	7.71E-01	LH1
ybhJ	putative hydratase	1.18	2.00E-04	0.14	5.54E-01	LH1
ybiI	DksA-type zinc finger protein	2.52	6.79E-08	0.99	2.93E-06	LH1
ybiJ	DUF1471 family putative periplasmic protein	1.63	1.92E-08	0.37	3.80E-03	LH1
ybiW	putative pyruvate formate lyase	-1.69	5.41E-08	-0.11	4.74E-01	LH1
ybiX	Fe(II)-dependent oxygenase superfamily protein	3.08	8.30E-06	-0.08	7.28E-01	LH1
ybjH	uncharacterized protein	1.56	2.07E-07	-0.29	9.99E-02	LH1

ybjX	DUF535 family protein	-1.02	2.48E-06	-0.77	1.51E-04	LH1
ycaD	putative MFS-type transporter	-1.13	2.47E-06	-0.17	2.43E-01	LH1
ycaO	ribosomal protein S12 methylthiotransferase accessory factor	1.25	1.15E-05	0.84	1.62E-04	LH1
ycbJ	protein kinase-like domain protein	-2.07	1.81E-10	-0.64	8.45E-05	LH1
yccJ	uncharacterized protein	-1.40	4.94E-10	0.92	2.95E-07	LH1
yccM	putative 4Fe-4S membrane protein	-2.74	4.15E-07	-0.25	3.41E-01	LH1
ycdT	diguanylate cyclase, membrane-anchored	-1.21	3.96E-05	-0.85	1.92E-03	LH1
ycdU	putative inner membrane protein	2.21	5.14E-06	-0.35	4.28E-01	LH1
yceI	secreted protein	2.82	2.01E-07	0.73	2.33E-03	LH1
yceJ	putative cytochrome b561	2.57	2.06E-05	0.56	8.34E-02	LH1
ycfJ	uncharacterized protein	2.32	1.96E-10	-0.23	2.18E-01	LH1
ycfL	uncharacterized protein	-1.15	4.30E-10	0.38	1.26E-04	LH1
ycfP	putative UPF0227 family esterase	-1.12	3.32E-06	-0.28	9.88E-02	LH1
ycgY	uncharacterized protein	1.36	1.60E-04	1.00	5.53E-03	LH1
ychH	DUF2583 family putative inner membrane protein	1.59	3.49E-10	0.71	2.78E-05	LH1
yciT	global regulator of transcription; DeoR family	-1.04	6.99E-06	-0.87	1.21E-05	LH1
ydaF	Rac prophage; uncharacterized protein	1.29	4.61E-02	-0.20	7.04E-01	LH1
ydaM	diguanylate cyclase, csgD regulator	-1.20	1.96E-05	0.54	7.51E-03	LH1
ydcA	putative periplasmic protein	-1.05	4.65E-06	-0.82	2.42E-05	LH1
ydcC	H repeat-associated putative transposase	1.35	2.34E-03	-0.32	5.19E-01	LH1
ydcF	DUF218 superfamily protein, SAM-binding	1.37	3.32E-06	-0.21	2.55E-01	LH1
ydcI	putative DNA-binding transcriptional regulator	1.36	2.08E-07	0.59	8.38E-04	LH1
ydcS	polyhydroxybutyrate (PHB) synthase, ABC transporter periplasmic binding protein homolog	1.28	2.60E-07	0.45	8.47E-03	LH1
ydcX	DUF2566 family protein	1.10	2.34E-03	0.19	5.31E-01	LH1
yddG	aromatic amino acid exporter	-1.50	8.79E-04	-0.66	4.81E-02	LH1
yddH	flavin reductase like-protein	1.43	2.29E-06	-0.38	3.18E-02	LH1
yddM	putative DNA-binding transcriptional regulator	1.80	7.20E-11	0.49	3.55E-05	LH1
ydeO	UV-inducible global regulator, EvgA-, GadE-dependent	1.89	1.43E-02	1.16	1.78E-01	LH1

ydeP	putative oxidoreductase	1.71	7.69E-09	-0.06	7.14E-01	LH1
ydeQ	putative fimbrial-like adhesin protein	3.42	1.44E-05	-0.01	9.93E-01	LH1
ydeR	putative fimbrial-like adhesin protein	2.35	2.00E-06	-0.85	7.50E-02	LH1
ydeS	putative fimbrial-like adhesin protein	3.04	3.66E-05	-0.81	3.87E-01	LH1
ydfA	Qin prophage; uncharacterized protein	2.39	4.11E-05	0.22	6.74E-01	LH1
ydfB	Qin prophage; uncharacterized protein	3.15	6.38E-04	-1.20	1.39E-01	LH1
ydfC	uncharacterized protein, Qin prophage	1.87	2.14E-05	0.09	7.95E-01	LH1
ydfD	Qin prophage; uncharacterized protein	2.23	3.63E-03	0.39	5.30E-01	LH1
ydfI	putative NAD-dependent D-mannonate oxidoreductase	1.11	7.86E-05	0.12	5.44E-01	LH1
ydfO	Qin prophage; uncharacterized protein	-3.38	8.56E-05	-1.17	5.44E-02	LH1
ydfR	Qin prophage; uncharacterized protein	2.20	2.33E-03	-0.05	9.48E-01	LH1
ydfU	Qin prophage; uncharacterized protein	1.68	3.28E-04	0.13	7.97E-01	LH1
ydfZ	selenoprotein, function unknown	-2.57	6.98E-05	-0.14	6.55E-01	LH1
ydhT	FNR, Nar, NarP-regulated protein; putative subunit of YdhYVWXUT oxidoreductase complex	-2.33	9.37E-08	0.26	1.85E-01	LH1
ydhU	putative cytochrome b subunit of YdhYVWXUT oxidoreductase complex	-2.10	4.91E-09	0.15	3.19E-01	LH1
ydhV	putative oxidoreductase subunit	-4.54	6.90E-12	-0.41	7.86E-02	LH1
ydhW	FNR, Nar, NarP-regulated protein; putative subunit of YdhYVWXUT oxidoreductase complex	-3.24	4.38E-11	-0.03	8.69E-01	LH1
ydhX	putative 4Fe-4S ferridoxin-type protein; FNR, Nar, NarP-regulated protein; putative subunit of YdhYVWXUT oxidoreductase complex	-3.46	4.86E-12	0.00	9.79E-01	LH1
ydiB	quininate/shikimate 5-dehydrogenase, NAD(P)-binding	1.56	2.60E-04	-0.14	6.75E-01	LH1
ydiF	putative acetyl-CoA:acetoacetyl-CoA transferase: alpha subunit/beta subunit	1.75	1.24E-04	0.06	9.17E-01	LH1
ydiN	MFS transporter superfamily protein	1.84	7.98E-03	0.24	7.58E-01	LH1
ydiO	putative acyl-CoA dehydrogenase	1.56	6.73E-05	0.18	6.15E-01	LH1
ydiU	UPF0061 family protein	1.07	9.73E-05	0.45	2.85E-02	LH1
ydiV	anti-FlhD4C2 factor, inactive EAL family phosphodiesterase	-1.49	5.24E-08	0.16	3.91E-01	LH1
ydjE	putative transporter	1.56	2.41E-04	-0.07	8.63E-01	LH1
ydjF	putative DNA-binding transcriptional regulator	1.17	2.32E-03	-0.57	3.68E-02	LH1

ydjM	inner membrane protein regulated by LexA	1.86	3.91E-08	-0.38	1.61E-01	LH1
ydjO	uncharacterized protein	1.65	3.10E-02	-1.03	1.36E-01	LH1
yeaJ	putative diguanylate cyclase	1.42	2.14E-05	0.38	5.02E-02	LH1
yeaL	UPF0756 family putative inner membrane protein	-1.19	3.99E-06	-0.56	7.90E-04	LH1
yeaN	putative transporter	-1.03	2.99E-04	-0.27	1.06E-01	LH1
yebF	extracellular Colicin M immunity family protein	2.53	2.62E-14	0.40	1.89E-04	LH1
yebG	DNA damage-inducible protein regulated by LexA	2.88	7.37E-12	-0.51	7.20E-03	LH1
yebV	uncharacterized protein	2.07	5.42E-10	0.83	5.80E-06	LH1
yebW	uncharacterized protein	1.14	4.22E-07	0.87	9.76E-07	LH1
yecF	DUF2594 family protein	1.02	2.95E-02	0.16	7.78E-01	LH1
yecT	uncharacterized protein	1.51	3.03E-03	-0.68	1.73E-01	LH1
yeeA	putative transporter, FUSC family inner membrane protein	1.70	7.20E-12	0.50	2.05E-05	LH1
yeeD	putative TusA family sulfurtransferase	2.06	3.31E-04	0.43	2.03E-01	LH1
yeeE	UPF0394 family inner membrane protein	1.63	1.69E-04	-0.26	3.91E-01	LH1
yeeY	LysR family putative transcriptional regulator	1.37	1.03E-09	0.83	1.76E-07	LH1
yefM	antitoxin of the YoeB-YefM toxin-antitoxin system	2.13	4.40E-07	-0.63	4.15E-03	LH1
yegD	Hsp70 chaperone family protein	1.20	9.57E-06	0.93	5.78E-06	LH1
yegH	inner membrane protein	-1.17	3.00E-10	0.36	1.45E-04	LH1
yegJ	uncharacterized protein	1.63	4.17E-02	0.16	8.56E-01	LH1
yegK	ser/thr phosphatase-related protein	1.61	5.33E-03	-0.14	7.30E-01	LH1
yegL	VMA domain protein	1.21	4.36E-03	-0.39	1.64E-01	LH1
yegP	UPF0339 family protein	1.24	1.15E-06	0.87	2.84E-05	LH1
yegR	uncharacterized protein	1.17	1.06E-03	-0.23	5.10E-01	LH1
yegT	nucleoside transporter, low affinity	1.16	4.06E-06	-0.36	1.95E-02	LH1
yehC	putative periplasmic pilin chaperone	-4.47	4.90E-04	-0.75	5.23E-01	LH1
yehD	putative fimbrial-like adhesin protein	-5.74	5.67E-06	-0.80	7.70E-02	LH1
yehL	putative ABC superfamily transporter ATP-binding subunit	1.38	8.45E-03	0.66	1.96E-01	LH1
yeiG	S-formylglutathione hydrolase	-1.16	1.75E-07	-0.30	1.53E-02	LH1

yeiS	DUF2542 family protein	-1.26	7.60E-05	-0.24	3.34E-01	LH1
yfbO	uncharacterized protein	1.15	3.30E-02	-0.04	9.53E-01	LH1
yfbS	putative transporter	-1.50	2.21E-08	-0.51	3.65E-04	LH1
yfcC	putative inner membrane transporter, C4-dicarboxylate anaerobic carrier family	-2.77	5.80E-09	-0.06	7.56E-01	LH1
yfcI	transposase_31 family protein	1.05	1.00E-03	-0.26	3.23E-01	LH1
yfcZ	UPF0381 family protein	-2.37	4.76E-10	-0.61	8.72E-04	LH1
yfdQ	CPS-53 (KpLE1) prophage; uncharacterized protein	1.03	2.36E-02	0.55	2.00E-01	LH1
yfdX	uncharacterized protein	4.75	5.29E-06	-0.63	3.00E-01	LH1
yfeN	putative outer membrane protein	1.91	1.72E-04	0.04	9.16E-01	LH1
yffL	CPZ-55 prophage; uncharacterized protein	1.60	2.63E-03	-0.36	3.20E-01	LH1
yfhH	putative DNA-binding transcriptional regulator	1.50	8.58E-07	-0.52	9.19E-03	LH1
yfhL	putative 4Fe-4S cluster-containing protein	1.69	1.07E-03	-0.82	1.14E-01	LH1
yfhR	putative S9 family prolyl oligopeptidase	1.28	1.04E-04	-0.06	8.51E-01	LH1
yfiL	lipoprotein	1.11	3.53E-04	0.32	2.08E-01	LH1
yfiP	DTW domain protein	-1.09	7.99E-05	-0.08	6.60E-01	LH1
yfjJ	CP4-57 prophage; uncharacterized protein	1.60	3.94E-02	0.46	6.07E-01	LH1
yfjK	DEAD/H helicase-like protein, CP4-57 putative defective prophage	-1.54	2.55E-09	0.30	1.77E-02	LH1
yfjL	CP4-57 putative defective prophage, DUF4297/DUF1837 polymorphic toxin family protein	-1.88	3.45E-12	-0.22	1.52E-02	LH1
yfjS	CP4-57 prophage; uncharacterized protein	-1.15	4.77E-02	0.60	2.07E-01	LH1
yfjW	CP4-57 prophage; putative inner membrane protein	-1.80	2.19E-06	-0.45	3.33E-02	LH1
ygaC	uncharacterized protein	2.42	4.67E-09	0.47	1.07E-02	LH1
ygaH	putative L-valine exporter, norvaline resistance protein	-1.15	9.38E-07	-0.31	6.85E-03	LH1
ygcP	putative antiterminator regulatory protein	-2.47	5.11E-09	-0.88	3.95E-05	LH1
ygdI	DUF903 family verified lipoprotein	1.46	1.35E-07	0.84	1.28E-04	LH1
ygdR	DUF903 family verified lipoprotein	1.09	2.16E-07	0.11	4.31E-01	LH1
ygfF	putative NAD(P)-dependent oxidoreductase with NAD(P)-binding Rossmann-fold domain	-1.32	2.72E-08	0.36	1.48E-03	LH1
ygfI	putative DNA-binding transcriptional regulator	-1.22	1.83E-06	-0.22	3.69E-01	LH1

ygfQ	putative purine permease	-3.24	1.21E-12	-0.42	3.68E-03	LH1
ygfS	putative 4Fe-4S ferredoxin-type oxidoreductase subunit	-3.71	3.98E-10	-0.99	4.61E-05	LH1
yggE	oxidative stress defense protein	-1.25	2.73E-08	0.12	3.79E-01	LH1
yggM	DUF1202 family putative secreted protein	-2.69	2.75E-07	-0.84	4.94E-02	LH1
yghA	putative oxidoreductase	1.13	5.20E-05	0.85	7.52E-04	LH1
yghJ	DUF4092 family putative lipoprotein peptidase	-1.91	3.18E-13	0.50	3.67E-06	LH1
yghR	putative ATP-binding protein	1.20	3.25E-02	-0.25	5.97E-01	LH1
ygjH	putative tRNA binding protein; putative tRNA corner chaperone	2.19	7.25E-03	-0.51	3.97E-01	LH1
ygjI	putative transporter	1.10	1.81E-03	-0.13	7.06E-01	LH1
yhaB	uncharacterized protein	-3.21	4.17E-03	-1.29	2.38E-01	LH1
yhaM	putative L-serine dehydratase alpha chain	-1.71	2.81E-08	-0.13	4.13E-01	LH1
yhaO	putative transporter	-1.78	1.54E-08	-0.51	5.01E-03	LH1
yhbS	putative acyl-CoA transferase	-1.33	7.09E-08	-0.68	1.01E-04	LH1
yhbT	SCP-2 sterol transfer family protein	-1.26	1.50E-07	-0.70	9.11E-05	LH1
yhbV	U32 peptidase family protein	-4.66	6.37E-10	-0.27	2.07E-01	LH1
yhdJ	DNA adenine methyltransferase, SAM-dependent	1.57	1.48E-04	-0.64	3.07E-02	LH1
yhdN	DUF1992 family protein	1.24	4.17E-05	-0.32	6.35E-02	LH1
yhdV	putative outer membrane protein	2.13	7.07E-07	0.01	9.71E-01	LH1
yheO	putative PAS domain-containing DNA-binding transcriptional regulator	-1.07	3.18E-09	-0.18	4.53E-02	LH1
yhfK	putative transporter, FUSC superfamily inner membrane protein, tandem domains	-1.08	1.21E-08	-0.01	9.47E-01	LH1
yhfL	small lipoprotein	2.00	7.81E-04	0.88	4.84E-02	LH1
yhfW	phosphopentomutase-related metalloenzyme superfamily protein	1.05	2.82E-02	-0.60	8.94E-02	LH1
yhhI	putative transposase	1.10	1.14E-02	-0.52	2.80E-01	LH1
yhhJ	inner membrane putative ABC transporter permease	-1.54	3.45E-06	-0.19	3.54E-01	LH1
yhhQ	DUF165 family inner membrane protein	2.04	2.14E-08	-0.17	2.59E-01	LH1
yhil	putative membrane fusion protein (MFP) of efflux pump	-1.22	5.11E-10	-0.36	8.72E-04	LH1
yhjA	putative cytochrome C peroxidase	-3.49	7.20E-12	-0.46	3.46E-02	LH1

yhjB	putative DNA-binding transcriptional response regulator	2.11	4.98E-06	0.65	3.64E-02	LH1
yhjC	LysR family putative transcriptional regulator	1.25	3.20E-05	-0.77	2.51E-04	LH1
yhjH	cyclic-di-GMP phosphodiesterase, FlhDC-regulated	1.61	4.33E-03	-0.46	2.66E-01	LH1
yiaA	YiaAB family inner membrane protein, tandem domains	2.32	1.94E-02	-0.78	5.47E-01	LH1
yiaD	multicopy suppressor of bamB; outer membrane lipoprotein	1.20	1.72E-06	-0.05	7.96E-01	LH1
yiaU	putative DNA-binding transcriptional regulator	1.37	1.55E-03	-0.94	3.99E-03	LH1
yiaV	membrane fusion protein (MFP) component of efflux pump, signal anchor	2.09	9.96E-06	0.73	1.51E-02	LH1
yiaW	DUF3302 family inner membrane protein	2.92	3.45E-03	1.02	2.77E-01	LH1
yibA	HEAT-domain lethality reduction protein; putative immunity protein for putative polymorphic toxin RhsA	1.05	1.96E-02	-0.17	6.00E-01	LH1
yibG	TPR-like repeat protein	1.99	3.73E-02	-0.77	4.56E-01	LH1
yibT	uncharacterized protein	2.61	1.07E-12	0.75	7.11E-06	LH1
yicG	UPF0126 family inner membrane protein	-1.20	9.75E-05	0.83	9.61E-03	LH1
yicO	putative adenine permease	-1.95	8.83E-08	-0.24	2.10E-01	LH1
yicS	putative periplasmic protein	1.26	4.98E-02	1.05	1.38E-01	LH1
yidB	DUF937 family protein	1.26	1.26E-04	0.24	2.81E-01	LH1
yidF	putative Cys-type oxidative YidJ-maturing enzyme	-1.01	4.88E-05	-0.58	1.16E-03	LH1
yidZ	putative DNA-binding transcriptional regulator	-1.35	9.28E-05	-0.84	2.60E-03	LH1
yieE	phosphopantetheinyl transferase superfamily protein	-1.14	9.43E-07	0.54	1.05E-03	LH1
yieP	putative transcriptional regulator	-1.36	6.19E-07	-0.50	5.95E-03	LH1
yifE	UPF0438 family protein	1.06	3.66E-06	-0.42	7.27E-03	LH1
yigI	4HBT thioesterase family protein	1.37	1.78E-07	0.75	3.83E-04	LH1
yihO	putative transporter	1.27	3.32E-03	0.06	8.75E-01	LH1
yihT	putative aldolase	-1.02	9.15E-04	-0.48	1.98E-02	LH1
yihU	gamma-hydroxybutyrate dehydrogenase, NADH-dependent	-1.26	2.75E-03	-0.50	5.01E-02	LH1
yijE	EamA-like transporter family protein	-1.99	7.20E-11	-0.29	1.65E-02	LH1
yjaA	stress-induced protein	2.52	3.67E-05	-0.28	7.12E-01	LH1

yjbE	extracellular polysaccharide production threonine-rich protein	2.32	1.89E-05	0.08	8.66E-01	LH1
yjbF	extracellular polysaccharide production lipoprotein	1.13	4.30E-02	0.00	9.99E-01	LH1
yjbM	uncharacterized protein	1.65	2.70E-02	-0.13	8.94E-01	LH1
yjcB	putative inner membrane protein	3.00	6.06E-08	0.22	4.63E-01	LH1
yjcC	putative membrane-anchored cyclic-di-GMP phosphodiesterase	1.21	4.24E-08	0.83	4.30E-06	LH1
yjcD	inner membrane putative guanine permease	1.43	1.08E-07	-0.13	1.81E-01	LH1
yjcE	putative cation/proton antiporter	-1.16	4.76E-09	0.02	8.15E-01	LH1
yjcF	pentapeptide repeats protein	2.03	3.10E-02	-0.14	8.83E-01	LH1
yjcS	metallo-beta-lactamase superfamily protein	1.17	1.69E-02	-0.27	5.22E-01	LH1
yjdF	DUF2238 family inner membrane protein	-1.17	1.11E-05	0.13	4.50E-01	LH1
yjdK	uncharacterized protein	-1.24	2.01E-02	-0.79	2.61E-01	LH1
yjdM	zinc-ribbon family protein	1.14	2.56E-03	0.76	2.69E-03	LH1
yjdO	uncharacterized protein	-1.41	2.02E-02	-0.20	8.43E-01	LH1
yjdP	putative periplasmic protein	1.67	8.56E-07	-0.20	2.10E-01	LH1
yjeV	uncharacterized protein	3.57	5.73E-04	-0.65	5.46E-01	LH1
yjfN	DUF1471 family periplasmic protein	2.08	2.80E-04	0.28	5.01E-01	LH1
yjfZ	uncharacterized protein	1.80	6.06E-04	0.31	5.47E-01	LH1
yjgH	UPF0131 family protein	1.15	1.13E-05	0.46	1.72E-02	LH1
yjgL	uncharacterized protein	-1.05	3.32E-05	-0.58	6.04E-03	LH1
yjgN	DUF898 family inner membrane protein	1.17	2.79E-02	0.44	5.19E-01	LH1
yjgZ	uncharacterized protein	2.63	7.68E-03	-0.85	2.72E-01	LH1
yjhB	putative transporter	1.30	1.51E-06	0.41	2.35E-02	LH1
yjhC	putative oxidoreductase	1.41	4.93E-07	0.29	9.94E-02	LH1
yjhF	putative transporter	1.05	7.93E-04	-0.42	1.73E-01	LH1
yjiH	nucleoside recognition pore and gate family putative inner membrane transporter	-1.73	3.55E-03	-0.30	7.28E-02	LH1
yjiR	putative DNA-binding transcriptional regulator/putative aminotransferase	-1.05	1.22E-06	0.43	3.88E-03	LH1
yjiQ	putative transcriptional regulator	3.51	1.32E-03	0.75	5.54E-01	LH1
yjiW	putative pyruvate formate lyase activating enzyme	-4.08	8.38E-10	-0.63	4.10E-03	LH1

yjz	uncharacterized protein	5.80	1.26E-06	0.53	1.66E-02	LH1
ykgH	putative inner membrane protein	2.04	1.20E-02	1.10	2.86E-01	LH1
ykgL	uncharacterized protein	1.65	2.66E-02	0.01	9.91E-01	LH1
ykgM	50S ribosomal protein L31 type B; alternative L31 utilized during zinc limitation	3.26	2.66E-05	-0.91	2.24E-01	LH1
yliE	putative membrane-anchored cyclic-di-GMP phosphodiesterase	-1.55	1.36E-07	-0.29	6.85E-02	LH1
ymcE	cold shock gene	-1.93	7.46E-05	-0.09	8.94E-01	LH1
ymfD	e14 prophage; putative SAM-dependent methyltransferase	1.68	9.62E-08	-0.90	8.63E-04	LH1
ymfI	e14 prophage; uncharacterized protein	1.82	1.01E-06	-0.69	6.47E-03	LH1
ymfL	e14 prophage; putative DNA-binding transcriptional regulator	4.01	8.38E-10	-1.17	2.22E-01	LH1
ymfM	e14 prophage; uncharacterized protein	4.54	1.94E-09	-0.63	4.86E-01	LH1
ynaK	Rac prophage; conserved protein	1.20	1.18E-02	-0.63	1.95E-01	LH1
ynbB	putative CDP-diglyceride synthase	4.12	1.09E-04	1.32	2.33E-01	LH1
yncE	ATP-binding protein, periplasmic, function unknown	4.04	4.71E-14	-0.66	8.98E-05	LH1
yncG	glutathione S-transferase homolog	1.53	3.71E-03	0.95	1.18E-02	LH1
yneE	bestrophin family putative inner membrane protein	-1.12	8.79E-03	-0.45	2.11E-01	LH1
yneM	inner membrane-associated protein	2.09	4.27E-06	0.66	1.64E-01	LH1
ynfD	DUF1161 family periplasmic protein	1.42	1.14E-05	0.30	1.50E-01	LH1
ynfE	putative selenate reductase, periplasmic	-5.13	1.83E-12	-0.99	6.78E-05	LH1
ynfF	S- and N-oxide reductase, A subunit, periplasmic	-5.52	1.60E-14	-0.63	5.45E-04	LH1
ynfG	oxidoreductase, Fe-S subunit	-5.01	1.84E-12	-0.71	1.59E-03	LH1
ynfH	oxidoreductase, membrane subunit	-3.95	6.25E-13	-0.40	1.38E-02	LH1
ynfK	putative dethiobiotin synthetase	-2.95	8.25E-08	-0.80	3.69E-03	LH1
yoaC	DUF1889 family protein	1.73	2.01E-09	0.99	1.45E-06	LH1
yoaE	putative membrane protein/conserved protein	-1.25	2.50E-08	-0.05	7.03E-01	LH1
yobH	uncharacterized protein	1.48	5.51E-04	-0.64	9.87E-02	LH1
yoeb	toxin of the YoeB-YefM toxin-antitoxin system	2.13	5.17E-07	-0.48	1.46E-02	LH1
yoel	uncharacterized protein	1.46	1.51E-05	-0.34	2.14E-01	LH1

yojI	microcin J25 efflux pump, TolC-dependent; fused ABC transporter permease and ATP-binding components	2.24	6.30E-10	-0.44	1.20E-03	LH1
ypdA	sensor kinase regulating yhjX; pyruvate-responsive YpdAB two-component system	-1.03	1.36E-07	0.23	2.67E-02	LH1
ypeC	DUF2502 family putative periplasmic protein	2.64	4.07E-07	-0.93	3.03E-03	LH1
ypfG	DUF1176 family protein	2.05	2.38E-09	-0.50	2.06E-03	LH1
ypfM	stress-induced small enterobacterial protein	-1.15	4.70E-03	-0.90	3.60E-03	LH1
yqaE	cyaR sRNA-regulated protein	2.01	4.08E-09	0.99	1.74E-05	LH1
yqeA	putative amino acid kinase	-4.39	1.64E-14	-0.64	1.28E-04	LH1
yqhD	aldehyde reductase, NADPH-dependent	-2.01	2.35E-12	-0.23	2.19E-02	LH1
yqiK	PHB family membrane protein, function unknown	1.08	5.82E-04	-0.93	9.15E-04	LH1
yqjH	putative siderophore interacting protein	3.01	6.65E-09	-0.74	6.24E-05	LH1
yqjI	PadR family putative transcriptional regulator	1.17	1.77E-04	-0.20	2.78E-01	LH1
yrbL	Mg(2+)-starvation-stimulated protein	1.20	1.56E-09	0.66	9.90E-06	LH1
yrhB	stable heat shock chaperone	2.15	1.37E-03	0.46	4.28E-01	LH1
ysaA	putative hydrogenase, 4Fe-4S ferredoxin-type component	-1.89	2.28E-05	-0.54	2.82E-02	LH1
ysaB	uncharacterized protein	1.41	7.28E-05	0.94	6.10E-03	LH1
ytfH	DUF24 family HxIR-type putative transcriptional regulator	1.30	1.99E-04	0.46	2.19E-02	LH1
ytfJ	putative transcriptional regulator	2.58	2.54E-10	-0.61	3.10E-04	LH1
ytfK	DUF1107 family protein	1.73	2.04E-08	0.97	3.21E-05	LH1
zraP	Zn-dependent periplasmic chaperone	2.42	2.89E-03	0.63	1.73E-01	LH1
zwf	glucose-6-phosphate 1-dehydrogenase	1.04	3.18E-09	0.31	2.20E-03	LH1
aceA	isocitrate lyase	0.08	7.00E-01	1.10	2.84E-04	LH2
aceK	isocitrate dehydrogenase kinase/phosphatase	-0.26	1.48E-01	1.02	1.14E-04	LH2
add	adenosine deaminase	-0.12	4.75E-01	-1.39	1.28E-06	LH2
ahr	aldehyde reductase, NADPH-dependent, Zn-containing, broad specificity	0.65	1.96E-05	1.15	5.21E-08	LH2
aidB	DNA alkylation damage repair protein; flavin-containing DNA binding protein, weak isovaleryl CoA dehydrogenase	-0.14	5.02E-01	2.11	5.73E-08	LH2
alaE	alanine exporter, alanine-inducible, stress-responsive	-0.74	1.33E-04	-1.23	5.04E-07	LH2

alsA	fused D-allose transporter subunits of ABC superfamily: ATP-binding components	0.52	1.41E-01	-1.06	2.99E-03	LH2
alsB	D-allose transporter subunit	0.57	5.86E-03	-1.60	1.85E-07	LH2
amyA	cytoplasmic alpha-amylase	0.37	2.57E-03	1.16	3.62E-08	LH2
aphA	acid phosphatase/phosphotransferase, class B, non-specific	-0.20	5.55E-02	-1.26	2.70E-09	LH2
appA	phosphoanhydride phosphorylase	-0.86	2.70E-05	1.17	2.33E-07	LH2
argH	argininosuccinate lyase	0.23	1.29E-01	1.13	2.38E-07	LH2
argR	l-arginine-responsive arginine metabolism regulon transcriptional regulator	-0.19	4.54E-01	-1.11	1.21E-04	LH2
arnA	fused UDP-L-Ara4N formyltransferase/UDP-GlcA C-4'-decarboxylase	0.87	5.42E-05	1.51	6.99E-08	LH2
arnB	uridine 5'-(beta-1-threo-pentapyranosyl-4-ulose diphosphate) aminotransferase, PLP-dependent	0.72	1.32E-03	1.65	1.99E-07	LH2
arnC	undecaprenyl phosphate-L-Ara4FN transferase	0.93	5.43E-05	2.21	3.06E-09	LH2
aroA	5-enolpyruvylshikimate-3-phosphate synthetase	-0.46	6.77E-04	1.19	1.93E-08	LH2
arsR	arsenical resistance operon transcriptional repressor; autorepressor	0.57	2.04E-01	-1.25	7.95E-05	LH2
asnA	asparagine synthetase A	0.24	2.03E-01	-1.98	4.07E-08	LH2
aspA	aspartate ammonia-lyase	-0.93	4.52E-05	-1.07	4.95E-05	LH2
aspT	tRNA-Asp	0.71	9.30E-04	1.07	9.59E-07	LH2
atoS	sensory histidine kinase in two-component regulatory system with AtoC	-0.57	3.03E-03	-1.24	1.76E-07	LH2
baeS	sensory histidine kinase in two-component regulatory system with BaeR	0.24	4.45E-01	1.14	7.57E-05	LH2
betA	choline dehydrogenase, a flavoprotein	0.22	5.21E-01	1.32	5.53E-04	LH2
betB	betaine aldehyde dehydrogenase, NAD-dependent	0.54	3.30E-02	1.45	1.93E-05	LH2
bioC	malonyl-ACP O-methyltransferase, SAM-dependent	0.87	4.81E-02	-1.05	4.24E-03	LH2
bioD	dethiobiotin synthetase	0.81	1.12E-02	-1.10	2.20E-04	LH2
borD	DLP12 prophage; putative lipoprotein	-0.44	5.36E-02	-2.92	8.52E-09	LH2
btuD	vitamin B12 transporter subunit : ATP-binding component of ABC superfamily	-0.27	6.44E-02	1.05	2.98E-07	LH2
carA	carbamoyl phosphate synthetase small subunit, glutamine amidotransferase	-1.00	2.89E-01	-3.54	4.78E-04	LH2
carB	carbamoyl-phosphate synthase large subunit	-0.47	5.42E-01	-2.90	5.17E-04	LH2

cbdX	putative cytochrome bd-II oxidase subunit	-0.87	1.72E-03	1.56	1.65E-07	LH2
cbpA	DnaK co-chaperone; curved DNA-binding protein	-0.80	2.40E-04	1.21	7.91E-06	LH2
cbpM	modulator of CbpA co-chaperone	-0.79	1.62E-03	1.16	2.63E-05	LH2
cfa	cyclopropane fatty acyl phospholipid synthase (unsaturated-phospholipid methyltransferase)	0.21	1.44E-01	1.16	1.68E-06	LH2
chaB	cation transport regulator	0.59	1.22E-03	1.43	4.86E-08	LH2
clsB	cardiolipin synthase 2	-0.65	3.49E-03	1.48	7.08E-07	LH2
cmoB	tRNA (cmo5U34)-carboxymethyltransferase, carboxy-SAM-dependent	-0.84	1.03E-06	1.04	3.50E-08	LH2
coaA	pantothenate kinase	-0.35	1.42E-01	-1.23	2.91E-05	LH2
codB	cytosine transporter	0.27	7.48E-01	-1.63	4.87E-03	LH2
csrA	pleiotropic regulatory protein for carbon source metabolism	0.67	2.68E-05	1.29	2.38E-08	LH2
cyoA	cytochrome o ubiquinol oxidase subunit II	0.42	2.66E-02	1.26	3.67E-06	LH2
cyoB	cytochrome o ubiquinol oxidase subunit I	0.34	1.51E-01	1.37	1.84E-05	LH2
cyoC	cytochrome o ubiquinol oxidase subunit III	0.63	1.81E-02	1.20	1.93E-04	LH2
cyoD	cytochrome o ubiquinol oxidase subunit IV	0.59	2.25E-02	1.14	2.23E-04	LH2
cyoE	protoheme IX farnesyltransferase	0.41	5.87E-02	1.15	4.30E-05	LH2
cysB	N-acetylserine-responsive cysteine regulon transcriptional activator; autorepressor	-0.24	4.07E-02	-1.08	7.26E-08	LH2
cysC	adenosine 5'-phosphosulfate kinase	0.87	1.66E-01	2.38	2.03E-05	LH2
cysD	sulfate adenylyltransferase, subunit 2	1.04	7.35E-02	1.42	3.70E-03	LH2
cysJ	sulfite reductase, alpha subunit, flavoprotein	0.59	9.05E-02	1.16	1.50E-03	LH2
cysM	cysteine synthase B (O-acetylserine sulfhydrylase B)	0.77	6.49E-03	1.40	2.92E-06	LH2
cysN	sulfate adenylyltransferase, subunit 1	0.79	7.88E-02	1.92	1.80E-04	LH2
dadA	D-amino acid dehydrogenase	0.08	4.71E-01	1.08	2.38E-07	LH2
dadX	alanine racemase, catabolic, PLP-binding	0.04	8.13E-01	1.25	1.17E-06	LH2
dbpA	ATP-dependent RNA helicase, specific for 23S rRNA	0.03	8.59E-01	1.05	2.59E-07	LH2
dctA	C4-dicarboxylic acid, orotate and citrate transporter	-0.38	1.96E-02	-1.13	2.87E-06	LH2
dps	Fe-binding and storage protein; stress-inducible DNA-binding protein	0.55	2.80E-03	1.57	4.30E-07	LH2
dsdC	dsd operon activator; autorepressor	0.54	2.02E-02	-1.25	1.64E-06	LH2

dsdX	D-serine transporter	-0.85	2.14E-03	-1.22	6.12E-06	LH2
elaB	DUF883 family protein, putative membrane-anchored ribosome-binding protein	0.75	1.30E-04	1.08	4.64E-06	LH2
elfA	laminin-binding fimbrin subunit	-0.49	2.98E-01	-1.15	4.75E-03	LH2
eptB	KDO phosphoethanolamine transferase, Ca(2+)-inducible	-0.18	2.10E-01	-1.22	1.15E-07	LH2
eutN	Ethanolamine catabolic microcompartment shell protein	0.13	8.67E-01	-1.19	7.81E-03	LH2
feoA	ferrous iron transporter, protein A	0.97	2.81E-03	-1.48	1.54E-06	LH2
feoB	fused ferrous iron transporter, protein B: GTP-binding protein/membrane protein	0.75	6.26E-08	-1.16	3.96E-09	LH2
fic	stationary-phase adenosine monophosphate-protein transferase domain protein	0.46	1.33E-04	1.36	7.23E-10	LH2
fixA	anaerobic carnitine reduction putative electron transfer flavoprotein subunit	0.40	2.10E-01	-1.24	1.62E-03	LH2
flgB	flagellar component of cell-proximal portion of basal-body rod	-0.70	2.74E-01	-1.35	3.89E-02	LH2
flgC	flagellar component of cell-proximal portion of basal-body rod	-0.86	9.65E-02	-1.02	4.07E-02	LH2
flhD	flagellar class II regulon transcriptional activator, with FlhC	-0.89	1.02E-04	-1.14	2.39E-07	LH2
focA	formate channel	-0.45	8.24E-04	-1.03	2.61E-07	LH2
frwC	putative enzyme IIC component of PTS	0.07	8.76E-01	-1.61	2.64E-05	LH2
ftnB	ferritin B, putative ferrous iron reservoir	-0.97	9.36E-05	-1.23	2.55E-06	LH2
fucP	L-fucose transporter	0.36	2.13E-01	-1.47	6.63E-06	LH2
fucR	l-fucose operon activator	-0.09	3.94E-01	-1.29	3.11E-09	LH2
gadA	glutamate decarboxylase A, PLP-dependent	0.64	2.87E-02	2.01	9.80E-06	LH2
gadB	glutamate decarboxylase B, PLP-dependent	0.11	7.04E-01	1.83	2.21E-05	LH2
gadC	glutamate:gamma-aminobutyric acid antiporter	-0.61	2.98E-02	1.75	3.37E-05	LH2
gadW	transcriptional activator of gadA and gadBC; repressor of gadX	-0.69	3.33E-04	1.91	4.16E-08	LH2
gcd	glucose dehydrogenase	-0.29	6.63E-03	2.32	3.80E-12	LH2
ggt	gamma-glutamyltranspeptidase	0.60	4.35E-03	1.17	1.00E-05	LH2
glnK	nitrogen assimilation regulatory protein for GlnL, GlnE, and AmtB	0.08	9.06E-01	2.37	9.97E-05	LH2
glpF	glycerol facilitator	0.89	1.17E-04	-1.69	1.57E-07	LH2

glpK	glycerol kinase	0.23	3.24E-02	-1.37	3.67E-09	LH2
glsA	glutaminase 1	-0.84	8.68E-04	1.44	1.11E-05	LH2
gpt	xanthine phosphoribosyltransferase; xanthine-guanine phosphoribosyltransferase	-0.10	6.19E-01	-1.88	9.36E-08	LH2
hdeA	stress response protein acid-resistance protein	0.18	4.73E-01	1.20	4.22E-04	LH2
hdeB	acid-resistance protein	-0.18	4.65E-01	1.33	9.71E-05	LH2
hdeD	acid-resistance membrane protein	0.57	2.35E-02	1.48	2.16E-05	LH2
hdhA	7-alpha-hydroxysteroid dehydrogenase, NAD-dependent	0.33	3.97E-03	1.09	4.59E-08	LH2
hisC	histidinol-phosphate aminotransferase	0.90	7.67E-04	1.43	2.53E-06	LH2
hisD	bifunctional histidinal dehydrogenase/ histidinol dehydrogenase	0.70	3.02E-03	1.44	1.77E-06	LH2
hisF	imidazole glycerol phosphate synthase, catalytic subunit with HisH	-0.09	7.53E-01	1.01	2.77E-04	LH2
hisG	ATP phosphoribosyltransferase	-0.42	9.24E-03	1.20	3.49E-07	LH2
ilvX	uncharacterized protein	0.52	2.65E-01	1.41	1.15E-02	LH2
intS	CPS-53 (KpLE1) prophage; putative prophage CPS-53 integrase	-0.60	2.31E-02	-1.10	3.56E-04	LH2
iraD	RpoS stabilizer after DNA damage, anti-RssB factor	-0.52	2.65E-01	1.22	1.16E-04	LH2
katE	catalase HPII, heme d-containing	0.97	4.69E-07	1.52	8.81E-09	LH2
kbaZ	tagatose 6-phosphate aldolase 1, kbaZ subunit	0.74	7.09E-04	-1.01	1.66E-05	LH2
ldcC	lysine decarboxylase 2, constitutive	-0.65	6.95E-05	1.06	5.67E-07	LH2
ldtA	L,D-transpeptidase linking Lpp to murein	0.03	8.22E-01	1.00	2.82E-07	LH2
ldtE	murein L,D-transpeptidase	0.90	7.49E-09	1.38	2.39E-10	LH2
lrhA	transcriptional repressor of flagellar, motility and chemotaxis genes	-0.74	5.80E-04	-1.66	1.32E-07	LH2
lysP	lysine transporter	0.00	9.67E-01	1.06	8.20E-09	LH2
lysV	tRNA-Lys	0.78	4.04E-03	-1.13	6.03E-04	LH2
malI	transcriptional repressor of Mal regulon	0.15	7.53E-01	-1.47	3.87E-04	LH2
malX	fused maltose and glucose-specific PTS enzymes: IIB component, IIC component	-0.40	5.45E-01	-2.72	1.31E-04	LH2
mdtA	multidrug efflux system, subunit A	1.27	1.59E-01	1.84	3.03E-02	LH2
mdtB	multidrug efflux system, subunit B	0.50	2.63E-01	1.96	1.04E-04	LH2

mdtC	multidrug efflux system, subunit C	0.78	5.55E-02	1.75	3.03E-05	LH2
mdtD	putative arabinose efflux transporter	0.73	4.39E-02	1.10	2.57E-04	LH2
melR	melibiose operon transcriptional regulator; autoregulator	0.90	3.57E-03	-1.23	7.71E-06	LH2
mepS	murein DD-endopeptidase, space-maker hydrolase, mutational suppressor of prc thermosensitivity, outer membrane lipoprotein	-0.50	4.30E-02	-1.97	7.42E-07	LH2
metT	tRNA-Met	-0.11	7.39E-01	1.05	3.12E-05	LH2
mhpB	2,3-dihydroxyphenylpropionate 1,2-dioxygenase	0.54	2.66E-01	1.29	7.70E-03	LH2
mscS	mechanosensitive channel protein, small conductance	-0.23	2.13E-01	1.02	2.14E-05	LH2
mtfA	anti-repressor for DgsA(Mlc)	0.17	1.61E-01	-1.36	9.25E-09	LH2
ompF	outer membrane porin 1a (Ia;b;F)	0.37	1.66E-02	-2.38	3.61E-10	LH2
ompT	DLP12 prophage; outer membrane protease VII (outer membrane protein 3b)	0.29	5.34E-02	-1.49	1.65E-07	LH2
opgC	osmoregulated periplasmic glucan succinylation membrane protein	0.31	1.53E-01	-1.07	3.13E-04	LH2
osmF	putative ABC superfamily transporter periplasmic-binding protein	0.33	2.11E-02	1.20	2.07E-07	LH2
otsA	trehalose-6-phosphate synthase	0.42	1.99E-03	1.77	1.15E-09	LH2
otsB	trehalose-6-phosphate phosphatase, biosynthetic	0.99	1.19E-06	1.87	9.74E-10	LH2
pabA	aminodeoxychorismate synthase, subunit II	0.05	6.83E-01	1.25	6.15E-09	LH2
pagP	phospholipid:lipid A palmitoyltransferase	0.26	2.49E-01	1.05	1.53E-05	LH2
paoD	moco insertion factor for PaoABC aldehyde oxidoreductase	0.54	2.12E-02	1.54	9.36E-08	LH2
patA	putrescine:2-oxoglutaric acid aminotransferase, PLP-dependent	0.43	7.41E-04	2.03	4.79E-11	LH2
phnK	carbon-phosphorus lyase complex subunit, putative ATP transporter ATP-binding protein	-0.13	8.52E-01	1.02	4.76E-02	LH2
phnP	5-phospho-alpha-D-ribosyl 1,2-cyclic phosphate phosphodiesterase	-0.37	3.63E-02	1.10	7.61E-07	LH2
phr	deoxyribodipyrimidine photolyase, FAD-binding	-0.23	3.46E-01	1.54	3.89E-06	LH2
pliG	periplasmic inhibitor of g-type lysozyme	-0.01	9.59E-01	-1.01	1.50E-04	LH2
pmrD	inactive two-component system connector protein	-0.14	6.58E-01	-1.02	8.01E-05	LH2
potG	putrescine transporter subunit: ATP-binding component of ABC superfamily	0.98	3.69E-04	1.38	2.02E-05	LH2

potH	putrescine transporter subunit: membrane component of ABC superfamily	0.35	2.03E-01	1.10	2.93E-04	LH2
poxB	pyruvate dehydrogenase (pyruvate oxidase), thiamine triphosphate-binding, FAD-binding	0.03	8.91E-01	1.63	3.44E-07	LH2
ppiA	peptidyl-prolyl cis-trans isomerase A (rotamase A)	-0.62	1.85E-02	-1.01	5.46E-04	LH2
proL	tRNA-Pro	-0.09	8.30E-01	1.46	2.69E-05	LH2
proM	tRNA-Pro	0.79	5.45E-02	-1.60	1.96E-03	LH2
psuG	pseudouridine 5'-phosphate glycosidase	0.75	1.22E-03	-1.20	4.91E-06	LH2
pykF	pyruvate kinase I	-0.22	8.77E-02	1.07	7.12E-07	LH2
pyrC	dihydro-orotase	0.00	9.89E-01	-1.73	6.67E-07	LH2
pyrD	dihydro-orotate oxidase, FMN-linked	-0.52	6.17E-02	-1.69	1.17E-06	LH2
pyrE	orotate phosphoribosyltransferase	0.23	4.68E-01	-1.30	4.32E-05	LH2
queD	6-pyruvoyl tetrahydrobiopterin synthase (PTPS)	-0.10	6.10E-01	-1.02	6.74E-05	LH2
rapA	RNA polymerase remodeling/recycling factor ATPase; RNA polymerase-associated, ATP-dependent RNA translocase	0.78	1.30E-06	1.66	4.61E-10	LH2
rbsB	D-ribose transporter subunit	-0.13	2.59E-01	-1.46	5.10E-09	LH2
rbsK	ribokinase	-0.81	4.48E-07	-1.12	1.91E-08	LH2
rscF	putative outer membrane protein	-0.92	2.20E-03	-1.09	5.96E-04	LH2
rdgC	nucleoid-associated ssDNA and dsDNA binding protein; competitive inhibitor of RecA function	0.29	2.89E-01	-1.11	2.52E-04	LH2
rhaR	transcriptional activator of rhaSR	-0.35	2.04E-01	-1.41	6.42E-07	LH2
rhIE	ATP-dependent RNA helicase	0.00	9.81E-01	1.33	2.40E-07	LH2
ridA	enamine/imine deaminase, reaction intermediate detoxification	-0.55	3.98E-03	-1.06	1.78E-05	LH2
rimL	ribosomal-protein-L7/L12-serine acetyltransferase	-0.25	1.62E-01	-1.07	3.04E-07	LH2
rluA	dual specificity 23S rRNA pseudouridine(746), tRNA pseudouridine(32) synthase, SAM-dependent	0.99	1.18E-04	1.65	3.70E-08	LH2
rsmJ	16S rRNA m(2)G1516 methyltransferase, SAM-dependent	0.45	1.39E-03	1.21	3.24E-08	LH2
rutB	ureidoacrylate amidohydrolase	0.66	4.23E-01	2.10	5.96E-03	LH2
rutC	putative aminoacrylate deaminase, reactive intermediate detoxification; weak enamine/imine deaminase activity	-0.47	4.05E-01	1.32	4.24E-03	LH2
rutD	putative aminoacrylate hydrolase, reactive intermediate detoxification	-0.37	3.98E-01	1.21	9.36E-04	LH2

sanA	vancomycin high temperature exclusion protein, DUF218 superfamily protein	-0.27	3.85E-01	-1.08	2.73E-03	LH2
secG	preprotein translocase membrane subunit	0.16	3.71E-01	-1.13	1.74E-05	LH2
serU	tRNA-Ser	0.46	1.24E-02	-1.38	5.05E-08	LH2
sgcB	putative enzyme IIB component of PTS	0.05	8.89E-01	-1.09	5.48E-05	LH2
sgcX	putative endoglucanase with Zn-dependent exopeptidase domain	0.38	2.43E-02	-1.07	2.43E-07	LH2
sieB	Rac prophage; phage superinfection exclusion protein	0.07	9.39E-01	-2.31	1.75E-03	LH2
sodC	superoxide dismutase, Cu, Zn, periplasmic	0.88	1.12E-06	1.03	1.66E-07	LH2
soxS	superoxide response regulon transcriptional activator; autoregulator	0.49	1.63E-04	-1.03	3.83E-06	LH2
speB	agmatinase	0.94	2.48E-06	1.13	3.59E-07	LH2
srlA	glucitol/sorbitol-specific enzyme IIC component of PTS	0.01	9.79E-01	-1.09	3.41E-04	LH2
srlB	glucitol/sorbitol-specific enzyme IIA component of PTS	0.06	7.58E-01	-1.20	8.18E-04	LH2
sufB	component of SufBCD Fe-S cluster assembly scaffold	0.75	1.45E-04	1.11	4.33E-06	LH2
sufC	SufBCD Fe-S cluster assembly scaffold protein, ATP-binding protein	0.54	7.54E-03	1.23	2.90E-06	LH2
sufD	component of SufBCD Fe-S cluster assembly scaffold	0.63	4.81E-03	1.20	1.71E-05	LH2
sufE	sulfur acceptor protein	0.47	3.34E-02	1.15	4.30E-06	LH2
sufS	cysteine desulfurase, stimulated by SufE; selenocysteine lyase, PLP-dependent	0.58	6.52E-03	1.19	1.02E-05	LH2
talA	transaldolase A	0.35	2.46E-02	1.62	4.95E-08	LH2
tdk	thymidine kinase/deoxyuridine kinase	0.25	3.64E-01	-1.02	1.39E-03	LH2
thrA	Bifunctional aspartokinase/homoserine dehydrogenase 1	0.67	7.12E-04	1.01	2.12E-05	LH2
tktB	transketolase 2, thiamine triphosphate-binding	0.54	4.12E-03	1.74	1.57E-07	LH2
torR	response regulator in two-component regulatory system with TorS	0.14	5.68E-01	-1.50	7.42E-07	LH2
tqsA	pheromone AI-2 transporter	0.87	1.02E-01	-2.03	2.64E-04	LH2
treF	cytoplasmic trehalase	0.69	2.15E-07	1.29	2.39E-10	LH2
treR	trehalose 6-phosphate-inducible trehalose regulon transcriptional repressor	0.21	2.83E-01	-1.23	1.48E-06	LH2

trpT	tRNA-Trp	0.89	9.48E-04	1.23	1.49E-06	LH2
tyrU	tRNA-Tyr	0.90	7.59E-04	-1.05	1.22E-04	LH2
ucpA	furfural resistance protein, putative short-chain oxidoreductase	-0.99	6.31E-06	-1.20	1.47E-06	LH2
ugpA	glycerol-3-phosphate transporter subunit	0.46	4.71E-02	1.52	1.63E-05	LH2
ugpE	glycerol-3-phosphate transporter subunit	0.33	1.82E-01	1.43	5.77E-05	LH2
ulaA	L-ascorbate-specific enzyme IIC permease component of PTS	-0.23	4.05E-01	-1.01	1.33E-04	LH2
upp	uracil phosphoribosyltransferase	-0.24	3.15E-01	-1.69	2.55E-06	LH2
uraA	uracil permease	-0.86	2.38E-01	-1.74	2.45E-02	LH2
valU	tRNA-Val	0.21	3.82E-01	-1.07	1.69E-04	LH2
valY	tRNA-Val	0.49	4.77E-02	-1.11	1.76E-04	LH2
yadI	putative PTS Enzyme IIA	-0.27	5.79E-02	-1.10	3.17E-08	LH2
yafT	lipoprotein	0.92	1.87E-02	-1.92	3.49E-03	LH2
yagN	CP4-6 prophage; uncharacterized protein	-0.32	3.47E-01	-1.14	2.86E-04	LH2
yahK	aldehyde reductase, NADPH-dependent, Zn-containing, broad specificity	0.10	6.04E-01	1.80	4.38E-08	LH2
yahL	uncharacterized protein	0.94	2.32E-02	1.51	1.44E-02	LH2
yahN	amino acid exporter for proline, lysine, glutamate, homoserine	-0.77	1.55E-03	-1.38	1.66E-05	LH2
yajG	putative lipoprotein	-0.77	3.18E-04	-1.51	3.95E-07	LH2
ybaV	putative competence-suppressing periplasmic helix-hairpin-helix DNA-binding protein	-0.53	5.87E-02	-1.32	2.08E-06	LH2
ybaY	outer membrane lipoprotein	0.54	5.13E-03	2.17	8.20E-09	LH2
ybbY	putative uracil/xanthine transporter	0.86	2.96E-03	1.22	1.05E-05	LH2
ybdJ	DUF1158 family putative inner membrane protein	-0.01	9.49E-01	1.02	8.72E-07	LH2
ybdK	weak gamma-glutamyl:cysteine ligase	0.05	6.02E-01	1.41	3.48E-10	LH2
ybdL	methionine aminotransferase, PLP-dependent	0.46	5.54E-02	-1.14	1.63E-06	LH2
ybfA	DUF2517 family protein	-0.54	1.65E-01	-2.07	2.69E-05	LH2
ybfC	putative periplasmic protein	0.72	3.18E-01	-2.69	6.87E-03	LH2
ybgA	DUF1722 family protein	-0.14	4.05E-01	1.48	7.25E-08	LH2
ybhA	pyridoxal phosphate (PLP) phosphatase	-0.60	4.14E-03	-1.02	8.77E-06	LH2

ybhN	UPF0104 family inner membrane protein	-0.43	3.70E-02	1.28	1.58E-06	LH2
ybhP	endo/exonuclease/phosphatase family protein	-0.46	2.65E-03	1.10	2.31E-07	LH2
ybiO	mechanosensitive channel protein, intermediate conductance	0.04	7.18E-01	1.02	8.85E-09	LH2
yccX	weak acylphosphatase	0.48	8.10E-02	1.13	6.72E-05	LH2
yceO	uncharacterized protein	0.23	7.02E-01	-1.66	1.61E-02	LH2
ycgG	putative membrane-anchored cyclic-di-GMP phosphodiesterase	0.15	4.71E-01	1.08	1.45E-04	LH2
ycgZ	RcsB connector protein for regulation of biofilm and acid-resistance	0.90	2.13E-04	1.70	2.32E-05	LH2
yciI	putative DGPF domain-containing enzyme	0.00	1.00E+00	-1.10	3.89E-05	LH2
yciW	putative oxidoreductase	0.66	3.01E-01	1.05	1.40E-02	LH2
ycjW	LacI family putative transcriptional repressor	-0.81	3.32E-02	-1.87	7.08E-05	LH2
ydcD	uncharacterized protein	-0.03	9.64E-01	-2.91	4.37E-03	LH2
ydcH	DUF465 family protein	-0.05	8.09E-01	-1.28	3.18E-06	LH2
ydcK	uncharacterized protein	0.54	4.36E-03	1.03	4.63E-06	LH2
ydeM	putative YdeN-specific sulfatase-maturing enzyme	-0.51	2.86E-01	-2.22	1.12E-03	LH2
ydgA	DUF945 family protein	-0.48	2.14E-05	1.09	6.93E-09	LH2
ydhS	putative oxidoreductase	0.29	2.66E-02	1.22	5.47E-08	LH2
ydiL	putative HTH domain DNA-binding protein	0.56	2.50E-01	-1.56	2.78E-03	LH2
ydiM	MFS superfamily sugar transport 1 family protein	-0.24	7.42E-01	-2.25	1.74E-02	LH2
ydiZ	uncharacterized protein	0.79	5.28E-04	1.29	5.60E-07	LH2
ydjX	TVP38/TMEM64 family inner membrane protein	-2.30	7.83E-02	-3.04	1.28E-04	LH2
ydjY	putative ferredoxin-like lipoprotein	-1.00	6.93E-02	-1.88	1.02E-05	LH2
yeaH	UPF0229 family protein	0.95	7.75E-08	1.53	1.04E-09	LH2
yeaQ	UPF0410 family protein	0.65	1.60E-04	1.32	2.43E-07	LH2
yecR	lipoprotein, function unknown	0.66	4.21E-01	-1.99	9.31E-03	LH2
yedA	amino acid exporter for phenylalanine, threonine	-0.19	2.07E-01	-1.06	1.40E-06	LH2
yedE	UPF0394 family sulfur transport domain-containing inner membrane protein	0.64	2.69E-02	-1.30	2.35E-06	LH2
yedF	putative Tusa family sulfurtransferase	0.98	1.66E-02	-1.08	8.31E-06	LH2
yedR	inner membrane protein	0.82	1.80E-02	1.22	2.51E-04	LH2

yeeN	UPF0082 family protein	-0.40	6.18E-02	-1.34	1.96E-06	LH2
yehW	inner membrane putative ABC superfamily transporter permease	0.53	2.13E-01	1.77	5.88E-05	LH2
yehX	putative ABC superfamily transporter ATP-binding subunit	0.14	6.72E-01	1.90	2.27E-06	LH2
yehY	inner membrane putative ABC superfamily transporter permease	-0.21	2.62E-01	1.69	6.90E-08	LH2
yeiL	putative transcriptional regulator	0.64	4.02E-02	-1.27	2.06E-04	LH2
yeiW	UPF0153 cysteine cluster protein	0.91	7.66E-02	-1.74	2.96E-02	LH2
yfbM	DUF1877 family protein	0.50	3.47E-01	-2.20	6.73E-06	LH2
yfcG	GSH-dependent disulfide bond oxidoreductase	0.38	3.60E-03	1.02	8.44E-08	LH2
yfcC	DUF1323 family putative DNA-binding protein	-0.94	4.40E-03	-1.13	1.84E-04	LH2
yfgJ	DUF1407 family protein	0.38	1.09E-01	1.09	5.31E-06	LH2
yfjH	CP4-57 prophage; uncharacterized protein	-0.35	2.89E-01	-1.13	3.49E-03	LH2
ygaM	DUF883 family protein, putative membrane-anchored ribosome-binding protein	0.96	2.09E-05	1.65	5.56E-08	LH2
ygbJ	putative dehydrogenase	-0.01	9.84E-01	-1.03	2.96E-04	LH2
ygcR	putative flavoprotein	0.87	2.66E-02	1.02	1.21E-03	LH2
ygcW	putative dehydrogenase	0.24	7.68E-01	-1.90	1.07E-02	LH2
ygeV	putative sigma-54-interacting transcriptional activator	-0.81	5.16E-06	-1.31	4.86E-08	LH2
yggI	Zn-dependent metalloprotease-related protein	-0.62	1.01E-01	-1.11	3.60E-03	LH2
ygiL	putative fimbrial-like adhesin protein	0.49	2.93E-01	-1.40	1.97E-02	LH2
ygiS	putative inner membrane ABC superfamily transporter permease	-0.21	4.43E-02	-1.43	2.15E-10	LH2
ygiV	transcriptional repressor for mcbR biofilm gene	-0.95	1.19E-04	1.04	2.07E-06	LH2
ygiW	hydrogen peroxide and cadmium resistance periplasmic protein; stress-induced OB-fold protein	-0.40	3.27E-02	1.22	5.55E-06	LH2
yhcO	putative barnase inhibitor	0.27	1.04E-01	1.23	2.38E-07	LH2
yhfG	putative Fic-binding protein	0.48	2.05E-04	1.19	4.10E-09	LH2
yhiD	putative Mg(2+) transport ATPase, inner membrane protein	0.29	1.66E-01	1.14	2.60E-05	LH2
yhjD	inner membrane putative BrbK family alternate lipid exporter	0.46	3.84E-05	1.15	9.01E-10	LH2
ylaL	DUF386 family protein	0.66	1.81E-01	-1.94	1.01E-03	LH2

yjiQ	DUF1454 family putative periplasmic protein	-0.81	2.98E-02	-1.12	2.87E-03	LH2
yjeJ	uncharacterized protein	0.39	2.13E-01	-1.54	3.99E-03	LH2
yjfJ	PspA/IM30 family protein	0.32	3.81E-01	-1.05	1.48E-02	LH2
yjhI	putative DNA-binding transcriptional regulator	0.77	1.93E-02	-1.07	3.64E-03	LH2
yjhP	putative methyltransferase	0.70	2.12E-03	-1.26	3.95E-06	LH2
yjhQ	putative acetyltransferase	0.45	7.25E-02	-1.35	4.10E-05	LH2
yjhX	UPF0386 family protein	0.86	7.09E-03	-1.60	2.78E-04	LH2
yjiK	SdiA-regulated family putative membrane-anchored protein; putative phytase-like esterase	-0.44	3.25E-01	-1.40	3.24E-04	LH2
yjiN	zinc-type alcohol dehydrogenase-like protein	0.15	1.12E-01	1.31	3.48E-10	LH2
yjjU	putative patatin-like family phospholipase	0.38	4.92E-02	1.17	5.79E-06	LH2
yjjV	putative DNase	0.21	3.48E-01	1.21	1.24E-05	LH2
ymfE	e14 prophage; putative inner membrane protein	0.42	7.66E-02	-1.63	1.44E-05	LH2
ymgC	Blue light, low temperature and stress induced protein	0.51	5.70E-03	3.40	8.52E-09	LH2
ynlL	stress-induced small inner membrane enterobacterial protein	0.83	1.80E-02	1.04	4.36E-04	LH2
ynfB	UPF0482 family putative periplasmic protein	-0.25	2.14E-01	-1.13	2.67E-05	LH2
ynfM	putative arabinose efflux transporter	0.71	2.00E-03	1.46	2.09E-07	LH2
yodC	uncharacterized protein	0.44	1.81E-02	1.40	4.90E-08	LH2
yohJ	UPF0299 family inner membrane protein	0.38	2.00E-01	1.36	3.95E-06	LH2
yohK	LrgB family inner membrane protein	0.35	1.84E-02	1.04	3.43E-08	LH2
yphA	DoxX family inner membrane protein	0.24	2.07E-01	1.12	3.63E-06	LH2
yqeI	putative transcriptional regulator	0.16	7.47E-01	-1.09	3.25E-02	LH2
yqiH	putative periplasmic pilin chaperone	-0.91	1.17E-01	-1.45	4.95E-02	LH2
yqiJ	DUF1449 family inner membrane protein	0.82	5.24E-02	-1.57	3.80E-03	LH2
yrbN	uncharacterized protein	0.62	1.99E-02	1.18	2.08E-05	LH2
ysgA	putative carboxymethylenebutenolidase	0.86	3.76E-05	1.14	1.49E-06	LH2
zinT	zinc and cadmium binding protein, periplasmic	-0.06	9.31E-01	-1.46	2.82E-02	LH2
abrB	regulator of aidB expression; inner membrane protein	-1.99	1.64E-02	-2.01	9.82E-04	both
acnA	aconitate hydratase 1	-1.26	3.67E-10	1.61	1.83E-10	both

acrR	transcriptional repressor	1.01	1.28E-03	-1.67	9.85E-05	both
acs	acetyl-CoA synthetase	2.02	3.77E-09	1.57	2.82E-07	both
actP	acetate transporter	2.11	5.36E-07	1.17	1.33E-04	both
adhP	ethanol-active dehydrogenase/acetaldehyde-active reductase	2.30	8.21E-08	1.64	4.30E-06	both
adiY	adi system transcriptional activator	-2.24	2.89E-05	-1.67	1.28E-04	both
allD	ureidoglycolate dehydrogenase	-1.01	8.29E-03	-1.66	2.52E-05	both
ansB	periplasmic L-asparaginase 2	-7.02	6.55E-14	-2.64	6.55E-09	both
ariR	RcsB connector protein for regulation of biofilm and acid-resistance	2.25	3.25E-10	2.82	5.26E-08	both
astA	arginine succinyltransferase	3.76	2.44E-12	2.49	9.01E-10	both
astB	succinylarginine dihydrolase	3.45	6.90E-12	2.03	5.23E-09	both
astC	succinylornithine transaminase, PLP-dependent	4.04	1.93E-14	2.55	2.77E-11	both
astD	succinylglutamic semialdehyde dehydrogenase	3.53	1.07E-11	2.13	7.16E-09	both
astE	succinylglutamate desuccinylase	3.51	5.22E-10	2.49	1.65E-08	both
atoC	fused response regulator of ato operon, in two-component system with AtoS: response regulator/sigma54 interaction protein	-1.47	1.45E-07	-1.30	1.53E-07	both
betI	choline-inducible betIBA-betT divergent operon transcriptional repressor	1.20	1.20E-05	1.59	5.78E-07	both
betT	choline transporter of high affinity	1.11	1.65E-03	1.09	8.70E-04	both
bglG	transcriptional antiterminator of the bgl operon	1.54	1.41E-02	-1.78	2.85E-02	both
bioA	7,8-diaminopelargonic acid synthase, PLP-dependent	1.34	1.71E-04	-1.76	7.74E-07	both
bioB	biotin synthase	1.24	1.17E-03	-1.58	1.61E-05	both
bolA	stationary-phase morphogene, transcriptional repressor for mreB; also regulator for dacA, dacC, and ampC	1.32	8.18E-09	1.20	8.51E-08	both
btuB	vitamin B12/cobalamin outer membrane transporter	-1.04	7.54E-08	-1.10	3.63E-08	both
caiF	cai operon transcriptional activator	-1.96	1.16E-06	-1.51	4.53E-06	both
cbdA	cytochrome bd-II oxidase, subunit I	-1.62	1.50E-07	1.65	1.15E-07	both
cbdB	cytochrome bd-II oxidase, subunit II	-1.19	2.40E-05	1.71	1.42E-07	both
cirA	colicin IA outer membrane receptor and translocator; ferric iron-catecholate transporter	4.44	3.92E-10	-1.05	1.67E-04	both

cpxP	inhibitor of the cpx response; periplasmic adaptor protein	2.46	4.05E-07	-1.52	1.03E-04	both
croE	e14 prophage; putative DNA-binding transcriptional regulator	4.69	2.80E-10	-2.99	1.12E-03	both
csgD	csgBAC operon transcriptional regulator	1.68	3.01E-07	1.25	5.92E-07	both
csgE	curlin secretion specificity factor	1.64	3.56E-04	1.35	9.23E-05	both
csgF	curli nucleation outer membrane protein	2.14	1.58E-05	1.84	4.05E-06	both
csiD	carbon starvation protein	2.79	1.11E-10	2.34	5.04E-09	both
csiE	stationary phase inducible protein	2.05	2.19E-12	1.11	2.38E-08	both
csiR	transcriptional repressor of csiD	1.60	6.13E-06	1.35	4.14E-06	both
cueR	copper-responsive regulon transcriptional regulator	-1.24	2.60E-07	1.16	2.43E-07	both
cydA	cytochrome d terminal oxidase, subunit I	-1.78	1.40E-11	-1.08	2.05E-07	both
cysA	sulfate/thiosulfate transporter subunit	1.69	1.39E-05	1.80	4.08E-06	both
cysH	phosphoadenosine phosphosulfate reductase; PAPS reductase, thioredoxin dependent	1.56	3.24E-04	2.05	7.91E-07	both
cysI	sulfite reductase, beta subunit, NAD(P)-binding, heme-binding	1.11	1.85E-03	1.91	9.59E-06	both
cysW	sulfate/thiosulfate ABC transporter subunit	1.42	5.72E-04	1.51	3.88E-05	both
dcuA	C4-dicarboxylate antiporter	-2.34	1.31E-13	-1.18	1.17E-08	both
dcuB	C4-dicarboxylate transporter, anaerobic; DcuS co-sensor	-6.40	1.93E-14	-1.79	6.67E-07	both
dcuC	anaerobic C4-dicarboxylate transport	-3.53	1.12E-07	-1.87	7.07E-06	both
ddpA	D-ala-D-ala transporter subunit	1.64	3.05E-07	1.40	5.44E-07	both
ddpX	D-ala-D-ala dipeptidase, Zn-dependent	2.22	3.93E-07	1.52	4.00E-06	both
deaD	ATP-dependent RNA helicase	1.30	9.43E-08	1.15	1.54E-06	both
dgcZ	diguanylate cyclase, zinc-sensing	3.06	8.16E-08	-1.28	3.09E-04	both
dinD	DNA damage-inducible protein	2.88	1.11E-10	-1.10	1.03E-04	both
dosC	diguanylate cyclase, cold- and stationary phase-induced oxygen-dependent biofilm regulator	3.50	3.98E-10	1.84	1.18E-07	both
dosP	oxygen sensor, c-di-GMP phosphodiesterase, heme-regulated; cold- and stationary phase-induced biofilm regulator	2.58	2.18E-08	2.42	1.65E-08	both
entD	phosphopantetheinyltransferase component of enterobactin synthase multienzyme complex	3.80	1.50E-06	-1.06	1.45E-05	both

fadD	acyl-CoA synthetase (long-chain-fatty-acid--CoA ligase)	2.57	9.45E-11	1.67	3.07E-08	both
fadE	acyl coenzyme A dehydrogenase	4.23	1.67E-11	1.42	1.72E-05	both
fadL	long-chain fatty acid outer membrane transporter	3.61	6.90E-12	1.11	1.59E-05	both
fimA	major type 1 subunit fimbrin (pilin)	1.91	3.28E-08	-1.16	1.84E-05	both
fimD	fimbrial usher outer membrane porin protein; FimCD chaperone-usher	2.79	2.04E-06	-1.15	1.11E-04	both
fimE	tyrosine recombinase/inversion of on/off regulator of fimA	3.92	1.51E-04	-1.08	2.99E-02	both
fimF	minor component of type 1 fimbriae	2.38	1.10E-04	-1.30	6.84E-05	both
fimG	minor component of type 1 fimbriae	2.09	2.66E-03	-1.47	2.84E-04	both
flxA	Qin prophage; uncharacterized protein	1.47	9.28E-03	2.05	4.88E-03	both
friA	putative fructoselysine transporter	2.21	1.12E-05	-1.26	2.11E-02	both
frwA	putative PTS enzyme, Hpr component/enzyme I component/enzyme IIA component	-1.17	1.58E-04	-1.18	4.08E-06	both
ftnA	ferritin iron storage protein (cytoplasmic)	-3.53	1.84E-11	-1.40	4.75E-05	both
fucA	L-fucose-1-phosphate aldolase	-1.05	1.62E-04	-1.22	1.11E-05	both
fucO	L-1,2-propanediol oxidoreductase	-2.52	2.11E-13	-1.67	1.03E-10	both
fumB	anaerobic class I fumarate hydratase (fumarase B)	-7.07	5.14E-16	-1.44	2.14E-07	both
gabD	succinate-semialdehyde dehydrogenase I, NADP-dependent	1.63	2.22E-06	2.12	3.22E-07	both
gabP	gamma-aminobutyrate transporter	2.23	1.08E-06	2.01	1.22E-06	both
gabT	4-aminobutyrate aminotransferase, PLP-dependent	1.87	8.64E-07	2.14	4.95E-07	both
gadE	gad regulon transcriptional activator	1.53	5.18E-07	1.03	5.70E-05	both
galS	galactose- and fucose-inducible galactose regulon transcriptional isorepressor; mgl operon transcriptional repressor; autorepressor	-1.71	6.31E-11	-1.60	1.82E-09	both
gatB	galactitol-specific enzyme IIB component of PTS	-1.94	5.89E-10	-1.27	7.42E-07	both
gatC	galactitol PTS permease - GatC subunit	-2.10	5.89E-10	-1.41	6.21E-07	both
gatD	galactitol-1-phosphate dehydrogenase, Zn-dependent and NAD(P)-binding	-1.12	1.12E-06	-1.05	9.65E-06	both
glcA	glycolate transporter	2.05	8.15E-09	1.17	1.20E-05	both
glcD	glycolate oxidase subunit, FAD-linked	2.89	3.43E-10	1.70	5.93E-07	both
glcE	glycolate oxidase FAD binding subunit	2.58	3.95E-08	1.61	2.64E-05	both

glpA	sn-glycerol-3-phosphate dehydrogenase (anaerobic), large subunit, FAD/NAD(P)-binding	-1.53	3.87E-02	-2.13	2.05E-03	both
glpB	sn-glycerol-3-phosphate dehydrogenase (anaerobic), membrane anchor subunit	-1.35	6.45E-04	-1.15	7.60E-04	both
glpT	sn-glycerol-3-phosphate transporter	-1.35	2.66E-04	-2.06	2.72E-06	both
gntP	fructuronate transporter	1.22	3.00E-07	-1.27	1.99E-07	both
grcA	autonomous glycyl radical cofactor	-4.60	4.30E-14	-1.24	2.85E-06	both
hchA	glyoxalase III and Hsp31 molecular chaperone	1.53	7.45E-08	1.18	4.95E-06	both
hiuH	hydroxyisourate hydrolase	-1.96	7.56E-06	1.65	5.52E-03	both
hyaA	hydrogenase 1, small subunit	-5.16	4.13E-11	1.57	1.75E-06	both
hyaB	hydrogenase 1, large subunit	-5.58	4.21E-12	1.54	1.43E-06	both
hyaC	hydrogenase 1, b-type cytochrome subunit	-5.17	8.53E-11	1.38	1.56E-06	both
hyaD	hydrogenase 1 maturation protease	-4.67	2.67E-10	1.39	1.16E-06	both
hyaE	putative HyaA chaperone	-4.72	2.81E-09	1.30	4.05E-06	both
hyaF	protein involved in nickel incorporation into hydrogenase-1 proteins	-4.72	1.46E-09	1.43	2.03E-06	both
hybA	hydrogenase 2 4Fe-4S ferredoxin-type component	-5.38	1.07E-11	-2.13	4.12E-07	both
hybB	putative hydrogenase 2 cytochrome b type component	-5.03	6.98E-12	-1.83	5.06E-07	both
hybC	hydrogenase 2, large subunit	-3.93	3.90E-13	-1.31	5.12E-07	both
hybO	hydrogenase 2, small subunit	-5.19	3.57E-12	-2.01	2.05E-07	both
hyi	hydroxypyruvate isomerase	1.23	1.72E-03	1.06	1.32E-02	both
hypA	protein involved in nickel insertion into hydrogenases 3	-3.51	7.72E-08	-1.37	4.12E-05	both
hypB	GTP hydrolase involved in nickel liganding into hydrogenases	-4.18	3.74E-10	-1.50	3.51E-06	both
hypC	hydrogenase maturation protein	-4.46	7.45E-08	-1.33	8.24E-05	both
hyuA	D-stereospecific phenylhydantoinase	-6.18	1.31E-12	-1.51	3.95E-06	both
ilvB	acetolactate synthase 2 large subunit	1.75	2.24E-08	1.51	3.35E-07	both
ilvN	acetolactate synthase 1 small subunit	2.42	1.08E-08	1.97	1.49E-07	both
intE	e14 prophage; putative integrase	3.74	8.58E-12	-1.07	1.42E-02	both
kdpB	potassium translocating ATPase, subunit B	2.45	3.98E-08	-1.38	4.13E-05	both
kdpC	potassium translocating ATPase, subunit C	2.42	1.19E-09	-1.17	4.37E-06	both

kdpF	potassium ion accessory transporter subunit	1.52	2.91E-03	-1.19	1.29E-02	both
lhgO	L-2-hydroxyglutarate oxidase	2.07	5.71E-08	2.37	4.16E-08	both
malE	maltose transporter subunit	3.32	3.00E-06	-1.75	5.00E-03	both
malK	fused maltose transport subunit, ATP-binding component of ABC superfamily/regulatory protein	4.02	1.07E-07	-1.51	1.91E-02	both
marA	multiple antibiotic resistance transcriptional regulator	2.12	4.47E-09	-1.43	1.97E-06	both
marR	transcriptional repressor of multiple antibiotic resistance	1.88	9.24E-06	-1.65	2.05E-04	both
mcbA	colanic acid mucoidy stimulation protein	2.03	2.94E-06	1.58	3.17E-07	both
mcbR	colanic acid and biofilm gene transcriptional regulator, MqsR-controlled	1.66	7.03E-09	1.07	3.28E-05	both
mcrA	putative 5-methylcytosine/5-hydroxymethylcytosine-specific restriction nuclease; 5-methylcytosine DNA binding protein; e14 prophage gene	3.51	1.78E-08	-1.04	3.25E-02	both
mcrB	5-methylcytosine-specific restriction enzyme McrBC, subunit McrB	-1.86	1.28E-07	-1.34	5.78E-06	both
mdtI	multidrug efflux system transporter	-1.83	2.98E-09	-1.44	9.62E-06	both
mdtJ	multidrug efflux system transporter	-2.13	2.20E-09	-1.87	3.67E-06	both
mdtL	multidrug efflux system protein	-3.45	2.40E-12	-1.37	3.53E-06	both
mepH	murein DD-endopeptidase, space-maker hydrolase	-1.32	1.70E-04	-1.80	2.66E-06	both
metA	homoserine O-transsuccinylase	1.19	1.33E-03	-1.19	1.40E-05	both
metF	5,10-methylenetetrahydrofolate reductase	2.17	1.90E-04	-1.67	1.56E-05	both
metN	DL-methionine transporter subunit	1.53	1.16E-06	-1.37	1.15E-07	both
metR	methionine biosynthesis regulon transcriptional regulator	1.71	2.16E-06	-1.37	2.91E-07	both
metV	tRNA-Met	1.21	1.31E-04	-1.26	1.29E-04	both
metW	tRNA-Met	1.17	2.29E-05	-1.19	1.98E-05	both
metZ	tRNA-Met	1.19	3.34E-06	-1.11	8.88E-06	both
mgIA	fused methyl-galactoside transporter subunits of ABC superfamily: ATP-binding components	-2.22	1.92E-08	-1.29	4.59E-05	both
mgIB	methyl-galactoside transporter subunit	-2.01	4.21E-08	-1.45	3.89E-06	both
mgIC	methyl-galactoside transporter subunit	-1.98	1.83E-06	-1.19	1.14E-03	both
mgtL	regulatory leader peptide for mgtA	1.81	1.87E-06	-1.06	1.59E-02	both

mrr	methylated adenine and cytosine restriction protein	-1.34	2.81E-06	-1.08	2.03E-05	both
nanC	N-acetylnuraminic acid outer membrane channel protein	1.40	2.78E-04	1.04	1.65E-02	both
napA	nitrate reductase, periplasmic, large subunit	-2.35	6.52E-09	-1.37	2.38E-06	both
napB	nitrate reductase, small, cytochrome C550 subunit, periplasmic	-1.80	2.88E-04	-1.30	4.83E-04	both
napD	assembly protein for periplasmic nitrate reductase	-2.50	4.45E-04	-1.47	2.51E-03	both
napF	ferredoxin-type protein, role in electron transfer to periplasmic nitrate reductase NapA	-2.24	4.28E-05	-1.65	6.33E-05	both
napG	ferredoxin-type protein essential for electron transfer from ubiquinol to periplasmic nitrate reductase (NapAB)	-2.04	5.39E-08	-1.21	3.14E-06	both
napH	ferredoxin-type protein essential for electron transfer from ubiquinol to periplasmic nitrate reductase (NapAB)	-1.87	2.91E-06	-1.32	9.02E-06	both
narU	nitrate/nitrite transporter	1.50	9.18E-08	1.64	1.06E-06	both
narY	nitrate reductase 2 (NRZ), beta subunit	1.29	3.42E-06	1.16	1.49E-05	both
narZ	nitrate reductase 2 (NRZ), alpha subunit	1.26	4.93E-06	1.29	9.00E-06	both
nikA	nickel-binding, heme-binding periplasmic protein	-5.11	3.91E-07	-1.81	2.69E-05	both
nrdE	ribonucleoside-diphosphate reductase 2, alpha subunit	5.05	7.00E-12	1.02	6.67E-06	both
nrdF	ribonucleoside-diphosphate reductase 2, beta subunit, ferritin-like protein	4.59	7.41E-06	1.17	3.28E-04	both
nudI	nucleoside triphosphatase	-2.10	7.84E-06	-1.20	2.99E-04	both
obgE	GTPase involved in cell partitioning and DNA repair	2.04	3.86E-12	1.14	1.02E-08	both
ompW	outer membrane protein W	-5.22	4.30E-14	-1.84	2.35E-08	both
osmB	lipoprotein	2.46	6.94E-12	1.10	1.56E-07	both
osmC	lipoyl-dependent Cys-based peroxidase, hydroperoxide resistance; salt-shock inducible membrane protein; peroxiredoxin	1.86	2.34E-10	1.08	3.35E-07	both
osmY	periplasmic protein	1.52	2.41E-09	2.40	7.33E-11	both
paoA	PaoABC aldehyde oxidoreductase, 2Fe-2S subunit	1.59	4.50E-06	1.59	1.38E-07	both
paoB	PaoABC aldehyde oxidoreductase, FAD-containing subunit	1.47	1.53E-06	1.75	1.17E-08	both
paoC	PaoABC aldehyde oxidoreductase, Moco-containing subunit	1.16	1.07E-04	1.65	2.66E-07	both

pdhR	pyruvate dehydrogenase complex repressor; autorepressor	-1.57	5.64E-07	-1.14	4.76E-05	both
pepE	(alpha)-aspartyl dipeptidase	-1.93	4.42E-09	-1.72	2.03E-08	both
phoH	ATP-binding protein; putative PhoH family P-loop ATPase	1.85	3.28E-09	2.10	3.21E-09	both
pmrR	putative membrane-bound BasS regulator	-1.13	4.57E-04	1.46	2.02E-05	both
potF	putrescine transporter subunit: periplasmic-binding component of ABC superfamily	1.55	1.67E-08	2.04	5.75E-09	both
ppdD	putative prepilin peptidase-dependent pilin	-1.35	2.85E-02	-1.42	1.01E-02	both
pphA	serine/threonine-specific protein phosphatase 1	1.13	2.42E-03	1.37	1.26E-04	both
pqqL	putative periplasmic M16 family zinc metalloendopeptidase	1.36	2.85E-03	-3.10	1.90E-08	both
preT	dihydropyrimidine dehydrogenase, NADH-dependent, subunit N	-4.21	4.94E-13	-1.21	1.55E-05	both
proP	proline/glycine betaine transporter	-1.21	9.59E-09	1.03	2.38E-07	both
prpR	propionate catabolism operon regulatory protein	2.01	4.44E-09	1.64	5.60E-09	both
psiF	PsiF family protein	1.29	4.61E-07	1.09	7.74E-07	both
pspA	regulatory protein for phage-shock-protein operon	4.28	1.93E-08	-2.58	7.41E-06	both
pspB	psp operon transcription co-activator	4.52	1.29E-07	-2.33	5.31E-05	both
pspC	psp operon transcription co-activator	4.52	2.40E-08	-2.21	2.97E-05	both
pspD	peripheral inner membrane phage-shock protein	4.85	3.66E-08	-2.19	3.24E-05	both
pspE	thiosulfate:cyanide sulfurtransferase (rhodanese)	2.13	4.76E-09	-1.96	3.97E-08	both
pspG	phage shock protein G	4.26	4.96E-06	-3.05	1.22E-04	both
psuK	pseudouridine kinase	1.39	3.41E-05	-1.07	3.58E-05	both
rciB	reactive chlorine species (RCS) stress resistance periplasmic protein	1.53	5.37E-03	1.80	1.95E-02	both
recN	recombination and repair protein	3.86	3.42E-15	-1.18	6.24E-08	both
rihC	ribonucleoside hydrolase 3	-1.99	4.81E-13	-1.36	2.39E-10	both
rutA	pyrimidine oxygenase, FMN-dependent	2.19	1.57E-02	1.84	1.47E-03	both
sfmA	FimA homolog	2.37	1.44E-04	1.11	3.72E-03	both
sodA	superoxide dismutase, Mn	4.42	8.36E-15	1.00	1.15E-06	both
sodB	superoxide dismutase, Fe	-3.58	5.93E-11	-1.01	3.00E-04	both

spy	periplasmic ATP-independent protein refolding chaperone, stress-induced	2.81	3.94E-02	4.05	6.37E-03	both
sra	stationary-phase-induced ribosome-associated protein	1.66	1.01E-05	1.19	1.56E-04	both
ssnA	putative chlorohydrolase/aminohydrolase	-7.49	9.25E-14	-2.64	4.60E-09	both
stpA	DNA binding protein, nucleoid-associated	2.09	8.84E-04	-2.42	9.32E-03	both
sufA	Fe-S cluster assembly protein	1.11	1.31E-06	1.05	8.47E-07	both
suhB	inositol monophosphatase	1.24	1.30E-07	-1.15	5.67E-07	both
tauA	taurine transporter subunit	3.18	6.30E-04	1.12	8.73E-03	both
tdcA	tdc operon transcriptional activator	-4.52	5.43E-11	-4.37	8.13E-10	both
tdcB	L-threonine dehydratase, catabolic	-6.46	1.54E-13	-4.69	4.84E-10	both
tdcC	L-threonine/L-serine transporter	-6.38	6.36E-15	-4.10	2.03E-11	both
tdcD	propionate kinase/acetate kinase C, anaerobic	-6.91	1.24E-14	-4.38	1.97E-10	both
tdcE	pyruvate formate-lyase 4/2-ketobutyrate formate-lyase	-6.96	2.22E-15	-3.73	4.79E-11	both
tdcF	putative reactive intermediate deaminase	-6.62	8.36E-15	-2.85	3.05E-09	both
tdcG	L-serine dehydratase 3, anaerobic	-5.91	4.40E-14	-2.72	8.67E-09	both
tnaA	tryptophanase/L-cysteine desulfhydrase, PLP-dependent	-5.27	4.32E-13	-2.74	1.82E-09	both
tnaB	tryptophan transporter of low affinity	-4.13	1.07E-09	-3.16	9.17E-08	both
tnaC	tryptophanase leader peptide	-4.89	6.36E-15	-2.46	2.93E-08	both
torA	trimethylamine N-oxide (TMAO) reductase I, catalytic subunit	-2.58	7.64E-15	6.67	2.16E-19	both
torC	trimethylamine N-oxide (TMAO) reductase I, cytochrome c-type subunit	-2.92	1.63E-11	6.86	1.46E-12	both
torD	TorA-maturation chaperone	-2.42	3.40E-13	5.17	6.75E-16	both
ttdR	transcriptional activator of ttdABT	-3.78	9.78E-08	-1.72	7.21E-06	both
uacT	uric acid permease	-5.82	3.71E-06	-2.39	6.85E-05	both
ugpB	glycerol-3-phosphate transporter subunit	1.94	9.40E-11	1.56	4.50E-09	both
ugpC	glycerol-3-phosphate transporter subunit	1.00	1.54E-04	1.22	2.05E-05	both
uspB	universal stress (ethanol tolerance) protein B	1.60	5.18E-11	1.41	3.48E-10	both
uvrA	ATPase and DNA damage recognition protein of nucleotide excision repair excinuclease UvrABC	1.37	2.34E-10	1.04	4.12E-08	both

xanQ	xanthine permease	-4.79	6.99E-13	-1.70	1.85E-07	both
xdhA	xanthine dehydrogenase, molybdenum binding subunit	-4.14	7.40E-14	-1.18	3.74E-07	both
xdhD	putative hypoxanthine oxidase, molybdopterin-binding/Fe-S binding	-5.58	4.76E-15	-1.46	3.95E-08	both
xylF	D-xylose transporter subunit	1.34	1.16E-07	-1.25	1.72E-07	both
xylG	fused D-xylose transporter subunits of ABC superfamily: ATP-binding components	1.38	1.92E-05	-1.06	1.56E-04	both
yahM	uncharacterized protein	1.15	8.21E-04	-1.15	4.81E-02	both
ybaA	DUF1428 family protein	3.04	2.73E-11	1.57	2.24E-08	both
ybaT	putative amino acid transporter	-1.32	2.70E-05	1.70	4.57E-06	both
ybcN	DLP12 prophage; uncharacterized protein	2.09	1.25E-02	-2.08	2.32E-02	both
ybcW	DLP12 prophage; uncharacterized protein	-1.52	1.22E-03	-1.17	1.70E-02	both
ybgS	putative periplasmic protein	3.73	1.71E-10	2.51	5.60E-09	both
ybiA	DUF1768 family protein	-1.36	7.37E-04	-1.36	1.54E-05	both
ybiH	DUF1956 domain-containing tetR family putative transcriptional regulator	1.33	1.87E-04	-1.14	2.06E-04	both
ybiU	DUF1479 family protein	2.10	3.48E-11	1.66	1.17E-08	both
ybiY	putative pyruvate formate lyase activating enzyme	-1.49	7.03E-03	-1.00	1.18E-02	both
ycgB	SpoVR family stationary phase protein	1.18	7.51E-10	1.47	4.00E-10	both
yciE	putative rubrerythrin/ferritin-like metal-binding protein	3.72	9.59E-11	1.74	5.88E-08	both
yciF	putative rubrerythrin/ferritin-like metal-binding protein	3.71	8.70E-11	1.65	1.53E-07	both
yciG	KGG family protein	4.03	5.76E-09	2.17	1.53E-07	both
yciX	uncharacterized protein	1.15	1.75E-03	-1.32	2.20E-03	both
ycjM	alpha amylase catalytic domain family protein	1.50	8.24E-06	-2.07	3.70E-05	both
yddA	putative multidrug transporter subunit of ABC superfamily, membrane component/ATP-binding component	3.72	1.51E-04	-2.43	9.74E-08	both
yddb	putative TonB-dependent outer membrane receptor	3.12	9.94E-05	-2.74	7.33E-08	both
ydeI	hydrogen peroxide resistance OB fold protein; putative periplasmic protein	3.28	2.78E-12	1.92	9.74E-10	both
ydeJ	inactive PncC family protein	2.90	1.62E-10	1.04	1.89E-06	both
ydeN	putative Ser-type periplasmic non-aryl sulfatase	-2.17	9.57E-10	-2.53	4.50E-09	both

ydhY	putative 4Fe-4S ferridoxin-type protein; FNR, Nar, NarP-regulated protein; putative subunit of YdhYVWXUT oxidoreductase complex	-5.11	2.77E-08	-1.74	1.09E-02	both
ydiE	hemin uptake protein HemP homolog	2.06	2.21E-08	-1.10	1.65E-07	both
yeaD	D-hexose-6-phosphate epimerase-like protein	-1.63	1.88E-09	-1.27	2.93E-08	both
yeaG	protein kinase, endogenous substrate unidentified; autokinase	1.18	2.36E-08	1.40	2.42E-08	both
yebE	DUF533 family inner membrane protein	3.11	2.59E-09	-1.18	2.41E-04	both
yeiQ	putative NAD-dependent D-mannonate oxidoreductase	1.20	9.15E-04	-1.08	1.36E-03	both
yfcV	putative fimbrial-like adhesin protein	2.98	1.07E-03	-2.12	2.82E-02	both
yfdE	acetyl-CoA:oxalate CoA-transferase	2.24	1.58E-06	1.04	8.74E-04	both
yfdV	putative transporter	3.07	1.87E-04	1.43	1.99E-02	both
yfeD	DUF1323 family putative DNA-binding protein	-1.32	2.14E-04	-1.31	9.75E-05	both
ygaU	uncharacterized protein	1.01	3.00E-07	1.33	3.30E-08	both
ygcN	putative oxidoreductase	-2.46	3.27E-11	-1.44	1.89E-08	both
ygcO	putative 4Fe-4S cluster-containing protein	-3.63	2.19E-08	-1.12	8.45E-05	both
ygeW	putative carbamoyltransferase	-7.58	6.80E-12	-2.22	1.04E-06	both
ygeX	2,3-diaminopropionate ammonia lyase, PLP-dependent	-7.70	3.90E-13	-2.00	2.37E-07	both
ygeY	putative peptidase	-6.76	4.40E-14	-1.84	9.91E-08	both
ygfK	putative Fe-S subunit oxidoreductase subunit	-7.45	1.93E-14	-2.61	3.96E-09	both
ygfM	putative oxidoreductase	-6.86	1.31E-13	-2.35	8.78E-09	both
ygfT	putative oxidoreductase, Fe-S subunit/nucleotide-binding subunit	-4.31	1.43E-11	-1.51	1.16E-06	both
yhbE	EamA family inner membrane putative transporter	1.44	9.45E-09	1.23	6.52E-08	both
yhbO	stress-resistance protein	1.47	3.69E-09	1.64	9.74E-10	both
yhbU	U32 peptidase family protein	-6.63	3.23E-07	-1.25	1.02E-03	both
yhcC	putative Fe-S oxidoreductase, Radical SAM superfamily protein	-2.33	1.32E-03	-1.29	1.91E-03	both
yhdU	putative membrane protein	1.52	1.02E-02	-3.45	7.94E-05	both
yhfX	putative pyridoxal 5'-phosphate binding protein	2.98	1.17E-04	-1.20	6.03E-03	both
yhfY	PRD domain protein	1.83	3.33E-02	-1.28	2.38E-02	both

yhfZ	putative DNA-binding transcriptional regulator	1.49	4.20E-03	-1.79	1.11E-04	both
yhhA	DUF2756 family protein	2.03	6.30E-10	1.03	1.36E-06	both
yhiM	acid resistance protein, inner membrane	1.67	1.29E-04	2.95	1.66E-07	both
yhjG	putative inner membrane-anchored periplasmic AsmA family protein	1.30	2.01E-09	1.57	5.42E-10	both
yiaG	HTH_CROC1 family putative transcriptional regulator	2.47	4.78E-11	1.79	3.67E-09	both
yiaK	2,3-diketo-L-gulonate reductase, NADH-dependent	1.40	1.83E-05	-1.45	2.55E-07	both
yiaM	2,3-diketo-L-gulonate TRAP transporter small permease protein	2.01	3.53E-02	-4.01	5.63E-04	both
yiaN	2,3-diketo-L-gulonate TRAP transporter large permease protein	1.54	2.75E-03	-1.30	1.84E-03	both
yidL	AraC family putative transcriptional regulator	1.90	4.67E-06	-1.20	3.44E-04	both
yjbl	stress-induced protein, UPF0337 family	2.02	5.10E-09	1.39	1.00E-06	both
yjcH	DUF485 family inner membrane protein	2.03	1.09E-05	1.02	1.34E-03	both
yjdN	metalloprotein superfamily protein	2.21	2.69E-10	1.28	2.38E-08	both
yjfl	UPF0719 family inner membrane protein	1.66	3.36E-03	2.33	4.67E-04	both
yjfY	YhcN family protein, periplasmic	2.87	2.90E-07	1.39	1.14E-05	both
yjiL	putative ATPase, activator of (R)-hydroxyglutaryl-CoA dehydratase	-1.85	4.26E-05	-1.12	4.37E-06	both
yjiM	putative 2-hydroxyglutaryl-CoA dehydratase	-1.71	8.36E-06	-1.19	5.92E-06	both
yjiY	putative transporter	-3.37	5.37E-09	1.77	1.88E-06	both
yjiI	DUF3029 family protein, putative glycine radical enzyme	-4.59	3.98E-10	-1.07	1.31E-04	both
yjiM	yjiMN operon transcriptional activator	1.13	4.40E-05	-1.27	2.91E-07	both
ykgO	RpmJ-like protein	3.76	1.89E-05	1.70	3.59E-02	both
ylaC	DUF1449 family inner membrane protein	1.76	9.46E-09	1.02	3.59E-06	both
ylcI	DUF3950 family protein, DLP12 prophage	-4.55	3.46E-05	-3.19	4.99E-04	both
ymdF	KGG family protein	3.49	2.64E-09	1.91	5.88E-08	both
ymfJ	e14 prophage; uncharacterized protein	4.76	1.54E-13	-1.70	1.94E-03	both
ymfQ	prophage e14 tail protein homolog	4.78	2.69E-10	1.01	7.47E-03	both
ymfR	e14 prophage; uncharacterized protein	4.52	5.78E-11	1.10	1.68E-02	both
ymgA	RcsB connector protein for regulation of biofilm	1.63	1.35E-07	2.37	7.15E-07	both

ymgD	uncharacterized protein	2.09	2.06E-05	-1.30	1.78E-04	both
ymgE	UPF0410 family putative inner membrane protein	2.11	1.52E-09	1.43	2.43E-08	both
ymgG	UPF0757 family protein	2.00	2.76E-05	-2.66	4.32E-06	both
ymgI	uncharacterized protein	2.10	1.71E-03	-2.32	8.63E-04	both
ymiA	uncharacterized protein	1.49	5.38E-04	-1.29	4.08E-03	both
yncJ	uncharacterized protein	4.62	2.09E-10	-1.18	1.36E-04	both
ynfO	uncharacterized protein, Qin prophage	-4.05	6.46E-06	-2.13	7.22E-04	both
ynjE	molybdopterin synthase sulfurtransferase	-2.16	1.06E-04	-1.53	1.92E-05	both
yodD	uncharacterized protein	1.71	1.94E-11	1.35	4.00E-10	both
yohC	Yip1 family inner membrane protein	3.75	2.47E-13	1.79	3.48E-10	both
yohF	putative oxidoreductase	1.18	1.01E-06	1.75	6.09E-09	both
yohP	uncharacterized protein	3.58	1.76E-07	2.27	1.16E-06	both
yqcE	MFS transporter family protein	-1.01	6.74E-03	-1.37	1.33E-03	both
yqeB	XdhC-CoxI family protein with NAD(P)-binding Rossman fold	-3.34	2.48E-12	-1.48	3.00E-07	both
yqeC	putative selenium-dependent hydroxylase accessory protein	-2.81	1.69E-09	-2.11	3.42E-07	both
yqfG	uncharacterized protein	-5.02	1.18E-05	-2.71	1.55E-03	both
yqgA	DUF554 family putative inner membrane protein	-1.69	1.41E-02	-1.31	3.72E-03	both
yqjG	putative S-transferase	1.01	3.53E-05	1.37	1.13E-06	both
ytjA	uncharacterized protein	1.45	7.57E-09	2.53	1.98E-10	both

VI. Significantly enriched terms in LH1 and LH2

Category	Term	Count	%	Genes	List Total	FDR	Sig	Reg
UP_KEY WORDS	Metal-binding	71	23.5	CUER, CBDB, CBDA, FUMB, YHCC, DOSP, CSID, HCHA, DDPX, NARY, NARZ, PAOC, FTNA, DGCZ, PAOA, KDPB, ILVB, HYBC, HYBA, HYBB, MGLB, SSNA, UVRA, FRWA, DOSC, HYBO, ASTE, NAPA, BTUB, NAPB, XDHD, BIOB, ACNA, TORC, XDHA,	298	0.00255	Both	Both

				FUCA, TORA, NAPF, NAPG, NAPH, HYAB, YBIY, HYAC, CYSI, HYAA, YGCO, OBGE, HYAD, FUCO, PPHA, YDEN, YJIL, HYPA, HYPB, NRDF, GATD, YGEY, CYDA, ACS, TDCG, YDHY, YGFT, ADHP, TDCD, PQQL, ENTD, YGFK, SUHB, SODB, HYUA, SODA				
UP_KEY WORDS	Signal	52	17.2	SFMA, CIRA, YHBU, NANC, YJFY, XYLF, YBCW, POTF, YNCJ, YBGS, SPY, PSPE, TAU, ANSB, FADL, UGPB, PAOA, MALE, HYBA, MEPH, MGLB, OSMY, FIMA, YNJE, FIMD, CPXP, HYBO, FIMF, FIMG, NAPA, OMPW, BTUB, NAPB, RCLB, PSIF, YDEI, TORA, NAPG, CSGF, CSGE, HYAA, YMGD, OSMB, YDEN, YHHA, YFCV, DDP, YQFG, MCBA, NIKA, HIUH, YMFQ	298	0.031196	Both	Both
UP_KEY WORDS	Oxidoreductase	47	15.6	NAPA, XDHD, CBDB, CBDA, LHGO, XDHA, TORA, YGCN, HYAB, YBIY, YIAK, CYSI, HYAA, CYSH, PRET, RUTA, FUCO, FADE, YEIQ, NARY, NARZ, OSMC, PAOC, FTNA, NRDE, PAOB, NRDF, GLCE, PAOA, GLCD, GATD, CYDA, METF, HYBC, HYBA, YGFT, ADHP, GLPB, GLPA, YQJG, ASTD, HYBO, SODB, YOHP, GABD, ALLD, SODA	298	0.002245	Both	Both
UP_KEY WORDS	Iron	38	12.6	NAPA, NAPB, XDHD, CBDB, CBDA, BIOB, FUMB, YHCC, DOSP, CIRA, TORC, ACNA, NAPF, NAPG, NAPH, YBIY, HYAC, CYSI, HYAA, YGCO, CSID, FUCO, YJIL, NARY, NARZ, FTNA, NRDF, PAOA, CYDA, HYBA, TDCG, HYBB, YDHY, YGFT, YGFK, DOSC, HYBO, SODB	298	2.57E-04	Both	Both
KEGG_PATHWAY	Microbial metabolism in diverse environments	29	9.6	NAPA, NAPB, FUMB, YEAD, ACNA, FUCA, XDHA, HYAB, CYSI, HYAA, CYSH, HCHA, FUCO, NARY, NARZ, PAOC, PAOB, GLCE, PAOA, GLCD, METF, HYBC, ACS, ADHP, HIUH, YNJE, HYBO, GABD, ALLD	102	0.021782	Both	Both
UP_KEY WORDS	Iron-sulfur	23	7.6	NAPA, XDHD, FUMB, BIOB, YHCC, PAOA, ACNA, NAPF, NAPG, NAPH, YBIY, HYBA, HYAA, TDCG, YGCO, CYSI, YDHY, YGFT, YGFK, HYBO, YJIL, NARY, NARZ	298	0.004998	Both	Both
UP_KEY WORDS	Stress response	22	7.3	RCLB, ASTA, GRCA, PSPB, PSPA, PSPD, YKGO, PSCP, PHOH, YHBO, HCHA, YOHP, CPXP, DEAD, BETT, ASTD, SPY, BOLA, PSPE, ASTE, ASTB, PSPG	298	0.013978	Both	Both
GOTERM_MF_DIRECTORY	4 iron, 4 sulfur cluster binding	21	7.0	NAPA, FUMB, BIOB, YHCC, ACNA, NAPF, NAPG, NAPH, YBIY, HYBA, HYAA, TDCG, CYSI, YDHY, YGFT, YGFK, SUFA, HYBO, YJIL, NARY, NARZ	220	0.005531	Both	Both

UP_KEY WORDS	4Fe-4S	20	6.6	NAPA, FUMB, BIOB, YHCC, ACNA, NAPF, NAPG, NAPH, YBIY, HYBA, HYAA, TDCG, CYSI, YDHY, YGFT, YGFK, HYBO, YJIL, NARY, NARZ	298	0.004692	Both	Both
GOTERM_CC_DIRECTORY	Periplasmic space	18	6.0	PAOC, NAPA, PAOB, NAPB, RCLB, ANSB, PAOA, YJFY, MALE, MCBA, HYBA, NIKA, OSMY, HIUH, YNJE, HYBO, PSPE, TAUA	204	0.008282	Both	Both
GOTERM_BP_DIRECTORY	Anaerobic respiration	16	5.3	NAPA, NAPB, TORC, ACNA, TORA, HYAB, HYBC, HYAC, HYBA, HYAA, HYBB, GLPB, GLPA, HYBO, NARY, NARZ	234	0.001281	Both	Both
GOTERM_MF_DIRECTORY	Iron ion binding	15	5.0	NAPA, XDHD, NRDF, BIOB, HYPC, TORC, ACNA, NAPF, NAPH, HYBC, HYAC, YGCO, CSID, YGFK, SODB	220	0.003852	Both	Both
UP_KEY WORDS	Heme	10	3.3	HYAC, NAPB, CBDB, CYSI, HYBB, CBDA, DOSP, TORC, DOSC, CYDA	298	0.014892	Both	Both
GOTERM_CC_DIRECTORY	[Ni-Fe] hydrogenase complex	7	2.3	HYBC, HYAB, HYAC, HYBA, HYAA, HYBB, HYBO	204	3.00E-05	Both	Both
UP_KEY WORDS	Purine metabolism	7	2.3	PAOC, PAOB, XDHD, HIUH, PAOA, XDHA, ALLD	298	0.005755	Both	Both
GOTERM_MF_DIRECTORY	Hydrogenase (acceptor) activity	6	2.0	HYBC, HYAB, HYBA, HYAA, HYBB, HYBO	220	0.003852	Both	Both
GOTERM_BP_DIRECTORY	L-threonine catabolic process to propionate	6	2.0	TDCG, TDCF, TDCE, TDCD, TDCB, TDCA	234	0.004652	Both	Both
GOTERM_MF_DIRECTORY	Oxidoreductase activity, acting on the aldehyde or oxo group of donors	5	1.7	PAOC, PAOB, XDHD, PAOA, XDHA	220	0.007204	Both	Both
GOTERM_BP_DIRECTORY	Arginine catabolic process to glutamate	5	1.7	ASTA, ASTD, ASTE, ASTB, ASTC	234	0.00842	Both	Both
GOTERM_BP_DIRECTORY	Arginine catabolic process to succinate	5	1.7	ASTA, ASTD, ASTE, ASTB, ASTC	234	0.00842	Both	Both
UP_KEY WORDS	Arginine metabolism	5	1.7	ASTA, ASTD, ASTE, ASTB, ASTC	298	0.013978	Both	Both
GOTERM_BP_DIRECTORY	Purine ribonucleoside salvage	5	1.7	PAOC, PAOB, XDHD, PAOA, XDHA	234	0.04204	Both	Both
UP_KEY WORDS	Transmembrane beta strand	20	2.6	NANC, CIRA, FHUE, SFMD, OMPN, FIU, FEPA, OMPG, BGLH, PHOE, FIMD, WZA, UIDC, HTRE, LAMB, FECA, OMPX, YBGQ, FADL, FHUA	743	0.001564	LH1	UP

UP_KEY WORDS	Stress response	48	6.3	PSPD, PSPC, PSPB, RCLB, PSPA, YHBO, HCHA, HSPQ, MQSA, RCLC, YDCX, PSPG, PHOE, YOHP, PSPE, HTPX, BETT, ASTA, PHOH, SPY, SBMC, YKGO, RMF, BSMA, YAFO, CPXP, HICA, IBPA, YOEI, BOLA, IBPB, RELE, HICB, MQSR, RELB, DEAD, YNEM, RECA, ASTD, ASTE, ASTB, IRAM, ISCR, HTRE, HSLJ, PSTS, IRAP, HSLO	743	1.06E-04	LH1	UP
UP_KEY WORDS	SOS response	17	2.2	RUVB, UVRD, RUVA, UVRA, UVRB, LEXA, POLB, RECA, RECX, YAFO, SULA, YAFO, UMUD, UMUC, YAFN, CHO, DINI	743	9.86E-08	LH1	UP
UP_KEY WORDS	Signal	120	15.8	NANC, FIU, RCLB, RZOR, YIBG, PHOA, MALE, BGLH, AIS, PHOE, YJFY, WZA, MALM, SPY, FECA, YIAV, NANM, FECB, ECNB, MALS, OSMY, ACRE, EFEO, YHHA, YSAB, YJFN, LIVJ, YDCS, YBCL, ARGT, YBJH, YGDI, HTRE, YGDR, SFMD, OMPN, SFMH, YTFJ, OMPG, YNFD, SFMA, DDPA, CPXP, LAMB, YPFG, YDEI, YIAD, TAU, SBP, YAHO, ASR, YDES, YAAX, YDER, YDEQ, MCBA, OMPX, PSTS, YOBH, FHUD, FHUE, FEPB, FEPA, YPEC, LDTC, PSPE, PROX, CSGA, CSGB, YMGD, CSGE, CSGF, YFDX, FHUA, LSRB, YBGD, UGPB, FIMD, XYLF, FIMC, YJBE, YJBF, FIMI, FIMF, ELFD, FIMG, YMFQ, YFCV, YBGQ, YBGS, FIMA, PSIF, CIRA, YADC, ECPB, EFEB, RCNB, YADK, YADN, YADM, YADL, UIDC, BSMA, ECPA, FADL, POTF, YEBF, YJCS, MLTF, YNCE, YBIJ, YNCJ, ZRAP, YCEI, BAME, YJDP, PAOA, OSMB, MLTD, CYSP	743	9.44E-04	LH1	UP
UP_KEY WORDS	rRNA-binding	30	4.0	RPLK, RPLF, RPLI, RPLB, RPLC, RPLD, RPLE, RPLA, OBGE, RMF, RELE, RPSD, RPSC, RPME, RPMC, RPSQ, RPSR, RPLW, RPSS, RPLV, RPSM, RPLP, RPSK, RPLO, RPSE, RPSF, RPSG, RPLS, RPLR, RPSH	743	3.44E-10	LH1	UP
UP_KEY WORDS	RNA-binding	41	5.4	RPLK, STPA, RPLF, RPLI, RPLB, RPLC, RPLD, DUSB, RPLE, BGLG, RPLA, OBGE, CASA, RMF, YAFO, HICA, RPSD, RELE, RPSC, YGJH, YOEB, DEAD, RPME, SYME, RPMC, RPSQ, RPSR, RPLW, RPSS, RPLV, RPSM, RPSI, RPLP, RPLO, RPSK, RPSE, RPSF, RPLS, RPSG, RPLR, RPSH	743	0.001003	LH1	UP
UP_KEY WORDS	Ribosomal protein	40	5.3	RPLK, RPLM, RPLF, RPLI, RPLB, RPLC, RPLD, RPLE, RPLA, YKGO, YKGM, RPSB, RPMJ, RPSD, RPSC, RPMH, RPME, RPF, RPMC, RPMD, RPSQ, RPSR, RPLW, RPSS, RPLV, RPSM, RPSN, RPSI, RPLQ, RPLP, RPSI, RPLO, RPSK, RPSE, RPSF, RPSG, RPLS, RPLR, RPSH	743	2.80E-15	LH1	UP

UP_KEY WORDS	Ribonucleoprotein	40	5.3	RPLK, RPLM, RPLF, RPLI, RPLB, RPLC, RPLD, RPLE, RPLA, YKGO, YKGM, RPSB, RPMJ, RPSD, RPSC, RPMH, RPME, RPMF, RPMC, RPMD, RPSQ, RPSR, RPLW, RPSS, RPLV, RPSM, RPSN, RPSP, RPSI, RPLQ, RPLP, RPSJ, RPLO, RPSK, RPSE, RPSF, RPSG, RPLS, RPLR, RPSH	743	3.67E-15	LH1	UP
UP_KEY WORDS	Iron transport	21	2.8	FHUC, FHUD, CIRA, FHUE, FECL, FIU, FECD, FEPB, FEPA, FECP, FEPC, AFUC, FEPC, FES, FEPC, FECA, FECA, FECC, FECC, FHUB, FIEF, FHUA	743	3.62E-08	LH1	UP
UP_KEY WORDS	Ion transport	39	5.1	FHUC, FHUD, NANC, CHAA, FHUE, CIRA, FIU, OMPN, FEPB, FEPA, KDPC, OMPG, FEPC, CORA, KDPF, FEPC, FES, BGLH, RCNA, PHOE, KDPB, KDPA, FEPC, WZA, NHAA, UIDC, MNTH, LAMB, FECA, FECC, FECC, FHUB, FIEF, FHUA, FECL, FECD, FECP, AFUC, ACTP	743	4.66E-04	LH1	UP
UP_KEY WORDS	Fimbrium	18	2.4	YADC, SFMH, YADK, YBGD, SFMA, YADN, YADM, CSGA, YADL, CSGB, FIMI, YDES, FIMF, YDER, FIMG, YDEQ, ECPA, FIMA	743	1.80E-05	LH1	UP
UP_KEY WORDS	Enterobactin biosynthesis	7	0.9	ENTE, ENTF, ENTC, ENTD, YBDZ, ENTA, ENTB	743	0.003399	LH1	UP
GOTERM_BP_DIRECTORY	SOS response	25	3.3	YEBG, RUVB, UVRD, RECN, RUVA, UVRA, UVRB, LEXA, POLB, RECA, SYME, RECX, YDJM, YAFP, SULA, YAFO, UMUD, UMCU, YAFN, DINB, CHO, DIND, DINI, DING, TISB	566	3.42E-11	LH1	UP
GOTERM_BP_DIRECTORY	Translation	36	4.7	RPLM, RPLI, SRA, RPLC, RPLD, RPLE, RPLA, YKGO, YKGM, RPSB, RPMJ, RPSC, RPMH, RPME, RPMF, RPMC, RPMD, RPSQ, RPSR, RPLW, RPSS, RPLV, RPSM, RPSN, RPSP, RPSI, RPLQ, RPLP, RPSJ, RPLO, RPSK, RPSF, RPSG, RPLS, RPLR, RPSH	566	1.83E-09	LH1	UP
GOTERM_BP_DIRECTORY	Iron ion homeostasis	19	2.5	FHUC, FHUD, FHUE, FECL, FIU, FECD, FEPB, FECP, FEPC, AFUC, FEPC, FES, FEPC, FECA, FECC, FECC, FHUB, FIEF, FHUA	566	1.19E-07	LH1	UP
GOTERM_BP_DIRECTORY	Ion transport	18	2.4	FHUC, FHUD, NANC, FECL, OMPN, FECD, FEPB, FECP, OMPG, FEPC, BGLH, PHOE, WZA, UIDC, LAMB, FECC, FECC, FHUB	566	4.74E-04	LH1	UP
GOTERM_BP_DIRECTORY	Enterobactin biosynthetic process	8	1.1	ENTE, ENTF, ENTC, ENTD, ENTH, YBDZ, ENTA, ENTB	566	0.003091	LH1	UP
GOTERM_BP_DIRECTORY	Cellular response to DNA damage stimulus	57	7.5	YOHC, PAAJ, FEPB, MALF, NARY, MALE, RECX, ENTS, BETT, YIBA, YDJM, UMUD, UMCU, YAFN, DINB, GLXR, DIND, EFEO, PUUP, RECN,	566	0.004599	LH1	UP

				LEXA, RECA, PURD, SYME, GLCD, YBCM, GABP, SULA, YCGB, ARGF, YADC, UXUA, EFEB, RCNB, RBFA, LLDR, SBMC, BSMA, LLDP, LAMB, CHO, YQJI, RUTE, EMRY, YJHC, ALDB, INSK, YBIJ, YIAA, ADHP, DINQ, YBIX, YCIE, YCIF, PSTS, PAOC, TISB				
GOTERM_BP_DIR ECT	Cell adhesion	16	2.1	SFMH, YBGD, SFMA, YADN, YADM, CSGA, YADL, CSGB, FIMI, YDES, FIMF, YDER, FIMG, YDEQ, YFCV, FIMA	566	0.010608	LH1	UP
GOTERM_BP_DIR ECT	Slime layer polysaccharide biosynthetic process	8	1.1	WCAK, WCAI, WCAF, WCAE, WCAC, WCAD, WCAA, WCAB	566	0.020817	LH1	UP
GOTERM_CC_DIR ECT	Cytosolic large ribosomal subunit	21	2.8	RPMJ, RPLK, RPLM, RPLF, RPLI, RPLB, RPLC, RPLD, RPLE, RPME, RPMF, RPMC, RPLA, RPMD, RPLW, RPLV, RPLQ, RPLP, RPLO, RPLS, RPLR	481	2.35E-07	LH1	UP
GOTERM_CC_DIR ECT	Cytosolic small ribosomal subunit	17	2.2	RPSB, RPSQ, RPSR, RPSD, RPSS, RPSC, RPSM, RPSN, RPSP, SRA, RPSI, RPSJ, RPSK, RPSE, RPSF, RPSG, RPSH	481	2.79E-06	LH1	UP
GOTERM_CC_DIR ECT	Pilus	19	2.5	YADC, SFMH, YADK, YBGD, SFMA, YADN, YADM, CSGA, YADL, CSGB, FIMI, YDES, FIMF, YDER, FIMG, YDEQ, ECPA, YFCV, FIMA	481	4.82E-05	LH1	UP
GOTERM_CC_DIR ECT	Periplasmic space	29	3.8	FHUD, RCLB, EFEB, YTFJ, PHOA, MALE, AIS, LDTC, YJFY, PSPE, PROX, FECB, MALS, OSMY, EFEO, YBIJ, FECR, TAUA, LSRB, YJFN, YAHO, ZRAP, ASR, YCEI, MCBA, PAOA, PSTS, PAOC, PAOB	481	0.026859	LH1	UP
GOTERM_CC_DIR ECT	Cell outer membrane	29	3.8	SFMD, FHUE, CIRA, FIU, OMPN, RZOR, FEPA, OMPG, BGLH, PHOE, YFEN, WZA, CSGB, UIDC, CSGE, CSGF, LAMB, FECA, FADL, FHUA, MLTF, RSXG, YIAD, FIMD, HTRE, OMPX, HSLJ, YBGQ, MLTD	481	0.040056	LH1	UP
GOTERM_MF_DIR ECT	Structural constituent of ribosome	41	5.4	RPLK, RPLM, RPLF, RPLI, RPLB, SRA, RPLC, RPLD, RPLE, RPLA, YKGO, YKGM, RPSB, RPMJ, RPSD, RPSC, RPMH, RPME, RPMF, RPMC, RPMD, RPSQ, RPSR, RPLW, RPSS, RPLV, RPSM, RPSN, RPSO, RPSI, RPLQ, RPLP, RPSJ, RPLO, RPSK, RPSE, RPSF, RPSG, RPLS, RPLR, RPSH	517	2.69E-17	LH1	UP
GOTERM_MF_DIR ECT	rRNA binding	26	3.4	RPLK, RPSD, RELE, RPSC, RPLF, RPLB, RPLC, RPLD, RPME, RPMC, RPLA, RPSQ, OBGE, RPSS, RLMN, RPLW, RPLV, RPSM, RPSN, RMF, RPLP, RPLO, RPSE, RPLS, RPSG, RPSH	517	9.10E-09	LH1	UP

KEGG_P ATHWA Y	Ribosome	40	5.3	RPLK, RPLM, RPLF, RPLI, RPLB, RPLC, RPLD, RPLE, RPLA, YKGO, YKGM, RPSB, RPMJ, RPSD, RPSC, RPMH, RPME, RPMF, RPMC, RPMD, RPSQ, RPSR, RPLW, RPSS, RPLV, RPSM, RPSN, RPSP, RPSI, RPLQ, RPLP, RPSJ, RPLO, RPSK, RPSE, RPSF, RPSG, RPLS, RPLR, RPSH	246	2.25E-11	LH1	UP
KEGG_P ATHWA Y	ABC transporters	43	5.7	FHUC, YOJI, FHUD, YDDA, MALF, FEPB, MALG, FEPD, MALE, FEPC, METN, FEPG, PROW, PROX, PROV, MALK, FECB, FECC, RBSD, FHUB, POTF, DPPF, LSRD, LSRC, FECD, TAUB, LSRB, TAUA, CYSA, LSRA, AFUC, UGPB, UGPC, LIVJ, SBP, ARGT, XYLF, CYSW, XYLG, XYLH, CYSU, PSTS, CYSP	246	0.031348	LH1	UP
UP_KEY WORDS	3Fe-4S	6	1.4	SDHB, FRDB, NARH, HYBO, HYAA, GLTB	415	0.006018	LH1	DO WN
UP_KEY WORDS	4Fe-4S	50	12.0	HYCF, FDHF, HYCG, HYCB, FRDB, TDCG, HYCE, FUMB, NRFC, ACNA, NARH, NARG, THIH, HYBA, HYBO, GLPC, HYFH, YSAA, YCCM, YHCC, FDOG, FDOH, THIC, YJJW, NAPG, NAPH, FDNG, NAF, FDNH, NAPA, YDHY, YNFE, YDHX, YNFF, YNFG, YDHV, DMSA, NRDG, HYAA, AEGA, YJIL, DMSB, HYDN, YGFK, NIRB, PREA, SDHB, YBIY, YGFS, YGFT	415	8.29E-21	LH1	DO WN
KEGG_P ATHWA Y	Citrate cycle (TCA cycle)	12	2.9	SDHA, SDHB, ACEF, FRDD, ACEE, FRDC, FRDB, FRDA, ACNA, PCK, LPD, FUMB	172	7.89E-04	LH1	DO WN
KEGG_P ATHWA Y	Glyoxylate and dicarboxylate metabolism	14	3.4	GARK, FDHF, FDOI, GCVP, DMLA, GLNA, ACNA, FUCO, GARR, GCVT, LPD, FDOG, FDOH, GCVH	172	0.002595	LH1	DO WN
KEGG_P ATHWA Y	Thiamine metabolism	7	1.7	THIF, THIE, THIH, THIG, THIK, THIM, THIC	172	0.007995	LH1	DO WN
KEGG_P ATHWA Y	Nitrogen metabolism	13	3.1	YQEA, HCP, NRFA, GLNA, NAPA, NAPB, NIRB, NIRD, NARH, NARG, NARI, NARK, GLTB	172	5.73E-05	LH1	DO WN
KEGG_P ATHWA Y	Microbial metabolism in diverse environments	49	11.8	YQEA, FDHF, LYSA, MAEB, FRDD, FRDC, FRDB, LYSC, FRDA, PCK, YEIG, FUMB, ACEF, ACEE, ACNA, NARH, NARG, NARI, YEAD, GLTB, PDXH, HYBC, HYBO, FDOI, HIUH, FDOG, FDOH, XDHA, XDHC, XDHB, NAPA, NAPB, YDHU, GALM, YNJE, HYAB, HYAA, SERA, ALLD, NRFA, TKTA, GLNA, FUCO, LPD, SDHA, NIRB, SDHB, NIRD, FUCA	172	8.48E-05	LH1	DO WN
KEGG_P ATHWA Y	Carbon metabolism	26	6.3	FDHF, YQEA, MAEB, FRDD, FRDC, TKTA, FRDB, FRDA, TDCG, PCK, LPD, YIHU, YEIG, FUMB, SDHA, SDHB, ACEF, ACEE, FDOI, GCVP,	172	0.001367	LH1	DO WN

				ACNA, GCVT, FDOG, FDOH, TDCB, SERA				
KEGG_PATHWAY	Two-component system	33	7.9	ATOC, NARQ, FRDD, FRDC, CITE, FRDB, DCUB, CITD, FRDA, CITC, FDNG, FDNI, FDNH, CITF, CBDB, CBDA, OMPC, NARH, NARG, NARI, NARI, UVRY, TORA, EVGA, GLNA, TORC, TORD, CYDA, CYDB, EVGS, AMPC, TORS, CITX	172	6.39E-04	LH1	DOWN
UP_KEY WORDS	Electron transport	42	10.1	HYCF, CYDX, NAPG, HYCB, FRDB, NAPH, FRDA, NAPF, NAPC, FDNI, FDNH, NAPA, NAPB, CBDB, CBDA, YNFG, NRFB, NRFC, NARH, HYAC, NARG, NARI, DMSB, YHJA, HCR, NRFA, TORC, HYBB, HYDN, GLPC, HYFH, YSAA, SDHA, GRXA, SDHB, YCCM, CYDA, CYDB, FDOI, YGFS, FDOH, YGCO	415	6.95E-16	LH1	DOWN
COGONTOLOGY	Energy production and conversion	10	2.4	YCCM, CYDB, HYCB, NAPC, YGFS, GLDA, CITF, CBDB, YGCO, YQHD	61	0.016305	LH1	DOWN
UP_KEY WORDS	Heme	19	4.6	YHJA, NRFA, TORC, HYBB, NAPC, FDNI, NAPB, CBDB, CBDA, NIRB, NRFB, CYDA, CYDB, FDOI, KATG, NRFF, HYAC, NARI, CCME	415	5.46E-08	LH1	DOWN
UP_KEY WORDS	Iron	80	19.2	FDHF, HYCF, HYCG, HYCB, FRDB, TDCG, HYCE, FUMB, FETB, FETA, NRFB, NRFC, KATG, NRFF, ACNA, NARH, NARG, NARI, GLTB, THIH, HYBA, HYBB, HYBO, GLPC, HYFH, YSAA, YCCM, CYDA, YHCC, FDOI, CYDB, FDOG, FDOH, YGCO, THIC, YJJW, NAPG, NAPH, XDHC, FDNG, NAPF, FDNI, NAPC, XDHD, FDNH, NAPA, YDHY, NAPB, YNFE, CBDB, CBDA, YNFF, YDHX, YNFG, YDHV, DMSA, HYAC, NRDG, HYAA, AEGA, YJIL, DMSB, HCR, YHJA, NRFA, HCP, TORC, GARL, FUCO, FTNA, HYDN, NIRB, YGFK, SDHB, PREA, YBIY, YGFS, CCME, SODB, YGFT	415	3.38E-23	LH1	DOWN
UP_KEY WORDS	Iron-sulfur	56	13.5	HYCF, FDHF, HYCG, HYCB, FRDB, TDCG, HYCE, FUMB, NRFC, ACNA, NARH, NARG, GLTB, THIH, HYBA, HYBO, GLPC, HYFH, YSAA, YCCM, YHCC, FDOG, FDOH, YGCO, THIC, YJJW, NAPG, NAPH, XDHC, FDNG, NAPF, XDHD, FDNH, NAPA, YDHY, YNFE, YDHX, YNFF, YNFG, YDHV, DMSA, NRDG, HYAA, AEGA, YJIL, DMSB, HCR, HYDN, NIRB, YGFK, SDHB, PREA, YBIY, YGFS, YGFT	415	2.38E-20	LH1	DOWN
UP_KEY WORDS	Metal-binding	128	30.8	FDHF, HYCF, HYCG, MAEB, HYCB, HYCE, GLDA, FUMB, THRS, GUDD, KATG, SRLQ, YQHD, GLTB, THIF, THIE, THIH, PDXK, HYBF, TOPB, HYBC, HYBD, HYBA, HYBB, HYBO, THIM, YSAA, YCCM, FDOI, LYSU, FDOG, FDOH, GATD, YGCO, THIC,	415	6.30E-16	LH1	DOWN

				YNFK, NAPG, NAPH, NAPF, NAPC, NAPA, HYUA, NAPB, CBDB, YNFE, CBDA, YNFF, YNFG, OMPC, NRDG, AEGA, YJIL, NRDD, BTUB, YGEY, TORA, NRFA, SSNA, TORC, GARL, FTNA, HYDN, GUAD, NIRB, YGFK, YGFS, YDEN, CCME, YGFT, TDCD, CITE, FRDB, CPDB, TDCG, PCK, FRWA, GSS, NRFB, NRFC, ACEE, MGLB, NRFF, ACNA, NARH, NARG, NARI, PEPD, GLPC, HYFH, PEPT, CYDA, CYDB, YHCC, YCDT, YJJW, XDHA, XDHC, FDNG, FDNI, XDHD, HYPD, CUER, FDNH, YDHY, HYPF, YDHX, HYPA, HYPB, YDHV, DMSA, HYAC, HYAB, HYAA, HYAD, DMSB, YHJA, HCR, MEND, HCP, TKTA, FUCO, NEI, YDAM, SDHB, PREA, YBIY, SODB, FUCA				
UP_KEY WORDS	Molybdenum	11	2.6	TORA, FDHF, DMSA, XDHA, FDNG, XDHD, NARG, FDOG, NAPA, YNFE, YNFF	415	6.39E-04	LH1	DO WN
UP_KEY WORDS	Nickel	14	3.4	HYBF, HYBC, HYBD, HYCE, HYPA, HYPB, HYAB, NIKD, NIKE, NIKB, NIKC, HYAF, HYAD, NIKA	415	3.27E-06	LH1	DO WN
UP_KEY WORDS	Nitrate assimilation	9	2.2	NIRB, NARQ, NIRD, NARH, NARG, NARI, NAPA, NARI, NARK	415	0.004397	LH1	DO WN
UP_KEY WORDS	Oxidoreductase	77	18.5	FDHF, HYCG, MAEB, HYCC, DMLA, FRDB, HYCD, FRDA, HYCE, GLDA, YIHU, NRFC, ACEE, KATG, NARH, NARG, NARI, YQHD, GLTB, PDXH, HYBC, GLPB, GLPA, HYBA, AHPF, HYBO, CYDA, CYDB, FDOG, GATD, YGCN, PNTB, YJJW, CYDX, XDHA, FDNG, PNTA, XDHB, XDHD, NAPA, YNFE, CBDB, CBDA, YNFF, YDHV, YNFH, DMSA, NRDG, HYAB, STHA, HYAA, AEGA, NRDD, PRET, SERA, DMSC, ALLD, TORA, HCR, YHJA, NRFA, HCP, FUCO, GARR, FTNA, LPD, WRBA, YGFF, NIRB, SDHA, SDHB, PREA, YBIY, GCVP, NIRD, SODB, YGFT	415	3.36E-10	LH1	DO WN
UP_KEY WORDS	Thiamine biosynthesis	7	1.7	THIF, THIE, THIH, THIG, THIM, THIC, THIS	415	0.004435	LH1	DO WN
UP_KEY WORDS	Transport	102	24.5	HYCF, GUDP, HYCB, FETB, FETA, DTPC, NIKD, NIKE, NIKB, NIKC, NIKA, HYBB, YSAA, GATA, YCCM, FDOI, ARGO, TNAB, YHHJ, FDOH, YGCO, GATB, CADB, YDDG, CYDX, NAPG, NAPH, GSIA, NAPF, NAPC, NAPA, NAPB, CBDB, CBDA, YNFG, OMPC, GALP, BTUB, NRFA, UACT, TORC, HYDN, YHAO, GARP, YCAD, CCMC, GRXA, CCMD, TORT, YBEX, YGFS, YAAJ, HSRA, TDCC, DCUA, DCUC, FRDB, DCUB, FRDA, FRWA, YEAN, MGLA, YJCE, NHAB, MGLC, NRFB, MGLB, NRFC, NARH, GLPT, PROP, NARG, MDTH, NARI, MDTL, NARK, CVRA, MDTI, MDTJ, GLPC, HYFH, CYDA, CYDB, SUGE, LOLB,	415	0.001937	LH1	DO WN

				LOLC, PGAA, AMPG, FDNI, FDNH, XANQ, YIJE, HYAC, DMSB, YHJA, YFBS, HCR, YBAT, SDHA, SDHB, ARAG, ARAF				
GOTERM_BP_DIRECTORY	anaerobic respiration	42	10.1	FRDD, FRDC, HYCB, FRDB, FRDA, FDNG, NAPC, FDNI, FDNH, NAPA, NAPB, YNFE, YNFF, YNFG, DMSA, ACNA, NARH, HYAC, NARG, HYAB, HYAA, NARI, DMSB, DMSB, TORA, HYBC, GLPB, GLPA, TORC, HYBA, HYBB, HYBO, HYDN, GLPC, YSAA, NIRB, FDOI, NIRD, TORS, YGFS, FDOG, FDOH	348	1.52E-26	LH1	DO WN
GOTERM_MF_DIRECTORY	4 iron, 4 sulfur cluster binding	51	12.3	HYCF, FDHF, HYCG, HYCB, FRDB, TDCG, HYCE, FUMB, NRFC, ACNA, NARH, NARG, THIH, HYBA, HYBO, GLPC, HYFH, YSAA, YCCM, YHCC, FDOG, FDOH, THIC, YJJW, NAPG, NAPH, FDNG, NAF, FDNH, HYPD, NAPA, YDHY, YNFE, YDHX, YNFF, YNFG, YDHV, DMSA, NRDG, HYAA, AEGA, YJIL, DMSB, HYDN, NIRB, YGFK, PREA, SDHB, YBIY, YGFS, YGFT	344	3.74E-18	LH1	DO WN
GOTERM_MF_DIRECTORY	electron carrier activity	43	10.3	FDHF, HYCB, FRDB, XDHC, FRDA, FDNG, NAPF, NAPC, FDNI, FDNH, NAPA, CBDB, YNFE, YNFF, CBDA, YDHU, YNFG, YDHV, DMSA, NRFB, NARH, HYAC, NARG, HYAB, HYAA, NARI, DMSB, TORA, YHJA, HCR, AHPF, TORC, HYDN, YSAA, GRXA, SDHA, SDHB, CYDA, CYDB, FDOI, YGFS, FDOG, FDOH	344	1.96E-15	LH1	DO WN
GOTERM_MF_DIRECTORY	metal ion binding	76	18.3	HYCF, HYCG, TDCD, HYCB, CPDB, FRDB, TDCG, FRWA, GLDA, FUMB, GSS, NRFB, NRFC, ACEE, MGLB, KATG, NRFF, ACNA, NARH, SRLQ, NARI, GLTB, THIF, THIE, PDXK, HYBD, HYBA, HYBB, HYBO, GLPC, HYFH, YSAA, YCCM, CYDA, YHCC, FDOI, CYDB, FDOH, YCDT, YJJW, NAPG, XDHA, XDHC, FDNI, NAPC, FDNH, YDHY, HYUA, NAPB, CBDB, CBDA, YDHX, YNFG, OMPC, YDHV, NRDG, HYAA, AEGA, YJIL, BTUB, HYAD, DMSB, HCR, YHJA, HCP, SSNA, HYDN, NIRB, SDHB, PREA, YDAM, YBIY, YGFS, YDEN, CCME, YGFT	344	1.20E-11	LH1	DO WN
GOTERM_MF_DIRECTORY	heme binding	17	4.1	YHJA, NRFA, TORC, NAPC, FDNI, CCMC, NIRB, NRFE, NRFB, CYDA, CYDB, FDOI, KATG, HYAC, NARI, CCME, NIKA	344	7.87E-06	LH1	DO WN
GOTERM_MF_DIRECTORY	iron-sulfur cluster binding	14	3.4	THIH, FRDB, HYBA, HYBO, GLPC, YNFE, YNFF, NIRB, PREA, SDHB, NARH, NRDG, YGCO, PRET	344	4.47E-05	LH1	DO WN
GOTERM_BP_DIRECTORY	protein maturation	11	2.6	HYBG, HYBE, HYBF, TORD, FDHE, HYPC, HYPD, HYPE, HYPF, HYPA, HYPB	348	1.27E-04	LH1	DO WN

GOTERM_CC_DIR ECT	ferredoxin hydrogenase complex	8	1.9	HYCF, HYCG, HYCB, HYCC, HYCD, HYCE, HYBO, HYAA	315	6.49E-05	LH1	DO WN
GOTERM_MF_DIR ECT	nickel cation binding	11	2.6	HYBF, HYBC, HYCE, HYAB, NIKD, NIKE, NIKB, NIKC, HYPA, NIKA, HYPB	344	1.13E-04	LH1	DO WN
GOTERM_MF_DIR ECT	oxidoreductase activity	26	6.3	YJJW, XDHA, HYCB, XDHC, HYCD, YDHY, YDHX, YNFG, YNFH, KATG, NARH, AEGA, DMSB, PDXH, HCP, HYBA, HYDN, YGFF, YSAA, YGFK, YBIY, YGFS, FDOH, SODB, YGCN, YGFT	344	2.90E-04	LH1	DO WN
GOTERM_BP_DIR ECT	formate oxidation	7	1.7	FDHF, FDOI, FDNG, FDNI, FDNH, FDOG, FDOH	348	0.001045	LH1	DO WN
GOTERM_CC_DIR ECT	[Ni-Fe] hydrogenase complex	7	1.7	HYBC, HYBA, HYBB, HYAC, HYBO, HYAB, HYAA	315	2.71E-04	LH1	DO WN
GOTERM_BP_DIR ECT	fermentation	7	1.7	FRDD, FRDC, FRDB, FRDA, HYAC, HYAB, HYAA	348	0.002854	LH1	DO WN
GOTERM_BP_DIR ECT	thiamine diphosphate biosynthetic process	8	1.9	THIF, THIE, THIH, THIG, THIK, THIM, THIC, THIS	348	0.002312	LH1	DO WN
GOTERM_BP_DIR ECT	oxidation-reduction process	19	4.6	PDXH, HYCF, HCP, HYCB, NAPG, NAPH, HYCD, NAPF, HYBB, LPD, YDHY, HYFH, YDHX, CCMC, SDHA, ACEF, YCCM, YGCO, SODB	348	0.001982	LH1	DO WN
GOTERM_CC_DIR ECT	formate dehydrogenase complex	6	1.4	FDOI, FDNG, FDNI, FDNH, FDOG, FDOH	315	0.001475	LH1	DO WN
GOTERM_MF_DIR ECT	formate dehydrogenase (quinone) activity	6	1.4	FDOI, FDNG, FDNI, FDNH, FDOG, FDOH	344	0.003634	LH1	DO WN
GOTERM_BP_DIR ECT	nitrate assimilation	10	2.4	NIRB, NARQ, NRFA, NIRD, NARH, NARG, NARJ, NAPA, NARI, NARK	348	0.007207	LH1	DO WN
GOTERM_BP_DIR ECT	anaerobic electron transport chain	7	1.7	NRFD, NRFB, NRFC, NRFA, NARI, DMSC, YNFH	348	0.008856	LH1	DO WN
GOTERM_BP_DIR ECT	L-threonine catabolic process to propionate	6	1.4	TDCE, TDCF, TDCD, TDCG, TDCB, TDCA	348	0.009118	LH1	DO WN
GOTERM_MF_DIR ECT	succinate dehydrogenase activity	6	1.4	SDHA, SDHB, FRDD, FRDC, FRDB, FRDA	344	0.010274	LH1	DO WN
GOTERM_MF_DIR ECT	hydrogenase (acceptor) activity	6	1.4	HYBC, HYBA, HYBB, HYBO, HYAB, HYAA	344	0.010274	LH1	DO WN

GOTERM_MF_DIRECTORY	NADH dehydrogenase activity	11	2.6	TORA, FDHF, DMSA, PREA, FDNG, NARG, FDOG, NAPA, YNFE, PRET, YNFF	344	0.015242	LH1	DO WN
GOTERM_MF_DIRECTORY	molybdenum ion binding	9	2.2	TORA, FDHF, DMSA, FDNG, NARG, FDOG, NAPA, YNFE, YNFF	344	0.014742	LH1	DO WN
GOTERM_BP_DIRECTORY	oxidative phosphorylation	5	1.2	CYDA, CYDB, CYDX, CBDB, CBDA	348	0.020379	LH1	DO WN
GOTERM_MF_DIRECTORY	3 iron, 4 sulfur cluster binding	6	1.4	SDHB, FRDB, NARH, HYBO, HYAA, GLTB	344	0.018662	LH1	DO WN
GOTERM_MF_DIRECTORY	dimethyl sulfoxide reductase activity	5	1.2	DMSA, YNFE, YNFF, DMSC, DMSB	344	0.01744	LH1	DO WN
GOTERM_BP_DIRECTORY	thiamine biosynthetic process	7	1.7	THIF, THIE, THIH, THIG, THIM, THIC, THIS	348	0.023373	LH1	DO WN
GOTERM_MF_DIRECTORY	iron ion binding	16	3.8	HYBG, THIH, NRFA, HYBC, NAPH, TORC, NAPF, HYPC, XDHD, HYPD, NAPA, YGFK, ACNA, HYAC, YGCO, SODB	344	0.023133	LH1	DO WN
GOTERM_CC_DIRECTORY	membrane	35	8.4	TDCE, RBBA, CADB, HYCB, CYDX, FRDB, NAPH, FRDA, FDNG, FDNH, CBDA, YNFG, ACEE, HDA, NARH, HYAB, NARG, HYAA, DMSB, LPP, GLNA, HYBO, LPD, HYDN, WRBA, YSAA, CYDA, CYDB, TNA, LYSU, YGFS, VIAA, FDOG, FDOH, SODB	315	0.021352	LH1	DO WN
GOTERM_MF_DIRECTORY	succinate dehydrogenase (ubiquinone) activity	5	1.2	SDHA, SDHB, FRDD, FRDC, FRDB	344	0.041016	LH1	DO WN
GOTERM_MF_DIRECTORY	formate dehydrogenase (NAD+) activity	5	1.2	FDHF, FDOI, FDNG, FDNI, FDOG	344	0.041016	LH1	DO WN
GOTERM_CC_DIRECTORY	[Ni-Fe] hydrogenase complex	49	17.4	GABD, THRA, YOHF, NARY, NARZ, LHGO, MHPB, KATE, ASTD, FADE, GLCE, AHR, GLCD, DADA, CBDB, YFCG, CBDA, DPS, RUTA, YQJG, BETB, HYAB, BETA, NRDF, HYAA, RUTC, NRDE, ARNA, TORA, CYSI, POXB, CYSI, HDHA, CYSH, ADHP, GCD, YAHK, HISD, AIDB, OSMC, PAOA, CYOA, PAOC, CYOB, SODA, PAOB, CYOC, SODC, CYOD	277	1.13E-04	LH2	UP
UP_KEY_WORDS	Sugar transport	21	6.8	GNTF, MALX, FRWC, FRWA, SRLA, SRLB, MALE, RBSB, MGLA, YADI, FUCP, ALSB, ALSA, MGLC, MGLB, XYLEF, XYLG, ULAA, MALK, GATB, SGCB	299	0.001094	LH2	DO WN

GOTERM_BP_DIRECTORY	aerobic electron transport chain	6	2.1	CYSJ, CYSI, CYSH, CYSD, CYSC, CYSN	219	0.001945	LH2	UP
COG_ONTOLOGY	Amino acid transport and metabolism	23	8.2	CBDX, BOLA, RCLB, YHBO, HCHA, DEAD, IRAD, ASTD, ASTE, YNCL, ASTB, YOHP, OTSA, ASTA, BETT, PHOH, SPY, YKGO, BAES, AIDB, ILVX, BETB, BETA	277	0.008043	LH2	UP
GOTERM_BP_DIRECTORY	L-threonine catabolic process to propionate	6	1.9	TDCE, TDCF, TDCD, TDCG, TDCB, TDCA	233	0.008657	LH2	DOWN
UP_KEYWORDS	Amino-acid biosynthesis	6	2.1	CYOA, CBDB, CBDA, CYOB, CYOC, CYOD	219	0.011471	LH2	UP
GOTERM_BP_DIRECTORY	aerobic respiration	5	1.8	ASTA, ASTD, ASTE, ASTB, ASTC	219	0.012358	LH2	UP
KEGG_PATHWAY	Alanine, aspartate and glutamate metabolism	5	1.8	ASTA, ASTD, ASTE, ASTB, ASTC	219	0.012358	LH2	UP
GOTERM_CC_DIRECTORY	ATP-binding cassette (ABC) transporter complex, substrate-binding subunit-containing	4	1.4	CYOA, CYOB, CYOC, CYOD	192	0.02086	LH2	UP
GOTERM_BP_DIRECTORY	anaerobic respiration	17	6.0	LDTE, RCLB, TAUA, LDTA, YJFY, HDEB, YGIW, APPA, GGT, HIUH, MCBA, PAOA, PAOC, PAOB, OSMY, SODC, OSMF	192	0.022615	LH2	UP
GOTERM_BP_DIRECTORY	arginine biosynthetic process via ornithine	5	1.8	ASTA, ASTD, ASTE, ASTB, ASTC	277	0.030114	LH2	UP
GOTERM_BP_DIRECTORY	arginine catabolic process to glutamate	6	2.1	CYSJ, CYSI, CYSW, CYSD, CYSC, CYSN	219	0.036191	LH2	UP
KEGG_PATHWAY	Arginine and proline metabolism	5	1.8	YEHY, YEHX, PROP, YEHW, OSMF	219	0.038357	LH2	UP
UP_KEYWORDS	Cysteine biosynthesis	10	3.6	SUFA, YHBO, ACNA, OSMC, CYSD, KATE, YFCG, SODA, SUFD, SUFE	219	0.044624	LH2	UP
GOTERM_MF_DIRECTORY	electron carrier activity	7	2.5	YEHY, UGPA, YEHX, UGPE, YEHW, OSMF, UGPC	192	0.046522	LH2	UP
GOTERM_BP_DIRECTORY	cellular response to acid chemical	4	1.4	BETI, BETT, BETB, BETA	219	0.049423	LH2	UP
GOTERM_MF_DIRECTORY	copper ion binding	4	1.4	UGPA, UGPE, UGPB, UGPC	219	0.049423	LH2	UP

VII. Significantly regulated metabolites table of CL1 and CL2

RT	m/z	Name	CL1_logFC	CL2_logFC	CL1_P.Value	CL2_P.Value	Col	mode	sig
3.54	152.0568	2-Hydroxyadenine	1.15	0.64	4.09E-05	0.000902	C18	pos	both
2.73	298.097	5_- Methylthioadenosine	3.32	-1.04	0.402901	0.004078	HILIC	pos	CL2
2.96	252.1094	5'-Deoxyadenosine	0.75	0.90	0.004196	0.001431	C18	pos	both
1.64	166.0724	7-Methylguanaine	1.21	1.00	0.000791	0.000439	C18	pos	both
16.22	325.2739	8,9-EE-14_Z_-E	2.51	0.95	0.010101	0.093652	C18	pos	CL1
2.97	136.0618	Adenine	0.71	0.53	0.004243	0.025706	C18	pos	CL1
12.29	131.1293	Agmatine	-1.01	1.55	0.005846	0.42265	HILIC	pos	CL1
3.71	203.1392	ALANYL-dl- LEUCINE	-1.43	0.00	6.80E-05	NA	C18	pos	CL1
11.79	162.0762	ALPHA- aminOADIPate	2.48	-0.76	0.38585	0.004895	HILIC	pos	CL2
14.63	304.1619	Arg Glu	-0.93	-0.68	0.008846	0.083426	HILIC	pos	CL1
11.83	288.2031	Arg Leu	-1.36	0.71	0.003377	0.123062	HILIC	pos	CL1
1.09	103.123	Cadaverine	-0.41	-6.85	0.013377	0.000129	C18	pos	CL2
5.89	768.1223	Coenzyme A	-0.91	1.56	0.000767	0.42265	C18	pos	CL1
8.08	211.1442	cyclo L-Leu-L-Pro	-0.22	0.72	0.046414	0.001029	C18	pos	CL2
8.31	245.1288	cyclo L-Phe-L-Pro	-0.22	0.71	0.124549	0.001181	C18	pos	CL2
6.83	197.1286	cyclo L-Val-L-Pro	-0.03	0.71	0.439562	0.007324	C18	pos	CL2
13.69	189.1599	delta- Trimethyllysine	-0.30	-0.91	0.053479	0.00178	HILIC	pos	CL2
7.22	457.112	FMN	0.61	-0.10	0.002822	0.29963	C18	pos	CL1
4.2	261.1446	Glu Ile	-0.97	-0.32	0.00474	0.046258	C18	pos	CL1
6.04	261.1446	Glu Leu_1	0.19	-0.94	0.030222	0.000105	C18	pos	CL2
10.82	261.1449	Glu Leu_2	-0.07	-0.95	0.783415	0.0002	HILIC	pos	CL2
3.12	279.1009	Glu Met	0.26	-1.10	0.023343	0.001006	C18	pos	CL2
6.51	295.1289	Glu Phe_1	0.19	-1.26	0.055057	0.000218	C18	pos	CL2

11.07	295.129	Glu Phe_2	0.04	-1.21	0.731795	0.000144	HILIC	pos	CL2
4.87	311.124	Glu Tyr	0.21	-1.20	0.061272	0.003909	C18	pos	CL2
15.36	261.0372	Glucose phosphate 1-	-1.01	0.12	0.014591	0.722435	HILIC	pos	CL1
12.91	306.0768	Glutathione	-0.99	-1.32	0.107757	0.045537	HILIC	neg	CL2
3.78	189.1235	Glycyl-L-leucine	-0.99	4.36	0.008875	0.000676	C18	pos	both
10.43	173.0924	Glycylproline	-0.88	0.01	0.008202	0.957361	HILIC	pos	CL1
2.33	152.0564	Guanine	-0.67	0.00	0.020867	NA	C18	pos	CL1
11.84	269.1609	His Leu	-1.00	0.47	0.004229	0.051724	HILIC	pos	CL1
1.87	137.0459	Hypoxanthine	1.19	-1.55	0.000486	1.50E-05	C18	pos	both
5.64	288.203	Ile Arg_1	-6.45	1.40	0.000109	0.42265	C18	pos	CL1
12.12	288.2032	Ile Arg_2	-1.62	3.37	0.016182	0.137877	HILIC	pos	CL1
5.45	332.1817	Ile Glu Ala	-0.82	0.00	0.005578	NA	C18	pos	CL1
2.33	261.1447	Ile Glu_1	-1.05	0.66	1.62E-06	0.003766	C18	pos	both
10.15	261.1451	Ile Glu_2	-0.99	0.34	0.02165	0.12806	HILIC	pos	both
6.08	358.1974	Ile Pro Glu	0.77	-0.20	0.008092	0.122091	C18	pos	CL1
1.93	233.1498	Ile Thr	-0.99	0.00	0.002224	NA	C18	pos	CL1
5.23	231.1704	Ile Val	-1.45	0.82	6.65E-05	0.04312	C18	pos	both
5.61	360.2131	Ile Val Glu	-1.55	0.78	0.000488	0.012335	C18	pos	both
2.81	269.0885	Inosine	-0.99	-0.16	0.005136	0.03655	C18	pos	CL1
12.91	179.0487	L-Cys-Gly	-0.83	0.00	0.023112	NA	HILIC	pos	CL1
5.07	390.187	Leu Glu Glu	-0.87	0.00	0.010954	NA	C18	pos	CL1
1.85	219.1341	Leu Ser	-1.46	3.19	1.35E-05	0.124688	C18	pos	CL1
5.62	231.1705	Leu Val_1	-1.72	0.61	2.89E-05	0.123392	C18	pos	CL1
5.28	231.1708	Leu Val_2	-1.93	2.76	0.03571	0.183689	HILIC	pos	CL1
7.21	245.186	Leucyl-leucine	-3.33	0.89	3.01E-06	0.006971	C18	pos	both
14.32	154.0625	L-Histidine	-0.94	-0.62	0.172866	0.010042	HILIC	neg	CL2
8.7	203.1394	L-Leucyl-L-Alanine	-2.33	-2.33	0.014657	0.00575	HILIC	pos	both
11.08	189.1346	L-NMMA	0.97	-0.11	0.002401	0.561134	HILIC	pos	CL1

16.04	440.2774	LPE 15:0	1.30	0.92	0.000463	0.04578	C18	pos	both
14.05	424.246	LPE_14:1	0.98	3.31	0.000862	0.243908	C18	pos	CL1
17.06	454.2931	LPE_16:0_	2.39	1.27	0.001453	0.026538	C18	pos	both
3.32	704.5221	PE_16:0_17:1	4.54	0.72	0.026481	0.383905	HILIC	pos	CL1
15.57	452.2775	LPE_16:1_	0.60	2.02	0.002869	8.53E-05	C18	pos	both
16.24	466.2932	LPE_17:1	2.45	0.97	0.008022	0.09666	C18	pos	CL1
16.99	480.309	LPE_18:1	2.42	2.43	0.002235	0.01017	C18	pos	both
18.04	495.2728	LPG_17:1	-1.31	1.24	0.681125	0.023359	C18	neg	CL2
19.49	509.2884	LPG_18:1	-1.50	2.88	0.634926	0.00081	C18	neg	CL2
6.52	166.0864	L-Phenylalanine	0.13	-1.01	0.332881	0.001313	C18	pos	CL2
14.79	276.1563	Lys Glu	-0.96	-1.62	0.02388	0.003839	HILIC	pos	both
12.86	260.1971	Lys Ile	-0.23	-0.69	0.111576	0.012403	HILIC	pos	CL2
1.24	166.0532	Methionine sulfoxide	0.82	0.34	0.005862	0.063702	C18	pos	CL1
10.37	217.1295	N_-Acetyl-L-arginine	-0.37	-0.71	0.177859	0.001964	HILIC	pos	CL2
12.51	188.1759	N1-Acetylspermidine	-0.65	-0.57	0.015444	0.001012	HILIC	pos	CL1
1.28	233.113	N2-Succinyl-L-ornithine	0.61	-0.35	0.006205	0.000643	C18	pos	CL1
6.68	145.1337	N-Acetylcadaverine	-0.11	-3.10	0.86085	3.96E-06	HILIC	pos	CL2
10.97	198.0875	N-Acetyl-L-Histidine	-0.21	-0.60	0.135338	0.024598	HILIC	pos	CL2
1.82	332.5625	NAD_1	-4.77	-0.27	5.88E-06	0.028356	C18	pos	both
16.16	664.1163	NAD_2	-2.26	-0.72	1.68E-05	0.001454	HILIC	pos	both
6.58	245.186	NH-DVal_NMe_-Val-OMe	-0.84	0.62	0.005831	0.01753	C18	pos	both
2.06	123.0555	NicOTINamide	-5.14	-0.09	6.08E-07	0.640551	HILIC	pos	CL1
1.3	124.0392	Nicotinic acid	-2.18	0.58	0.000484	0.008649	C18	pos	CL1
1.27	162.0761	N-Methyl-L-glutamate	0.69	-0.87	0.002557	0.000683	C18	pos	both
1.7	290.1348	Ophthalmic acid_1	0.13	0.80	0.017185	4.48E-05	C18	pos	CL2
12.73	290.1349	Ophthalmic acid_2	-0.09	0.65	0.488192	0.000374	HILIC	pos	CL2

14.76	133.0976	Ornithine	-0.68	-1.00	0.004427	0.036831	HILIC	pos	both
10.52	359.1039	Pantetheine phosphate 4_-	0.65	0.00	0.011295	NA	HILIC	pos	CL1
4.37	295.1289	Phe Glu	-0.72	0.00	0.001144	NA	C18	pos	CL1
7.88	279.1704	Phe Ile	-1.15	0.56	0.00079	0.028643	C18	pos	CL1
5.25	253.118	Phe Ser	-1.73	0.00	0.030171	NA	C18	pos	CL1
6.48	265.1547	Phe Val	-0.92	3.84	0.011433	0.161848	C18	pos	CL1
12.66	103.1231	Piperidine	-0.57	-1.36	0.063267	0.00012	HILIC	pos	CL2
10.89	245.1135	Pro Glu	-0.67	-0.73	0.006145	0.0014	HILIC	pos	both
6.79	358.1974	Pro Glu Leu	-1.04	-0.51	0.000147	0.012956	C18	pos	CL1
5.69	344.1817	Pro Glu Val	-1.51	-1.05	6.55E-06	0.001416	C18	pos	both
2.82	286.1761	Pro Gly Ile	-0.86	0.00	0.005981	NA	C18	pos	CL1
13.66	253.1293	Pro His	-1.31	-2.73	0.008218	0.188401	HILIC	pos	CL1
9.48	358.1976	Pro Ile Glu	-0.66	0.32	0.004693	0.17042	HILIC	pos	CL1
7.97	342.2389	Pro Ile Ile	-1.76	0.56	6.79E-05	0.066503	C18	pos	CL1
7.11	328.2231	Pro Ile Val	-1.70	0.18	7.71E-05	0.263639	C18	pos	CL1
4.25	229.1548	Pro Ile_1	-1.61	-0.13	0.000113	0.229492	C18	pos	CL1
4.76	229.1548	Pro Ile_2	-2.07	-0.12	0.025849	0.260873	HILIC	pos	CL1
3.74	286.1763	Pro Leu Gly	-1.77	0.27	2.93E-05	0.072643	C18	pos	CL1
8.56	342.2388	Pro Leu Leu	-0.33	6.00	0.012899	6.81E-05	C18	pos	CL2
8.18	328.2232	Pro Leu Val	-0.24	0.65	0.097129	0.034402	C18	pos	CL2
13.51	244.1657	Pro Lys	-1.53	-1.28	0.000899	0.000398	HILIC	pos	both
2.64	247.1114	Pro Met_1	-1.57	-0.30	0.000435	0.067769	C18	pos	CL1
6.74	247.1114	Pro Met_2	-1.72	-0.46	0.017198	0.030473	HILIC	pos	CL1
6.42	334.1764	Pro Phe Ala	-6.53	0.00	1.10E-05	NA	C18	pos	CL1
6.31	263.1392	Pro Phe_1	-1.92	0.69	0.000337	0.004029	C18	pos	both
5.72	263.1393	Pro Phe_2	-2.25	0.34	0.006164	0.095029	HILIC	pos	both
6.81	326.2076	Pro Pro Ile	-1.14	0.05	4.61E-06	0.76278	C18	pos	CL1
7.61	360.1925	Pro Pro Phe	-1.24	0.68	6.04E-05	0.037063	C18	pos	both
6.05	312.192	Pro Pro Val	-1.39	-0.16	0.006984	0.441812	C18	pos	CL1

10.51	217.1187	Pro Thr	-1.35	-0.03	0.001219	0.858994	HILIC	pos	CL1
3.86	279.1342	Pro Tyr_1	-1.53	0.54	5.02E-05	0.003349	C18	pos	CL1
8.52	279.1342	Pro Tyr_2	-1.70	0.46	0.042487	0.004386	HILIC	pos	CL1
2.67	344.1817	Pro Val Glu	-1.10	0.13	1.34E-06	0.132539	C18	pos	CL1
7.39	328.2232	Pro Val Ile_1	-1.94	0.31	2.47E-05	0.1259	C18	pos	CL1
4.9	328.2237	Pro Val Ile_2	-2.31	0.35	0.041321	0.226938	HILIC	pos	CL1
6.4	314.2074	Pro Val Val	-6.63	0.00	0.000232	NA	C18	pos	CL1
2.18	215.1392	Pro Val_1	-1.49	-0.61	3.29E-05	0.002487	C18	pos	both
5.58	215.1395	Pro Val_2	-1.78	-0.80	0.006359	0.017859	HILIC	pos	both
1.08	89.10735	Putrescine	-0.60	1.57	0.006811	0.42265	C18	pos	CL1
1.71	130.0499	Pyrrolidonecarboxylic acid	-0.21	0.73	0.001812	0.008351	C18	pos	CL2
7.64	377.1455	Riboflavin_1	2.34	0.35	1.80E-06	0.123682	C18	pos	CL1
8.93	377.1458	Riboflavin_2	1.98	0.69	0.005885	0.756179	HILIC	pos	CL1
13.41	385.1292	S-_5_-AdenOSyl_-L-HOMOCYSTEine	-2.89	-3.50	0.001199	0.116931	HILIC	pos	CL1
1.23	399.1447	S-Adenosylmethionine	0.70	-0.77	0.004489	0.022546	C18	pos	both
3.29	219.1341	Ser Ile	-1.49	2.13	5.57E-06	0.290419	C18	pos	CL1
2.17	290.1711	Ser Ile Ala	-4.49	0.00	9.94E-05	NA	C18	pos	CL1
2.13	348.1765	Ser Ile Glu	-4.95	0.00	0.00149	NA	C18	pos	CL1
3.01	276.1564	Ser Ile Gly	-3.60	4.33	0.120335	0.000849	C18	pos	CL2
7.54	332.2181	Ser Leu Ile	-0.68	0.14	0.000887	0.351347	C18	pos	CL1
2.34	380.1124	S-Lactoylglutathione	3.45	-0.03	0.001005	0.932886	C18	pos	CL1
6.08	362.1922	Thr Glu Leu	-1.29	0.00	0.011731	NA	C18	pos	CL1
6.33	233.1497	Thr Ile	-0.30	0.60	0.032907	0.001081	C18	pos	CL2
3.98	304.1867	Thr Ile Ala	-5.43	0.00	0.00042	NA	C18	pos	CL1
3.81	362.192	Thr Ile Glu	-4.34	0.00	0.000833	NA	C18	pos	CL1
2.32	311.1238	Tyr Glu	-0.92	0.00	0.000429	NA	C18	pos	CL1
6.79	295.1654	Tyr Leu	-1.43	0.45	3.60E-05	0.100122	C18	pos	CL1

6.76	378.2023	Tyr Pro Val	-0.85	-0.26	0.007438	0.906017	C18	pos	CL1
1.25	565.0476	UDP-D-galactose	0.00	-0.97	NA	0.006422	C18	neg	CL2
1.75	167.0212	Uric acid	-2.43	2.73	0.491583	0.029956	C18	neg	CL2
1.66	243.0625	Uridine	-3.56	0.63	0.339778	0.028089	C18	neg	CL2
12.93	274.1875	Val Arg	-1.04	-0.11	0.000126	0.962003	HILIC	pos	CL1
6.05	231.1703	Val Ile	-1.64	0.95	4.97E-05	0.031426	C18	pos	both
5.07	281.1497	Val Tyr	-1.19	4.15	0.003452	0.000496	C18	pos	both
2.78	217.1547	Val Val	-0.61	2.41	0.00821	0.239498	C18	pos	CL1
4.05	285.0827	Xanthosine	0.59	-0.06	0.003935	0.718422	C18	pos	CL1

VIII. Significantly regulated metabolites table of LH1 and LH2

RT	m/z	Name	LH1_log ₂ FC	LH2_log ₂ FC	LH1_P.Value	LH2_P.Value	Col	mode	Sig
7.34	231.1130	1,2,3,4-Tetrahydro-1-methyl-beta-carboline-3-carboxylic acid	0.75	0.61	1.13E-03	1.18E-02	C18	pos	both
5.88	242.0658	2,3-Dihydroxybenzoylserine	-0.40	1.47	6.13E-02	7.33E-04	C18	pos	LH2
6.52	146.0926	4-GuaNIDinobutanoate	1.01	0.25	3.93E-03	4.70E-01	HILIC	pos	LH1
3.11	144.0479	4-Methyl-5-thiazoleethanol	-0.62	5.69	8.22E-03	9.60E-05	C18	pos	both
4.02	252.1093	5_-Deoxyadenosine	10.61	-1.68	1.59E-05	5.99E-01	HILIC	pos	both
12.66	219.0978	5-L-Glutamyl-L-alanine	-0.93	-0.21	9.01E-03	2.63E-01	HILIC	pos	LH1
1.64	166.0724	7-Methylguanine	-1.10	0.23	1.10E-03	1.49E-02	C18	pos	LH1
16.22	325.2739	8,9-EE-14_Z_-E	1.42	-0.25	7.04E-04	6.60E-01	C18	pos	LH1
2.97	136.0618	Adenine	0.54	1.26	1.41E-02	1.16E-03	C18	pos	LH2
6.99	348.0706	Adenosine monophosphate	-0.96	-0.03	4.45E-04	7.88E-01	C18	pos	LH1
12.29	131.1293	Agmatine	3.03	0.01	5.55E-05	9.96E-01	HILIC	pos	LH1
3.71	203.1392	ALANYL-dl-LEUCINE	1.46	1.52	1.68E-03	4.23E-01	C18	pos	LH1
11.79	162.0762	ALPHA-aminOADIPate	0.69	0.62	1.35E-03	3.32E-02	HILIC	pos	both
14.63	304.1619	Arg Glu	2.13	-1.58	2.86E-03	4.32E-01	HILIC	pos	LH1

11.83	288.2031	Arg Leu	1.98	0.31	4.81E-05	4.18E-01	HILIC	pos	LH1
4.56	304.1506	Asp Ile Gly	-1.07	0.93	1.53E-03	1.81E-06	C18	pos	both
6.85	118.0864	Betaine	0.16	-1.30	1.85E-01	8.26E-03	HILIC	pos	LH2
18.08	742.0684	BETA-NicOTINamide ADenine DINUCLEOTide phosphate	-4.55	0.74	4.64E-04	2.28E-01	HILIC	neg	LH1
1.09	103.1230	Cadaverine	1.17	1.87	3.15E-03	4.23E-01	C18	pos	LH1
5.37	162.1127	Carnitine	0.85	-1.20	1.34E-02	6.53E-03	HILIC	pos	both
1.25	104.1070	Choline	0.82	-0.44	1.01E-02	5.26E-02	C18	pos	LH1
2.9	104.1071	Choline	0.84	-0.34	1.41E-02	2.10E-01	HILIC	pos	LH1
13.05	176.1031	Citrulline	1.22	-4.77	2.42E-03	1.35E-01	HILIC	pos	LH1
5.89	768.1223	Coenzym A	-8.33	-1.56	7.40E-05	4.23E-01	C18	pos	LH1
8.08	211.1442	cyclo L-Leu-L-Pro	1.01	0.87	1.72E-04	8.05E-06	C18	pos	both
8.31	245.1288	cyclo L-Phe-L-Pro	1.12	1.50	1.11E-04	4.53E-04	C18	pos	both
6.83	197.1286	cyclo L-Val-L-Pro	0.66	0.75	9.29E-04	1.06E-03	C18	pos	both
1.68	197.1286	cyclo L-Val-L-Pro	0.76	0.95	2.92E-03	5.99E-03	HILIC	pos	both
13.69	189.1599	delta-Trimethyllysine	0.68	0.01	4.78E-03	9.71E-01	HILIC	pos	LH1
4.24	252.1093	Deoxyadenosine	-8.93	-0.31	1.03E-04	6.84E-01	HILIC	pos	LH1
3.42	146.1177	DEoxyCARNITine	1.62	-3.72	1.36E-04	1.67E-01	HILIC	pos	LH1
7.51	228.0982	Deoxycytidine	1.19	0.27	3.09E-03	6.85E-01	HILIC	pos	LH1
5.88	344.5815	Dephospho-CoA	1.62	1.95	7.42E-04	5.60E-01	C18	pos	LH1
11.22	201.0161	D-Erythrose 4-phosphate	1.43	0.00	2.29E-03	NA	HILIC	pos	LH1
15.78	259.0227	D-Fructose 1-phosphate	1.79	-0.73	8.40E-04	8.96E-02	HILIC	neg	LH1
15.7	276.1557	E- γ -Glutamyl-lysine	0.88	-2.81	5.09E-03	2.48E-01	HILIC	pos	LH1
7.22	457.1120	Flavin mononucleotide _FMN_	0.71	-0.20	2.62E-05	2.28E-02	C18	pos	LH1
5.84	261.1446	Gamma-Glu-Leu	1.17	-0.82	2.81E-05	5.21E-03	C18	pos	both
14.5	218.1501	gamma-L-Glutamylputrescine	-1.09	0.67	2.14E-03	8.25E-03	HILIC	pos	both
1.5	219.0977	Glu Ala	-1.04	-0.09	1.55E-03	4.20E-01	C18	pos	LH1

14.06	262.1036	Glu Gly Gly	-1.28	0.23	2.73E-03	3.51E-01	HILIC	pos	LH1
4.2	261.1446	Glu Ile	1.86	0.67	2.27E-03	7.54E-04	C18	pos	both
6.04	261.1446	Glu Leu	1.71	-1.21	1.47E-05	1.34E-04	C18	pos	both
10.82	261.1449	Glu Leu	1.74	-0.76	5.93E-03	1.70E-02	HILIC	pos	both
3.12	279.1009	Glu Met	1.09	-0.72	4.13E-04	3.66E-03	C18	pos	both
11.07	295.1290	Glu Phe	1.68	-2.87	3.49E-03	2.57E-01	HILIC	pos	both
6.51	295.1289	Glu Phe	1.72	-0.99	8.83E-06	3.86E-04	C18	pos	both
4.87	311.1240	Glu Tyr	1.66	-1.06	5.52E-05	8.39E-03	C18	pos	both
15.36	261.0372	Glucose 1-phosphate	0.67	-2.10	2.34E-02	3.62E-01	HILIC	pos	LH1
12.91	306.0768	Glutathione	0.86	-7.15	1.76E-03	2.53E-03	HILIC	neg	both
16.82	613.1592	Glutathione, oxidized	-2.84	0.61	3.13E-05	1.42E-01	HILIC	pos	both
16.83	611.1448	Glutathione, oxidized	-1.94	1.33	3.23E-04	3.43E-02	HILIC	neg	both
13.42	173.0211	Glycerol 2-phosphate	1.43	-1.41	3.66E-04	5.92E-01	HILIC	pos	LH1
3.78	189.1235	Glycyl-L-leucine	1.84	-0.10	8.98E-04	4.91E-01	C18	pos	LH1
10.43	173.0924	Glycylproline	1.76	-0.26	1.17E-04	2.15E-01	HILIC	pos	LH1
2.33	152.0564	Guanine	3.71	0.00	6.65E-06	NA	C18	pos	LH1
8.05	183.0919	Harman	1.19	0.61	3.46E-04	1.34E-03	C18	pos	both
11.84	269.1609	His Leu	1.64	-0.04	9.06E-04	9.20E-01	HILIC	pos	LH1
10.63	382.2451	His Leu Leu	4.54	0.00	2.03E-03	NA	HILIC	pos	LH1
6.9	131.0715	Hydroxyisocaproic acid	2.84	-2.11	4.70E-01	1.12E-02	C18	neg	LH2
1.87	137.0459	Hypoxanthine	-1.03	3.28	2.62E-03	6.43E-06	C18	pos	both
5.8	137.0460	Hypoxanthine	-0.77	3.67	1.29E-02	2.42E-03	HILIC	pos	both
12.12	288.2032	Ile Arg	1.18	-4.83	3.18E-02	6.44E-03	HILIC	pos	both
5.64	288.2030	Ile Arg	4.94	-1.40	3.85E-04	4.23E-01	C18	pos	both
2.41	247.1290	Ile Asp	-0.92	-0.30	1.41E-04	3.20E-03	C18	pos	LH1
10.92	247.1291	Ile Asp	-0.78	-0.13	5.19E-03	5.28E-01	HILIC	pos	LH1
10.15	261.1451	Ile Glu	2.00	-1.56	2.42E-03	4.47E-01	HILIC	pos	LH1
2.33	261.1447	Ile Glu	2.32	0.00	4.62E-04	9.88E-01	C18	pos	LH1
5.45	332.1817	Ile Glu Ala	2.16	1.33	1.35E-04	4.23E-01	C18	pos	LH1

6.08	358.1974	Ile Pro Glu	0.93	0.85	1.30E-05	8.18E-04	C18	pos	both
1.93	233.1498	Ile Thr	1.59	1.21	1.35E-03	4.23E-01	C18	pos	LH1
5.23	231.1704	Ile Val	2.63	0.27	2.15E-05	3.39E-02	C18	pos	LH1
5.61	360.2131	Ile Val Glu	2.26	0.59	2.78E-05	8.31E-03	C18	pos	both
2.81	269.0885	Inosine	1.33	0.04	4.71E-04	8.21E-01	C18	pos	LH1
8.57	267.0734	Inosine	1.18	0.30	8.85E-04	5.51E-01	HILIC	neg	LH1
8.41	307.0442	Inosine	1.03	0.44	3.32E-03	3.84E-01	HILIC	pos	LH1
6.71	190.0500	Kynurenic acid	-1.41	1.28	1.07E-05	9.76E-05	C18	pos	both
1.28	116.0705	L-2-Amino-5-hydroxypentanoic acid	1.22	0.48	9.85E-03	2.51E-02	C18	pos	LH1
1.58	147.0301	L-2-Hydroxyglutaric acid	2.05	1.93	5.22E-01	4.96E-03	C18	neg	LH2
8.51	132.1021	L-Alloisoleucine	0.59	-0.20	6.16E-03	6.30E-01	HILIC	pos	LH1
11.13	175.1190	L-Arginine	0.92	-6.72	8.79E-04	2.33E-05	HILIC	pos	both
12.99	132.0305	L-Aspartic acid	1.76	-3.25	9.97E-04	8.31E-03	HILIC	neg	both
13.01	134.0449	L-Aspartic acid	1.97	-5.69	2.28E-03	8.05E-02	HILIC	pos	both
12.91	179.0487	L-Cys-Gly	1.19	0.00	1.43E-02	NA	HILIC	pos	LH1
5.07	390.1870	Leu Glu Glu	1.85	1.46	1.22E-03	4.23E-01	C18	pos	LH1
7.2	360.2109	Leu Ile Asp	0.88	-1.90	1.47E-03	3.07E-01	C18	pos	LH1
5.67	357.2132	Leu Pro Gln	1.34	-0.26	2.21E-04	9.19E-01	C18	pos	LH1
1.85	219.1341	Leu Ser	1.94	0.71	5.88E-04	1.51E-02	C18	pos	both
5.28	231.1708	Leu Val	2.34	-0.04	2.45E-04	9.86E-01	HILIC	pos	LH1
5.62	231.1705	Leu Val	2.36	0.64	9.74E-06	9.79E-02	C18	pos	LH1
7.21	245.1860	Leucyl-leucine	1.91	0.02	6.23E-04	8.96E-01	C18	pos	LH1
12.3	148.0606	L-Glutamic acid	-0.70	0.18	1.12E-02	5.98E-01	HILIC	pos	LH1
1.23	148.0605	L-Glutamic acid	-1.06	0.25	1.12E-02	3.67E-02	C18	pos	LH1
14.34	156.0769	L-Histidine	0.59	-0.42	6.23E-03	1.36E-01	HILIC	pos	LH1
14.32	154.0625	L-Histidine	0.83	0.24	8.04E-03	5.61E-01	HILIC	neg	LH1
8.7	203.1394	L-Leucyl-L- Alanine	0.53	1.04	1.61E-02	4.83E-02	HILIC	pos	LH2
5.13	227.1401	L-Leucyl-L-proline_	5.25	0.67	1.43E-01	3.68E-02	C18	neg	LH2

14.56	147.1130	L-Lysine	0.85	-1.58	1.22E-02	3.99E-02	HILIC	pos	both
11.08	189.1346	L-NMMA	2.04	0.58	1.17E-03	1.25E-01	HILIC	pos	LH1
8.17	118.0863	L-Norvaline	1.06	0.06	5.82E-03	7.98E-01	C18	pos	LH1
16.04	440.2774	LPE 15:0	0.86	0.76	4.66E-03	9.16E-02	C18	pos	LH1
14.05	424.2460	LPE_14:1	2.55	-0.22	2.06E-04	2.96E-01	C18	pos	LH1
15.57	452.2775	LPE_16:1	-0.81	1.61	6.95E-04	3.76E-03	C18	pos	both
16.24	466.2932	LPE_17:1	1.44	-0.26	4.35E-04	6.43E-01	C18	pos	LH1
7.67	466.2934	LPE_17:1	1.25	0.16	1.86E-04	8.60E-01	HILIC	pos	LH1
16.99	480.3090	LPE_18:1	-1.03	0.77	1.70E-03	2.62E-01	C18	pos	LH1
18.04	495.2728	LPG_17:1	5.78	-1.32	1.71E-01	2.65E-02	C18	neg	LH2
6.52	166.0864	L-Phenylalanine	1.70	-5.86	5.14E-04	3.97E-05	C18	pos	both
9.71	116.0707	L-Proline	1.29	0.30	1.10E-04	1.50E-01	HILIC	pos	LH1
9.52	118.0864	L-Valine	0.59	-0.40	1.81E-02	2.98E-01	HILIC	pos	both
14.79	276.1563	Lys Glu	3.06	-1.56	1.73E-03	4.19E-01	HILIC	pos	LH1
12.86	260.1971	Lys Ile	1.83	-1.13	7.41E-04	1.74E-02	HILIC	pos	both
1.29	246.1811	Lys Val	1.87	-0.28	1.64E-03	1.90E-01	C18	pos	LH1
12.85	246.1814	Lys Val	2.50	-0.07	9.54E-05	7.51E-01	HILIC	pos	LH1
11.29	359.2653	Lys Val Ile	5.06	0.00	2.89E-04	NA	HILIC	pos	LH1
7.59	133.0145	Malic acid	1.29	0.32	2.08E-02	5.71E-01	HILIC	neg	LH1
1.24	166.0532	Methionine sulfoxide	-4.27	3.74	1.10E-04	5.76E-04	C18	pos	both
10.37	217.1295	N_-Acetyl-L-arginine	1.26	0.00	6.25E-03	9.93E-01	HILIC	pos	LH1
12.51	188.1759	N1-Acetylspermidine	0.63	0.17	1.54E-02	1.91E-01	HILIC	pos	LH1
11.13	275.1351	N2-Succinyl-L-arginine	0.70	-2.39	2.21E-02	9.78E-03	HILIC	pos	both
1.3	275.1348	N2-Succinyl-L-arginine	1.15	-2.11	1.11E-02	1.02E-04	C18	pos	both
1.28	233.1130	N2-Succinyl-L-ornithine	-1.46	0.41	9.16E-03	5.05E-02	C18	pos	LH1
9.33	188.1759	N8-Acetylspermidine	0.62	-1.67	3.81E-03	4.44E-01	HILIC	pos	LH1
6.68	145.1337	N-Acetylcadaverine	-0.01	1.33	9.12E-01	2.16E-02	HILIC	pos	LH2
9.49	222.0973	N-Acetyl-D-glucosamine	-1.71	-1.42	8.66E-04	4.91E-01	HILIC	pos	LH1

2.17	192.0691	N-Acetyl-L-methionine	-1.80	-0.39	2.64E-05	1.96E-01	HILIC	pos	LH1
5.84	214.0510	N-Acetyl-L-methionine	-1.68	-0.71	1.60E-03	8.90E-04	C18	pos	both
1.82	332.5625	NAD	-5.30	0.18	2.89E-04	2.82E-01	C18	pos	LH1
16.16	664.1163	NAD	-4.73	-0.46	1.80E-04	2.94E-01	HILIC	pos	LH1
10.58	189.1236	N-Alpha-acetyllysine	0.60	-0.90	3.26E-02	2.71E-02	HILIC	pos	both
6.58	245.1860	NH-DVal_NMe_-Val-OMe	2.45	0.27	3.29E-04	1.05E-01	C18	pos	LH1
1.77	123.0553	Niacinamide	-1.46	0.22	3.09E-03	2.29E-01	C18	pos	LH1
1.3	124.0392	NicOTINate	0.73	1.71	4.38E-03	3.28E-05	C18	pos	both
1.27	162.0761	N-Methyl-L-glutamate	0.39	0.66	2.86E-02	1.39E-02	C18	pos	LH2
2.65	169.0767	Norharman	0.81	0.31	2.99E-03	2.99E-01	HILIC	pos	LH1
1.7	290.1348	Ophthalmic acid	-0.73	0.24	1.19E-03	4.71E-02	C18	pos	LH1
14.76	133.0976	Ornithine	-0.91	0.12	7.09E-04	7.71E-01	HILIC	pos	LH1
5.27	359.1038	Pantetheine phosphate 4_-	2.76	0.75	3.39E-04	5.53E-02	C18	pos	LH1
10.51	357.0892	Pantetheine phosphate 4_-	3.07	0.00	7.67E-04	NA	HILIC	neg	LH1
10.52	359.1039	Pantetheine phosphate 4_-	3.16	0.00	6.67E-04	NA	HILIC	pos	LH1
4.85	218.1034	Pantothenic acid	3.11	1.49	4.76E-01	1.25E-02	C18	neg	LH2
4.86	220.1182	Pantothenic acid	-0.56	1.38	6.16E-03	3.34E-04	C18	pos	LH2
3.27	718.5375	PE 34:1	-0.88	0.35	3.52E-02	5.96E-01	HILIC	pos	LH1
3.26	732.5501	PE_13:0_22:1_11Z_	0.97	-0.90	1.70E-02	2.43E-01	HILIC	pos	LH1
4.37	295.1289	Phe Glu	1.64	0.00	1.67E-03	NA	C18	pos	LH1
7.88	279.1704	Phe Ile	1.06	0.18	6.10E-04	8.46E-02	C18	pos	LH1
6.48	265.1547	Phe Val	1.45	0.22	9.07E-04	2.02E-01	C18	pos	LH1
12.69	168.9899	phosphoenol pyruvate	-7.42	-0.25	5.31E-05	5.53E-01	HILIC	pos	LH1
12.69	166.9754	phosphoenol pyruvate	-7.81	0.40	2.38E-04	2.74E-01	HILIC	neg	LH1
14.57	130.0864	Pipelicolic acid	0.83	-1.64	1.17E-02	4.51E-02	HILIC	pos	both
12.66	103.1231	Piperidine	0.82	0.68	1.63E-02	1.00E-02	HILIC	pos	both
13.5	272.1721	Pro Arg	5.77	-1.98	1.83E-05	4.30E-01	HILIC	pos	LH1
1.48	245.1133	Pro Glu	1.43	-0.22	5.64E-04	7.47E-02	C18	pos	LH1

10.89	245.1135	Pro Glu	1.70	-0.20	2.00E-04	2.47E-01	HILIC	pos	LH1
6.79	358.1974	Pro Glu Leu	3.07	1.16	6.19E-06	8.49E-04	C18	pos	both
5.69	344.1817	Pro Glu Val	2.74	0.51	9.35E-07	6.27E-02	C18	pos	LH1
2.82	286.1761	Pro Gly Ile	2.10	1.24	1.59E-04	4.23E-01	C18	pos	LH1
13.66	253.1293	Pro His	1.74	0.10	1.54E-03	9.65E-01	HILIC	pos	LH1
4.25	229.1548	Pro Ile	3.03	0.32	4.54E-06	2.63E-02	C18	pos	LH1
4.76	229.1548	Pro Ile	3.15	0.83	2.24E-04	5.26E-02	HILIC	pos	LH1
6.38	344.1818	Pro Ile Asp	0.10	-1.03	5.63E-01	1.81E-03	C18	pos	LH2
9.48	358.1976	Pro Ile Glu	1.72	-1.29	6.67E-04	6.16E-01	HILIC	pos	LH1
7.97	342.2389	Pro Ile Ile	2.68	0.62	1.13E-05	3.22E-03	C18	pos	both
7.11	328.2231	Pro Ile Val	2.67	0.58	1.59E-06	6.02E-03	C18	pos	LH1
7.59	229.1548	Pro Leu	1.76	-1.40	2.85E-05	4.78E-01	HILIC	pos	LH1
6.94	229.1548	Pro Leu	1.24	0.01	1.61E-04	9.54E-01	C18	pos	LH1
3.74	286.1763	Pro Leu Gly	2.87	1.01	3.30E-05	6.21E-04	C18	pos	both
8.56	342.2388	Pro Leu Leu	1.34	0.11	1.06E-05	2.43E-01	C18	pos	LH1
8.18	328.2232	Pro Leu Val	1.28	0.31	5.97E-04	6.54E-02	C18	pos	LH1
13.51	244.1657	Pro Lys	2.44	-0.30	3.74E-04	4.04E-01	HILIC	pos	LH1
6.74	247.1114	Pro Met	2.99	-1.01	3.25E-03	6.01E-01	HILIC	pos	LH1
2.64	247.1114	Pro Met	3.05	0.44	6.73E-05	4.09E-03	C18	pos	LH1
6.31	263.1392	Pro Phe	2.71	0.30	2.54E-05	1.91E-02	C18	pos	LH1
5.72	263.1393	Pro Phe	2.78	0.45	4.90E-04	1.16E-01	HILIC	pos	LH1
6.42	334.1764	Pro Phe Ala	6.94	0.00	2.16E-05	NA	C18	pos	LH1
6.81	326.2076	Pro Pro Ile	2.99	1.23	4.70E-06	5.80E-04	C18	pos	both
7.61	360.1925	Pro Pro Phe	2.27	0.44	7.69E-06	1.16E-01	C18	pos	LH1
6.05	312.1920	Pro Pro Val	2.71	0.69	9.74E-04	2.72E-03	C18	pos	both
10.51	217.1187	Pro Thr	2.88	-1.21	1.27E-03	1.73E-02	HILIC	pos	both
3.86	279.1342	Pro Tyr	2.45	0.23	1.29E-04	3.40E-02	C18	pos	LH1
8.52	279.1342	Pro Tyr	2.34	0.41	8.72E-05	1.65E-01	HILIC	pos	LH1
2.18	215.1392	Pro Val	3.03	0.17	1.50E-05	1.60E-02	C18	pos	LH1

5.58	215.1395	Pro Val	3.05	0.49	1.21E-03	1.17E-01	HILIC	pos	LH1
2.67	344.1817	Pro Val Glu	2.29	1.08	9.08E-04	6.70E-03	C18	pos	both
7.39	328.2232	Pro Val Ile	3.20	1.00	2.33E-06	8.63E-04	C18	pos	both
4.9	328.2237	Pro Val Ile	2.81	1.08	5.96E-04	7.98E-02	HILIC	pos	both
6.4	314.2074	Pro Val Val	8.14	1.82	5.21E-05	4.23E-01	C18	pos	LH1
1.08	89.1074	Putrescine	-1.06	-1.57	7.79E-03	4.23E-01	C18	pos	LH1
5.9	229.1184	Pyro Glu Val	1.13	-0.16	7.36E-04	2.91E-01	C18	pos	LH1
12.56	147.0767	Pyroglutamic acid	-1.33	-0.51	5.20E-04	9.90E-02	HILIC	pos	LH1
1.71	130.0499	Pyrrolidonecarboxylic acid	1.19	-0.02	1.99E-03	8.53E-01	C18	pos	LH1
7.64	377.1455	Riboflavin	1.76	-0.12	7.80E-07	6.85E-01	C18	pos	LH1
8.93	377.1458	Riboflavin	2.08	1.73	1.31E-03	3.96E-01	HILIC	pos	LH1
15.46	399.1450	S-Adenosylmethionine	1.13	-0.24	7.18E-03	5.32E-01	HILIC	pos	LH1
3.29	219.1341	Ser Ile	2.01	0.67	4.04E-03	4.89E-02	C18	pos	both
2.13	348.1765	Ser Ile Glu	5.61	0.00	8.18E-04	NA	C18	pos	LH1
3.01	276.1564	Ser Ile Gly	4.25	-4.33	9.11E-02	8.49E-04	C18	pos	LH2
2.24	306.1661	Ser Ile Ser	0.94	-1.34	7.37E-04	4.23E-01	C18	pos	LH1
4.53	320.1818	Ser Ile Thr	0.44	-0.61	3.48E-02	7.33E-03	C18	pos	LH2
7.54	332.2181	Ser Leu Ile	1.60	-0.21	5.66E-05	2.94E-01	C18	pos	LH1
6.97	318.2025	Ser Val Leu	0.66	-0.57	2.84E-03	5.13E-04	C18	pos	LH1
8.83	318.2023	Ser Val Leu	1.25	0.10	3.83E-03	6.02E-01	HILIC	pos	LH1
2.34	380.1124	S-Lactoylglutathione	-1.59	-0.59	2.43E-02	1.65E-01	C18	pos	LH1
1.09	146.1653	Spermidine	1.00	0.21	3.01E-03	1.97E-02	C18	pos	LH1
6.08	362.1922	Thr Glu Leu	1.92	1.58	6.67E-03	4.23E-01	C18	pos	LH1
6.33	233.1497	Thr Ile	1.11	0.03	3.34E-03	8.07E-01	C18	pos	LH1
3.98	304.1867	Thr Ile Ala	4.96	0.00	7.27E-04	NA	C18	pos	LH1
3.81	362.1920	Thr Ile Glu	4.79	0.00	7.12E-04	NA	C18	pos	LH1
4.69	265.0797	Thymidine	-0.20	1.40	1.30E-01	2.17E-03	C18	pos	LH2
3.32	281.0536	Thymidine	-0.41	1.55	5.22E-02	3.63E-02	HILIC	pos	LH2
4.7	127.0503	Thymine	-0.23	1.28	7.20E-02	2.61E-04	C18	pos	LH2

3.32	127.0504	Thymine	-0.27	1.39	7.55E-02	4.99E-02	HILIC	pos	LH2	
12.06	311.1242	Tyr Glu	1.62	-1.42	1.22E-02	4.23E-01	HILIC	pos	LH1	
2.32	311.1238	Tyr Glu	1.42	0.00	1.56E-03	NA	C18	pos	LH1	
6.76	378.2023	Tyr Pro Val	2.43	2.02	5.48E-05	2.79E-01	C18	pos	LH1	
1.6	113.0346	Uracil	0.06	0.60	5.80E-01	4.30E-03	C18	pos	LH2	
1.75	167.0212	Uric acid	2.55	-1.15	4.74E-01	1.53E-03	C18	neg	LH2	
6.22	243.0626	Uridine	0.75	-0.20	1.16E-02	7.01E-01	HILIC	neg	both	
1.81	189.1234	Val Ala	0.70	0.99	1.25E-02	4.35E-03	C18	pos	both	
12.93	274.1875	Val Arg	1.71	1.42	1.94E-04	5.21E-01	HILIC	pos	LH1	
10.7	247.1293	Val Glu	1.17	2.03	3.84E-04	3.25E-01	HILIC	pos	both	
6.05	231.1703	Val Ile	2.48	0.37	1.70E-05	2.06E-01	C18	pos	LH1	
2.18	205.1185	Val Ser	1.11	-0.73	4.50E-04	4.48E-03	C18	pos	both	
5.07	281.1497	Val Tyr	1.99	-0.11	5.83E-04	5.47E-01	C18	pos	LH1	
2.78	217.1547	Val Val	1.79	0.37	1.62E-04	8.94E-02	C18	pos	LH1	
2.06	151.0263	Xanthine	3.88	0.73	4.21E-01	2.37E-02	C18	neg	LH2	
2.07	153.0408	Xanthine	-0.17	0.79	1.65E-01	6.92E-03	C18	pos	LH2	
14.67	243.0278	β -L-Fucose phosphate	1-	-0.66	4.25	3.69E-02	1.70E-01	HILIC	neg	LH1

IX. Over-representation analysis for differentially regulated metabolites in LH1 and LH2

Pathway	Total	Count	FDR	Enrichment score	Reg	Compounds
Glutathione metabolism	28	10	2.81E-05	7.1	LH1	Glutathione; Oxidized glutathione; NADP; L-Glutamic acid; Pyroglutamic acid; Ornithine; Putrescine; Spermidine; Cadaverine

Arginine and proline metabolism	38	9	0.00251	4.7	LH1	L-Arginine; Agmatine; Putrescine; S-Adenosylmethionine; Spermidine; L-Proline; L-Glutamic acid; Ornithine; 4-Guanidinobutanoic acid
Arginine biosynthesis	14	5	0.0106	7.2	LH1	L-Glutamic acid; L-Arginine; Citrulline; L-Aspartic acid; Ornithine
Nicotinate and nicotinamide metabolism	15	5	0.0115	6.7	LH1	L-Aspartic acid; NAD; Niacinamide; NADP; Nicotinic acid
Aminoacyl-tRNA biosynthesis	48	8	0.0297	3.3	LH1	L-Histidine; L-Phenylalanine; L-Arginine; L-Aspartic acid; L-Valine; L-Lysine; L-Proline; L-Glutamic acid
D-Glutamine and D-glutamate metabolism	6	3	0.0297	10.0	LH1	L-Glutamic acid; Pyrrolidonecarboxylic acid
Aminoacyl-tRNA biosynthesis	48	5	0.0466	6.9	Both	L-Phenylalanine; L-Arginine; L-Aspartic acid; L-Valine; L-Lysine

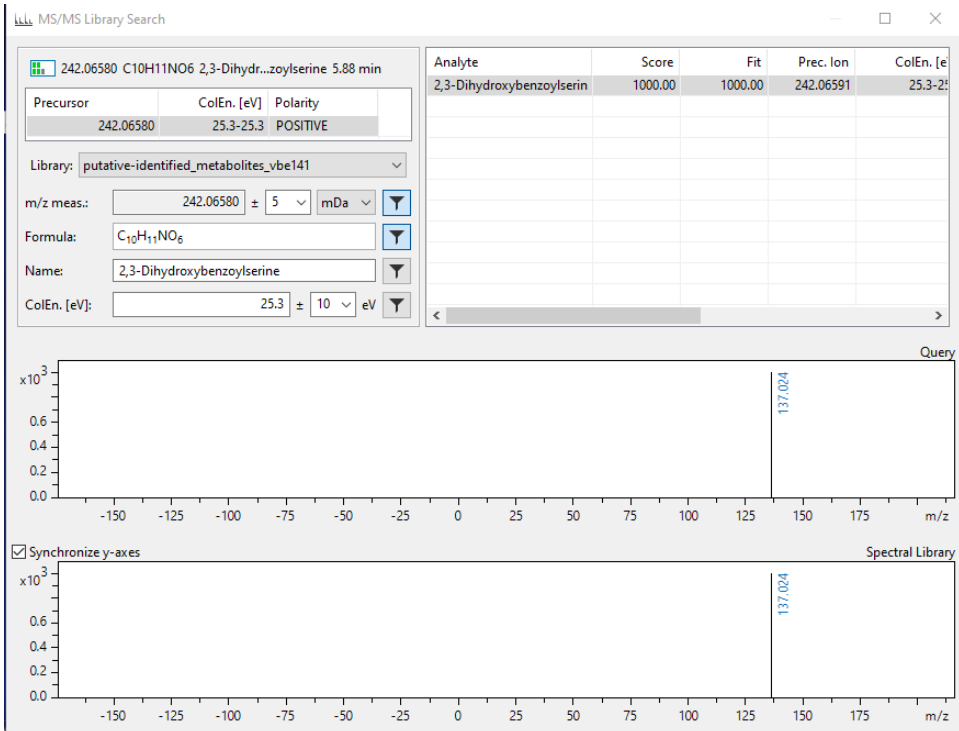
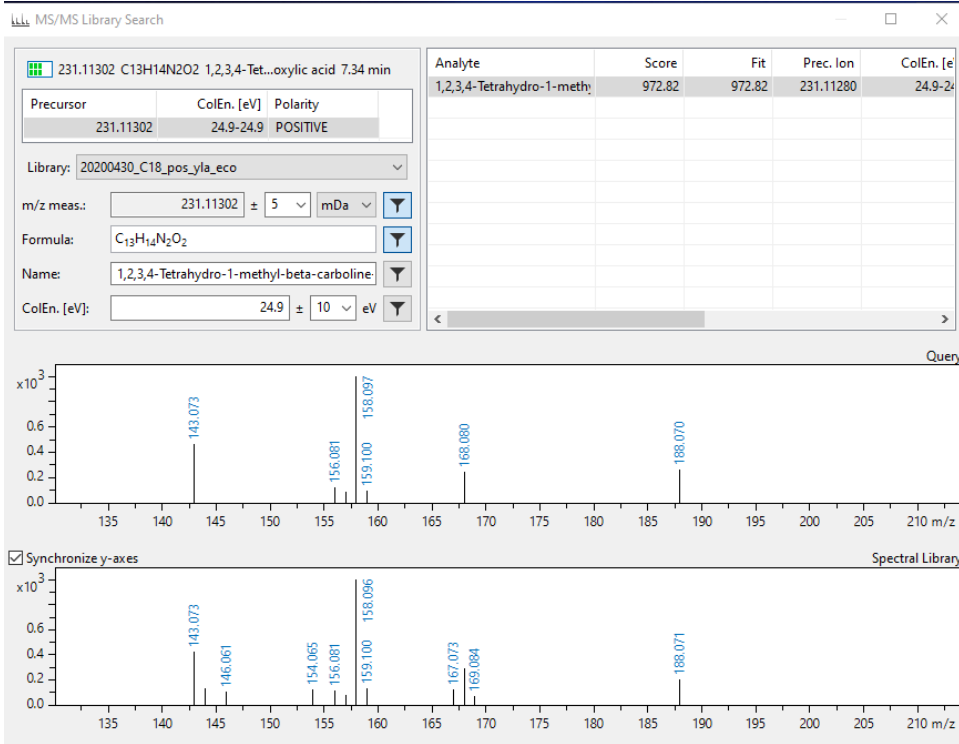
X. Top 100 differential pathways

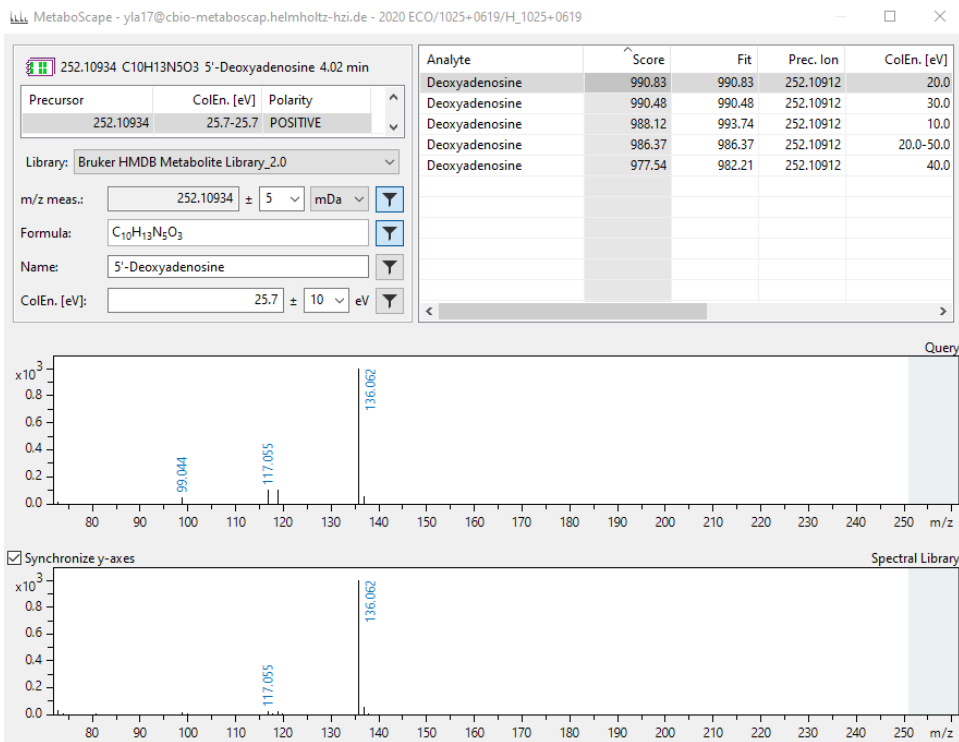
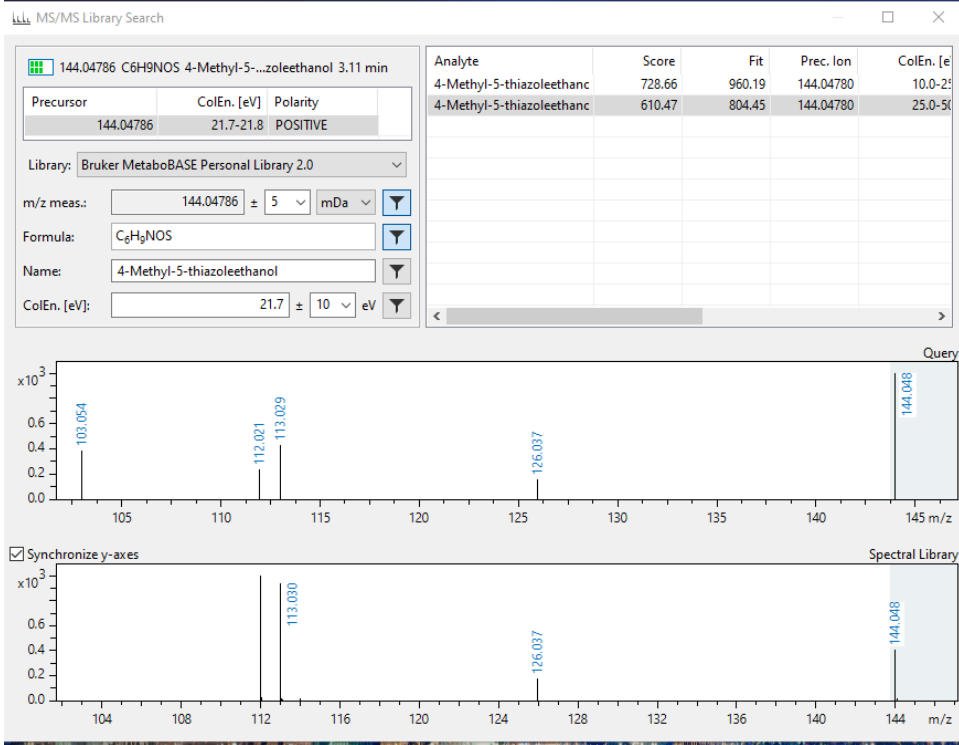
Pathway	DPPS	Pathway	DPPS	Pathway	DPPS	Pathway	DPPS
Cadaverine biosynthesis	9.0	Glycerol degradation V	6.4	Mixed acid fermentation	5.4	L-cysteine biosynthesis I	4.8
Biotin biosynthesis from 8-amino-7-oxononanoate I	8.9	Enterobactin biosynthesis	6.3	Superpathway of thiamine diphosphate biosynthesis I	5.4	Glyoxylate cycle	4.8
Lipoate biosynthesis and incorporation II	8.7	Heme- biosynthesis II (oxygen-independent)	6.3	L-cysteine biosynthesis VII (from sulfo-L-cysteine)	5.3	CDP-diacylglycerol biosynthesis I	4.8
4-amino-2-methyl-5-diphosphomethylpyrimidine biosynthesis I	8.7	Methylphosphonate degradation I	6.3	Hydrogen to fumarate electron transfer	5.3	2-methylcitrate cycle I	4.8
Lipoate biosynthesis and incorporation I	8.7	Ethanol degradation I	6.2	Citrate degradation	5.3	Fatty acid & beta;-oxidation I (generic)	4.8
Hydrogen to trimethylamine N-oxide electron transfer	8.6	L-threonine degradation II	6.2	Biotin biosynthesis I	5.2	Thiazole component of thiamine	4.8

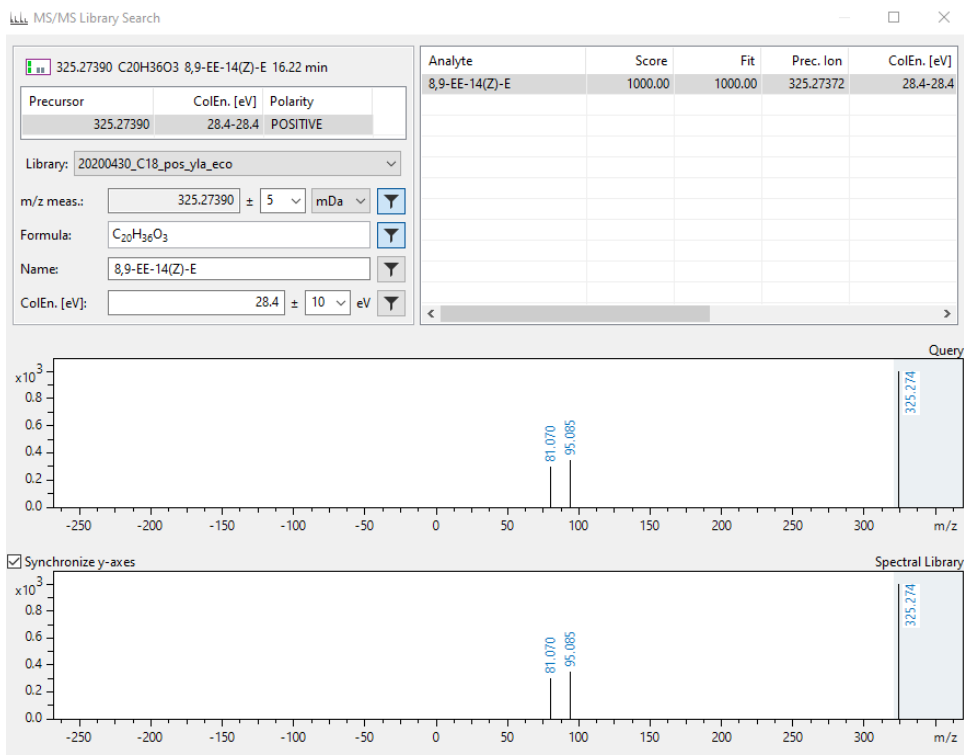
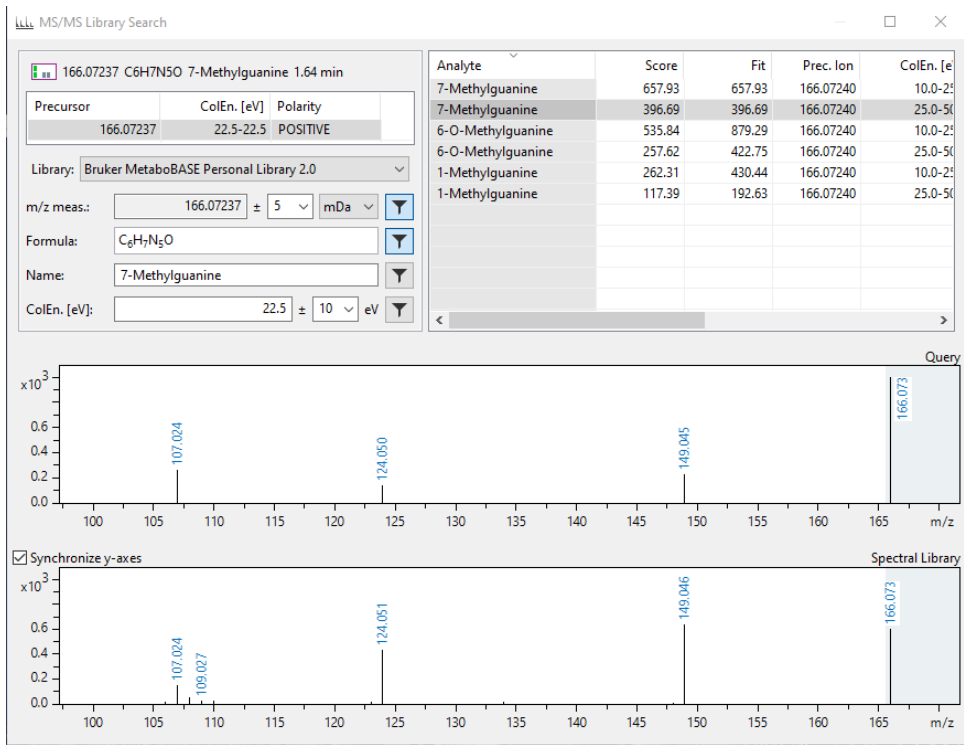
						diphosphate biosynthesis I	
Glutathionylspermidine biosynthesis	8.0	2,3-dihydroxybenzoate biosynthesis	6.0	Superpathway of methylglyoxal degradation	5.2	Superpathway of arginine and polyamine biosynthesis	4.8
Arsenate detoxification II (glutaredoxin)	8.0	NADH to dimethyl sulfoxide electron transfer	6.0	Superpathway of heme biosynthesis from uroporphyrinogen-III	5.2	Cinnamate and 3-hydroxycinnamate degradation to 2-hydroxypentadienoate	4.8
NADH to trimethylamine-oxide electron transfer	7.9	L-arginine degradation III (arginine decarboxylase/agmatinase pathway)	5.8	(Aminomethyl)phosphonate degradation	5.1	Nitrate reduction III (dissimilatory)	4.7
Superpathway of L-aspartate and L-asparagine biosynthesis	7.7	Putrescine biosynthesis I	5.8	Molybdopterin biosynthesis	5.1	Superpathway of glyoxylate bypass and TCA	4.7
Superpathway of L-asparagine biosynthesis	7.7	Glutathione biosynthesis	5.7	3-dehydroquinate biosynthesis I	5.1	Formate to nitrite electron transfer	4.7
L-asparagine degradation I	7.7	Superpathway of purine deoxyribonucleosides degradation	5.7	Pyruvate decarboxylation to acetyl coa I	5.1	TCA cycle I (prokaryotic)	4.7
β-alanine biosynthesis III	7.7	Nitrate reduction VIII (dissimilatory)	5.7	Formate to dimethyl sulfoxide electron transfer	5.1	Superpathway of polyamine biosynthesis I	4.7
L-asparagine biosynthesis I	7.7	Nitrate reduction viiib (dissimilatory)	5.7	2-oxoglutarate decarboxylation to succinyl-coa	5.0	L-arginine degradation II (AST pathway)	4.6
L-asparagine biosynthesis II	7.7	Glutathione-glutaredoxin redox reactions	5.7	L-threonine degradation I	5.0	2-carboxy-1,4-naphthoquinol biosynthesis	4.5
L-aspartate biosynthesis	7.7	Superpathway of acetate utilization and formation	5.6	Ethanolamine utilization	5.0	NAD de novo biosynthesis I (from aspartate)	4.5

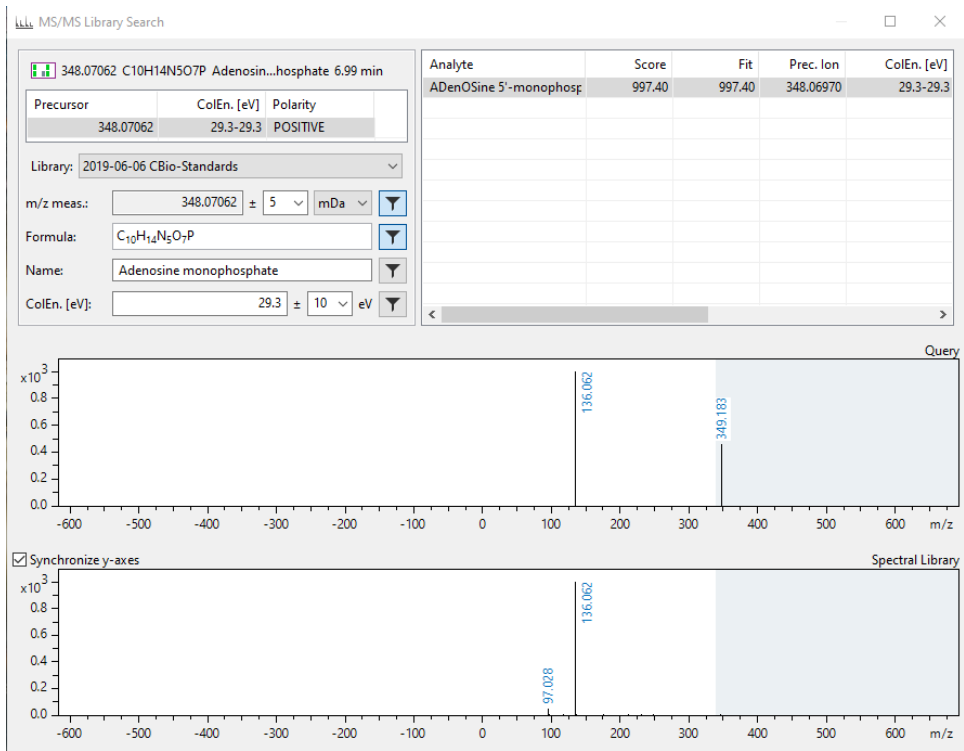
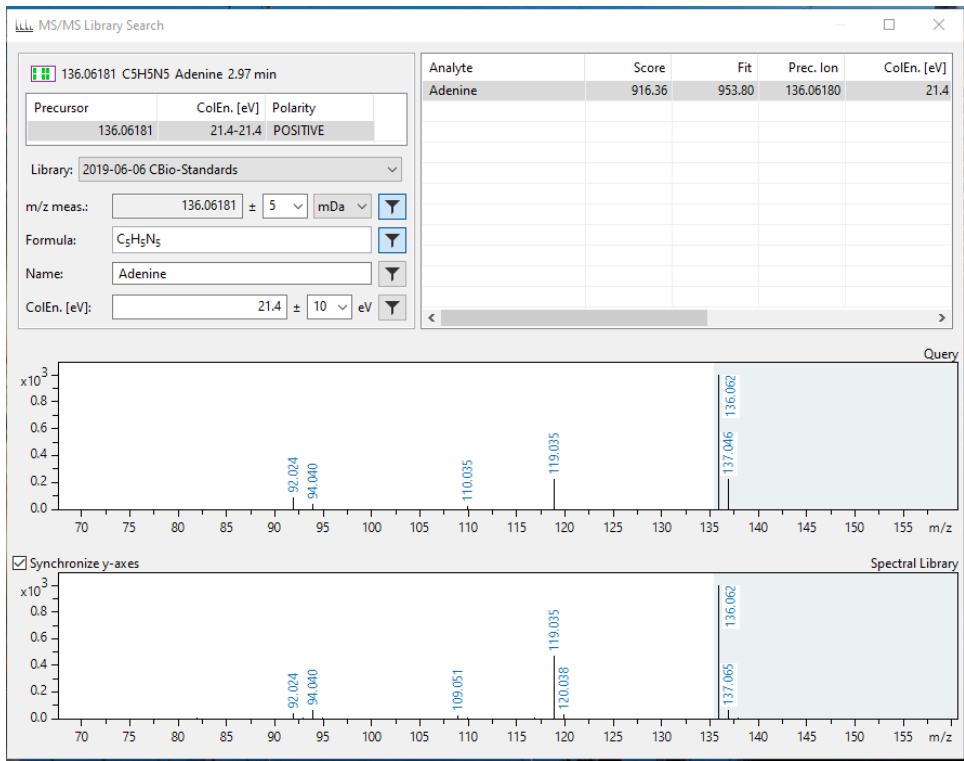
L-glutamate degradation II	7.7	Fatty acid biosynthesis initiation (type II)	5.5	Acyl carrier protein metabolism	5.0	NADH to cytochrome <i>bd</i> oxidase electron transfer I	4.5
Arginine dependent acid resistance	7.6	D-malate degradation	5.5	Acetate and ATP formation from acetyl-coa I	4.9	NADH to cytochrome <i>bd</i> oxidase electron transfer II	4.5
Formate to trimethylamine-oxide electron transfer	7.3	UDP- α -D-glucuronate biosynthesis (from UDP-glucose)	5.5	Oleate β -oxidation	4.9	D-gulosides conversion to D-glucosides	4.5
Hydrogen to dimethyl sulfoxide electron transfer	6.8	NAD phosphorylation and dephosphorylation	5.5	Acetoacetate degradation (to acetyl coa)	4.9	L-phenylalanine biosynthesis I	4.5
Acetate conversion to acetyl-coa	6.8	Ethylene glycol degradation	5.5	Fatty acid biosynthesis initiation II	4.9	Adenosine ribonucleotides <i>de novo</i> biosynthesis	4.5
Purine deoxyribonucleosides degradation I	6.7	D-sorbitol degradation II	5.5	L-threonine degradation IV	4.9	Superpathway of glycolysis, pyruvate dehydrogenase, TCA, and glyoxylate bypass	4.5
Methylglyoxal degradation I	6.5	Mannitol degradation I	5.5	Glycolate and glyoxylate degradation II	4.9	Superpathway of glycol metabolism and degradation	4.5
Formaldehyde oxidation II (glutathione-dependent)	6.5	L-lactaldehyde degradation (anaerobic)	5.5	Superpathway of fatty acid biosynthesis initiation (<i>E. coli</i>)	4.8	L-homoserine biosynthesis	4.4
Aminopropylcadaverine biosynthesis	6.4	L-galactonate degradation	5.5	L-arginine biosynthesis I (via L-ornithine)	4.8	Superpathway of L-threonine biosynthesis	4.4

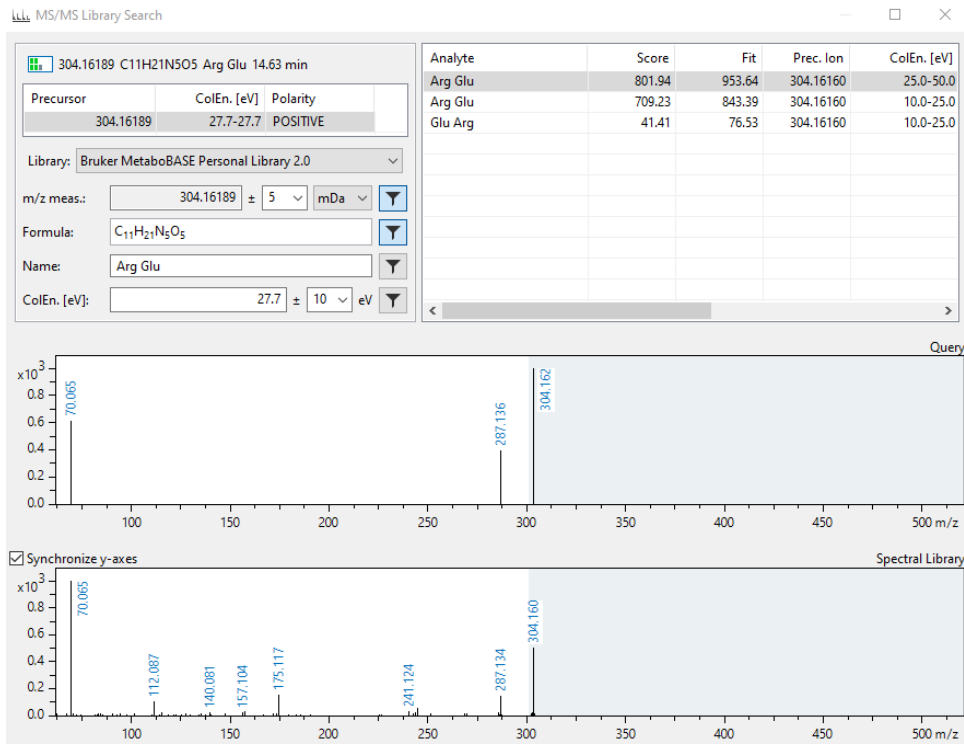
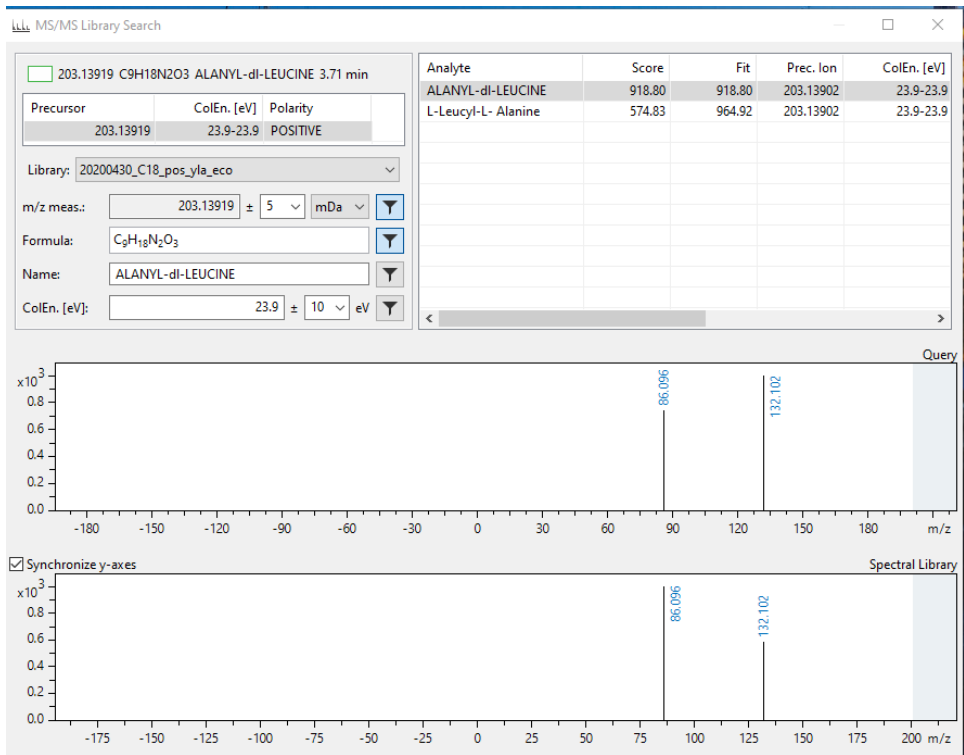
XI. MS and MS/MS identification











288.20305 C₁₂H₂₅N₅O₃ Arg Leu 11.83 min

Precursor	ColEn. [eV]	Polarity
288.20305	27.1-27.1	POSITIVE

Library: Bruker MetaboBASE Personal Library 2.0

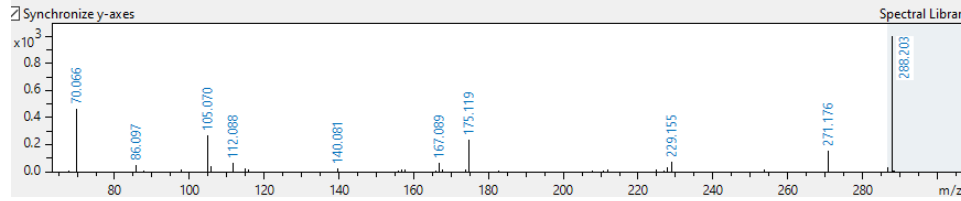
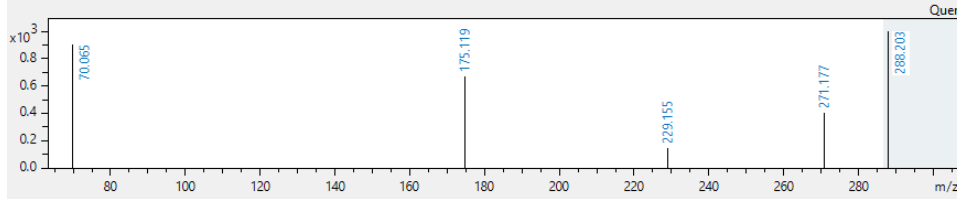
m/z meas.: 288.20305 ± 5 mDa

Formula: C₁₂H₂₅N₅O₃

Name: Arg Leu

ColEn. [eV]: 27.1 ± 10 eV

Analyte	Score	Fit	Prec. Ion	ColEn. [eV]
Arg Leu	857.93	857.93	288.20300	10.0-25.0
Arg Leu	834.38	840.16	288.20300	25.0-50.0
Ile Arg	693.78	698.59	288.20300	10.0-25.0
Leu Arg	684.14	684.14	288.20300	10.0-25.0
Ile Arg	672.90	719.30	288.20300	25.0-50.0
Leu Arg	168.13	256.02	288.20300	25.0-50.0
Arg Ile	80.71	86.27	288.20300	10.0-25.0
Arg Ile	21.93	38.76	288.20300	25.0-50.0



304.15056 C₁₂H₂₁N₃O₆ Asp Ile Gly 4.56 min

Precursor	ColEn. [eV]	Polarity
304.15056	27.7-27.7	POSITIVE

Library: 20200430_C18_pos_yla_eco

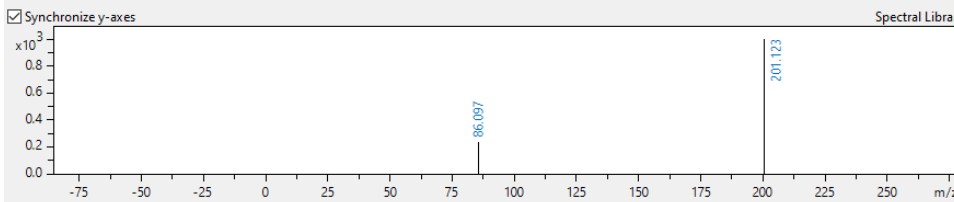
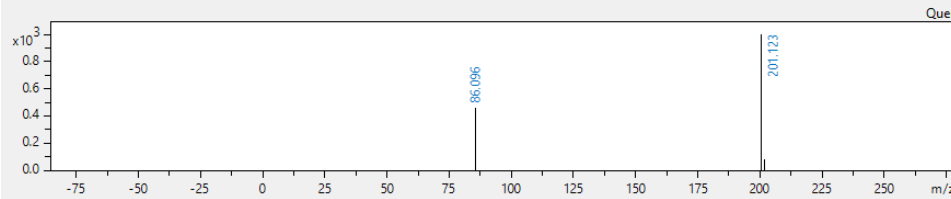
m/z meas.: 304.15056 ± 5 mDa

Formula: C₁₂H₂₁N₃O₆

Name: Asp Ile Gly

ColEn. [eV]: 27.7 ± 10 eV

Analyte	Score	Fit	Prec. Ion	ColEn. [eV]
Asp Ile Gly	977.67	979.87	304.15031	27.7-27.7



MS/MS Library Search

118.08639 C5H11NO2 Betaine 6.85 min

Precursor	ColEn. [eV]	Polarity
235.16740	25.1-25.1	POSITIVE

Library: 20200430_C18_pos_yla_eco

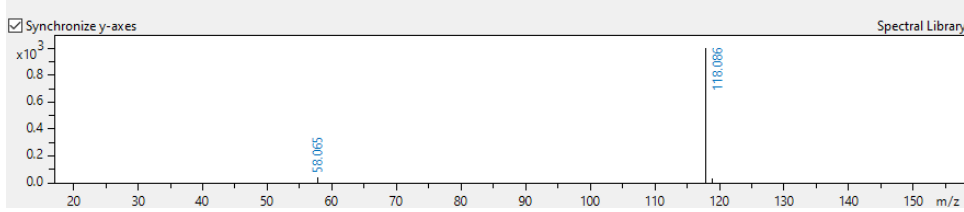
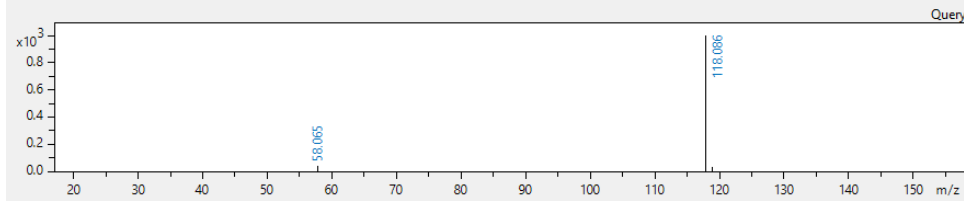
m/z meas.: 235.16740 ± 5 mDa

Formula: C₅H₁₁NO₂

Name: Betaine

ColEn. [eV]: 25.1 ± 10 eV

Analyte	Score	Fit	Prec. Ion	ColEn. [eV]
Betaine	1000.00	1000.00	235.16523	25.1-25.1



MS/MS Library Search

103.12303 C5H14N2 Cadaverine 1.09 min

Precursor	ColEn. [eV]	Polarity
103.12303	20.1-20.1	POSITIVE

Library: Bruker HMDB Metabolite Library_2.0

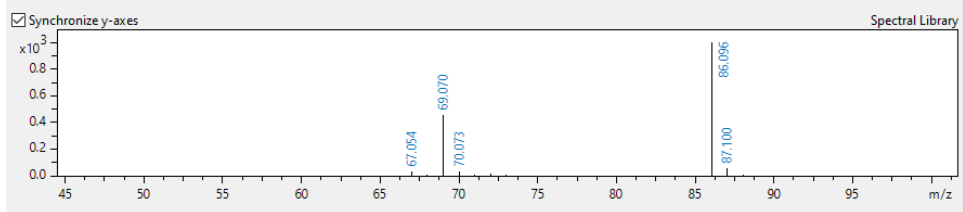
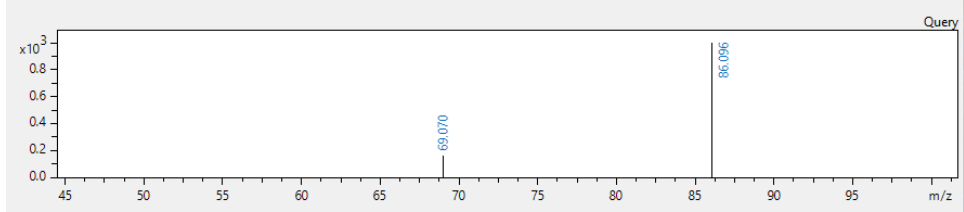
m/z meas.: 103.12303 ± 5 mDa

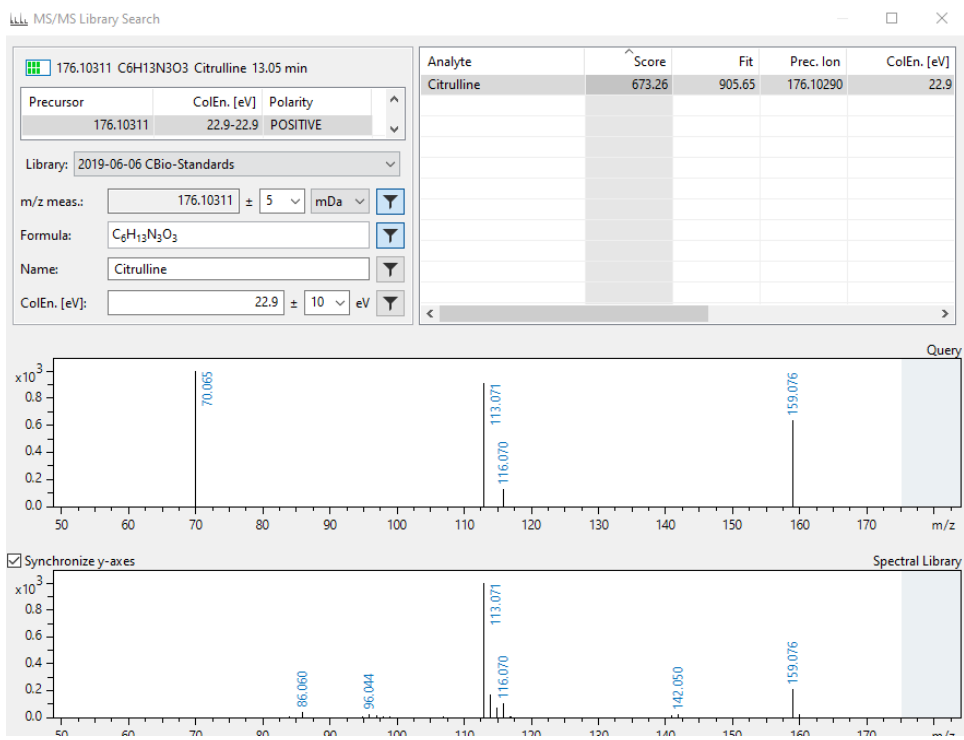
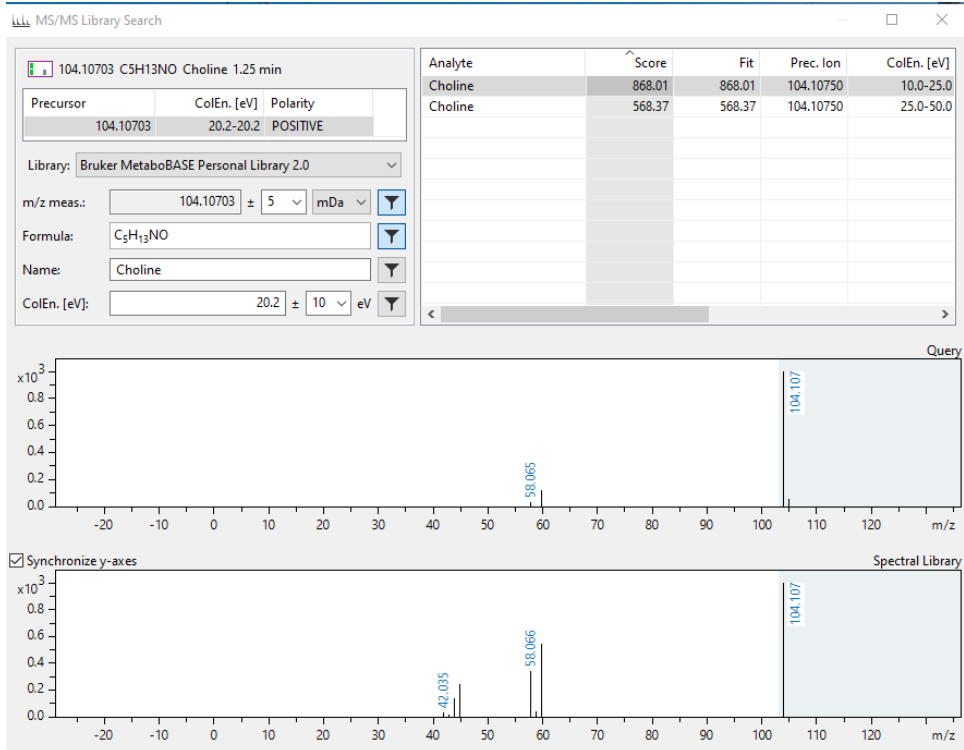
Formula: C₅H₁₄N₂

Name: Cadaverine

ColEn. [eV]: 20.1 ± 10 eV

Analyte	Score	Fit	Prec. Ion	ColEn. [eV]
Cadaverine	993.69	993.69	103.12297	10.0
Cadaverine	961.10	961.10	103.12297	20.0-50.0
Cadaverine	958.98	958.98	103.12297	20.0
Cadaverine	134.96	864.37	103.12297	30.0





768.12230 C21H36N7O16P3S Coenzym A 5.89 min

Precursor	ColEn. [eV]	Polarity
768.12230	45.7-45.7	POSITIVE

Library: 20200430_C18_pos_yla_eco

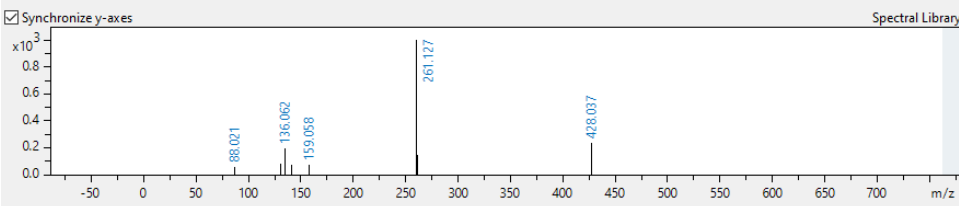
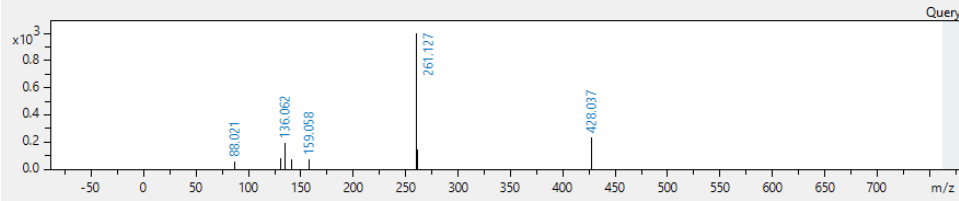
m/z meas.: 768.12230 ± 5 mDa

Formula: C₂₁H₃₆N₇O₁₆P₃S

Name: Coenzym A

ColEn. [eV]: 45.7 ± 10 eV

Analyte	Score	Fit	Prec. Ion	ColEn. [eV]
Coenzym A	1000.00	1000.00	768.12249	45.7-45.7



211.14424 C11H18N2O2 cyclo L-Leu-L-Pro 8.08 min

Precursor	ColEn. [eV]	Polarity
211.14424	24.2-24.2	POSITIVE

Library: 20200430_C18_pos_yla_eco

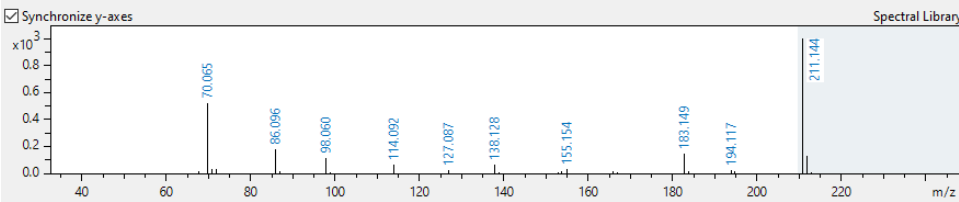
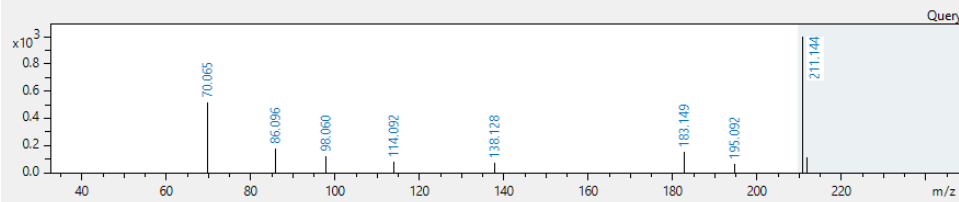
m/z meas.: 211.14424 ± 5 mDa

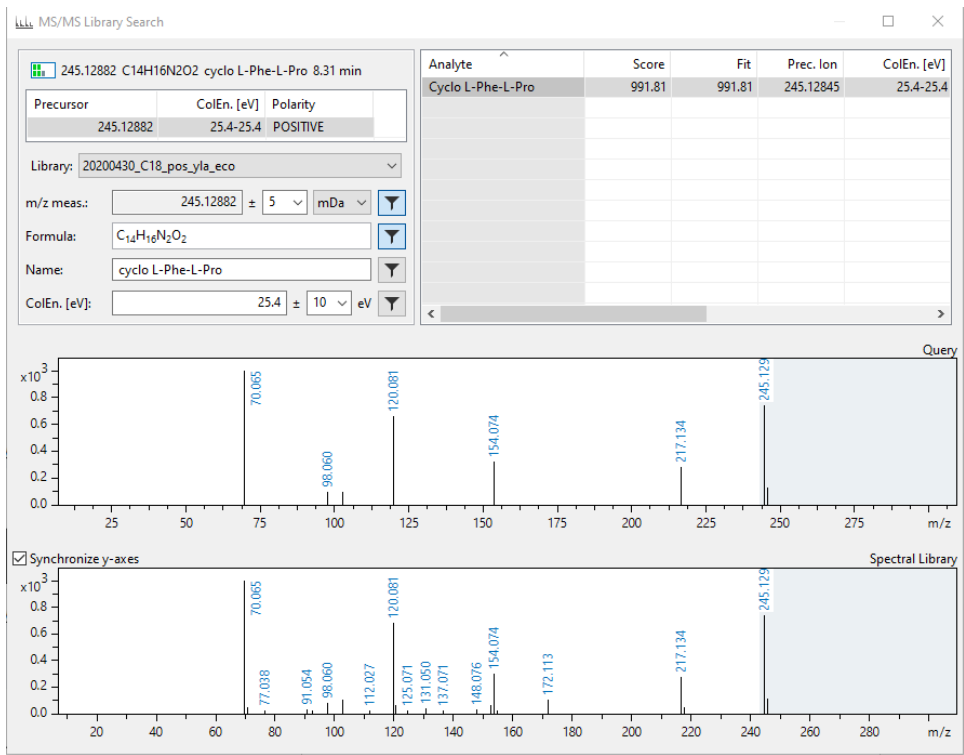
Formula: C₁₁H₁₈N₂O₂

Name: cyclo L-Leu-L-Pro

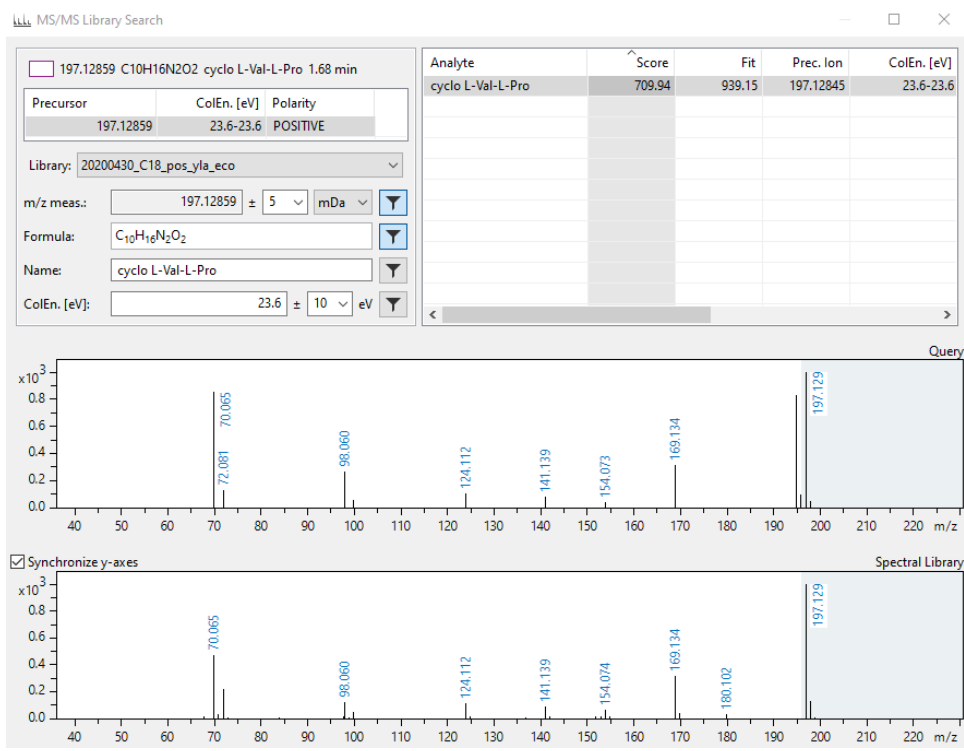
ColEn. [eV]: 24.2 ± 10 eV

Analyte	Score	Fit	Prec. Ion	ColEn. [eV]
cyclo L-Leu-L-Pro	989.66	989.66	211.14410	24.2-24.3





5



189.15994 C₉H₂₀N₂O₂ delta-Trimethyllysine 13.69 min

Precursor	ColEn. [eV]	Polarity
189.15994	23.3-23.3	POSITIVE

Library: 2019-06-06 CBio-Standards

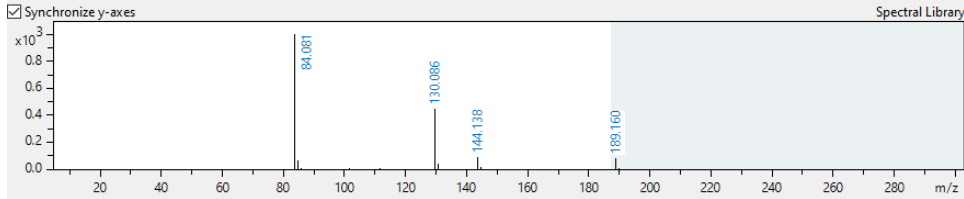
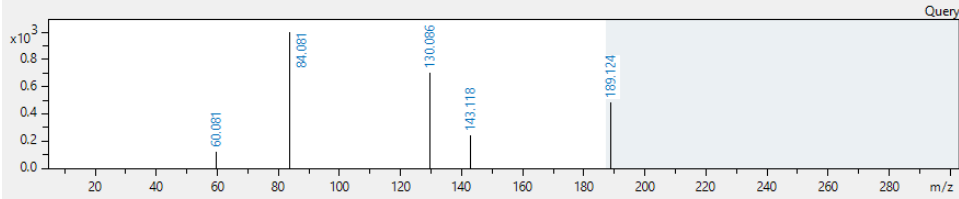
m/z meas.: 189.15994 ± 5 mDa

Formula: C₉H₂₀N₂O₂

Name: delta-Trimethyllysine

ColEn. [eV]: 23.3 ± 10 eV

Analyte	Score	Fit	Prec. Ion	ColEn. [eV]
NEP:siION;NEP:siION;NEP:si	891.22	976.79	189.15930	23.3-23.3



252.10934 C₁₀H₁₃N₅O₃ Deoxyadenosine 4.24 min

Precursor	ColEn. [eV]	Polarity
252.10934	25.7-25.7	POSITIVE

Library: Bruker MetaboBASE Personal Library 2.0

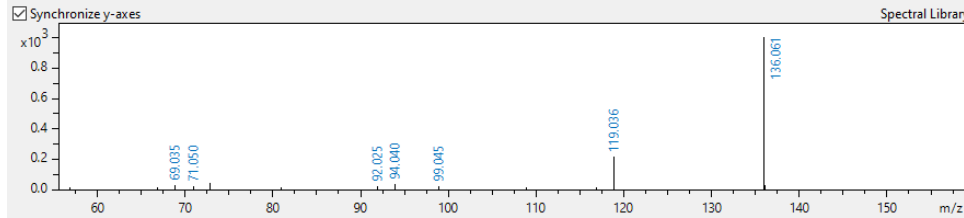
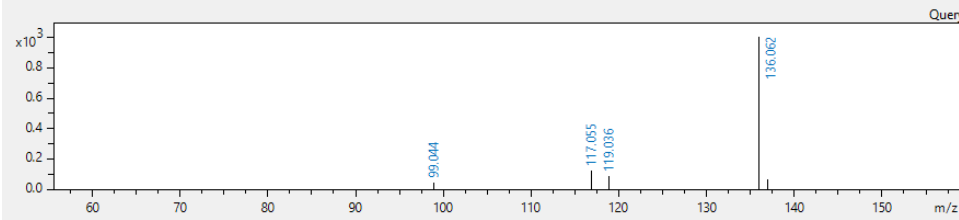
m/z meas.: 252.10934 ± 5 mDa

Formula: C₁₀H₁₃N₅O₃

Name: Deoxyadenosine

ColEn. [eV]: 25.7 ± 10 eV

Analyte	Score	Fit	Prec. Ion	ColEn. [eV]
Deoxyadenosine	977.11	979.02	252.10910	25.0-50.0
Deoxyadenosine	985.89	990.90	252.10910	10.0-25.0
5'-Deoxyadenosine	986.25	999.30	252.10900	10.0-25.0
5'-Deoxyadenosine	987.09	996.99	252.10900	25.0-50.0



146.11770 C7H15NO2 DEoxyCARNITine 3.42 min

Precursor	ColEn. [eV]	Polarity
146.11770	21.7-21.7	POSITIVE

Library: 2019-06-06 CBio-Standards

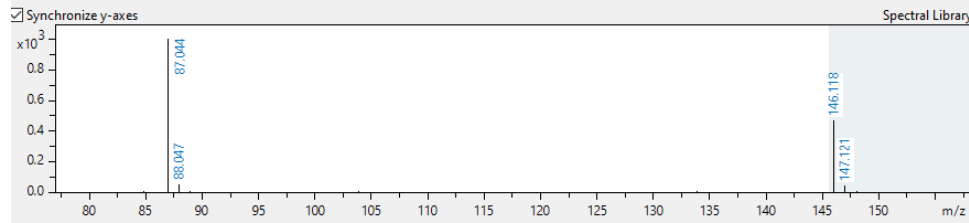
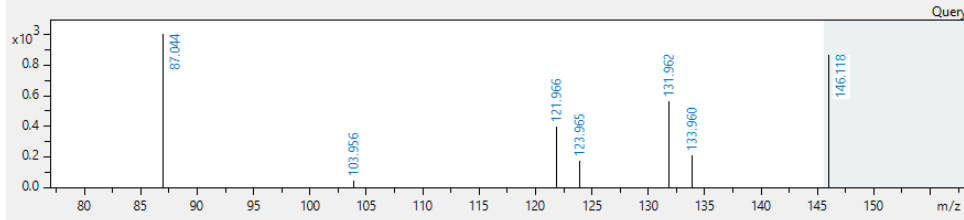
m/z meas.: 146.11770 ± 5 mDa

Formula: C₇H₁₅NO₂

Name: DEoxyCARNITine

ColEn. [eV]: 21.7 ± 10 eV

Analyte	Score	Fit	Prec. Ion	ColEn. [eV]
DEoxyCARNITine	745.04	998.88	146.11720	21.7



228.09821 C9H13N3O4 Deoxycytidine 7.51 min

Precursor	ColEn. [eV]	Polarity
228.09821	24.8-24.8	POSITIVE

Library: Bruker MetaboBASE Personal Library 2.0

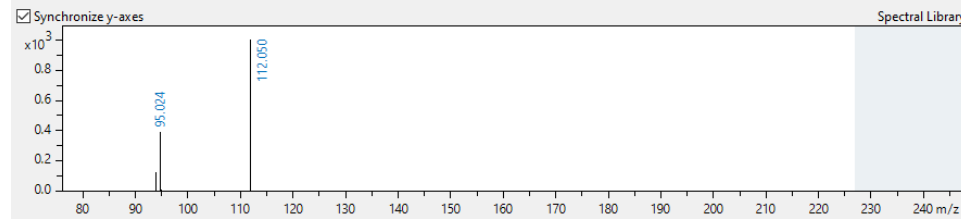
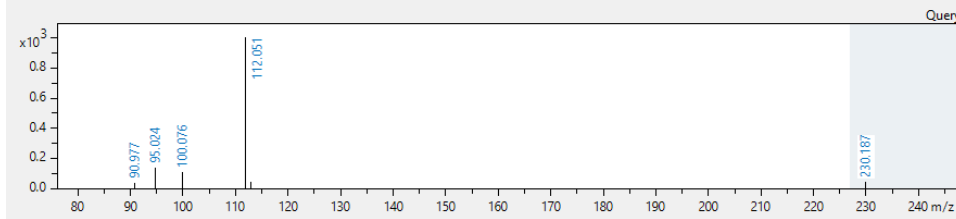
m/z meas.: 228.09821 ± 5 mDa

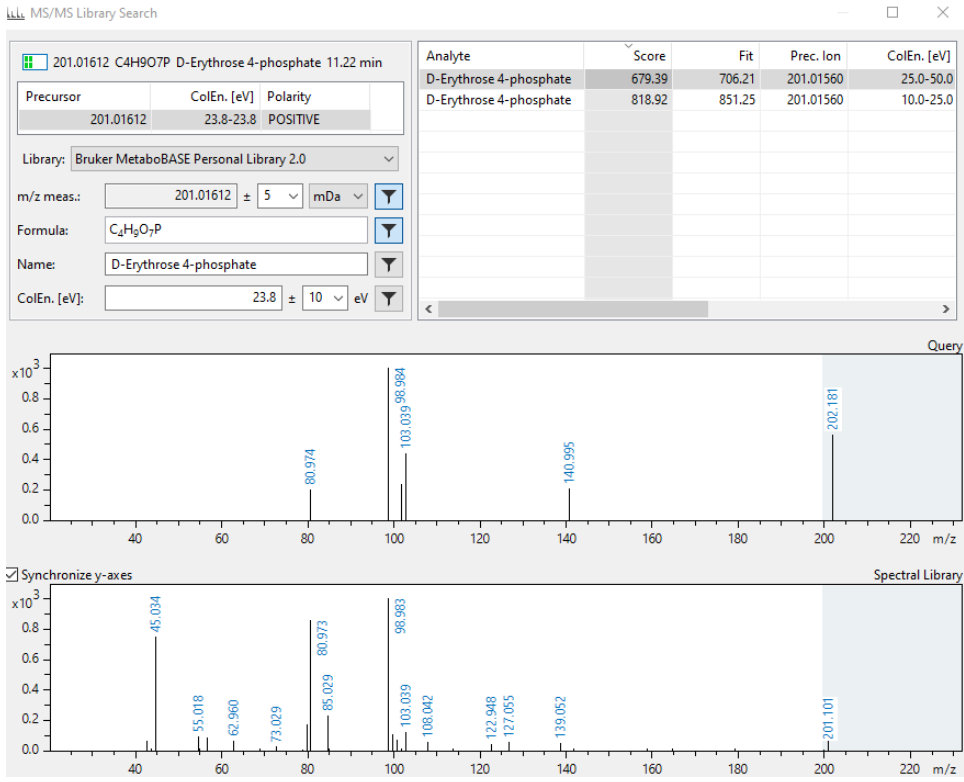
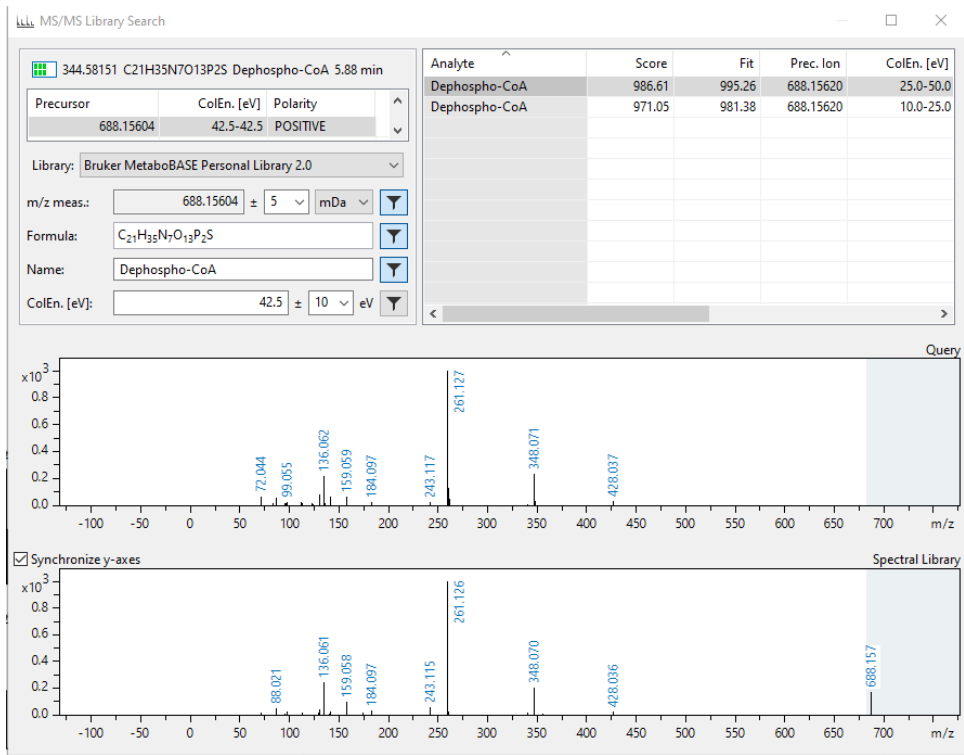
Formula: C₉H₁₃N₃O₄

Name: Deoxycytidine

ColEn. [eV]: 24.8 ± 10 eV

Analyte	Score	Fit	Prec. Ion	ColEn. [eV]
Deoxycytidine	952.29	958.43	228.09790	25.0-50.0
Deoxycytidine	991.49	997.87	228.09790	10.0-25.0





276.15571 C₁₁H₂₁N₃O₅ E-(gamma-...l)-lysine 15.70 min

Precursor	ColEn. [eV]	Polarity
276.15571	26.6-26.7	POSITIVE

Library: Bruker MetaboBASE Personal Library 2.0

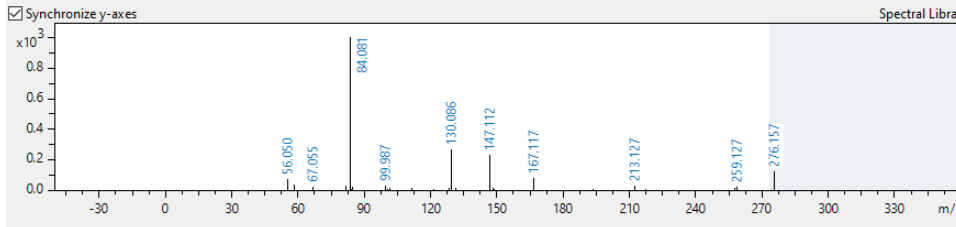
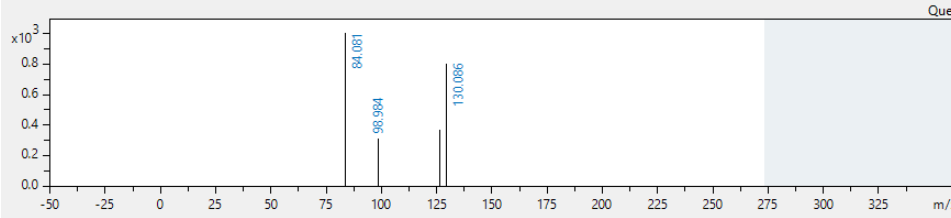
m/z meas.: 276.15571 ± 5 mDa

Formula: C₁₁H₂₁N₃O₅

Name: E-(gamma-Glutamyl)-lysine

ColEn. [eV]: 26.6 ± 10 eV

Analyte	Score	Fit	Prec. Ion	ColEn. [eV]
E-(gamma-Glutamyl)-lysir	817.13	872.50	276.15540	25.0-50.0
Lys Glu	724.42	991.20	276.15540	25.0-50.0
Glu Lys	702.42	750.01	276.15540	25.0-50.0
Lys Glu	696.64	743.84	276.15540	10.0-25.0
E-(gamma-Glutamyl)-lysir	642.39	685.91	276.15540	10.0-25.0
Glu Lys	465.08	496.59	276.15540	10.0-25.0
Gly Val Thr	5.35	7.33	276.15540	25.0-50.0



457.11203 C₁₄H₁₃N₁₄O₃P Flavin m...de (FMN) 7.22 min

Precursor	ColEn. [eV]	Polarity
457.11203	33.4-33.4	POSITIVE

Library: 20200430_C18_pos_yla_eco

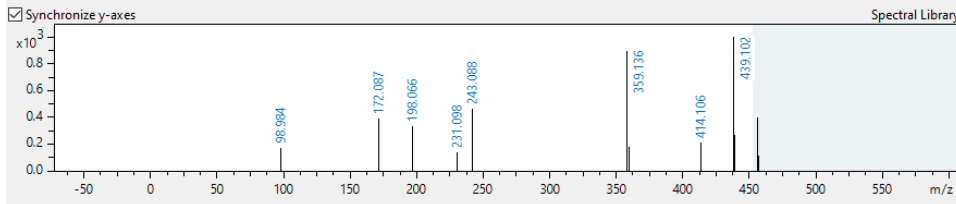
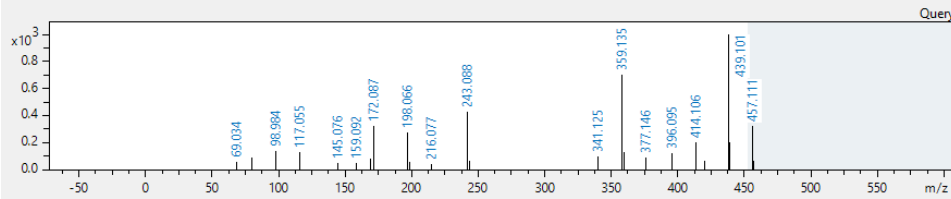
m/z meas.: 457.11203 ± 5 mDa

Formula: C₁₄H₁₃N₁₄O₃P

Name: Flavin mononucleotide (FMN)

ColEn. [eV]: 33.4 ± 10 eV

Analyte	Score	Fit	Prec. Ion	ColEn. [eV]
Flavin mononucleotide (FMN)	668.51	797.24	457.11054	33.4-33.4



261.14464 C11H20N2O5 Gamma-Glu-Leu 5.84 min

Precursor	ColEn. [eV]	Polarity
261.14464	26.0-26.0	POSITIVE

Library: Bruker MetaboBASE Personal Library 2.0

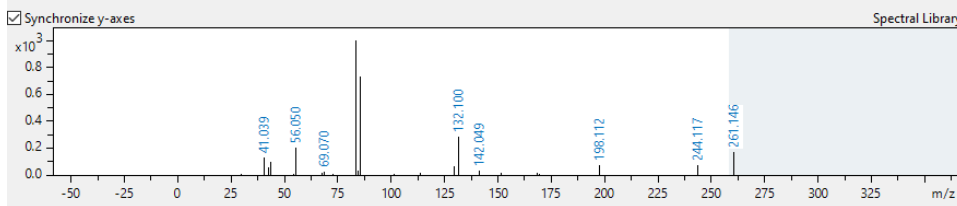
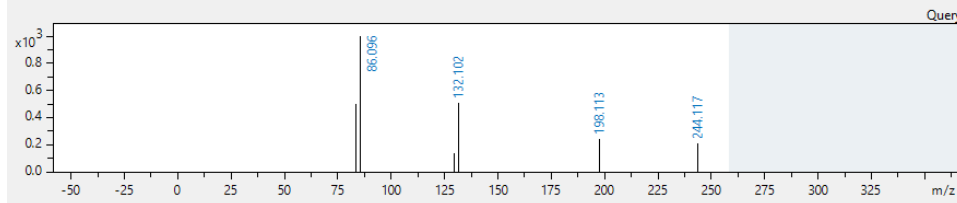
m/z meas.: 261.14464 ± 5 mDa

Formula: C₁₁H₂₀N₂O₅

Name: Gamma-Glu-Leu

ColEn. [eV]: 26.0 ± 10 eV

Analyte	Score	Fit	Prec. Ion	ColEn. [eV]
Gamma-Glu-Leu	843.89	849.42	261.14441	25.0-50.0
Gamma-Glu-Leu	815.25	892.39	261.14441	10.0-25.0



218.15011 C9H19N3O3 gamma-L-G...utrescine 14.50 min

Precursor	ColEn. [eV]	Polarity
218.15011	24.4-24.4	POSITIVE

Library: 20200430_C18_pos_yla_eco

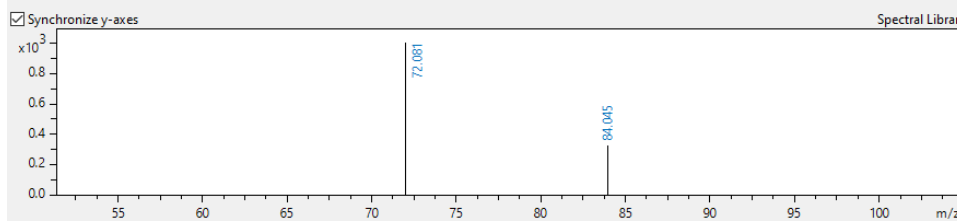
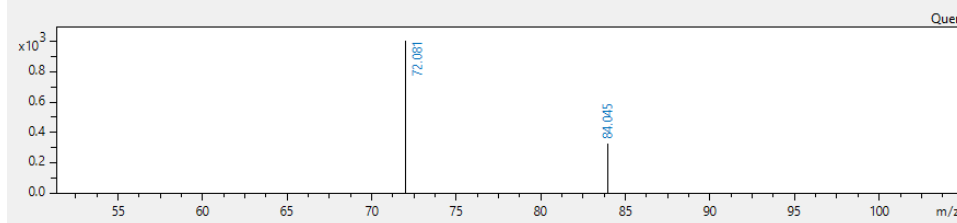
m/z meas.: 218.15011 ± 5 mDa

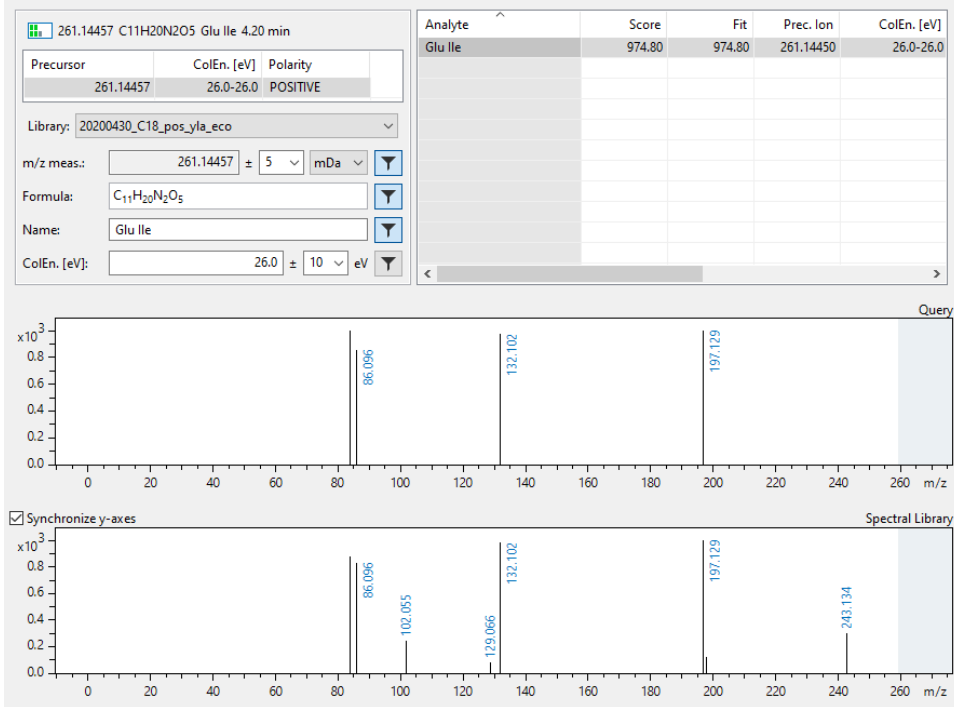
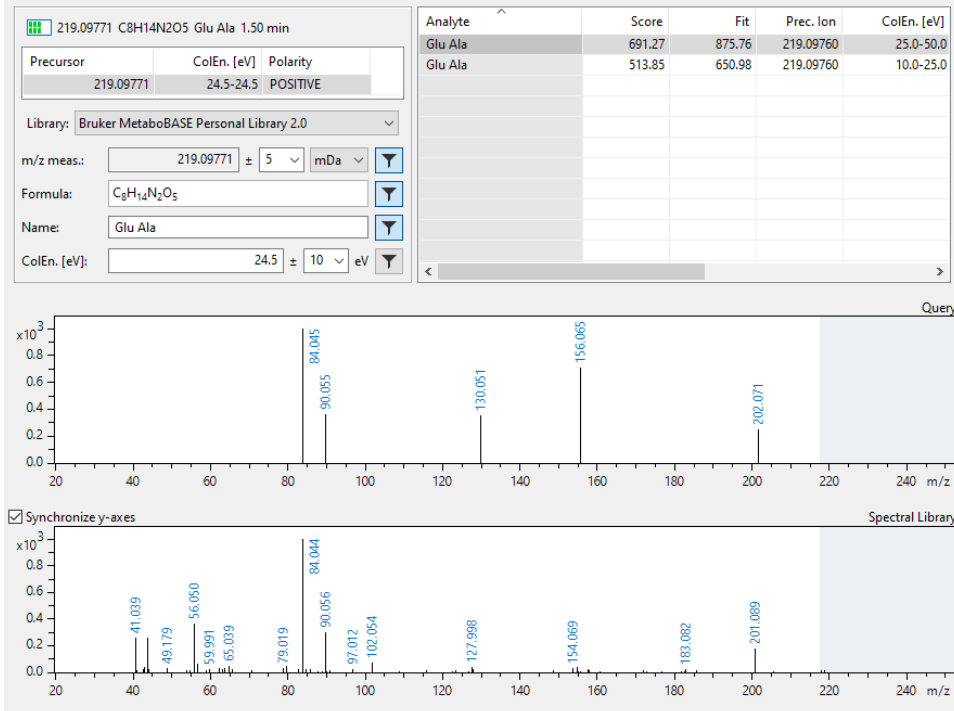
Formula: C₉H₁₉N₃O₃

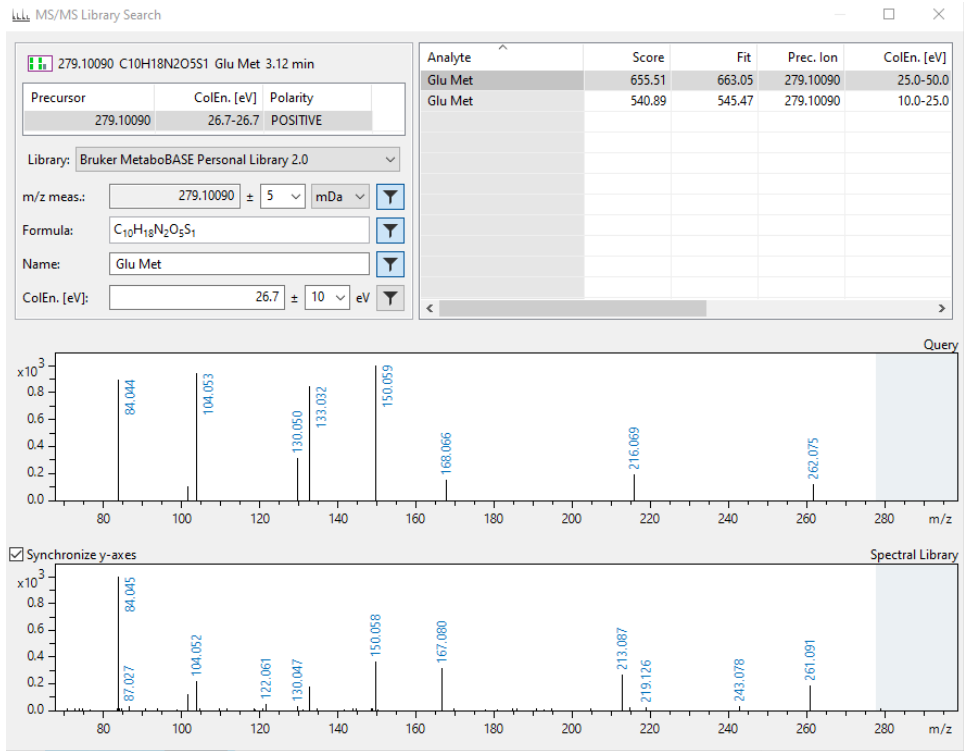
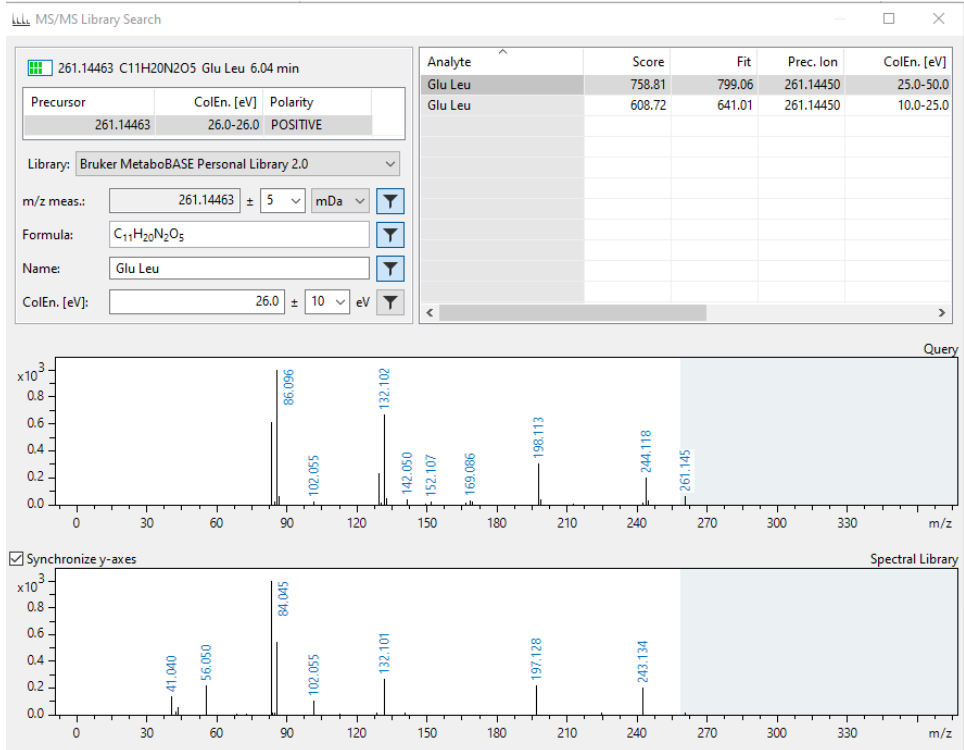
Name: gamma-L-Glutamylputrescine

ColEn. [eV]: 24.4 ± 10 eV

Analyte	Score	Fit	Prec. Ion	ColEn. [eV]
gamma-L-Glutamylputrescine	1000.00	1000.00	218.14992	24.4-24.4







295.12892 C₁₄H₁₈N₂O₅ Glu Phe 6.51 min

Precursor	ColEn. [eV]	Polarity
295.12892	27.3-27.4	POSITIVE

Library: Bruker MetaboBASE Personal Library 2.0

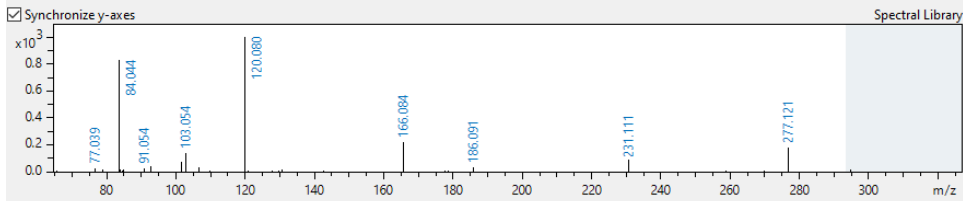
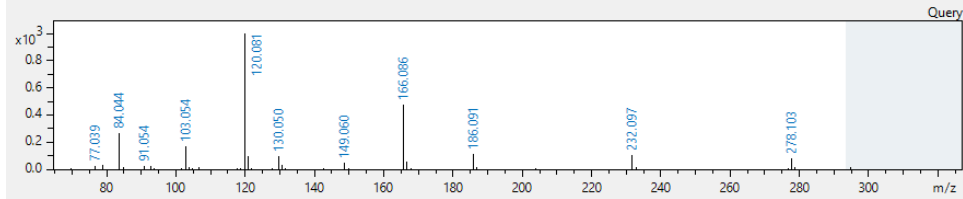
m/z meas.: 295.12892 ± 5 mDa

Formula: C₁₄H₁₈N₂O₅

Name: Glu Phe

ColEn. [eV]: 27.3 ± 10 eV

Analyte	Score	Fit	Prec. Ion	ColEn. [eV]
Glu Phe	808.65	820.31	295.12890	25.0-50.0
Glu Phe	623.31	629.64	295.12890	10.0-25.0



311.12399 C₁₄H₁₈N₂O₆ Glu Tyr 4.87 min

Precursor	ColEn. [eV]	Polarity
311.12399	27.9-27.9	POSITIVE

Library: Bruker MetaboBASE Personal Library 2.0

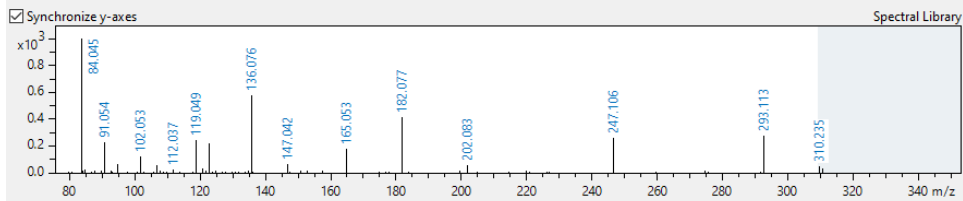
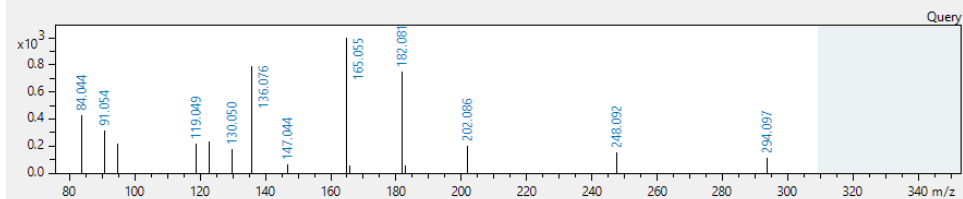
m/z meas.: 311.12399 ± 5 mDa

Formula: C₁₄H₁₈N₂O₆

Name: Glu Tyr

ColEn. [eV]: 27.9 ± 10 eV

Analyte	Score	Fit	Prec. Ion	ColEn. [eV]
Glu Tyr	652.44	661.11	311.12380	25.0-50.0
Glu Tyr	409.53	414.97	311.12380	10.0-25.0



613.15918 C20H32N6O12S2 Glutathi...oxidized 16.82 min

Precursor: 307.08360 ColEn. [eV]: 23.7-23.7 Polarity: POSITIVE

Library: 20200430_C18_pos_yla_eco

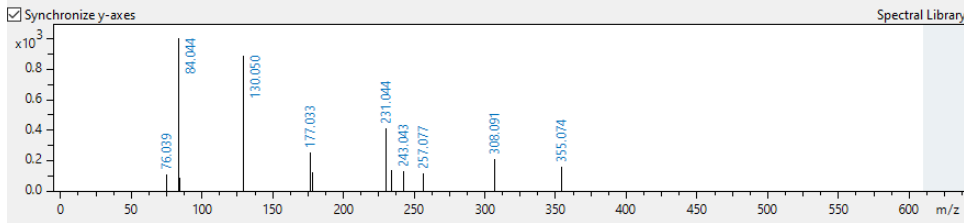
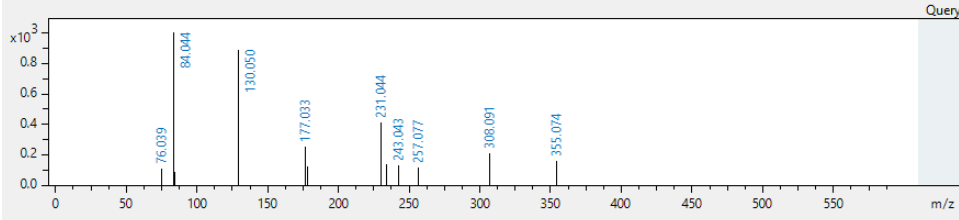
m/z meas.: 307.08360 ± 5 mDa

Formula: C₂₀H₃₂N₆O₁₂S₂

Name: Glutathione, oxidized

ColEn. [eV]: 23.7 ± 10 eV

Analyte	Score	Fit	Prec. Ion	ColEn. [eV]
Glutathione, oxidized	1000.00	1000.00	307.08326	23.7-23.7



189.12345 C8H16N2O3 Glycyl-L-leucine 3.78 min

Precursor: 189.12345 ColEn. [eV]: 23.3-23.3 Polarity: POSITIVE

Library: Bruker HMDB Metabolite Library_2.0

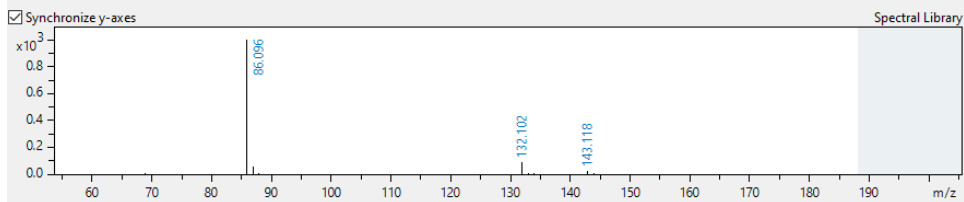
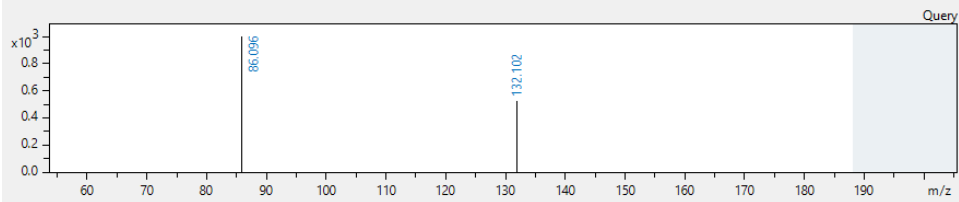
m/z meas.: 189.12345 ± 5 mDa

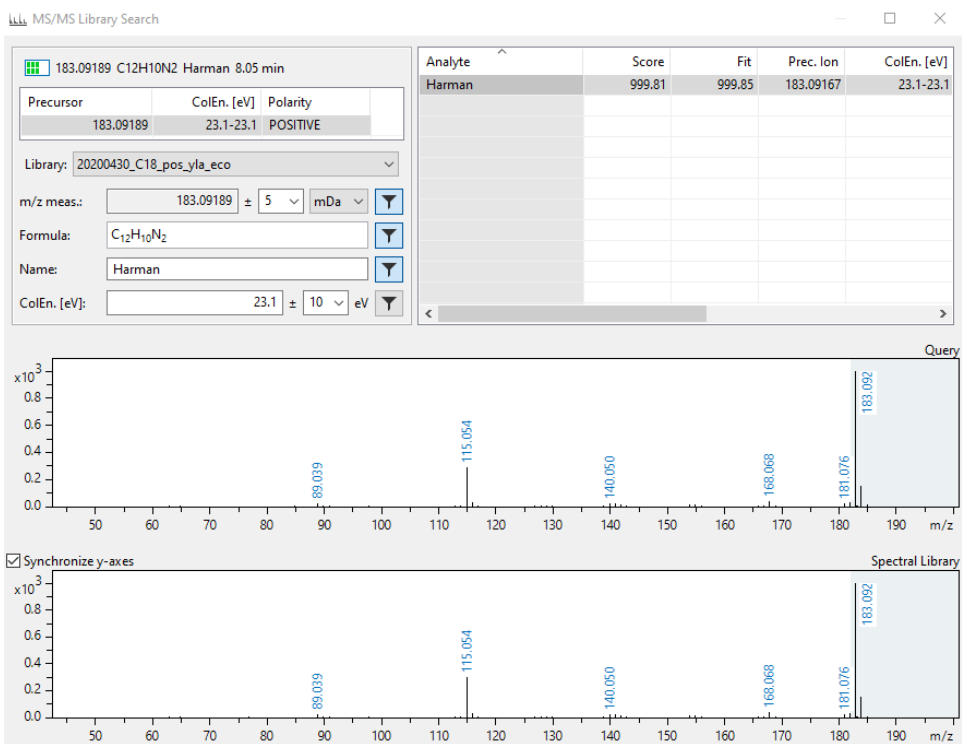
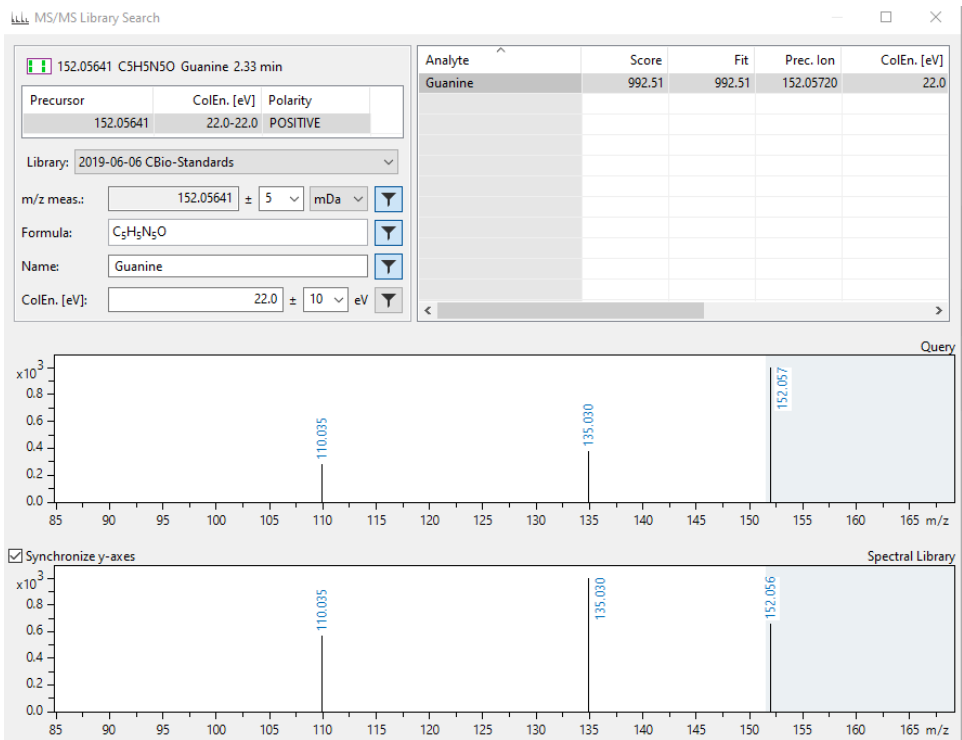
Formula: C₈H₁₆N₂O₃

Name: Glycyl-L-leucine

ColEn. [eV]: 23.3 ± 10 eV

Analyte	Score	Fit	Prec. Ion	ColEn. [eV]
Glycyl-L-leucine	920.64	920.64	189.12337	20.0
Glycyl-L-leucine	919.91	919.91	189.12337	20.0-50.0
Glycyl-L-leucine	893.91	893.91	189.12337	30.0
Glycyl-L-leucine	837.51	837.51	189.12337	10.0
Glycyl-L-leucine	819.36	819.36	189.12337	40.0





131.07146 C6H12O3 Hydroxyisocaproic acid 6.90 min

Precursor	ColEn. [eV]	Polarity
131.07146	20.8-20.8	POSITIVE

Library: Bruker HMDB Metabolite Library_2.0

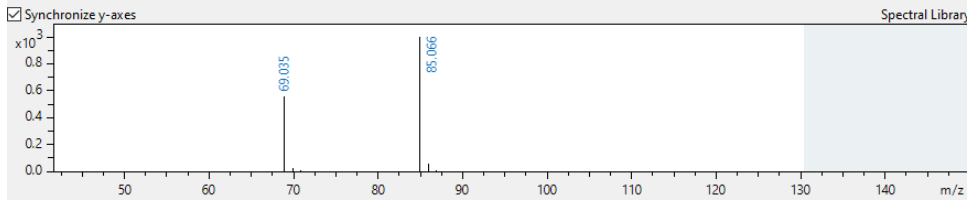
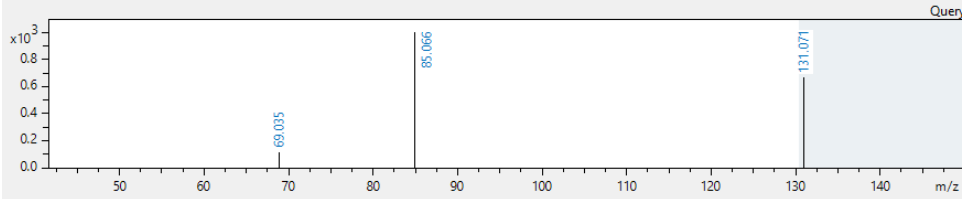
m/z meas.: 131.07146 ± 5 mDa

Formula: C₆H₁₂O₃

Name: Hydroxyisocaproic acid

ColEn. [eV]: 20.8 ± 10 eV

Analyte	Score	Fit	Prec. Ion	ColEn. [eV]
Leucinic acid	994.47	994.47	131.07137	1
2-Ethyl-2-hydroxybutyric acid	992.90	998.48	131.07137	2
2-Ethyl-2-hydroxybutyric acid	992.45	998.03	131.07137	1
2-Hydroxycaproic acid	992.33	997.91	131.07137	1
2-Hydroxycaproic acid	989.89	995.46	131.07137	2
Leucinic acid	958.40	958.40	131.07137	2
Leucinic acid	945.49	945.49	131.07137	20.0-5
Hydroxyisocaproic acid	943.15	943.15	131.07137	2
Hydroxyisocaproic acid	920.48	920.48	131.07137	20.0-5
Hydroxyisocaproic acid	105.52	999.03	131.07137	3
Leucinic acid	105.52	999.03	131.07137	3



137.04588 C5H4N2O Hypoxanthine 1.87 min

Precursor	ColEn. [eV]	Polarity
137.04588	21.4-21.4	POSITIVE

Library: 2019-06-06 CBio-Standards

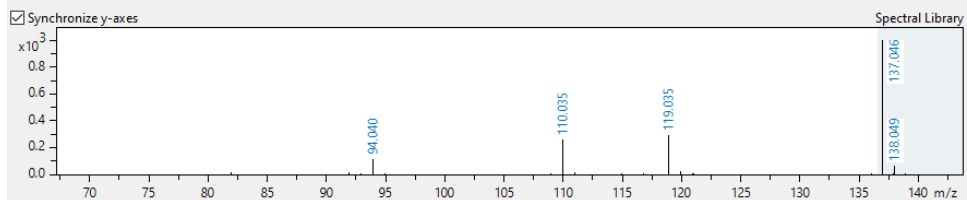
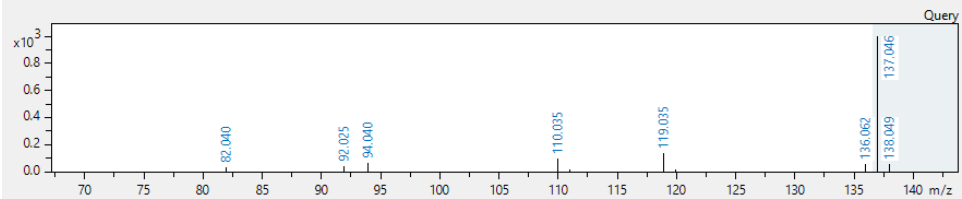
m/z meas.: 137.04588 ± 5 mDa

Formula: C₅H₄N₂O

Name: Hypoxanthine

ColEn. [eV]: 21.4 ± 10 eV

Analyte	Score	Fit	Prec. Ion	ColEn. [eV]
Hypoxanthine	585.89	735.60	137.04580	21.4



288.20302 C12H25N5O3 Ile Arg 5.64 min

Precursor	ColEn. [eV]	Polarity
288.20302	27.1-27.1	POSITIVE

Library: Bruker MetaboBASE Personal Library 2.0

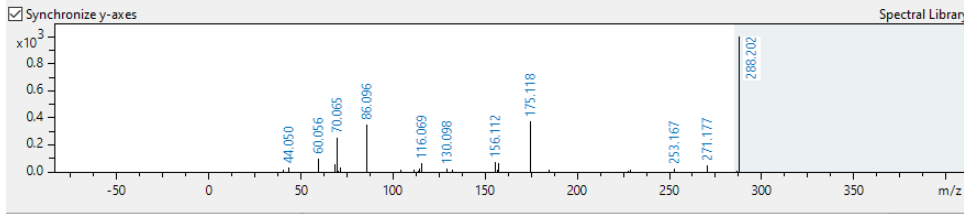
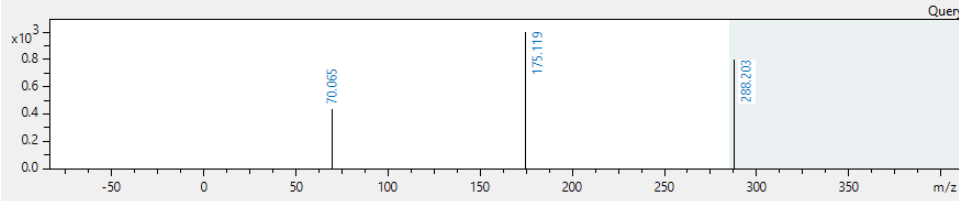
m/z meas.: 288.20302 ± 5 mDa

Formula: C₁₂H₂₅N₅O₃

Name: Ile Arg

ColEn. [eV]: 27.1 ± 10 eV

Analyte	Score	Fit	Prec. Ion	ColEn. [eV]
Ile Arg	748.31	748.31	288.20300	10.0-25.0
Ile Arg	539.65	539.65	288.20300	25.0-50.0



247.12903 C10H18N2O5 Ile Asp 2.41 min

Precursor	ColEn. [eV]	Polarity
247.12903	25.5-25.5	POSITIVE

Library: 20200430_C18_pos_yla_eco

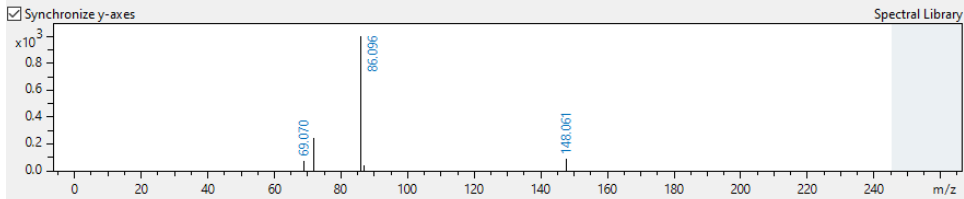
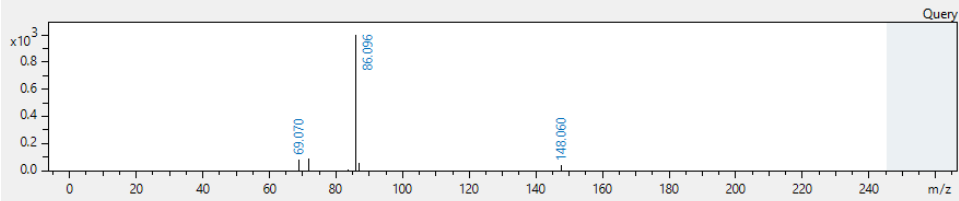
m/z meas.: 247.12903 ± 5 mDa

Formula: C₁₀H₁₈N₂O₅

Name: Ile Asp

ColEn. [eV]: 25.5 ± 10 eV

Analyte	Score	Fit	Prec. Ion	ColEn. [eV]
Ile Asp	987.70	987.70	247.12885	25.5-25.5



358.19742 C₁₆H₂₇N₃O₆ Ile Pro Glu 6.08 min

Precursor	ColEn. [eV]	Polarity
358.19742	29.7-29.7	POSITIVE

Library: Bruker MetaboBASE Personal Library 2.0

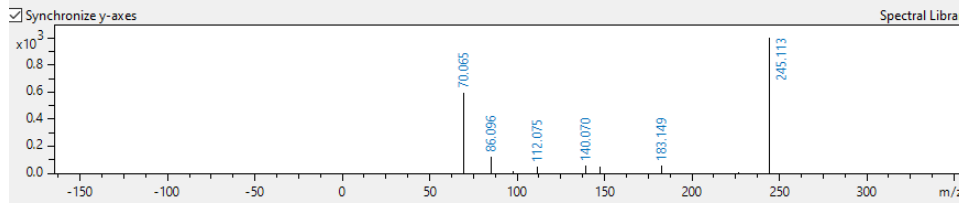
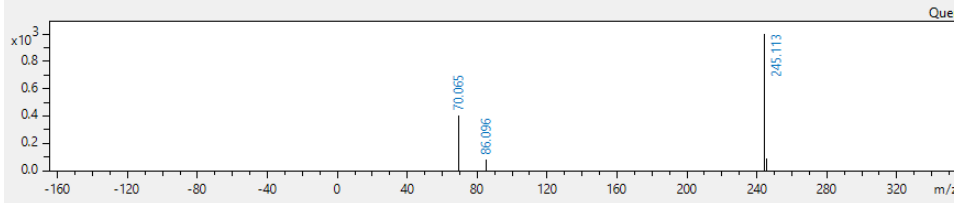
m/z meas.: 358.19742 ± 5 mDa

Formula: C₁₆H₂₇N₃O₆

Name: Ile Pro Glu

ColEn. [eV]: 29.7 ± 10 eV

Analyte	Score	Fit	Prec. Ion	ColEn. [eV]
Ile Pro Glu	981.05	984.09	358.19730	10.0-25.0
Ile Pro Glu	721.92	724.15	358.19730	25.0-50.0



233.14976 C₁₀H₂₀N₂O₄ Ile Thr 1.93 min

Precursor	ColEn. [eV]	Polarity
233.14976	25.1-25.1	POSITIVE

Library: 20200430_C18_pos_ylla_eco

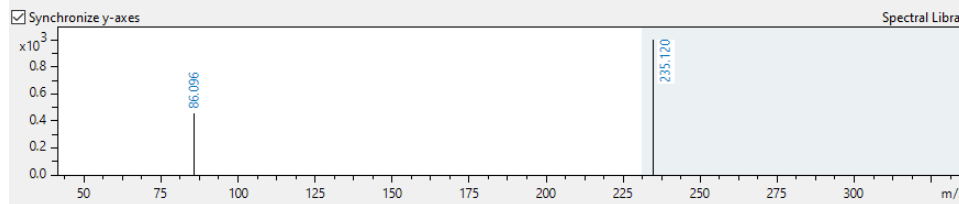
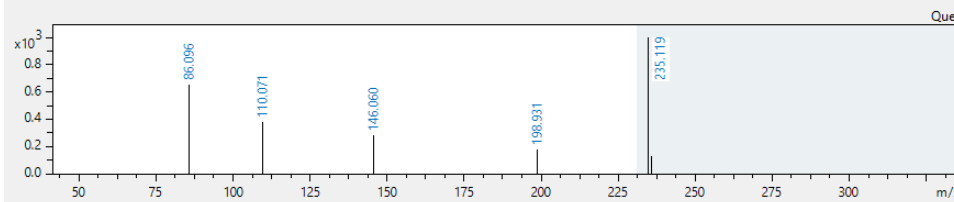
m/z meas.: 233.14976 ± 5 mDa

Formula: C₁₀H₂₀N₂O₄

Name: Ile Thr

ColEn. [eV]: 25.1 ± 10 eV

Analyte	Score	Fit	Prec. Ion	ColEn. [eV]
Ile Thr	792.82	1000.00	233.14958	25.1-25.1



360.21312 C16H29N3O6 Ile Val Glu 5.61 min

Precursor	ColEn. [eV]	Polarity
360.21312	29.8-29.8	POSITIVE

Library: Bruker MetaboBASE Personal Library 2.0

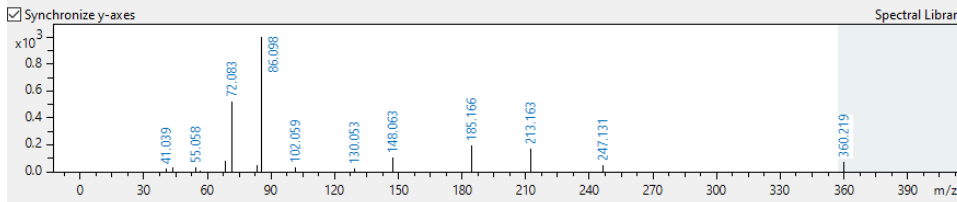
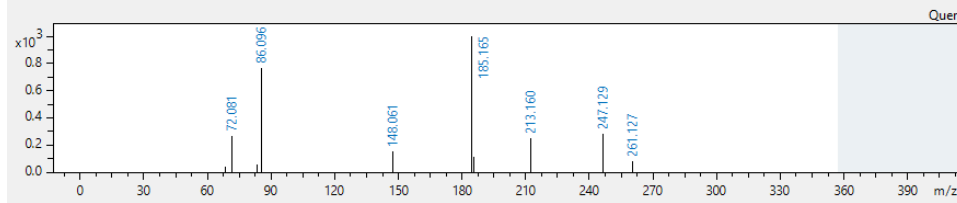
m/z meas.: 360.21312 ± 5 mDa

Formula: C₁₆H₂₉N₃O₆

Name: Ile Val Glu

ColEn. [eV]: 29.8 ± 10 eV

Analyte	Score	Fit	Prec. Ion	ColEn. [eV]
Ile Val Glu	614.09	923.09	360.21290	25.0-50.0
Ile Val Glu	517.43	777.79	360.21290	10.0-25.0



233.14976 C10H20N2O4 Ile Thr 1.93 min

Precursor	ColEn. [eV]	Polarity
233.14976	25.1-25.1	POSITIVE

Library: 20200430_C18_pos_yla_eco

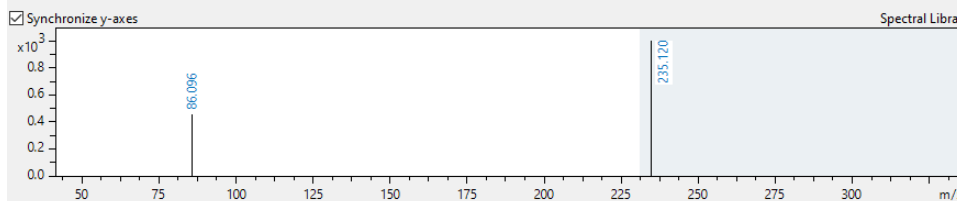
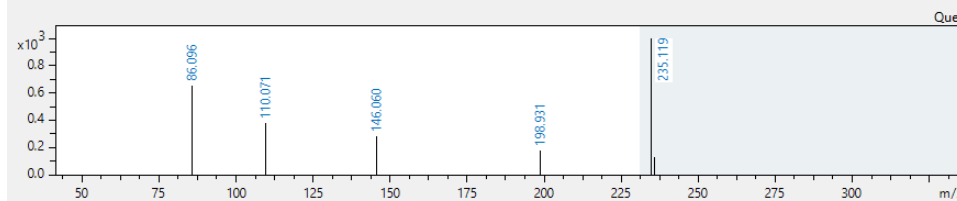
m/z meas.: 233.14976 ± 5 mDa

Formula: C₁₀H₂₀N₂O₄

Name: Ile Thr

ColEn. [eV]: 25.1 ± 10 eV

Analyte	Score	Fit	Prec. Ion	ColEn. [eV]
Ile Thr	792.82	1000.00	233.14958	25.1-25.1



307.04415 C₁₀H₁₂N₄O₅ Inosine 8.41 min

Precursor	ColEn. [eV]	Polarity
307.04415	27.8-27.8	POSITIVE

Library: 20200430_C18_pos_yla_eco

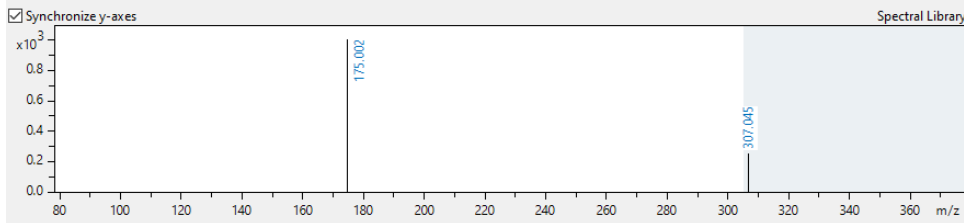
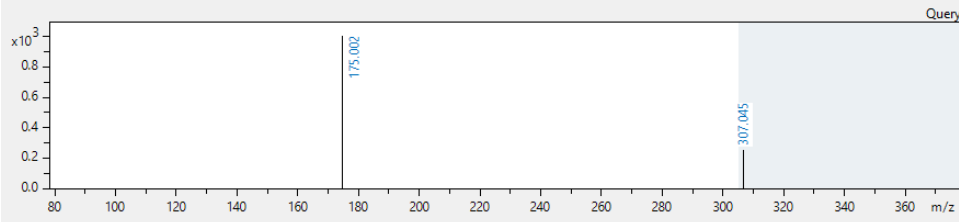
m/z meas.: 307.04415 ± 5 mDa

Formula: C₁₀H₁₂N₄O₅

Name: Inosine

ColEn. [eV]: 27.8 ± 10 eV

Analyte	Score	Fit	Prec. Ion	ColEn. [eV]
Inosine	1000.00	1000.00	307.04393	27.8-27.8



190.04999 C₁₀H₇NO₃ Kynurenic acid 6.71 min

Precursor	ColEn. [eV]	Polarity
190.04999	23.4-23.4	POSITIVE

Library: Bruker HMDB Metabolite Library_2.0

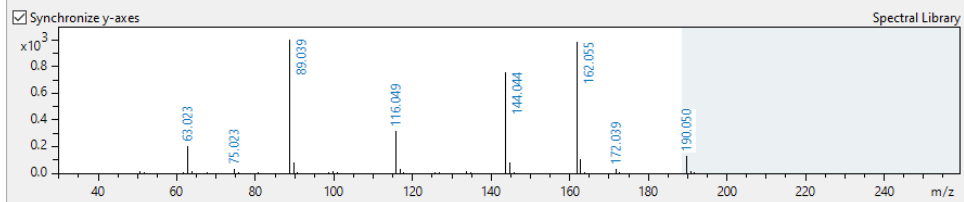
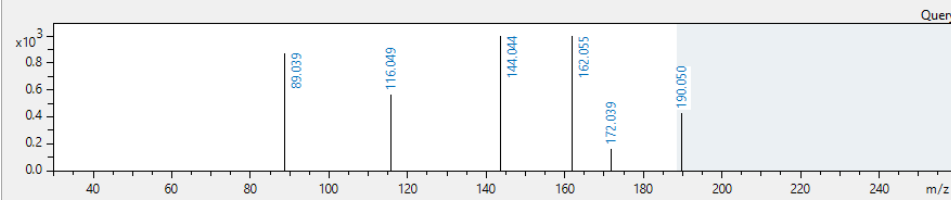
m/z meas.: 190.04999 ± 5 mDa

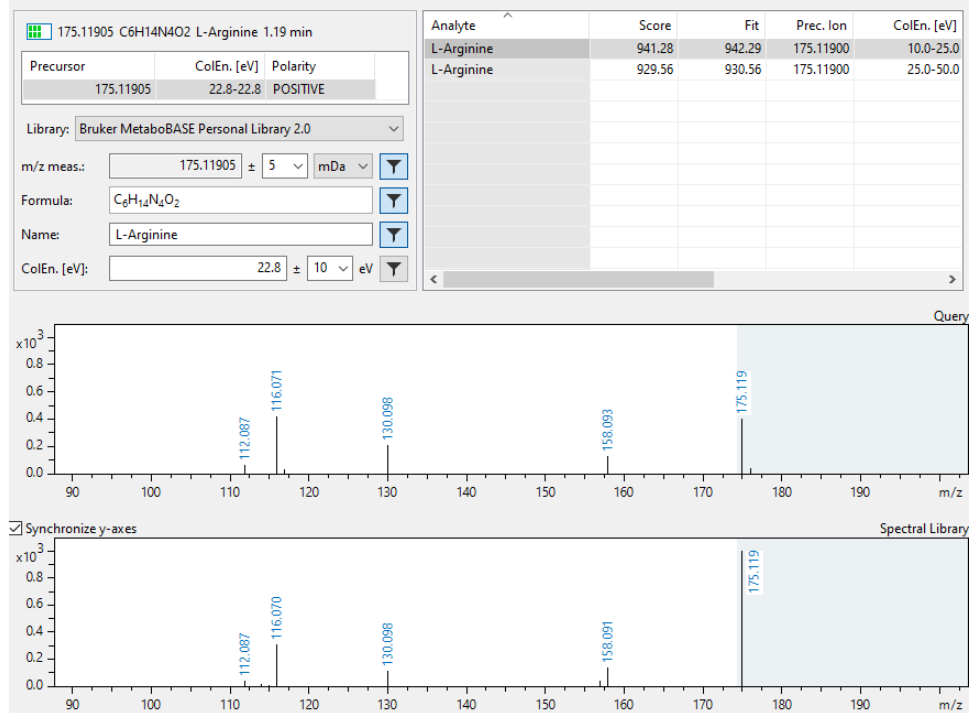
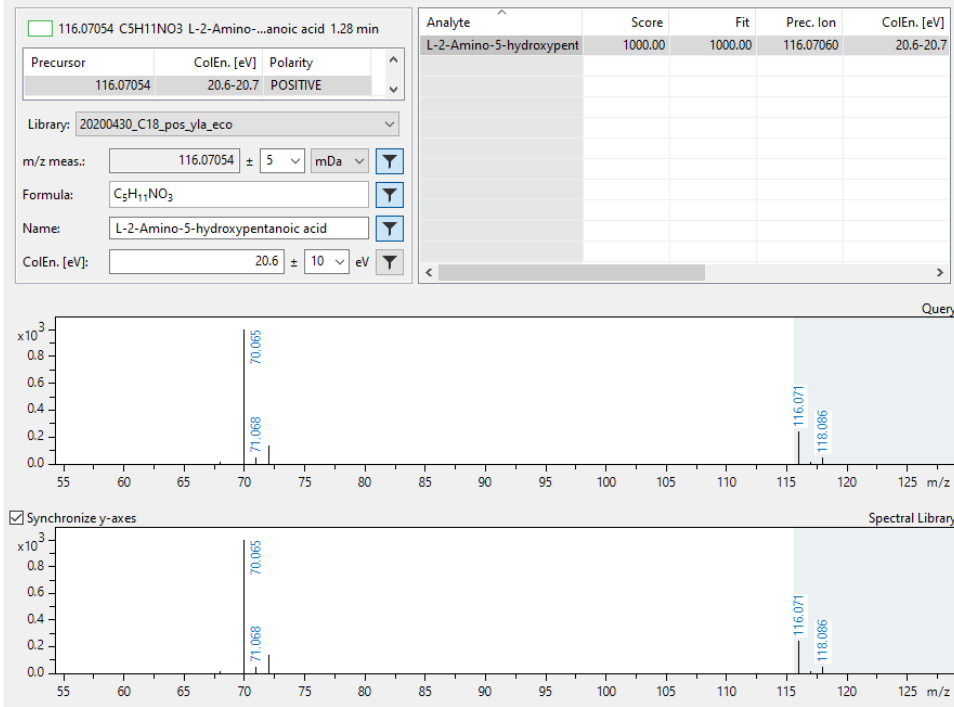
Formula: C₁₀H₇NO₃

Name: Kynurenic acid

ColEn. [eV]: 23.4 ± 10 eV

Analyte	Score	Fit	Prec. Ion	ColEn. [eV]
Kynurenic acid	964.06	964.06	190.04987	20.0-50.0
Kynurenic acid	927.55	931.21	190.04987	30.0
Kynurenic acid	807.00	928.92	190.04987	20.0
Kynurenic acid	727.96	900.95	190.04987	10.0
Kynurenic acid	720.67	723.52	190.04987	40.0





134.04493 C4H7NO4 L-Aspartic acid 13.01 min

Precursor	ColEn. [eV]	Polarity
134.04493	21.2-21.3	POSITIVE

Library: 20200430_C18_pos_yla_eco

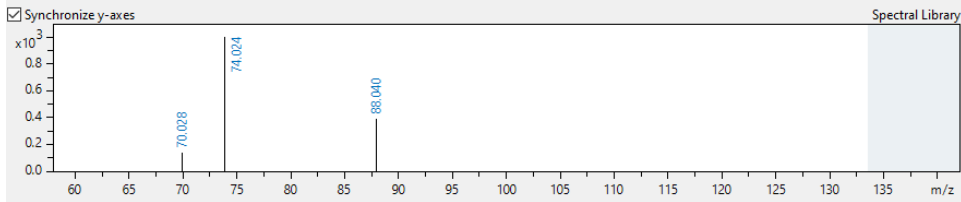
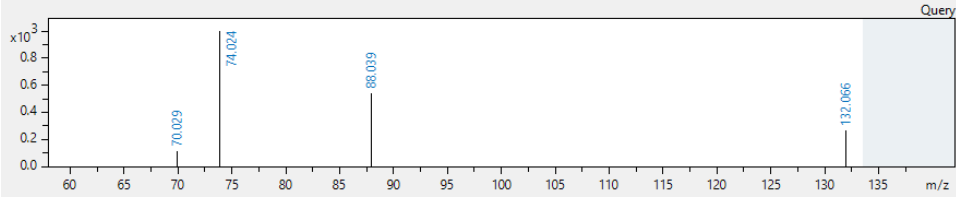
m/z meas.: 134.04493 ± 5 mDa

Formula: C₄H₇NO₄

Name: L-Aspartic acid

ColEn. [eV]: 21.2 ± 10 eV

Analyte	Score	Fit	Prec. Ion	ColEn. [eV]
L-Aspartic acid	966.12	992.18	134.04478	21.3-21.3



179.04870 C5H10N2O3S L-Cys-Gly 12.91 min

Precursor	ColEn. [eV]	Polarity
179.04870	23.0-23.0	POSITIVE

Library: Bruker MetaboBASE Personal Library 2.0

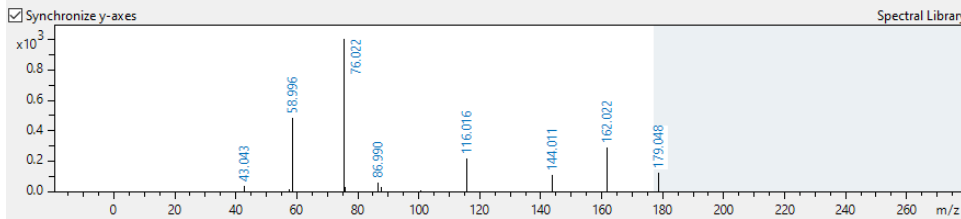
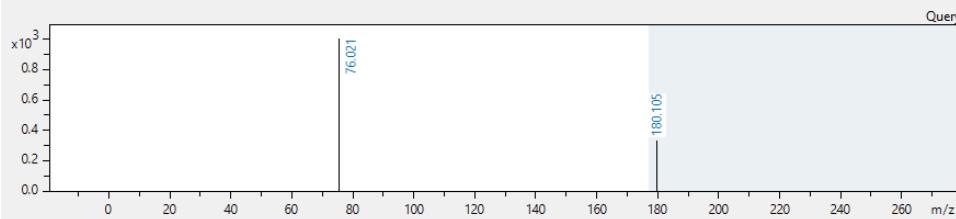
m/z meas.: 179.04870 ± 5 mDa

Formula: C₅H₁₀N₂O₃S

Name: L-Cys-Gly

ColEn. [eV]: 23.0 ± 10 eV

Analyte	Score	Fit	Prec. Ion	ColEn. [eV]
L-Cys-Gly	852.65	852.65	179.04850	10.0-25.0
L-Cys-Gly	545.81	545.81	179.04850	25.0-50.0



390.18703 C₁₆H₂₇N₃O₈ Leu Glu Glu 5.07 min

Precursor	ColEn. [eV]	Polarity
390.18703	30.9-30.9	POSITIVE

Library: 20200430_C18_pos_yla_eco

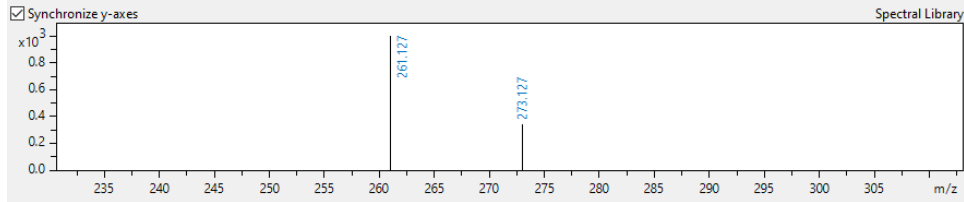
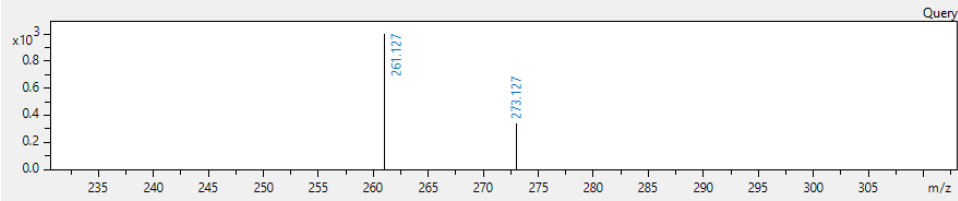
m/z meas.: 390.18703 ± 5 mDa

Formula: C₁₆H₂₇N₃O₈

Name: Leu Glu Glu

ColEn. [eV]: 30.9 ± 10 eV

Analyte	Score	Fit	Prec. Ion	ColEn. [eV]
Leu Glu Glu	1000.00	1000.00	390.18709	30.9-30.9



357.21321 C₁₆H₂₈N₄O₅ Leu Pro Gln 5.67 min

Precursor	ColEn. [eV]	Polarity
357.21321	29.6-29.6	POSITIVE

Library: 20200430_C18_pos_yla_eco

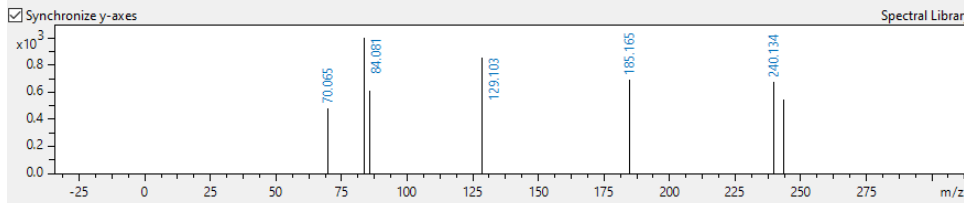
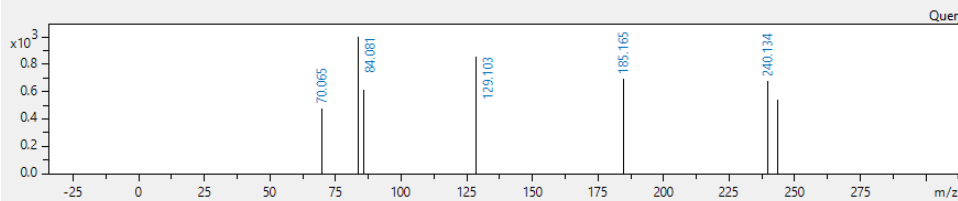
m/z meas.: 357.21321 ± 5 mDa

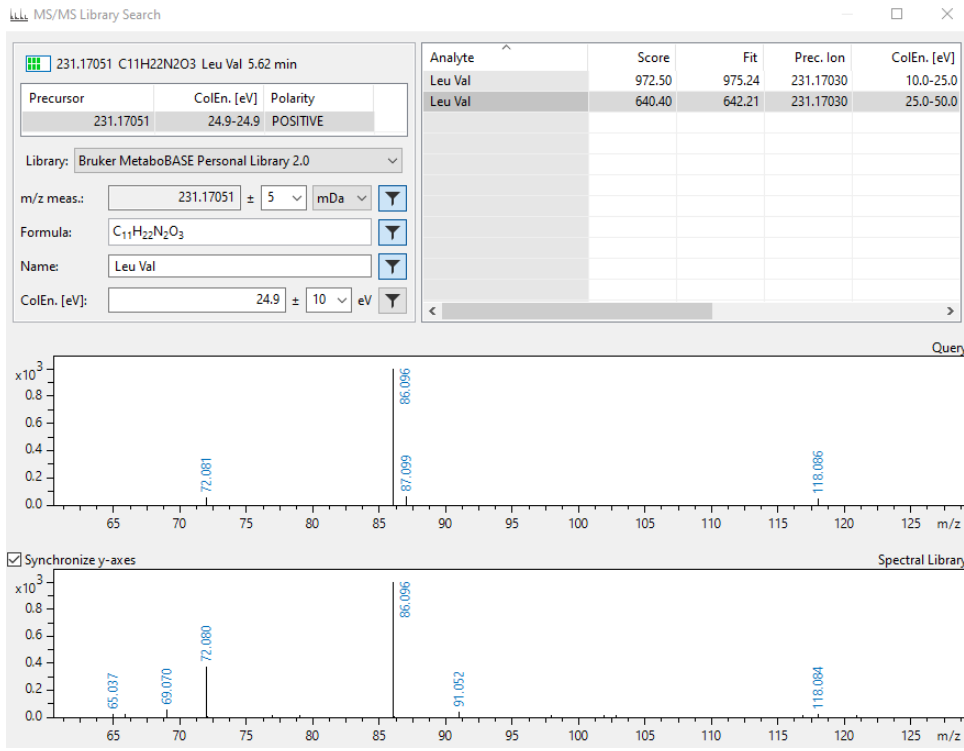
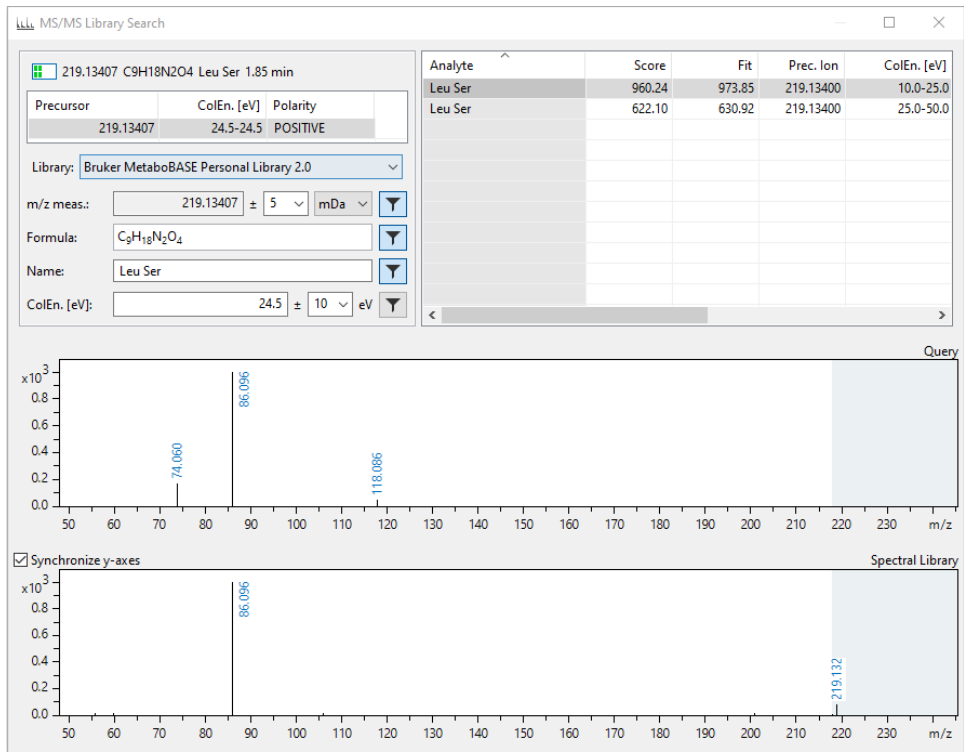
Formula: C₁₆H₂₈N₄O₅

Name: Leu Pro Gln

ColEn. [eV]: 29.6 ± 10 eV

Analyte	Score	Fit	Prec. Ion	ColEn. [eV]
Leu Pro Gln	1000.00	1000.00	357.21325	29.6-29.6





245.18603 C12H24N2O3 Leucyl-leucine 7.21 min

Precursor	ColEn. [eV]	Polarity
245.18603	25.4-25.4	POSITIVE

Library: 20200430_C18_pos_yla_eco

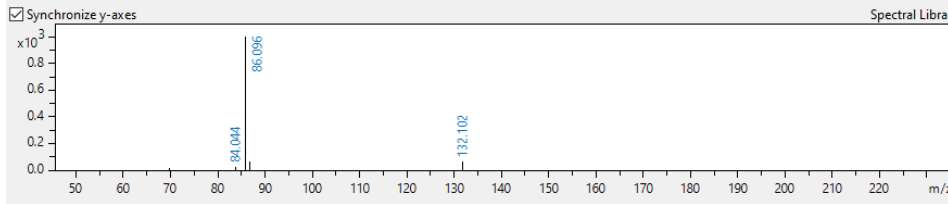
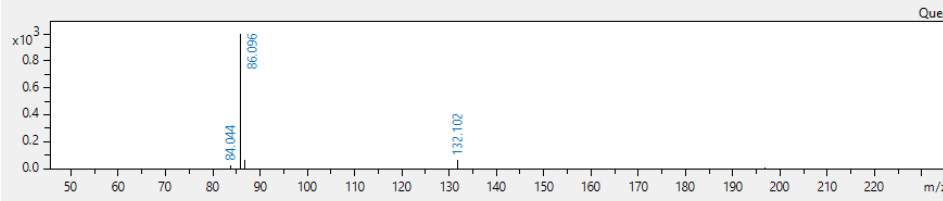
m/z meas.: 245.18603 ± 5 mDa

Formula: C₁₂H₂₄N₂O₃

Name: Leucyl-leucine

ColEn. [eV]: 25.4 ± 10 eV

Analyte	Score	Fit	Prec. Ion	ColEn. [eV]
Leucyl-leucine	999.90	999.92	245.18597	25.4-25.4



148.06049 C5H9NO4 L-Glutamic acid 1.23 min

Precursor	ColEn. [eV]	Polarity
148.06049	21.8-21.8	POSITIVE

Library: 20200430_C18_pos_yla_eco

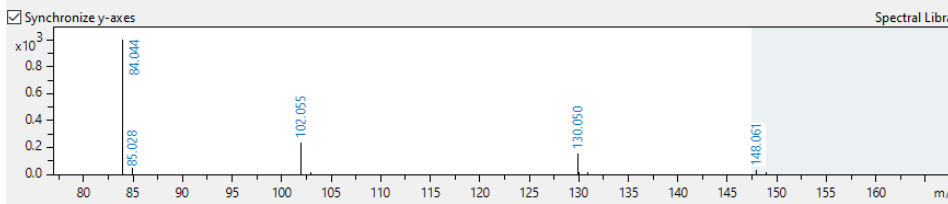
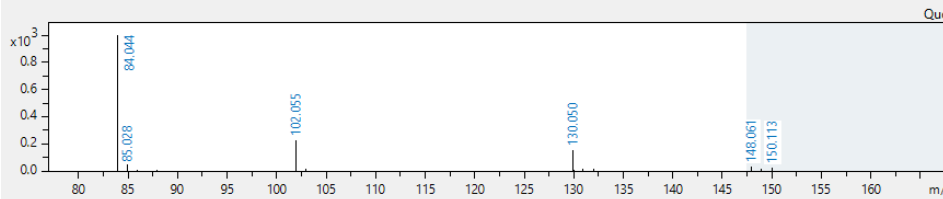
m/z meas.: 148.06049 ± 5 mDa

Formula: C₅H₉NO₄

Name: L-Glutamic acid

ColEn. [eV]: 21.8 ± 10 eV

Analyte	Score	Fit	Prec. Ion	ColEn. [eV]
L-Glutamic acid	999.73	999.84	148.06043	21.8-21.8



156.07694 C6H9N3O2 L-Histidine 14.34 min

Precursor	ColEn. [eV]	Polarity
156.07694	22.1-22.1	POSITIVE

Library: 2019-06-06 CBio-Standards

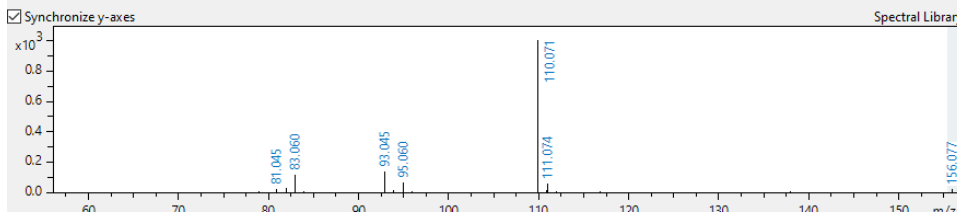
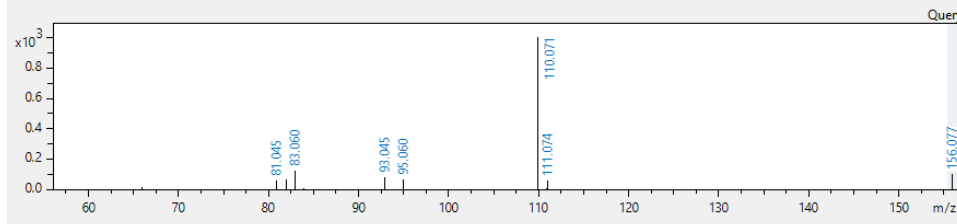
m/z meas.: 156.07694 ± 5 mDa

Formula: C₆H₉N₃O₂

Name: L-Histidine

ColEn. [eV]: 22.1 ± 10 eV

Analyte	Score	Fit	Prec. Ion	ColEn. [eV]
L-Histidine	996.81	996.89	156.07670	22.1
Histidin	995.90	995.97	156.07640	22.1



203.13935 C9H18N2O3 L-Leucyl-L- Alanine 8.70 min

Precursor	ColEn. [eV]	Polarity
203.13935	23.9-23.9	POSITIVE

Library: 20200430_C18_pos_yla_eco

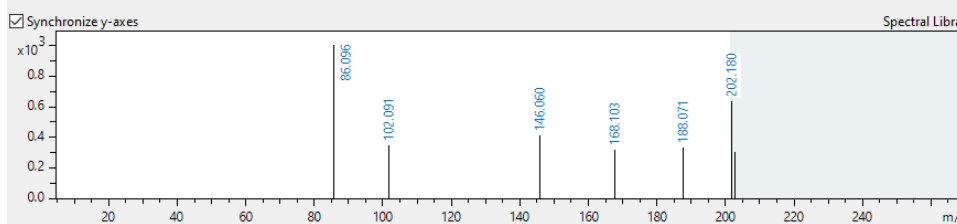
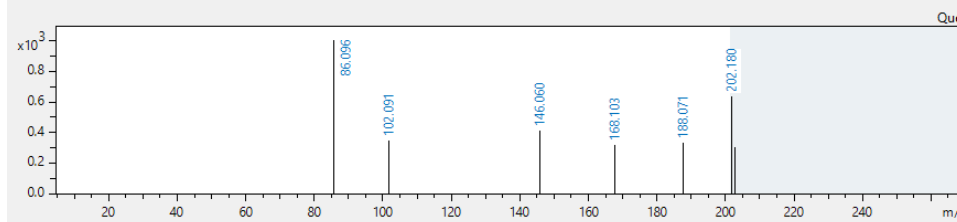
m/z meas.: 203.13935 ± 5 mDa

Formula: C₉H₁₈N₂O₃

Name: L-Leucyl-L- Alanine

ColEn. [eV]: 23.9 ± 10 eV

Analyte	Score	Fit	Prec. Ion	ColEn. [eV]
L-Leucyl-L- Alanine	1000.00	1000.00	203.13902	23.9-23.9
L-Leucyl-L- Alanine	700.95	964.92	203.13902	23.9-23.9
ALANYL-dl-LEUCINE	627.93	864.40	203.13902	23.9-23.9



Analyte	Score	Fit	Prec. Ion	ColEn. [eV]
L-Leucyl-L-proline_	1000.00	1000.00	227.14012	23.1-23.2

Precursor	ColEn. [eV]	Polarity
227.14011	23.1-23.2	NEGATIVE

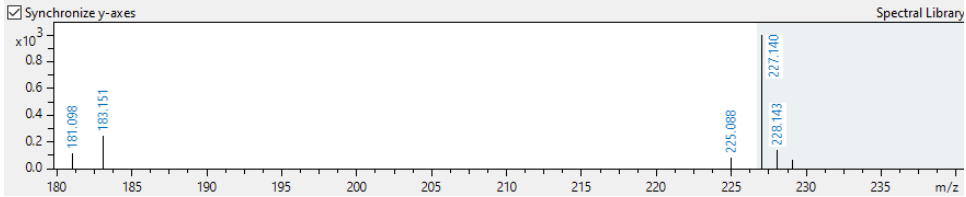
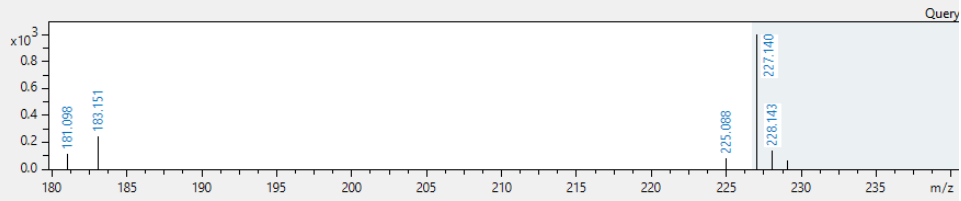
Library: 20200430_C18_pos_ylla_eco

m/z meas.: 227.14011 ± 5 mDa

Formula: C₁₁H₂₀N₂O₃

Name: L-Leucyl-L-proline_

ColEn. [eV]: 23.1 ± 10 eV



Analyte	Score	Fit	Prec. Ion	ColEn. [eV]
L-NMMA	764.55	963.28	189.13460	25.0-50.0
L-NMMA	689.98	869.32	189.13460	10.0-25.0

Precursor	ColEn. [eV]	Polarity
189.13464	23.3-23.3	POSITIVE

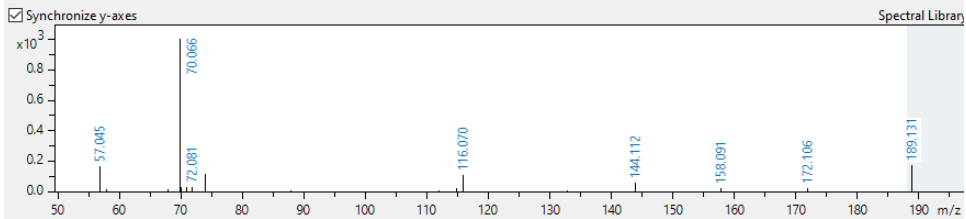
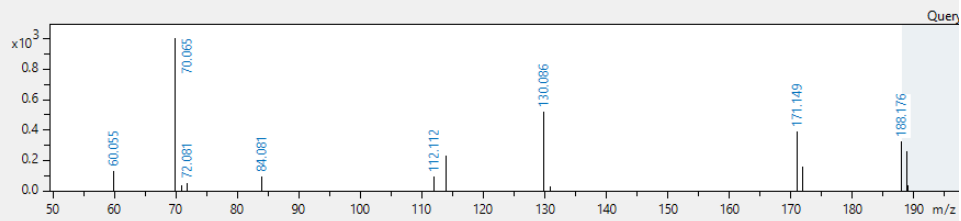
Library: Bruker MetaboBASE Personal Library 2.0

m/z meas.: 189.13464 ± 5 mDa

Formula: C₇H₁₆N₄O₂

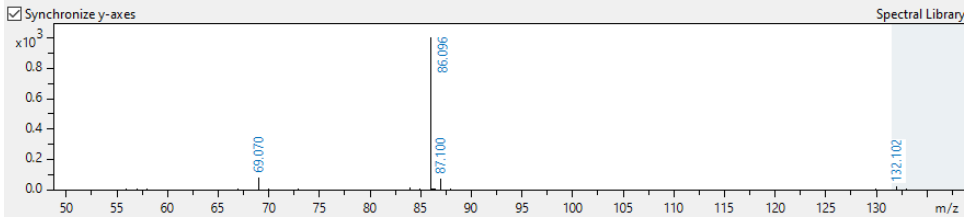
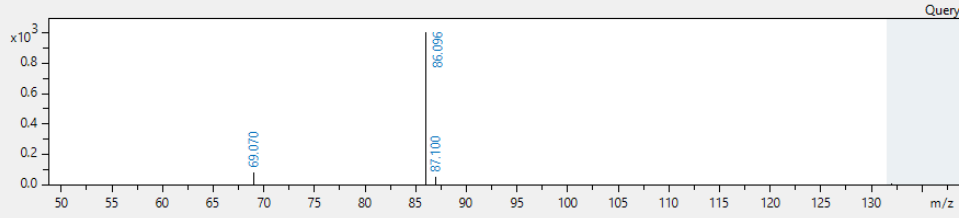
Name: L-NMMA

ColEn. [eV]: 23.3 ± 10 eV



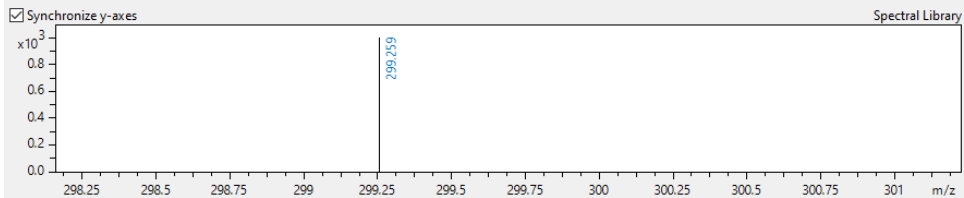
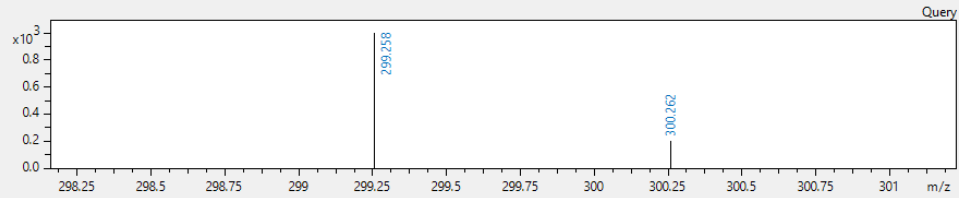
Analyte	Score	Fit	Prec. Ion	ColEn. [eV]
L-Norleucine	999.70	999.70	132.10191	21.2-21.2

Precursor: 132.10206 ColEn. [eV]: 21.2-21.2 Polarity: POSITIVE
 Library: 20200430_C18_pos_yla_eco
 m/z meas.: 132.10206 ± 5 mDa
 Formula: C₆H₁₃NO₂
 Name: L-Norleucine
 ColEn. [eV]: 21.2 ± 10 eV



Analyte	Score	Fit	Prec. Ion	ColEn. [eV]
LPE 15:0; [M+H] ⁺	980.84	1000.00	440.27771	

Precursor: 440.27743 ColEn. [eV]: 32.8-32.8 Polarity: POSITIVE
 Library: LipidBlast
 m/z meas.: 440.27743 ± 5 mDa
 Formula: C₂₀H₄₂NO₂P
 Name: LPE 15:0
 ColEn. [eV]: 32.8 ± 10 eV



424.24596 C19H38NO7P LPE(14:1)9Z 14.05 min

Precursor	ColEn. [eV]	Polarity
424.24596	32.2-32.2	POSITIVE

Library: putative-identified_metabolites_vbe141

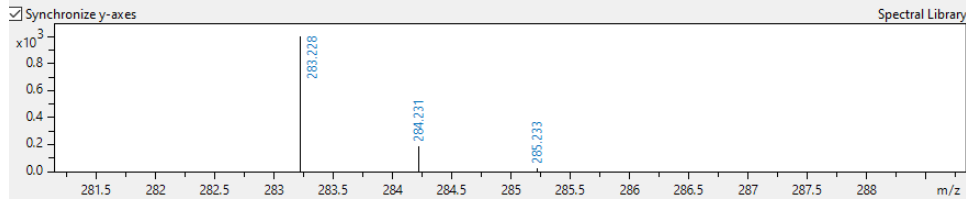
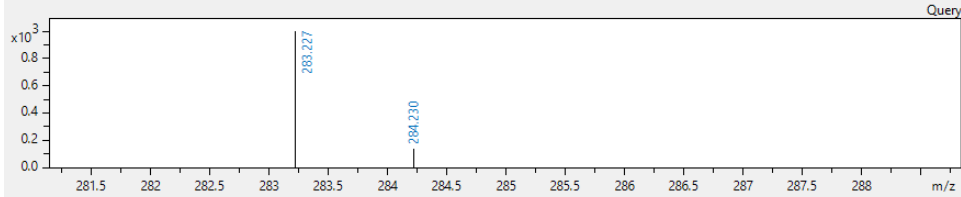
m/z meas.: 424.24596 ± 5 mDa

Formula: C₁₉H₃₈NO₇P

Name: LPE(14:1)9Z

ColEn. [eV]: 32.2 ± 10 eV

Analyte	Score	Fit	Prec. Ion	ColEn. [eV]
LPE(14:1)9Z	991.94	991.94	424.24690	32.2



452.27747 C21H42NO7P LPE(16:1) 15.57 min

Precursor	ColEn. [eV]	Polarity
474.25940	34.0-34.0	POSITIVE

Library: 20200430_C18_pos_yla_eco

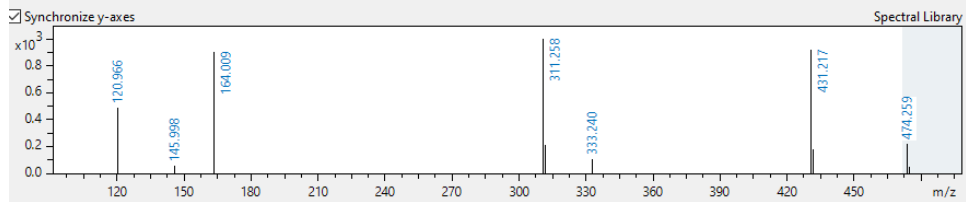
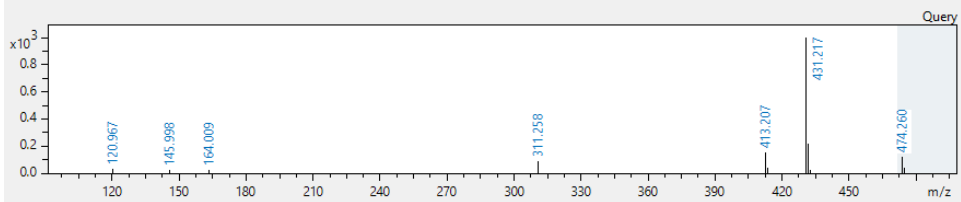
m/z meas.: 474.25940 ± 5 mDa

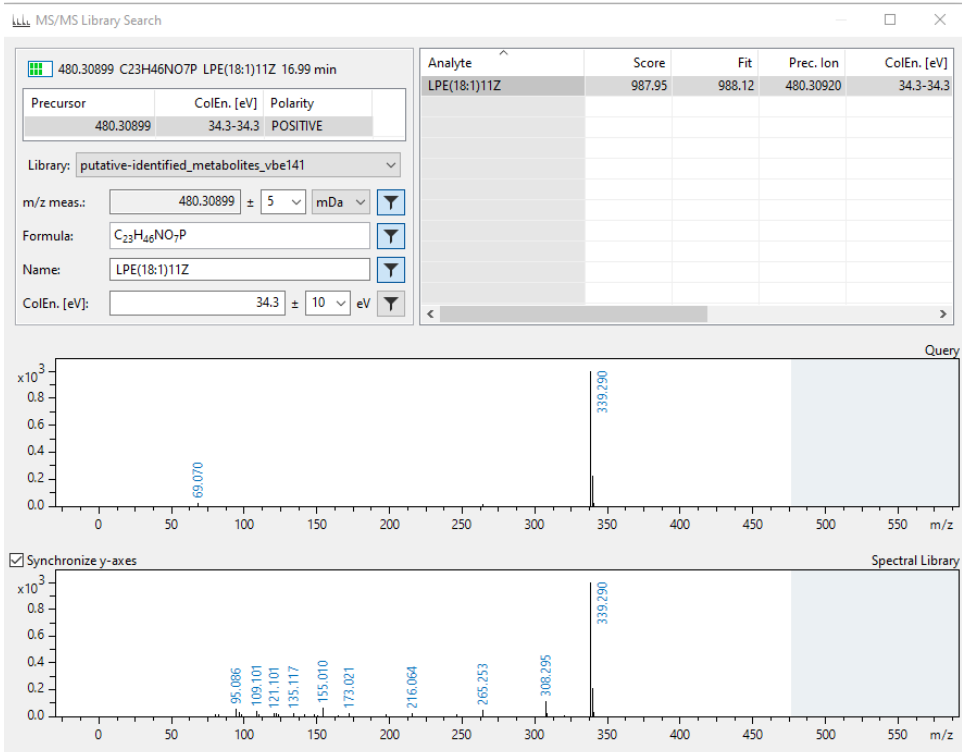
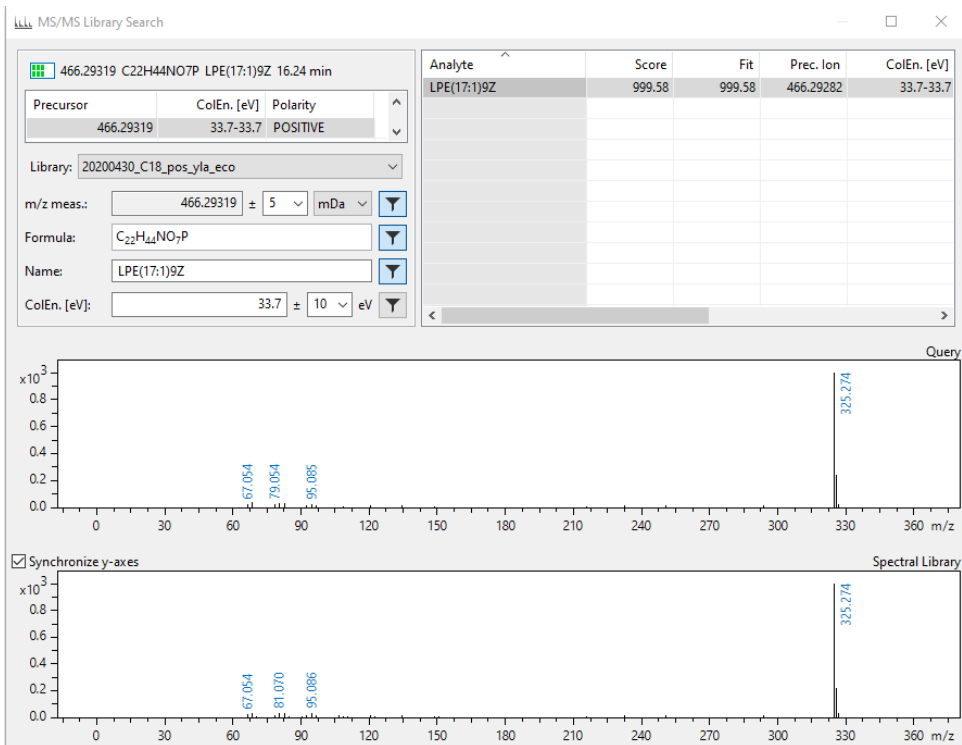
Formula: C₂₁H₄₂NO₇P

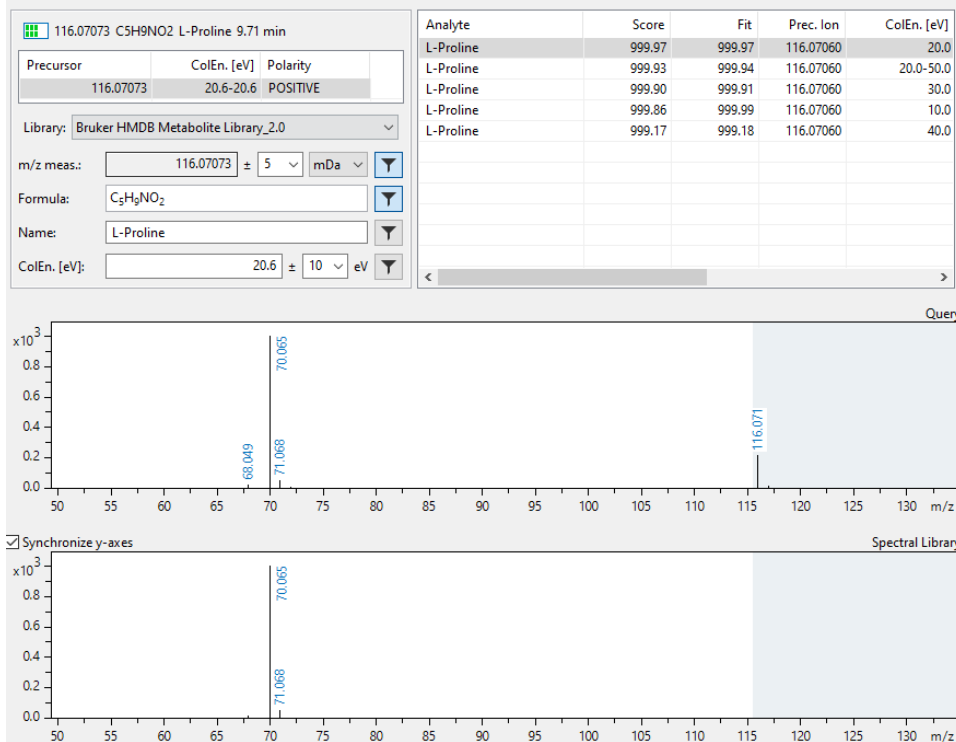
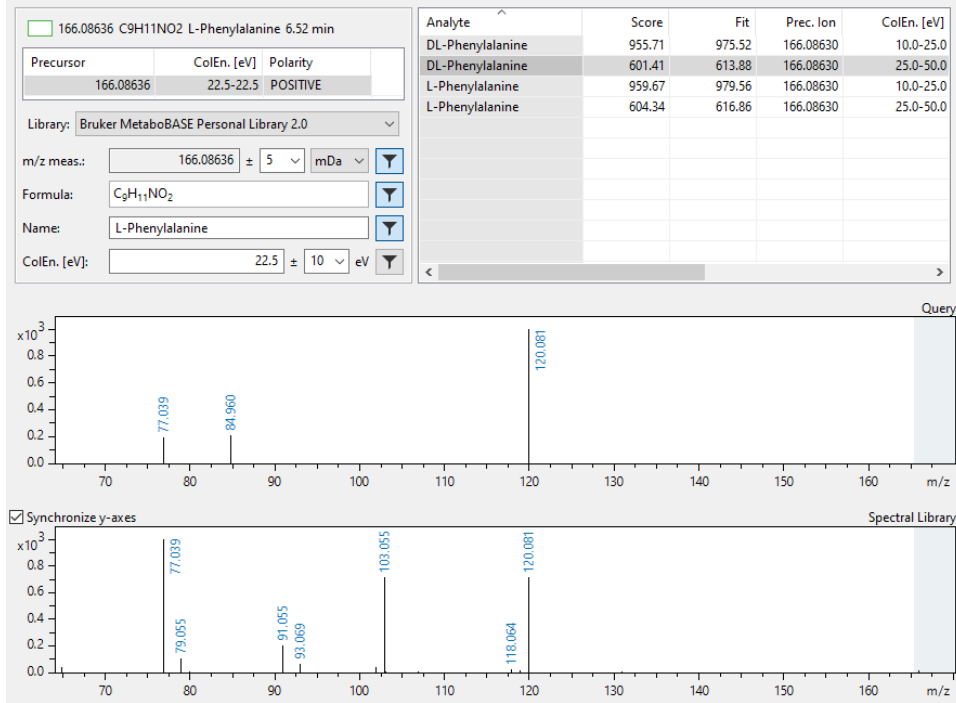
Name: LPE(16:1)

ColEn. [eV]: 34.0 ± 10 eV

Analyte	Score	Fit	Prec. Ion	ColEn. [eV]
LPE(16:1)	595.41	602.25	474.25911	34.0-34.0







118.08620 C5H11NO2 L-Valine 1.28 min

Precursor	ColEn. [eV]	Polarity
118.08620	20.7-20.7	POSITIVE

Library: 20200430_C18_pos_yla_eco

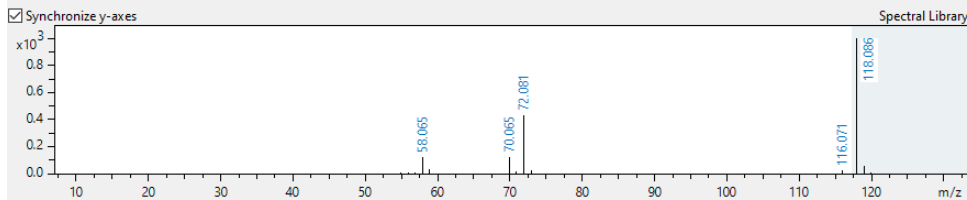
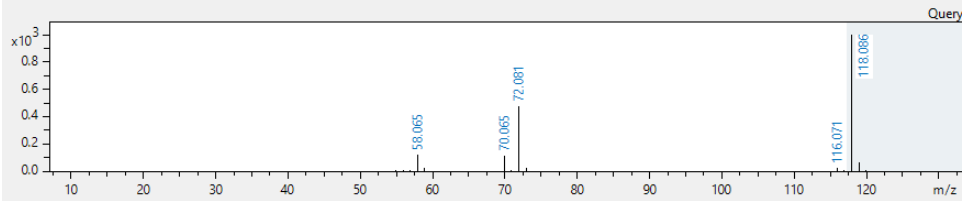
m/z meas.: 118.08620 ± 5 mDa

Formula: C₅H₁₁NO₂

Name: L-Valine

ColEn. [eV]: 20.7 ± 10 eV

Analyte	Score	Fit	Prec. Ion	ColEn. [eV]
L-Valine	882.99	930.89	118.08626	20.7-20.7



276.15634 C11H21N3O5 Lys Glu 14.79 min

Precursor	ColEn. [eV]	Polarity
276.15634	26.6-26.7	POSITIVE

Library: Bruker MetaboBASE Personal Library 2.0

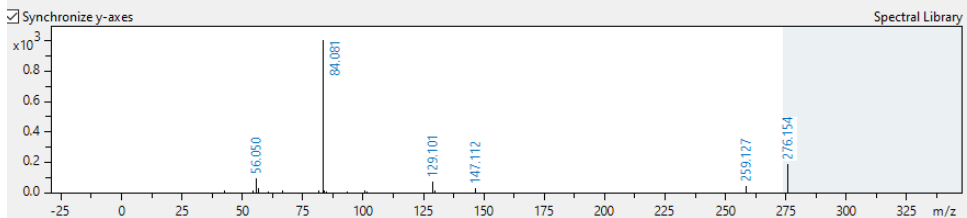
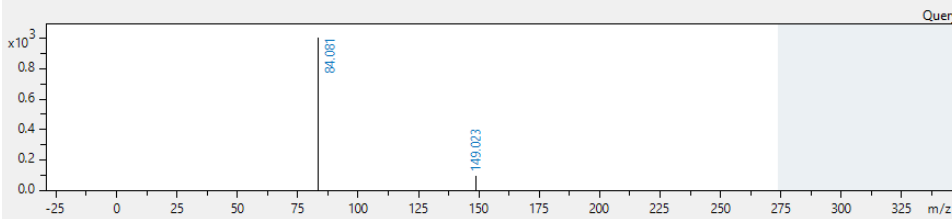
m/z meas.: 276.15634 ± 5 mDa

Formula: C₁₁H₂₁N₃O₅

Name: Lys Glu

ColEn. [eV]: 26.6 ± 10 eV

Analyte	Score	Fit	Prec. Ion	ColEn. [eV]
Lys Glu	986.94	991.20	276.15540	25.0-50.0
Lys Glu	938.94	942.99	276.15540	10.0-25.0
E-(gamma-Glutamyl)-lysir	920.62	920.62	276.15540	25.0-50.0
Glu Lys	834.84	838.44	276.15540	25.0-50.0
E-(gamma-Glutamyl)-lysir	553.29	555.68	276.15540	10.0-25.0
Glu Lys	500.95	503.11	276.15540	10.0-25.0
Gly Val Thr	7.30	7.33	276.15540	25.0-50.0



260.19709 C₁₂H₂₅N₃O₃ Lys Ile 12.86 min

Precursor	ColEn. [eV]	Polarity
260.19709	26.0-26.0	POSITIVE

Library: Bruker MetaboBASE Personal Library 2.0

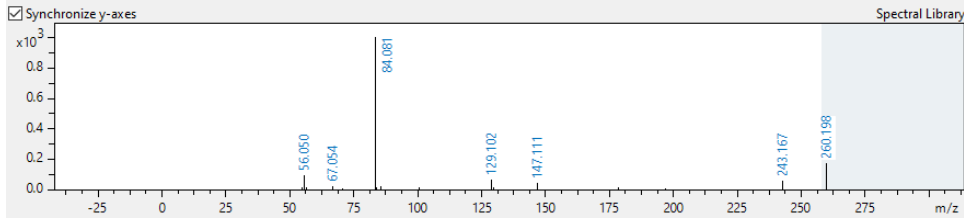
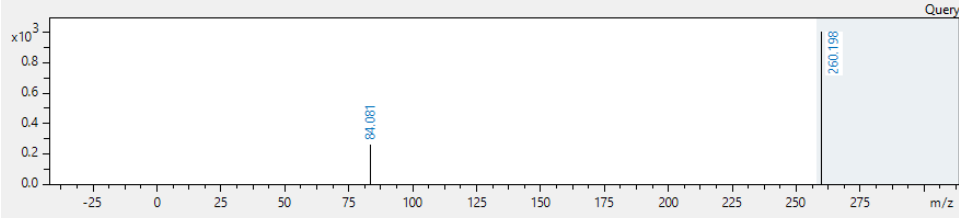
m/z meas.: 260.19709 ± 5 mDa

Formula: C₁₂H₂₅N₃O₃

Name: Lys Ile

ColEn. [eV]: 26.0 ± 10 eV

Analyte	Score	Fit	Prec. Ion	ColEn. [eV]
Lys Ile	991.54	991.54	260.19690	25.0-50.0
Lys Leu	990.09	990.09	260.19690	25.0-50.0
Lys Leu	948.13	948.13	260.19690	10.0-25.0
Lys Ile	927.50	927.50	260.19690	10.0-25.0
Leu Lys	810.66	810.66	260.19690	25.0-50.0
Ile Lys	742.88	742.88	260.19690	25.0-50.0
Leu Lys	445.84	445.84	260.19690	10.0-25.0
Ile Lys	435.86	435.86	260.19690	10.0-25.0



246.18114 C₁₁H₂₃N₃O₃ Lys Val 1.29 min

Precursor	ColEn. [eV]	Polarity
246.18114	25.4-25.4	POSITIVE

Library: 20200430_C18_pos_yla_eco

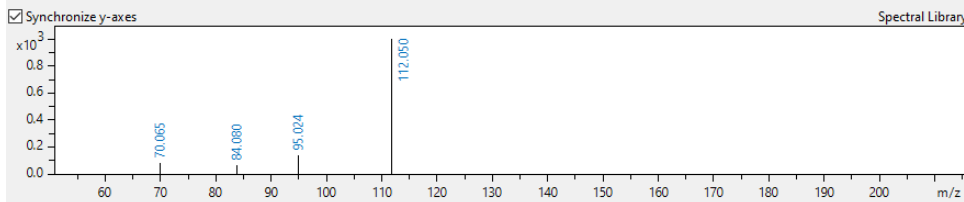
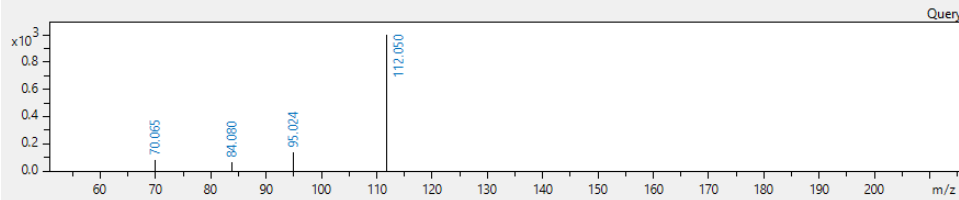
m/z meas.: 246.18114 ± 5 mDa

Formula: C₁₁H₂₃N₃O₃

Name: Lys Val

ColEn. [eV]: 25.4 ± 10 eV

Analyte	Score	Fit	Prec. Ion	ColEn. [eV]
Lys Val	1000.00	1000.00	246.18122	25.4-25.4



166.05321 C5H11NO3S Methionine sulfoxide 1.24 min

Precursor	ColEn. [eV]	Polarity
166.05321	22.5-22.5	POSITIVE

Library: Bruker HMDB Metabolite Library_2.0

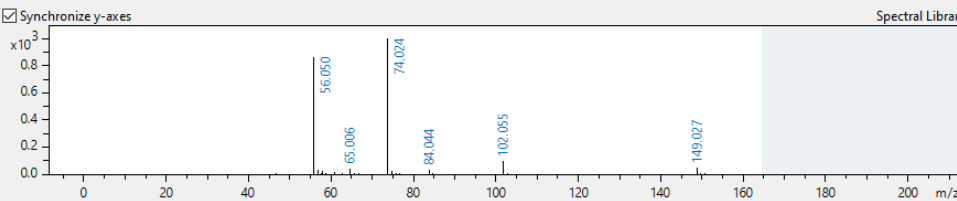
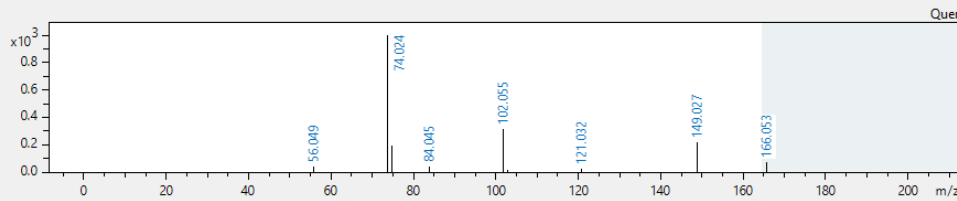
m/z meas.: 166.05321 ± 5 mDa

Formula: C₅H₁₁NO₃S

Name: Methionine sulfoxide

ColEn. [eV]: 22.5 ± 10 eV

Analyte	Score	Fit	Prec. Ion	ColEn. [eV]
Methionine sulfoxide	901.72	940.44	166.05324	10.0
Methionine sulfoxide	725.31	756.45	166.05324	20.0
Methionine sulfoxide	633.50	660.70	166.05324	20.0-50.0
Methionine sulfoxide	388.52	405.20	166.05324	30.0
Methionine sulfoxide	171.58	182.77	166.05324	40.0



188.17589 C9H21N3O N1-Acetylspermidine 12.51 min

Precursor	ColEn. [eV]	Polarity
188.17589	23.2-23.3	POSITIVE

Library: Bruker MetaboBASE Personal Library 2.0

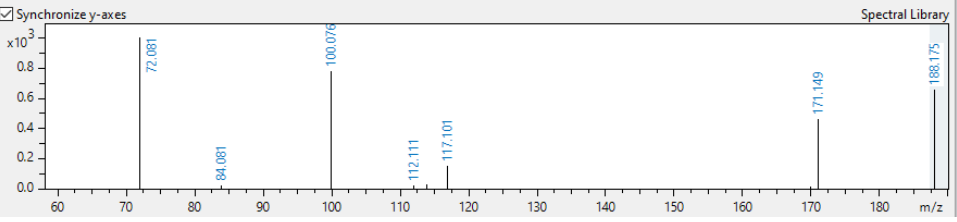
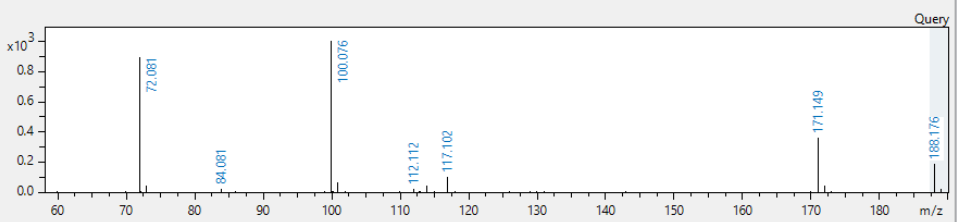
m/z meas.: 188.17589 ± 5 mDa

Formula: C₉H₂₁N₃O

Name: N1-Acetylspermidine

ColEn. [eV]: 23.2 ± 10 eV

Analyte	Score	Fit	Prec. Ion	ColEn. [eV]
N1-Acetylspermidine	978.67	980.44	188.17580	10.0-25.0
N1-Acetylspermidine	878.77	880.36	188.17580	25.0-50.0
N8-Acetylspermidine	361.58	363.22	188.17580	10.0-25.0
N8-Acetylspermidine	356.32	515.00	188.17580	25.0-50.0



275.13479 C10H18N4O5 N2-Succinyl-L-arginine 1.30 min

Precursor	ColEn. [eV]	Polarity
275.13479	26.6-26.6	POSITIVE

Library: 20200430_C18_pos_yla_eco

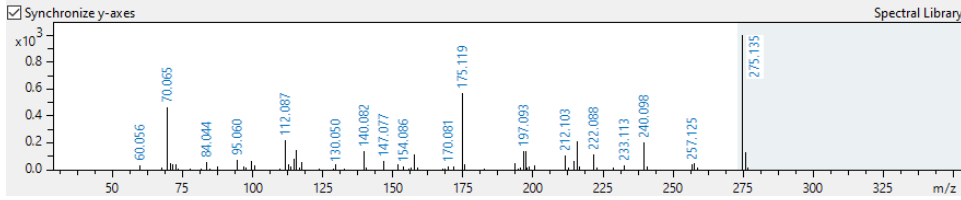
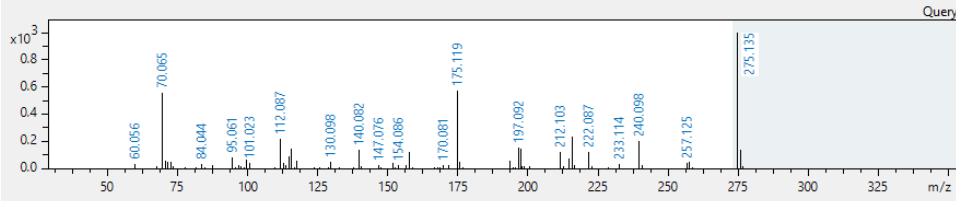
m/z meas.: 275.13479 ± 5 mDa

Formula: C₁₀H₁₈N₄O₅

Name: N2-Succinyl-L-arginine

ColEn. [eV]: 26.6 ± 10 eV

Analyte	Score	Fit	Prec. Ion	ColEn. [eV]
N2-Succinyl-L-arginine	994.36	994.51	275.13500	26.6-26.6



188.17591 C9H21N3O N8-Acetylsermidine 9.33 min

Precursor	ColEn. [eV]	Polarity
188.17591	23.3-23.3	POSITIVE

Library: Bruker MetaboBASE Personal Library 2.0

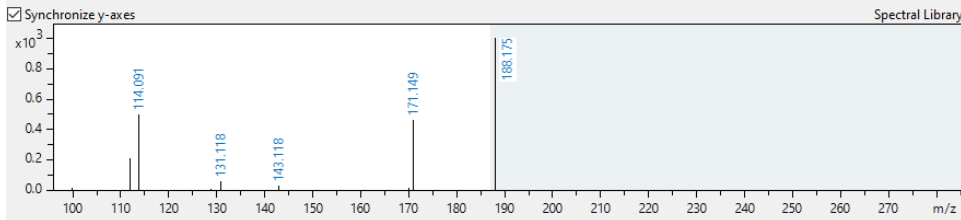
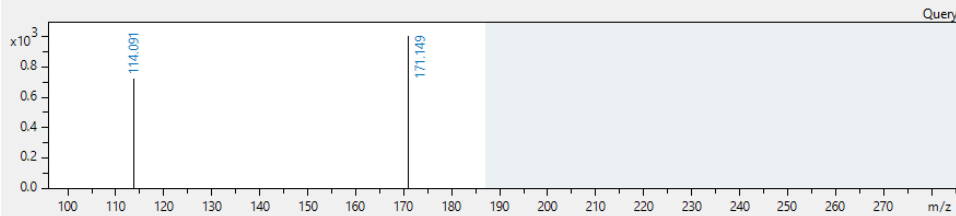
m/z meas.: 188.17591 ± 5 mDa

Formula: C₉H₂₁N₃O

Name: N8-Acetylsermidine

ColEn. [eV]: 23.3 ± 10 eV

Analyte	Score	Fit	Prec. Ion	ColEn. [eV]
N8-Acetylsermidine	704.13	704.13	188.17580	10.0-25.0
N8-Acetylsermidine	295.78	295.78	188.17580	25.0-50.0
N1-Acetylsermidine	284.79	284.79	188.17580	10.0-25.0
N1-Acetylsermidine	94.32	94.32	188.17580	25.0-50.0



145.13372 C7H16N2O N-Acetylcadaverine 6.68 min

Precursor	ColEn. [eV]	Polarity
145.13372	21.7-21.7	POSITIVE

Library: 20200430_C18_pos_yla_eco

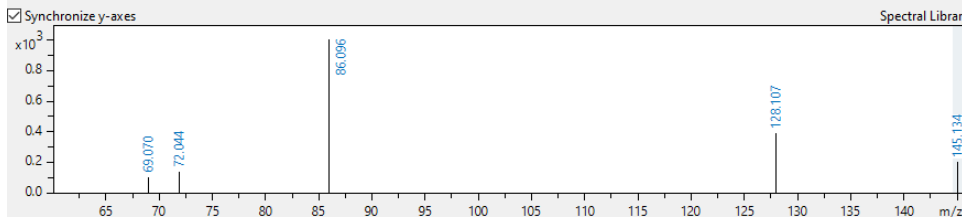
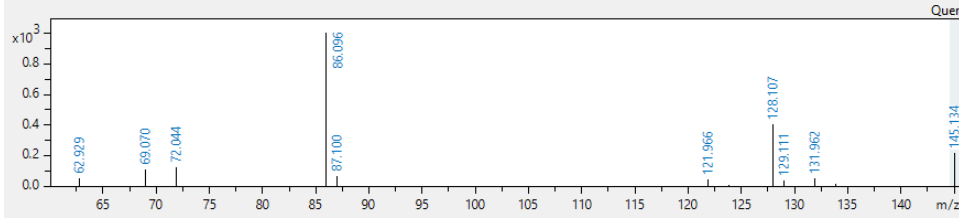
m/z meas.: 145.13372 ± 5 mDa

Formula: C₇H₁₆N₂O

Name: N-Acetylcadaverine

ColEn. [eV]: 21.7 ± 10 eV

Analyte	Score	Fit	Prec. Ion	ColEn. [eV]
N-Acetylcadaverine	995.17	999.79	145.13354	21.7-21.7



222.09732 C8H15NO6 N-Acetyl-D-glucosamine 9.49 min

Precursor	ColEn. [eV]	Polarity
222.09732	24.6-24.6	POSITIVE

Library: Bruker MetaboBASE Personal Library 2.0

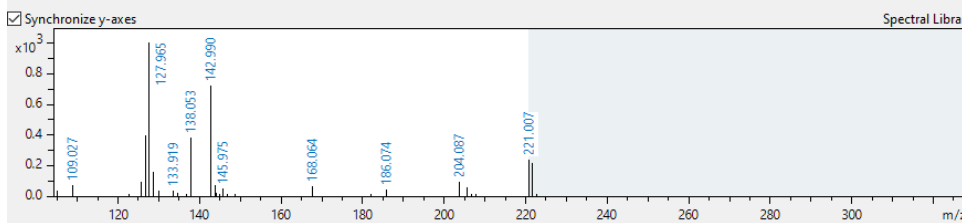
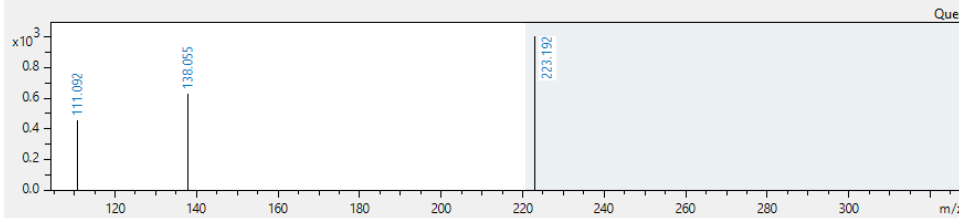
m/z meas.: 222.09732 ± 5 mDa

Formula: C₈H₁₅NO₆

Name: N-Acetyl-D-glucosamine

ColEn. [eV]: 24.6 ± 10 eV

Analyte	Score	Fit	Prec. Ion	ColEn. [eV]
N-Acetyl-D-glucosamine	696.44	858.21	222.09720	10.0-25.0
N-Acetyl-β-D-mannosami	406.77	501.26	222.09770	10.0-25.0
N-Acetyl-D-glucosamine	229.56	282.88	222.09720	25.0-50.0
N-Acetyl-β-D-mannosami	208.43	256.85	222.09770	25.0-50.0



214.05096 C7H13NO3S N-Acetyl-L-methionine 5.84 min

Precursor: 192.06890 ColEn. [eV]: 23.5-23.5 Polarity: POSITIVE

Library: 2019-06-06 CBio-Standards

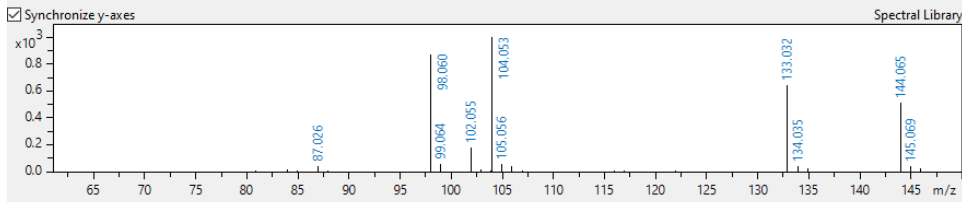
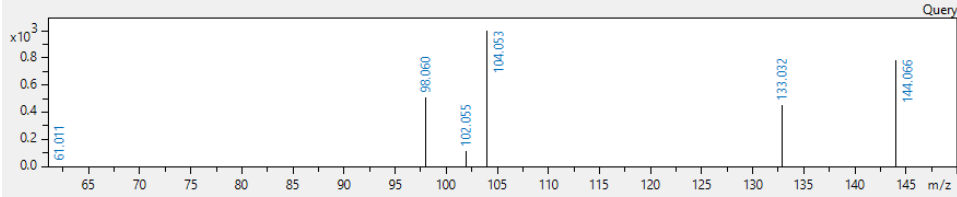
m/z meas.: 192.06890 ± 5 mDa

Formula: C₇H₁₃NO₃S

Name: N-Acetyl-L-methionine

ColEn. [eV]: 23.5 ± 10 eV

Analyte	Score	Fit	Prec. Ion	ColEn. [eV]
N-Acetyl-DL-methionine	919.40	938.49	192.06860	23.5-23.5



332.56248 C₂₁H₂₇N₇O₁₄P₂ NAD 1.82 min

Precursor: 332.56248 ColEn. [eV]: 24.6-24.6 Polarity: POSITIVE

Library: 20200430_C18_pos_yla_eco

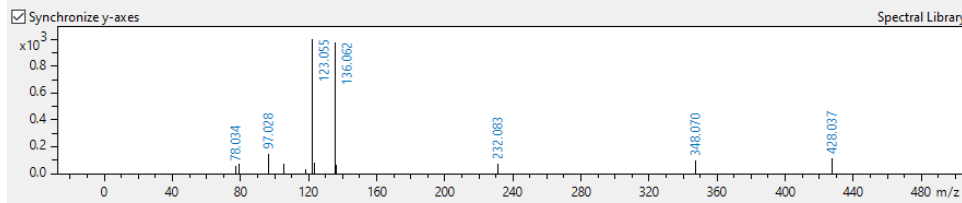
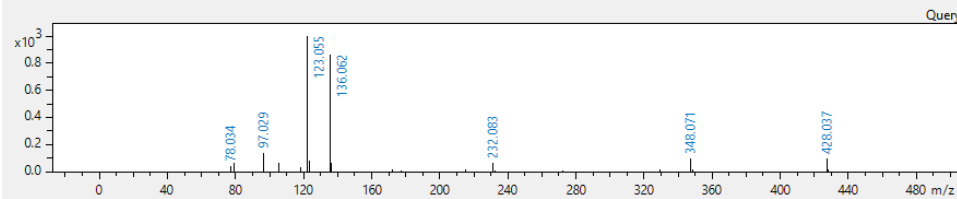
m/z meas.: 332.56248 ± 5 mDa

Formula: C₂₁H₂₇N₇O₁₄P₂

Name: NAD

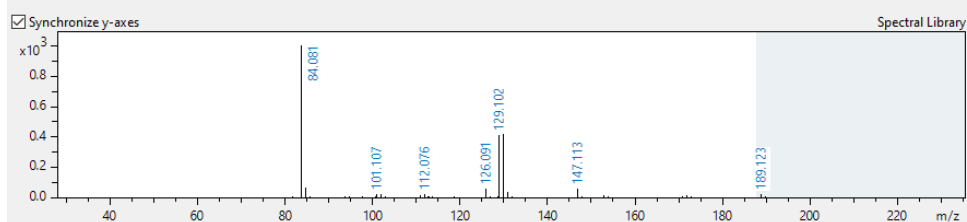
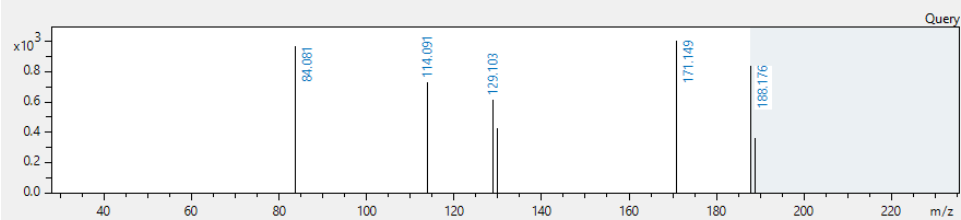
ColEn. [eV]: 24.6 ± 10 eV

Analyte	Score	Fit	Prec. Ion	ColEn. [eV]
NAD	997.83	998.04	332.56184	24.6-24.6



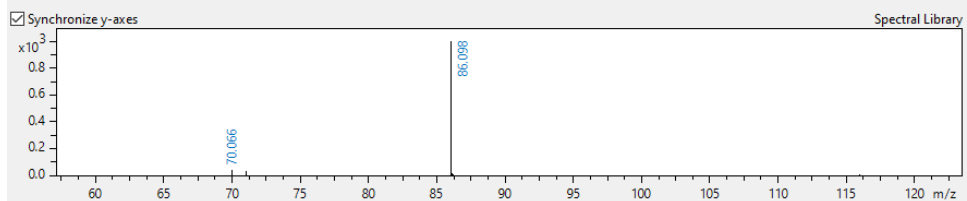
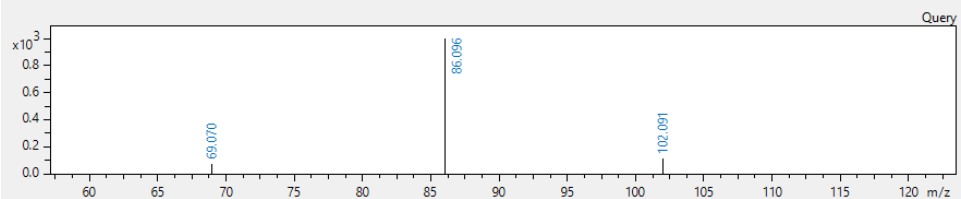
Analyte	Score	Fit	Prec. Ion	ColEn. [eV]
NALPHA-acetyl-L-LYSine	620.63	981.75	189.12340	23.3-23.3

Precursor: 189.12363 ColEn. [eV]: 23.3-23.3 Polarity: POSITIVE
 Library: 2019-06-06 CBio-Standards
 m/z meas.: 189.12363 ± 5 mDa
 Formula: C₈H₁₆N₂O₃
 Name: N-Alpha-acetyllysine
 ColEn. [eV]: 23.3 ± 10 eV



Analyte	Score	Fit	Prec. Ion	ColEn. [eV]
NH-DVal(NMe)-Val-OMe	988.70	996.61	245.18600	10.0-25.0
Ile Ile	986.24	992.01	245.18600	10.0-25.0
Ile Leu	982.89	988.64	245.18600	10.0-25.0
Leu Ile	973.02	978.71	245.18600	10.0-25.0
Leu Leu	969.51	977.27	245.18600	10.0-25.0
NH-DVal(NMe)-Val-OMe	968.79	976.54	245.18600	25.0-50.0
Ile Ile	885.39	890.57	245.18600	25.0-50.0
Ile Leu	849.39	854.35	245.18600	25.0-50.0
Leu Ile	763.01	767.47	245.18600	25.0-50.0
Leu Leu	725.89	730.14	245.18600	25.0-50.0

Precursor: 245.18604 ColEn. [eV]: 25.4-25.4 Polarity: POSITIVE
 Library: Bruker MetaboBASE Personal Library 2.0
 m/z meas.: 245.18604 ± 5 mDa
 Formula: C₁₂H₂₄N₂O₃
 Name: NH-DVal(NMe)-Val-OMe
 ColEn. [eV]: 25.4 ± 10 eV



123.05532 C6H6N2O z_Niacinamide 1.77 min

Precursor	ColEn. [eV]	Polarity
123.05532	20.9-20.9	POSITIVE

Library: 2019-06-06 CBio-Standards

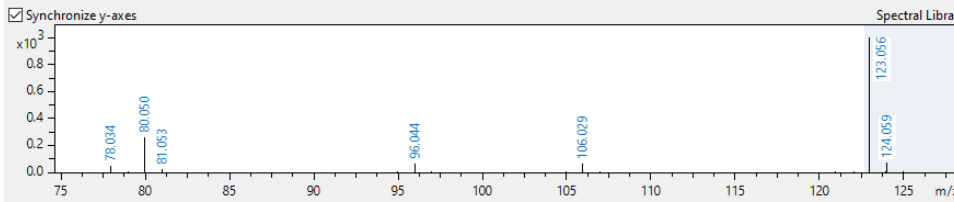
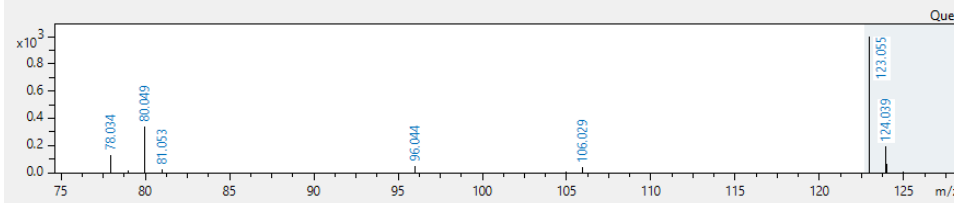
m/z meas.: 123.05532 ± 5 mDa

Formula: C₆H₆N₂O

Name: z_Niacinamide

ColEn. [eV]: 20.9 ± 10 eV

Analyte	Score	Fit	Prec. Ion	ColEn. [eV]
NicOTINamide	970.02	970.02	123.05500	20.9



124.03922 C6H5NO2 NicOTINate 1.30 min

Precursor	ColEn. [eV]	Polarity
124.03922	20.9-20.9	POSITIVE

Library: 2019-06-06 CBio-Standards

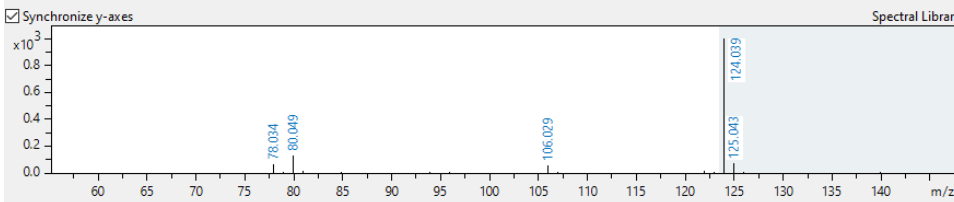
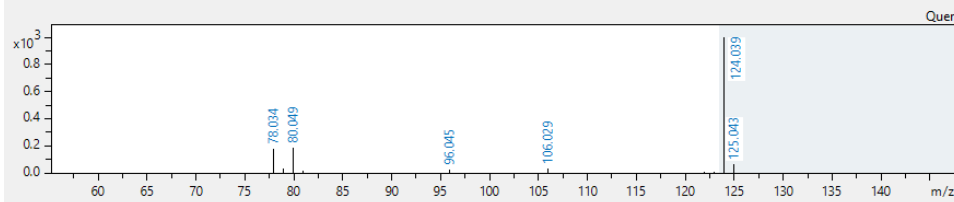
m/z meas.: 124.03922 ± 5 mDa

Formula: C₆H₅NO₂

Name: NicOTINate

ColEn. [eV]: 20.9 ± 10 eV

Analyte	Score	Fit	Prec. Ion	ColEn. [eV]
NicOTINate	916.76	917.13	124.03930	20.9
Picolinic acid	606.69	864.76	124.03910	20.9-20.9



162.07606 C6H11NO4 N-Methyl-L-glutamate 1.27 min

Precursor	ColEn. [eV]	Polarity
162.07606	22.3-22.3	POSITIVE

Library: 2019-06-06 CBio-Standards

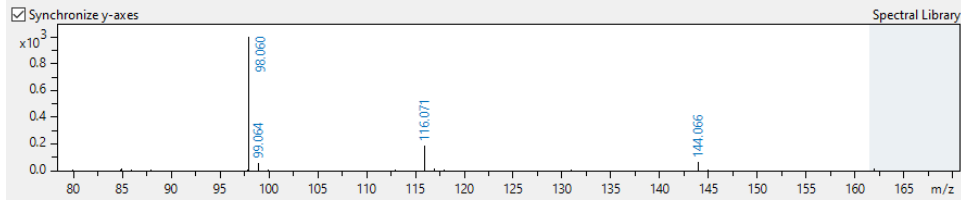
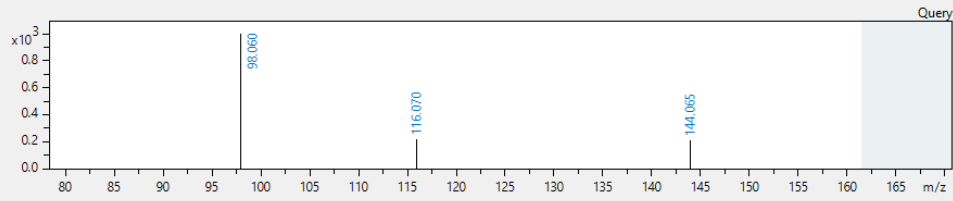
m/z meas.: 162.07606 ± 5 mDa

Formula: C₆H₁₁NO₄

Name: N-Methyl-L-glutamate

ColEn. [eV]: 22.3 ± 10 eV

Analyte	Score	Fit	Prec. Ion	ColEn. [eV]
N-Methyl-L-glutamate	988.33	988.33	162.07590	22.3-22.3
ALPHA-aminOADIPate	984.13	984.13	162.07540	22.3-22.3



169.07673 C11H8N2 Norharman 2.65 min

Precursor	ColEn. [eV]	Polarity
169.07673	22.6-22.6	POSITIVE

Library: Bruker MetaboBASE Personal Library 2.0

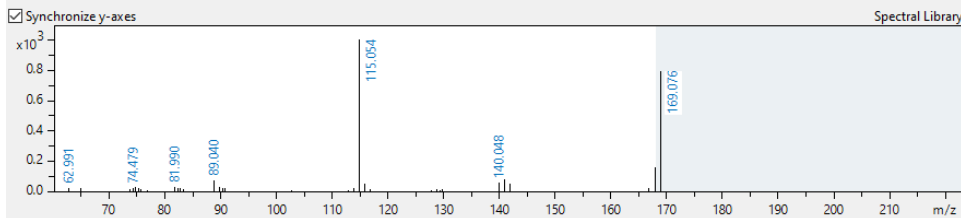
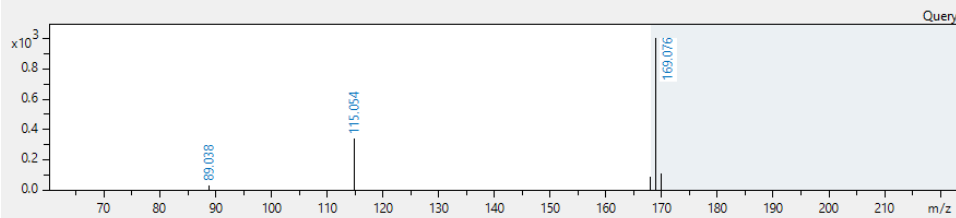
m/z meas.: 169.07673 ± 5 mDa

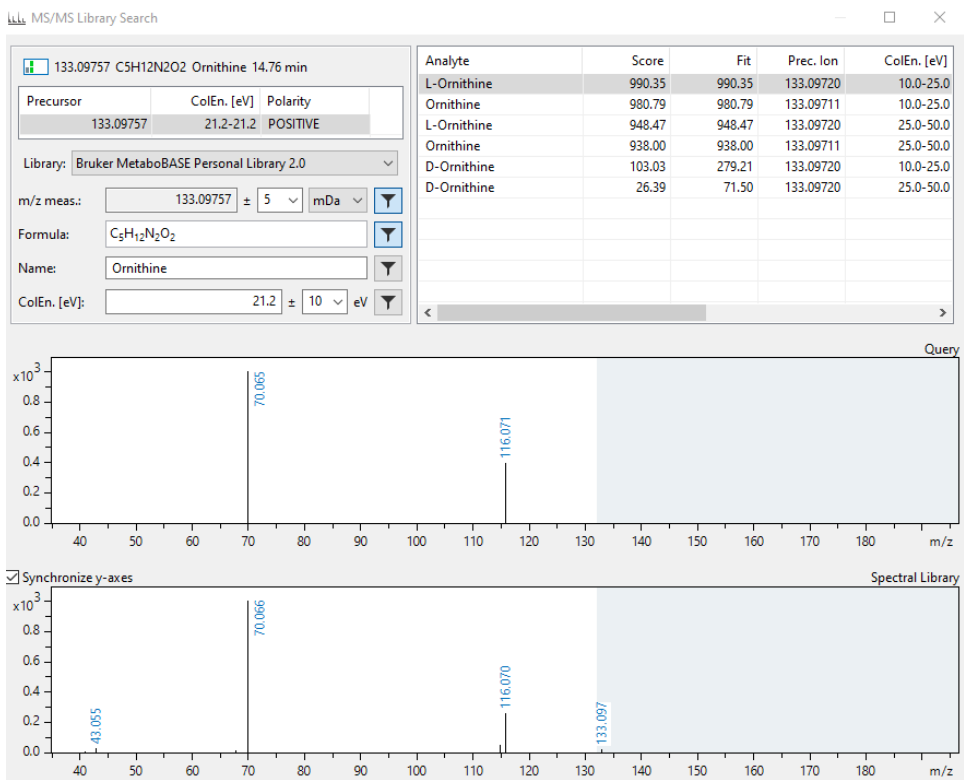
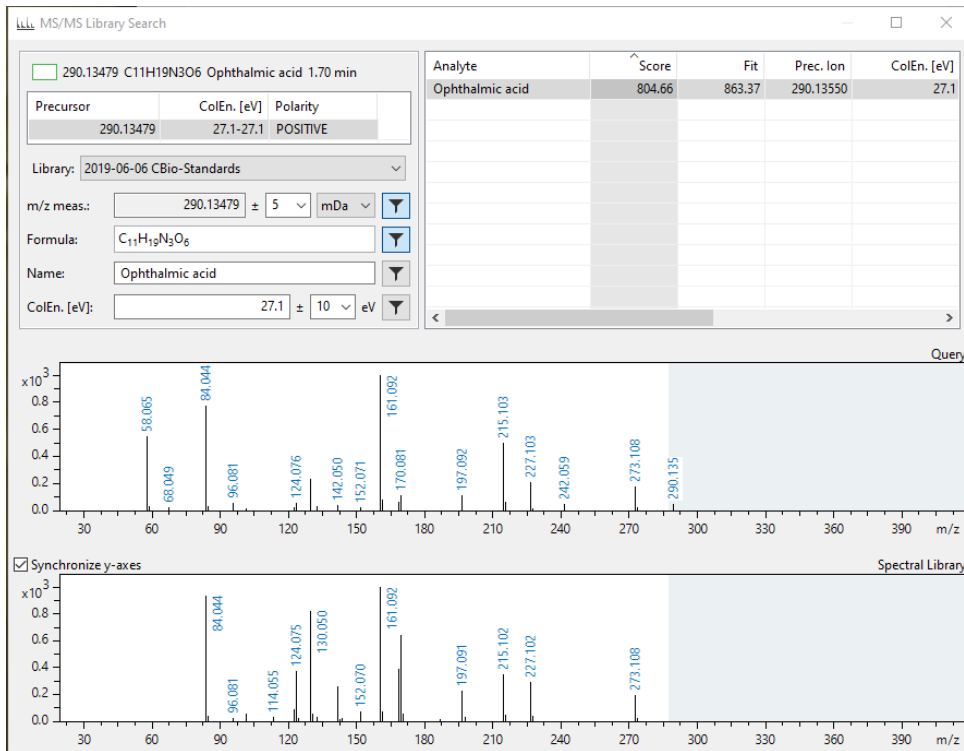
Formula: C₁₁H₈N₂

Name: Norharman

ColEn. [eV]: 22.6 ± 10 eV

Analyte	Score	Fit	Prec. Ion	ColEn. [eV]
Norharman	987.56	987.56	169.07651	25.0-50.0
Norharman	925.30	925.30	169.07651	10.0-25.0





220.11818 C₉H₁₇NO₅ Pantothenic acid 4.86 min

Precursor	ColEn. [eV]	Polarity
220.11818	24.5-24.5	POSITIVE

Library: Bruker MetaboBASE Personal Library 2.0

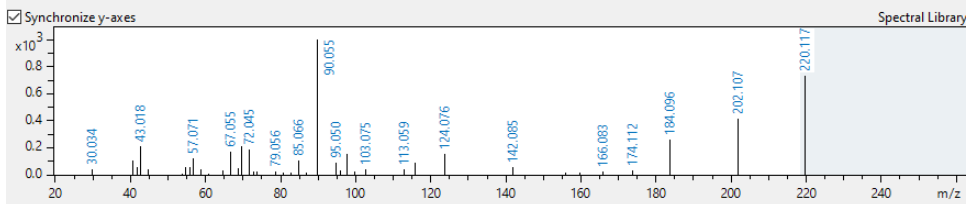
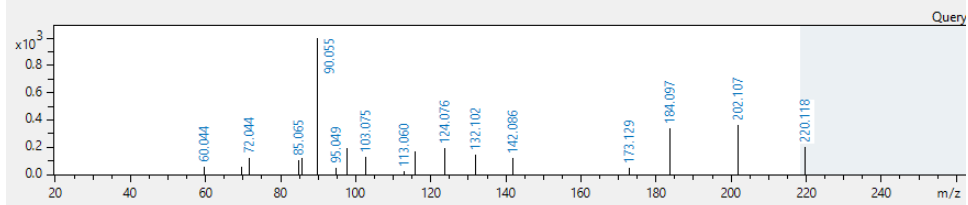
m/z meas.: 220.11818 ± 5 mDa

Formula: C₉H₁₇NO₅

Name: Pantothenic acid

ColEn. [eV]: 24.5 ± 10 eV

Analyte	Score	Fit	Prec. Ion	ColEn. [eV]
Pantothenic acid	901.45	926.29	220.11790	10.0-25.0
Pantothenic acid	424.42	433.92	220.11790	25.0-50.0



732.55008 C₄₀H₇₈ON₁O₈PE(1...1Z) 3.26 min

Precursor	ColEn. [eV]	Polarity
732.55008	44.3-44.3	POSITIVE

Library: 20200430_C18_pos_yla_eco

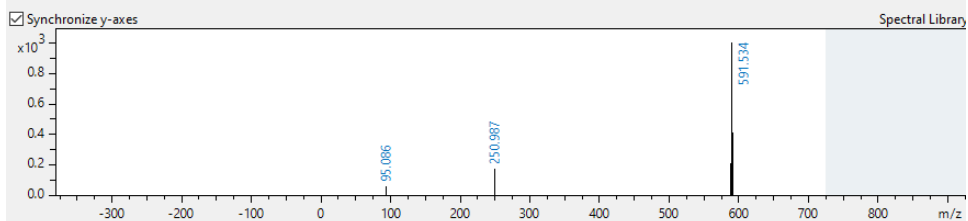
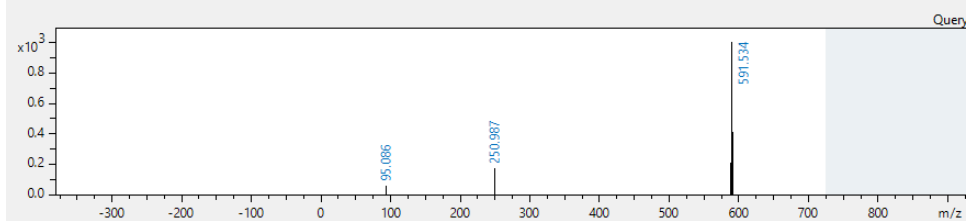
m/z meas.: 732.55008 ± 5 mDa

Formula: C₄₀H₇₈ON₁O₈PE(1...1Z)

Name: PE(13:0/22:1(11Z))

ColEn. [eV]: 44.3 ± 10 eV

Analyte	Score	Fit	Prec. Ion	ColEn. [eV]
PE(13:0/22:1(11Z))	1000.00	1000.00	732.55378	44.3-44.3



279.17042 C₁₅H₂₂N₂O₃ Phe Ile 7.88 min

Precursor	ColEn. [eV]	Polarity
279.17042	26.7-26.7	POSITIVE

Library: Bruker MetaboBASE Personal Library 2.0

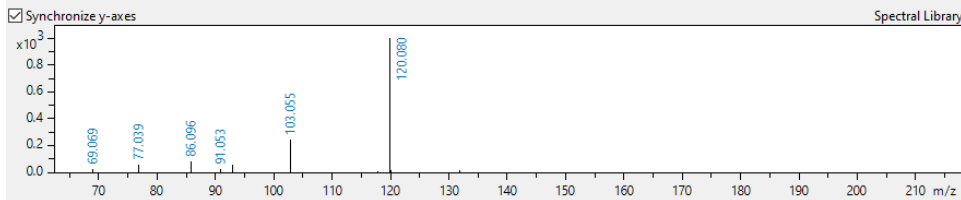
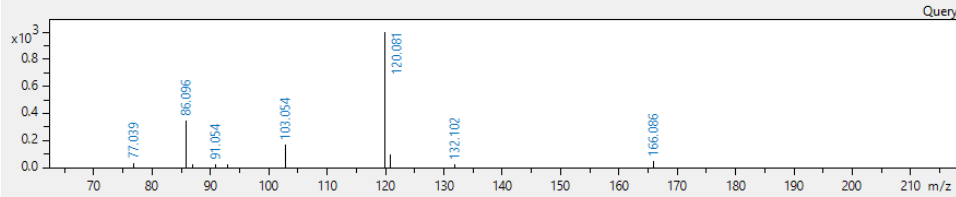
m/z meas.: 279.17042 ± 5 mDa

Formula: C₁₅H₂₂N₂O₃

Name: Phe Ile

ColEn. [eV]: 26.7 ± 10 eV

Analyte	Score	Fit	Prec. Ion	ColEn. [eV]
Phe Ile	958.46	963.21	279.17030	25.0-50.0
Phe Ile	954.78	959.50	279.17030	10.0-25.0
Phe Leu	948.82	953.52	279.17030	25.0-50.0
Phe Leu	946.45	951.14	279.17030	10.0-25.0
Leu Phe	585.87	588.34	279.17030	25.0-50.0
Leu Phe	453.00	455.23	279.17030	10.0-25.0
Ile Phe	428.61	430.42	279.17030	25.0-50.0



265.15474 C₁₄H₂₀N₂O₃ Phe Val 6.48 min

Precursor	ColEn. [eV]	Polarity
265.15474	26.2-26.2	POSITIVE

Library: Bruker MetaboBASE Personal Library 2.0

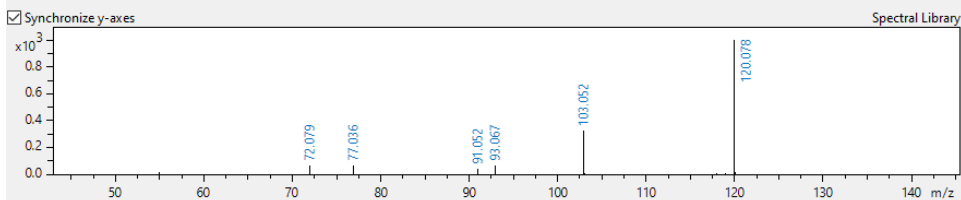
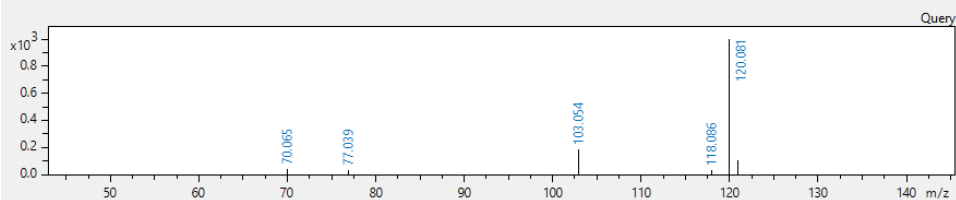
m/z meas.: 265.15474 ± 5 mDa

Formula: C₁₄H₂₀N₂O₃

Name: Phe Val

ColEn. [eV]: 26.2 ± 10 eV

Analyte	Score	Fit	Prec. Ion	ColEn. [eV]
Phe Val	987.54	993.14	265.15470	10.0-25.0
Phe Val	980.80	986.35	265.15470	25.0-50.0
Val Phe	149.87	150.78	265.15470	25.0-50.0
Val Phe	85.11	85.63	265.15470	10.0-25.0
SAHA	12.15	66.93	265.15470	25.0-50.0



168.98985 C₃H₅O₆P phosphoenol pyruvate 12.69 min

Precursor	ColEn. [eV]	Polarity
168.98985	22.6-22.6	POSITIVE

Library: Bruker MetaboBASE Personal Library 2.0

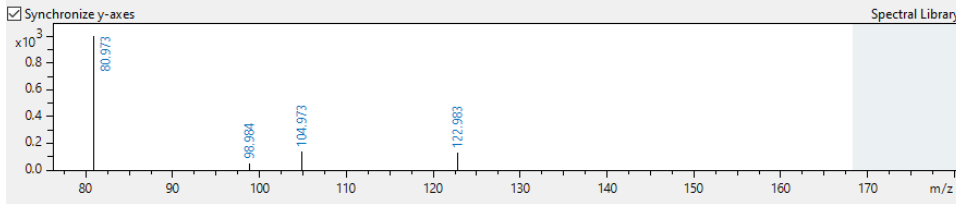
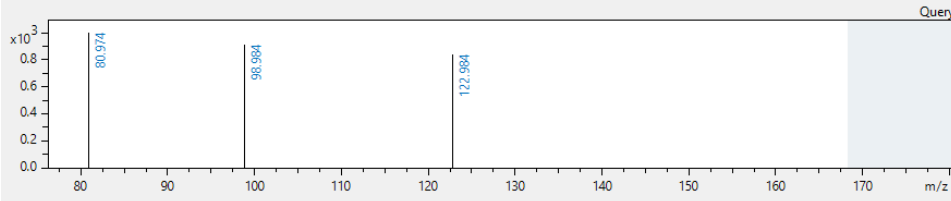
m/z meas.: 168.98985 ± 5 mDa

Formula: C₃H₅O₆P

Name: phosphoenol pyruvate

ColEn. [eV]: 22.6 ± 10 eV

Analyte	Score	Fit	Prec. Ion	ColEn. [eV]
phosphoenol pyruvate	654.91	654.91	168.98940	25.0-50.0
phosphoenol pyruvate	499.02	499.02	168.98940	10.0-25.0



130.08641 C₆H₁₁NO₂ Pipecolic acid 14.57 min

Precursor	ColEn. [eV]	Polarity
130.08641	21.1-21.1	POSITIVE

Library: Bruker HMDB Metabolite Library_2.0

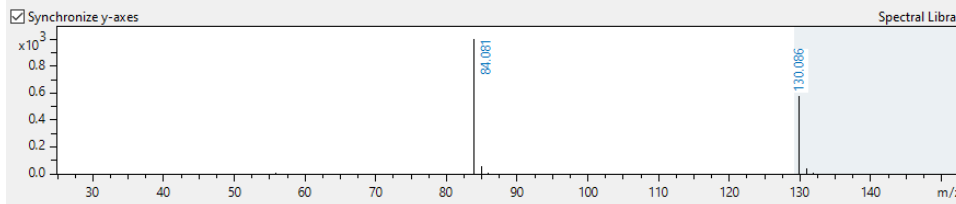
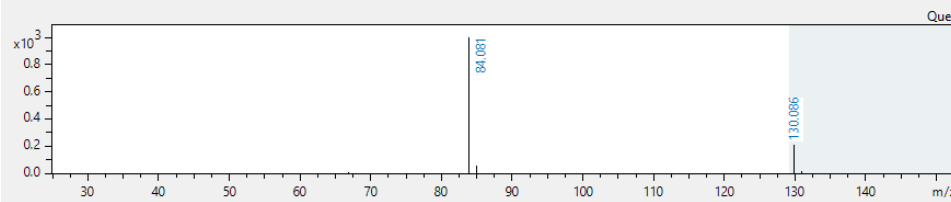
m/z meas.: 130.08641 ± 5 mDa

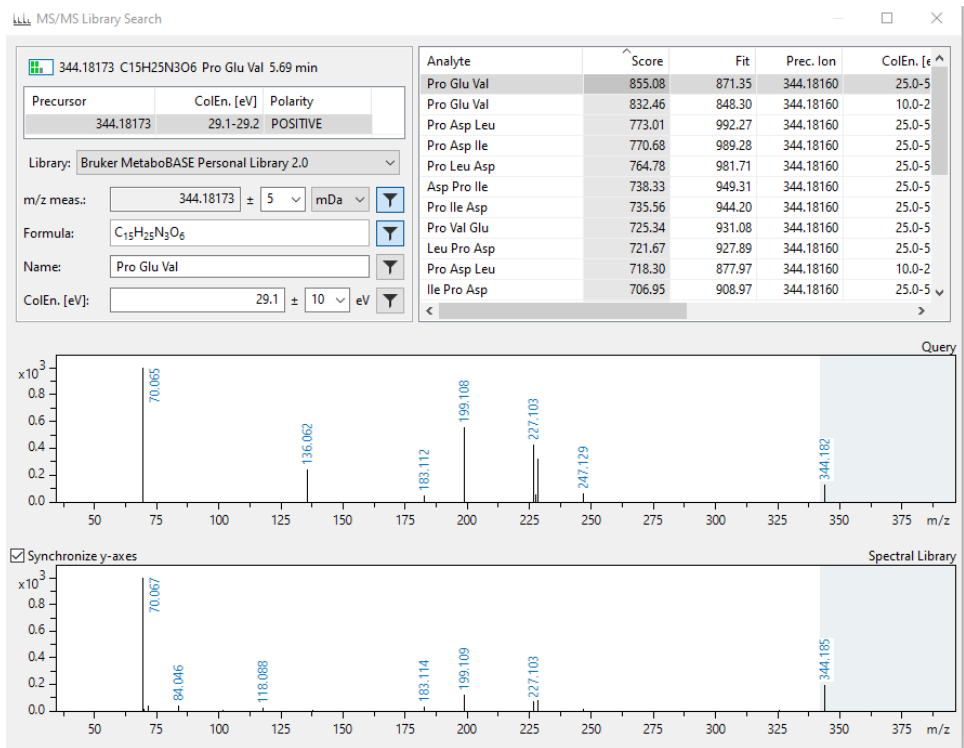
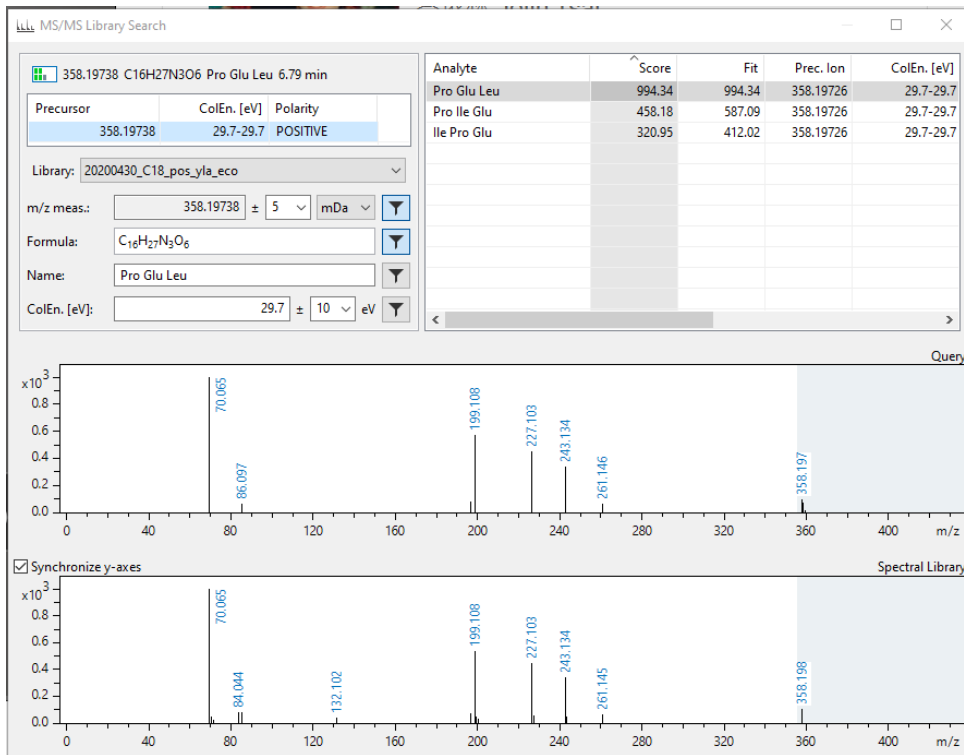
Formula: C₆H₁₁NO₂

Name: Pipecolic acid

ColEn. [eV]: 21.1 ± 10 eV

Analyte	Score	Fit	Prec. Ion	ColEn. [eV]
L-Pipecolic acid	634.39	634.39	130.08626	40.0
Pipecolic acid	999.97	999.98	130.08626	10.0
Pipecolic acid	995.24	995.24	130.08626	20.0
Pipecolic acid	961.22	961.22	130.08626	20.0-50.0
Pipecolic acid	885.96	885.96	130.08626	30.0
Pipecolic acid	493.21	493.21	130.08626	40.0





245.11348 C₁₀H₁₆N₂O₅ Pro Glu 10.89 min

Precursor	ColEn. [eV]	Polarity
245.11348	25.4-25.5	POSITIVE

Library: Bruker MetaboBASE Personal Library 2.0

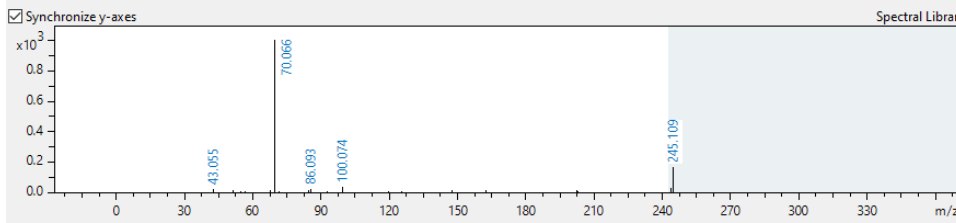
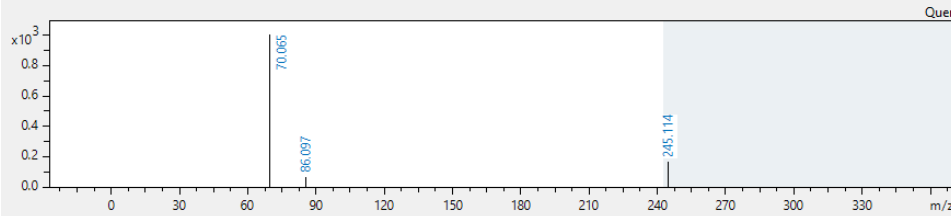
m/z meas.: 245.11348 ± 5 mDa

Formula: C₁₀H₁₆N₂O₅

Name: Pro Glu

ColEn. [eV]: 25.4 ± 10 eV

Analyte	Score	Fit	Prec. Ion	ColEn. [eV]
Pro Glu	996.37	998.39	245.11320	25.0-50.0
Pro Glu	985.61	987.61	245.11320	10.0-25.0



344.18175 C₁₅H₂₅N₃O₆ Pro Ile Asp 6.38 min

Precursor	ColEn. [eV]	Polarity
344.18175	29.2-29.2	POSITIVE

Library: Bruker MetaboBASE Personal Library 2.0

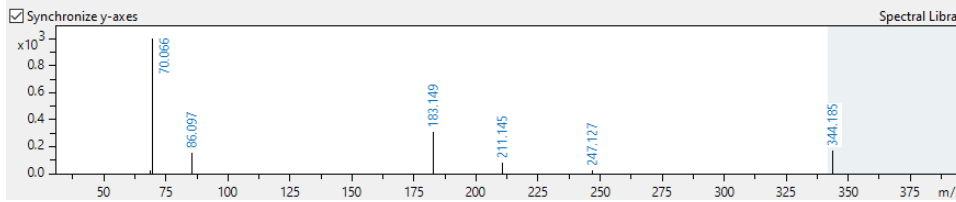
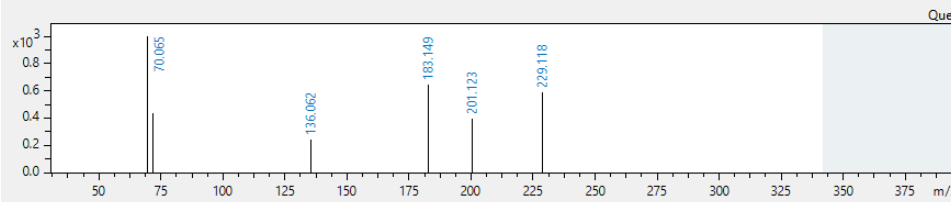
m/z meas.: 344.18175 ± 5 mDa

Formula: C₁₅H₂₅N₃O₆

Name: Pro Ile Asp

ColEn. [eV]: 29.2 ± 10 eV

Analyte	Score	Fit	Prec. Ion	ColEn. [eV]
Pro Ile Asp	767.59	948.46	344.18160	25.0-5
Pro Ile Asp	742.53	917.49	344.18160	10.0-2
Pro Leu Asp	732.73	905.39	344.18160	25.0-5
Pro Leu Asp	729.01	900.79	344.18160	10.0-2
Pro Glu Val	710.94	844.20	344.18160	25.0-5
Pro Asp Leu	676.90	924.90	344.18160	25.0-5
Pro Asp Ile	673.38	989.29	344.18160	25.0-5
Pro Glu Val	667.26	792.33	344.18160	10.0-2
Pro Val Glu	665.81	898.37	344.18160	25.0-5
Val Pro Glu	653.92	882.34	344.18160	25.0-5
Asp Pro Ile	648.73	801.59	344.18160	25.0-5



342.23889 C17H31N3O4 Pro Ile Ile 7.97 min

Precursor	ColEn. [eV]	Polarity
342.23889	29.1-29.2	POSITIVE

Library: Bruker MetaboBASE Personal Library 2.0

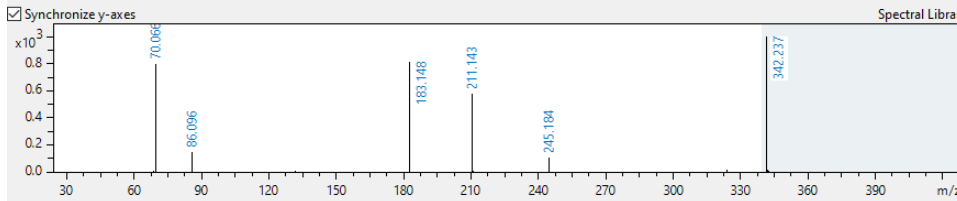
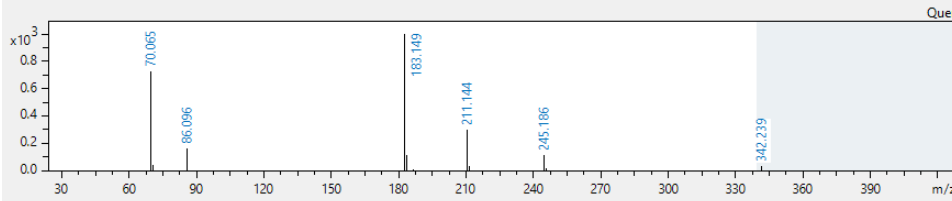
m/z meas.: 342.23889 ± 5 mDa

Formula: C₁₇H₃₁N₃O₄

Name: Pro Ile Ile

ColEn. [eV]: 29.1 ± 10 eV

Analyte	Score	Fit	Prec. Ion	ColEn. [eV]
Pro Ile Ile	952.57	959.96	342.23880	10.0-2
Pro Leu Leu	930.23	934.29	342.23880	10.0-2
Pro Leu Ile	862.70	862.75	342.23880	10.0-2
Pro Ile Ile	828.28	834.70	342.23880	25.0-5
Pro Leu Leu	777.95	781.34	342.23880	25.0-5
Pro Leu Ile	762.01	786.19	342.23880	25.0-5
Leu Pro Ile	576.18	580.65	342.23880	25.0-5
Leu Pro Leu	572.25	576.69	342.23880	25.0-5
Ile Pro Ile	552.21	556.50	342.23880	25.0-5
Leu Pro Ile	442.27	445.70	342.23880	10.0-2
Leu Pro Leu	419.31	422.57	342.23880	10.0-2



328.22313 C16H29N3O4 Pro Ile Val 7.11 min

Precursor	ColEn. [eV]	Polarity
328.22313	28.6-28.6	POSITIVE

Library: Bruker MetaboBASE Personal Library 2.0

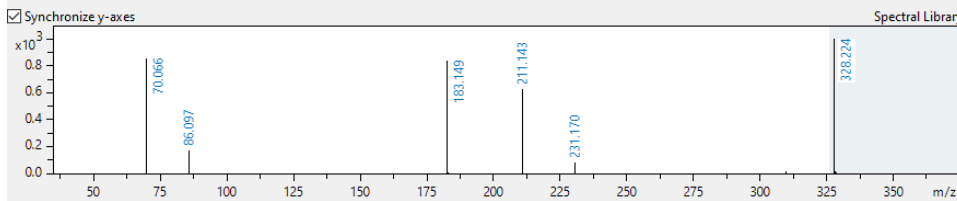
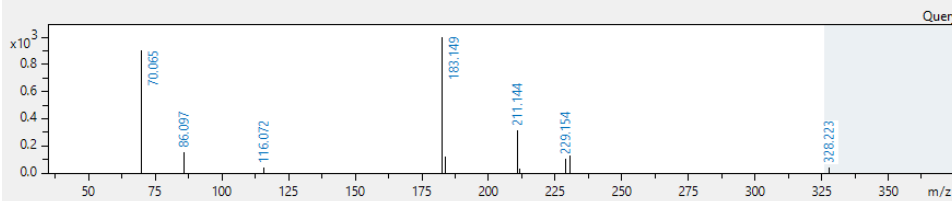
m/z meas.: 328.22313 ± 5 mDa

Formula: C₁₆H₂₉N₃O₄

Name: Pro Ile Val

ColEn. [eV]: 28.6 ± 10 eV

Analyte	Score	Fit	Prec. Ion	ColEn. [eV]
Pro Ile Val	960.74	967.08	328.22310	10.0-2
Pro Ile Val	862.53	868.22	328.22310	25.0-5
Pro Leu Val	831.23	836.71	328.22310	10.0-2
Pro Leu Val	742.96	747.86	328.22310	25.0-5
Ile Pro Val	613.58	619.97	328.22310	25.0-5
Val Pro Ile	612.27	635.04	328.22310	25.0-5
Pro Val Leu	608.16	924.35	328.22310	25.0-5
Pro Val Ile	607.28	923.02	328.22310	25.0-5
Val Pro Leu	577.98	898.79	328.22310	25.0-5
DIPROTIN B	577.88	885.97	328.22310	25.0-5
Pro Val Leu	458.73	697.23	328.22310	10.0-2



229.15484 C₁₁H₂₀N₂O₃ Pro Ile 4.25 min

Precursor	ColEn. [eV]	Polarity
229.15484	24.8-24.8	POSITIVE

Library: Bruker MetaboBASE Personal Library 2.0

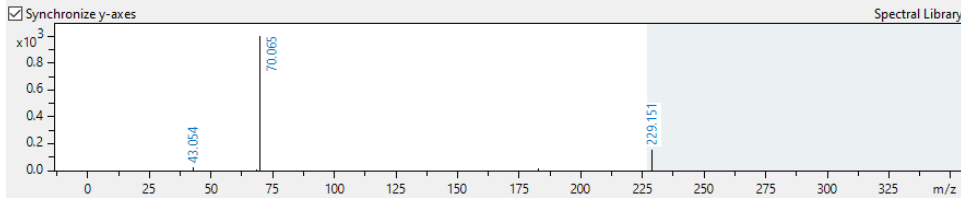
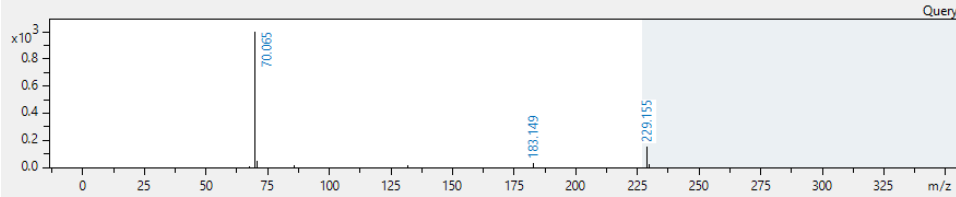
m/z meas.: 229.15484 ± 5 mDa

Formula: C₁₁H₂₀N₂O₃

Name: Pro Ile

ColEn. [eV]: 24.8 ± 10 eV

Analyte	Score	Fit	Prec. Ion	ColEn. [eV]
Pro Ile	998.47	999.68	229.15470	25.0-50.0
Pro Leu	998.32	999.87	229.15470	25.0-50.0



286.17633 C₁₃H₂₃N₃O₄ Pro Leu Gly 3.74 min

Precursor	ColEn. [eV]	Polarity
286.17633	26.9-27.0	POSITIVE

Library: Bruker MetaboBASE Personal Library 2.0

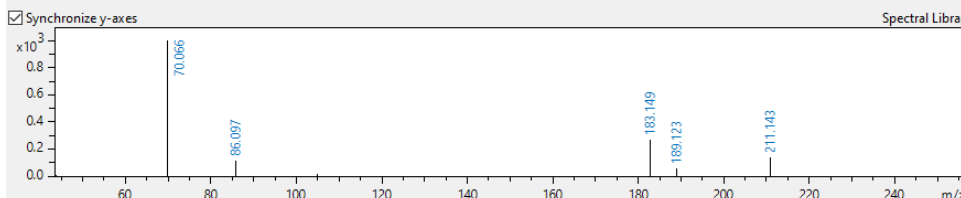
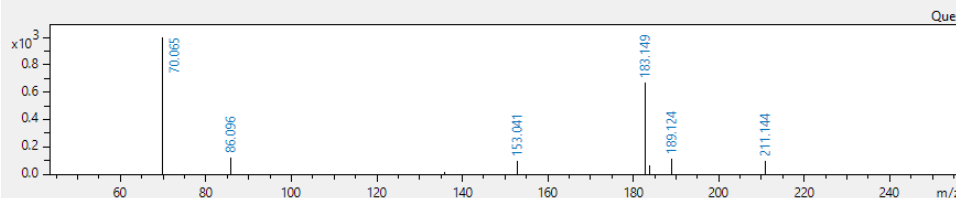
m/z meas.: 286.17633 ± 5 mDa

Formula: C₁₃H₂₃N₃O₄

Name: Pro Leu Gly

ColEn. [eV]: 26.9 ± 10 eV

Analyte	Score	Fit	Prec. Ion	ColEn. [eV]
Pro Leu Gly	941.38	945.34	286.17620	25.0-5
Pro Leu Gly	937.36	940.15	286.17620	10.0-2
Pro Ile Gly	907.94	914.35	286.17620	25.0-5
Pro Ile Gly	896.83	900.61	286.17620	10.0-2
Pro Gly Ile	820.05	989.51	286.17620	25.0-5
Pro Ala Val	806.64	973.33	286.17620	25.0-5
Pro Val Ala	803.04	968.99	286.17620	25.0-5
Pro Gly Ile	798.02	962.92	286.17620	10.0-2
Pro Gly Leu	795.19	959.52	286.17620	25.0-5
Gly Pro Ile	772.31	937.06	286.17620	25.0-5
Gly Pro Leu	767.60	931.35	286.17620	25.0-5



229.15480 C₁₁H₂₀N₂O₃ Pro Leu 6.94 min

Precursor	ColEn. [eV]	Polarity
229.15480	24.8-24.9	POSITIVE

Library: Bruker MetaboBASE Personal Library 2.0

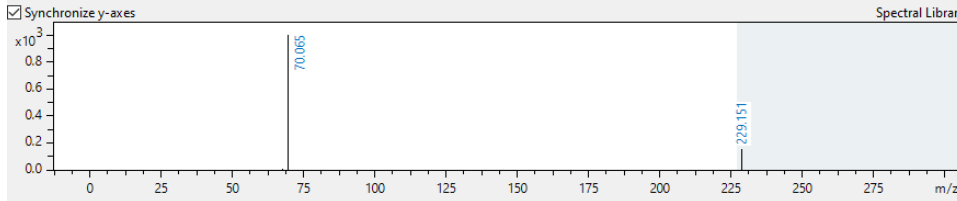
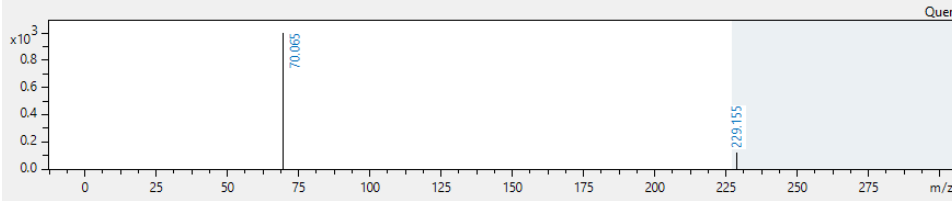
m/z meas.: 229.15480 ± 5 mDa

Formula: C₁₁H₂₀N₂O₃

Name: Pro Leu

ColEn. [eV]: 24.8 ± 10 eV

Analyte	Score	Fit	Prec. Ion	ColEn. [eV]
Pro Leu	999.85	999.85	229.15470	25.0-50.0
Pro Ile	999.77	999.77	229.15470	25.0-50.0



244.16571 C₁₁H₂₁N₃O₃ Pro Lys 13.51 min

Precursor	ColEn. [eV]	Polarity
244.16571	25.4-25.4	POSITIVE

Library: 20200430_C18_pos_yla_eco

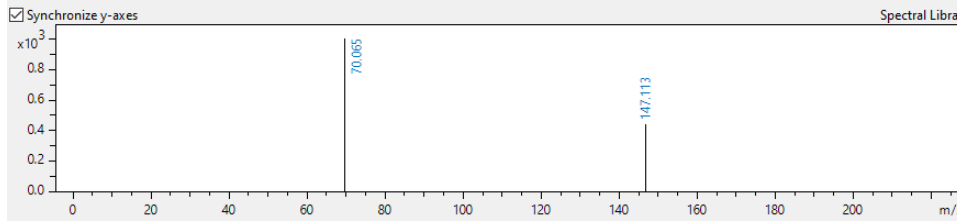
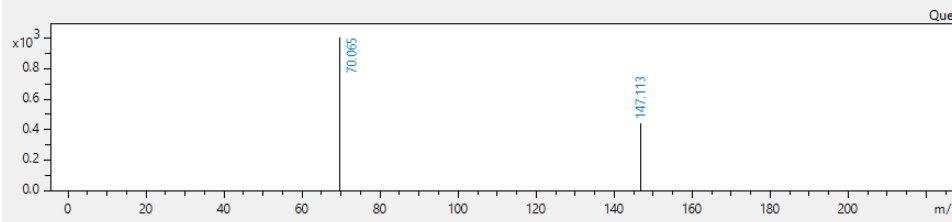
m/z meas.: 244.16571 ± 5 mDa

Formula: C₁₁H₂₁N₃O₃

Name: Pro Lys

ColEn. [eV]: 25.4 ± 10 eV

Analyte	Score	Fit	Prec. Ion	ColEn. [eV]
Pro Lys	1000.00	1000.00	244.16557	25.4-25.4



247.11139 C10H18N2O3S1 Pro Met 2.64 min

Precursor	ColEn. [eV]	Polarity
247.11139	25.5-25.5	POSITIVE

Library: Bruker MetaboBASE Personal Library 2.0

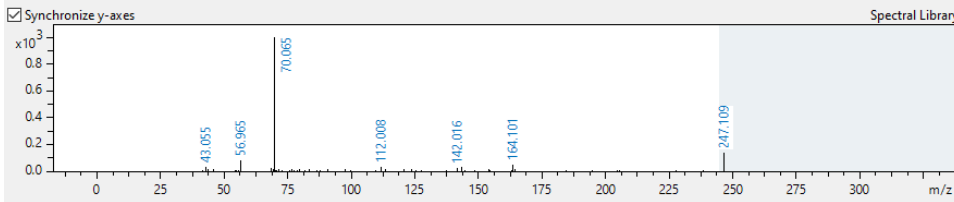
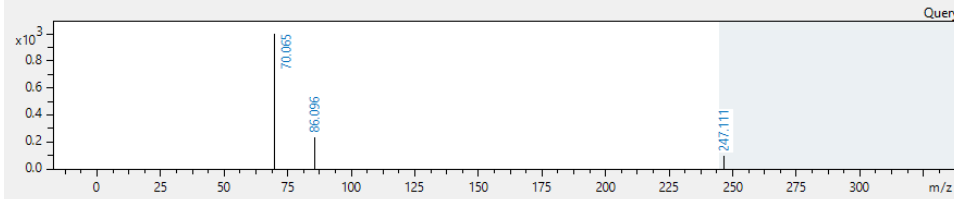
m/z meas.: 247.11139 ± 5 mDa

Formula: C₁₀H₁₈N₂O₃S₁

Name: Pro Met

ColEn. [eV]: 25.5 ± 10 eV

Analyte	Score	Fit	Prec. Ion	ColEn. [eV]
Pro Met	965.89	991.53	247.11110	25.0-50.0
Pro Met	952.18	977.46	247.11110	10.0-25.0



334.17635 C17H23N3O4 Pro Phe Ala 6.42 min

Precursor	ColEn. [eV]	Polarity
334.17635	28.8-28.8	POSITIVE

Library: 20200430_C18_pos_yla_eco

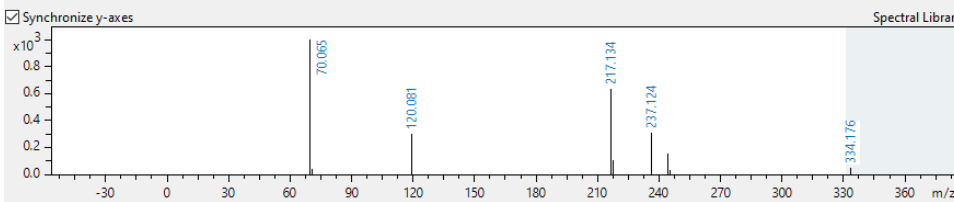
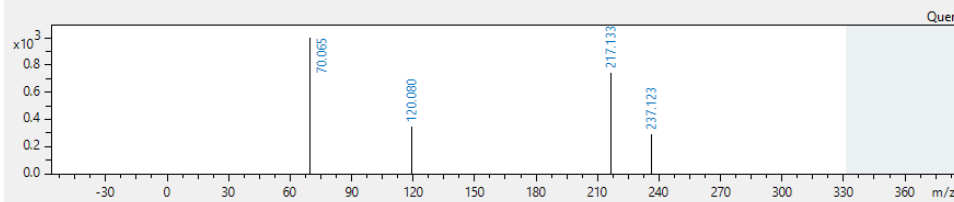
m/z meas.: 334.17635 ± 5 mDa

Formula: C₁₇H₂₃N₃O₄

Name: Pro Phe Ala

ColEn. [eV]: 28.8 ± 10 eV

Analyte	Score	Fit	Prec. Ion	ColEn. [eV]
Pro Phe Ala	390.02	596.76	334.17613	28.8-28.8



263.13919 C14H18N2O3 Pro Phe 6.31 min

Precursor	ColEn. [eV]	Polarity
263.13919	26.0-26.1	POSITIVE

Library: Bruker MetaboBASE Personal Library 2.0

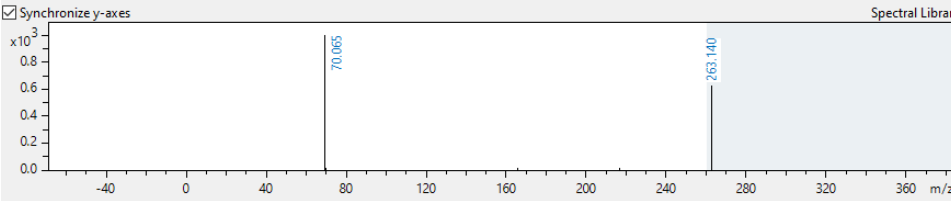
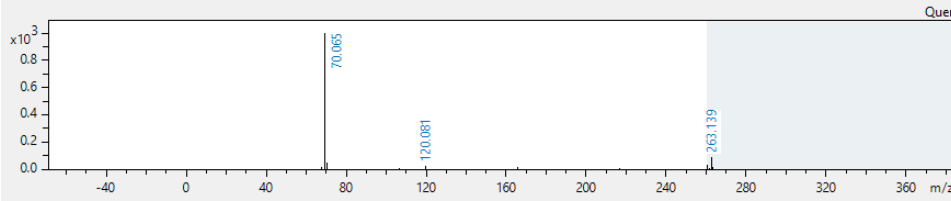
m/z meas.: 263.13919 ± 5 mDa

Formula: C₁₄H₁₈N₂O₃

Name: Pro Phe

ColEn. [eV]: 26.0 ± 10 eV

Analyte	Score	Fit	Prec. Ion	ColEn. [eV]
Pro Phe	998.28	999.89	263.13900	10.0-25.0
Pro Phe	998.17	999.93	263.13900	25.0-50.0
L-phenylalanyl-L-proline	508.14	508.93	263.13900	25.0-50.0
L-phenylalanyl-L-proline	13.57	671.59	263.13900	10.0-25.0



326.20763 C16H27N3O4 Pro Pro Ile 6.81 min

Precursor	ColEn. [eV]	Polarity
326.20763	28.5-28.5	POSITIVE

Library: Bruker MetaboBASE Personal Library 2.0

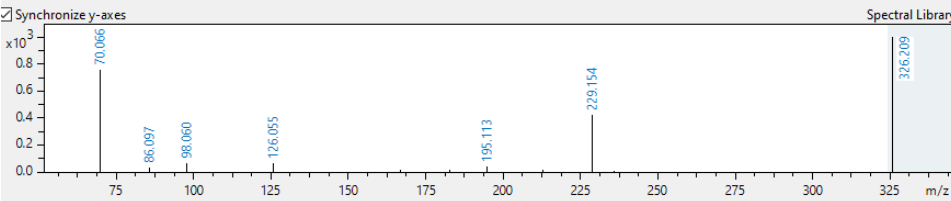
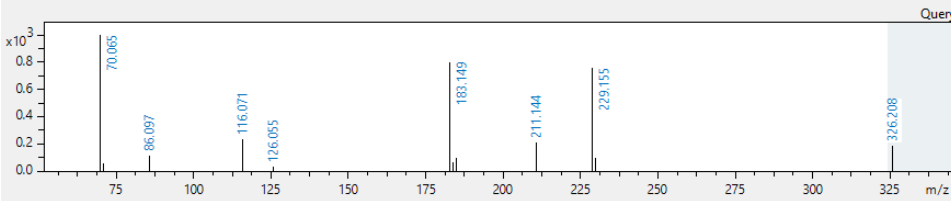
m/z meas.: 326.20763 ± 5 mDa

Formula: C₁₆H₂₇N₃O₄

Name: Pro Pro Ile

ColEn. [eV]: 28.5 ± 10 eV

Analyte	Score	Fit	Prec. Ion	ColEn. [eV]
Pro Pro Ile	777.26	797.91	326.20750	10.0-25.0
Pro Pro Ile	771.73	792.24	326.20750	25.0-50.0
Pro Pro Leu	523.72	537.74	326.20750	25.0-50.0
Pro Pro Leu	496.91	511.62	326.20750	10.0-25.0



360.19251 C19H25N3O4 Pro Pro Phe 7.61 min

Precursor	ColEn. [eV]	Polarity
360.19251	29.8-29.8	POSITIVE

Library: Bruker MetaboBASE Personal Library 2.0

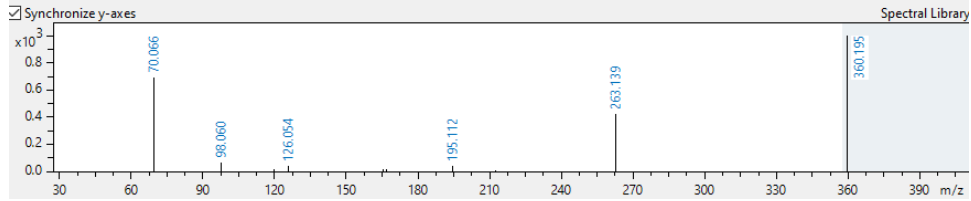
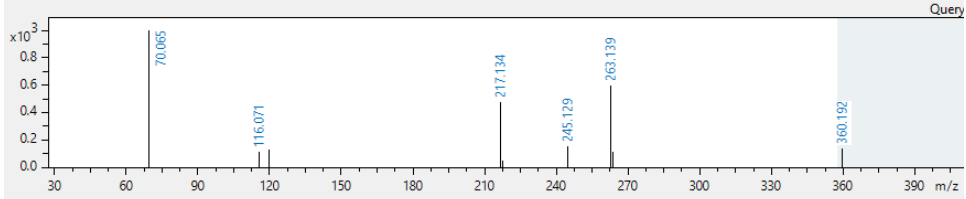
m/z meas.: 360.19251 ± 5 mDa

Formula: C₁₉H₂₅N₃O₄

Name: Pro Pro Phe

ColEn. [eV]: 29.8 ± 10 eV

Analyte	Score	Fit	Prec. Ion	ColEn. [eV]
Pro Pro Phe	903.51	989.80	360.19180	10.0-25.0
Pro Pro Phe	880.26	964.33	360.19180	25.0-50.0



312.19198 C15H25N3O4 Pro Pro Val 6.05 min

Precursor	ColEn. [eV]	Polarity
312.19198	28.0-28.0	POSITIVE

Library: 20200430_C18_pos_yla_eco

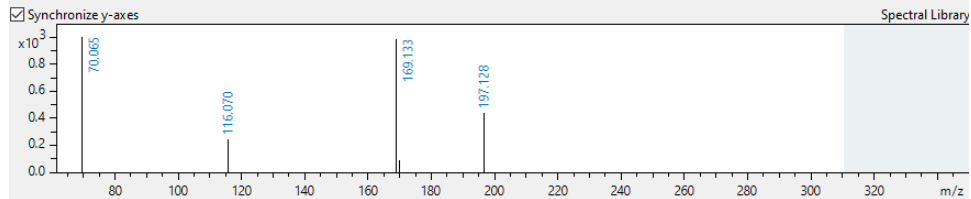
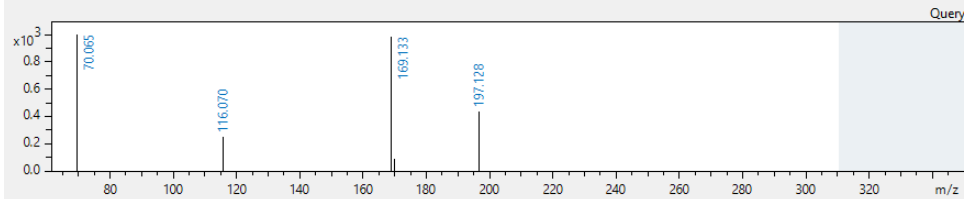
m/z meas.: 312.19198 ± 5 mDa

Formula: C₁₅H₂₅N₃O₄

Name: Pro Pro Val

ColEn. [eV]: 28.0 ± 10 eV

Analyte	Score	Fit	Prec. Ion	ColEn. [eV]
Pro Pro Val	1000.00	1000.00	312.19178	28.0-28.0



279.13420 C14H18N2O4 Pro Tyr 3.86 min

Precursor	ColEn. [eV]	Polarity
279.13420	26.7-26.7	POSITIVE

Library: Bruker MetaboBASE Personal Library 2.0

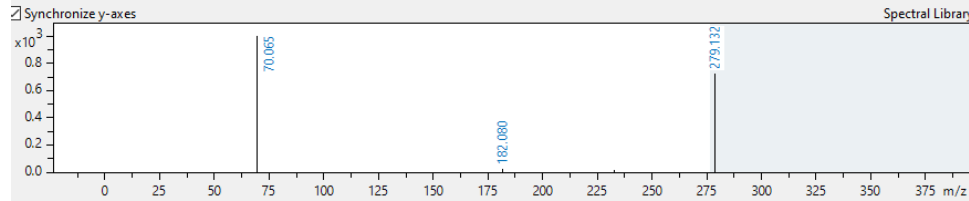
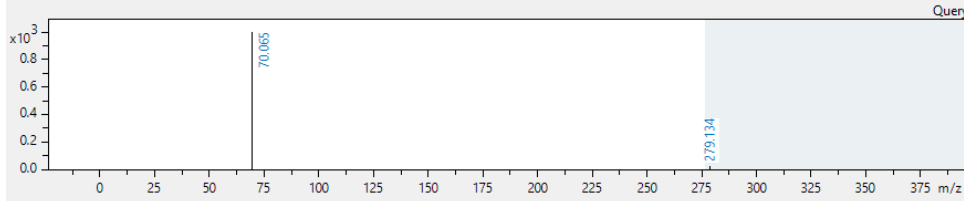
m/z meas.: 279.13420 ± 5 mDa

Formula: C₁₄H₁₈N₂O₄

Name: Pro Tyr

ColEn. [eV]: 26.7 ± 10 eV

Analyte	Score	Fit	Prec. Ion	ColEn. [eV]
Pro Tyr	999.50	999.50	279.13400	10.0-25.0
Carboxy-PTIO	23.60	23.60	279.13400	25.0-50.0
Carboxy-PTIO	13.74	13.74	279.13400	10.0-25.0



344.18172 C15H25N3O6 Pro Val Glu 2.67 min

Precursor	ColEn. [eV]	Polarity
344.18172	29.2-29.2	POSITIVE

Library: 20200430_C18_pos_ylla_eco

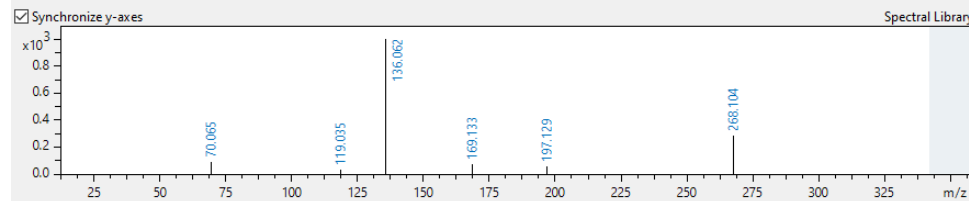
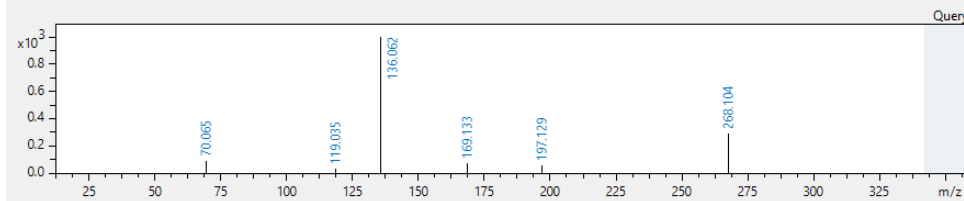
m/z meas.: 344.18172 ± 5 mDa

Formula: C₁₅H₂₅N₃O₆

Name: Pro Val Glu

ColEn. [eV]: 29.2 ± 10 eV

Analyte	Score	Fit	Prec. Ion	ColEn. [eV]
Pro Val Glu	1000.00	1000.00	344.18161	29.2-29.2
Pro Glu Val	63.59	769.88	344.18161	29.2-29.2



328.22322 C16H29N3O4 Pro Val Ile 7.39 min

Precursor	ColEn. [eV]	Polarity
328.22322	28.6-28.6	POSITIVE

Library: Bruker MetaboBASE Personal Library 2.0

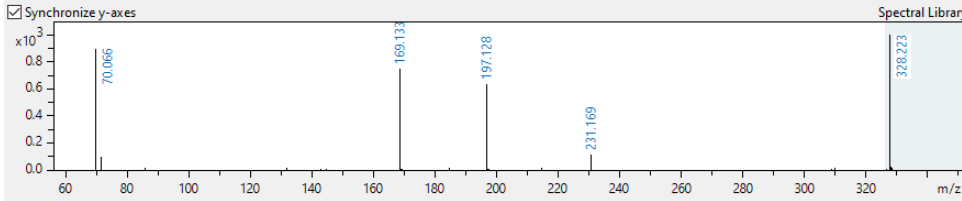
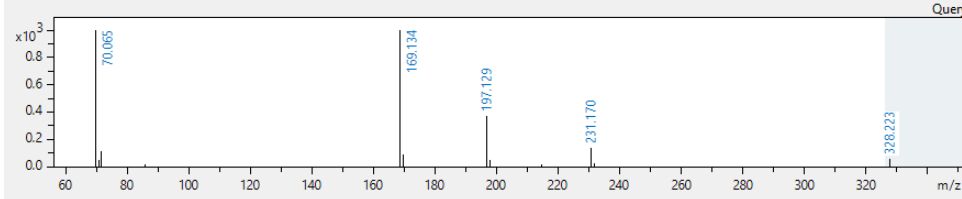
m/z meas.: 328.22322 ± 5 mDa

Formula: C16H29N3O4

Name: Pro Val Ile

ColEn. [eV]: 28.6 ± 10 eV

Analyte	Score	Fit	Prec. Ion	ColEn. [eV]
Pro Val Leu	965.30	999.96	328.22310	10.0-2
Pro Val Ile	965.19	967.66	328.22310	10.0-2
Pro Val Ile	886.02	888.34	328.22310	25.0-5
Pro Val Leu	867.54	898.69	328.22310	25.0-5
Val Pro Ile	668.93	673.35	328.22310	25.0-5
Pro Leu Val	668.82	972.36	328.22310	25.0-5
Val Pro Leu	664.15	668.57	328.22310	25.0-5
DIPROTIN B	657.68	662.02	328.22310	25.0-5
Pro Ile Val	632.91	920.16	328.22310	25.0-5
Ile Pro Val	611.24	635.83	328.22310	25.0-5
Pro Leu Val	555.84	813.19	328.22310	10.0-2



314.20742 C15H27N3O4 Pro Val Val 6.40 min

Precursor	ColEn. [eV]	Polarity
314.20742	28.0-28.0	POSITIVE

Library: Bruker MetaboBASE Personal Library 2.0

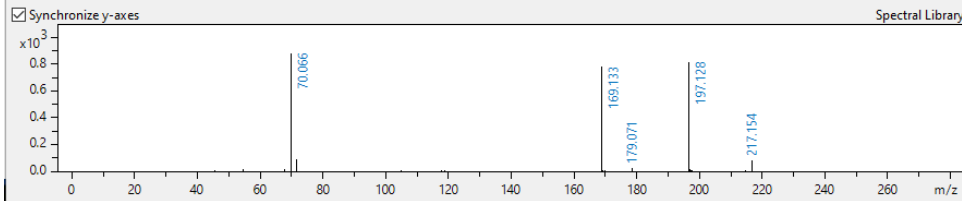
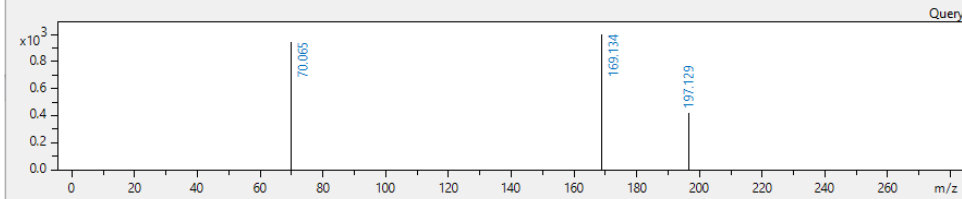
m/z meas.: 314.20742 ± 5 mDa

Formula: C15H27N3O4

Name: Pro Val Val

ColEn. [eV]: 28.0 ± 10 eV

Analyte	Score	Fit	Prec. Ion	ColEn. [eV]
Pro Val Val	946.37	946.37	314.20750	10.0-25.0
Pro Val Val	874.93	874.93	314.20750	25.0-50.0
Val Pro Val	602.50	602.50	314.20750	25.0-50.0
Val Pro Val	343.60	478.82	314.20750	10.0-25.0



215.13920 C10H18N2O3 Pro Val 2.18 min

Precursor	ColEn. [eV]	Polarity
215.13920	24.3-24.3	POSITIVE

Library: 20200430_C18_pos_yla_eco

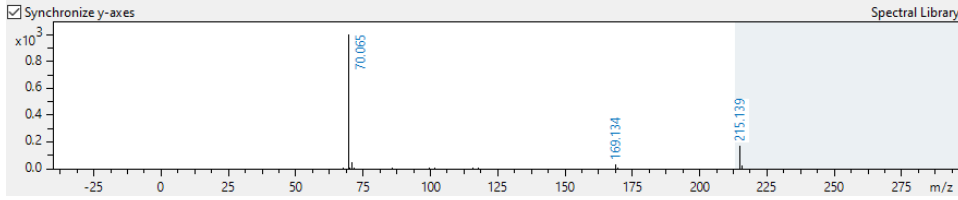
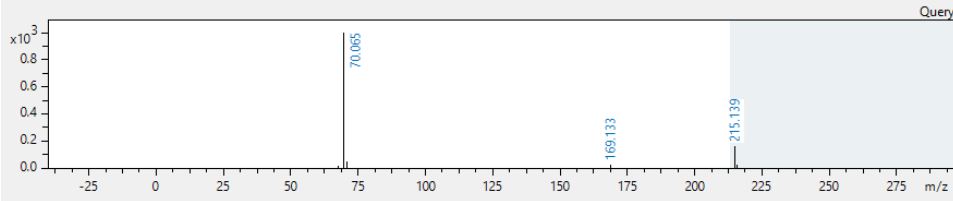
m/z meas.: 215.13920 ± 5 mDa

Formula: C₁₀H₁₈N₂O₃

Name: Pro Val

ColEn. [eV]: 24.3 ± 10 eV

Analyte	Score	Fit	Prec. Ion	ColEn. [eV]
Pro Val	999.97	999.97	215.13902	24.3-24.3



229.11840 C10H16N2O4 Pyro Glu Val 5.90 min

Precursor	ColEn. [eV]	Polarity
229.11840	24.8-24.8	POSITIVE

Library: 20200430_C18_pos_yla_eco

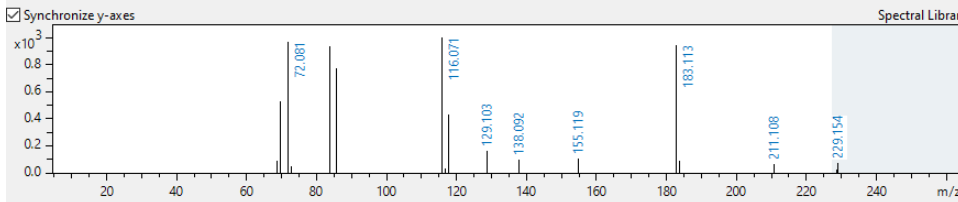
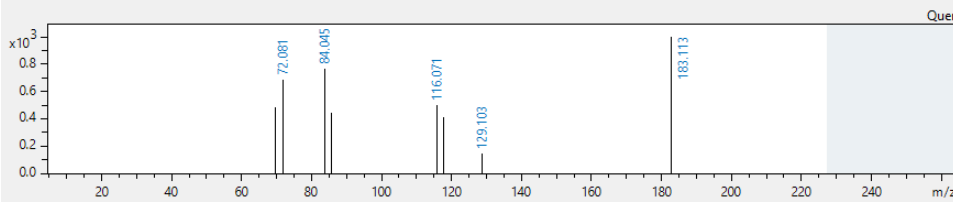
m/z meas.: 229.11840 ± 5 mDa

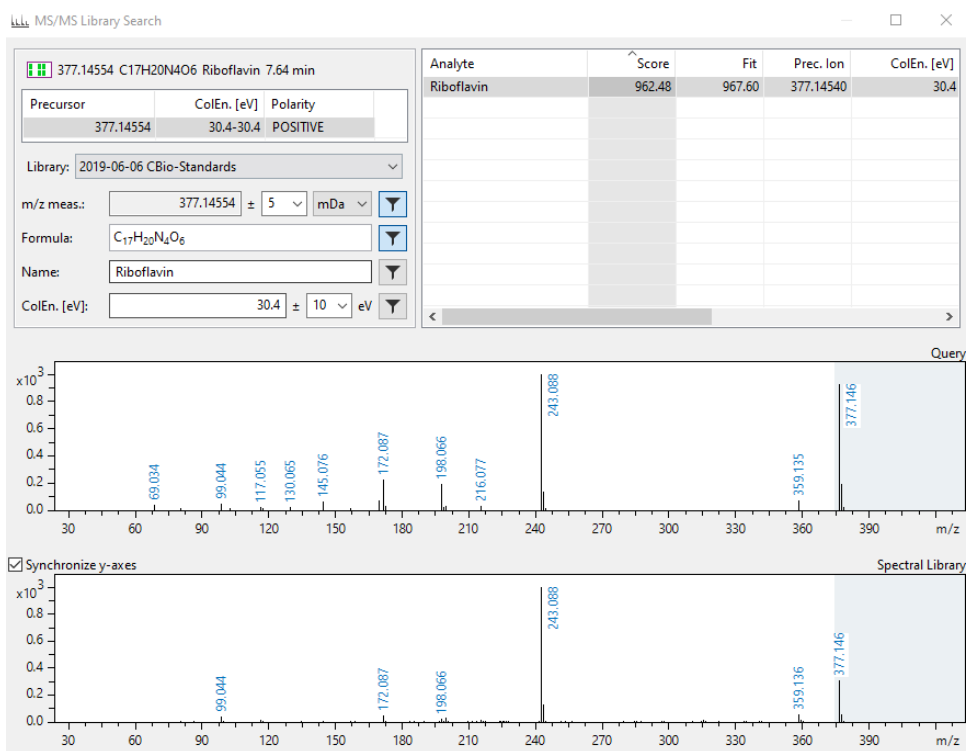
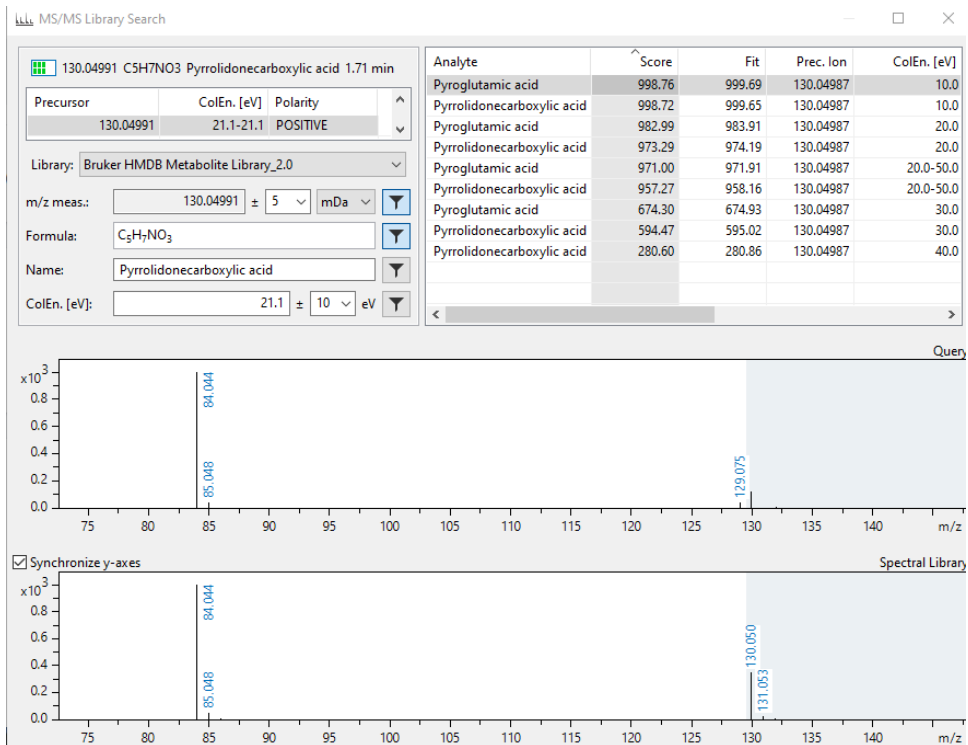
Formula: C₁₀H₁₆N₂O₄

Name: Pyro Glu Val

ColEn. [eV]: 24.8 ± 10 eV

Analyte	Score	Fit	Prec. Ion	ColEn. [eV]
Pyro Glu Val	895.50	933.30	229.11828	24.8-24.8





399.14467 C₁₅H₂₂N₆O₅S S-Adenosylmethionine 1.23 min

Precursor	ColEn. [eV]	Polarity
399.14467	31.2-31.2	POSITIVE

Library: Bruker MetaboBASE Personal Library 2.0

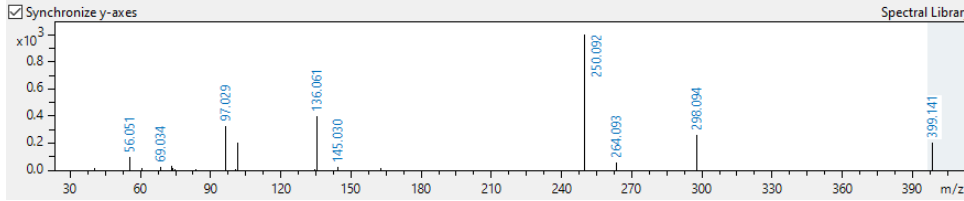
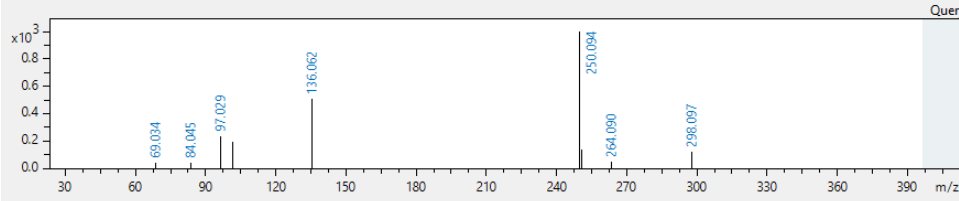
m/z meas.: 399.14467 ± 5 mDa

Formula: C₁₅H₂₂N₆O₅S

Name: S-Adenosylmethionine

ColEn. [eV]: 31.2 ± 10 eV

Analyte	Score	Fit	Prec. Ion	ColEn. [eV]
S-Adenosylmethionine	952.22	963.55	399.14450	10.0-25.0
S-Adenosylmethionine	736.58	745.05	399.14450	25.0-50.0



348.17649 C₁₄H₂₅N₃O₇ Ser Ile Glu 2.13 min

Precursor	ColEn. [eV]	Polarity
348.17649	29.3-29.3	POSITIVE

Library: 20200430_C18_pos_yla_eco

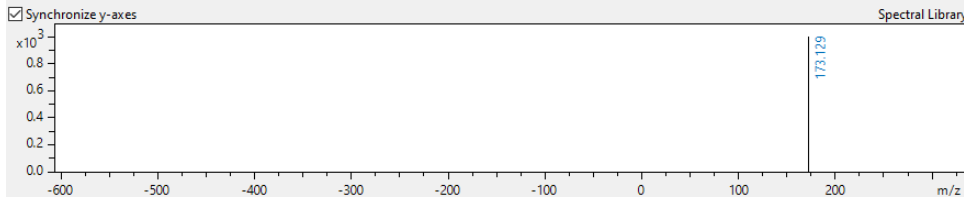
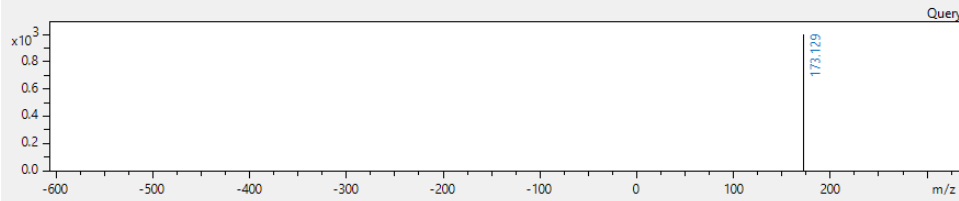
m/z meas.: 348.17649 ± 5 mDa

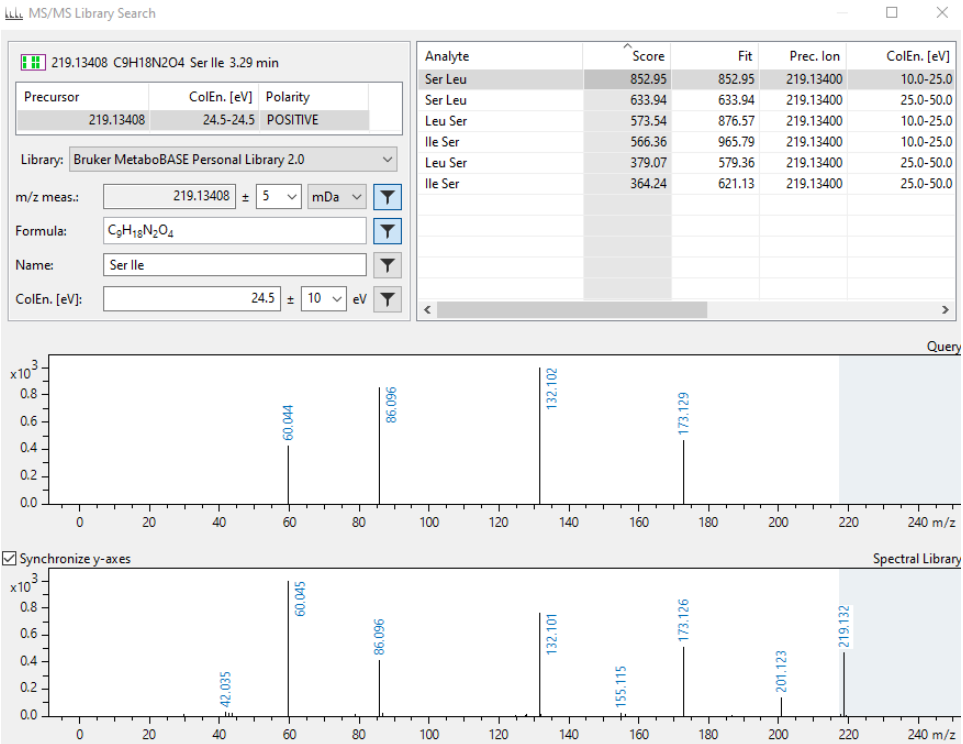
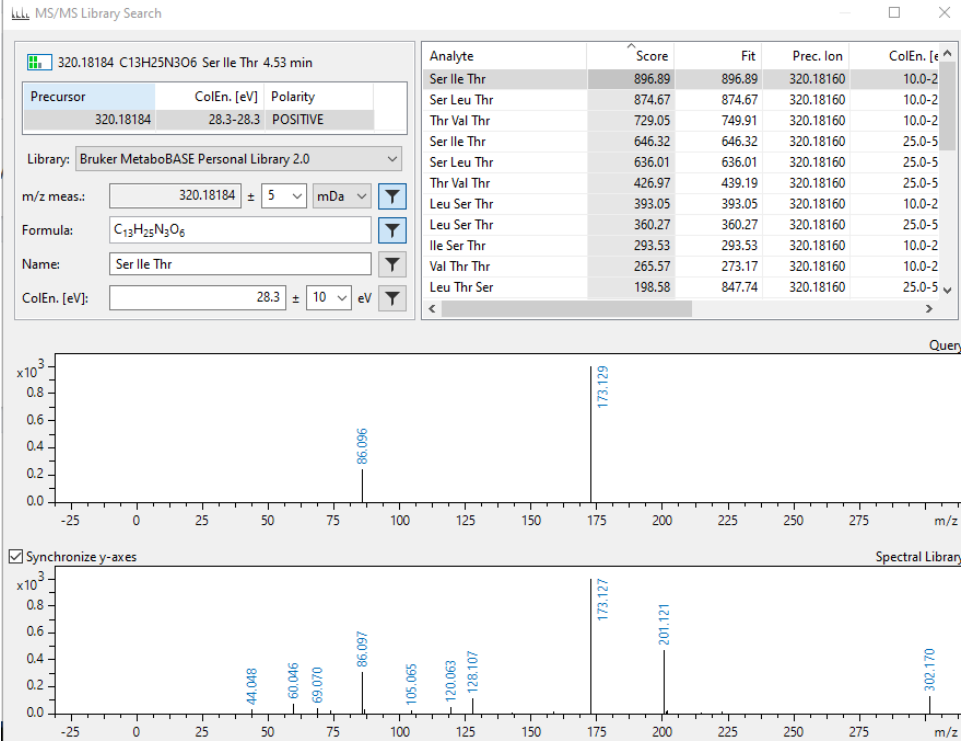
Formula: C₁₄H₂₅N₃O₇

Name: Ser Ile Glu

ColEn. [eV]: 29.3 ± 10 eV

Analyte	Score	Fit	Prec. Ion	ColEn. [eV]
Ser Ile Glu	1000.00	1000.00	348.17653	29.3-29.3





318.20254 C₁₄H₂₇N₃O₅ Ser Val Leu 6.97 min

Precursor	ColEn. [eV]	Polarity
318.20254	28.1-28.2	POSITIVE

Library: Bruker MetaboBASE Personal Library 2.0

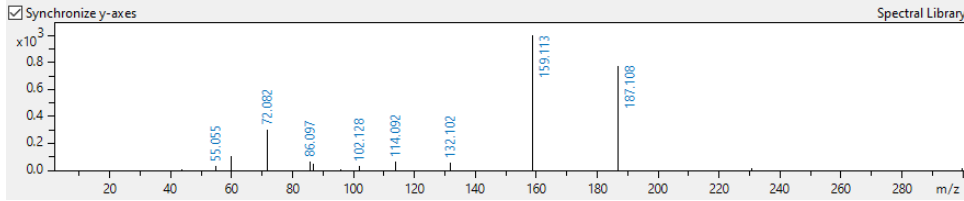
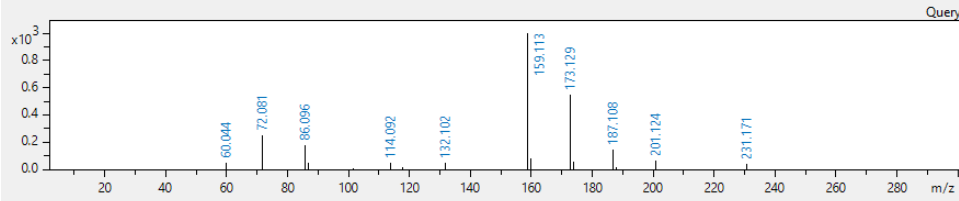
m/z meas.: 318.20254 ± 5 mDa

Formula: C₁₄H₂₇N₃O₅

Name: Ser Val Leu

ColEn. [eV]: 28.1 ± 10 eV

Analyte	Score	Fit	Prec. Ion	ColEn. [eV]
Ser Val Leu	770.05	870.49	318.20240	10.0-2
Ser Val Ile	761.28	860.67	318.20240	10.0-2
Ser Val Leu	609.51	689.42	318.20240	25.0-5
Ser Val Ile	603.34	682.11	318.20240	25.0-5
Val Ser Ile	458.00	459.93	318.20240	10.0-2
Thr Val Val	449.75	890.14	318.20240	10.0-2
Ser Leu Val	434.87	826.86	318.20240	10.0-2
Val Ser Ile	402.21	403.62	318.20240	25.0-5
Thr Val Val	369.27	733.57	318.20240	25.0-5
Ser Leu Val	361.38	685.62	318.20240	25.0-5
Leu Ser Val	322.22	323.78	318.20240	25.0-5



146.16529 C₇H₁₉N₃ Spermidine 1.09 min

Precursor	ColEn. [eV]	Polarity
146.16529	21.7-21.7	POSITIVE

Library: Bruker MetaboBASE Personal Library 2.0

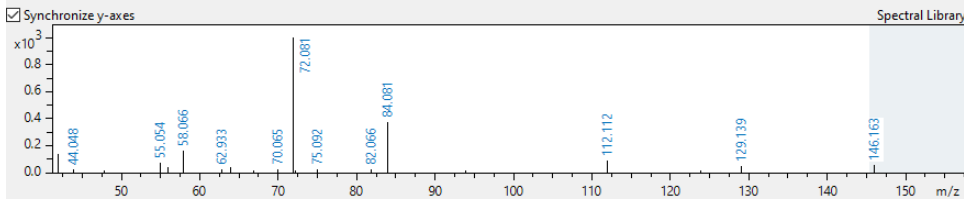
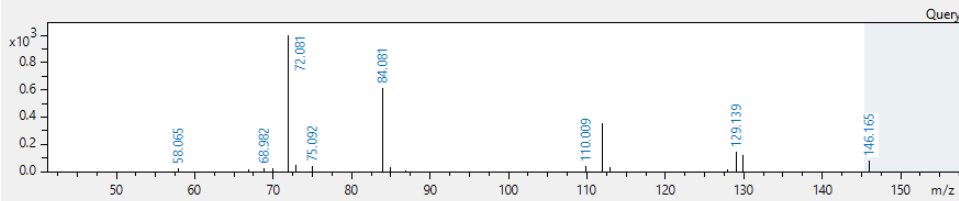
m/z meas.: 146.16529 ± 5 mDa

Formula: C₇H₁₉N₃

Name: Spermidine

ColEn. [eV]: 21.7 ± 10 eV

Analyte	Score	Fit	Prec. Ion	ColEn. [eV]
Spermidine	931.07	937.04	146.16521	25.0-50.0
Spermidine	902.53	908.45	146.16521	10.0-25.0



362.19218 C₁₅H₂₇N₃O₇ Thr Glu Leu 6.08 min

Precursor	ColEn. [eV]	Polarity
362.19218	29.8-29.8	POSITIVE

Library: 20200430_C18_pos_yla_eco

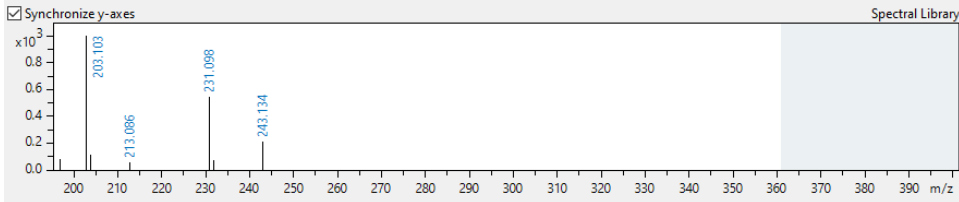
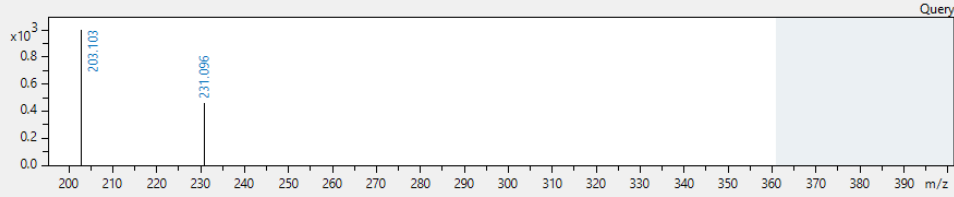
m/z meas.: 362.19218 ± 5 mDa

Formula: C₁₅H₂₇N₃O₇

Name: Thr Glu Leu

ColEn. [eV]: 29.8 ± 10 eV

Analyte	Score	Fit	Prec. Ion	ColEn. [eV]
Thr Glu Leu	925.26	925.26	362.19218	29.8-29.8



304.18669 C₁₃H₂₅N₃O₅ Thr Ile Ala 3.98 min

Precursor	ColEn. [eV]	Polarity
304.18669	27.7-27.7	POSITIVE

Library: 20200430_C18_pos_yla_eco

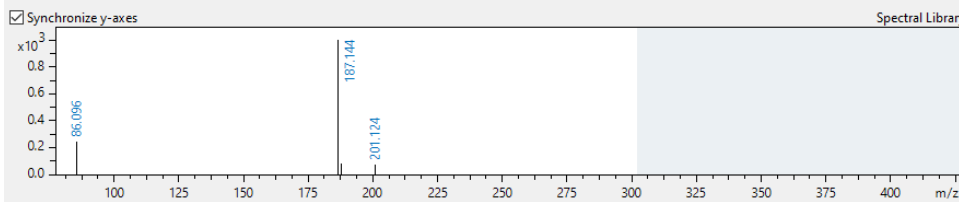
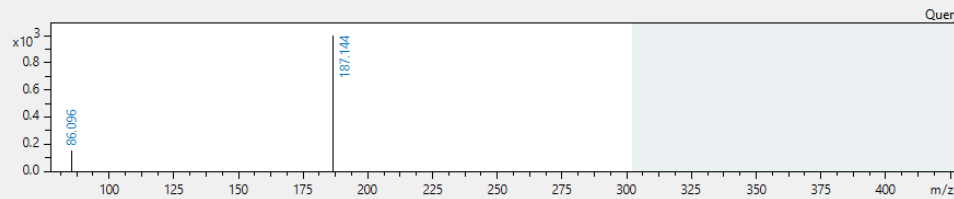
m/z meas.: 304.18669 ± 5 mDa

Formula: C₁₃H₂₅N₃O₅

Name: Thr Ile Ala

ColEn. [eV]: 27.7 ± 10 eV

Analyte	Score	Fit	Prec. Ion	ColEn. [eV]
Thr Ile Ala	988.52	988.52	304.18670	27.7-27.7



233.14968 C₁₀H₂₀N₂O₄ Thr Ile 6.33 min

Precursor	ColEn. [eV]	Polarity
233.14968	25.0-25.0	POSITIVE

Library: Bruker MetaboBASE Personal Library 2.0

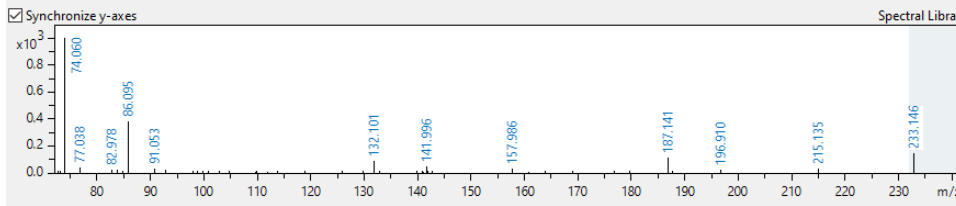
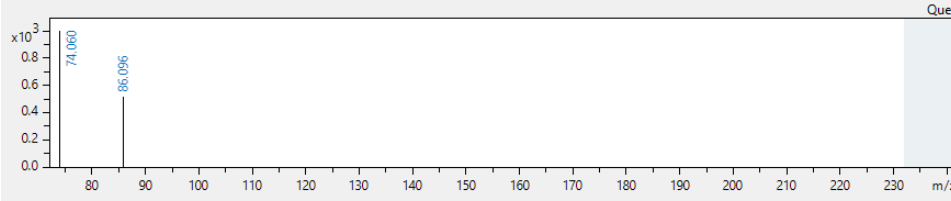
m/z meas.: 233.14968 ± 5 mDa

Formula: C₁₀H₂₀N₂O₄

Name: Thr Ile

ColEn. [eV]: 25.0 ± 10 eV

Analyte	Score	Fit	Prec. Ion	ColEn. [eV]
Thr Ile	890.97	890.97	233.14960	25.0-50.0
Thr Leu	882.03	882.03	233.14960	10.0-25.0
Thr Ile	844.17	844.17	233.14960	10.0-25.0
Thr Leu	767.27	767.27	233.14960	25.0-50.0
Ile Thr	427.24	427.24	233.14960	25.0-50.0
Leu Thr	343.27	343.27	233.14960	25.0-50.0



265.07971 C₁₀H₁₄N₂O₅ Thymidine 4.69 min

Precursor	ColEn. [eV]	Polarity
243.09808	25.3-25.4	POSITIVE

Library: Bruker MetaboBASE Personal Library 2.0

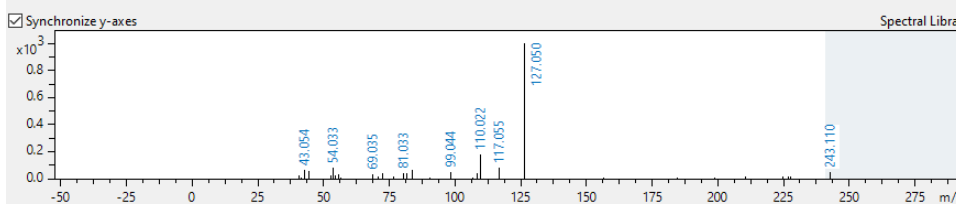
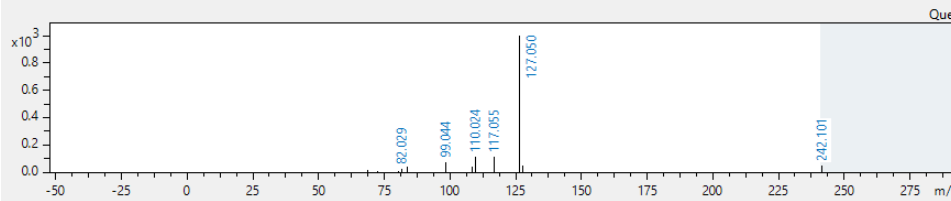
m/z meas.: 243.09808 ± 5 mDa

Formula: C₁₀H₁₄N₂O₅

Name: Thymidine

ColEn. [eV]: 25.3 ± 10 eV

Analyte	Score	Fit	Prec. Ion	ColEn. [eV]
Thymidine	984.59	987.11	243.09750	10.0-25.0
Thymidine	786.77	788.79	243.09750	25.0-50.0



127.05029 C₅H₆N₂O₂ Thymine 4.70 min

Precursor	ColEn. [eV]	Polarity
127.05029	21.0-21.0	POSITIVE

Library: Bruker MetaboBASE Personal Library 2.0

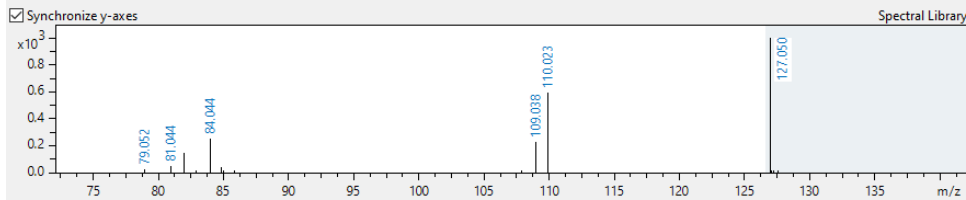
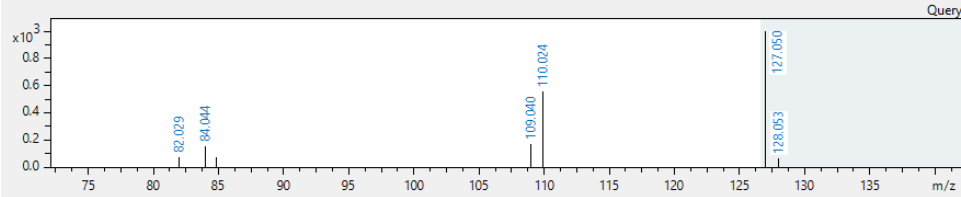
m/z meas.: 127.05029 ± 5 mDa

Formula: C₅H₆N₂O₂

Name: Thymine

ColEn. [eV]: 21.0 ± 10 eV

Analyte	Score	Fit	Prec. Ion	ColEn. [eV]
Thymine	751.93	751.93	127.05020	10.0-25.0
Thymine	347.21	347.21	127.05020	25.0-50.0



181.10123 C₁₄H₁₂ trans-Stilbene 14.27 min

Precursor	ColEn. [eV]	Polarity
181.10123	23.0-23.0	POSITIVE

Library: Bruker MetaboBASE Personal Library 2.0

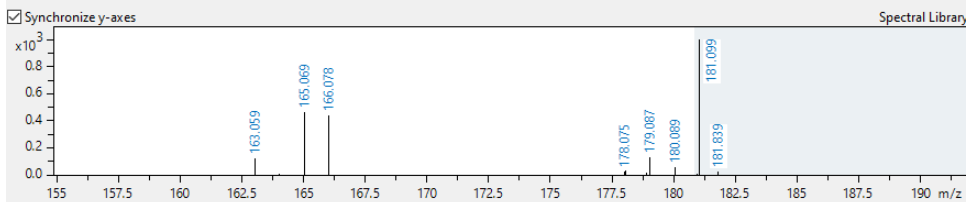
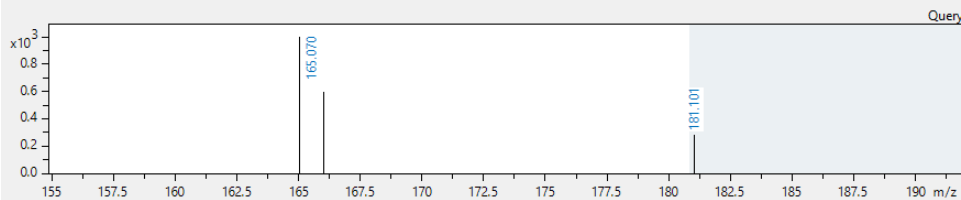
m/z meas.: 181.10123 ± 5 mDa

Formula: C₁₄H₁₂

Name: trans-Stilbene

ColEn. [eV]: 23.0 ± 10 eV

Analyte	Score	Fit	Prec. Ion	ColEn. [eV]
trans-Stilbene	685.19	685.19	181.10120	10.0-25.0
trans-Stilbene	591.99	591.99	181.10120	25.0-50.0



311.12381 C₁₄H₁₈N₂O₆ Tyr Glu 2.32 min

Precursor	ColEn. [eV]	Polarity
311.12381	27.9-27.9	POSITIVE

Library: Bruker MetaboBASE Personal Library 2.0

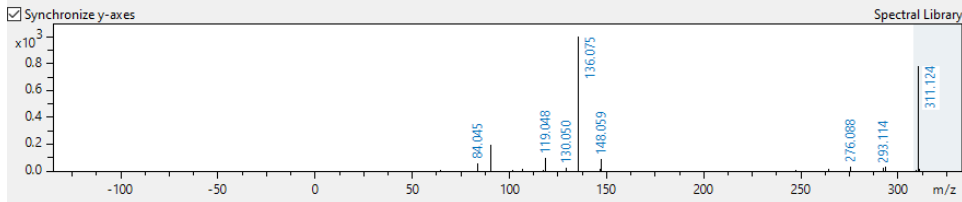
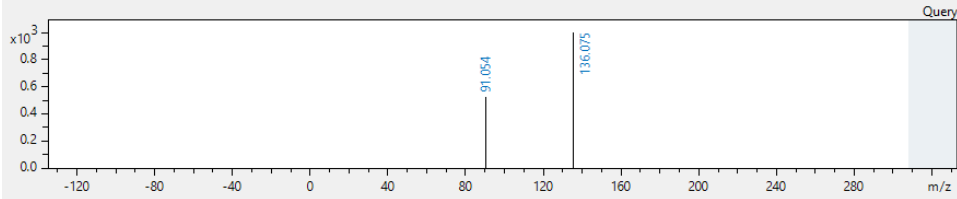
m/z meas.: 311.12381 ± 5 mDa

Formula: C₁₄H₁₈N₂O₆

Name: Tyr Glu

ColEn. [eV]: 27.9 ± 10 eV

Analyte	Score	Fit	Prec. Ion	ColEn. [eV]
Tyr Glu	947.67	947.67	311.12380	10.0-25.0
Tyr Glu	936.47	936.47	311.12380	25.0-50.0
Glu Tyr	428.81	428.81	311.12380	25.0-50.0
Glu Tyr	174.12	174.12	311.12380	10.0-25.0
Abu-Val-OH	14.93	32.22	311.12380	25.0-50.0



378.20226 C₁₉H₂₇N₃O₅ Tyr Pro Val 6.76 min

Precursor	ColEn. [eV]	Polarity
378.20226	30.4-30.4	POSITIVE

Library: 20200430_C18_pos_yla_eco

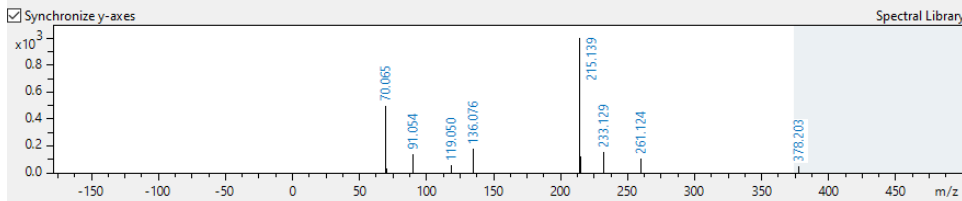
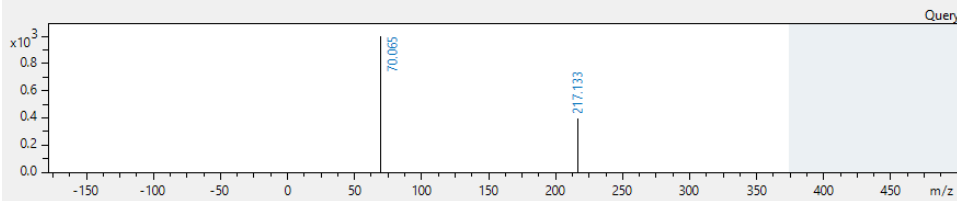
m/z meas.: 378.20226 ± 5 mDa

Formula: C₁₉H₂₇N₃O₅

Name: Tyr Pro Val

ColEn. [eV]: 30.4 ± 10 eV

Analyte	Score	Fit	Prec. Ion	ColEn. [eV]
Tyr Pro Val	397.93	427.66	378.20235	30.4-30.4



113.03459 C4H4N2O2 Uracil 1.60 min

Precursor	ColEn. [eV]	Polarity
113.03459	20.5-20.5	POSITIVE

Library: Bruker MetaboBASE Personal Library 2.0

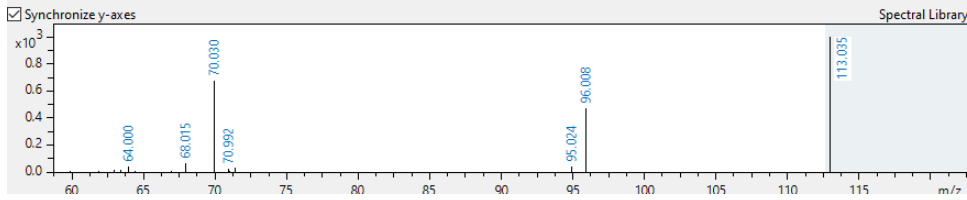
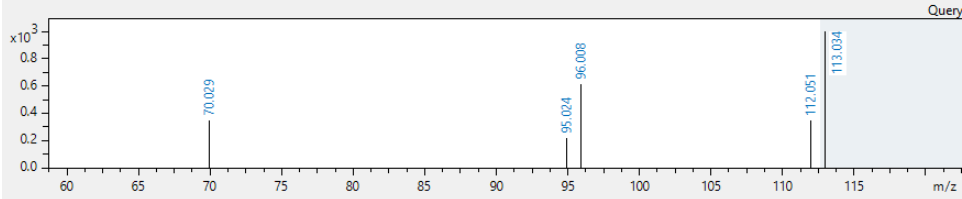
m/z meas.: 113.03459 ± 5 mDa

Formula: C₄H₄N₂O₂

Name: Uracil

ColEn. [eV]: 20.5 ± 10 eV

Analyte	Score	Fit	Prec. Ion	ColEn. [eV]
Uracil	725.91	801.38	113.03450	10.0-25.0
Uracil	411.39	454.16	113.03450	25.0-50.0



189.12344 C8H16N2O3 Val Ala 1.81 min

Precursor	ColEn. [eV]	Polarity
189.12344	23.3-23.3	POSITIVE

Library: Bruker MetaboBASE Personal Library 2.0

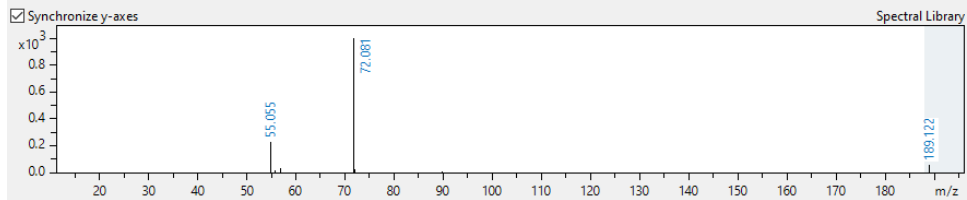
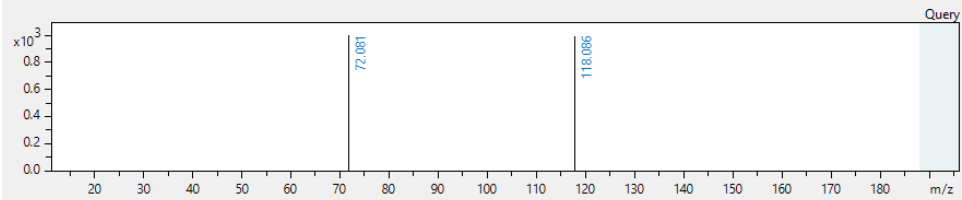
m/z meas.: 189.12344 ± 5 mDa

Formula: C₈H₁₆N₂O₃

Name: Val Ala

ColEn. [eV]: 23.3 ± 10 eV

Analyte	Score	Fit	Prec. Ion	ColEn. [eV]
Val Ala	693.47	975.02	189.12340	10.0-25.0
Ala Val	683.91	683.91	189.12340	10.0-25.0
Val Ala	511.47	719.13	189.12340	25.0-50.0
Ala Val	340.93	340.93	189.12340	25.0-50.0



231.17025 C11H22N2O3 Val Ile 6.05 min

Precursor	ColEn. [eV]	Polarity
231.17025	24.8-24.9	POSITIVE

Library: Bruker MetaboBASE Personal Library 2.0

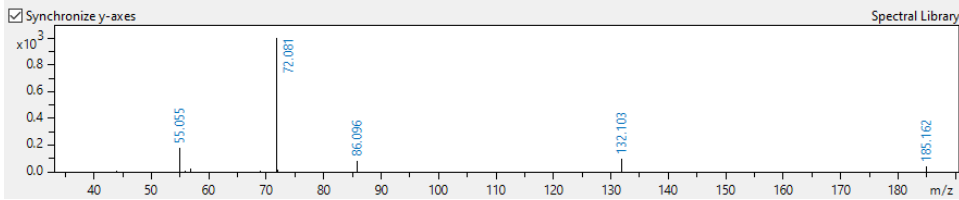
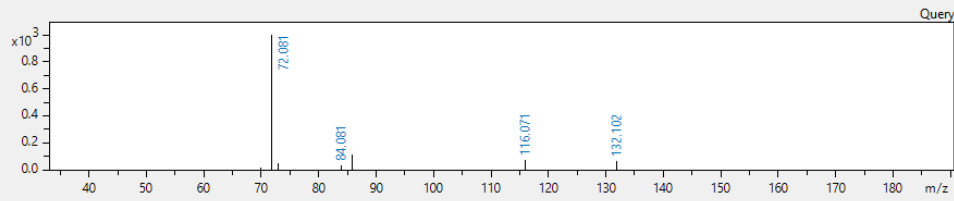
m/z meas.: 231.17025 ± 5 mDa

Formula: C₁₁H₂₂N₂O₃

Name: Val Ile

ColEn. [eV]: 24.8 ± 10 eV

Analyte	Score	Fit	Prec. Ion	ColEn. [eV]
Val Ile	979.66	983.19	231.17030	10.0-25.0
Val Leu	979.51	983.04	231.17030	10.0-25.0
Val Leu	863.29	866.40	231.17030	25.0-50.0
Val Ile	856.21	859.29	231.17030	25.0-50.0
Leu Val	297.40	299.00	231.17030	25.0-50.0
Leu Val	188.26	189.28	231.17030	10.0-25.0
Ile Val	159.20	160.04	231.17030	25.0-50.0



205.11849 C8H16N2O4 Val Ser 2.18 min

Precursor	ColEn. [eV]	Polarity
205.11849	23.9-23.9	POSITIVE

Library: Bruker MetaboBASE Personal Library 2.0

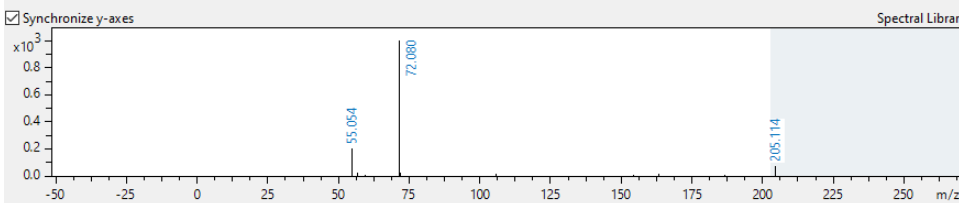
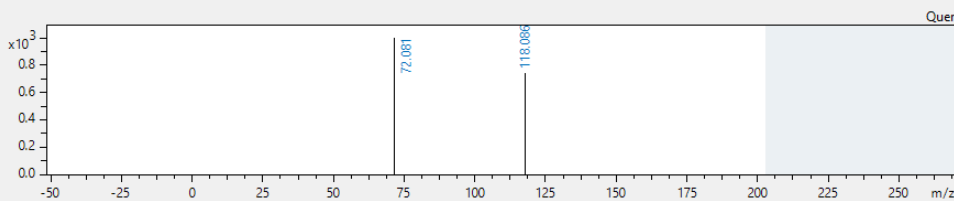
m/z meas.: 205.11849 ± 5 mDa

Formula: C₈H₁₆N₂O₄

Name: Val Ser

ColEn. [eV]: 23.9 ± 10 eV

Analyte	Score	Fit	Prec. Ion	ColEn. [eV]
Val Ser	787.39	980.26	205.11830	10.0-25.0
Val Ser	636.58	792.51	205.11830	25.0-50.0
Ser Val	523.45	523.45	205.11830	10.0-25.0
Ser Val	472.84	472.84	205.11830	25.0-50.0
Suberohydroxamic Acid	22.37	27.85	205.11830	25.0-50.0
Suberohydroxamic Acid	6.09	7.58	205.11830	10.0-25.0



281.14970 C₁₄H₂₀N₂O₄ Val Tyr 5.07 min

Precursor	ColEn. [eV]	Polarity
281.14970	26.8-26.8	POSITIVE

Library: 20200430_C18_pos_yla_eco

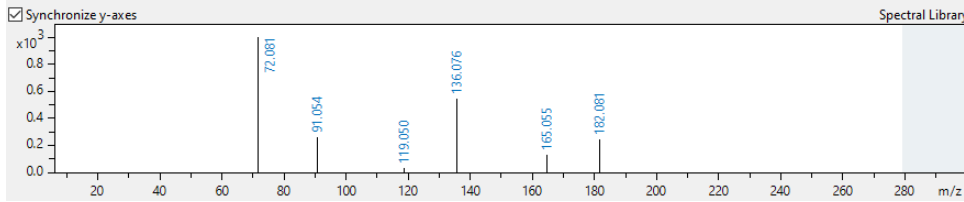
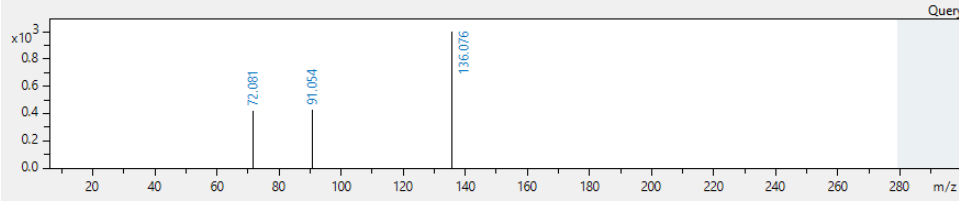
m/z meas.: 281.14970 ± 5 mDa

Formula: C₁₄H₂₀N₂O₄

Name: Val Tyr

ColEn. [eV]: 26.8 ± 10 eV

Analyte	Score	Fit	Prec. Ion	ColEn. [eV]
Val Tyr	764.69	764.69	281.14958	26.8-26.8



153.04080 C₅H₄N₄O₂ Xanthine 2.07 min

Precursor	ColEn. [eV]	Polarity
153.04080	22.0-22.0	POSITIVE

Library: Bruker MetaboBASE Personal Library 2.0

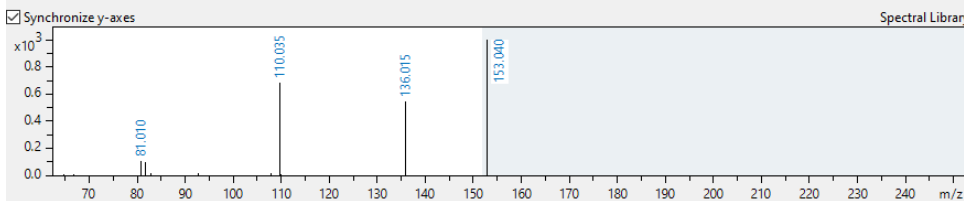
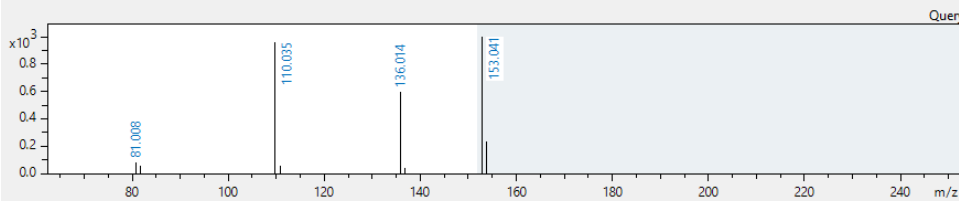
m/z meas.: 153.04080 ± 5 mDa

Formula: C₅H₄N₄O₂

Name: Xanthine

ColEn. [eV]: 22.0 ± 10 eV

Analyte	Score	Fit	Prec. Ion	ColEn. [eV]
Xanthine	626.30	627.32	153.04060	10.0-25.0
Xanthine	414.19	414.86	153.04060	25.0-50.0



Acknowledgment

I would like to thank my doctoral supervisor Prof. Dr. Mark Brönstrup who has supported me over the years. I would also like to thank Prof. Dr. Ursula Bilitewski and Prof. Dr. Till Strowig who gave me many supports for my research project and advice during my PhD as a member of my Thesis Committee.

Additionally, I would like to thank Dr. Raimo Franke who gave me great support and idea for the omics project. I would also thank Ulrike Beutling for supporting me to conduct LC-MS/MS measurements. Moreover, I would like to express my gratitude to the other members of CBIO: Dr. Mariel García, Dr. Federica Fiorini and Dr. Hans Prochnow who greatly supported me in terms of scientific ideas and PhD student life. I am very grateful to Aditya Shekhar, Jana Krull, Virginia Njau, Dr. Volker Berndt, Dr. Tobias Depke, Dr. Aamna Habib, Dr. Charlotte Grandclaudon, Dr. Kevin Ferreira, Dr. Christian Lentz and Dr. Tiankun Ren who have a good time with during the lunch breaks and on several occasions. Moreover, I would thank Heike Overwin, Dr. Sven-Kevin Hotop, Dr. Werner Tegge, Bettina Mehner and express my thanks to the other people in CBIO and COPS.

Furthermore, I would also like to acknowledge the HZI Graduate School for organizing a great PhD program including the scientific training, fellowship and several nice events for PhD students.

Last but not least I would thank my family and friends together with the above-mentioned for their support all the time, making my PhD life a wonderful journey: this work is dedicated to you.

Curriculum vitae

Name Yi-Hui Lai
Date of Birth 1989.11.18
Place of Birth Taipei, Taiwan

Education

Leibniz University Hannover Hannover, Germany
Ph.D. candidate in Chemistry Oct. 2017- present

National Taiwan University Taipei, Taiwan
M.S. in Molecular Medicine Sept. 2012-July 2014

GPA: thesis 4.3/4.3, overall 4.05/4.3

Taipei Medical University Taipei, Taiwan
B.S. in Medical Laboratory Science and Biotechnology Sept. 2008-June 2012

GPA: thesis 4.0/4.0, major 4.0/4.0, overall 3.79/4.0

Experience

Helmholtz Centre for Infection Research Braunschweig, Germany
Doctoral candidate, Department of Chemical Biology Oct. 2017- present

- Advisor: Prof. Mark Brönstrup
- Thesis: The uptake mechanism of synthetic siderophore conjugates in Gram-negative bacteria

National Taiwan University Taipei, Taiwan
Master and Research assistant, Graduate Institute of Molecular Medicine Jul. 2012-Sep. 2017

- Thesis: The role of a novel DEAD-box protein in NLRP3 inflammasome activation.

Publications and Poster Presentations

W.T. Tsai, Y.C. Lo, M. Wu, C.Y. Li, Y.P. Kuo, **Y.H. Lai**, Y. Tsai, K.C. Chen, T.H. Chuang, C.H. Yao, J.C. Lee, L.C. Hsu, John T.-A. Hsu, G. Y. Yu. (2016) Mycotoxin Patulin Suppresses Innate Immune Responses by Mitochondrial Dysfunction and p62/Sequestosome-1-Dependent Mitophagy. *J Biol Chem.* 2016 Sep 9;291 (37):19299-311.

Y.H. Lai, L.Pinkert, M. Brönstrup. The uptake mechanism of synthetic siderophore-conjugate in Gram-negative bacteria. (2019) EMBL Symposium: New Approaches and Concepts in Microbiology, Heidelberg, Germany

Y.H. Lai, C.H. Yang, S.W. Lin, L.C. Hsu. (2017) The role of a novel DEAD-box protein in NLRP3 inflammasome activation. National Health Research Institutes and Institute of Biomedical Sciences Joint International Conference on Inflammation & Disease, Taipei, Taiwan (selected short talk and First Place Award for Poster)

Y.H. Lai, L.C. Hsu. (2015) The role of a novel DEAD-box protein in NLRP3 inflammasome activation. The 30th Joint Annual Conference of Biomedical Science, Taipei, Taiwan (Outstanding Poster Award)

Yi-Hui Lai